

**Risk to Buried Gas Pipelines in Landslide Areas**

**by**

**Nelson John Ferreira**

**A Thesis submitted to the Faculty of Graduate Studies of**

**The University of Manitoba**

**in partial fulfilment of the requirements of the degree of**

**Doctor of Philosophy**

**Department of Civil Engineering**

**University of Manitoba**

**Winnipeg**

**Copyright © 2016 by Nelson John Ferreira**

## Abstract

Natural Hazards are a risk to buried gas pipeline infrastructure, but these risks are difficult to assess and quantify. This can often lead to the risks not being properly identified by pipeline owners. The risk to pipelines within landslide areas are particularly difficult to assess given the complex nature of landslide movements and the soil-pipeline interaction mechanisms imposing loads on a pipeline. This thesis research examines the relationship between ground movements and strains/stresses in buried pipelines through field measured ground movements and *in-situ* measured pipe strains/stresses. The pipe stresses and strains are then used to estimate probability of pipeline failure and risk based on RBDA limit states approaches.

Within Manitoba Hydro's pipeline network, three at-risk landslide areas (riverbank and deep river valleys) were selected for detailed studies. A field investigation and monitoring program was undertaken to assess possible sources of load and stresses on pipelines. Soil, ground, and pipe instrumentation were installed at the sites and monitored over a four year period.

Monitoring results identified soil near the pipeline does not freeze, and ground movements at valley sites are slow moving (<50 mm/year) landslides. The monitoring results also showed pipe stresses and behaviour were affected by backfilling, changes in river levels, thermal affects, soil-pipe relaxation, and ground movements. Pipe push tests were conducted in conjunction with FEM modelling to examine pipe adhesion and to possible explain the pipe behaviour observed.

Several ultimate and serviceability limit states pipe failure modes were assessed using the measured pipe stresses. Statistical analysis was undertaken to calculate the probability of pipeline failure for the various limit states failure modes and compared against limit states targets for several scenarios (backfill loads, initial stress-state of the pipeline, other pipelines within Manitoba Hydro network). Overall, the probability of failure estimates were generally insignificant or low due to a postulated soil-pipe relaxation mechanism which is causing a repeated release in longitudinal pipe stresses as the landslide continues to accumulate ongoing ground movements. Three mechanisms are presented and discussed. The statistical analysis indicate pipelines within Manitoba Hydro's network may exceed limit states targets for yielding and local buckling depending on the loading scenario and the class of the pipeline within the landslide area.

The outcome of the research was used to develop a risk managements system to examine geotechnical hazards within Manitoba Hydro's pipeline network. Specifically, risks associated with ground movements along natural slopes and at river crossings are examined within the system.

## **Acknowledgements**

I would like to thank Dr. J. Blatz, P.Eng. for his patience and guidance during my time at post-graduate studies. I am proud to say that I was one of his graduate students, twice!

Manitoba Hydro provided financial support along with technical support and company resources and for this I'm grateful. Specifically, I would like following Hydro personnel who helped with all or parts of my research, Kevin Klym, Jeff Tutkaluk, Lindsay Gigian, and especially Tim Starodub.

I acknowledge and appreciate financial support from the Natural Sciences and Engineering Research Council of Canada, the department of Civil Engineering, and the Canadian Geotechnical Society.

Special thanks go to my work colleagues at TREK Geotechnical who have helped where they can and provided me with an opportunity complete my research, sometimes with personnel and company sacrifices.

I would like to finally thank my parents João Carlos and Maria dos Anjos Ferreira who might not necessarily understand what I do for a living, but have always been supportive. Finally, I would like to especially thank Kelly Teixeira who took my mind off my research as much as possible and for her endless patience, encouragement, and support during my research.



# Table of Contents

Chapter 1 Introduction .....	1
1.1 Introduction .....	1
1.1.1 Justification for Research .....	2
1.2 Background .....	3
1.2.1 Standard of Practice, Regulations for Design and Operation of Gas Pipelines.....	3
1.2.2 Manitoba Hydro Gas Pipeline System and “At Risk” Sites .....	4
1.3 Hypothesis and Objectives .....	4
1.4 Organization of Thesis .....	5
Chapter 2 Literature Review.....	7
2.1 Introduction .....	7
2.2 Geohazards and Risk to Gas Pipelines .....	7
2.3 Limit States Approaches and RBDA Design for Onshore Pipelines .....	11
2.4 Applied Loads and Principal Stresses on Pipes.....	16
2.4.1 Applied Loads to Buried Pipeline.....	16
2.4.2 Stresses on Pipes.....	17
2.5 Ultimate and Serviceability Limit States Failure Modes for Buried Pipelines ..	20
2.5.1 Yielding Criteria .....	22
2.5.2 Tensile Rupture.....	23
2.5.3 Buckling.....	25
2.6 Statistical Analysis and RBDA Application.....	35
2.6.1 Probability Theory .....	36

2.6.2 Probability Theory Research Application in RBDA .....	40
2.7 Pipelines in Landslide (Current State-of-the-Art) .....	42
Chapter 3 Methodology .....	66
3.1 Information Gathering and Review .....	66
3.2 Selection of Research Sites .....	67
3.3 Field Program .....	67
3.3.1 Contributors to Strains/Stresses on Pipe.....	67
3.3.2 Field Program Details .....	69
3.4 Monitoring of Instrumentation and Ground Movements .....	70
3.5 Interpretation of Monitoring Data, Pipe Stresses, and Probability Calculations .....	71
3.6 Development of Risk Management System .....	72
Chapter 4 Research Sites and Field Work .....	73
4.1 Site Visits and Selection of Research Sites .....	73
4.2 Geology, Site Description, Sub-Surface Conditions, and Pipe Information .....	74
4.2.1 Riverbank Site - Plum River.....	74
4.2.2 Valley Sites – Harrowby and St-Lazare .....	76
4.2.3 Pipeline Information at the Research Sites.....	82
4.3 Field Instrumentation and Set-up .....	83
4.3.1 Riverbank Instrumentation Layout (Plum River).....	84
4.3.2 Valley Instrumentation Layout (Harrowby and St-Lazare).....	85
4.3.3 Strain Gauge and Temperature Gauge Set-up .....	85
4.3.4 Data Acquisition System and Solar Panel Set-Up.....	87

4.3.5 Monitoring Pin Installation.....	88
4.4 Abandoned Pipe Push Test (St-Lazare) Set-up .....	88
Chapter 5 Instrumentation Monitoring Results.....	117
5.1 Monitoring Disruptions, Instrument Noise, and Equipment Issues .....	117
5.1.1 Ground Movement Issues.....	118
5.1.2 Data Filtering Techniques .....	120
5.1.3 Results of Post-Processing of Noisy Monitoring Data.....	126
5.2 Ground Movement Results.....	127
5.3 Groundwater Results .....	127
5.4 Temperature Results.....	128
5.5 Strain Gauge Measurements.....	128
5.5.1 Laboratory Pipe Tests.....	128
5.5.2 Calculating Stresses from Strain Gauge Measurements.....	130
5.5.3 Understanding Raw Strain Gauge Data.....	134
5.5.4 Axial, Bending and Shear Stress Monitoring Results .....	134
5.6 St-Lazare Pipe Push Test Results .....	135
Chapter 6 Interpretation of Monitoring Data and Observations .....	171
6.1 Ground Movements.....	171
6.2 Temperature.....	173
6.2.1 Axial Pipe Stress due to Thermal Expansion .....	174
6.3 Pipe Stresses .....	177
6.3.1 Backfilling .....	177
6.3.2 Stress Relaxation After Pipeline Abandonment .....	178

6.3.3 Ground Movements, and Environmental and Regional Affects.....	179
6.3.4 Distinct Changes in Stresses at the Valley Sites.....	186
6.4 Pipe Push Tests.....	187
6.5 Summary .....	190
Chapter 7 Statistical Analysis and Probability of Pipeline Failure Estimates .....	204
7.1 Limit States Reliability Targets.....	204
7.1.1 Ultimate Limit States Reliability Targets.....	204
7.1.2 Serviceability Limit States Reliability Targets.....	207
7.2 Statistical Analysis Results.....	208
7.2.1 Statistical and Probability of Failure Results at Research Sites .....	208
7.2.2 Probability of Failure Estimates without “locked-in” Stresses and Beyond the Set-Ups .....	211
7.2.3 Standard Error Estimates .....	213
7.2.4 Initial Pipe Stress-State.....	214
7.3 Manitoba Hydro Pipeline Network Assessment .....	215
7.4 Summary .....	216
Chapter 8 Changes in Pipe Stresses due to Ground Movements or Other Mechanisms .	230
8.1 Changes Pipe Stresses Attributed to Ground Movements.....	231
8.2 Soil-Pipe Relaxation Mechanisms.....	232
8.2.1 Upward Block Movement .....	234
8.2.2 Soil Displaces around the Pipeline .....	236
8.2.3 Loss of Soil-Pipe Contact Due to Soil Volume Change.....	237
8.3 Summary .....	238

Chapter 9 Risk Management System .....	242
9.1 Phased Approach to PipeHaz .....	243
9.1.1 Phase 1 – Information Gathering and Review .....	244
9.1.2 Phase 2 – Hazard Inventory, Probability of Pipeline Failure Estimations, and Risk Evaluation .....	245
9.1.3 Phase 3 – Risk control analysis and cost-benefit analysis .....	246
9.1.4 Phase 4 – Action - remedial works, monitoring and re-evaluation ...	246
9.1.5 Phase 5 – System Maintenance .....	250
9.2 Quantitative Risk Indexing Method .....	251
9.2.1 Determination of Parameter Uncertainty .....	251
9.2.2 Subjective Probability of Failure Estimates for Geotechnical Hazard .....	252
9.3 Summary .....	254
Chapter 10 Summary, Conclusions and Recommendations for Future Research .....	261
10.1 Summary .....	261
10.2 Conclusions .....	264
10.3 Recommendations for Future Research.....	266
Chapter 11 References .....	269

## **Appendices**

Appendix A – Test Hole Logs

Appendix B – DA Programming

Appendix C – DA Monitoring Results (Raw and Filtered)

Appendix D – Statistical Results

Appendix E – Example of Application of the Risk Indexing Method

Digital Appendix - Monitoring and Statistical Data and Probability of Failure Estimator spreadsheet

## List of Tables

Table 4-1	Plum River Soil Properties .....	109
Table 4-2	St-Lazare Soil Properties – Silt Clay .....	110
Table 4-3	St-Lazare Soil Properties – Clay Shale.....	111
Table 4-4	Harrowby Soil Properties – Silt Clay .....	112
Table 4-5	Harrowby Soil Properties – Silt Clay with Varying Amounts of Organics .....	113
Table 4-6	Harrowby Soil Properties – Clay Shale.....	114
Table 4-7	Pipe Information at the Research Sites (based on original construction specifications) .....	115
Table 4-8	St-Lazare Soil Properties – Pipe Push Test Soil Backfill .....	115
Table 5-1	Interruptions to Instrumentation Monitoring.....	162
Table 5-2	Slope Inclinometer Operation Details .....	166
Table 5-3	Summary of Post-Processing of Monitoring Data .....	167
Table 5-4	St-Lazare Pipe Push Test Results .....	170
Table 6-1	Summary of Monitoring Pin Results for St. Lazare and Harrowby .....	201
Table 6-2	Distinct Changes in Pipe Stress over Relatively Short Durations (Valley Sites) .....	202
Table 6-3	Maximum Pipe Adhesion Estimates .....	203
Table 7-1	Class Location Designations (Adapted from Table 4.1, CSA Z662-15)....	222
Table 7-2	Population Density by Location Class (Adapted from Table O.2, CSA Z662-15) .....	223

Table 7-3	Predicted Probability of Failure (per km-yr) for Various Limit States Failure Mode.....	224
Table 7-4	Probability of Failure with and without “locked-in” stresses and % increased required to exceed limit states reliability targets .....	225
Table 7-5	Bootstrapping standard error estimates on predicated probability of failures for yield and local buckling at the research sites.....	226
Table 7-6	Potential exceedance of limit states for re-backfilled pipeline within slow moving valley and riverbank landslide areas.....	227
Table 7-7	Potential exceedance of limit states for pipelines within slow moving valley and riverbank landslide areas .....	229
Table 9-1	Level of Knowledge at a Site Index .....	258
Table 9-2	Level of Value of Information.....	259
Table 9-3	Landslides Probability of Pipeline Failure Estimate Index .....	259
Table 9-4	Ground Settlement, Subsidence and Soil Heave Probability of Pipeline Failure Estimate Index.....	260
Table 9-5	Subjective Probability (in a Given Year) .....	260



## List of Figures

Figure 2-1	Schematic Illustration of Typical Geotechnical Hazards in Manitoba (adapted from Porter and Savigny, 2002) .....	54
Figure 2-2	Schematic Representation of Expected Extent of Damage versus Movement Rate (adapted from Mansour et al. 2009) .....	54
Figure 2-3	Relationship between Probability of Failure versus Consequence.....	55
Figure 2-4	Principle Stresses acting on a Hollow Cylinder .....	55
Figure 2-5	Histogram Example .....	56
Figure 2-6	Histogram with Probability Density Function and Cumulative Probability Distribution Function.....	56
Figure 2-7	Schematics of Common Probability Distributions .....	57
Figure 2-8	Example of Probability of Tensile Rupture .....	58
Figure 2-9	Road Map of Predictive Models for Pipelines Subjected to Landslides .....	59
Figure 2-10	Spring/Slider Model for Axial Soil-Pipeline Interface Forces (O'Rourke Nordberg 1992) .....	60
Figure 2-11	Assumed Axial Force vs. Relative Displacement Relation for Elastic Spring/Slider Model of the Soil-Pipeline Interface (O'Rourke Nordberg 1992) .....	60
Figure 2-12	Pipeline Subjected to Longitudinal Transitional Slide: (a) plan view, (b) cross-section view. (Rajani et al. 1995) .....	61
Figure 2-13	Free Body Diagram Transitional Slide Limit Equilibrium Approach (Rajani et al. 1995) .....	61

Figure 2-14 (a) axial soil resistance, elastic-perfectly plastic (b) stress versus strain relation for typical steel pipeline (Rajani et al. 1995) .....	62
Figure 2-15 Longitudinal pull on pipeline due to planar slide (Rajani et al. 1995) .....	62
Figure 2-16 Non-dimensional characteristic curve for axial displacement for longitudinal soil-pipeline interaction (Rajani et al. 1995) .....	63
Figure 2-17 Non-dimensional characteristic curve for axial load-displacement for different values of the soil-pipeline stiffness parameter, .....	63
Figure 2-18 Comparison of $\alpha$ -Cu between theoretical model (CGL, 1984) and experimental data by Rizkalla et al. (1996) noted as NGTL, and Cappelletto et al. (1998) noted as SNAM .....	64
Figure 2-19 Recommend bounds for adhesion factors (modified from D.G. Honegger Consulting et al., 2009).....	64
Figure 2-20 Idealized Soil Movement Patterns: (a) shallow planar slip in plan view (b) deep-seated planar slip side view, (c) circular slip in side view. $\delta$ resultant soil .....	65
Figure 4-1 Location of Research Sites .....	92
Figure 4-2 Plum River Site Plan and Cross-Section .....	93
Figure 4-3 St-Lazare Site Plan and Cross-Section .....	94
Figure 4-4 Harrowby Site Plan and Cross-Section .....	95
Figure 4-5 Plum River Riverbank (2009) .....	96
Figure 4-6 St-Lazare Research Site.....	96
Figure 4-7 St-Lazare Research Site.....	97
Figure 4-8 Harrowby Research Site .....	97

Figure 4-9	Harrowby Research Site .....	98
Figure 4-10	Riverbank Site Test Hole and Instrumentation Layout Schematic (Plum River) .....	99
Figure 4-11	Valley Sites Test Hole and Instrumentation Layout Schematic .....	100
Figure 4-12	Assumed Direction Ground Movement at Research Sites .....	101
Figure 4-13	Strain Gauge Configuration .....	101
Figure 4-14	Strain Gauges (a) Uniaxial (Vishay WK-06-250bg-350) and (b) Torsion (Vishay WK-06-125TR-10CW) .....	102
Figure 4-15	Epoxied Unaxial Strain Gauge.....	102
Figure 4-16	Epoxied Torsion Strain Gauge.....	103
Figure 4-17	Strain Gauge and Pipe Temperature Gauge Installation Sequence.....	104
Figure 4-18	Data Acquisition (DA) System, with auxiliary components and Solar Panel Set-Up.....	105
Figure 4-19	Location of Three Pipe Push Tests.....	106
Figure 4-20	Schematic of Pipe Push Test Figure .....	107
Figure 4-21	Fabricated Strike Plate and Pipe Attachment .....	108
Figure 4-22	Excavator Pushing on Abandoned Pipe.....	108
Figure 5-1	(a) Frequency spectrum (hypothetical) of a waveform including desired signal and unwanted higher frequency noise, (b) filter response of low pass filter used to attenuate the noise (c) filter output spectrum where higher frequency noise is severely attenuated while the desired signal is relatively unchanged with only slight distortion in transition zone (modified from Winter 2009). .....	137

Figure 5-2	Hypothetical Application of Low Frequency and High Frequency Filter to a Data Set .....	138
Figure 5-3	Residual plot vs cut-off frequencies used to determine optimal frequency, $f'_c$ (Winter 2009) .....	138
Figure 5-4	Example of Filtered Monitoring Data with a Butterworth Filter.....	139
Figure 5-5	Example of Residual Cut-Off Frequency Plot showing .....	139
Figure 5-6	Monitoring Pin Results St-Lazare .....	140
Figure 5-7	Monitoring Pin Results Harrowby.....	141
Figure 5-8	Overall Monitoring Pin Results St-Lazare .....	142
Figure 5-9	Overall Monitoring Pin Results Harrowby.....	143
Figure 5-10	St. Lazare – Pin Movement Parallel to Pipe Alignment .....	144
Figure 5-11	St. Lazare – Pin Movement Perpendicular to Pipe Alignment .....	144
Figure 5-12	Harrowby – Pin Movement Parallel to Pipe Alignment .....	145
Figure 5-13	Harrowby – Pin Movement Perpendicular to Pipe Alignment .....	145
Figure 5-14	Plum River Pipe and Ground Temperatures.....	146
Figure 5-15	St-Lazare Top of Valley Pipe and Ground Temperatures .....	146
Figure 5-16	St-Lazare Bottom of Valley Ground Temperatures .....	147
Figure 5-17	Harrowby Top of Valley Pipe and Ground Temperatures .....	147
Figure 5-18	Harrowby Bottom of Valley Ground Temperatures.....	148
Figure 5-19	Laboratory Pipe Load Test Results .....	148
Figure 5-20	Understanding Stresses Induced on the Pipe Using Two Uniaxial Strain Gauges .....	149

Figure 5-21	Example of Monitoring Results from Uniaxial Strain Gauges (Harrowby Top of Valley).....	150
Figure 5-22	Pipe Stresses Plum River Beyond the Crest.....	151
Figure 5-23	Pipe Stresses Plum River Along Slope.....	152
Figure 5-24	Pipe Stresses St-Lazare Top of Valley .....	153
Figure 5-25	Pipe Stresses St-Lazare Middle of Valley .....	154
Figure 5-26	Pipe Stresses St-Lazare Bottom of Valley .....	155
Figure 5-27	Pipe Stresses Harrowby Top of Valley .....	156
Figure 5-28	Pipe Stresses Harrowby Middle of Valley .....	157
Figure 5-29	Pipe Stresses Harrowby Bottom of Valley .....	158
Figure 6-1	Measured Axial Stress and Axial Stresses without Thermal Affects at the Valley Sites.....	192
Figure 6-2	Plum River Bending and Axial Stresses with Time and Seasons.....	193
Figure 6-3	St-Lazare Bending and Axial Stresses with Time and Seasons .....	194
Figure 6-4	Harrowby Bending and Axial Stresses with Time and Seasons.....	195
Figure 6-5	Bending Stress with Time and Season for the Valley Sites .....	196
Figure 6-6	Comparison of $\alpha$ -Su from St-Lazare pipe push test (modified from D.G. Honegger Consulting et al., 2009).....	197
Figure 6-7	Example of Pipe Adhesion Simulation FEM model Output .....	197
Figure 6-8	Modelled Axial Pipe Stress along the Pipe for St-Lazare .....	198
Figure 6-9	Modelled Horizontal Soil Stress at Soil-Pipe Interface for St-Lazare.....	198
Figure 6-10	Modelled Horizontal Soil Stress versus Young's Modules for Plum River .....	199

Figure 6-11	Modelled Horizontal Soil Stress versus Young's Modules for St-Lazare	199
Figure 6-12	Modelled Horizontal Soil Stress versus Young's Modules for Harrowby	200
Figure 7-1	Target Probability of Failure (Pf) for Varying Consequences	218
Figure 7-2	Yield Statistics and Best-Fit Theoretical Distribution (Harrowby Middle of Valley Histogram)	219
Figure 7-3	Tensile Rupture Statistics and Best-Fit Theoretical Distribution (Harrowby Middle of Valley Histogram)	219
Figure 7-4	CSA Strain Buckling Statistics and Best-Fit Theoretical Distribution (Harrowby Middle of Valley Histogram)	220
Figure 7-5	DNV Strain Buckling Statistics and Best-Fit Theoretical Distribution (Harrowby Middle of Valley Histogram)	220
Figure 7-6	DNV (2000) Load Controlled Buckling Statistics and Best-Fit Theoretical Distribution (Harrowby Middle of Valley Histogram)	221
Figure 7-7	DNV (2012) Load Controlled Buckling Statistics and Best-Fit Theoretical Distribution (Harrowby Middle of Valley Histogram)	221
Figure 8-1	Landslide Related Ground Movements at Research Sites	239
Figure 8-2	Free Body Diagram of Pipe Response to Downward Soil Displacements	240
Figure 8-3	Upward Block Mechanism	240
Figure 8-4	Soil Displaces Around the Pipe Mechanism	241
Figure 8-5	Loss of Soil-Pipe Contact Due to Soil Volume Change Mechanism	241

Figure 9-1	PipeHaz Risk Management Process .....	255
Figure 9-2	PipeHaz Detailed Site Monitoring Process .....	256
Figure 9-3	Risk Level for Site Probability Targets .....	257
Figure 9-4	Priority Sites Flow Chart .....	257

## **List of Copyrighted Material for which Permission was Obtained**

“Figure 2 Schematic Illustrations of Geotechnical Hazards” from Porter, M, Savigny, W. 2002. Natural Hazard and Risk Management for South American Pipelines. *In Proceedings 4th International Pipeline Conference*, Calgary, Alberta, 2002. Appears as Figure 2-1 on page 54.

“Figure 3-6 Schematic Representation of the Developed Scales Showing the Degree of Damage and the Consequence Factor versus Movement Rate” from Mansour, M.F. 2009. *Characteristic Behaviour of Slow Moving Slides*, Ph.D. Thesis. University of Alberta:Canada. Appears as Figure 2-2 on page 54.

“Figure 7. Pipeline subjected to a longitudinal planar slide: (a) plan view, (b) section view.” from Rajani, B.B, Robertson, P.K., Morgenstern, N.R. 1995. *Simplified Design Methods for Pipelines Subject to Transverse and Longitudinal Soil Movements*. *Canadian Geotechnical Journal*. Volume 32, 309 – 323. Appears as Figure 2-12 on page 61.

“Figure 8. Pipeline – planar slide force system.” from Rajani, B.B, Robertson, P.K., Morgenstern, N.R. 1995. *Simplified Design Methods for Pipelines Subject to Transverse and Longitudinal Soil Movements*. *Canadian Geotechnical Journal*. Volume 32, 309 – 323. Appears as Figure 2-13 on page 61.

“Figure 9. (a) Typical soil resistance vs. displacement at the soil-pipeline interface, and (b) stress vs. strain relation for typical pipeline steel.” from Rajani, B.B, Robertson, P.K., Morgenstern, N.R. 1995. *Simplified Design Methods for Pipelines Subject to Transverse*



and Longitudinal Soil Movements. Canadian Geotechnical Journal. Volume 32, 309 – 323.  
Appears as Figure 2-14 on page 62.

“Figure 10. Longitudinal pull on pipeline due to planar slide.” from Rajani, B.B, Robertson, P.K., Morgenstern, N.R. 1995. Simplified Design Methods for Pipelines Subject to Transverse and Longitudinal Soil Movements. Canadian Geotechnical Journal. Volume 32, 309 – 323. Appears as Figure 2-15 on page 62.

“Figure 11. Nondimensional characteristic curve for axial load-displacement for longitudinal soil-pipeline interaction.” from Rajani, B.B, Robertson, P.K., Morgenstern, N.R. 1995. Simplified Design Methods for Pipelines Subject to Transverse and Longitudinal Soil Movements. Canadian Geotechnical Journal. Volume 32, 309 – 323. Appears as Figure 2-16 on page 63.

“Figure 11. Nondimensional characteristic curve for axial load-displacement for different values of the soil-pipeline stiffness parameter,  $\kappa$ .” from Rajani, B.B, Robertson, P.K., Morgenstern, N.R. 1995. Simplified Design Methods for Pipelines Subject to Transverse and Longitudinal Soil Movements. Canadian Geotechnical Journal. Volume 32, 309 – 323. Appears as Figure 2-17 on page 63.

“Figure 10  $\alpha$ -Cu comparison between theoretical model proposed by CGL (1984) and experimental data on pipelines.” from Cappelletto, A., Tagliaferri, R., Gianmario, G., Giuseppe, A., Furlani, G., Scarpelli, G. 1998. Field full scale tests on longitudinal pipeline-soil interaction. *In Proceedings International Pipeline Conference, Calgary, Alberta, 1998.* Appears as Figure 2-18 on page 64.

“Fig. 5. Idealized soil movement patterns: (a) shallow planar slip in plan view, (b) deep-seated planar slip in side view, and (c) circular slip in side view.  $\delta$ , resultant soil movement;  $\delta_L$  and  $\delta_P$ , soil longitudinal and transverse movement components, respectively;  $\delta_t$ , rotational (tangential) displacement.” from Chan, P.D.S, Wong, R.C.K. 2004. Performance Evaluation of Buried Steel Pipe in a Moving Slope: A Case Study. Canadian Geotechnical Journal. Volume 41, 894-907. Appears as Figure 2-20 on page 65.

“Figure 2.16 (a) Hypothetical frequency spectrum of a waveform consisting of a desired signal and unwanted higher frequency noise. (b) Response of low-pass filter  $X_o(f)/X_i(f)$ , introduced to attenuate the noise. (c) Spectrum of the output waveform, obtained by multiplying the amplitude of the input by the filter response at each frequency. Higher-frequency noise is severely attenuated, while the signal is passed with only minor distortion in transition region around  $f_c$ .” from Winter, D. 2009. Biomechanics and Motor Control of Human Movement, 4th edition, John Wiley and Sons Inc. Appears as Figure 5-1 on page 137.

“Figure 3.20 Plot of the residual between a filtered and an unfiltered signal as a function of the filter cutoff frequency. See text for the interpretation as to where to set the cutoff frequency of the filter.” from Winter, D. 2009. Biomechanics and Motor Control of Human Movement, 4th edition, John Wiley and Sons Inc. Appears as Figure 5-3 on page 138.

“Tables 4.1 Class Location Designators and Table O.2 Population Density by Location Class ” from Canadian Standards Association. (2015). CSA Z662-15 Oil and Gas Pipeline Systems. Appears as Table 7-1 on page 222 and Table 7-2 on page 223.

## List of Symbols

$P_f$	=	Probability of Failure in a given period of time, per km-yr
$P_t$	=	limit states target reliability in the form of a probability of failure, per km-yr
$H$	=	Likelihood of a hazard occurring as a probability
$V$	=	Vulnerability of a system as a probability of failure
$\sigma_h$	=	hoop stress due to pressure differential, MPa
$p_i$	=	internal pressure of pipe, MPa
$p_e$	=	external hydrostatic pressure, MPa
$E$	=	Young's modulus of steel, MPa
$D$	=	outside diameter, mm or m
$t$	=	pipe wall thickness, mm or m
$r$	=	radius, mm or m
$\sigma_L$	=	longitudinal stress, MPa
$M$	=	bending moment, MN per m
$S$	=	section Modulus of hollow pipe, m <sup>3</sup>
$P_A$	=	axial force, MN
$A$	=	cross-sectional radius, m <sup>2</sup>
$F_y$	=	effective specified minimum yield strength, MPa
SMYS	=	Specified minimum yield strength, MPa
$\sigma_{ef}$	=	combined equivalent stress (von Mises), MPa
$\sigma_h$	=	hoop stress, MPa
$\sigma_L$	=	longitudinal stress, MPa
$\tau$	=	tangential shear stress, MPa

- $\varepsilon_t^{\text{crit}}$  = ultimate tensile strain capacity (pipe wall or weldment)  
 $\varepsilon_t$  = tensile strains  
 $\varepsilon_c^{\text{crit}}$  = ultimate compressive strain capacity (pipe wall or weldment)  
 $\varepsilon_c$  = compressive strains  
 $\alpha_h$  = yield to ultimate stress ratio in axial tension  
 $\alpha_{gw}$  = girth weld reduction factor (=1.0 if no girth weld)  
 $p_b(t)$  = burst pressure, MPa  
 $R_{t0.5}$  = yield strength at 0.5% of test specimen, MPa  
 $R_m$  = ultimate strength of test specimen, MPa  
 $f_y$  = characteristic yield tensile strength, MPa  
 $f_u$  = characteristic ultimate tensile strength, MPa  
 $S_{Sd}$  = design effective force, MN  
 $M_{Sd}$  = design bending moment  
 $S_p(t_2)$  = characteristic plastic force resistance, MN  
 $M_p(t_2)$  = plastic moment resistance, MN per m  
 $p_b(t_2)$  = pressure containment resistance, MPa  
 $t_2$  = net pipe wall thickness free of possible corrosion, mm  
 $\alpha_c$  = flow stress parameter accounting for strain hardening  
 $\alpha_p$  = parameter accounting for effect of  $D/t_2$   
 $F(x)$  = cumulative distribution function (CDF)  
 $X$  = random variable  
 $x$  = discrete values of  $x$  (statistics)  
 $f(x)$  = probability density function (PDF)

- $\mu$  = mean value of random variable X
- $\sigma$  = standard deviation of random variable X
- $\lambda$  = mean of  $\ln(X)$
- $\zeta$  = standard deviation of  $\ln(X)$
- $l_s$  = the limit states resistance (critical) value for a particular failure mode
- $F_x$  = axial adhesion load on the pipe, kN
- $\alpha$  = adhesion factor between the pipe and soil
- $C_u$  = undrained shear strength of the soil, kPa
- $S_u$  = undrained shear strength of the soil, kPa
- $L$  = buried pipe length, m
- $K_o$  = coefficient of lateral earth pressure at rest soil
- $\gamma'$  = average effective unit weight of the soil, kN/m<sup>3</sup>
- $H$  = depth below ground surface to centerline of the pipe, m
- $\delta$  = interface angle of friction between the pipe and the soil, degrees
- $x$  = the measured or recorded signal or unfiltered raw data (data filtering)
- $\hat{x}$  = is the true signal of interest
- $e$  = error or noise introduce into the recorded signal
- $R(f_c)$  = residual value for a specific cut-off frequency
- $x_i$  = unfiltered (raw) data at the  $i$ th sample
- $x'_n$  = Butterworth filtered data at the  $i$ th sample
- $N$  or  $n$  = number of sample points
- $V_o$  = voltage output, volts
- $V_o$  = excitation voltage, volts

$GF$	=	Gauge Factor
$\varepsilon_o$	=	measured strain
$\varepsilon$	=	temperature corrected strain
$\varepsilon_T$	=	strain due to temperature change (based on manufacturers formula and measured pipe temperatures)
$\sigma$	=	pipe stress, MPa
$\tau$	=	shear stress, MPa
$\nu$	=	poisson's ratio of steel, 0.3
$T$	=	shaft torsion, MN per m
$d_o$	=	outside diameter of pipe, m
$d_i$	=	inside diameter of pipe, m
$\sigma_T$	=	axial stress due temperature differential, MPa
$\alpha_T$	=	coefficient of thermal expansion of steel, $12 \times 10^{-6}$ m/m/°C
$T_2$	=	measured pipe temperature, °C
$T_1$	=	initial pipe temperature, °C
$R_{TLS}$	=	limit states target reliability, per km-yr
$P$	=	pipeline pressure, MPa
$\rho$	=	average population density per hectare

# **Chapter 1 Introduction**

## **1.1 Introduction**

Natural hazards (often referred to as geohazards) are recognized by the pipeline industry as a risk to gas pipeline infrastructure, but these hazards are often underestimated and are not properly incorporated into design and operation of gas pipelines. This lack of consideration is due to the fact that geohazards are not a major contributor to pipeline failures as documented in several studies where only 7 to 9% of pipeline incidents are reported to be attributed to geohazards (European Gas Pipeline Incident Data Group, 2011; US DOT., 2004; Allergro Energy Consulting, 2005; National Energy Board, 2011). The major causes of pipeline incidents are external interference (40 to 50%), corrosion (15 to 25%) and construction (15 to 20%). However, the risk posed by natural hazards is proportionally significant, especially in active geological terrain where pipelines cross or run parallel to unstable slopes (landslides), meandering rivers or fault lines. Pipeline failures due to geohazards tend to result in catastrophic failures and complete loss of service (high consequence) while other hazards may result in failures with lower consequences such as slow leaks due to corrosion.

This research focuses on developing a better understanding of the risk of geotechnical hazards (landslides) impacting Manitoba Hydro's natural gas pipelines using a limit states reliability approach to ascertain risk for pipelines in active landslides. This was done through monitoring of in-service pipelines to determine stresses and strains acting on a pipeline subjected to known (measured) ground movements. A landslide is defined

in thesis as any slope movement (lateral and downward) irrespective of soil volume, rate, and magnitude of movement.

Manitoba Hydro is the primary supplier of natural gas in the Province Manitoba, on average supplying 2.1 billion cubic meters of natural gas annually to almost 270,000 customers and nearly 100 communities across the province. The pipeline system consists of over 1,800 km of transmission pipelines and almost 8,100 km of distribution pipelines, almost exclusively comprised of steel pipe. These transmission and distribution lines often traverse and run parallel to many rivers, streams and valleys. At these locations, there is a risk of damage to the pipelines due to geotechnical hazards, specifically the potential for ground movements due to landslides, either transverse or longitudinal to the pipeline. These movements can lead to costly repairs, disruption of service to customers, and dangerous gas leaks. Pipeline crossing replacements can range from \$50,000 to \$100,000 (relatively inexpensive) to \$1,000,000 or more depending on the pipe size, the pipeline operating pressure and length of pipeline to be replaced. Consequently, there is great value in being able to proactively assess the risk of pipeline failure within potential landslide areas, thus having the ability to defer replacement/repair of a pipeline until it is necessary from a risk perspective.

### *1.1.1 Justification for Research*

Due to the complexity and limited knowledge of soil/pipe interaction, currently there are no generally accepted methods to assess the transmission of strains and stresses onto buried pipelines in landslide areas. This limits the ability of pipeline risk management methods to properly characterize and classify all risks associated with pipeline



infrastructure. Manitoba Hydro recognizes that part of its pipeline system may be exposed to geotechnical hazards, and in this regard, Manitoba Hydro has supported this research to examine the risk of such geotechnical hazards. The intent of the research is to develop a better understanding of the risk of geotechnical hazards impacting Manitoba Hydro's natural gas pipelines, in particular landslide areas where pipelines run parallel to the direction of movement (*e.g.* landslides moving along the longitudinal direction of the pipeline).

The outcome of the research was used to develop a geotechnical risk management tool for Manitoba Hydro that is simple to understand, implement, use, and maintain, but is founded on a higher level understanding of the soil-pipe interactions for pipelines subjected to landslides through a Reliability Based Design Analysis (RBDA) approach. The RBDA approach utilizes probabilistic theory to determine the risk of pipeline failure using several limit states failure conditions based on measured ground movements and measured pipe strains at a few at-risk landslide areas.

## **1.2 Background**

### *1.2.1 Standard of Practice, Regulations for Design and Operation of Gas Pipelines*

The Manitoba Hydro natural gas distribution system is primarily regulated by the Manitoba Public Utilities Board (PUB) while a small portion of the system with a pipeline originating in Saskatchewan is regulated by The National Energy Board of Canada. Through Board Order 18/12, the PUB has adopted the Canadian Standard (CSA Z662-15) for Oil and Gas Pipelines as the minimum standard for the design, construction,

operation and maintenance of gas pipelines in Manitoba. Similarly, regulations outlined by the National Energy Board (Canada Regulation *SOR/99-294*) stipulate the design, construction, and operations of onshore pipelines are to adhere to applicable standards such as CSA Z662-15.

### *1.2.2 Manitoba Hydro Gas Pipeline System and “At Risk” Sites*

Within Manitoba Hydro’s natural gas pipeline network, there are more than 300 locations where these pipelines cross rivers and streams, and many more locations where pipelines run parallel to rivers and streams, and traverse other slopes. At these locations, there is a potential for ground movements (typically landslides) which could damage the pipelines.

An external geotechnical risk assessment of Manitoba Hydro's gas transmission pipeline system was conducted in 2006. The assessment identified a total of 35 moderate to high risk sites that are subjected to geohazards. Eighteen (18) of the 35 sites were identified as being at-risk to landslide ground movements while the remainder were exposed to other geohazards such as erosion (scour) and insufficient cover. The ground movements identified at the 18 sites were either shallow creep movements or related to more significant landslide movements.

## **1.3 Hypothesis and Objectives**

This research is based upon investigating the following fundamental hypothesis:

*“A relationship between ground movements (in landslide areas) and strains/stresses in buried pipeline infrastructure can be developed through comparison of field measured*

*ground movements and pipe strains/stresses to develop a probabilistic evaluation of pipeline risk”.*

The research objectives are as follows:

- 1) Gain a better understanding of the influence of landslide movements (ground movements) along the longitudinal direction of a pipeline for various types of pipes in different soil conditions. In particular, understanding the causes of pipe stresses due to small movements (*e.g.* creep), slope instabilities, and freeze-thaw ground movements.
- 2) Use probabilistic methods to determine the relationship between ground movements and pipe stresses to ultimately enable calculations of probability of pipeline failure using RBDA for various limit states failure modes.
- 3) Use the outcome of 1) and 2) to develop a risk management system that is comprehensive, progressive, effective and easily integrated into Manitoba Hydro’s risk practices, policies and procedures.

#### **1.4 Organization of Thesis**

This thesis commences with a literature review (Chapter 2) where theories, current state-of-art practices and engineering fundamentals related to the thesis research are presented and discussed. Chapter 3 describes the methodology of the thesis research program while Chapter 4 describes at risk pipeline sites selected for monitoring, the field work conducted and site conditions including local geology and geotechnical sub-surface conditions. A description of the monitoring program and monitoring results are presented

in Chapter 5 with the results being interpreted and discussed in Chapter 6. Chapter 7 presents the outcome of the probability statistical analysis for various limit states failure modes. Chapter 8 discusses the soil-pipe interaction behaviour inferred from the monitoring results including mechanisms that maybe causing the observed behaviour. The risk management system developed through the thesis research is presented in Chapter 9. Chapter 10 summarizes the thesis research and conclusions and presents recommendations for future research.

Background information is included in the appendices such as additional monitoring plots, test holes logs, etc. Monitoring and statistical data is included in the attached digitized appendix. The digitized appendix also includes a spreadsheet tool to predict probability of pipeline failure and compliance with limit states reliability targets for pipelines in landslide areas when pipeline information is inputted.

## **Chapter 2 Literature Review**

### **2.1 Introduction**

The main focus of this research is to evaluate risk to a pipeline when subjected to a landslide. There are several components to the research that are required to fully capture the nature of the topic examined and to satisfy the thesis objectives. This chapter provides a review and background of geohazards, risk fundamentals, loading and stresses on pipes, and limit states design. This chapter also describes in detail the reliability based design and analysis (RBDA) approach used in the thesis research and applicable limit states failure modes. Historical engineering methods used to predict pipeline response in landslide areas and the current state-of-the-art are discussed to provide context as to the previous work completed to better illustrate the uniqueness of this thesis research approach.

### **2.2 Geohazards and Risk to Gas Pipelines**

There are numerous natural hazards (geohazards) that can impact the safe operation of gas pipelines within Canada. Geohazards can be divided into three general groups, geotechnical, hydrotechnical, and seismic tectonic. Geotechnical hazards include landslides, debris flow, and ground movements associated with settlement, subsidence, and soil heave (Figure 2-1). Landslides and debris flows are location specific hazards which occur at river crossings and along natural slopes while settlement, subsidence and soil heave can occur at any point along a pipeline.

A hazard is a condition with the potential for causing an undesirable consequence such as the potential for pipeline failure or affecting the safe operation of a pipeline. The occurrence of geotechnical hazards, such as a landslide, results in ground movements that may induce large strains/stresses on a pipeline causing structural failure or serviceability issues.

Geotechnical mechanisms that trigger these hazards include removal of toe support along slopes (erosion), change in groundwater conditions, piping of soil particles, thawing of permafrost, changes in moisture condition (wetting/drying), and freezing of frost susceptible soils. The occurrence of a geotechnical hazard does not necessarily result in an undesirable effect such a product loss on a pipeline system since other factors influence the vulnerability of a pipeline to a hazard (Zimmerman *et al.*, 1995; Rajani *et al.*, 1995). Some of these factors include: type, magnitude and mechanism of the hazard; the proximity of the pipeline to the potential zone of ground movement; the condition, size and material properties of the pipeline; and pipeline operations. There has been substantial research in determining vulnerability of buried pipelines subjected to ground movements including landslides (Section 2.7).

The definition of vulnerability (V) is a measure of the susceptibility of a pipeline to failure if a hazard (H) occurs. The likelihood of a hazard occurring and the vulnerability (chance of pipeline failure) can be expressed as a probability. Typically, the probability of a hazard occurring is related to an annual probability while the vulnerability of a pipeline is associated with the probability of a particular failure mode occurring. The overall probability of failure is simply the product of the vulnerability of the system and the likelihood of the hazard occurring:

$$P_f = H * V \quad \text{eq. 2.1}$$

In a historically active landslide area, the likelihood of a hazard occurring is either close to or at 1. Thus, the overall probability of failure is approximately equal to the vulnerability of the pipeline.

$$P_f \approx V \quad \text{eq. 2.2}$$

Mansour *et al.* (2009) studied the vulnerability of critical infrastructure to slow moving landslides in a qualitative manner by examining more than 50 cases of slow moving landslides from the literature. A useful relationship between rate of ground movements and expected extent of damage for various types of infrastructure is presented in the paper (Figure 2-2). Four pipeline infrastructure cases were examined in the study where sufficient data was available in the literature. Pipelines were not included as an infrastructure category in the relationship between rate of ground movements and expected extent of damage because of the limited number of case studies available to properly assesses the relationship.

Reliability of a pipeline is defined as the probability the pipeline will meet the operational requirements without failure during a specified period of time, typically annually and can be expressed as follows (Porter *et al.*, 2004):

$$\text{Reliability} = 1 - P_f \quad \text{eq. 2.3}$$

Reliability based design analysis (RBDA) is utilized in this research and is discussed in detail in Section 2.3.

Pipeline failure is defined as a rupture, leak, and loss of service or condition that causes unsafe operation of the pipeline. A pipeline failure may cause various unacceptable impacts. These impacts may include injury, death, product loss, environmental impacts, costs, and even reputational damage to the stakeholders. Additionally, natural gas customers rely on an reliable supply of gas for residences (space and water heating) and commercial and industrial purposes.

The consequence of failure (C) is defined as the collective summation of these unacceptable impacts, usually expressed in monetary or potential loss of life terms. Risk is typically defined as the probability of failure (eq. 2.1) multiplied by the consequence of failure, which can be expressed as follows (Porter *et al.*, 2004):

$$\text{Risk} = P_f * C \quad \text{eq. 2.4}$$

The risk to a buried pipeline may be deemed acceptable depending on the consequences. Acceptable risk has been studied by many authors (Fell, 1993; Zimmerman *et al.*, 1996; Finlay and Fell, 1997; Nessim *et al.*, 2004) in terms of individual risk and societal risk. Societal risk represents the risk level carried by a society due to pipeline failure incidents while individual risk is the amount of risk to specific individuals who are exposed to pipeline failure incidents.

Acceptable individual risk levels, regardless of the number of lives lost, varies between an annual probability of failure of about  $10^{-3}$  for voluntary risk and about  $10^{-6}$  for involuntary risk which is similar to an individual's risk exposure to fatal disease (annual mortality rate of  $10^{-3}$ ) and natural disasters (annual mortality rate of  $10^{-6}$ ), respectively (Fell, 1993; Nessim, 2004). Acceptable risk levels for society are directly related to



number of lives lost, aversion to low probability incidents with a high loss of life, and cultural influences. Societal acceptable risk levels can be lower than for an individual with respect to onshore gas pipelines. Specifically, the societal acceptable annual probability of failure can be as low as  $10^{-9}$  (per km of pipeline per year) where there is a high loss of life (100 to 1000 lives).

CSA Z662-15 handles acceptable risk by specifying limit states reliability targets for gas pipelines based indirectly on the consequences of failure. Risk of a pipeline failure is then deemed acceptable if the calculated reliability is less than the target reliability as illustrated in Figure 2-3. CSA Z662-15 reliability target process is described in detail in Section 7.1.

### **2.3 Limit States Approaches and RBDA Design for Onshore Pipelines**

A structural element must be designed to withstand all anticipated loads and deformations with an adequate level of safety for a specified design life which is referred to as ultimate limit states. Structural performance of the element must also satisfy any functional or operational requirements which is referred to as serviceability limit states (Zimmerman *et al.*, 1992). An active pipeline has two design requirements based on limit states, the probability of excessive deformation causing an unserviceable line (serviceability limit states) and the probability of burst where there is a loss of product (ultimate limit states) is sufficiently low for both limit states (*i.e.* acceptable safety margin or reliability).

CSA Z662-15 defines limit states requirements for oil and gas pipelines systems. According to the standard, limit states methods for design and operations are recommended, but are not mandatory for oil and gas pipelines. Limit states methods are fundamentally based on reliability analysis where variations in the loads and resistances are handled through a probabilistic approach to quantify an acceptable safety margin. Three levels of analysis are recommended in CSA Z662-15 to analyze that the probability of excessive deformations (serviceability limit states) and burst (ultimate limit states) are within an acceptable structural safety margin. Each level is discussed in detail below and the complexity of each method increases with each level:

#### *Level 1*

A semi-probabilistic approach where the probabilistic qualities of the design parameters are handled through defining partial safety factors associated with the inherent characteristic attributes of loads and structural resistance. This approach is typically used in pipeline design and is commonly referred to as Limit States design. Structural loads are calculated using deterministic approaches. Partial safety factors for loads are greater than unity while partial safety factors for resistance are less than unity.

#### *Level 2*

Level 2 incorporates a probabilistic design approach that includes approximation of design parameter probability distributions. Loads and strengths are defined by their known or estimated probability distribution using statistical parameters. The probability distributions assigned are typically, simply expressed by the statistical form of distribution through the mean and standard deviation for a particular parameter. Level 2

methods are best suited for use in economic planning, pipeline monitoring, structural integrity assessments, and maintenance decision making and are not usually used for pipeline design. Level two is also useful for vulnerability ranking of wide-area systems. The Level 2 approach is recommended for onshore non-sour natural gas pipelines systems and CSA Z662-15 provides guidelines for using Level 2 methods.

### *Level 3*

The Level 3 approach uses a full probabilistic analysis design of the pipeline by defining probabilistic distributions of load and strength parameters as well as uncertainties in the analysis. Level 3 methods are the most complex and have limited applications making this approach impractical for general use (Zimmerman *et al.*, 1992; Nessim, 2012). This method is typically used under certain circumstances, such as active landslide areas, where a higher level of analysis is required due to system sensitivity or where cost savings outweigh the additional expense of implementing a complex analysis procedure. However, considerable and detailed amount of data is required which may not be available and fully understanding the interdependent factors influencing landslide may not be straight forward in assessing pipeline risk in landslide areas (D.G. Honegger Consulting *et al.*, 2009).

Level 2 and Level 3 methods are well suited for Reliability-based Design and Assessment (RBDA) of pipelines, in particular onshore non-sour natural gas pipelines. RBDA methods evaluate structural competence of a pipeline through a well-defined estimate of its reliability for various limit states. RBDA methods do not consider consequences explicitly, but indirectly through a comparison to target reliability values (stipulated in

CSA Z662-15) which can vary based on the anticipated consequence of failure (Zhou *et al.*, 2009). Level 2 is often referred to as a partial RBDA approach while Level 3 is a full RBDA approach.

All engineering analysis related to structural reliability and integrity of a pipeline can be handled by RBDA methods from design of new pipelines, evaluation of existing pipelines (fitness-for-service), and other design assessments due to changes in operations. The benefits of RBDA methods include consistent safety margins between various limit states failure modes, optimized solutions using the best information available, and flexibility in assessing non-standard engineering problems (Nessim *et al.*, 2002). RBDA methods are particularly useful for pipelines subjected to large uncertainties, comprised of new materials and technologies, unique loading situations (*e.g.* geotechnical hazards), and severe failure consequences (CSA Z662-15). RBDA methods are attractive for use in risk management systems for evaluating the integrity and performance of existing pipelines since RBDA methods can be easily incorporated into established systems and are useful tools in identifying and classifying risks within a pipeline system. This allows the pipeline owners/operators to manage their assets more effectively in terms of having a better understanding of how pipeline integrity is affected by operations, maintenance, and the local environment by using a RBDA approach.

RBDA approaches are becoming more widely accepted by gas pipeline operators in Canada and internationally as a rationale design approach of varying complexity (Porter *et al.*, 2004; Nessim *et al.*, 2002), but its use is relatively limited. Within the RBDA processes, assessing the reliability of the pipelines (likelihood of hazard occurring and the structural response to these hazards resulting in failure) is generally better defined

for corrosion, internal factors (pressure, temperature change), external interference, and construction. Determining reliability of a pipeline subjected to ground movements, however, is not well defined.

Estimating when ground movements may occur and once triggered, the rate, magnitude, direction of movement is difficult and highlights our limited engineering understanding. There are established methods to assess ground movements such as landslides, typically through global factor of safety methods. These methods are strongly influenced by engineering experience rather than probabilistic reliability values. Selection of design parameters, design loads, analysis methods are, for the most part, determined from experience and are reflective of the judgement of the design engineer. Recently, RBDA approaches based on probabilistic analysis have become more commonly used to assess pipelines subjected to ground movements, but are typically utilized in specific cases where the consequences necessitate a higher level of understanding (Porter *et al*, 2004). This is due to complexity of RBDA approaches, the lack of understanding of probability theory, especially when examining the natural variability of soils and the amount of design information required has limited its general acceptance in practice (Nessim *et al.*, 2002; Nessim, 2012). CSA Z662-15 has highlighted this limited understanding by allowing both the limit states approach (including RBDA) and the global factor of safety design approach to be selected at the discretion of the design engineer with the only stipulation that geotechnical parameters and analysis methods are selected in accordance with good engineering practice.

## 2.4 Applied Loads and Principal Stresses on Pipes

### 2.4.1 Applied Loads to Buried Pipeline

Buried Pipelines are subjected to various applied loads from different sources.

CSA Z662-15 has categorized applied loads as either:

- **Permanent** – self-weight of the pipeline, weight of permanent equipment, permanent portion of overburden loads, and external hydrostatic pressure (if constant).
- **Operational** – internal pressure, thermal forces due to temperature differential, weight of temporary equipment, and variable portion of overburden loads.
- **Environmental** – variations in ambient temperature, ground movements, and earthquakes.
- **Accident** – outside force during construction and operation, fire and explosion, and loss of pressure control.

Permanent loads remain constant for long periods of time while operational and environmental loads generally vary over time and can be static or dynamic in nature.

Accidental loads are event based caused by humans, nature, or mechanical failures.

Applied loads induce internal forces within the pipe member which may or may not diminish if structural deformation of the pipe section occurs. Applied loads where internal forces are sustained following deformation are referred to as *primary loads* (CSA Z662-15; Khatib *et al.*, 1992). Primary loads impose internal forces within the pipeline member that are necessary to satisfy the laws of static equilibrium (Khatib *et al.*, 1992).

Primary loads are referred to as non-self-limiting meaning internal forces act as long as loads are applied through yielding and plastic deformation of the pipeline section up until failure. Primary loads include the following applied loads: internal pressure, self-weight of the pipe, soil overburden, external hydrostatic pressure and buoyancy.

*Secondary loads* are those which diminish once yielding occurs. Secondary loads are related to structural deformations (or resistance to) in the pipeline where loads are applied to the pipeline by the constraint of adjacent parts or the self-constraint of the pipeline. The internal forces within member in this scenario are required to satisfy the laws of compatibility of strains and deformations. These loads are self-limiting and tend to dissipate as the pipeline deforms through yielding. Secondary loads include differential temperature loads and vibration loads.

Applied environmental (geotechnical) loads associated with ground movements are classified as secondary loads within CSA Z662-15 where the loads are considered to be self-limiting because these loads tend to decrease if the pipeline yields, distorts, moves through the soil, or a combination thereof through either gross failure of the soil or plastic permanent deformation of the pipeline (D.G. Honegger Consulting *et al.*, 2009).

#### *2.4.2 Stresses on Pipes*

Primary and secondary loads applied to pipelines induce strains and stresses within a pipeline member. Pipelines are essentially open ended hollow cylinders from an analytical standpoint. The behaviour of cylinders is covered by many text books

(Timoshenko and Goodier, 1970; Young, 2002). For hollow cylinders, the three principal stresses acting on the exterior are:

- Circumferential or hoop stress
- Radial Stresses
- Longitudinal Stresses

Hoop stress and radial stresses are caused by the difference between the internal (gas pressure) and external pressures applied to the wall of the cylinder and act in the directions shown in Figure 2-4. Longitudinal stresses are induced by internal pressures if the cylinder has closed ends or are a result of external loading on the cylinder due to axial loading (compression/tension) or bending, or a combination thereof.

Hoop Stress:

The hoop stress is calculated using the following equation (adapted Barlow's Equation):

$$\sigma_h = \frac{(p_i - p_e)D}{2t} \quad \text{eq. 2.5}$$

Where:

$\sigma_h$  = hoop stress due to pressure differential, MPa

$p_i$  = internal pressure of pipe, MPa

$p_e$  = external hydrostatic pressure, MPa

$D$  = outside diameter, mm



$t$  = pipe wall thickness, mm

Radial Stress:

For thin-walled cylinders, the radial stress is negligible when compared to the other principal stresses and therefore is typically ignored when (Young 2002):

$$\frac{r}{t} \geq 10 \quad \text{eq. 2.6}$$

Where:

$r$  = radius, mm

$t$  = pipe wall thickness, mm

Gas pipelines are considered to be thin-walled members and typically satisfy the above equation. Therefore, radial stresses are usually ignored when calculating stresses acting on pipelines.

Longitudinal Stress:

Longitudinal stress is calculated using the following equation:

$$\sigma_L = \frac{M}{S} + \frac{P_A}{A} \quad \text{eq. 2.7}$$

Where:

$\sigma_L$  = longitudinal stress, MPa

$M$  = bending moment, MN per m

$S$  = section modulus,  $m^3$

$P_A$  = axial force, MN

$A$  = cross-sectional radius,  $m^2$

## **2.5 Ultimate and Serviceability Limit States Failure Modes for Buried Pipelines**

Historically, working stress design, also referred to as allowable stress, has been used by the pipeline industry for design of buried pipelines due to its simplicity since the design is based on linear elastic analysis. A limitation of working stress design is it does not examine failure modes directly. Working stress design uses a factor of safety approach under normal conditions to control undesirable effects indirectly (Yoosef-Ghodsi, 1994). For buried pipeline design, the factor of safety against yielding is assessed exclusively and results in varying levels of safety for different failure modes. Limit states design, evaluates each of the limit states failure modes directly resulting in a more uniform level of safety. In this regard, limit states design provides greater clarity and a more rational approach to the safe and economic design of buried pipelines (Yoosef-Ghodsi, 1994).

Geotechnical loads are typically associated with serviceability limit states since a reduction of loading occurs once plastic deformation of the pipe is initiated and ultimate failure due to applied stress may not be reached because the loads can diminish. However, failure can occur if pipe deformations exceed the limit of the pipe material or connections (welded, fastened). Ground movements may induce deformations large enough to exceed the stress or strain limit of the pipe material either in one instance or cumulatively. The applicable failure modes due to ground movements include yielding,

rupture (tensile strain limit), and local buckling (compressive strain limit). Yielding due to geotechnical loads is considered a serviceability limit state (SLS) since yielding of the pipe would not result in restrictions to normal operations of the pipeline and/or affect the durability of the pipeline. Yielding may be considered an ultimate limit states failure (ULS) mode if excessive yielding occurs to a point where there is loss of product (CSA Z662-15). Yielding of a pipeline can also occur based on a combination of primary (internal pressure) and secondary loads (geotechnical). Tensile rupture (burst) is categorized as ULS since there is a potential for human and product losses. Local buckling (collapse) is categorized as either a SLS or ULS depending on the mechanics of the buckling mode and the nature of ground movement.

A modified form of level 2 limit states approach (Section 2.3) is used in this research to determine if limit states failure modes are satisfied. Typically, partial safety factors (safety margin) are applied to loads and structural resistance to determine if limit states are satisfied. However, partial factors are not required when using a RBDA approach since probabilistic analysis is used to determine the limit states which inherently provides an acceptable margin of safety. The RBDA approach for this research entails calculating the probability that a strain or stress limit states (capacity) is exceeded for a failure mode based on pipe monitoring results which will then be compared to reliability targets stipulated in CSA Z662-15 to determine compliance. Probability distributions representing the structural resistance will not be used since failure modes examined either have slight variations in their capacity (*e.g.* yield) which would not significantly alter the outcome probability of limit states failure calculations or the approaches used to determine capacity (*e.g.* buckling, tensile rupture) are not deterministic and are complex

estimates. Local buckling, for example, can be predicted using various methods with a range of different outcomes since this failure mode is complex and difficult to predict and therefore a probabilistic distribution associated with this failure mode for a particular method cannot realistically be determined with reasonable certainty.

### 2.5.1 Yielding Criteria

The von Mises stress theory is used to determine if the minimum yielding stress of the pipe is exceeded based on the following formula:

$$\sigma_{ef} \leq F_y \quad \text{eq. 2.8}$$

Where:

$F_y$  = effective specified minimum yield strength, MPa

$\sigma_{ef}$  = combined equivalent stress (von Mises), MPa

#### von Mises Combined Equivalent Stress:

The von Mises stress theory calculates a combined equivalent (tensile) stress,  $\sigma_{ef}$ , from a combination of the three principal pipe stresses and shear stress (torque) acting on member. The equivalent tensile stress is considered a scalar stress value. The minimum specified yield strength value,  $F_y$ , is obtained from uniaxial testing of the material in tension within a lab environment. Failure of the member occurs when the equivalent tensile stress exceeds the specified minimum yield strength (SMYS) of the material at the

on-set of plastic deformation. The von Mises stress theory is well suited to analyze stresses in ductile materials such as metals (Paglietti, 2007).

The combined equivalent stress for a thin walled cylinder is calculated using the following equation:

$$\sigma_{ef} = \sqrt{\sigma_h^2 + \sigma_L^2 - \sigma_h\sigma_L + 3\tau^2} \quad \text{eq. 2.9}$$

Where:

$\sigma_{ef}$  = combined equivalent stress, MPa

$\sigma_h$  = hoop stress, MPa

$\sigma_L$  = longitudinal stress, MPa

$\tau$  = tangential shear stress, MPa

### 2.5.2 Tensile Rupture

Rupture is caused by exceeding the longitudinal axial strain limit of the pipe wall or weldment and this failure mode is governed by the following formula:

$$\varepsilon_t \leq \varepsilon_t^{crit} \quad \text{eq. 2.9}$$

Where:

$\varepsilon_t^{crit}$  = ultimate tensile strain capacity (pipe wall or weldment)

$\varepsilon_t$  = tensile axial strains

Buried steel pipelines are typically comprised of girth-welded steel pipe, including the vast majority of Manitoba Hydro's pipelines. The strain capacity of a girth-weld typically governs the longitudinal tensile strain capacity,  $\epsilon_t^{crit}$ , of a steel pipeline. The girth-weld capacity depends on size and location of the girth-weld flaw, pipeline geometry, material toughness, yield and tensile strengths for the pipe body, weld metal, and internal pressure (Yoosef-Ghodsi, 1994; Wang *et al.*, 2003; Zhou, 2012). There is on-going research in developing analytical methods to determine girth-weld capacity that do not require finite element analysis (DNV-OS-F101-2013; Zhou, 2012) In this regard, the ultimate tensile strain capacity is not well defined in the CSA Z662-11, but the standard does provide recommendations and guidelines for two approaches. The first approach (Tier I) is the ultimate tensile strain capacity should be determined using "*sound and proven fracture mechanics analysis and physical tests*". The standard also provides some general information on strain capacities values from some experimental tests suggesting the critical strain can be between 0.2% to as high as 4% tensile strain.

The second approach (Tier II) utilizes two empirical formulas for pipes with weld defects requiring various inputs. The two empirical formulas are representative for pipes with either a surface-breaking defect or a buried defect. The use of these equations requires the assumption that the pipe will fail along the weld and several of the input parameters are also assumed, in particular the weld defect length. The approach also requires an integration process which is computationally intense. The Tier II approach is also recognized to be "*generally conservative, and sometimes highly conservative*" (CSA Z662-11; Lee *et al.*, 2014). This may be due to internal pressure not being considered in the Tier II approach which is known to influence tensile strain capacity

(Wang *et al.*, 2004). The Tier II approach was removed from the latest CSA Z662 standard (CSA Z662-15).

Other standards, guidelines and published literature was reviewed to determine an appropriate tensile strain capacity given the CSA Z662-15 does not explicitly specify methods to calculate tensile strain capacity and conducting fracture mechanics using finite element analysis is beyond the scope of this research. Recommended critical tensile strains values in the literature generally ranged between 0.5% and 2.0%. A tensile strain capacity of 0.5% is considered to be a conservative lower bound (Triggs and Rizkalla, 1994) while tensile strain limit of 1.0% and 2.0% are more representative of tensile strain capacities for average (1.0%) and good (2.0%) quality girth-welds (Zhou, 2012). American Lifelines Alliance and American Society of Civil Engineers (2001) suggests a tensile strain limit of 2.0%. A tensile strain capacity of 2% was selected based on a review of published values.

### 2.5.3 *Buckling*

Local buckling occurs when a wrinkle forms in the wall of a pipeline due large bending moments. A local buckle can progress to global buckling of a pipeline as a result of excessive plastic deformation, thus, limiting the axial capacity of the pipeline. A wrinkle is a localized plastic deformation of the pipe wall which forms on the compression side of the pipe for a pipe subjected to bending and potentially other loads (internal pressure, temperature changes, torque). The buckling mechanism is typically associated with the compressive limit of a pipe. It is recognized by researchers that pipelines can function following plastic deformations and, to certain degree, following local buckling under

non-sustained secondary loads (Zimmerman, 1995; Bai and Bai, 2014). As such, CSA Z662-15 considers a local buckle in a pipeline as a serviceability limit state at the start which may progress to an ultimate limit state. In the context of the thesis research, local buckling is considered to be an ultimate limit state failure mode.

Numerous studies over the last 30 years have been conducted to determine local buckling response of pipelines and predictive models (equations) have been developed by either analytical (Mohareb, 2002; Mohareb, 2003), experimental (Gresnigt, 1986; Gresnigt, 1998) and numerical means (Bruschi and Monti *et al.*, 1995; Mahdavi *et al.*, 2014) or combination thereof (Yooesef-Ghodsi *et al.*, 1994; Dorey *et al.*, 2001; Ozkan, 2008). These equations estimate buckling based on either critical bending moments, critical strains, or critical stresses for various loading combinations. These models also differ in their assumption of material behaviour in terms of simple elastic deformations or including plastic deformations past yield, critical conditions assumed, and critical points. There is no industry-wide accepted single equation for predicting compressive limit due to buckling (Mahdavi, 2013).

Many of these equations allow for plastic deformation of pipe to occur prior to buckling if specific loading conditions and pipe properties are satisfied. In particular, many equations include strain hardening beyond yield and use the plastic bending moment capacity expression in lieu of the elastic bending moment capacity to predict buckling in thin walled, slender pipes. Distinguishing between elastic and plastic deformation that leads to local buckling is a key consideration in predicating buckling capacity of a pipe and the selection of an appropriate equation to be used in design is also key. For pure axial and pure bending cases, pipes will attain their full plastic moment capacity at the



onset of buckling when,  $D/t \leq 23,000/F_y$ , and  $D/t \leq 18,000/F_y$ , respectively (CSA S16-01). Karbasian *et al.* (2012) examined 59 data sets from full-scale buckling tests with various loading conditions and suggests that when  $D/t < \sim 70$ , a plastic moment develops and buckling is governed by local plastic deformations, otherwise buckling will occur due to elastic instability of the pipe.

Karbasian *et al.* (2012) also compared six known buckling equations to the results of the 59 full-scale tests for various loading conditions to determine the predictive capabilities of each equation against measured buckling failures. The six equations examined in the study include; Yosef-Ghodsi *et al.* (1994), Mohareb *et al.* (1994), Zimmerman *et al.* (1995), Bruschi and Monti *et al.* (1995), DNV-OS-F101-2000, Gresnigt (1986) and Brüggemann *et al.* (2005). The study recommended which equations provided the best fit for different loading conditions based on the experimental data. The best equation for predicating buckling when subjected to axial and bending loads including internal pressure is the DNV-OS-F101-2000 stress based equation. When axial force is omitted, Gresnigt (1986) and Brüggemann *et al.* (2005) as well as DNV-OS-F101-2000 stress based equation were deemed to be the most accurate in the study.

The CSA Z662-15 standard has essentially adopted the Gresnigt (1986) equation with a slight modification. The DNV-OS-F101 standard also includes a strain based equation which accounts for girth-welds. The DNV-OS-F101-2000 stress based equation has been modified since 2000 and the new equation is included in the most recent DNV-OS-F101-2013 standard. Based on the results of the Karbasian *et al.* (2012) study and the preference to use equations recommended in well recognized standards, buckling

predications within the research will utilize the strain based equations from CSA Z662-15 and DNV-OS-F101-2013 standard and stress based equations in DNV-OS-F101 (2000, 2013). The applicable buckling equations are discussed in detail in section 2.5.3.1

The affects of torsion on buckling are not well defined in the literature. Torsion has been examined in combination with bending by several researchers in experimental studies (Gresnigt and Steenbergen, 1998; Ozkan and Mohareb, 2003; Ozkan, 2008). Research on buckling under a combination of internal pressure, axial, bending, and torsion appears to have not been investigated. Ozkan (2008) did however conduct experiment tests on pipe sections subjected to internal pressure in addition to bending and torsion. Ozkan (2008) concluded that increasing torsion reduced the critical buckling strain very slightly, but no definite trends can be inferred given the limited number of specimens tested. Ozkan (2008) also investigated other load combinations (internal pressure, axial tension, and bending) and determined the influence of several parameters on the ability of a pipe to develop its plastic moment capacity prior to buckling:

- Axial load (most important parameter)
- $D/t$  ratio (strong dependence)
- Internal pressure (weak dependence)
- Torsion (negligible)

### 2.5.3.1 Applicable Buckling Equations

The following equations are considered to be suitable for predicting pipeline buckling:

#### 1) CSA Stain Based Equation:

The CSA Z662-15 buckling failure mode is governed by the following formula:

$$\varepsilon_c \leq \varepsilon_c^{crit} \quad \text{eq. 2.10}$$

Where:

$\varepsilon_c^{crit}$  = ultimate compressive strain capacity (pipe wall or weldment)

$\varepsilon_c$  = compressive strains

The CSA Z662-15 equation used to determine  $\varepsilon_c^{crit}$  is a modified version of the Gresnigt equation (Gresnigt, 1986) and is defined as follows:

$$\varepsilon_c^{crit} = 0.5 \frac{t}{D} - 0.0025 + 3000 \left[ \frac{(p_i - p_e)D}{2tE} \right]^2 \quad \text{for } \frac{D(p_i - p_e)}{2tF_y} < 0.4 \quad \text{eq. 2.11}$$

and

$$\varepsilon_c^{crit} = 0.5 \frac{t}{D} - 0.0025 + 3000 \left[ \frac{0.4F_y}{E} \right]^2 \quad \text{for } \frac{D(p_i - p_e)}{2tF_y} \geq 0.4 \quad \text{eq. 2.12}$$

Where:

$\varepsilon_c^{crit}$  = ultimate compressive strain capacity (pipe wall or weldment)

$t$  = pipe wall thickness, mm

$D$  = outside pipe diameter, mm

$p_i$  = internal pressure, MPa

$p_e$  = external pressure, MPa

$E$  = Young's modulus of steel, MPa

$F_y$  = effective specified minimum yield strength, MPa

The Gresnigt (1986) model is a semi-empirical equation based on elastic-plastic pipe material for pipes subjected to internal pressure, axial forces, and bending moments. The difference between the CSA Z662-15 strain equation and Gresnigt (1986) is CSA Z662-15 does not include ovalization effects and the outside wall diameter is used in lieu of the mid-wall diameter. The CSA equation also limits the maximum critical buckling strain calculated, does not account for strain-hardening characteristics of the pipe material, and does not specify a gauge length associated with the predicted strain capacity. The CSA equation is considered to be generally conservative (Yoosef-Ghodsi, 2014).

## 2) DNV Strain Equation

DNV-OS-F101-2013 proposed the following equation (with safety factors removed) to calculate critical buckling strains,  $\varepsilon_c^{crit}$  for pipelines subjected to internal pressure, axial forces and bending moments:

$$\varepsilon_c^{crit} = 0.78 \left( \frac{t}{D} - 0.01 \right) \left( 1 + 5.75 \frac{p_i - p_e}{p_b(t)} \right) \alpha_h^{-1.5} \alpha_{gw} \quad \text{eq. 2.13}$$

for  $D/t \leq 45, p_i \geq p_e$

Where:

$\alpha_h$  = yield to ultimate stress ratio in axial tension given by:

$$\alpha_h = \frac{R_{t0.5}}{R_m}$$

$\alpha_{gw}$  = girth weld reduction factor (=1.0 if no girth weld) given by:

$$\alpha_{gw} = 1.2 - 0.01 \frac{D}{t}$$

$p_b(t)$  = burst pressure given by:

$$p_b(t) = \frac{2t}{D-t} f_{cb} \frac{2}{\sqrt{3}}$$

$$f_{cb} = \min \left[ f_y, \frac{f_u}{1.15} \right]$$

$R_{t0.5}$  = yield strength at 0.5% of test specimen, MPa

$R_m$  = ultimate strength of test specimen, MPa

$f_y$  = characteristic yield tensile strength, MPa

$f_u$  = characteristic ultimate tensile strength, MPa

The DNV strain equation somewhat allows for plastic straining to occur through a yield to ultimate stress ratio and makes a distinction for pipe with girth-weld, recognizing work by Yoosef-Ghodsi *et al.* (1994). Yoosef-Ghodsi (2014) noted the DNV strain equation (without the safety factors) can lead to unconservative predictions depending on the D/t ratio and if the pipe is pressurized or unpressurized.

### 3) DNV (2000) Stress Based Equation

DNV-OS-F101-2000 included a load controlled buckling condition expression which is a stress based approach for pipelines subjected to internal pressure, axial force and bending moment. The stress based equation (without safety factors) is as follows:

$$\left( \frac{S_{sd}}{\alpha_c S_p(t_2)} \right)^2 + \left( \frac{|M_{sd}|}{\alpha_c M_p(t_2)} \sqrt{1 - \left( \frac{p_i - p_e}{\alpha_c p_b(t_2)} \right)^2} \right) + \left( \frac{p_i - p_e}{\alpha_c p_b(t_2)} \right)^2 \leq 1 \quad \text{eq. 2.14}$$

For  $D/t \leq 45, p_i \geq p_e$

where:

$S_{sd}$  = design effective force, MN

$M_{sd}$  = design bending moment, MN per m

$p_i - p_e =$  design differential overpressure, MPa

$S_p(t_2) =$  characteristic plastic force resistance given by:

$$S_p(t_2) = f_y \pi (D - t_2) t_2 \quad \text{note: } D, t_2 \text{ are in meters}$$

$M_p(t_2) =$  plastic moment resistance given by:

$$M_p(t_2) = f_y \pi (D - t_2)^2 t_2 \quad \text{note: } D, t_2 \text{ are in meters}$$

$p_b(t_2) =$  pressure containment resistance given by:

$$p_b(t_2) = \min(p_{b,s}(t_2); p_{b,u}(t_2))$$

Yield Limit State

$$p_{b,s}(t_2) = \frac{2t_2}{D - t_2} f_y \frac{2}{\sqrt{3}}$$

Bursting Limit State

$$p_{b,u}(t_2) = \frac{2t_2}{D - t_2} \frac{f_u}{1.15} \frac{2}{\sqrt{3}}$$

$t_2 =$  net pipe wall thickness free of possible corrosion, mm

$\alpha_c =$  flow stress parameter accounting for strain hardening given by:

$$\alpha_c = (1 - \beta) + \beta \frac{f_u}{f_y} \quad \alpha_c \text{ is not to be taken larger than 1.20}$$

$$\beta = \begin{cases} 0.4 + q_h & \text{for } (D/t_2 < 15) \\ (0.4 + q_h)(60 - D/t_2)/45 & \text{for } 15 \leq D/t_2 \leq 60 \\ 0 & \text{for } D/t_2 \geq 60 \end{cases}$$

$$q_h = \begin{cases} \frac{(p_i - p_e) 2}{p_b(t_2) \sqrt{3}} & \text{for } p_i > p_e \\ 0 & \text{for } p_i \leq p_e \end{cases}$$

The DNV (2000) stress based equation, in essence, normalizes the internal pressure, axial force, and bending to the plastic capacity of each loading condition, except for pressure containment resistance where both elastic and plastic limiting conditions are evaluated. Local buckling is predicted to occur when the summation of the terms is equal to or exceeds 1.0.

#### 4) DNV (2012) Stress Based Equation

The stress based equation was updated in DNV-OS-F101-2012 with the no changes in the latest DNV standard (DNV-OS-F101-2013) The updated stress based equation (without safety factors) is as follows:

$$\left\{ \frac{|M_{Sd}|}{\alpha_c M_p(t_2)} + \left( \frac{S_{Sd}}{\alpha_c S_p(t_2)} \right)^2 \right\}^2 + \left( \alpha_p \frac{p_i - p_e}{\alpha_c p_b(t_2)} \right)^2 \leq 1 \quad \text{eq. 2.15}$$

For  $15 \leq D/t \leq 45, p_i \geq p_e, |S_{Sd}|/S_p(t_2) < 0.4$

where:

$\alpha_c$  = flow stress parameter accounting for strain hardening given by:

$$\alpha_c = (1 - \beta) + \beta \frac{f_u}{f_y}$$



$$\beta = \frac{60 - D/t_2}{90}$$

$\alpha_p$  = parameter accounting for effect of  $D/t_2$  given by:

$$\alpha_p = \begin{cases} 1 - \beta & \text{for } \frac{p_i - p_e}{p_b(t_2)} < \frac{2}{3} \\ 1 - 3\beta \left(1 - \frac{p_i - p_e}{p_b(t_2)}\right) & \text{for } \frac{p_i - p_e}{p_b(t_2)} \geq \frac{2}{3} \end{cases}$$

## 2.6 Statistical Analysis and RBDA Application

Uncertainty in engineering is always present to a certain degree and it is important engineers recognize the major sources of uncertainty in practice. Uncertainty can be classified into two general types: Aleatory and Epistemic. Aleatory uncertainties are associated with natural randomness while epistemic uncertainties are associated with inaccuracies in predictive tools and estimations of reality (Ang and Tang, 2007). Many engineering processes and phenomena contain variable randomness meaning the numerical outcome of an event or experiment cannot be predicted with certainty in advance

(Van Helden, 2014).

Epistemic uncertainty is related to imperfect or limited knowledge as result of idealized models used by engineers to predict or estimate real world situations. Idealized models are usually mathematical or simulation based such as empirical formulas, numerical algorithms, and computer programs or can be laboratory models which attempt to mimic

the real world. The outcome of these idealized models is not perfectly accurate with some unknown degree of error resulting in uncertainty associated with the outcome.

The traditional process for predicting pipeline response subjected to landslides contains both aleatory and epistemic uncertainties. The nature of the landslides, the soil-structure interaction, soil and pipeline properties contain random variables and the idealization models and analytical approaches used to predict pipe response to ground movements contain epistemic uncertainties. By measuring pipelines strains directly and using probability theory to determine the likelihood of failure, epistemic uncertainties associated with idealization models do not play a role in the prediction of pipeline failure. Measured pipeline strain is the physical outcome of a combination of highly variables conditions acting on a pipeline and therefore is also highly unpredictable. In this regard, probability theory is well suited to define pipeline response and ultimately pipeline failure using RBDA approaches. The probability theory used in the research is discussed briefly in Section 2.6.1.

### *2.6.1 Probability Theory*

A phenomena (or random variables) are often characterized by field or experimental data where the variability due natural randomness of the random variable is captured through measurement. Measurements can vary between observations, tests, or between similar experiments due to random variables. This results in a range of results. In a test or experiment, the random variable to be characterized can be denoted by  $X$  while the observed or measured values can be denoted by  $x$ , and varies between 1 and the total number of observations  $n$ , resulting in a measured data set  $\{x_1 \text{ to } x_n\}$ .

When measuring a random variable, within a set of observations, certain values may occur more frequently than others (Ang and Tang, 2007) and can be represented by statistics. A histogram can be used to illustrate the measured data in a statistical form. The frequency of differing observed values within a specific range or referred to as bins are plotted graphically as shown in Figure 2-5 either by number of observations or by frequency of occurrence for the hypothetical data set in the figure. The summation of the frequency must be equal to unity.

Theoretical probability distributions can be used to statistically represent the shape of a histogram. Theoretical probability distributions allow for the predication of specific outcomes of future observations. A theoretical distribution is expressed as:

$$F(x) = P(-\infty < X \leq x) = \int_{-\infty}^x f(x)dx \quad \text{eq. 2.16}$$

Where:

$F(x)$  = cumulative distribution function (CDF)

$X$  = random variable

$x$  = discrete values of  $x$

$f(x)$  = probability density function (PDF)

The probability density function (PDF),  $f(x)$ , is a relative probability since a specific value of  $x$  is never really equal to a particular value, but rather a probability is calculated over some range of  $x$  (Van Helden 2012). The integration of  $f(x)$  creates the cumulative

distribution function (CDF). Both the PDF and CDF can be represented graphically and compared to the observed data set as shown in Figure 2-6.

It may be difficult to fully specify the CDF since the exact form of the probability distribution is not known (Ang and Tang 2007). Theoretical probability distribution functions based on random variables main descriptors can be used to approximate a probability distribution. The main contributors include parameters to describe the central values and dispersion of the data set. A sample mean,  $\mu$ , (central value) and the sample standard deviation,  $\sigma_x$  (data dispersion) or forms thereof are used in the more common probability distribution functions. The sample mean is an estimate of the expected central value of the random variable defined as:

$$\mu = \frac{1}{n} \sum_{i=1}^n x_i \quad \text{eq. 2.17}$$

The sample variance,  $\sigma_x^2$ , is a measure of the dispersion of the values of the random variable in terms of how widely or narrowly the data is dispersed around the mean and is the summation of the average square deviation from the sample mean for the data set. The samples deviation is the square root of the variance expressed as:

$$\sigma_x = \sqrt{\sigma_x^2} = \sqrt{\frac{1}{n-1} \sum_i^n (x_i - \mu)^2} \quad \text{eq. 2.18}$$

The sample mean and standard deviation approach the actual real value of the mean,  $E[X]$ , and the standard deviation,  $\sigma[X]$  as the sample size,  $n$ , increases.

Common theoretical probability distribution functions include normal distribution, log normal, and gamma. Each of these distributions has slightly different shapes. The normal distribution is symmetric on either side of the sample mean. The lognormal distribution is skewed below the sample's mean while the gamma distribution looks very similar to the normal distribution but is not quite symmetric (Figure 2-7). The skewness of lognormal and gamma distribution are influenced by a shape factor within the distribution formulations. The probability distributions are as follows:

Normal Distribution

$$f_x(x) = \frac{1}{\sigma\sqrt{2\pi}} \exp\left[-\frac{1}{2}\left(\frac{x-\mu}{\sigma}\right)^2\right] \quad -\infty < x < \infty \quad \text{eq. 2.19}$$

Where:

$f_x(x)$  = probability density

$x$  = discrete values of X

$\mu$  = mean value of random variable X

$\sigma$  = standard deviation of random variable X

Lognormal Distribution

$$f_x(x) = \frac{1}{\sigma\sqrt{2\pi}(\zeta x)} \exp\left[-\frac{1}{2}\left(\frac{x-\lambda}{\zeta}\right)^2\right] \quad x \geq 0 \quad \text{eq. 2.20}$$

Where:

$\lambda$  = mean of  $\ln(X)$

$\zeta$  = standard deviation of  $\ln(X)$

### Gamma Distribution

$$f_x(x) = \frac{1}{\beta^\alpha \Gamma(\alpha)} x^{\alpha-1} e^{-\frac{x}{\beta}} \quad x, \beta, \alpha \geq 0 \quad \text{eq. 2.21}$$

Where:

$$\beta = \sigma^2 / \mu$$

$$\alpha = \mu^2 / \sigma^2$$

$$\Gamma(\alpha) = \int_0^{\infty} x^{\alpha-1} e^{-x} dx \quad x, \alpha \geq 0$$

### 2.6.2 Probability Theory Research Application in RBDA

The three theoretical probability distribution functions can be applied to a set of observed data, such as measured pipe tensile strains, and the cumulative probability distributions of each function can be plotted against the cumulative frequency of the observed data. This allows for visual comparison of the observed data to each of the distribution functions to assess which function is the best fit. The probability of a random variable being less than or equal to specific tensile value can then be determined based on the CDF of the selected distribution using the following equation:

$$F_x(x) = P(X \leq x) = \int_{-\infty}^x f_x(t) dt \quad \text{eq. 2.22}$$

Conversely, the probability that a specific value is exceeded is:

$$P(X > x) = 1 - F_x(x) \quad \text{eq. 2.23}$$

In terms of limit states failure modes, eq.2.23 can be noted as:

$$P_f = 1 - F_x(ls) = \int_{-\infty}^{ls} f_x(ls) dls \quad \text{eq. 2.24}$$

Where:

$ls$  = the limit states resistance (critical) value for a particular failure mode

Determining the limit states critical resistance values for various failure modes are discussed Section 2.5. A visual example of eq. 2.24 for tensile rupture is presented in Figure 2-8. In a full RBDA approach, a probability distribution would also be determined for the critical resistance value of the pipeline for a particular failure mode. However, within this research, the loads are only represented by a probability distribution while the resistance is represented by a single limit state critical value calculated using the equations presented herein.

## 2.7 Pipelines in Landslide (Current State-of-the-Art)

Pipeline infrastructure subjected to ground movements has been studied with more of a focus over the last 30 years to advance the understanding of the complex nature of the subject with the goal of developing better design tools to improve safety and reliability of pipeline systems. Once the nature of ground movements and magnitudes of movements are understood or assumed for a pipeline subjected to ground movements, determining structural loading due to ground movements is very complex and there is considerable uncertainty in available methods (Bruschi and Tomassini *et al.*, 1995; D.G Honegger Consulting *et al.*, 2009). The complexity is a result of the pipe-soil interaction where loads are induced on the pipeline by the surrounding soil. A moving soil mass can apply lateral (transverse), vertical and longitudinal forces resulting in bending, shear (torsion) and axial loads within the pipe as the ground tries to displace the pipeline. There is no generally accepted approach for estimating the magnitude of stresses induced on a pipeline within a moving soil mass although there are soil-spring based soil-pipe interaction analysis.

This section focuses on research conducted on pipelines subjected to landslide movements along the longitudinal direction of the pipeline. Figure 2-9 illustrates the differing methodologies and approaches implemented by researchers to determine the pipeline response due to landslides. Figure 2-9 is considered to be a road map of the process starting with selection of one of the input parameters from each of the various bins to define the pipe and landslide scenario, then the analysis types that can be implemented, and the desired outcome. The road map is not inclusive of all analytical approaches that may be used to assess pipeline stresses/strains due to landslides, but does



provide a relatively comprehensive illustration of the process based on current published research. The evolution of research on pipelines subjected to landslides (current state-of-the-art) is described in detail in this section.

Researchers have studied stresses/strains induced on pipelines due ground movements predominantly through either analytical, numerical, or experimental means, often in combination where one approach is used to supplement or verify the outcome of another approach (Calvetti *et al.*, 2004; Cocchetti *et al.*, 2009 part 1 and part 2; Wijewickreme *et al.*, 2009). Early studies focused on analytical methods to determine stresses on pipelines. In relation to landslides, research in the 1980s and 1990s study the response of buried pipelines to lateral and longitudinal movements (O'Rourke and Nordberg, 1992; Triggs and Rizkalla, 1994; Rajani *et al.*, 1995). Analytical methods developed during this time were intended to be simple methods to be used as planning tools or identify areas where pipelines may be at risk within a risk management system. These methods typically assumed simple soil deformation patterns where an elastic pipeline is buried in a homogenous elastic-plastic soil medium.

O'Rourke and Nordberg (1992) developed analytical models to determine the response of buried pipeline to longitudinal permanent ground deformation following earthquakes. In particular, focusing on earthquake induced landslides and liquefaction causing lateral spreading areas. The ground movements were assumed to be translational and infinite, resulting in purely axial loading on the pipe. Four idealized permanent ground deformation (PGD) patterns were developed and applied to the pipeline using a spring-slider model to determine the force at the soil-pipe interface (Figure 2-10). The spring represents the stiffness of the soil ( $k$ ). The soil-pipe interaction used is elastic-perfectly plastic where

slippage occurs when the soil force reaches the maximum adhesion ( $f_m$ ) between the pipe and the soil at a specific relative displacement ( $D_s$ ) as illustrated in Figure 2-11. The soil in the model assumes coarse grained non-cohesive soil and the maximum adhesion,  $f_m$ , is calculated based on a coefficient of friction, the soil friction angle, overburden stresses while the relative displacement where slippage occurs ( $D_s$ ) is the ratio of  $f_m/k$ . Reference tables with maximum pipe strains for each of the four idealized PGD patterns is presented in O'Rourke and Nordberg (1992) for differing pipe diameters, pipe wall thickness, cover, slope angle, and length of movement.

Rajani *et al.* (1995) developed two simple analytical solutions to predict pipe loads for pipelines undergoing transverse (bending loads) and longitudinal (axial loads) slope movements. Non-dimensional relationships related to pipe loading were developed in the form of charts. These charts allow quick hand calculations and verification of structural loading on pipelines and ultimately, again as with O'Rourke and Nordberg (1992), can be used in pipeline design as a planning tool or determining capacity of pipeline subjected to landslide movements. Some knowledge of soil parameters (sub-grade modulus, soil strength) and pipe (geometry, burial depth, pipe stiffness) is required.

Relationships developed by Rajani *et al.* (1995) for longitudinal movements assumed a translational slide mass as illustrated in Figure 2-12. Two approaches were presented; a limit equilibrium approach and a force-displacement approach. The limit equilibrium approach calculated the maximum axial load on a pipeline assuming a factor of safety of unity where the driving and resisting forces are balanced as illustrated in the free body diagram in Figure 2-13 and there is no slip between the soil and the pipe. The failure criteria for the surrounding soil are assumed to be Mohr-Coulomb and the height of the

translational slide mass is determined using slope stability analysis. The mathematical solution for the limit equilibrium approach is provided in the research paper and is not presented herein.

The second approach developed by Rajani et al. (1995) estimates net force ( $P_o$ ) acting on the pipeline in the longitudinal direction by examining the soil-pipe interaction resulting from axial displacements. The soil-pipe interaction models presented are similar to O'Rourke and Nordberg (1992) with the soils resistance being represented with an elastic-perfectly plastic material (Figure 2-14 (a.)) However, the pipeline response to loading is assumed to follow a stress-strain relationship with strain hardening typical of steel pipeline (Figure 2-14 (b.)). This differs from O'Rourke and Nordberg (1992), where design tables related to pipeline strain were provided by the authors, leaving the calculation of load (stress) due to strains to the constitutive model selected by the designer. In Figure 2-14 (a.), the limiting maximum axial resistance per unit length ( $F_x$ ) provided by the soil can be expressed with equations presented by the Committee on Gas and Liquid Fuel Lifelines (1984), while  $k_x$  is related to the axial sub-grade modulus which can be estimated from typical values for various soils or based on empirical calculations. Young's modulus of steel ( $E_1$ ) and hardening modulus of steel are either known for a pipeline section or can be estimated. Using the soil-pipe interaction models presented in the paper, three distinct stages of soil-pipeline interaction to displacements can be assessed based on the analytical solutions developed by the authors in a separate paper. The three distinct stages are; (1) elastic response of both the soil and pipeline, (2) the soil is in a plastic state and the pipeline is elastic, (3) both the soil and pipe are in the plastic state. Analytical solutions for the various distinct stages were determined for non-

dimensional longitudinal displacements and load parameters with various input parameters. The objective of the analytical solutions is to determine the maximum load ( $P_o$ ) based on the displacement ( $u_o$ ) at the interface of moving and stationary soil mass as illustrated in Figure 2-15. The analytical solutions by Rajani *et al.* (1995) are presented graphically in Figure 2-16 and 2-17. The input parameters required to determine the load ( $P_o$ ) and displacement ( $u_o$ ) at the landslide interface include; pipeline diameter ( $b$ ), unit weight of the soil ( $\gamma$ ), axial sub-grade modulus ( $k_x$ ), moduli of pipe ( $E_1, E_2$ ), and pipe stiffness ( $\kappa$ ) which is related to the sub-grade modulus and  $\epsilon_y$ , pipeline strain at yield. This approach is useful in determining the maximum displacement ( $u_o$ ) for a load ( $P_o$ ) that would yield the pipe.

The early methods for determining pipe stresses due to landslide movements were founded on essentially a base framework with similar assumptions related to direction of movements, soil conditions, and constitutive models to represent the interaction between soil and a pipeline. Research following these early methods verified or expanded on these concepts with increasing complexity.

Trigg and Rizkalla (1994) applied the simplified design methods developed by Rajani *et al.* (1995) to known and unknown landslide locations. The intent of the authors was to demonstrate the applicability and validity of the method presented by Rajani *et al.* (1995) as a preliminary design tool and risk integrity first cut approach to identify potential critical landslide locations. Trigg and Rizkalla (1994) also compared predicted strains to selected critical tensile and compressive strain limit deemed unacceptable by the authors. Case studies were presented where the time to reach critical

strain limit were calculated and at which time, mitigation measures are warranted by the authors such as pipe relaxation.

Becchi *et al.* (1994) applied work completed by O'Rourke and Nordberg (1992) and the soil-pipe interaction equations developed by the Committee on Gas and Liquid Fuel Lifelines (1984) by using a numerical finite element method (FEM) approach in lieu of idealized permanent ground deformation patterns to assess pipeline response to ground movements. Results of the FEM model were then compared to a case study with known ground movements and field measured axial strains in the pipe to determine how well these simplified methods predicts axial strain. Becchi *et al.* (1994) examined buried steel pipelines subjected to both transverse and longitudinal translational movement in their FEM model. The FEM model predicted strains compared well to measured strains at two locations, but was poor at two other locations where FEM calculated strains significantly over predicted field measured strains. Due to simplified assumptions required in the analysis, the authors could not determine any firm conclusions in regards to validity of their methodology for predicting pipeline stresses due to landslides. However, the authors concluded the methodology presented would be useful as a screening tool within a risk management system. Bruschi *et al.* (1996) used 3-D FEM methods to compare predicted pipe strains using simplified methods to represent soil-pipe interaction for nine case studies where field measured pipeline strain and ground movement data was available. The analysis included both longitudinal and transverse movements applied to buried steel pipelines focusing solely on axial loading. As with Becchi *et al.* (1994), the results from the method presented by Bruschi *et al.* (1996) over predicted measured strains along the pipelines. Bruschi *et al.* (1996) concluded that there is “*a problem in consistency between*

*the basic assumption of the structural modelling and what has actually occurred in the studied areas*". The authors also concluded the inconsistency is due to the uncertainties in both the actual geometry of the landslide and the soil-pipe interaction.

To accurately predict pipeline stresses due to landslides, research began to focus on gaining a better understanding of key input parameters and developing more complex methods (models) to capture the geometry of the landslide and interaction between to the soil and pipe interface. The soil stiffness and associated pipe interaction is a key input parameter in the methods presented. Theoretical predications of the maximum adhesion force presented by CGL (1984) were determined to over predict forces on the pipeline due to soil displacements for most types of soil backfill (Rizkalla *et al.* 1996; Cappelletto *et al.* 1998; Scarpelli *et al.* 1999) and under predict in the case of dense sand backfill (Wijewickreme *et al.*, 2009). CGL (1984) recommended using two equations to predict the maximum axial adhesion load per unit length of the pipe for both total stress (undrained) and effective stress (drained) conditions as follows:

$$F_x = \alpha S_u (\pi DL) \qquad \text{Total Stress} \qquad \text{eq. 2.25}$$

$$F_x = 0.5(1 + K_o)\gamma' H \tan(\delta) (\pi DL) \qquad \text{Effective Stress} \qquad \text{eq. 2.26}$$

Where:

$F_x$  = axial adhesion load on the pipe, kN

$\alpha$  = adhesion factor between the pipe and soil

$S_u$  = undrained shear strength of the soil (alternatively denoted as  $C_u$ ), kPa

$D$  = pipe diameter, m

$L$  = buried pipe length, m

$K_o$  = coefficient of lateral earth pressure at rest soil

$\gamma'$  = average effective unit weight of the soil, kN/m<sup>3</sup>

$H$  = depth below ground surface to centerline of the pipe, m

$\delta$  = interface angle of friction between the pipe and the soil, degrees

The parameters associated with geometry ( $H$ ,  $D$ ,  $L$ ) and material properties ( $S_u$ ,  $\gamma'$ ) can be easily measured or estimated reasonably well. However,  $\alpha$ ,  $K_o$ ,  $\delta$ , are more uncertain and are difficult to determine. Scarpelli *et al.* (1999) conducted field experiment and laboratory testing to better define  $\delta$  for different pipe coatings and backfill types and Wijewickreme *et al.*, 2009 focused on examining  $K_o$  for loose and dense sand backfill through laboratory testing and numerical FEM modelling. Total stress analysis is typically used when fine grained cohesive soils (silts and clays) is used as backfill which generally apply larger axial pipe loads than non-cohesive soils (sands and gravels). The adhesion factor,  $\alpha$ , is key in predicting loads transferred from cohesive soil to a pipeline. Rizkalla *et al.* (1996) conducted laboratory and full-scale field tests to assess  $\alpha$ -values for different undrained shear strength results and compare these results to published values by CGL (1984). The adhesion values published by CGL (1984) significantly overestimated  $\alpha$  values (and in turn overestimate pipe adhesion loading) when compared to results determined in research conducted by Rizkalla *et al.* (1996). Cappelletto *et al.* (1998) expanded on work completed by Rizkalla *et al.* (1996) and

confirmed  $\alpha$ -values published by CGL (1984) over estimated  $\alpha$ -values as shown in Figure 2-18. Additional work has been conducted on understanding and measuring pipe adhesion values since the 1990s and Figure 2-19 from D.G Honegger Consulting *et al.* (2009) presents more recent data and relationships between pipe adhesion and undrained shear strength. The use of CGL (1984) within the simplified methods presented herein may explain the discrepancy between predicted strains using simple models to field measured strain as noted by Becchi *et al.* (1994) and Bruschi *et al.* (1996).

The simplified methods developed in the mid-1990s were limited in their ability to properly predict pipeline stresses/strains due to landslides, especially where field conditions did not match well with the assumptions used in the models (*e.g.* assumptions of translational slides, pure axial pipe loading). In this regard, these simplified methods were expanded by several researchers to incorporate more complex numerical modelling techniques, comprehensive soil-pipe stress-strain relationships, different combinations of ground movements, and pipe loading scenarios and on occasion, limit states failure modes. Challamel and Buhar (2003) proposed a method similar to the limit equilibrium method (Approach 1) presented by Rajani *et al.* (1995) using a “mixed modelling” technique. A kinematic approach is used to predict axial stresses in the pipeline subjected to rotational landslides moving away the assumption of translational slides. Chan and Wong (2004) also examined different landslide types (Figure 2-20) such as deep-seated planar slip (block movement), circular slip (rotational) in addition to traditional translational type movement referred to as shallow planer slip in Figure 2-20. Chan and Wong (2004) also proposed analytical solutions that improved and presented modified solutions to the simplified methods proposed by O’Rourke and Nordberg



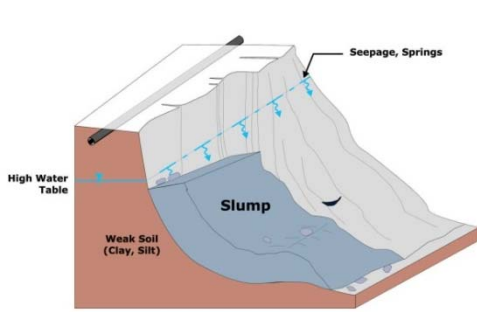
(1992) and Rajani *et al.* (1995). Chan and Wong (2004) used a case study to illustrate how to apply their method, but independent verification of the predicted axial and bending stresses and strains from their model was not undertaken. Cocchetti *et al.* (2009) in two companion papers proposed a different approach to capture ground movements not necessarily perpendicular or parallel to a pipeline in either plan or cross-section for translational slides. The author's approach used FEM modelling where the pipeline is discretized as a 3D beam element, the soil is assumed to behave as elastic-perfectly plastic, and the soil-pipe interaction is modelled using macro-element theory which the authors consider to be the main novelty of their approach. Both large and small displacement approaches are presented and several case studies are examined to verify the two approaches. The two approaches are deemed by authors to reliably predicted stresses in the pipeline for the case studies examined. Yoosef-Ghodsi *et al.* (2008) improved on work carried out by Rajani *et al.* (1995) by incorporating the effects of internal pressure, pipe temperature change, and pipe bends on the strain demand on a pipeline in a closed-form solution. A limiting scenario was included in the analytical model to prevent overestimation of axial strains in the pipe, common to early simplified methods. The analytical model was validated against finite element solutions.

Examining limit states failure modes (yield, tensile rupture, buckling) for pipelines within landslides in the literature is relatively limited and tends to focus on one failure mode, yielding. Limit states design methods and failure modes for pipelines are discussed in detail in Section 2.3 and Section 2.5. Simmonds *et al.* (1996) introduced tensile rupture and buckling limit states failure modes in their research to determine if predicted strains from simple methods (Trigg and Rizkall, 1994) and FEM analysis are acceptable.

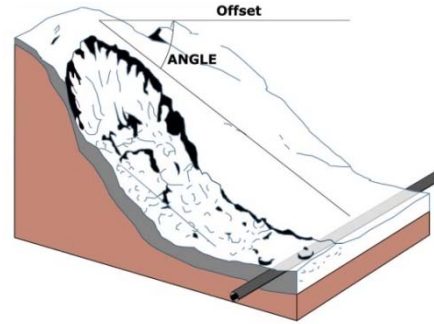
Bruschi and Monti *et al.* (1995) also compared predicted pipeline strains/stresses using FEM analysis to examine scenarios where limit states failure modes (tensile rupture, buckling) may occur.

Research focusing on probabilistic approaches to determine limit states failure modes for pipelines subjected to ground movements is even more limited (Zhou, 2012). Wijewickreme *et al.* (2005) analyzed failure probability of tensile rupture for gas pipelines subjected to longitudinal ground movement following earthquakes. Nobahar *et al.* (2007) examined the probability of ice gouging inducing local buckling of buried offshore pipeline. Zhou (2012) presented a strain based methodology to determine the probability of tensile rupture and local buckling of a buried pressurised pipeline subjected to longitudinal movements. Zhou's methodology uses the analytical model developed by Yoosef-Ghodsi *et al.* (2008) (which is an enhancement of the simplified model presented by Rajani *et al.*, 1995), and assumes the pipe is elastic-plastic with strain hardening, the soil-pipe interaction is perfectly plastic, and includes internal pressure. The spatial variability of the soil and pipe properties is also included in calculating the probability of failure for the two limit states failure modes assessed. The probabilistic calculations used a Monte-Carlo simulation on some of the input parameters into the Yoosef-Ghodsi *et al.* (2008) analytical model represented with known or estimated probability distribution functions. The calculated probability of failures can then be compared to limit states failure criteria to determine the reliability of the pipeline. A hypothetical example to illustrate the methodology was presented in the paper. The methodology proposed by Zhou (2012) is deemed by the author to be well suited for a reliability or risk-based pipeline integrity management system.

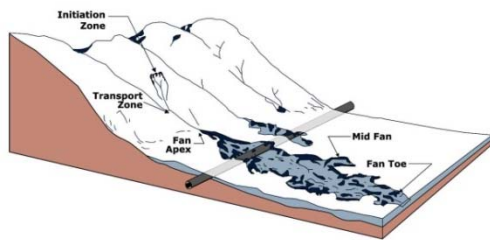
The simplified and more complex methods discussed are intended to demonstrate the variations, applicability, and limitations of these methods. The simplified methods are easy to implement requiring minimal input parameters, but should only be used as a preliminary design tool since predicted stress/strains are generally overestimated, and conservative. Complex models provide better predictions of pipeline stresses/strains, but require a higher level of understanding and knowledge to properly use these analytical models. All of these methods are limited as they cannot fully capture the response of a pipeline subjected to ground movements given the numerous combinations of factors and scenarios that would be required to fully define a particular landslide and corresponding pipeline response. Assumptions, estimates, and idealizations will always be required. These methods approach the problem starting from the soil/ground movement perspective and work towards determining the response of the pipeline as a final outcome. This thesis research approaches understanding of stress/strains induced on pipelines due to landslides starting from the pipeline and working towards linking it to ground movements. This is achieved by measuring strains on in-service pipelines in actively moving ground and using probability theory to determine if reliability based limit states failure criteria are exceeded for certain magnitudes of ground movements. Measuring of active pipelines is not new (Greenwood *et al.*, 1986; Couperthwaite and Marshall, 1989; Braun *et al.* 1998; Dinovitzer *et al.* 2014). But historically, strains in pipelines are measured as a mitigation measure for pipelines at risk or used to calibrate analytical methods presented herein. The approach undertaken in this research, however, is unique as no known research has been conducted in this manner.



On-Row Instability



Off-Row Instability/Fall



Off-Row Debris Flow

Figure 2-1 Schematic Illustration of Typical Geotechnical Hazards in Manitoba (adapted from Porter and Savigny, 2002).

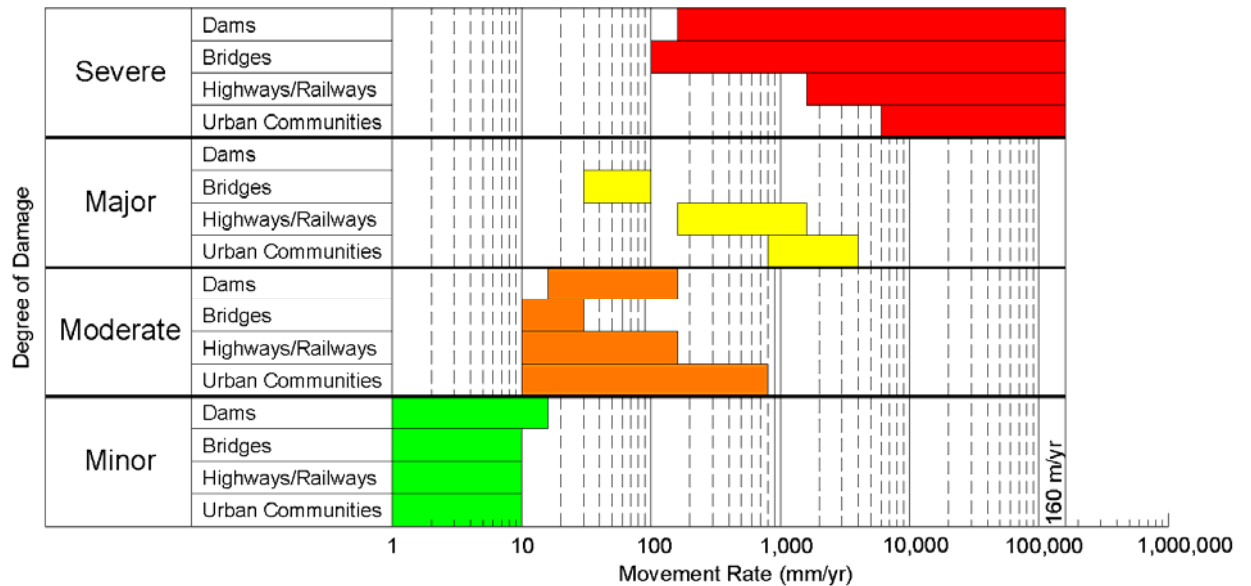


Figure 2-2 Schematic Representation of Expected Extent of Damage versus Movement Rate (adapted from Mansour *et al.*, 2009).

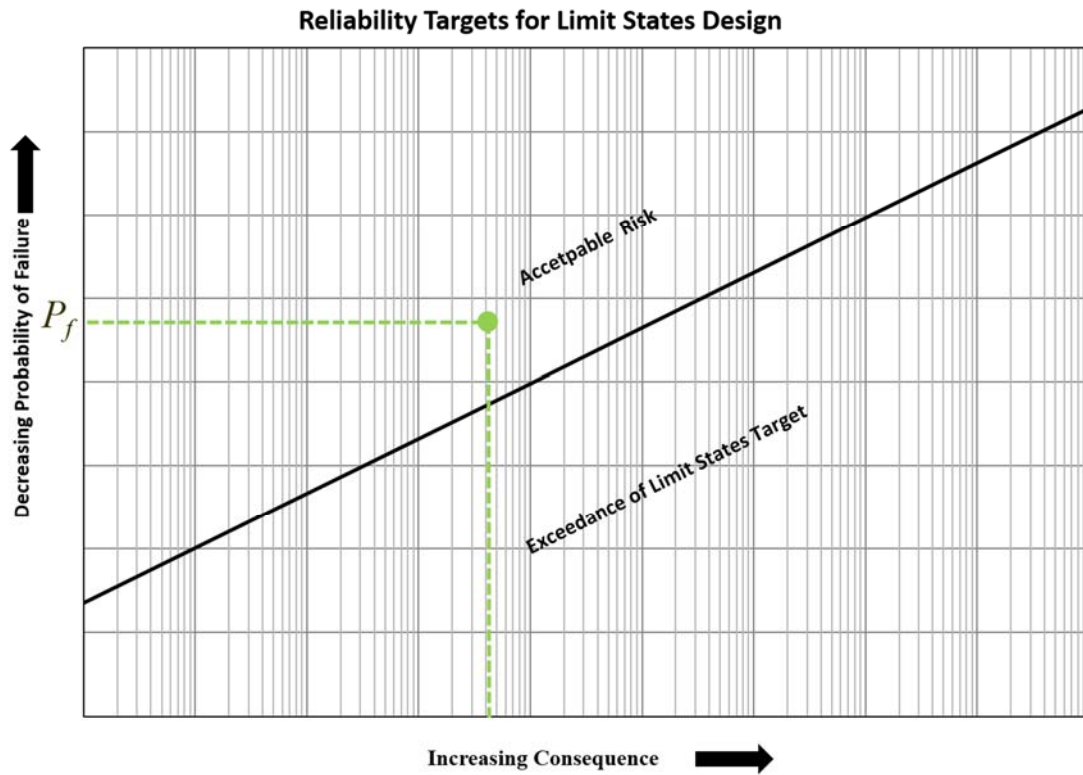


Figure 2-3 Relationship between Probability of Failure *versus* Consequence.

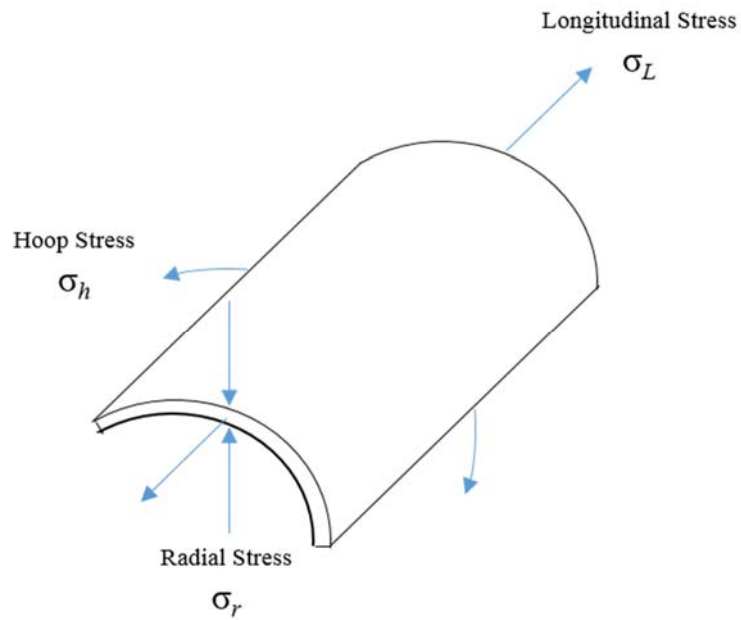


Figure 2-4 Principle Stresses acting on a Hollow Cylinder.

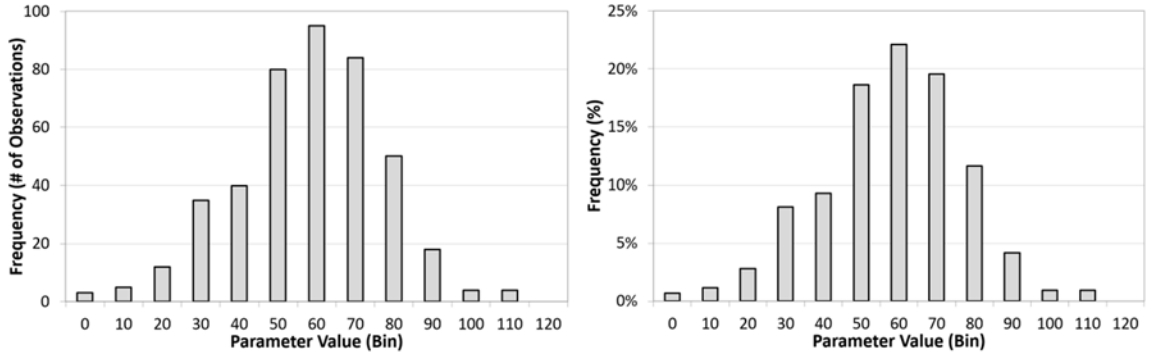


Figure 2-5 Histogram Example.

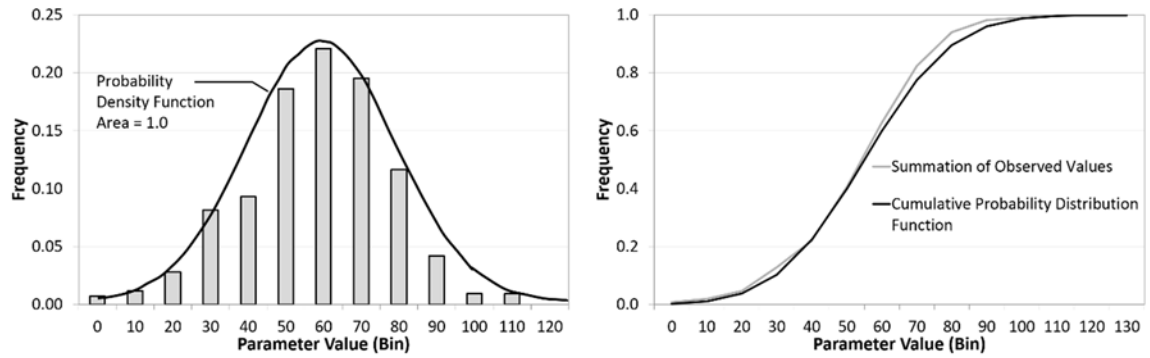


Figure 2-6 Histogram with Probability Density Function and Cumulative Probability Distribution Function

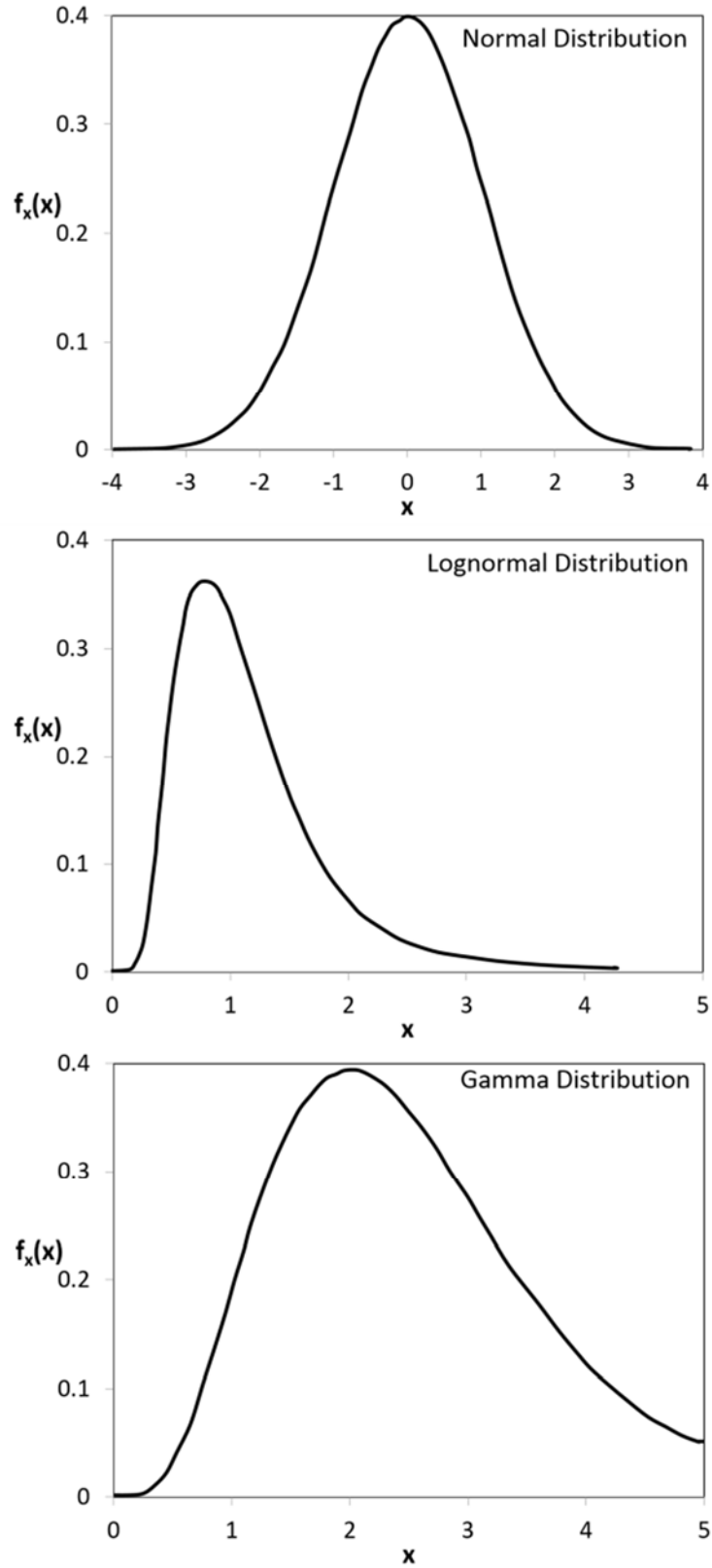


Figure 2-7 Schematics of Common Probability Distributions.

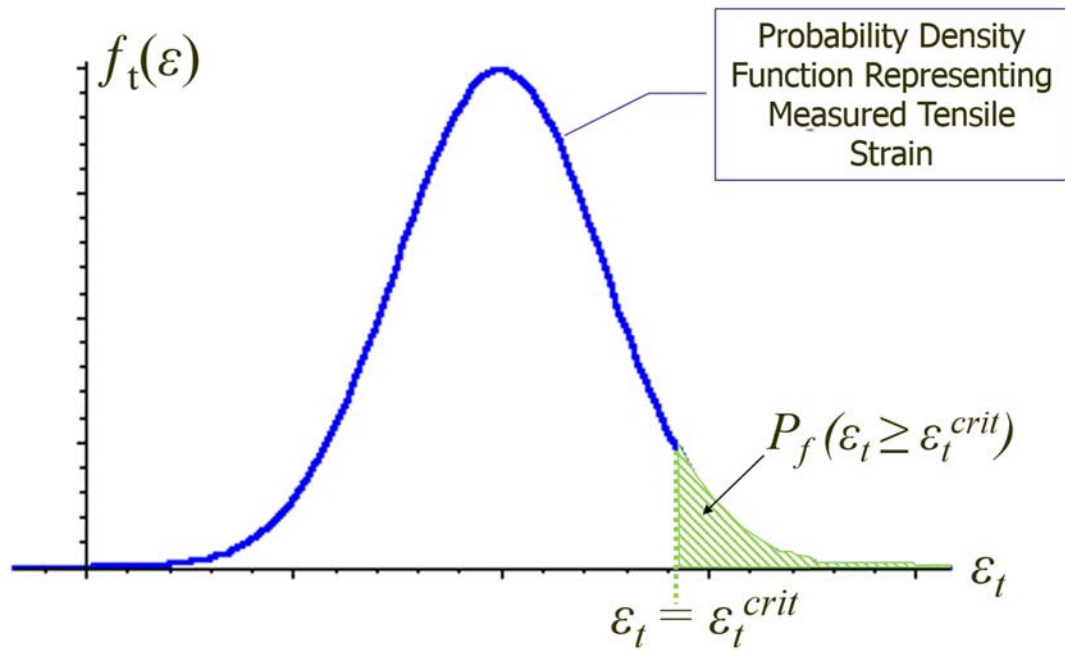


Figure 2-8 Example of Probability of Tensile Rupture.



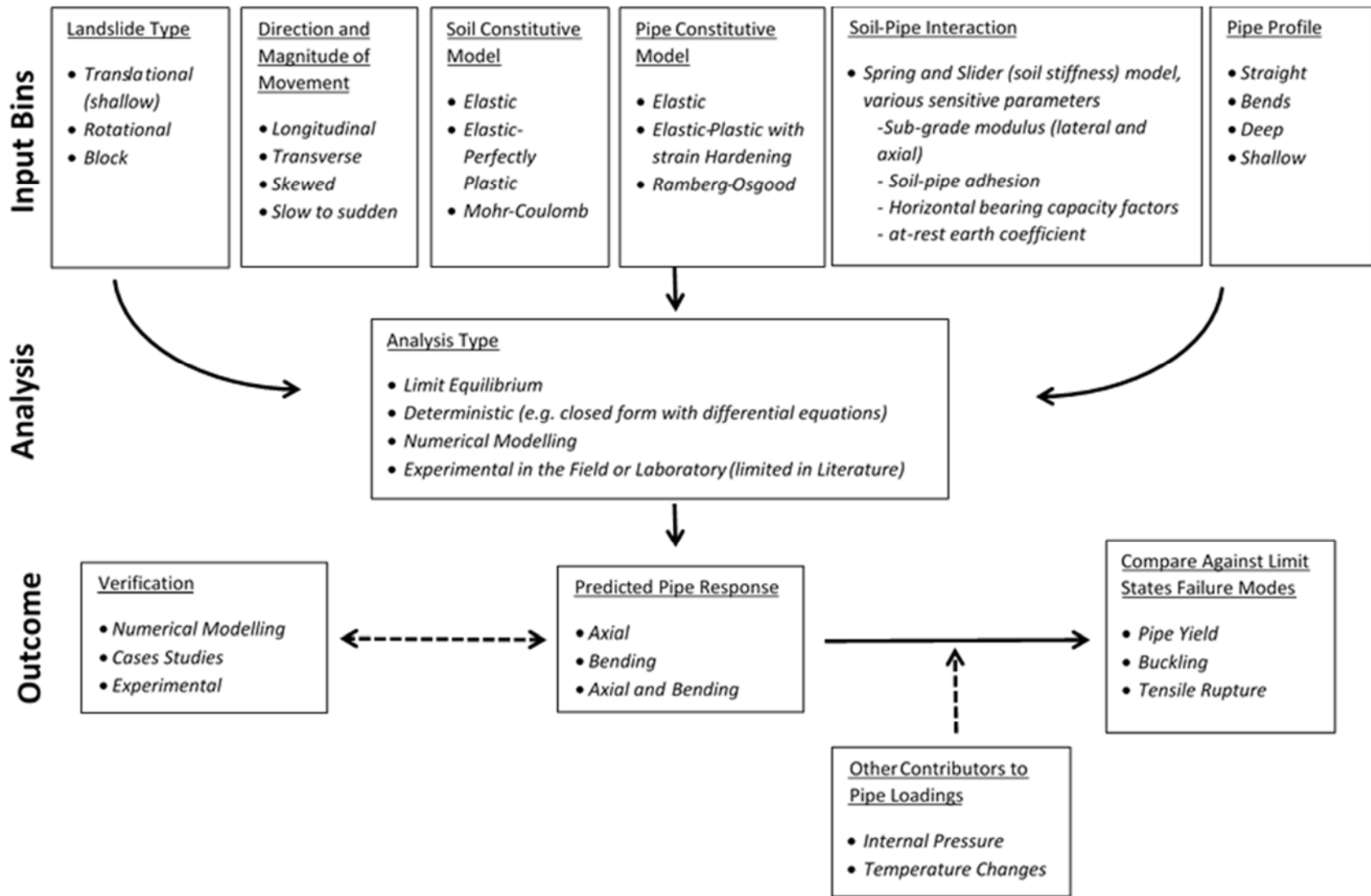


Figure 2-9 Road Map of Predictive Models for Pipelines Subjected to Landslides.

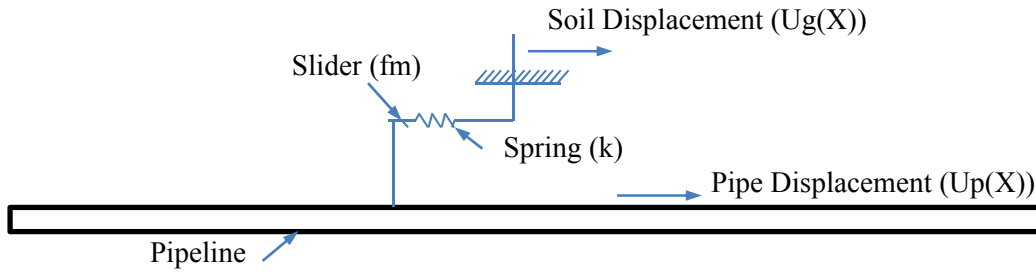


Figure 2-10 Spring/Slider Model for Axial Soil-Pipeline Interface Forces.

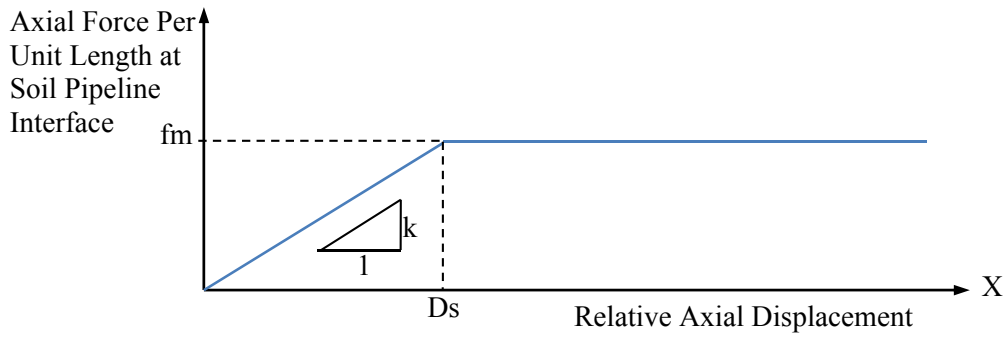


Figure 2-11 Assumed Axial Force vs. Relative Displacement Relation for Elastic Spring/Slider Model of the Soil-Pipeline Interface.

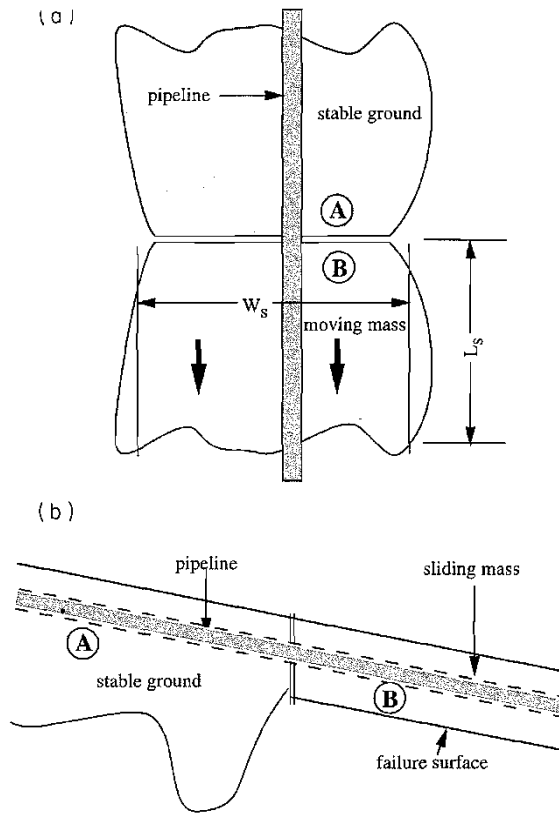


Figure 2-12 Pipeline Subjected to Longitudinal Translational Slide: (a) plan view, (b) longitudinal cross-section view. (Rajani *et al.* 1995).

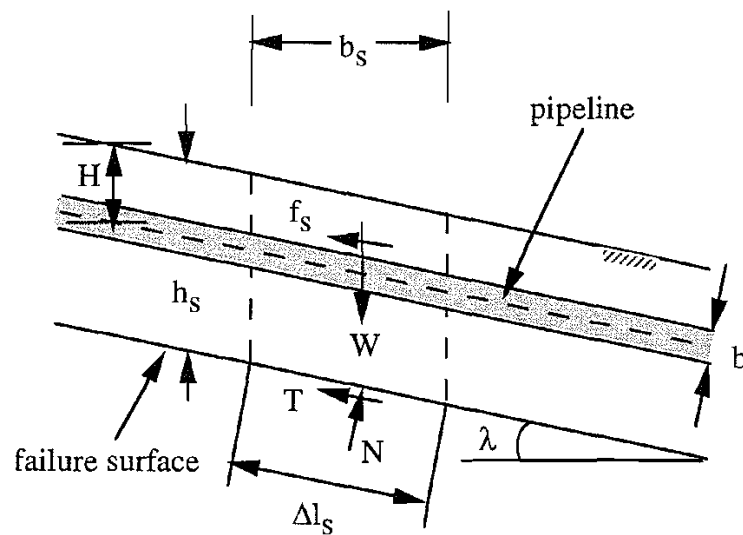


Figure 2-13 Free Body Diagram Transitional Slide Limit Equilibrium Approach (Rajani *et al.* 1995).

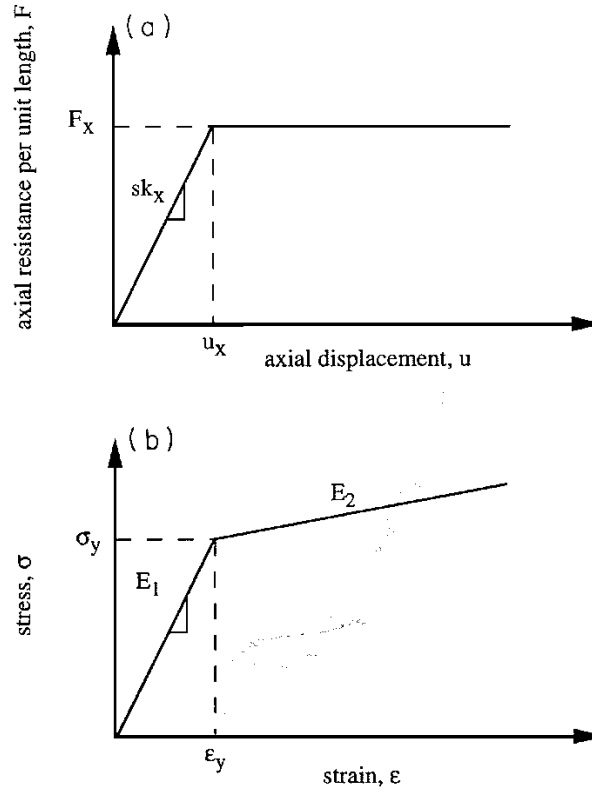


Figure 2-14 (a) axial soil resistance, elastic-perfectly plastic (b) stress *versus* strain relation for typical steel pipeline (Rajani *et al.* 1995).

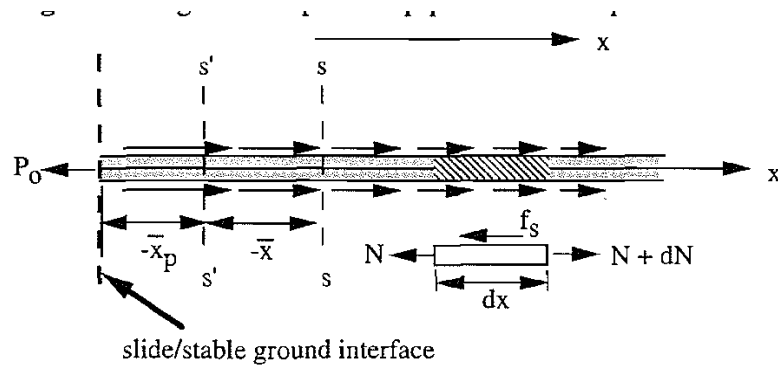


Figure 2-15 Longitudinal pull on pipeline due to planar slide (Rajani *et al.* 1995).

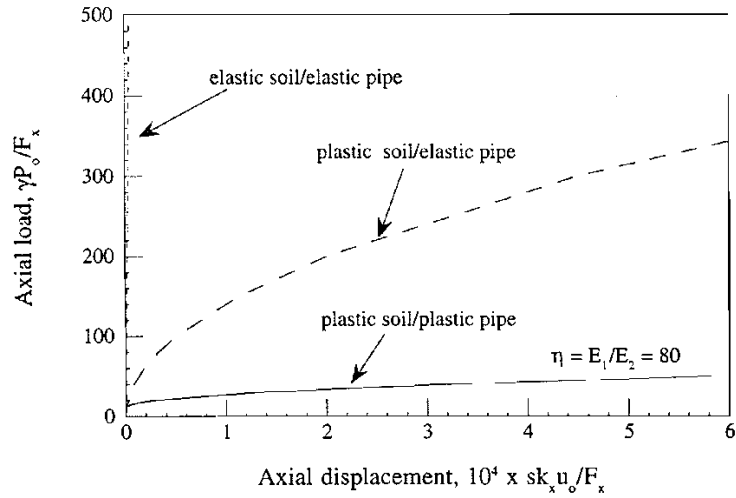


Figure 2-16 Non-dimensional characteristic curve for axial displacement for longitudinal soil-pipeline interaction (Rajani *et al.* 1995).

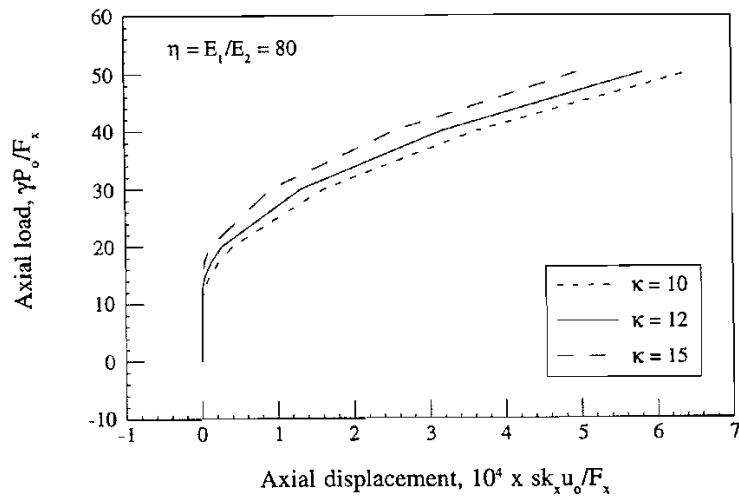


Figure 2-17 Non-dimensional characteristic curve for axial load-displacement for different values of the soil-pipeline stiffness parameter,  $\kappa$  (Rajani *et al.* 1995).

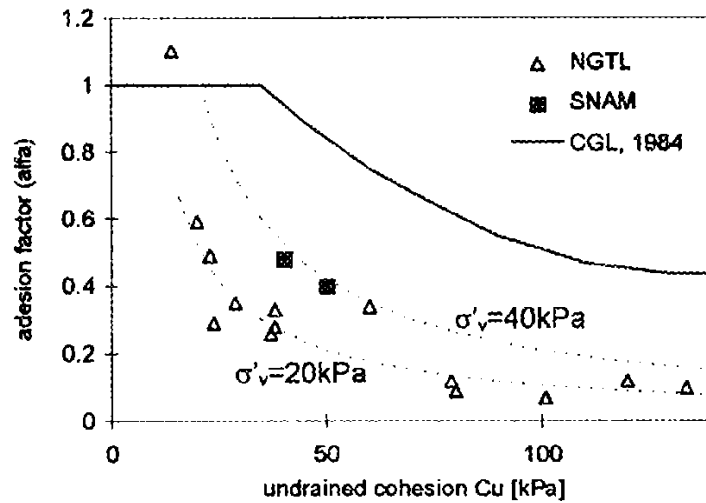


Figure 2-18 Comparison of  $\alpha$ - $S_u$  between theoretical model (CGL, 1984) and experimental data NGTL (Rizkalla *et al.*, 1996), and SNAM (Cappelletto *et al.*, 1998)

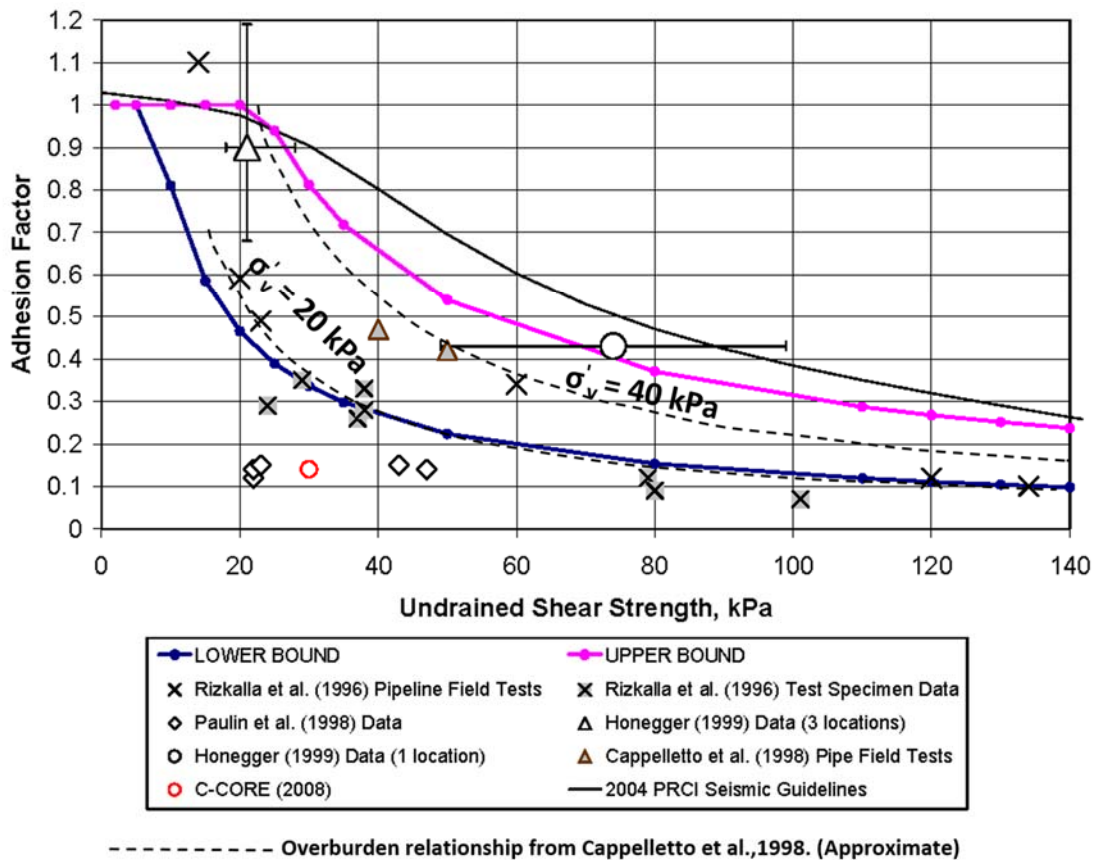


Figure 2-19 Recommend bounds for adhesion factors (modified from D.G. Honegger Consulting *et al.*, 2009).

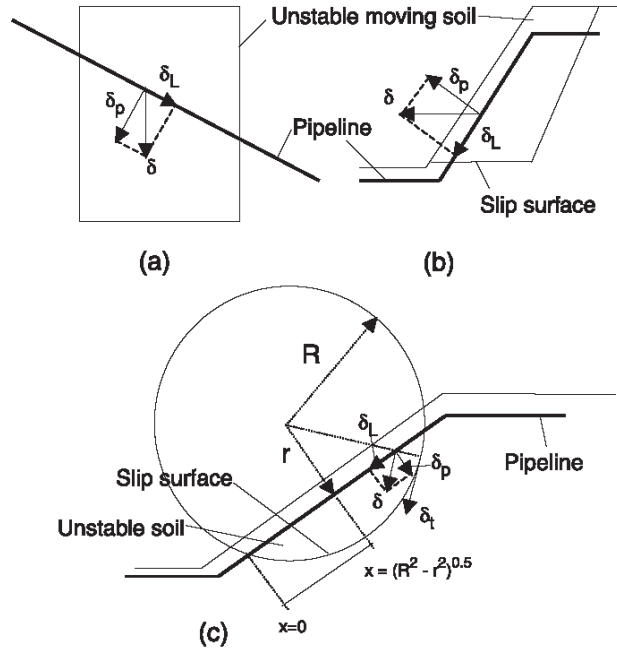


Figure 2-20 Idealized Soil Movement Patterns: (a) shallow planar slip in plan view (b) deep-seated planar slip side view, (c) circular slip in side view.  $\delta$  resultant soil movement;  $\delta_L$  and  $\delta_p$ , soil longitudinal and transverse movement components, respectively;  $\delta_t$  rotational (tangential) displacement (Chan and Wong, 2004).

## Chapter 3 Methodology

The research program was developed to test the thesis hypothesis and complete the research objectives outlined in Chapter 1. The overall program includes the following major components:

- Information gathering and review.
- Selection of research field sites for *in-situ* testing.
- Field Program – sub-surface investigation, ground survey, instrumentation installation, *in-situ* stress release tests, and pipe push test.
- Monitoring of instrumentation and ground movements.
- Interpretation of monitoring results, strain/stress calculations and probability failure calculations for various limit states failure modes.
- Development of a risk management system for decision support.

The major components of the thesis research are discussed briefly in this chapter to provide a better understanding and outline of the research process undertaken.

### 3.1 Information Gathering and Review

Manitoba Hydro's internal information was reviewed for pertinent information related to the thesis research project. In particular, Manitoba Hydro's at-risk sites catalogued in a previous report was reviewed. The review process provided an understanding of Manitoba Hydro's Gas Pipeline network and further insight into previously identified at-risk sites which was beneficial in the development and implementation of the field program and instrumentation installation.



## **3.2 Selection of Research Sites**

The intent of the site visits was to become familiar with at-risk sites catalogued in a previous report and identify and select potential key at-risk landslide sites that are well suited for the detailed field investigation, ground monitoring and pipeline monitoring. Information gathered during the site visits included the nature and level of the risk, visual evidence of ground movements and possible pipeline failure mechanisms, classification of surficial soils, estimates of slope heights and angles, site photos, and other pertinent information.

## **3.3 Field Program**

### *3.3.1 Contributors to Strains/Stresses on Pipe*

In order to determine the strains/stresses induced on a pipe solely due to ground movements, other possible sources of load that may be inducing strains/stresses on the pipe needed to be determined. Four primary sources have been identified to be potentially applying strains/stresses on pipelines (stress-state) in landslide areas within Manitoba. Other sources that may be applying load to a pipeline were reviewed, but were deemed not to be significant in comparison to the four primary load factors identified. While the four sources may induce stresses on the pipe, soil-pipe interaction (*e.g.* adhesion) can affect and limit the magnitude of axial pipe stresses due to ground movements as discussed in Section 2.7. These four sources may occur individually or in combination and may change seasonally. The four primary sources affecting the stress-state of the pipe are:

- Landslides movements.
- Soil volume changes due to freezing/thawing of the soil around the pipe or moisture changes in expansive soils (*e.g.* fine grained cohesive soils).
- Soil Creep.
- Elongation/Compression of the pipe due to temperature change (thermal effects).

Three of the four stresses are due to soil displacement around the pipe either due to ground movements or related to volume change associated with water. Stress change in the pipe related to temperature and soil volume changes is variable and transient, while the change in stress due to ground movements are cumulative, unless the soil fails and allows the pipe to displace, pipe slips (axial soil force exceeds adhesion) or the pipe permanently deforms (plastic behaviour).

Soil volume changes due to moisture changes are difficult to measure or estimate, especially since gas pipelines are typical buried at shallow depths (<1 m), within the vadose zone, in Manitoba. Soil moisture within the vadose zone is transient and can increase (rainfall events) or decrease (evapotranspiration) over short periods of time in non-winter months, but is relatively constant over the winter. Although transient in non-winter months, soil moisture within the vadose zone would trend towards a natural moisture content if measured over a large enough period of time in an established environment. This would result in a relatively constant volume where notable changes in volume would be due to extreme events such as draught or significant long-term low-intensity rainfall events. In this regard, the magnitude of applied stresses due to moisture changes was assumed to be minor most of the time when compared to the other sources

of load identified and therefore stresses induced on the pipe due to moisture related soil volume changes was not examined in this research.

### *3.3.2 Field Program Details*

The field program was developed in a manner to measure, directly or indirectly, the possible sources of stresses on the pipes and to determine soil-pipe adhesion characteristics. The field program included:

- Drilling of test holes – Test hole drilling provides information related to sub-surface soil and groundwater conditions. The sub-surface information can be used to calculate or estimate potential for landslide to occur (slope stability), freeze/thaw potential, soil creep, and soil-pipe adhesion.
- Installation of slope inclinometers and vibrating piezometers – Slope inclinometers (SI) measure ground movements with depth and are useful for identifying landslide movements and measuring soil creep. Vibrating wire piezometers (VW) measure groundwater levels which influence the stability of natural slopes and can be a main cause triggering landslides.
- Installation of strain gauges – Strain gauges were installed directly on the active gas pipelines to measure pipe strains and are used to determine axial, bending, and torsional shear stresses with time.
- Installation of temperature gauges – Placing temperature gauges on the pipe and within the ground in the vicinity of the pipe is used to calculate structural stresses resulting from temperature changes and used to assess freezing/thawing conditions.

- Ground survey – A ground survey provides topographic information (slope angle, length). The location of the instrumentation and test holes were also captured in the survey. The SI's became inoperable due ground movements early on and the method of monitoring ground movements was switched to surveying of monitoring pins installed at ground surface. Section 5.1.1 provides further information.
- Field pipe push tests –Pipe push tests on abandoned gas pipelines was conducted to provide direct measurements of soil-pipe adhesion characteristics under field conditions.

Although changes in stress affecting the pipe can be easily calculated following installation of strain gauges, it is likely that existing buried pipelines are under the influence of cumulative stresses from past ground movements. In this regard, the initial stress state of the pipe needs to be determined in order to evaluate the remaining capacity of the monitored pipeline. An understanding of the initial stress state of the pipelines is required to properly assess the risk of pipeline failure. Research sites where pipelines were to be replaced were selected which allowed pre-installed strain gauges to capture any stress release resulting from cutting (abandoning) and the subsequent stress relaxation of the pipeline. In addition, abandoned pipelines were used in the field push tests to assess soil-pipe adhesion.

### **3.4 Monitoring of Instrumentation and Ground Movements**

A minimum of three years of monitoring was selected as an appropriate amount of time for the monitoring program. The selection of a minimum of three years duration was intended to gather information for a sufficient amount of time to in order to properly

assess the probability of failure for various limit failure modes and the associated measured ground movements. In the end, site monitoring lasted four years.

A data acquisition (DA) system was used to record strains on the pipelines, ground and pipe temperatures, and ground water levels on an hourly basis for the duration of monitoring. The slope inclinometers and ground monitoring pins were monitored manually several times a year.

### **3.5 Interpretation of Monitoring Data, Pipe Stresses, and Probability Calculations**

Monitoring data gathered was reduced and noise in the data was filtered using appropriate techniques (discussed in Section 5.1.2). Pipe longitudinal and torsional stresses are calculated from the monitoring data in conjunction with internal pipe pressure monitoring data provided by Manitoba Hydro. The calculated pipe stresses data sets were then evaluated to determine trends, outliers, and other important results. The temperature data was used to apply a temperature correction to the measured strains and to evaluate freeze/thaw conditions.

Methods outlined in Chapter 2 were used to calculate probability of failure of the various applicable limit state failure modes to determine if limit states criteria are exceeded. The results of probability analysis are compared against the ground movement monitoring data, and is examined for any notable trends or correlations between ground movements and pipe stresses, especially for instances when limit states failure modes are exceeded.

### **3.6 Development of Risk Management System**

The outcome of the thesis research was used to develop a risk management system, referred to as the PipeHaz risk management system. The intent of PipeHaz risk management system (PipeHaz) is to provide a simple and flexible risk management approach for gas pipelines in Manitoba that may be at-risk due to potential ground movements (geotechnical hazards). Specifically, the system evaluates risks associated with ground movements along natural slopes and at river crossings. PipeHaz uses a multi-phase approach which can be applied in full or in parts and was developed to comply with CSA standards for onshore gas pipelines (CSA Z662-15). The system has been calibrated and validated using the measurements from this thesis which are strictly behavioural based on the monitoring approaches identified. Although quantitative elements are introduced to take into account the stress state in the pipe structure, the intent of the management systems is to be used in a qualitative manner to compare relative risk of installations along the network to aid in the pipeline owner/operators ability to make operational decisions.

## **Chapter 4 Research Sites and Field Work**

### **4.1 Site Visits and Selection of Research Sites**

Over ten of Manitoba Hydro's at-risk landslide sites were visited in the Fall of 2009 to select preferred sites for the field work and monitoring. The term landslide can also be referred to as slope instabilities or slope failures, while potential landslide areas are often referred to as unstable slopes or banks. The majority of the at-risk sites are located in the SW corner of the province of Manitoba within the Parkland, Westman and Winkler District regions of the Manitoba Hydro's gas pipeline network. Three research sites were selected that best captured a range of landslide types (translational, rotational), different geological features, and are considered to be high-risk among other parameters considered in the selection process. The three research sites selected are the Plum River crossing, Harrowby Assiniboine River valley, and St-Lazare Assiniboine River valley sites. The Plum River site represents the condition where a gas pipeline is buried parallel to a riverbank slope (a river crossing) that has undergone past riverbank landslide activity and is likely to still be moving. A past riverbank instability encompassing the gas pipeline at the crossing was visually evident during the initial site visit and the instability is predominantly rotational in nature. The Harrowby and St-Lazare valley sites represent conditions where a gas pipeline transverses a potential landslide area (unstable slope) or a slope undergoing creep movements on a larger scale since the pipelines run along a long valley wall within a deep river valley. The potential for ground movements at the valley sites were deemed to be either translational (assumed to be relatively shallow) or rotational associated with deep seated movements or combination thereof. Figure 4-1

illustrates the site locations within Manitoba. Site plans and cross-sections for the three research sites are plotted on Figure 4-2 to 4-4.

## **4.2 Geology, Site Description, Sub-Surface Conditions, and Pipe Information**

### *4.2.1 Riverbank Site - Plum River*

The Plum river site is located about 10 km south of Morris, Manitoba and just southwest of the town St. Jean Baptiste (Figure 4-1). The Plum River is a tributary within the Red River valley system and flows into the Red River just north east of St. Jean Baptiste. The surficial geology of the area is dominated by de-glaciation activities where a large ice-dam lake was created known as Lake Agassiz (Teller *et al.*, 1996). The glacial lake was formed about 12,000 years ago depositing lake sediments (mostly lacustrine deposits of silt and clay sizes) for about 4,000 years before the lake drained to the north into the Hudson Bay. The Red River along with its tributaries formed within the flat lakebed created by Lake Agassiz. Rivers and tributaries, including the Plum River, are slow moving and have meandered over time due to the flatness of the lakebed. The on-going meandering of a river causes erosion at the toe of riverbanks along the outside bends of the river which becomes over-steepened and can trigger riverbank instabilities.

The riverbank at the Plum River site is about 4 to 5 m high from toe to crest and is sloped at approximately 3.7Horizontal(H):1Vertical(V). The riverbank has experienced riverbank landslides in the past with larger slump blocks evident along this stretch of riverbank (Figure 4-5).



The ideal location for ground and pipe instrumentation is within the past riverbank instability (slump block). Therefore, a test hole (TH10-01) was drilled near the top of bank, along the riverbank slope, within one of the larger slump blocks at the location noted on Figure 4-2.

Soil units encountered during drilling were logged and classified using the Unified Classification System (ASTM D2487) and disturbed and relatively undisturbed soil samples (Shelby Tube) were obtained for each soil unit. Laboratory soil testing was conducted on select samples in general accordance with applicable ASTM standards. Laboratory testing included moisture content (ASTM D2216) determination, bulk unit weights measurements, undrained shear strength (ASTM D2166) unconfined compression tests, and grain-size distribution using mechanical sieve and hydrometer methods (ASTM D6913 and ASTM D422), and Atterberg Limits (ASTM D4318).

The riverbank soil stratigraphy consists of a thin veneer of topsoil (<0.5 m thick) overlying lacustrine clay to the maximum depth drilled of 12.8 m. The lacustrine clay is silty, brown, becoming grey with depth, moist, firm to stiff, becoming soft with depth, and of high plasticity. Table 4-1 summarizes the soil properties of the lacustrine clay based on the laboratory testing.

Test hole logs have been prepared for all seven test holes drilled at the three research sites and are included in Appendix A. Each test hole log includes a description and elevation of soil units encountered, sample type, sample location, results of field and laboratory testing, and other pertinent information such as sloughing, groundwater seepage, drilling method and equipment used, and UTM location of the test hole.

The Plum River site is an ideal site to represent typical riverbank conditions for a gas pipeline crossing considered to be at-risk. The advantages of the Plum River site compared to other at-risk riverbank sites examined is the proximity to the City of Winnipeg which made it attractive in terms of the field and site monitoring work. Additionally, the gas pipeline river crossing was scheduled to be replaced following instrumentation installation which provided an opportunity to measure any release in pre-existing pipe strains/stresses once the pipeline is cut and abandoned to gain an understanding of the stress-state of the pipeline prior to instrumentation installation. The response of the pipeline after being abandoned is discussed in Section 6.3.2.

#### *4.2.2 Valley Sites – Harrowby and St-Lazare*

The Harrowby and St-Lazare valley sites are located near the Saskatchewan/Manitoba border (Figure 4-1). The Harrowby valley site is located adjacent to the community with the same name which is about 12 km directly west of Russell, Manitoba while the St-Lazare valley site is located about 1.3 km southwest of the town of St-Lazare. The sites are about 37 km apart, roughly north–south of each other.

Both sites are located within the Assiniboine river valley and lie within the same regional geology. The Assiniboine river valley (along with the Qu`Appelle River valley) system was largely established following glaciation during the early Wisconsin period (100,000 to 55,000 Before Present (BP)) through glacial meltwater erosion where spillways and meltwater channels were formed. The cutting of the ancient Assiniboine river valley was then followed by a period infilling of the valley system with alluvium and colluvium deposits (Klassen, 1972).

The modern valley system was not formed until between 15,000 and 12,000 BP following the last ice age where, again, glacial meltwater and drainage from postglacial lakes carved out the modern valley, but this process occurred essentially within confinements of the ancestral valley. Terraces were formed as the river incised within the ancestral valley over several phases until about 13,000 years BP at which time infilling of the valley bottom occurred with alluvium material for a second time, but with significantly less deposition (Klassen, 1972).

The geological activities have created a trench-shaped valley where the Assiniboine River is underfit and meanders within the wider ancestral valley. The valley is generally between 50 to 85 m deep and 250 to 450 m across. The walls are mainly cut into bedrock. Bedrock at the two research sites is from the Millwood geological member within the Riding Mountain Formation from the Upper Cretaceous period and consists of greenish grey bentonitic clay shale (Klassen, 1966:Map). The surficial geology along the valley walls consists of undifferentiated deposits of glacial drift, colluvium and alluvium (Klassen, 1979:Map).

The Assiniboine valley in the vicinity of the research sites is prone to landslides of the valley walls due to the nature of the geology of the area and the geometry of the valley. The Assiniboine valley walls are visually scarred with historical landslides, and active landslides still occur within the valley. Steeper sections of the valley walls where bentonitic shales (Millwood member) are present along or near the valley wall are particularly susceptible to landslide failures, especially following significant rainfall events. Bentonitic clay shale is a highly sensitive material in terms of shear strength of the material. The shear strength of bentonitic clay shales varies significantly with changes

in moisture conditions, weathering and overburden pressure and the material can exhibit low strengths under certain conditions.

The bentonitic shales are well-known to be problematic and have been attributed to many landslide failures within the Assiniboine River Valley between and near the two valley sites (Klassen, 1979; Baldwin, 2007; Blatz *et al.*, 2004). The landslides tend to be retrogressive and can have shallower slides within larger/deeper slump block type movements. Manitoba Infrastructure and Transportation (MIT) has catalogued, monitored, and studied four large landslides affecting highways in the area and these failures have also been attributed to the presence of bentonitic shales within the valley walls (Baldwin, 2007).

One of these MIT monitored sites is a large known active landslide area affecting Highway PTH 41 within the community of St-Lazare (Acres Manitoba, 2000), directly north of the research site, on the opposite side of the valley. This landslide has impacted the highway and Canadian National's main rail line since the early 1970s and been studied and monitored by Manitoba Infrastructure and Transportation (Acres Manitoba, 2000).

Rail lines within the valley have also experienced movements attributed to the presence of shales. Three kilometres south of the Harrowby site, landslide activity along Canadian Pacific (CP Rail) main line has affected track performance since the 1980s (Yong, 2003). Clifton Associates have studied this landslide in depth since the mid-1980s and this landslide was the focus of a Masters Thesis by the Yong in 2003 from the University of

Calgary. Remedial works at both sites (MIT and CP) have been implemented with mixed success.

The major advantage of the Harrowby and St-Lazare sites are the sites are relatively accessible when compared to other high-risk sites examined within the Assiniboine Valley. As with Plum River, the gas pipeline river crossing at St-Lazare was scheduled to be replaced following instrumentation installation which provided an opportunity to measure any release in pipe strains/stresses once the pipeline was abandoned. St-Lazare was also selected because a considerable portion of pipe was to be abandoned and is an ideal location for conducting pipe-push tests. The response of the pipeline after being abandoned (stress release) is discussed in Section 6.3.2 and details of the pipe-push set-up and results are discussed in Section 4.4, and Section 6.4, respectively.

#### 4.2.2.1 St-Lazare Research Site Description

The St-Lazare research site runs along the southern valley wall of Assiniboine River, just south of the town of St-Lazare. The valley wall is approximately 55m high and is sloped at approximately 5.5H:1V (Figure 4-6 and Figure 4-7).

There are several indicators that the valley wall has undergone previous slope movements (landslides) and may still be active at the St-Lazare research site. There are two distinct terraces along the slope which are indicative of large slump block movements (Figure 4-3) and tension cracks were identified outside of Manitoba Hydro's right-of-way in the vicinity of the lower slump block in 2005. There is also visual evidence of creep movements just outside of the right-of-way.

Three test holes were drilled along the valley wall; one near the top of the valley (TH10-02), one near the middle of the valley (TH10-03), and one near the toe (TH10-04) at the locations indicated on Figure 4-3. Soil classification techniques, sampling methods, and laboratory testing undertaken at St-Lazare were consistent with those undertaken at Plum River. The test holes were located in areas best suited for ground and pipe instrumentation to capture pipe stresses due to ground movements. The test holes were drilled within the two terraces (middle and near the top of valley) where ground movements are most likely to occur since they are located within the top horizontal portion of the ancestral slump blocks.

The test holes near the top and bottom of the valley were drilled to depths between 20 to 25 m while the middle test hole was drilled to a depth of 11 m. In general, the soil stratigraphy consists of a thin veneer of topsoil (<0.3 m thick) overlying 6 to 7 m thick silty clay layer (till or colluvium). Clay shale is present below the silty clay to the maximum depth drilled in the test holes. The silty clay contains trace amounts of sand and gravel, brown and grey, moist, stiff to very stiff and of high plasticity. The clay shale is dark grey to black, damp, very stiff, and of high plasticity. The clay shale for the most part is non-cemented (“soil-like”), but two thin layers of cemented shale (“rock-like”) were encountered in the test holes drilled near the top and bottom of the valley wall. Table 4-2 and Table 4-3 summarize the soil properties of the major soil units encountered (silty clay and clay shale) based on laboratory testing. Test hole logs have been prepared and are included in Appendix A.

#### 4.2.2.1 Harrowby Research Site Description

The pipeline at the Harrowby research site runs along the west valley wall of Assiniboine River directly east of the town of Harrowby, Manitoba. The valley wall is approximately 84 m high and is sloped at approximately 6H:1V (Figure 4-8 and Figure 4-9).

The valley wall appears to have undergone retrogressive failures in the past and at least three large slump blocks are easily identified (Figure 4-4). More recent evidence of movement was identified outside of the right-of-way along the lower slump block in 2004. Large storage retention ponds have been constructed within the last 15 years near the crest of the valley wall and additional surcharge weight of the water may be reducing the stability of the valley wall.

Three test holes were drilled along the valley wall; one near the top of the valley (TH10-05), one near the middle of the valley (TH10-06), and one near the toe (TH10-07) at the locations shown on Figure 4-4. The soil classification techniques, sampling methods, and laboratory testing undertaken at Harrowby were consistent with those undertaken at St-Lazare and Plum River. The test holes were drilled within the three terraces (near the bottom, middle and near the top of the valley) where ground movements and larger pipe stresses are most expected to occur being located within the top horizontal portion of the ancestral slump blocks.

The test holes near the top and bottom of the valley were drilled to approximately 30m depth while the middle test hole was drilled to a depth of 11 m. In general, the soil stratigraphy is similar to St-Lazare and consists of a thin veneer of topsoil (<0.3m thick) overlying about 10 m of thick silty clay layer (till or colluvium). Clay shale is present

below the silty clay to the maximum depth drilled in the test holes. The silty clay contains trace amounts of sand and gravel, is brown and grey, moist, soft to stiff and of intermediate to high plasticity. The clay shale is dark grey, very stiff, and of high plasticity. The clay shale is non-cemented (“soil-like”).

The soil stratigraphy at the bottom of valley (TH10-07) differs slightly then the upper portion of the valley. Two clay layers containing varying amounts of organics (including rootlets) were encountered at a depth of 10 m (Elev. 414.1 m) to about a depth of about 17 m (406.9 m). Based on the organic composition of these layers and the elevation it was encountered, which is relatively consistent with the current river elevation, the clay layers with varying amounts of organics are likely alluvial material suspected to be remnants from an old river bed. The clay layers contain trace to with organics, are dark grey, soft to stiff and of high plasticity. Table 4-4 to Table 4-6 summarizes the soil properties of the major soil units (silty clay, clay with varying organics, and clay shale) based on laboratory testing. Test hole logs and are included in Appendix A.

#### *4.2.3 Pipeline Information at the Research Sites*

The pipelines at the research sites consist of thin-walled ( $r/t \leq 10$ ) ductile steel pipe ( $D/t < 70$ ). Therefore, pipe radial stresses can be ignored and the plastic bending moment capacity will govern if buckling occurs. The pipeline properties for each site are included in Table 4.7. The steel pipelines have been operational for 30+ years at Harrowby, and 50+ years at Plum River and St-Lazare. The yield strength varies between 241 MPa for the oldest pipe to 345 MPa for the newest pipe highlighting manufactures



ability to produce better quality steel over the years. The operating pressure varies depending on the service demand which in turn influences the pipe diameter used.

The pipelines were installed using an open cut method where the pipe was installed at a shallow depth (~ 1 m) and backfilled with excavated material which is cohesive in nature for all three sites. The pipeline cover at the valley sites is about  $\pm 1$  m in general while the cover at Plum River is a bit deeper below natural prairie (a couple of meters), increasing in depth towards the river. The ground surface and pipeline profile for the three research sites are plotted on Figures 4-2 to 4-4.

### **4.3 Field Instrumentation and Set-up**

The field instrumentation program was developed to most effectively monitor ground movements, groundwater conditions, pipe strains, and ground/pipe temperatures required to assess the potential sources of stress and overall, the stress-state of the pipeline at the three research sites. A total of 6 temperature gauges, 7 SIs, 10 VW piezometers and 23 strain gauges were installed between the three research sites. Figures 4-10 and 4-11 illustrate the test hole and instrumentation schematic layout of the instrumentation installed at riverbank and valley research sites.

The slope inclinometers (SIs) used were manufactured by DGSI and are 70 mm standard casing. The VW's were also purchased from DGSI and are also standard ~350 kPa (3.5 psi) piezometers. Two types of foil gauges were used from Vishay Technology, a uniaxial foil gauge (WK-06-250bg-350), and a two element torque rosetta (WK-06-125TR-10CW). The soil temperature gauges used are a Campbell Scientific 109B-L soil/water temperature gauge with a range of -50°C to 70°C.

The field instrumentation was installed between August 2010 and May 2012. Instrumentation to measure ground movements (SI) and groundwater levels (VW piezometers) were installed within the test holes drilled in the fall to early winter of 2010 as part of the sub-surface investigation at all three sites. The following year (2011), the majority of strain gauges and temperature gauges were installed on the pipelines at the three research sites between July and September. A set of strain gauges could not be installed within the riverbank at Plum River until 2012 due to high river levels during 2011. Ground monitoring pins were installed at the valley sites in May 2011 following the discovery of the inoperable SIs.

#### *4.3.1 Riverbank Instrumentation Layout (Plum River)*

At Plum River, a single SI (SI-01) was installed within the riverbank instability to measure ground movements and determine the depth to the landslide slip surface. Two vibrating wire piezometers (VW-1A and VW-1B) were attached to the outside of the SI casing. The vibrating wire piezometers were staggered vertically. Staggering the vibrating wire piezometers vertically allows for measurement of the vertical groundwater flow gradients within and below the landslide.

Two sets of three strain gauges were installed on the pipeline; one set was installed on the pipe within the riverbank landslide (referred to as along the slope set-up) while the other was installed beyond the bank crest (referred to as beyond the crest set-up) outside of the riverbank instability (Figure 4-10). Two temperature gauges were also installed beyond the crest; one on the pipeline and one within the soil mass, about 1.2 to 1.5m away from the pipeline at roughly the same elevation as the pipeline. One strain gauge (torsion

gauge) was not successfully attached to the pipe for the beyond the crest setup due the epoxy not properly curing, likely due to excessive moisture (sweating) of the pipe during installation of the strain gauges.

Silty clay soils were encountered at the beyond the crest set-up location which is consistent with the soil stratigraphy at the test hole location.

#### *4.3.2 Valley Instrumentation Layout (Harrowby and St-Lazare)*

The instrumentation at each valley research site included installing three slope inclinometers, four vibrating wire piezometers, three sets of three strain gauges, and three temperature gauges (one on the pipe and two within the soil mass) as shown in Figure 4-11. The SIs near the top and bottom of the valley wall were installed to depths ranging between 20 and 30 m to capture shallow and deep seated ground movements while the SI near the middle of the valley is intended to only capture shallower ground movements (<11 m depth). The VW piezometers were installed in sets of two and attached to the outside of the SI pipe near the top and bottom of the valley. The VW piezometer sets were installed in sets of two, staggered vertically in elevation between the top of and bottom of the valley to measure the groundwater flow regime within the valley wall.

#### *4.3.3 Strain Gauge and Temperature Gauge Set-up*

Foil type gauge strain gauges were used in the research which were physically attached to the pipeline using epoxy glue. Protective casing along the outside of the pipeline, referred to as “yellow jacket”, was cut away and any adhesive, oil or dirt was removed from a

section of pipe prior to attaching the strain gauges to the pipeline. The epoxy was allowed to cure for at least 12 hours under an applied pressure using hose clamps.

Strain gauges were installed in a manner to capture compression, tension, bending along one plane, and torsion. It was assumed that ground movements occurred downslope, parallel to pipeline as shown in Figure 4-12 and the gauges were oriented accordingly based on this assumption. A schematic of the strain gauge layout is illustrated in Figure 4-13 and sketches of the strain gauges used are shown in Figure 4-14. Two uniaxial strain gauges and one torsion strain gauge (two element 45° rosette) were installed as a set per location per site; three locations at the valley sites and two at the riverbank site. Figure 4-15 and Figure 4-16 are photos of installed gauges on a pipeline in the field.

Lead wires were carefully soldered onto the strain gauges (Figure 4-17 Step 1). The strain gauges and the ends of the lead wires were then protected using a using a layered system of Teflon tape, butyl rubber, neoprene rubber covered with aluminium tape (Figure 4-17 Step 2 to 5). A temperature gauge was then installed near the strain gauges. The pipe and instrumentation (strain gauges and temperature gauge) was then wrapped using a shrink sleeve overlapping the yellow jacket and heated to create a water tight seal (Steps 6 and 7).

Temperature gauges were either attached to the pipe with the temperature probe in direct contact with the outside of the pipe or inserted into soil at the same elevation as the pipeline within about 1.2 m to 1.5 m of the pipeline depending on the location of the set-up (Figure 4-10 and Figure 4-11). The temperature gauge on the pipeline measures pipeline temperature changes along with the temperature changes affecting the strain

gauges. This information was used to apply a temperature correction to strain measurements as well as allow for calculations of strains/stresses induced on the pipe due to thermal expansion/contraction (one of the four sources of stresses outlined). The temperature gauge in the soil is intended to determine if the soil mass within the vicinity of the pipeline freezes, possibly applying stresses to the pipeline (one of the four sources of stresses outlined).

#### *4.3.4 Data Acquisition System and Solar Panel Set-Up*

The DA/Solar Panel set-up is essentially the same for all the research sites. Field instrumentation was connected to a data acquisition (DA) system excluding the SIs and ground monitoring pins which are manually read or surveyed. Manitoba Hydro and Campbell Scientific assisted in the layout and programming of the DA system. The DA system was sealed within a fiberglass enclosure with power being supplied through a 12-volt car type battery trickle charged using a 20-watt solar panel and controller (Figure 4-18). The solar panel and enclosure were mounted on steel or aluminium poles and the entire system was grounded to a grounding rod. Lead wires from the instrumentation were fed through flexible conduit to protect the wiring from the elements and wildlife. Data was recorded using a Campbell Scientific CR10X DA system with auxiliary components required to measure vibrating wire piezometers (Vibrating Wire Spectrum Analyzer AVW 200) and for the riverbank set-up, where additional channels (AM16/32 Channel Multiplexer) were required due to the high number of connections. Wiring diagrams and CR10X programs for differing set-ups are included in Appendix B.

#### 4.3.5 Monitoring Pin Installation

At the valley sites, monitoring pins (12.5 mm rebar) were installed at ground surface to measure ground movements by survey due to the SIs becoming inoperable early on. A set of eight pins were installed at each of the valley sites on May 31, 2011 with an additional 7 pins and 14 pins installed at St-Lazare and Harrowby, respectively on September 15, 2011 and November 11, 2011. Monitoring pins were concentrated within the vicinity of the terraces along the valley walls where the pipeline instrumentation was to be installed in the future and ground movements are most likely to occur. The initial sets of monitoring pins were installed using RTK GPS survey equipment while the second sets of pins were installed using Total Station survey equipment.

#### 4.4 Abandoned Pipe Push Test (St-Lazare) Set-up

The intent of the pipe push tests is to measure soil-pipe adhesion to determine the adhesion factor,  $\alpha$ , a key parameter in calculating the maximum applied axial pipe load due to the soil backfill before pipe slippage occurs. The benefit of conducting field pipe push test in lieu of a laboratory set-up is measuring directly the soil-adhesion values for a pipeline that has been active for over 50 years in field conditions. The adhesion factor measured during the pipe push test is assumed to be representative for all three research sites. Thus, the maximum axial load to pipe can be easily calculated based on the undrained shear strength of the soil backfill at the research sites contingent on if the pipe push test results are comparable to  $\alpha - S_u$  relationships published in literature (D.G. Honegger Consulting *et al.*, 2009).

A new pipeline river crossing was installed in the summer/fall of 2013 at the St-Lazare research site. The new pipeline river crossing consisted of a 169.3mm diameter steel gas pipe installed using directional drilling techniques near the banks of the Assiniboine River. Figure 4-19 shows the location of the new pipeline in plan and cross-section, the tie in points to the existing gas pipeline and the profile of the existing pipeline. The switch over to the newly installed pipeline occurred in summer of 2015 and about 130 m of existing gas pipelines was abandoned between the two tie points.

Three pipe push tests were conducted on the abandoned pipeline on the north side of the river, between ~STA 1+26 to ~STA 1+43 (Figure 4-19), on the opposite side of the river relative to the St-Lazare research site. The portion of abandoned pipe tested was about 1.5 m below natural ground for all three tests. The pipe tested was asbestos wrapped for the most part, with a short portion of the last section of pipe tested consisting of yellow jacket. Proper safe handling of asbestos was undertaken during the pipe push test in accordance with Manitoba Hydro safety protocols. The soil backfill around the pipe is cohesive consisting of alluvial silt and clay containing trace to some fine sand. The backfill was moist, firm and of intermediate plasticity. Disturbed and relatively undisturbed soil samples (Shelby Tube) were obtained for the soil backfill in around the pipeline. Laboratory soil testing was conducted with a focus on determining the index properties (Atterberg Limit and Grain Size Distribution) and the undrained shear strength of the soil backfill. Undrained shear strength testing was conducted on relatively undisturbed samples, representing *in-situ* conditions and a reconstituted sample which was tested based on a single point Proctor at the moisture content sampled to represent

the undrained shear strength of compacted backfill. Table 4-8 summarizes the soil properties of the alluvial silt and clay from the laboratory testing.

A schematic illustrating the pipe push test set-up is presented in Figure 4-20. The test consisted of excavating and exposing about 3 m of the abandoned pipeline at two locations, leaving a portion of the soil and abandoned pipeline intact between the two excavated pits, referred to as jacking pits. The pipe push test was conducted on the portion of intact ground and pipeline to determine the amount of load required to displace the pipe in its natural state, and in turn, the adhesion value between the pipe and soil can be calculated. The length of intact ground or test length, between the jacking pits varied between 4.4 m and 5.6 m. The slopes of the jacking pits were excavated as steep as possible while still maintaining a safe excavation. After excavation of the jacking pits, about a 1 m to 1.5 m portion of pipe was then cut out at both ends. A fabricated metal bracket with a load cell was attached to one end of the pipe while an extensometer was attached to the other end to measure displacement. Figure 4-21 is photo of the fabricated bracket. The fabricated bracket has a strike plate where an excavator bucket can press against. The strike plate rests against a load cell and is able to move along a set of threaded rods allowing load to be applied to the load cell. The amount the strike plate can move is dictated by a set of nuts that are adjustable. The fabricated bracket is attached to pipe with a 0.3 m deep sleeve that slips over end of the pipe and is fixed using set-screws. A draw wire displacement sensor (extensometer) is attached and fully drawn at the other end of the pipe. An excavator was then used to push on the pipe (Figure 4-22). The excavator was positioned on the portion of intact ground between the two jacking pits, straddling the pipeline and with the excavator bucket on the power side of the boom, the



pipe was pushed in a slow, controlled manner as much as possible. Given the type of equipment used and the manner in which the push tests were conducted, there was likely some component of force that was not necessarily uniaxial acting on the end the abandoned pipe. However, this force is assumed not be significant enough to affect the validity of the test. The remaining two push tests were conducted in similar manner. Results of the pipe push tests are discussed in Section 6.4.

A Vishay Technology 50,000 lbs compression load cell (Model 92,93) and 750 mm range Micro-Epsilon draw wire displacement sensor was used in the tests. Test data was recorded using a Campbell Scientific CR10X DA system. Unfortunately, the extensometer was damaged after being installed for the first push test.

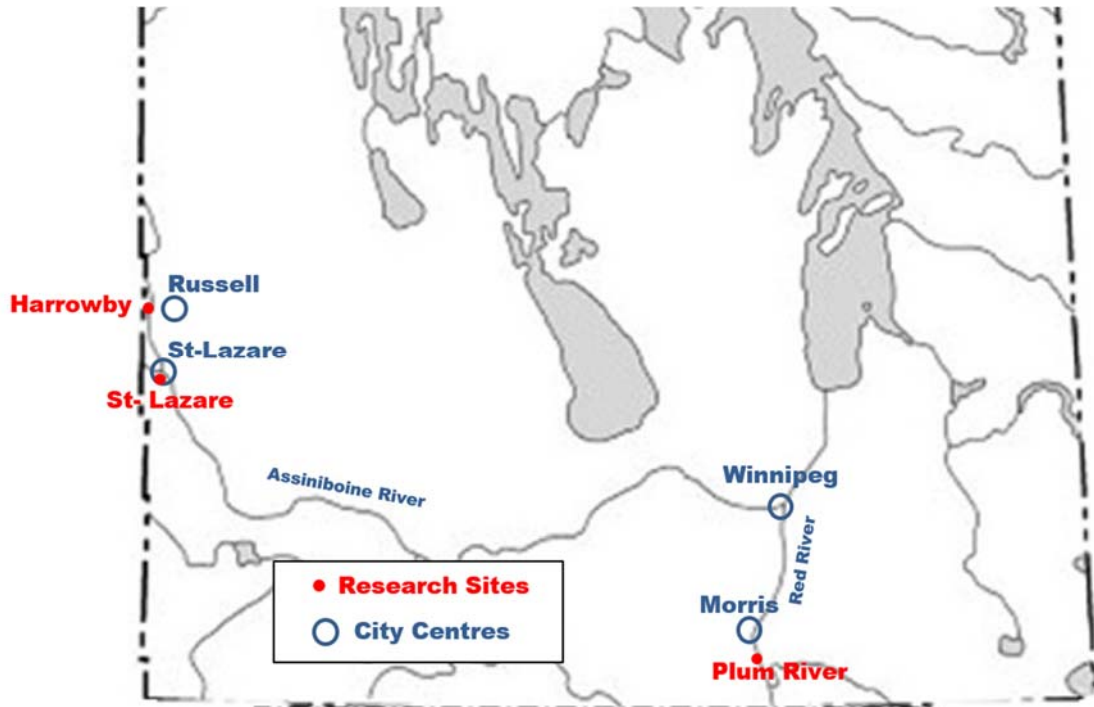


Figure 4-1 Location of Research Sites.

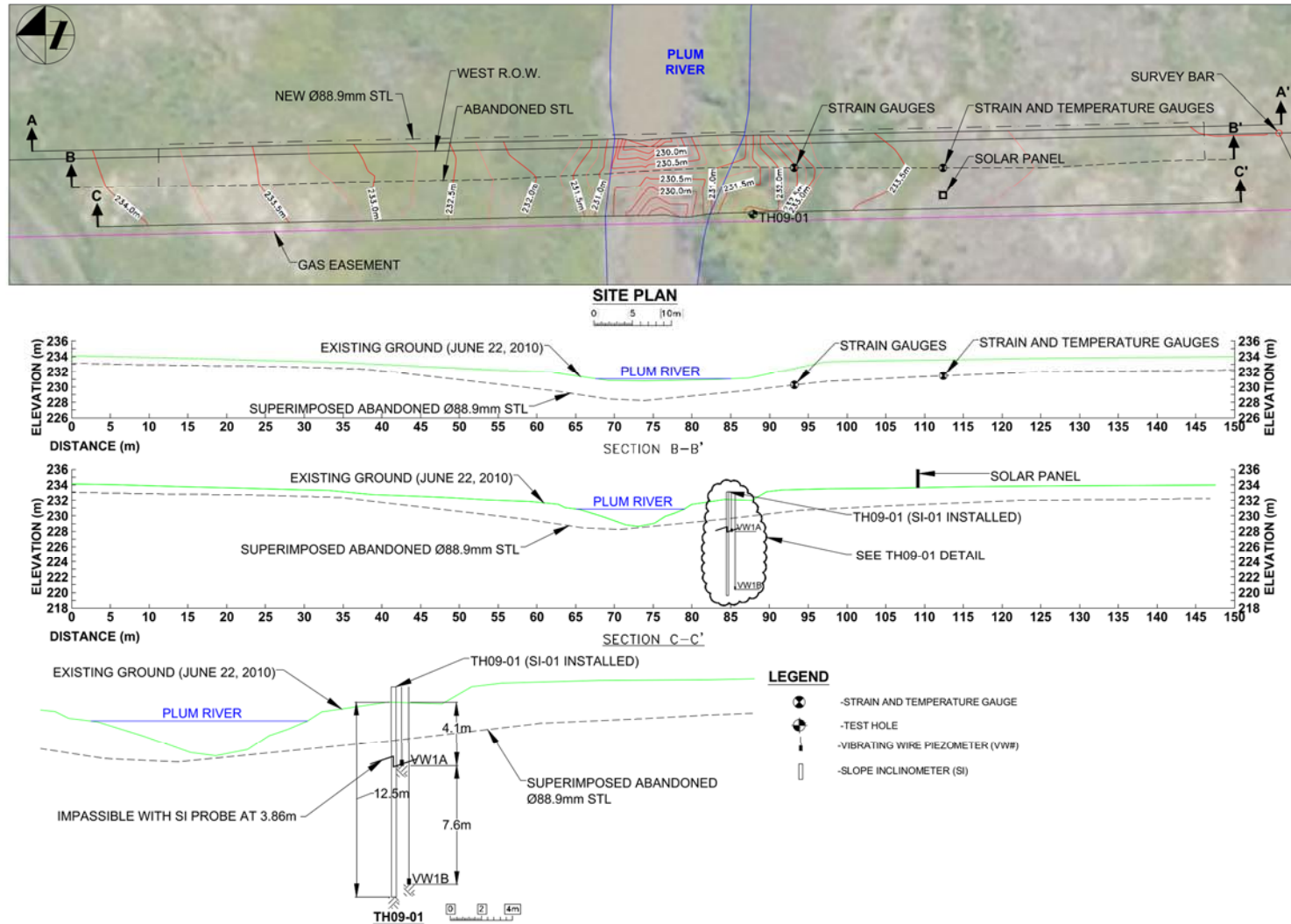
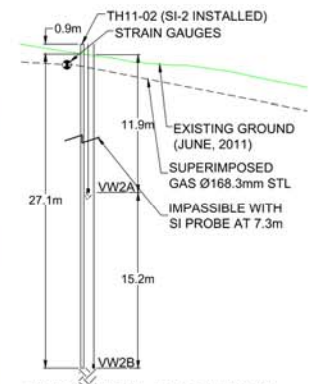
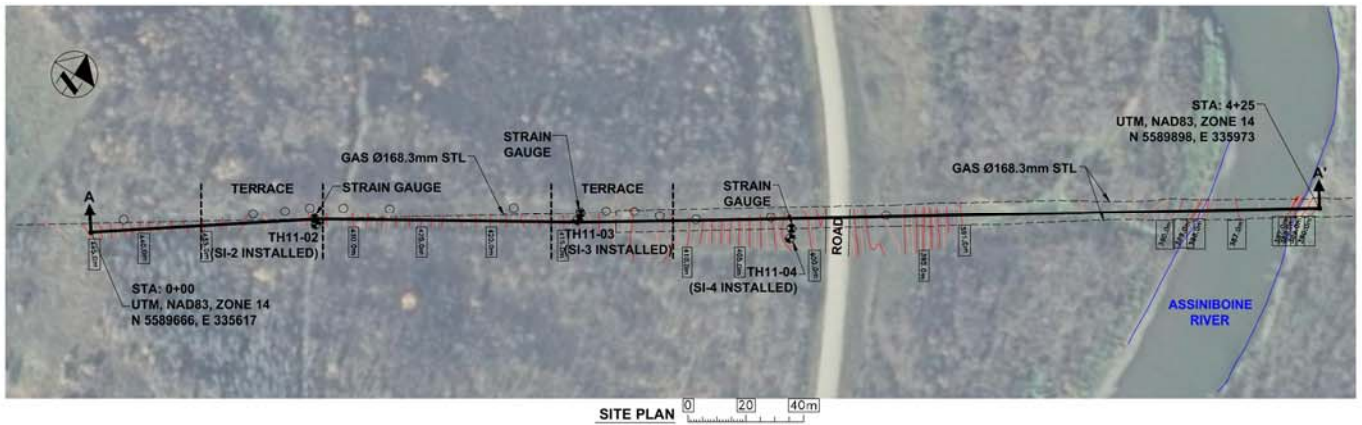
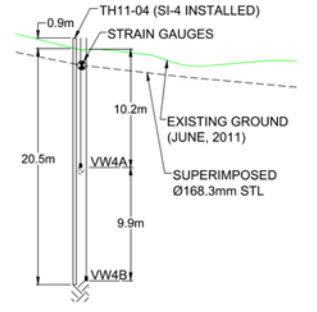
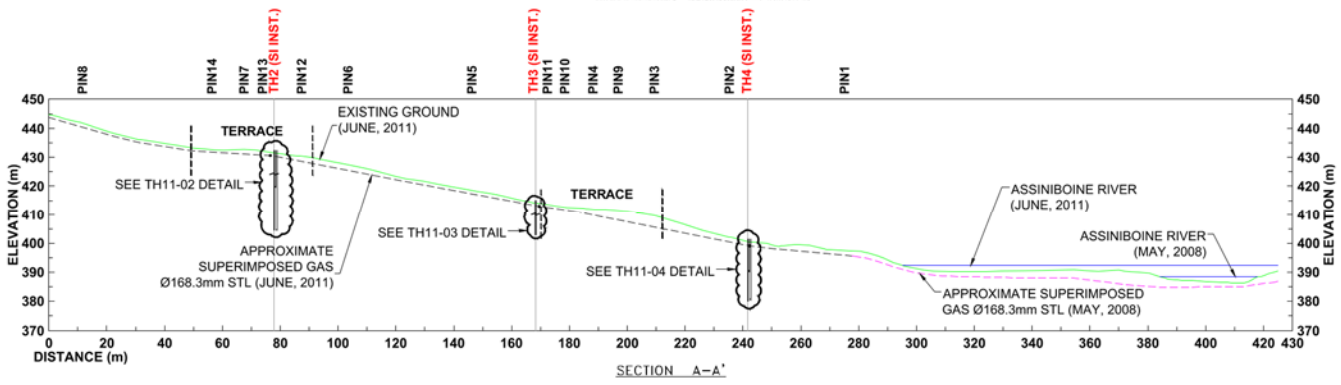


Figure 4-2 Plum River Site Plan and Cross-Section.

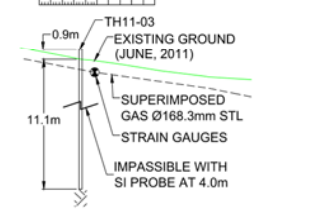


TH11-02 DETAIL - TOP OF VALLEY



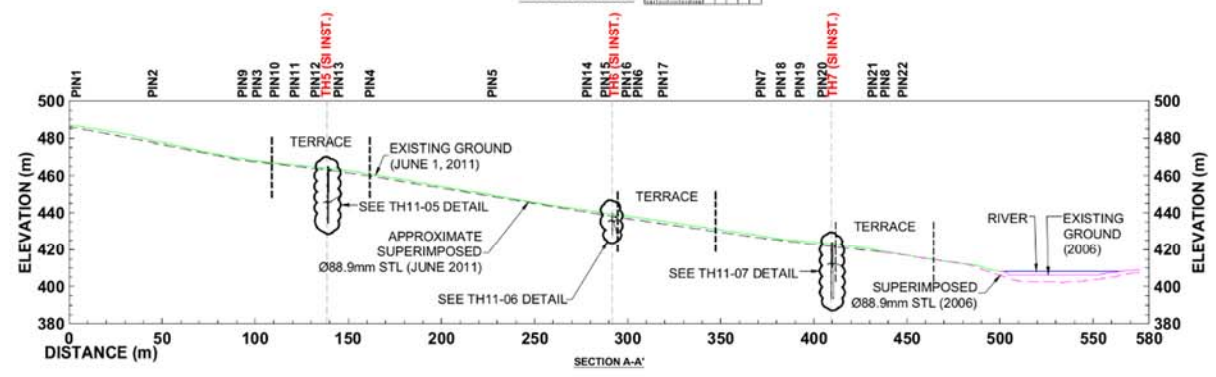
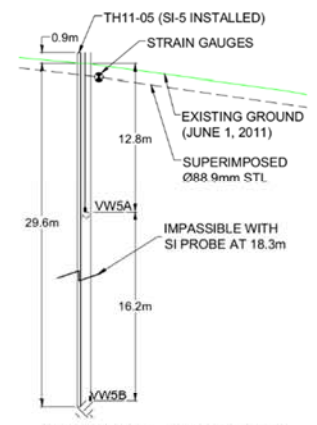
TH11-04 DETAIL - BOTTOM OF VALLEY

- LEGEND**
- TEST HOLE AND SLOPE INCLINOMETER
  - STRAIN GAUGE
  - MONITORING PIN
  - VIBRATING WIRE PIEZOMETER (VW#)
  - SLOPE INCLINOMETER (SI)



TH11-03 DETAIL - MIDDLE OF VALLEY

Figure 4-3 St-Lazare Site Plan and Cross-Section.



- LEGEND**
- STRAIN GAUGES
  - TEST HOLE AND SLOPE INCLINOMETER
  - MONITORING PIN
  - FENCE
  - VIBRATING WIRE PIEZOMETER (VW#)
  - SLOPE INCLINOMETER (SI)

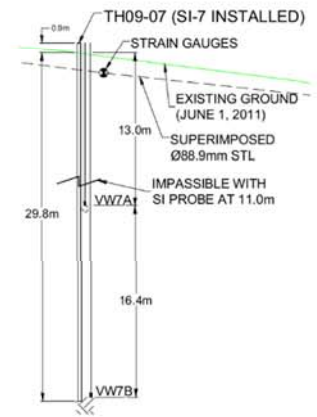
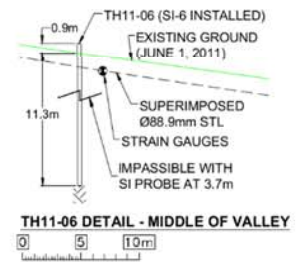


Figure 4-4 Harrowby Site Plan and Cross-Section.





Figure 4-5 – Plum River Riverbank (2009).



Figure 4-6 – St-Lazare Research Site.



Figure 4-7 – St-Lazare Research Site.



Figure 4-8 – Harrowby Research Site.





Figure 4-9– Harrowby Research Site.



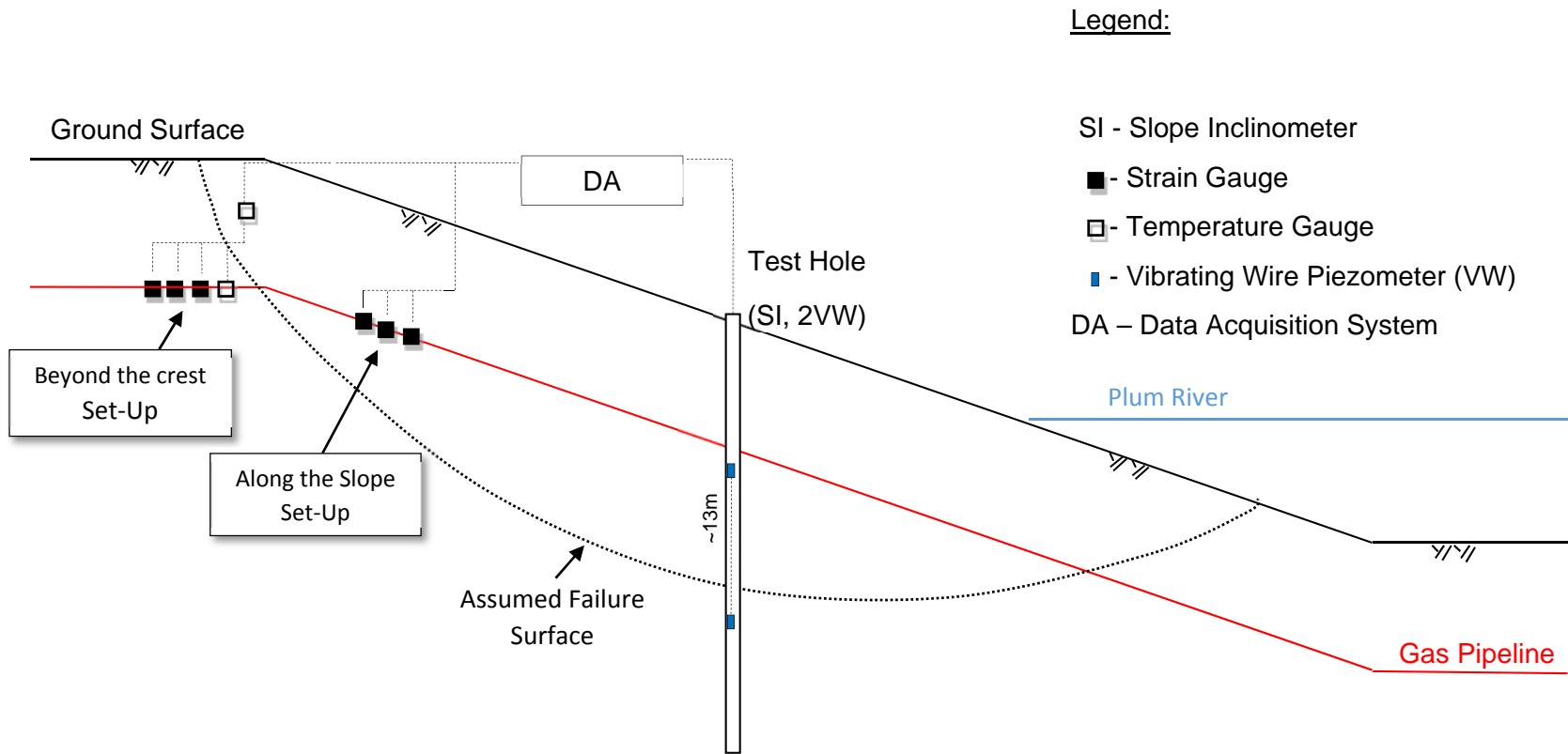


Figure 4-10 Riverbank Site Test Hole and Instrumentation Layout Schematic (Plum River).

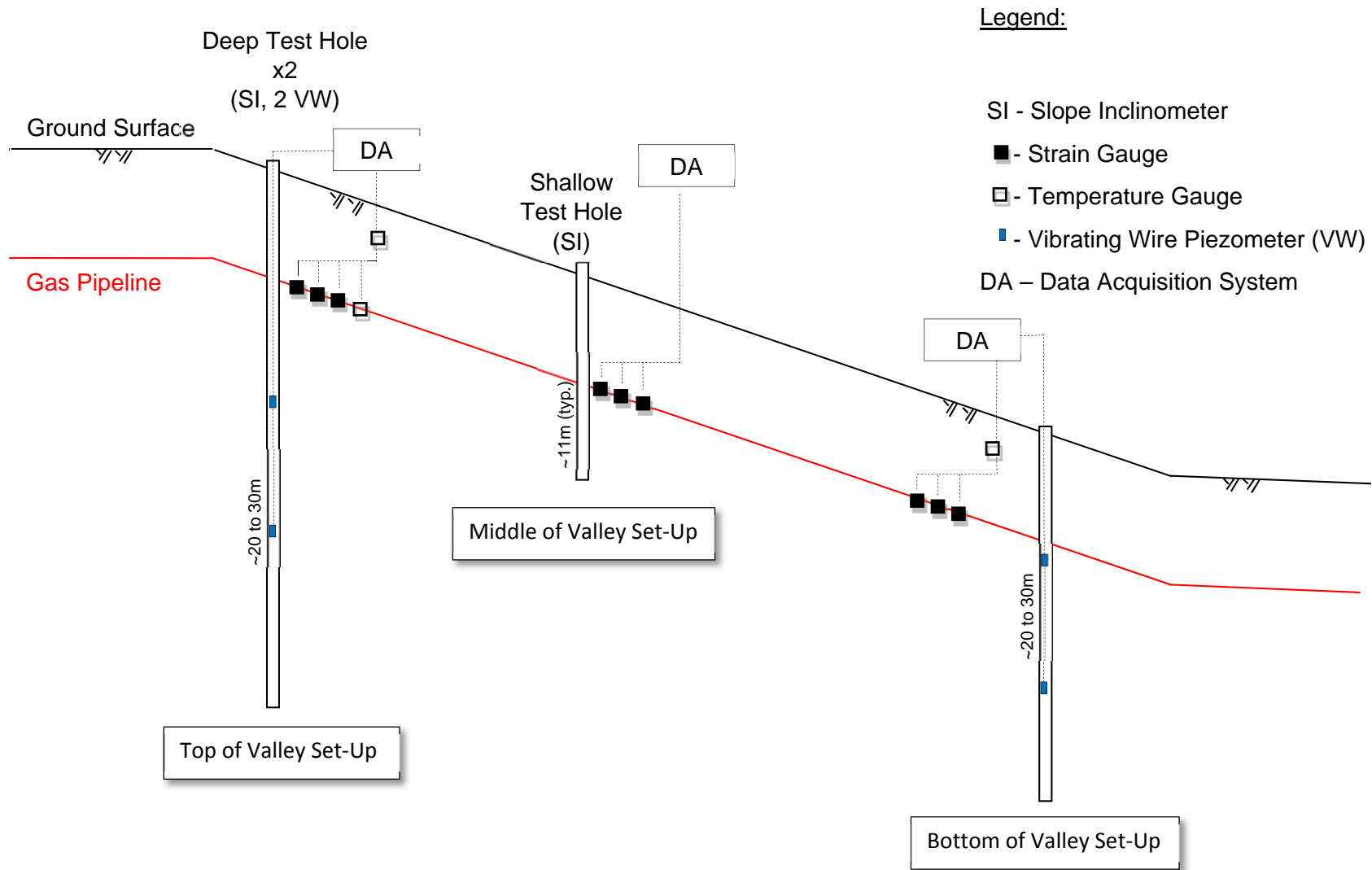


Figure 4-11 Valley Sites Test Hole and Instrumentation Layout Schematic.

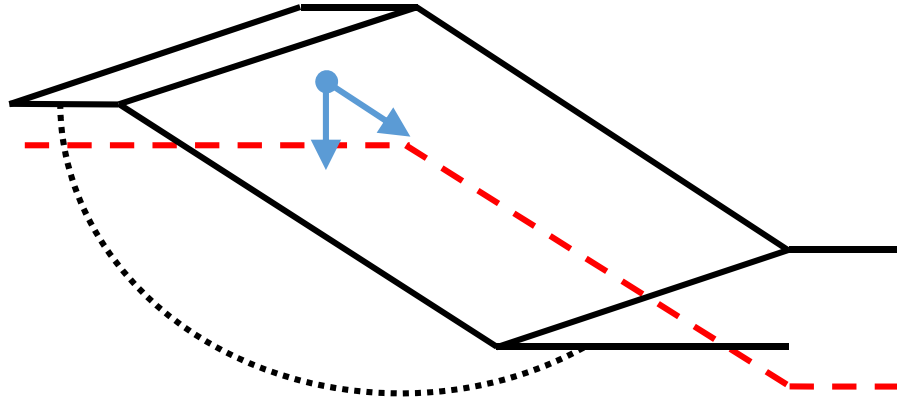


Figure 4-12 Assumed Direction Ground Movement at Research Sites.

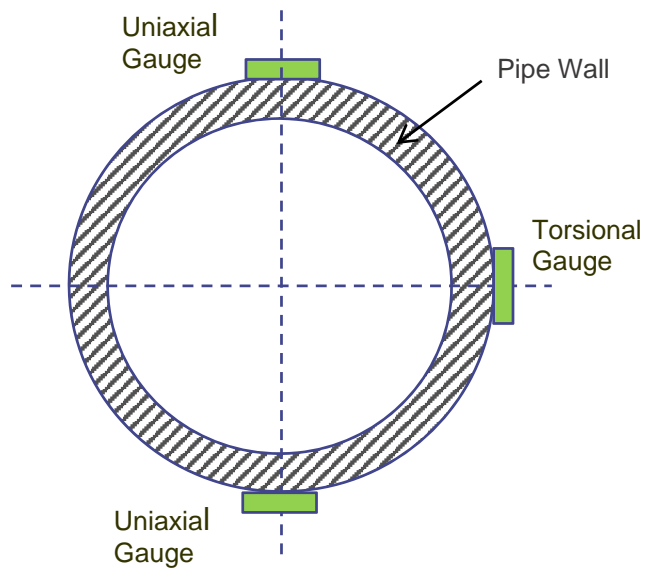


Figure 4-13 Strain Gauge Configuration.

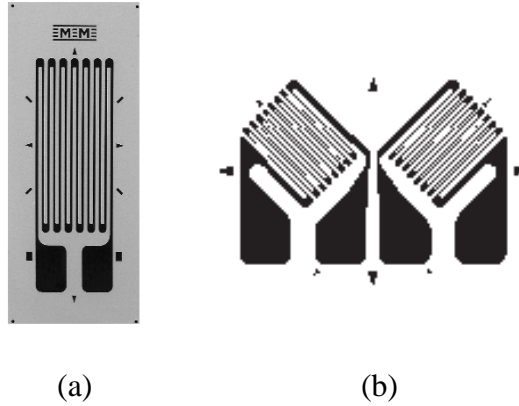


Figure 4-14 Strain Gauges (a) Uniaxial (Vishay WK-06-250bg-350) and (b) Torsional (Torque Vishay WK-06-125TR-10CW).



Figure 4-15 Epoxied Uniaxial Strain Gauge.



Figure 4-16 Epoxied Torsion Strain Gauge



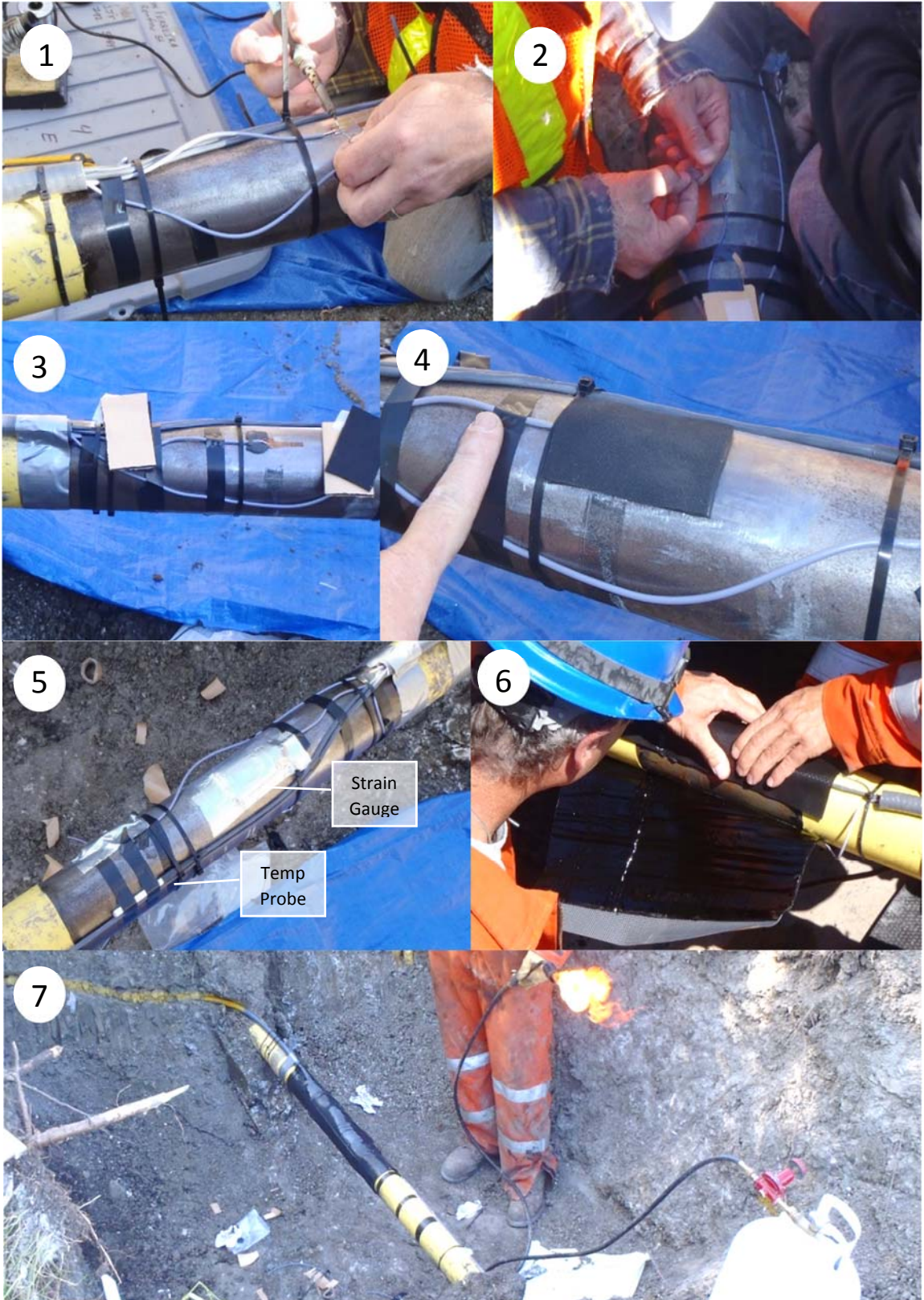


Figure 4-17 Strain Gauge and Pipe Temperature Gauge Installation Sequence.





Figure 4-18 Data Acquisition (DA) System, with auxiliary components and Solar Panel Set-Up.

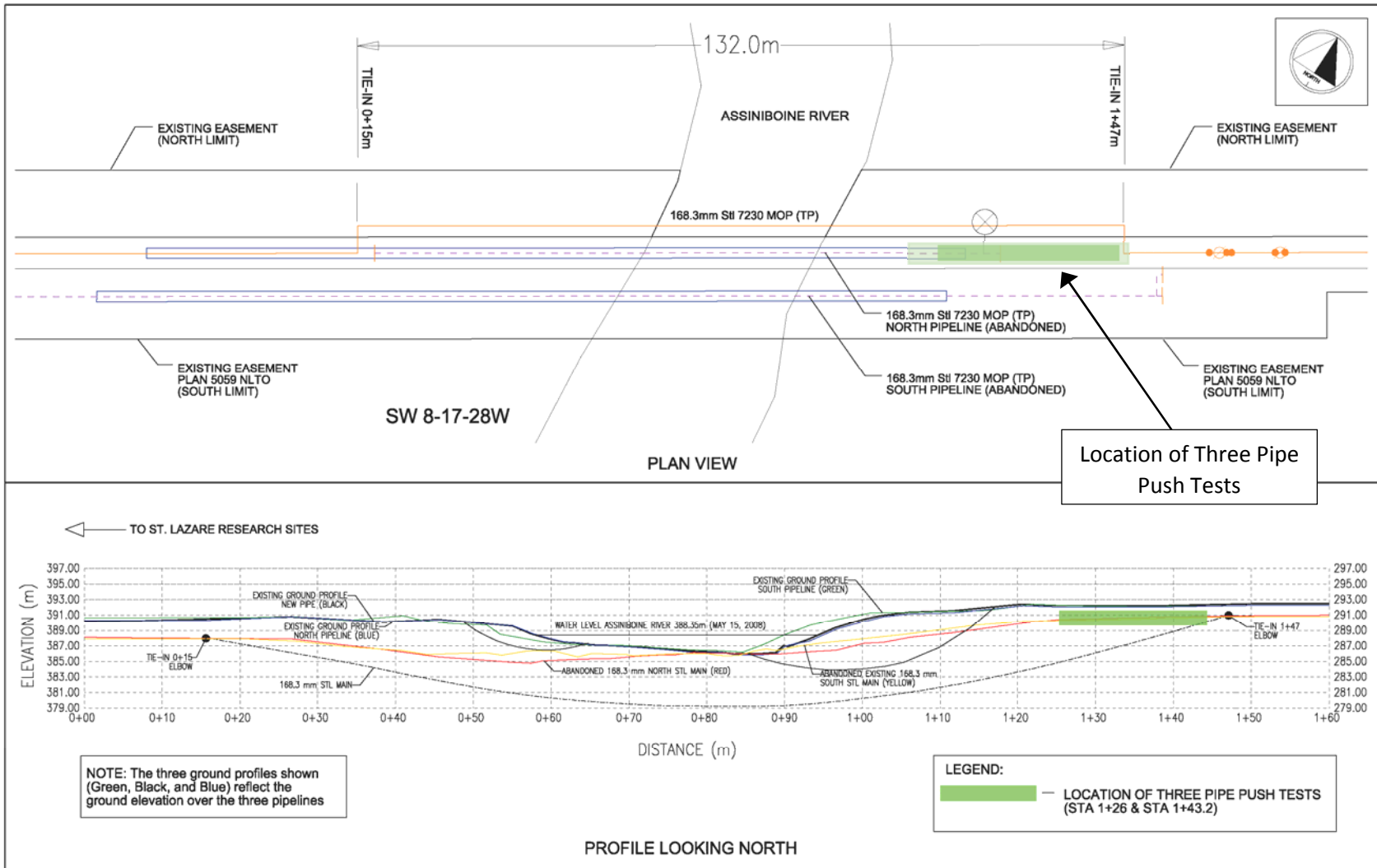


Figure 4-19 Location of Three Pipe Push Tests.



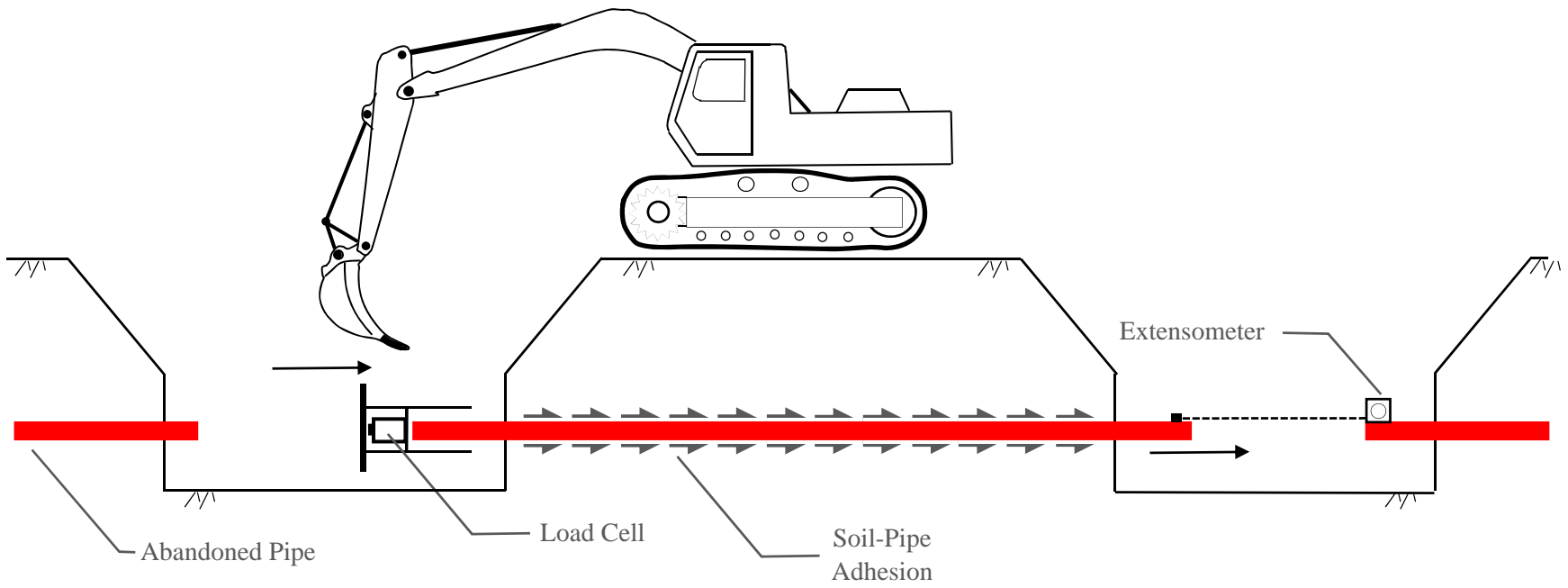


Figure 4-20 Schematic of Pipe Push Test.

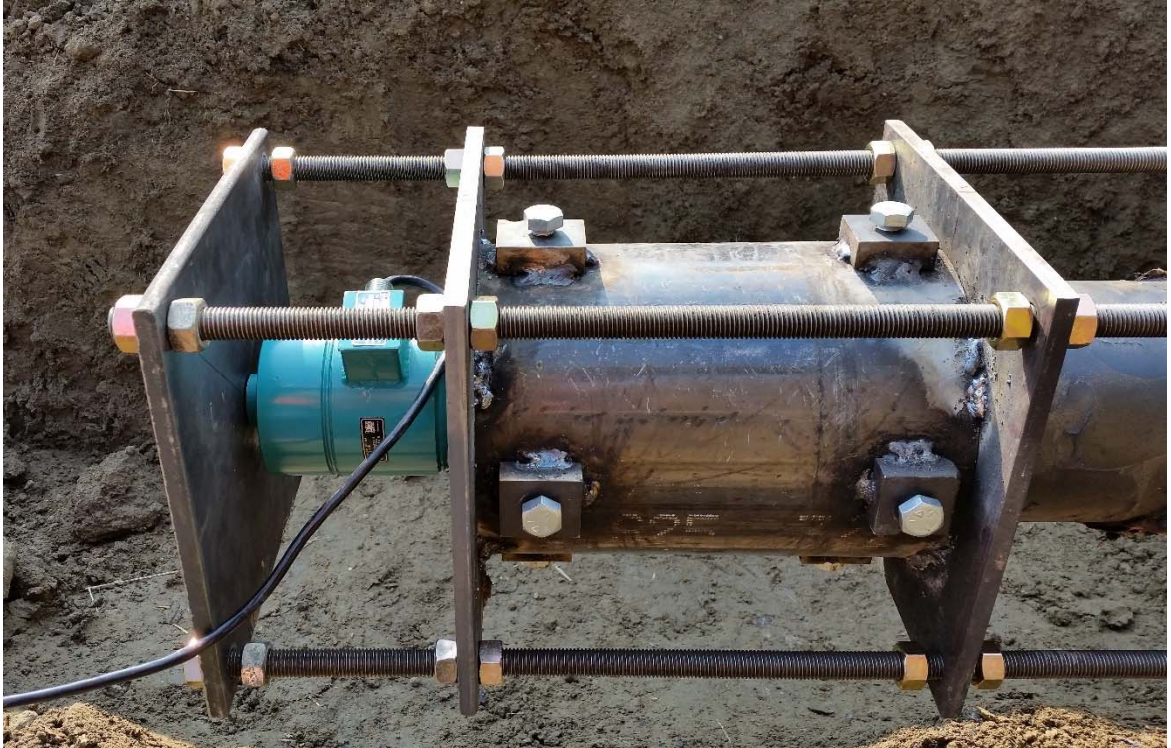


Figure 4-21 Fabricated Strike Plate and Pipe Attachment.



Figure 4-22 Excavator Pushing on Abandoned Pipe.

Table 4-1 Plum River Soil Properties.

Soil Property	Units	Number of Tests	Minimum Value	Maximum Value	Average Value
<b>Lacustrine Clay</b>					
Unit Weight	kN/m <sup>3</sup>	3	16.7	17.3	16.9
Moisture Content	%	15	34.9	51.0	46.0
Undrained Shear Strength <sup>1</sup>	kPa	-	-	-	-
<i>Atterberg Limits</i>		5			
Liquid Limit	LL		74	92	83
Plastic Limit	PL		22	35	27
Plasticity Index	PI		40	67	56
<i>Grain Size Distribution</i>		3			
Clay	%		64	80	73
Silt	%		20	27	36
Sand	%		0	0	0
Gravel	%		0	0	0

<sup>1</sup> – based on unconfined compression tests

Table 4-2 St-Lazare Soil Properties – Silt Clay.

Soil Property	Units	Number of Tests	Minimum Value	Maximum Value	Average Value
<b>Silty Clay</b>					
Unit Weight	kN/m <sup>3</sup>	-	-	-	-
Moisture Content	%	15	27.1	34.0	30.6
Undrained Shear Strength <sup>1</sup>	kPa	-	-	-	-
<i>Atterberg Limits</i>		11			
Liquid Limit	LL		52	81	73
Plastic Limit	PL		22	32	26
Plasticity Index	PI		25	55	34
<i>Grain Size Distribution</i>		11			
Clay	%		45	68	59
Silt	%		31	39	35
Sand	%		0	22	6
Gravel	%		0	0	0

<sup>1</sup> – based on unconfined compression tests

Table 4-3 St-Lazare Soil Properties – Clay Shale.

Soil Property	Units	Number of Tests	Minimum Value	Maximum Value	Average Value
<b>Clay Shale</b>					
Unit Weight	kN/m <sup>3</sup>	-	-	-	-
Moisture Content	%	21	11.0	34.0	23.5
Undrained Shear Strength <sup>1</sup>	kPa	-	-	-	-
<i>Atterberg Limits</i>		7			
Liquid Limit	LL		69	140	99
Plastic Limit	PL		20	23	21
Plasticity Index	PI		56	118	82
<i>Grain Size Distribution</i>		7			
Clay	%		51	73	66
Silt	%		27	42	7
Sand	%		0	7	1
Gravel	%		0	0	0

<sup>1</sup> – based on unconfined compression tests

Table 4-4 Harrowby Soil Properties – Silt Clay.

Soil Property	Units	Number of Tests	Minimum Value	Maximum Value	Average Value
<b>Silty Clay</b>					
Unit Weight	kN/m <sup>3</sup>	3	17.3	18.2	17.9
Moisture Content	%	16	18.0	37.0	30.1
Undrained Shear Strength <sup>1</sup>	kPa	1	-	-	62.7
<i>Atterberg Limits</i>		7			
Liquid Limit	LL		50	70	65
Plastic Limit	PL		18	20	19
Plasticity Index	PI		32	51	46
<i>Grain Size Distribution</i>		7			
Clay	%		38	56	48
Silt	%		30	50	40
Sand	%		7	15	13
Gravel	%		0	0	0

<sup>1</sup> – based on unconfined compression tests

Table 4-5 Harrowby Soil Properties – Silt Clay with Varying Amounts of Organics.

Soil Property	Units	Number of Tests	Minimum Value	Maximum Value	Average Value
<b>Silty Clay (Organics)</b>					
Unit Weight	kN/m <sup>3</sup>	2	18.8	18.9	18.9
Moisture Content	%	6	30.0	63.0	38.2
Undrained Shear Strength <sup>1</sup>	kPa	-	-	-	-
<i>Atterberg Limits</i>		3			
Liquid Limit	LL		55	74	67
Plastic Limit	PL		18	20	19
Plasticity Index	PI		37	54	47
<i>Grain Size Distribution</i>		3			
Clay	%		42	49	47
Silt	%		37	41	39
Sand	%		10	21	14
Gravel	%		0	0	0

<sup>1</sup> – based on unconfined compression tests

Table 4-6 Harrowby Soil Properties – Clay Shale.

Soil Property	Units	Number of Tests	Minimum Value	Maximum Value	Average Value
<b>Clay Shale</b>					
Unit Weight	kN/m <sup>3</sup>	-	-	-	-
Moisture Content	%	18	14.0	42.0	31.1
Undrained Shear Strength <sup>1</sup>	kPa	-	-	-	-
<i>Atterberg Limits</i>		6			
Liquid Limit	LL		48	70	60
Plastic Limit	PL		14	22	18
Plasticity Index	PI		34	51	42
<i>Grain Size Distribution</i>		6			
Clay	%		41	52	47
Silt	%		26	38	33
Sand	%		11	33	20
Gravel	%		0	5	1

<sup>1</sup> – based on unconfined compression tests



Table 4-7 Pipe Information at the Research Sites (based on original specifications).

Site	Date Installed	Diameter	Wall Thickness	Grade (Yield Strength)	Max. Operating Pressure
Plum River	January 1, 1962	88.9 mm	3.17 mm	241 MPa	6070 kPa
St-Lazare	October 5, 1965	168.3 mm	4.78 mm	345 MPa	7230 kPa
Harrowby	August 21, 1982	88.9 mm	3.18 mm	290 MPa	3450 kPa

Table 4-8 St-Lazare Soil Properties – Pipe Push Test Soil Backfill.

Soil Property	Units	# of Tests	Minimum	Maximum	Average
<b>Alluvial Silt and Clay</b>					
Unit Weight	kN/m <sup>3</sup>	3	17.5	17.8	18.1
Moisture Content	%	5	27.6	30.2	33.2
Undrained Shear Strength <sup>1</sup>	kPa	6	41.2	43.4	45
<i>Atterberg Limits</i>		8			
Liquid Limit	LL		36	42.8	47
Plastic Limit	PL		17	18.1	19
Plasticity Index	PI		18	24.6	29

Table 4-8 St-Lazare Soil Properties – Pipe Push Test Soil Backfill (cont'd).

Soil Property	Units	# of Tests	Minimum	Maximum	Average
<i>Grain Size</i>					
<i>Distribution</i>					
		6			
Clay	%		32	34.2	37
Silt	%		50	53.8	61
Sand	%		7	12.2	17
Gravel	%		0	0	0
<b>Reconstituted</b>					
<b>Sample</b>					
Unit Weight	kN/m <sup>3</sup>	1	-	18.8	-
Moisture Content	%	1	-	26	-
Undrained Shear Strength <sup>1</sup>	kPa	1	-	65.8	-

<sup>1</sup> – based on unconfined compression tests

## **Chapter 5 Instrumentation Monitoring Results**

Monitoring of field instrumentation occurred between 2010 and 2015. SIs and ground monitoring pins were monitored several times a year for approximately five years while hourly monitoring of pipe strains, pipe/soil temperatures, and groundwater levels occurred for a duration of approximately four years with about 270,000 hours of monitoring recorded. This chapter discusses the quality of the monitoring data, techniques used to filter poor or noisy data, and presents the monitoring results. The monitoring results are discussed and interpreted in detail in Chapter 6.

### **5.1 Monitoring Disruptions, Instrument Noise, and Equipment Issues**

In general, the instrumentation worked well. Some instrumentation issues were anticipated due to the complexity of the field program and DA system set-up, and the delicate nature of strain gauges. In this regard, the quantity and layout of the instrumentation was developed to provide redundancy in case of instrumentation malfunctions or failure. Table 5-1 summarizes instrumentation issues or disruptions which occurred at the research sites. Terminology used in the table specific to the research includes false readings, unrealistic readings and noise. False readings are readings which are recorded by the DA indicating a bad or poor connection or faulty instrumentation such as a value measured by the DA of -99999. Unrealistic readings are those that are not false, but are improbable due to physical limitations associated with the value measured. An example of this includes anomalous readings which drastically change to show a large strain on the pipe (possibly exceeding the yield capacity of the pipe) with subsequent reading(s) being in-line with measurements before the noise in the

data appeared or in-line with strains and trends measured on other similar gauges (companion uniaxial gauge).

#### *5.1.1 Ground Movement Issues*

One issue that arose during SI monitoring early on that was not anticipated was the magnitude of ground movements at the sites, especially the valley sites. The SI at Plum River became inoperable within two months after installation while 6 of the 7 SIs at the valley sites were inoperable within seven to nine months due to excessive ground movements. The depths at which the SI probe could not pass are indicated within the details on Figures 4-2 to 4-4 and likely coincide to the depths where ground movements are occurring (Table 5-2).

Unfortunately, the valley movements occurred shortly after the SIs were installed during the fall and early winter months and not one round of monitoring was completed before the vast majority SIs were inoperable by the time spring monitoring occurred. The short duration of time for the SIs to become inoperable indicated that the riverbank and valley movements are on-going and ground movements are not limited to creep movements and ground movements are of sufficient magnitude to cause the SIs to become inoperable. This magnitude and rate of ground movement was unexpected at the valley sites as landslide movements were thought to be ancestral and not particularly active.

At the valley sites, monitoring pins (12.5 mm rebar) were installed at ground surface to measure ground movements by survey going forward as further installation of SIs would not be appropriate given the cost in relation to the limited displacement range they can measure. The ground surface method of measurement was deemed an appropriate

alternative to SIs to measure ground movements given the magnitude of movement inferred by the failed SI installations. Although the measurement error per survey event (typically  $< \pm 20$  mm) would not be as precise as an SI (typically  $< \pm 6$  mm), the suspected cumulative magnitude of movements occurring at the valley sites would eventually be larger than the random survey error and with numerous measurements over a long duration, these errors would become less significant and average out over time. Alternative approaches at the Plum River riverbank site were considered for measuring ground movements, but were deemed inappropriate, difficult to implement/maintain, or too costly to be used routinely by Manitoba Hydro in the future to monitor other at-risk sites, which is one of the key considerations of the research.

The first set of ground monitoring pins were installed on May 31, 2011 with additional pins being installed in the fall of 2011 at both valley sites. The initial set of pins were installed using RTK GPS survey equipment (baseline) while the second set of pins were installed using Total Station equipment. Subsequently, five surveys were undertaken using total station survey equipment over the next two years before it was confirmed that there was survey based error in the monitoring results. It is suspected that the total station set-up, methodology and the combination of larger horizontal and vertical distances may be contributing to the errors. This suspicion is based on conversations with experienced surveyors within Manitoba Hydro and industry. Once the survey error was identified, the method of surveying was switched to RTK GPS survey equipment which was used for the remaining monitoring surveys.

### 5.1.2 Data Filtering Techniques

Three types of data filtering were applied to the monitoring data recorded by the DA's either individually or in combination, and are as follows:

- False readings are removed, omitted from the data set
- Filtering of unrealistic data (truncated from data based on a specific value or omitted using statistics)
- A digital filter is used to remove noise

False readings were simply manually removed from the raw monitoring data recorded using the DA's. Filtering of unrealistic data varied depending on the type of data measured and the noise in the data. For example, uniaxial strain gauge measurements with unrealistic data were typically removed based on a specific loading condition, as those readings would result in pipe loading switching from tension to compression or from downward pipe bending to upward pipe bending. A pipe switching from tension to compression over short durations (hours) and back again is considered to be unrealistic especially when the other companion uniaxial gauge does not exhibit similar behaviour or trends. Torsion gauges tended to have the most noise and readings that were greater than the shear stress yield of the pipe member ( $\sim 0.577F_y$ ) were considered to be unrealistic as shear stress yielding due to torsion is unlikely since buried pipelines typically do not yield in this manner.

Another form of unrealistic data is data which oscillates significantly between hourly readings. Measured pipe loading is generally cumulative and sustained until additional loading occurs or the pipe distorts or displaces. Sudden increases and decreases and back

again in loading (or temperature changes) are questionable. This is especially true over a short duration. Oscillating data is considered unrealistic when the difference between hourly readings is significantly large to a point where the change between readings makes the legitimacy of the data improbable. This type of unrealistic data was filtered from the data set using statistics to determine improbable differences between hourly data.

For oscillating data, the 68-95-99.7 empirical rule (Ang, and Tang, 2007) was used to remove data which exceed a specified confidence level based on the standard deviation of the difference between hourly readings. The standard deviation was calculated on the difference between hourly readings for a data set before the noisy readings occurred to represent true data if possible, otherwise the standard deviation was calculated on the entire noisy data set. In some cases, the data set from the companion uniaxial gauge was used to calculate the standard deviation of the difference between hourly readings. A standard deviation of  $\pm 3\sigma$ , was used to filter unrealistic readings from a noisy data set. This results in a confidence of level of 99.7, meaning there is a 99.7% chance that the difference in data measured back to back is within  $\pm 3\sigma$  of the mean difference in hourly readings for the entire data set. A difference in hourly readings which exceeded  $\pm 3\sigma$ , or a 0.3% chance of representing real data, was filtered out. This filtering approach results in the removal of data where extreme changes between hourly data occurs.

#### 5.1.2.1 Digital Filters

Some data sets still contained noise after false and unrealistic data were removed and furthering filtering was required to produce usable data. For these cases, a digital filter was used to distinguish true signal from random or systematic noise. While digital filters

can reveal the true signal by attenuating noise that obscures the true signal, digital filters can also distort the true signal by altering or eliminating important data. In this regard, selecting the appropriate digital filtering technique is key to maximizing the amount of noise filtered from the data without compromising true data. A measured data set with noise can be expressed as follows:

$$x = \hat{x} + e \quad \text{eq. 5.1}$$

Where:

$x$  = the measured or recorded signal

$\hat{x}$  = is the true signal of interest

$e$  = error or noise introduced into the recorded signal

Digital filters use mathematical procedures that are applied to digital data with four basic types of filters: low pass, high pass, band-pass and band-stop. Low pass filter assumes the true signal occupies the lower end of the frequency and data noise is usually in the higher frequency with overlap between the two as shown in Figure 5-1 (Winter, 2009). The aim of a low pass filter is to selectively accept or reject certain frequencies. Figure 5-2 presents the application of a hypothetical low and high frequency filter to a data set to illustrate how the differences in frequency affects the amount of true data and noise captured by the outcome of the filters.

A Butterworth filter is a type of low pass filter, which is basically a sophisticated moving average filter. It is commonly used in biomechanics which use instruments to measure



acceleration, force signals from transducers or from Electromyography (EMG) recording devices which measure low volt signals (0.1–2000 mV amplitude) from muscle response. These types of measurements are also common to this thesis research and therefore, a Butterworth filter was used to filter noise in the recorded monitored data. A Butterworth filter is a recursive digital filter where the output data is a weighted version of the immediate and past raw data with also a weighted contribution of past filtered data (Winter, 2009). A recursive 2<sup>nd</sup> order digital filter is as follows:

$$x'_n = a_0x_n + a_1x_{n-1} + a_2x_{n-2} + b_1x'_{n-1} + b_2x'_{n-2} \quad \text{eq. 5.2}$$

Where:

$x'_n$  = filtered output data

$x$  = unfiltered (raw) input data

$n$  =  $n^{th}$  sample

$n - 1$  = 1 sample before  $n$

$n - 2$  = 2 samples before  $n$

$a_0, \dots, b_0, \dots$  = filter coefficients

The filter coefficients are constants which vary depending on the type digital filter, their order within the filter, and the ratio of the sampling frequency to a cut-off frequency value. The following is used to calculate the filter coefficients for a Butterworth digital filter:

$$\omega_c = \frac{(\tan(\pi f_c/f_s))}{C}$$

Where C is a correction factor depending on the number of times the data set is passed through the filter,  $C = (2^{1/2n} - 1)^{0.25}$ . C equals unity (1) for a single pass and 0.802 for a second pass.

$$K_1 = \sqrt{2}\omega_c, \quad K_2 = \omega_c^2, \quad a_o = \frac{K_2}{(1 + K_1 + K_2)}, \quad a_1 = 2a_o, \quad a_2 = a_o$$

$$K_3 = \frac{2a_o}{K_2}, \quad b_1 = -2a_o + K_3, \quad b_2 = 1 - 2a_o - K_3,$$

The sampling frequency,  $f_s$ , is either known or assumed while the cut-off frequency,  $f_c$ , is related to the amount that the data set is attenuated and is selected based on a desired outcome of the filtering processes.

Reverting back to Figure 5-1, the filter response is the ratio of the filter output data,  $X_o(f)$  over its input data,  $X_i(f)$  at each frequency present (Winter, 2009). A filter response of 1.0 means the input signal (raw data) passes through the filter unaltered or is commonly termed as unattenuated. There is a point at which the filter response has a sharp transition referred to as the cut-off frequency,  $f_c$ . Signals above the cut-off frequency are severely attenuated as illustrated in Figure 5-1. The resulting filter output associated based on a selected cut-off frequency is illustrated in Figure 5-1 (c).

There are several ways to determine the optimal cut-off frequency such as harmonic analysis, using second order derivatives (Yu *et al*, 1999) or residual analysis (Winter 2009). The residual analysis calculates a form of the mean square error for different cut-

off frequencies based on the filtered and unfiltered data and uses a graphical method to determine the optimal cut-off frequency. The residual for any cut-off frequency is calculated using the following equation:

$$R(f_c) = \sqrt{\frac{1}{N} \sum_{i=1}^N (x_i - x'_i)^2} \quad \text{eq. 5.3}$$

Where:

$R(f_c)$  = residual value for a specific cut-off frequency

$x_i$  = unfiltered (raw) data at the  $i$ th sample

$x'_i$  = Butterworth filtered data at the  $i$ th sample

$N$  = number of sample points

The residual values at different cut-off frequencies are plotted as shown on Figure 5-3. The  $d-e$  line on the graph represents the best estimate of the residual noise and this line is drawn until it intercepts the  $y$ -axis, at  $a$ . Above the dashed line  $a-d-e$ , signal (data altering) distortion is introduced into the filter as the cut-off frequency,  $f_c$ , decreases. A decision on the location of the optimal cut-off frequency,  $f'_c$ , is required taking into consideration the amount of signal distortion and noise desired to be allowed through the filter. A straight line is projected from  $a$  until it intersects the residual line at  $b$  and the corresponding frequency at  $b$  is the optimal cut-off frequency for an equal amount of signal distortion and noise allowed to pass through the filter. The signal distortion and noise allowed through the filter is represented by  $b-c$ .

A Butterworth filter produces a phase shift of the output filtered data relative to the raw input data. The phase shift is about 90° forward or graphically to the right of the plotted data. The phase shift can be cancelled out by filtering the data again, but in the reverse direction. This results in the second time filtered data to shift back 90°, resulting in a zero shift (zero lag). This process is referred to as a fourth order zero lag Butterworth filter. The second pass of the filtering processes requires the correction factor,  $C$  to be introduced into the calculations.

### *5.1.3 Results of Post-Processing of Noisy Monitoring Data*

Noisy monitoring data recorded with the DA systems were post-processed using the three filtering techniques described. Table 5-3 summarizes the monitoring data that was post-processed and the filter techniques applied to noisy data sets. Figure 5-4 and Figure 5-5 are examples of the application of a Butterworth 4<sup>th</sup> order filter applied to noisy torsion gauge data following the noisy data first being filtered for unrealistic data. The filtering of unrealistic data included truncating the data set to be below torsional pipe yield and the difference between hourly monitoring data was limited to three standard deviations of the difference based on the recorded data before noisy data appeared. Monitoring plots showing the raw and filtered data along with residual frequency plots are included in Appendix C. Monitoring results of unfiltered raw data are also included in in Appendix C. The post-processed data is of good quality and is suitable to used in statistical analysis.

## **5.2 Ground Movement Results**

Ground pin monitoring results are illustrated on Figures 5-6 to 5-13. Figure 5-6 and 5-7 show the results of each survey while Figure 5-8 and Figure 5-9 plot the total displacement over the four years of monitoring. A graphic representation of the horizontal pin movements are presented in plan view using vectors (direction and magnitude) of the ground movements to illustrate movements and allows for easy comparison between monitoring events in terms of pins or areas that may be moving more or less than others. The ground movement vectors are magnified by 50 or 100 times for illustration purposes. The figures also include a table with measured downslope movements and differences in elevations between monitoring events for each pin. A summation of the movements is also provided in the table within the figures. Figures 5-10 to Figure 5-13 plots pin ground movements parallel and perpendicular to the pipeline at the both valley sites and the figures do not include Pins 1, 4, 9 and 11 for St-Lazare and Pin 20 from Harrowby since the monitoring results are questionable for these pins as discussed in Section 6.1.

## **5.3 Groundwater Results**

Fluctuations or high ground water levels can negatively impact the stability of natural slopes. Therefore, monitoring of groundwater levels is an important aspect in assessing site conditions and the potential for landslides to occur. In conjunction with SI monitoring, changes in groundwater levels may be directly or strongly linked to landslide movements usually determined through slope stability analysis. With the SIs becoming inoperable, the influence of groundwater conditions on landslide activity cannot be as

easily made with measurements of surficial ground movements. Therefore, the groundwater monitoring data was not used directly to determine the risk to buried gas pipelines as part of this research.

The groundwater monitoring results for the research sites are included Appendix C for completeness. The groundwater data is plotted by geodetic piezometric elevation *versus* time. A schematic of the soil stratigraphy based on test hole information is included on the left hand side of the plot while the tip of the piezometers has been included as the first data point of each series. Pertinent notes have also been included on the plots for clarification and aid in interpretation of the monitoring results.

## **5.4 Temperature Results**

Figures 5-14 to 5-18 plot the ground and pipe temperature monitoring results for the three research sites. The graph plots temperature in degrees Celsius *versus* time.

## **5.5 Strain Gauge Measurements**

### *5.5.1 Laboratory Pipe Tests*

Strain gauge measurements are converted into stresses to determine the stress-state on the pipe. The theoretical Young's modulus of steel pipe is well established, but the actual Young's modulus of manufactured steel may vary depending on the tolerances and quality control established by the manufacturer. Specimens of steel gas pipeline used by Manitoba Hydro were load tested in the lab to confirm the Young's modulus of steel pipe used by Manitoba Hydro. A load frame apparatus at the University of Manitoba

structures lab was used to perform the test with the load frame having the capabilities of measuring load and displacement accurately.

Test specimens were provided by Manitoba Hydro. The test specimens were prepared by cutting the ends of the pipe square at a length twice the diameter. Uniaxial strain gauges were installed in the middle of the specimens to measure axial compression during the load test to confirm the uniaxial strain gauges used in the research are working properly and are consistent with the load frame test results as a validation exercise. The specimens were loaded in nine increments between 5 kN and 200 kN and the load was held at each increment until the strain gauge measurements stabilized.

Originally, only one specimen was tested and the results suggested the Young's modulus was notably lower than the theoretical Young's modulus of steel. It was suspected that the strain gauge measurements had not stabilized at each increment. A second round of testing was undertaken where additional specimens of differing diameters were tested along with the original specimen. Fortunately, two field specimens from a pipe repair near the Harrowby research site (from the other side of the Assiniboine valley) were provided by Manitoba Hydro. The field specimens were taken from a pipeline which was originally installed in the 1960s and would have been exposed to the installed environment for over 50 years. It was suspected that the Young's modulus of existing pipe may be different than the theoretical value which is important to establish in order to properly calculate pipe stresses at the research sites.

The results of the pipe tests are plotted on Figure 5-19. The measured Young's modulus from the specimens were at or near the theoretical value with measurements above and below the theoretical line. These results suggest the theoretical Young's modulus can be

considered an average and therefore was deemed appropriate to be used in determining stresses from measured strain values. The Young's modulus was assumed to be constant (linear elastic) when calculating pipe stresses since specific stress-strain relationship information was not available for the pipelines at the research sites. This is a conservative assumption when calculating yielding and stress based local buckling limit states since pipe stresses will be over predicted for measured strains close to or beyond pipe yield.

### *5.5.2 Calculating Stresses from Strain Gauge Measurements*

Strain gauges are measured using a wheatstone bridge circuit that includes a combination of four gauges (full bridge) wired in a manner to measure changes in strain. Using a complete wheatstone bridge can be impractical and costly (as is the case for this research). Half bridges and quarter bridges are commonly used over a complete wheatstone bridge where a full bridge is not feasible or practical. Half bridge (two active gauges) or quarter bridge (one active gauge) requires fixed resistors (commonly referred to as completion resistors or completion block) to occupy the remaining portion of the wheatstone bridge. An excitation voltage is applied to the wheatstone bridge and the output voltage from the bridge is measured. As strain is applied to the active gauge(s), the resistance of the bridge changes and unbalances the wheatstone bridge which results in a signal output (output voltage). With a known resistance, input and output voltage across a gauge, the strain applied to the gauge can be measured. The uniaxial gauges (one active gauge) require a quarter bridge while the torsion gauge (two active gauges) uses a half bridge to measure strains. The stress and strain calculations for the uniaxial and torsion gauges are as follows:



Uniaxial Gauge Strain and Stress Calculations

**Strain - 1/4 Bridge Calculations:**

$$\frac{V_o}{V_E} = \frac{GF(\varepsilon_o)}{4} \quad \text{eq. 5.4}$$

Where:

$V_o$  = voltage output, volts

$V_E$  = excitation voltage, volts

$GF$  = Gauge Factor

$\varepsilon_o$  = measured strain

**Temperature Corrected Strain:**

$$\varepsilon = \varepsilon_o + \varepsilon_T \quad \text{eq. 5.5}$$

Where:

$\varepsilon$  = temperature corrected strain

$\varepsilon_o$  = measured strain

$\varepsilon_T$  = strain due to temperature change (based on manufacturers formula and measured pipe temperatures)

### **Stress Calculations from Strain:**

$$\sigma = E(\varepsilon) \quad \text{eq. 5.6}$$

Where:

$\sigma$  = stress, MPa

$E$  = Young's modulus of steel, 207 GPa

$\varepsilon$  = temperature corrected strain

### *Torsion Gauge Strain and Stress Calculations*

### **Strain – 1/2 Bridge Calculations:**

$$\frac{V_o}{V_E} = \frac{GF(\varepsilon_o)}{2} \quad \text{eq. 5.7}$$

### **Temperature Corrected Strain:**

No temperature correction is required since the configuration and wiring nulls the effect of temperature changes on the strain gauge rosetta.

### **Shear Stress Calculations:**

$$\tau = \frac{\varepsilon(E)}{1 + \nu} \quad \text{eq. 5.8}$$

Where:

$\tau$  = torque shear stress, MPa

$\varepsilon$  = measured strain

$E$  = Young's modulus of steel, 207 MPa

$\nu$  = poisson's ratio of steel, 0.3

**Torsion Calculations:**

$$T = \tau (S); S = \frac{\pi}{16} \left( \frac{d_o^4 - d_i^4}{d_o} \right) \quad \text{eq. 5.8}$$

Where:

$T$  = shaft torsion, MN per m

$\tau$  = shear stress, MPa

$S$  = section modulus of hollow pipe, m<sup>3</sup>

$d_o$  = outside diameter of pipe, m

$d_i$  = inside diameter of pipe, m

Although pipe stresses or torsion were not directly measured, but are calculated based on measured strains at the research sites, calculated pipe stresses are referred to as monitored or observed pipe stresses in this thesis.

### 5.5.3 *Understanding Raw Strain Gauge Data*

Understanding axial and bending strains (and ultimately the calculated stresses) acting on the pipe based on two uniaxial measurements requires interpretation of the results to ultimately determine the longitudinal stresses acting on the pipe. Figure 5-20 provides illustrations on how to interpret the axial and bending stresses and the behaviour with time based on the strain gauge data. Tension axial forces in the pipe and bending in the downwards direction are assumed to be positive for the sign convention selected. An example plot of the uniaxial strain gauge monitoring stress results are presented in Figure 5-21 and all the strain gauge monitoring results are included in Appendix C. Monitoring results for the torsion gauge are presented as pipe torsion and not shear stress in Appendix C. Pertinent notes have also been included on the monitoring plots for clarification and to aid in interpretation of the monitoring results, in particular where notable or distinct changes in measurements occur, *i.e.* strains.

### 5.5.4 *Axial, Bending and Shear Stress Monitoring Results*

The strain gauge data has been reduced to produce plots of axial, bending and shear stress with time (Figures 5-22 to 5-29). The stresses plotted are absolute stresses measured in the pipe. The axial stresses are calculated by taking the summation of the two uniaxial strain gauges and dividing it by two since each uniaxial gauge measurement includes a component of axial (doubling of measurements). Bending is calculated as the difference between the top and bottom gauges divided by two. For example, if the top strain gauge measures -20 MPa and the bottom gauge measures +10 MPa, the axial and bending components are calculated as follows:

$$Axial = \frac{Bottom\ Gauge\ (+10) + Top\ Gauge\ (-20)}{2} = -5\ MPa$$

$$Bending = \frac{Bottom\ Gauge\ (+10) - Top\ Gauge\ (-20)}{2} = 15\ MPa$$

## 5.6 St-Lazare Pipe Push Test Results

The pipe push test results are summarized in Table 5.4. The table provides details related to the three tests performed along with the calculated force required per meter to exceed the soil-pipe adhesion and the maximum adhesion value measured for each test. Adhesion factors based on undrained strength measurement of the *in-situ* backfill ( $S_u = 43.4$  kPa) and reconstituted compacted backfill ( $S_u = 65.8$  kPa) are also provided in the table. The adhesion factor,  $\alpha$ , is the ratio between soil-pipe adhesion and the undrained shear strength of the soil.

The position of the excavator (straddling the abandoned pipe) may be adding a surcharge load on the pipe during the push tests. A simple finite element analysis was undertaken to estimate the surcharge load at the pipe location due to the excavator. The surcharge was modeled as two ground pressures over the width of each track and the surcharge load at the pipe was calculated using a total stress analysis. A surcharge load of about 10 kPa was calculated based on ground pressure of 42 kPa for the type of excavator used and this magnitude of loading is considered to be relatively small.

Figures 5-30 to 5-32 plot load versus time for the three push tests. The three pipe segments were pushed between 0.25 to 0.38 m resulting in strains between 4.7 to 15.6%. Based on the distance travelled and time to complete the tests, the average loading rate

ranged between 9.9 to 14.3 mm/sec which equates to an average strain rate of 0.22 to 0.40% /sec.

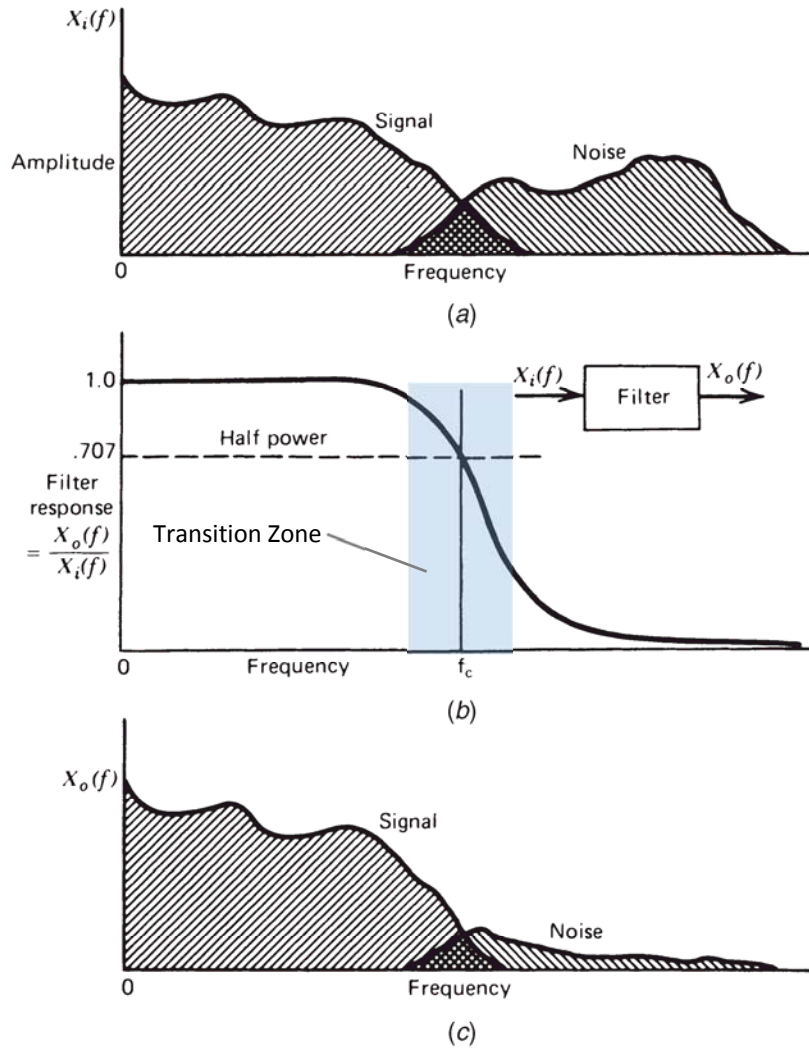


Figure 5-1 (a) Frequency spectrum (hypothetical) of a waveform including desired signal and unwanted higher frequency noise, (b) filter response of low pass filter used to attenuate the noise (c) filter output spectrum where higher frequency noise is severely attenuated while the desired signal is relatively unchanged with only slight distortion in transition zone (modified from Winter 2009).

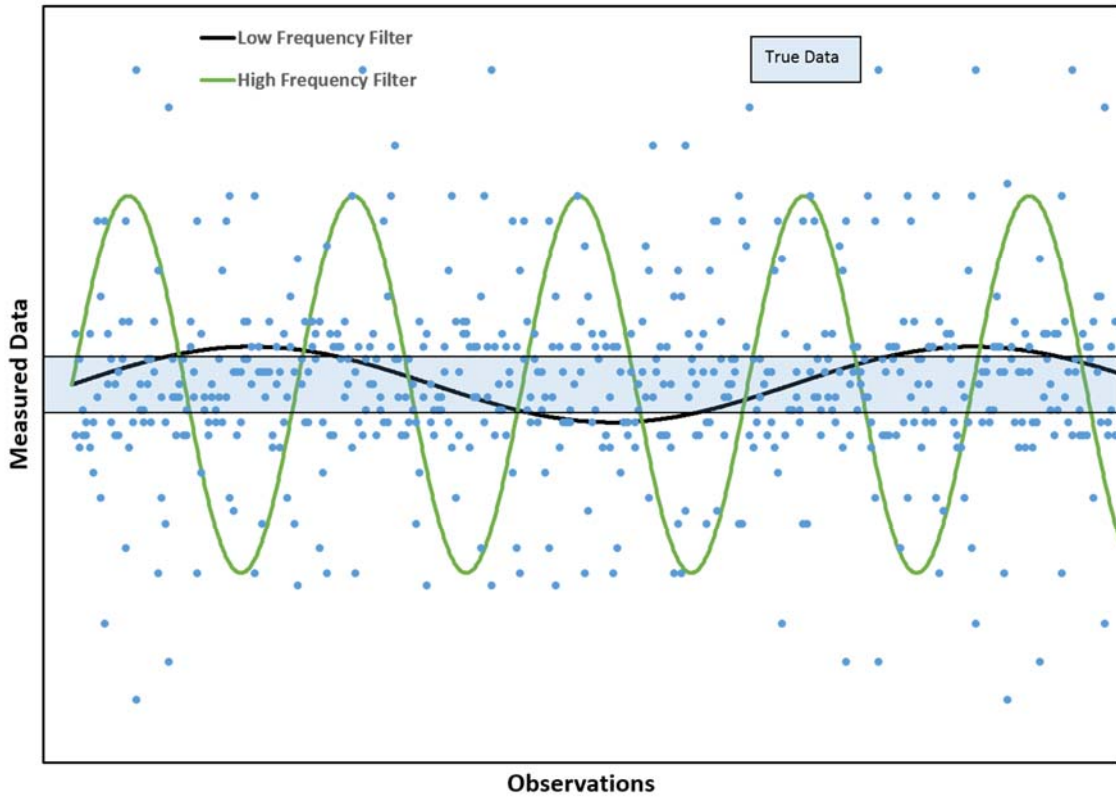


Figure 5-2 Hypothetical Application of Low Frequency and High Frequency Filter to a Data Set.

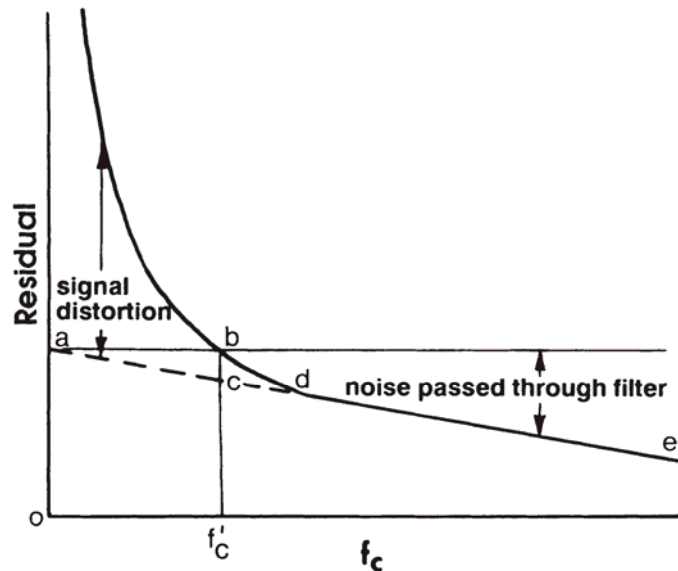


Figure 5-3 Residual Plot vs Cut-off Frequencies Used to Determine Optimal Frequency,  $f'_c$  (Winter 2009).



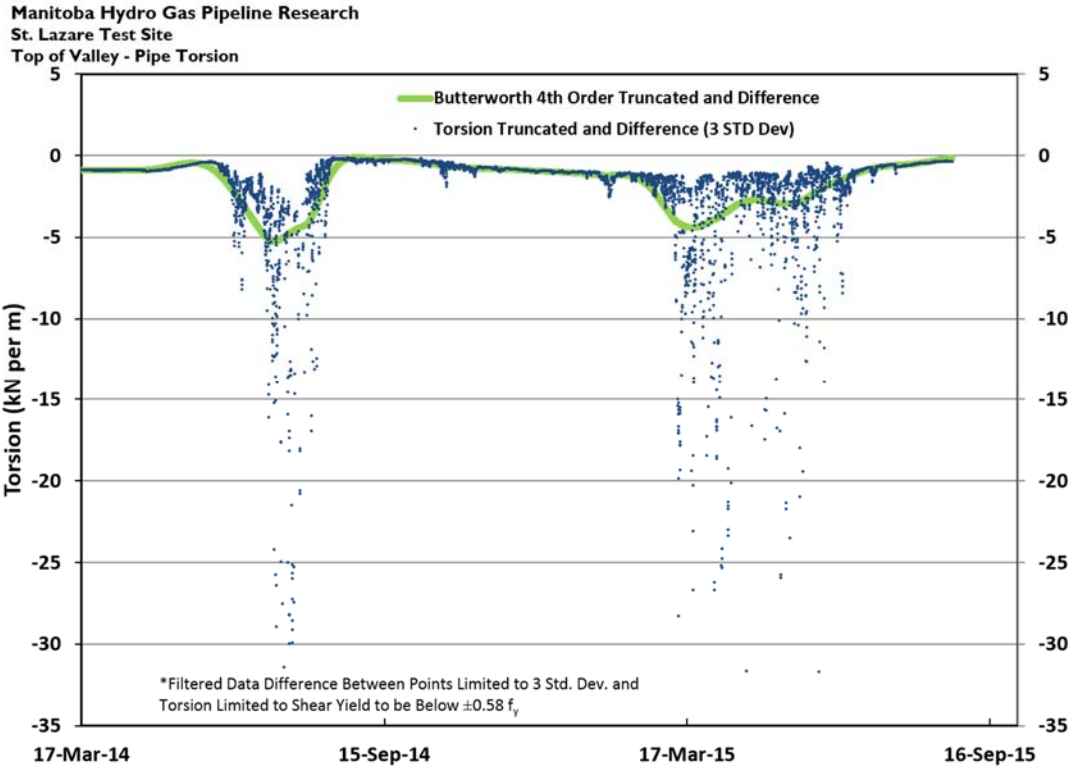


Figure 5-4 Example of Filtered Monitoring Data with a Butterworth Filter.

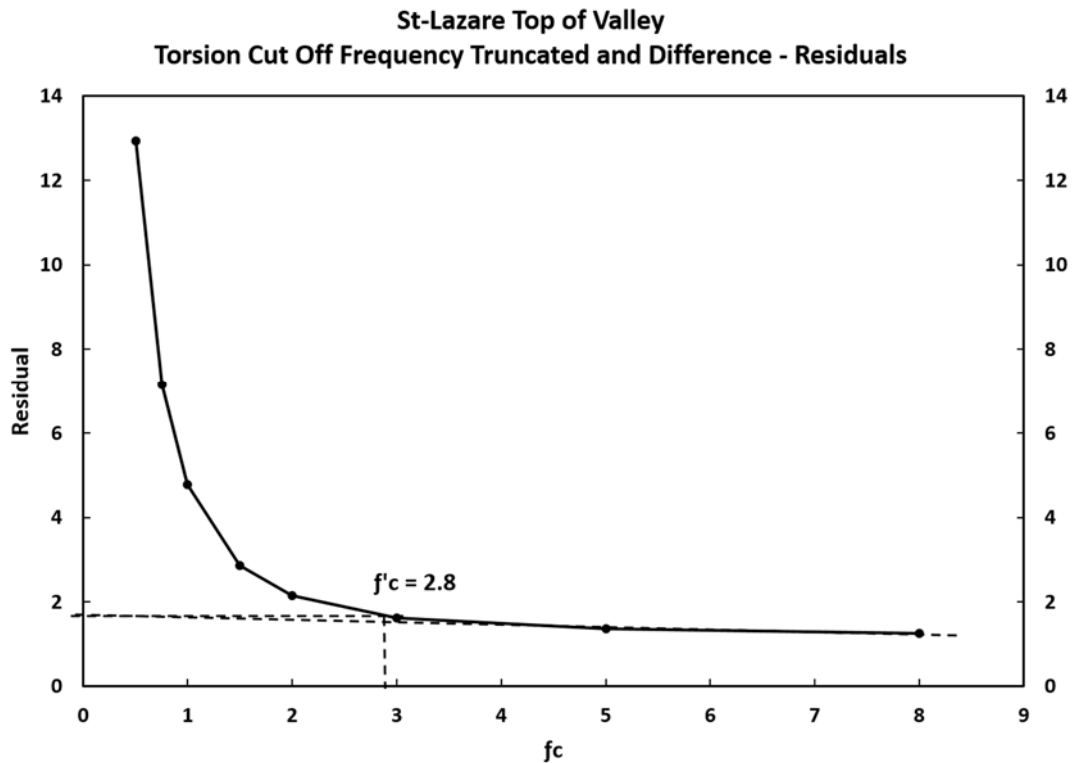
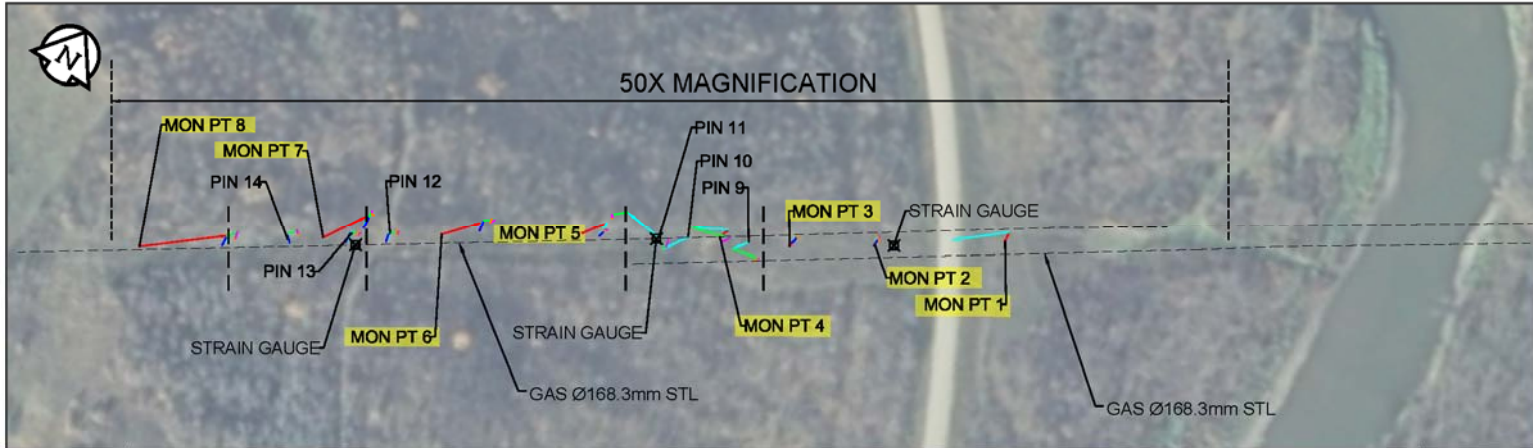


Figure 5-5 Example of Residual Cut-Off Frequency Plot Showing Optimal Frequency.



DOWNSLOPE MOVEMENTS / Δ ELEVATIONS

LEGEND	DATES	MON PT8		PIN 14		MON PT7		PIN 13		PIN 12		MON PT6		MON PT5		PIN 11		PIN 10		MON PT4		PIN 9		MON PT3		MON PT2		MON PT1		
		MOVEMENTS (mm)	Δ ELEVATIONS (mm)	MOVEMENTS (mm)	Δ ELEVATIONS (mm)	MOVEMENTS (mm)	Δ ELEVATIONS (mm)	MOVEMENTS (mm)	Δ ELEVATIONS (mm)	MOVEMENTS (mm)	Δ ELEVATIONS (mm)	MOVEMENTS (mm)	Δ ELEVATIONS (mm)	MOVEMENTS (mm)	Δ ELEVATIONS (mm)	MOVEMENTS (mm)	Δ ELEVATIONS (mm)	MOVEMENTS (mm)	Δ ELEVATIONS (mm)	MOVEMENTS (mm)	Δ ELEVATIONS (mm)	MOVEMENTS (mm)	Δ ELEVATIONS (mm)	MOVEMENTS (mm)	Δ ELEVATIONS (mm)	MOVEMENTS (mm)	Δ ELEVATIONS (mm)	MOVEMENTS (mm)	Δ ELEVATIONS (mm)	
Red diagonal line	MAY 31, 2011 to JUNE 18, 2013	+547.1	-231.0	-	-	+268.3	-52.0	-	-	-	-	+246.7	-34.0	+146.4	-39.0	-	-	-	-	-	+54.7	-6.0	-	-	+41.7	-12.0	+23.5	-1.0	+25.0	-3.0
Cyan diagonal line	JUNE 18, 2013 to OCT 10, 2013	-42.9	+9.0	+10.0	+51.0	-19.8	+5.0	-39.1	+8.0	-24.1	+15.0	-16.9	+28.0	-44.4	-12.0	-191.7	+3.0	-156.4	-31.0	-219.9	-120.0	-98.5	-51.0	-25.8	+19.0	-30.6	+9.0	-347.7	+68.0	
Blue diagonal line	OCT 10, 2013 to MAY 29, 2014	+26.5	-34.0	-14.0	-5.0	+32.4	-13.0	+31.1	+32.0	+17.4	-19.0	+25.6	-22.0	+37.9	+14.0	-	-	-	-	-	-	-	-	-	+34.7	-28.0	+38.8	-10.0	-	
Green diagonal line	MAY 29, 2014 to OCT 07, 2014	+66.3	-19.0	+60.5	-3.0	+18.2	+17.0	+60.1	-27.0	+59.6	-65.0	+68.1	+14.0	+9.9	-15.0	+19.1	+109.0	-4.3	+82.0	+137.8	+131.0	+133.0	+80.0	-11.9	-5.0	-8.9	-28.0	-	-	
Purple diagonal line	OCT 07, 2014 to JUNE 10, 2015	-14.9	+19.0	+5.3	+18.0	-3.5	+2.0	-25.3	-36.0	-11.4	-5.0	-28.0	-25.0	-28.9	+20.0	-0.3	+35.0	-13.1	+21.0	-48.0	0.0	-25.3	-14.0	+17.0	+4.0	+3.9	+34.0	-	-	
Orange diagonal line	JUNE 10, 2015 to SEPT 2, 2015	-0.1	-23.0	+4.4	-40.0	+14.8	-38.0	+12.3	-1.0	0.0	-14.0	+8.9	-3.0	+13.9	-46.0	-0.8	-142.0	-	-	-	-	+17.0	+11.0	-19.5	+8.0	-9.4	-7.0	-	-	
	TOTAL	+582.0	-279.0	+66.2	+21.0	+310.4	-79.0	+39.1	-24.0	+41.5	-88.0	+304.4	-42.0	+134.8	-78.0	-173.7	+5.0	-173.9	+72.0	-75.4	+5.0	+26.2	+26.0	+36.2	-14.0	+17.3	-3.0	-322.7	+65.0	

NOTES:

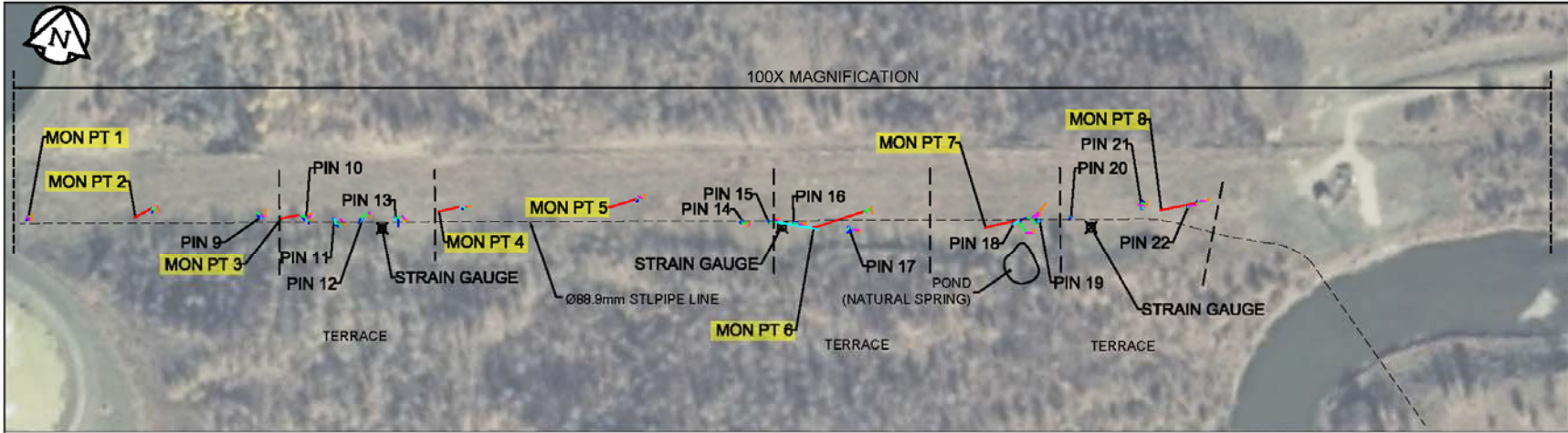
- MON PT1 TO MON PT8 BASELINED (INSTALLED) USING RTK GPS ON MAY 31, 2011
- MON PT9 TO MON PT14 BASELINED (INSTALLED) USING TOTAL STATION ON SEPTEMBER 15, 2011, AND RE-BASELINED (INSTALLED) USING RTK GPS ON JUNE 18, 2013
- MON PT1, MON PT4, PIN 9, PIN 10 AND PIN 11 WERE DESTROYED AND NOTICED DURING MAY 29, 2014 SURVEY PERFORMED
- MON PT4, PIN 9, PIN 10 AND PIN 11 WERE REINSTALLED IN NOVEMBER 2014



LEGEND:

- + DOWNSLOPE MOVEMENT / INCREASE IN ELEVATION
- UPSLOPE MOVEMENT / DECREASE IN ELEVATION

Figure 5-6  
Monitoring Pin Results - May 31, 2011 to September 2, 2015  
St-Lazare, MB



DOWNSLOPE MOVEMENTS / Δ ELEVATIONS

LEGEND	DATES	MON PT1	MON PT2	PIN 9	MON PT3	PIN 10	PIN 11	PIN 12	PIN 13	MON PT4	MON PT5	PIN 14	PIN 15	PIN 16	MON PT6	PIN 17	MON PT7	PIN 18	PIN 19	PIN 20	PIN 21	MON PT8	PIN 22																						
		MOVEMENTS (mm)	Δ ELEVATIONS (mm)	MOVEMENTS (mm)	Δ ELEVATIONS (mm)	MOVEMENTS (mm)	Δ ELEVATIONS (mm)	MOVEMENTS (mm)	Δ ELEVATIONS (mm)	MOVEMENTS (mm)	Δ ELEVATIONS (mm)	MOVEMENTS (mm)	Δ ELEVATIONS (mm)	MOVEMENTS (mm)	Δ ELEVATIONS (mm)	MOVEMENTS (mm)	Δ ELEVATIONS (mm)	MOVEMENTS (mm)	Δ ELEVATIONS (mm)	MOVEMENTS (mm)	Δ ELEVATIONS (mm)	MOVEMENTS (mm)	Δ ELEVATIONS (mm)	MOVEMENTS (mm)	Δ ELEVATIONS (mm)																				
Red line	MAY 31, 2011 to JUNE 18, 2013	+0.3	0.0	+67.3	44.0	-	-	-75.7	-15.0	-	-	-	-	-	-	-	-	-	-	-	-	-	-	-																					
Cyan line	JUNE 18, 2013 to OCT 10, 2013	-8.6	-3.0	-3.2	-10.0	-8.4	-31.0	+13.5	-41.0	+10.1	-10.0	+7.8	-33.0	-14.9	-24.0	+11.5	-40.0	+4.9	-2.0	-5.5	+9.0	-11.0	-27.0	+2.0	-16.0	+12.2	-15.0	+2.4	-32.0	-5.2	-23.0	-3.8	-11.0	+27.7	-10.0	-12.4	-2.0	-6.8	-7.0	+5.1	-14.0	+0.4	-9.0	-2.3	-1.0
Blue line	OCT 10, 2013 to MAY 29, 2014	+15.4	+7.0	+7.4	0.0	-10.2	+6.0	+10.3	+24.0	-0.3	-4.0	+13.6	-13.0	+8.5	+17.0	+2.8	+30.0	+12.0	-3.0	+10.9	+18.0	+10.5	+21.0	+5.5	+12.0	-8.4	+24.0	-7.2	+10.0	+21.6	+21.0	+15.5	+17.0	-1.7	+26.0	-1.8	+1.0	+2.8	+36.0	+10.0	+10.0	-2.5	+8.0	-0.7	+10.0
Green line	MAY 29, 2014 to OCT 07, 2014	-12.6	-39.0	+12.6	-2.0	+16.1	+8.0	+24.4	-1.0	+2.8	+17.0	+1.6	+52.0	-30.2	+20.0	+16.6	-1.0	+5.6	-22.0	+9.2	-7.0	+28.3	+6.0	+19.6	-2.0	+16.9	-28.0	+25.7	+4.0	+2.5	-98.0	+21.4	-43.0	+21.2	-135.0	-16.8	+4.0	-	-	-27.8	-98.0	+15.5	+6.0	+4.1	-2.0
Purple line	OCT 07, 2014 to JUNE 10, 2015	+15.8	-3.0	+2.4	+24.0	+16.2	-15.0	+13.2	+8.0	+10.0	-22.0	+21.6	-39.0	+8.4	-31.0	+18.0	-13	+5.2	-30.0	+18.5	-28.0	-7.0	-21.0	+18.1	-15.0	+25.1	+4.0	+4.7	-25.0	+24.6	-6.0	+29.6	-42.0	+30.2	-24.0	+30.0	+23.0	-	-	+30.6	+28.0	+24.7	-9.0	+33.1	-16.0
Orange line	JUNE 10, 2015 to SEPT 2, 2015	+4.7	+8.0	-7.0	+18.0	+1.4	+26.0	-14.5	-22.0	-6.2	+13.0	-7.2	+13.0	-3.6	+22.0	-4.6	+4.0	+10.4	+23.0	+6.3	+30.0	+1.2	+8.0	-14.1	+13.0	-15.7	+21.0	-3.7	+11.0	-5.0	+1.0	-4.9	-4.0	-2.1	+13.0	+22.8	+9.0	-	-	+4.0	-3.0	+10.0	+6.0	-3.0	+9.0
	TOTAL	+15.0	-30.0	+78.7	-62.0	+15.1	-6.0	+102.0	-47.0	+16.4	-6.0	+37.4	-20.0	+28.6	+4.0	+38.7	-20.0	+120.4	+9.0	+134.4	0.0	+22.0	-13.0	+31.1	-8.0	+30.1	+6.0	+221.8	-44.0	+38.5	-105.0	+207.6	-159.0	+75.5	-130.0	+21.8	+35.0	-4.0	+29.0	+19.9	-77.0	+183.5	-58.0	+31.2	0.0

**NOTES:**

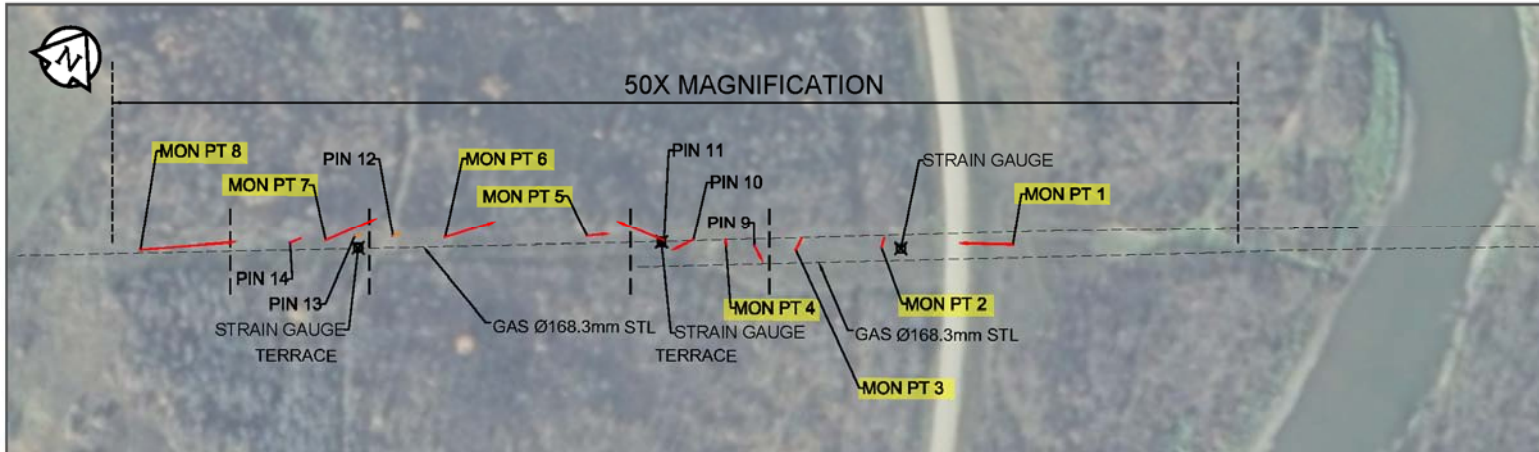
- MON PT1 TO MON PT8 BASELINED (INSTALLED) USING RTK GPS ON MAY 31, 2011
- MON PT 9 TO MON PT22 BASELINED (INSTALLED) USING TOTAL STATION ON NOVEMBER 15, 2011 AND RE-BASELINED (INSTALLED) USING RTK GPS ON JUNE 18, 2013
- PIN 20 DESTROYED AND WAS NOTICED DURING OCTOBER 07, 2014 SURVEY

**LEGEND:**

- + DOWNSLOPE MOVEMENT / INCREASE IN ELEVATION
- UPSLOPE MOVEMENT / DECREASE IN ELEVATION



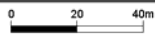
**Figure 5-7**  
**Monitoring Pin Results - May 31, 2011 to September 2, 2015**  
**Harrowby, MB**



	DOWNSLOPE MOVEMENTS / Δ ELEVATIONS																											
	MON PT 8		PIN 14		MON PT 7		PIN 13		PIN 12		MON PT 6		MON PT 5		PIN 11		PIN 10		MON PT 4		PIN 9		MON PT 3		MON PT 2		MON PT 1	
	MOVEMENTS (mm)	Δ ELEVATIONS (mm)	MOVEMENTS (mm)	Δ ELEVATIONS (mm)	MOVEMENTS (mm)	Δ ELEVATIONS (mm)	MOVEMENTS (mm)	Δ ELEVATIONS (mm)	MOVEMENTS (mm)	Δ ELEVATIONS (mm)	MOVEMENTS (mm)	Δ ELEVATIONS (mm)	MOVEMENTS (mm)	Δ ELEVATIONS (mm)	MOVEMENTS (mm)	Δ ELEVATIONS (mm)	MOVEMENTS (mm)	Δ ELEVATIONS (mm)	MOVEMENTS (mm)	Δ ELEVATIONS (mm)	MOVEMENTS (mm)	Δ ELEVATIONS (mm)	MOVEMENTS (mm)	Δ ELEVATIONS (mm)	MOVEMENTS (mm)	Δ ELEVATIONS (mm)	MOVEMENTS (mm)	Δ ELEVATIONS (mm)
TOTAL MOVEMENTS UP TO SEPT 2, 2015	+582.0	-279.0	+68.2	+21.0	+310.4	-79.0	+39.1	-24.0	+41.5	-88.0	+304.4	-42.0	+134.8	-78.0	-173.7	+5.0	-173.9	+72.0	-75.4	+5.0	+26.2	+26.0	+36.2	-14.0	+17.3	-3.0	-322.7	+65.0

**NOTES:**

1. MON PT1 TO MON PT8 BASELINED (INSTALLED) USING RTK GPS ON MAY 31, 2011
2. MON PT9 TO MON PT14 BASELINED (INSTALLED) USING TOTAL STATION ON SEPTEMBER 15, 2011, AND RE-BASELINED (INSTALLED) USING RTK GPS ON JUNE 16, 2013
3. MON PT1, MON PT4, PIN 9, PIN 10 AND PIN 11 WERE DESTROYED AND NOTICED DURING MAY 29, 2014 SURVEY PERFORMED
4. MON PT4, PIN 9, PIN 10 AND PIN 11 WERE REINSTALLED IN NOVEMBER 2014

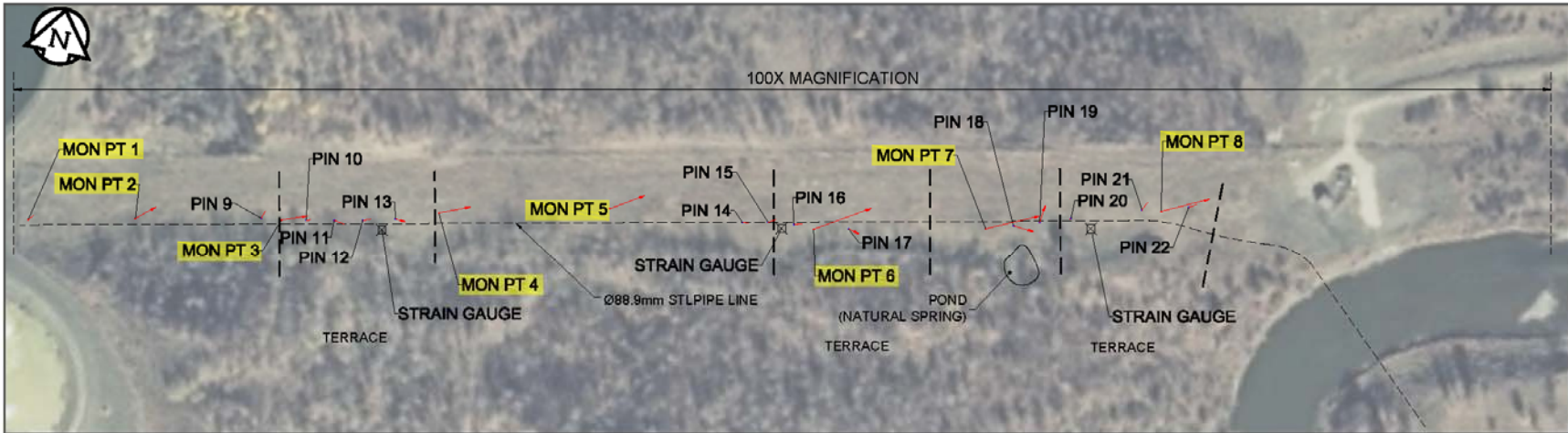


**LEGEND :**

- + DOWNSLOPE MOVEMENT / INCREASE IN ELEVATION
- UPSLOPE MOVEMENT / DECREASE IN ELEVATION

Figure 5-8  
Monitoring Pin Results - September 2, 2015  
St-Lazare, MB





		DOWNSLOPE MOVEMENTS / Δ ELEVATIONS																																											
		MON PT1	MON PT2	PIN 9	MON PT3	PIN 10	PIN 11	PIN 12	PIN 13	MON PT4	MON PT5	PIN 14	PIN 15	PIN 16	MON PT6	PIN 17	MON PT7	PIN 18	PIN 19	PIN 20	PIN 21	MON PT8	PIN 22																						
MOVEMENTS (mm)	Δ ELEVATIONS (mm)																																												
TOTAL MOVEMENTS UP TO SEPT 2, 2015		+15.0	-30.0	+78.7	-62.0	+15.1	-6.0	+102.0	-47.0	+16.4	-6.0	+37.4	-20.0	+28.6	+4.0	+38.7	-20.0	+120.4	+9.0	+134.4	0.0	+22.0	-13.0	+31.1	-8.0	+30.1	+6.0	+221.8	-44.0	+38.5	-105.0	+207.6	-159.0	+75.3	-130.0	+21.8	+36.0	-4.0	+29.0	+19.9	-77.0	+183.5	-38.0	+31.2	0.0

**NOTES:**

1. MON PT1 TO MON PT8 BASELINED (INSTALLED) USING RTK GPS ON MAY 31, 2011
2. MON PT 9 TO MON PT22 BASELINED (INSTALLED) USING TOTAL STATION ON NOVEMBER 15, 2011 AND RE-BASELINED (INSTALLED) USING RTK GPS ON JUNE 18, 2013
3. PIN 20 DESTROYED AND WAS NOTICED DURING OCTOBER 07, 2014 SURVEY

**LEGEND :**

- + DOWNSLOPE MOVEMENT / INCREASE IN ELEVATION
- UPSLOPE MOVEMENT / DECREASE IN ELEVATION



**Figure 5-9**  
Monitoring Pin Results - September 2, 2015  
Harrowby, MB

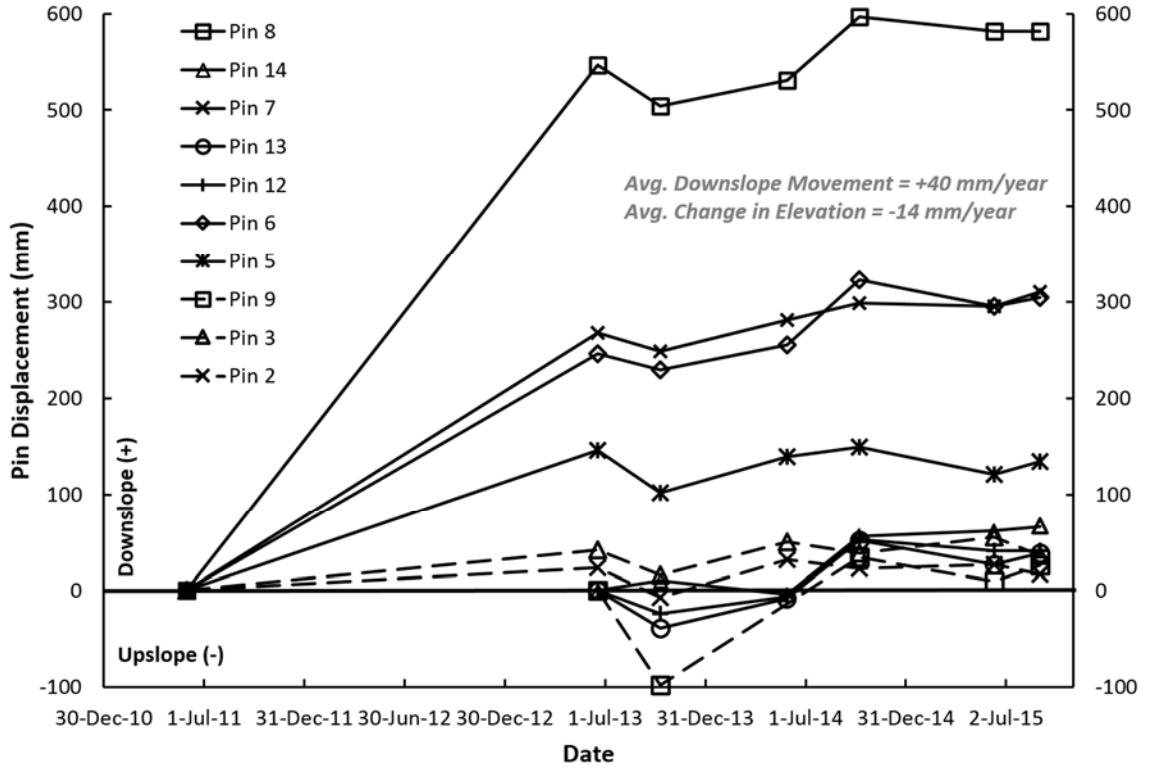


Figure 5-10 St. Lazare – Pin Movement Parallel to Pipe Alignment

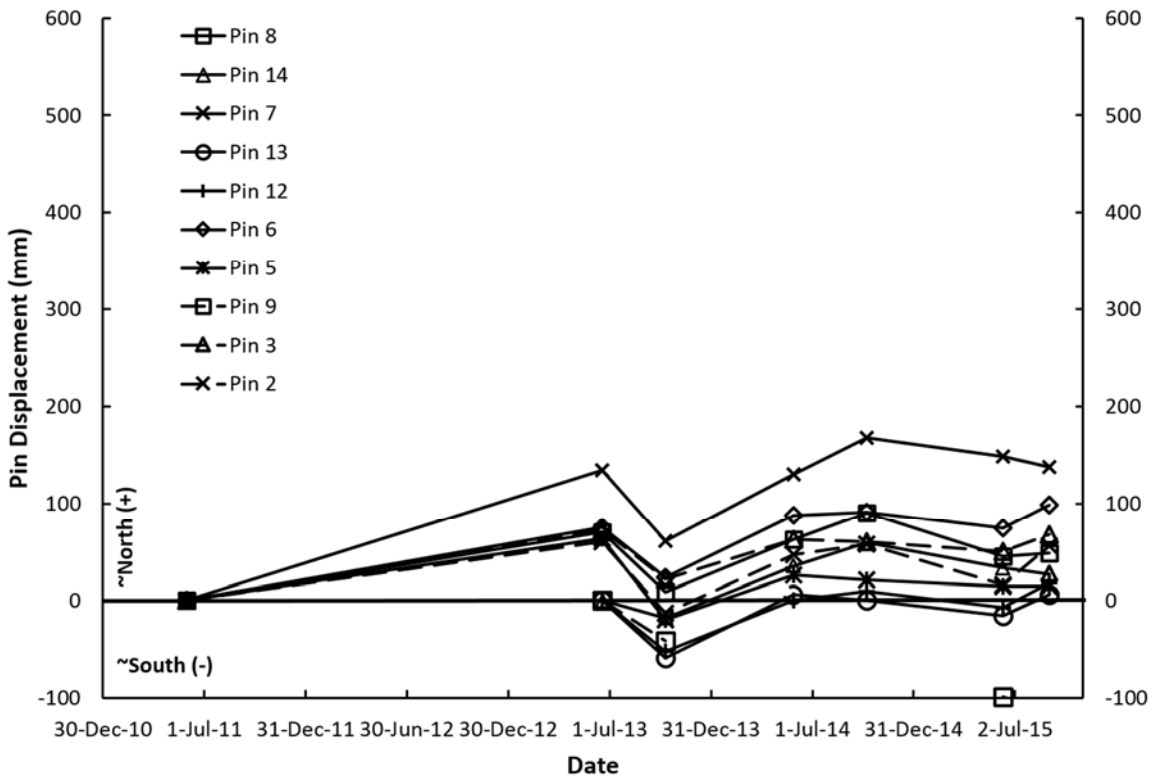


Figure 5-11 St. Lazare – Pin Movement Perpendicular to Pipe Alignment

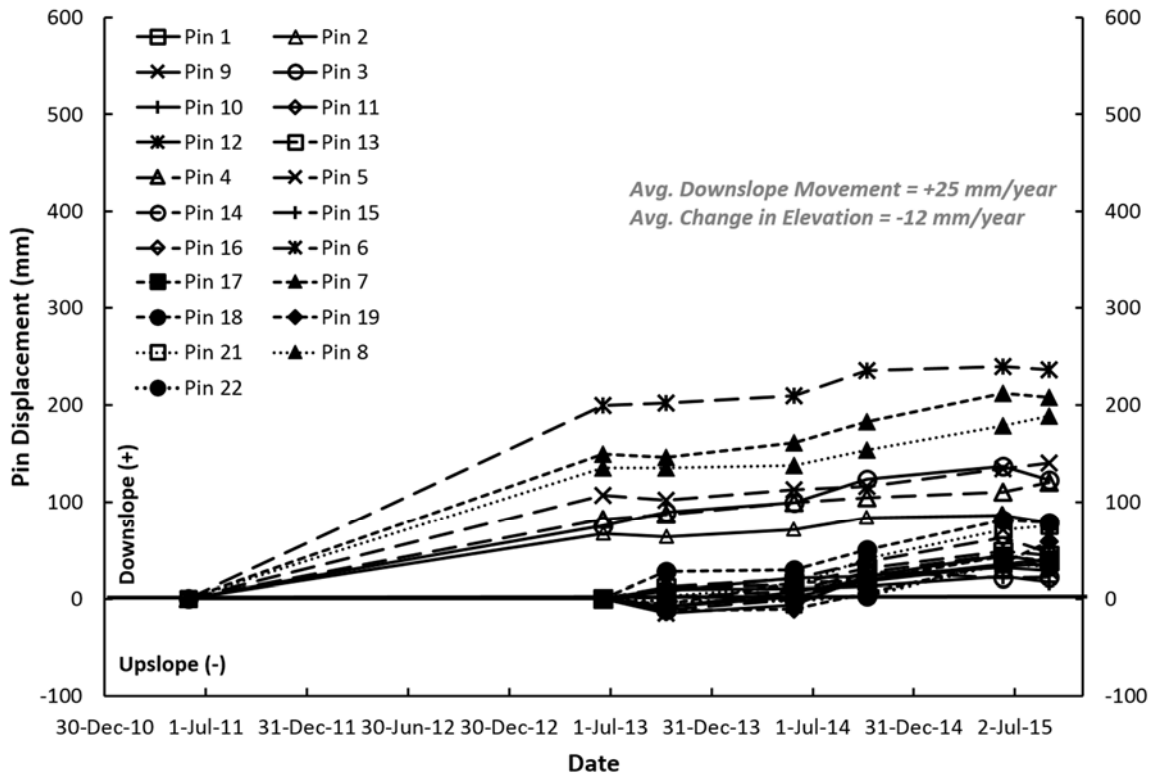


Figure 5-12 Harrowby – Pin Movement Parallel to Pipe Alignment

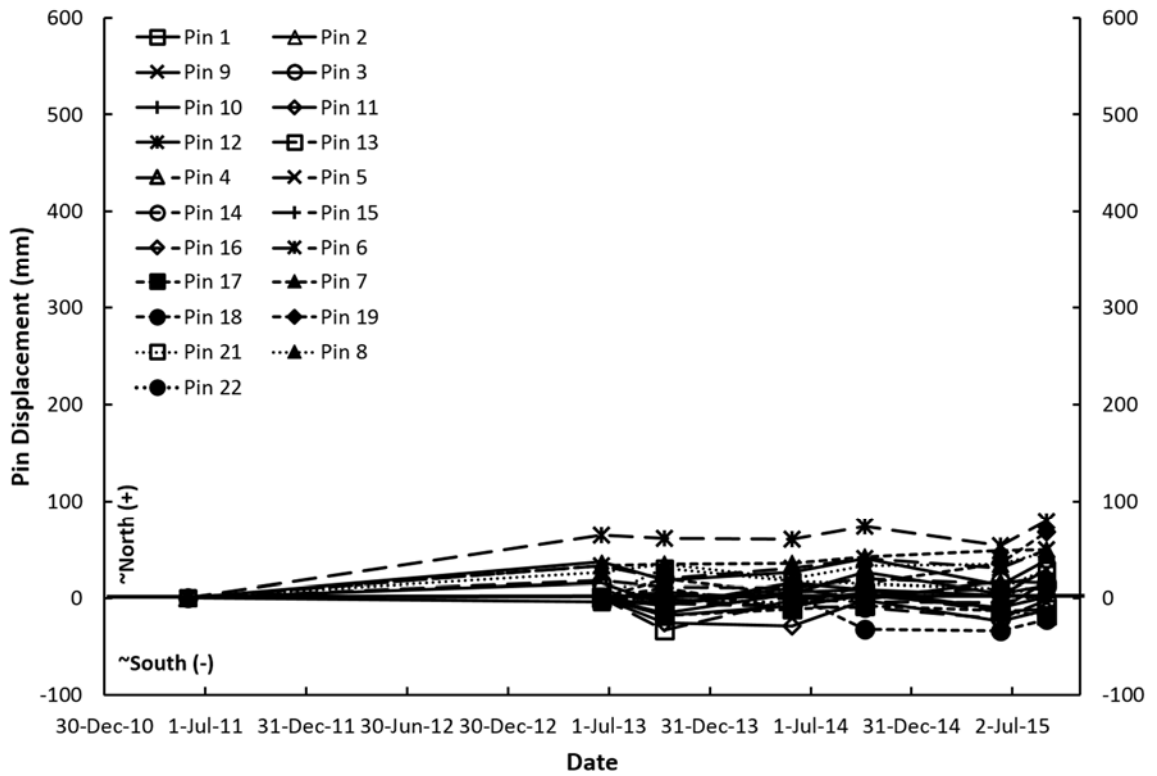


Figure 5-13 Harrowby – Pin Movement Perpendicular to Pipe Alignment

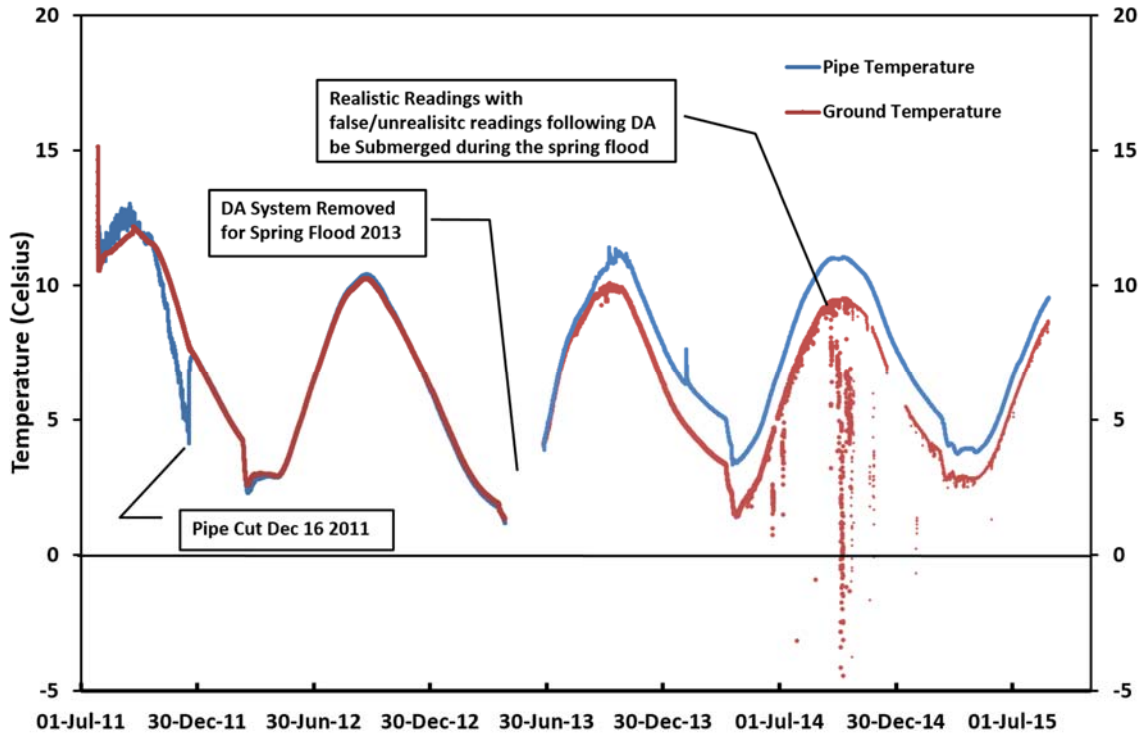


Figure 5-14 Plum River Pipe and Ground Temperatures.

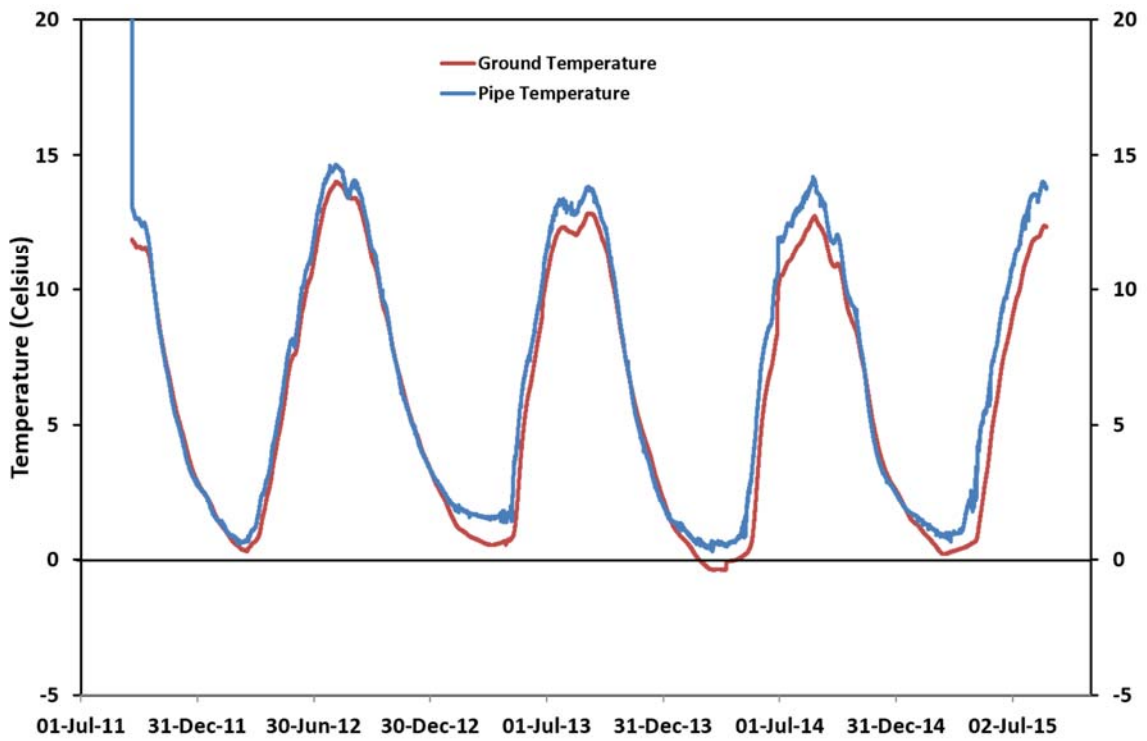


Figure 5-15 St-Lazare Top of Valley Pipe and Ground Temperatures.



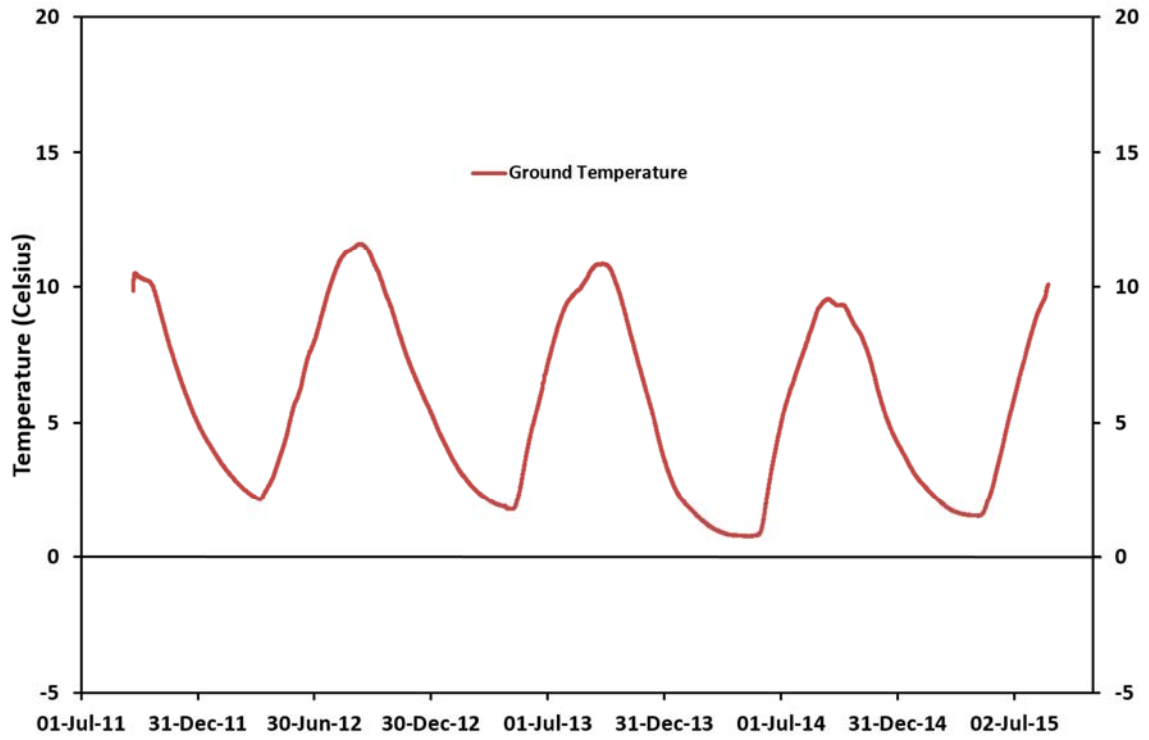


Figure 5-16 St-Lazare Bottom of Valley Ground Temperatures.

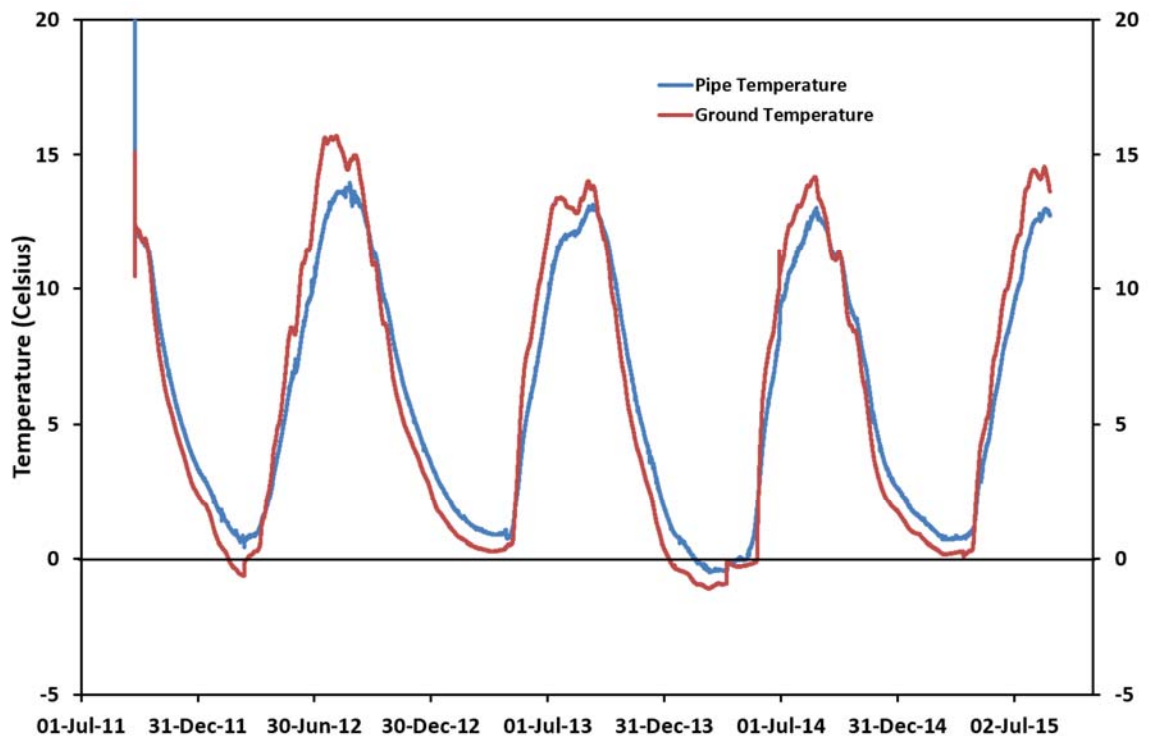


Figure 5-17 Harrowby Top of Valley Pipe and Ground Temperatures

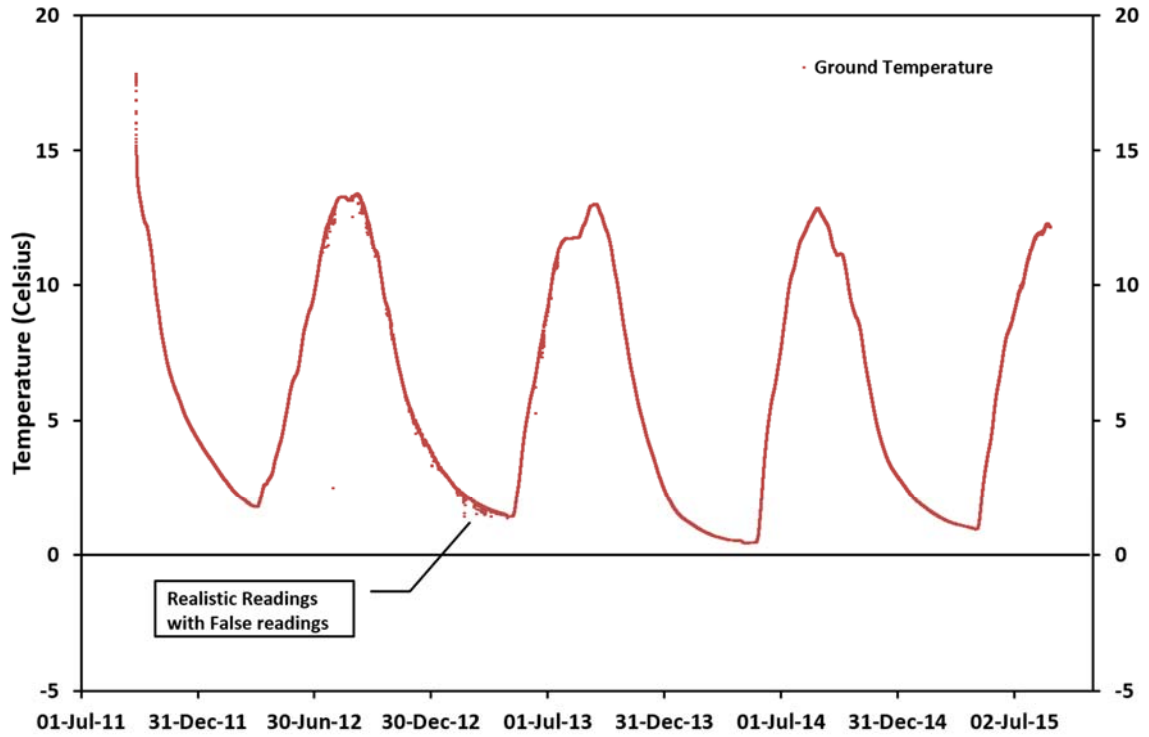


Figure 5-18 Harrowby Bottom of Valley Ground Temperatures.

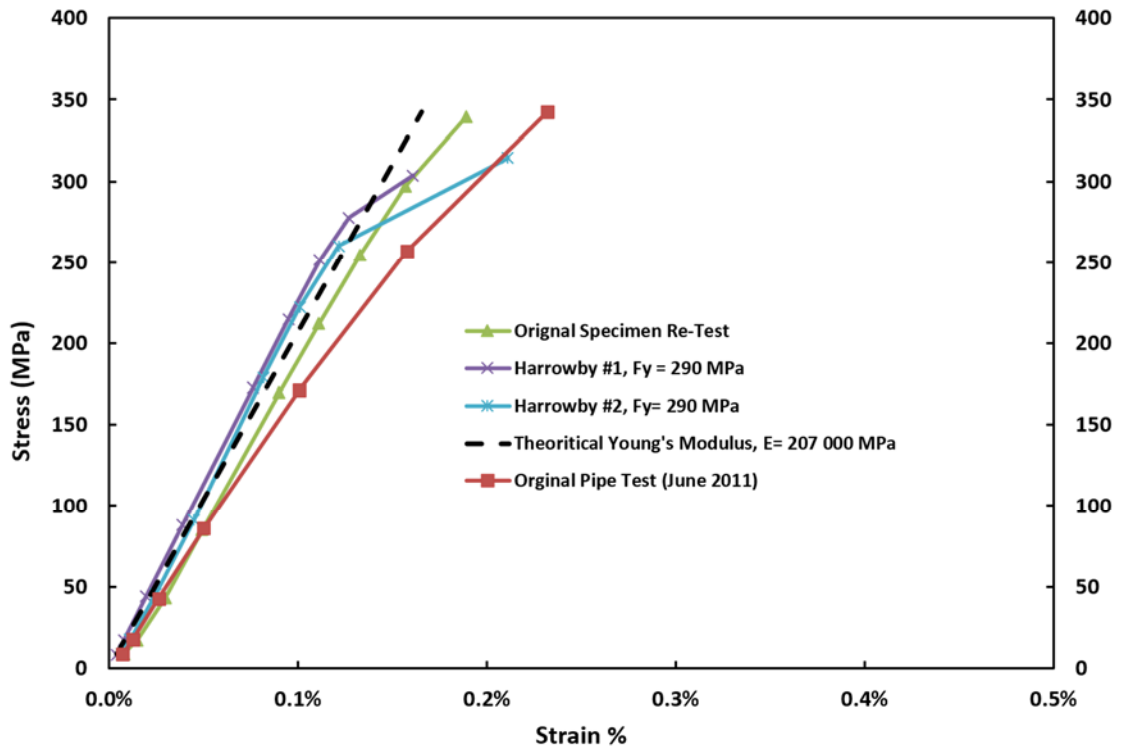


Figure 5-19 Laboratory Pipe Load Test Results.

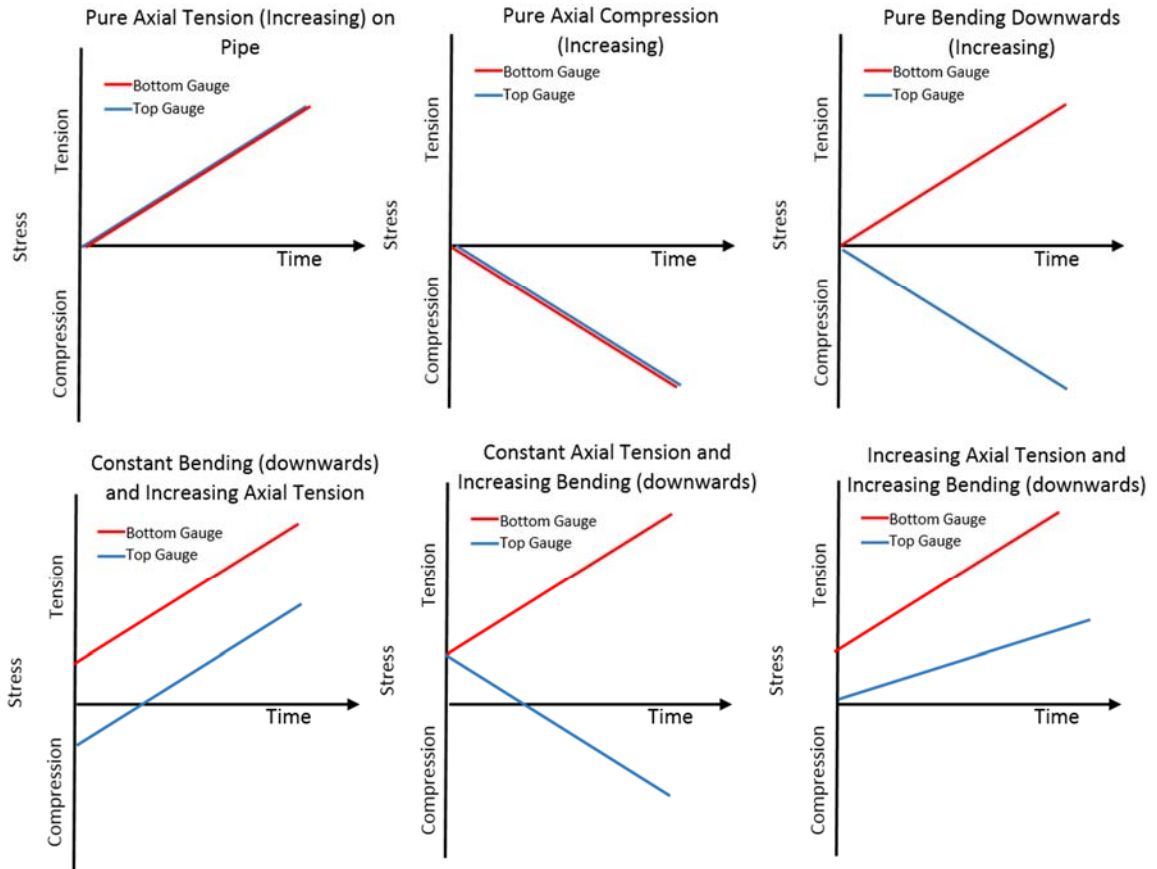


Figure 5-20 Understanding Stresses Induced on the Pipe Using Two Uniaxial Strain Gauges.

Manitoba Hydro Gas Pipeline Research  
 Harrowby Test Site  
 Top of Valley - Pipe Stresses

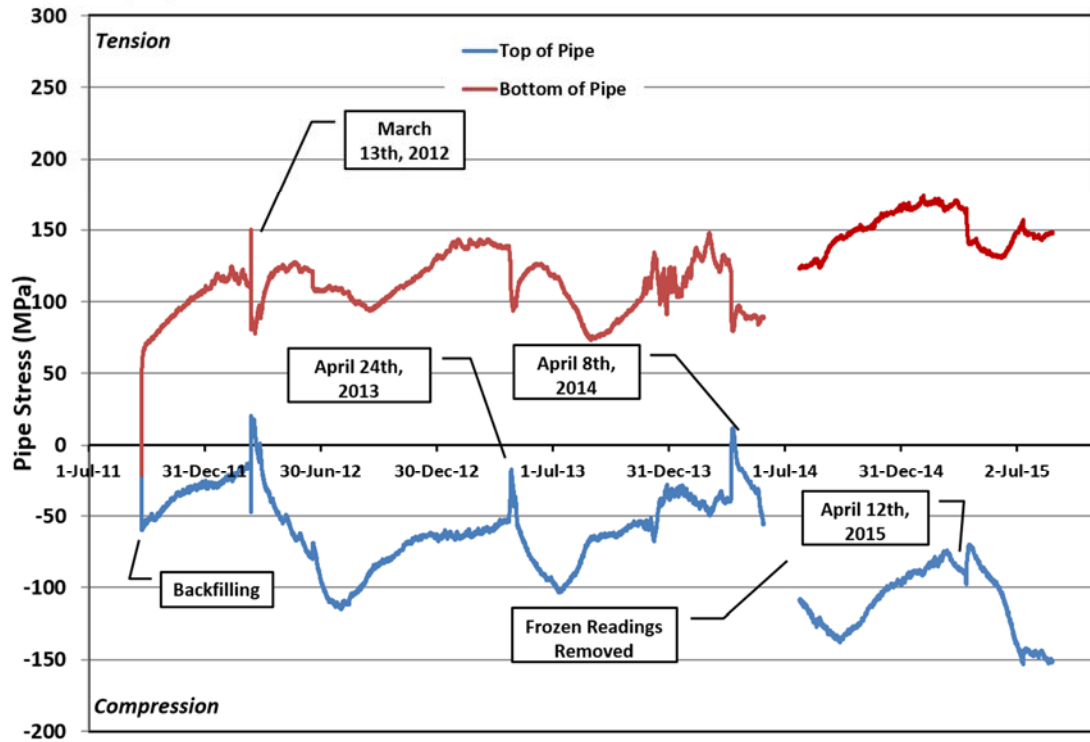


Figure 5-21 Example of Monitoring Results from Uniaxial Strain Gauges (Harrowby top of valley).

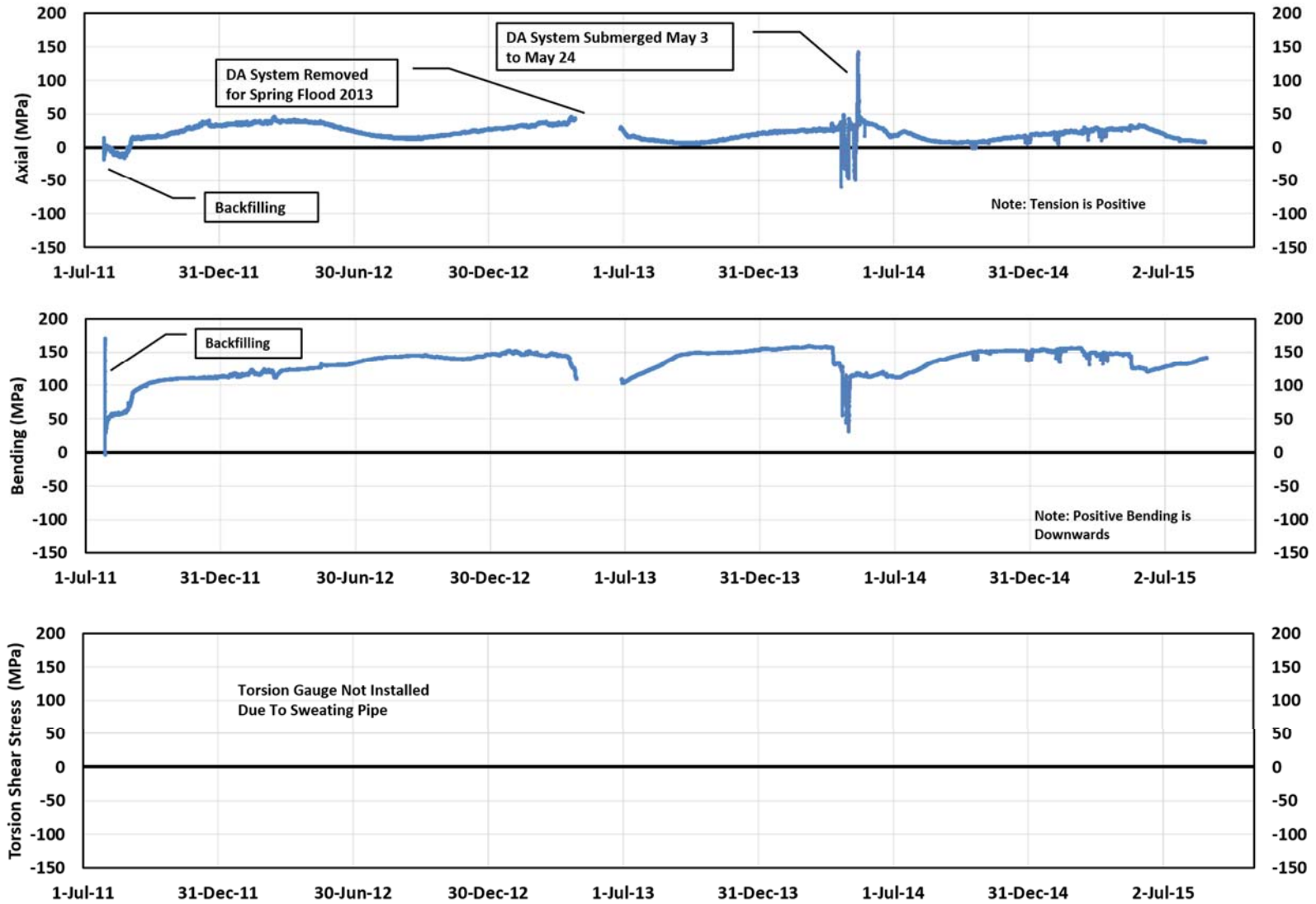


Figure 5-22 Pipe Stresses Plum River Beyond the Crest.

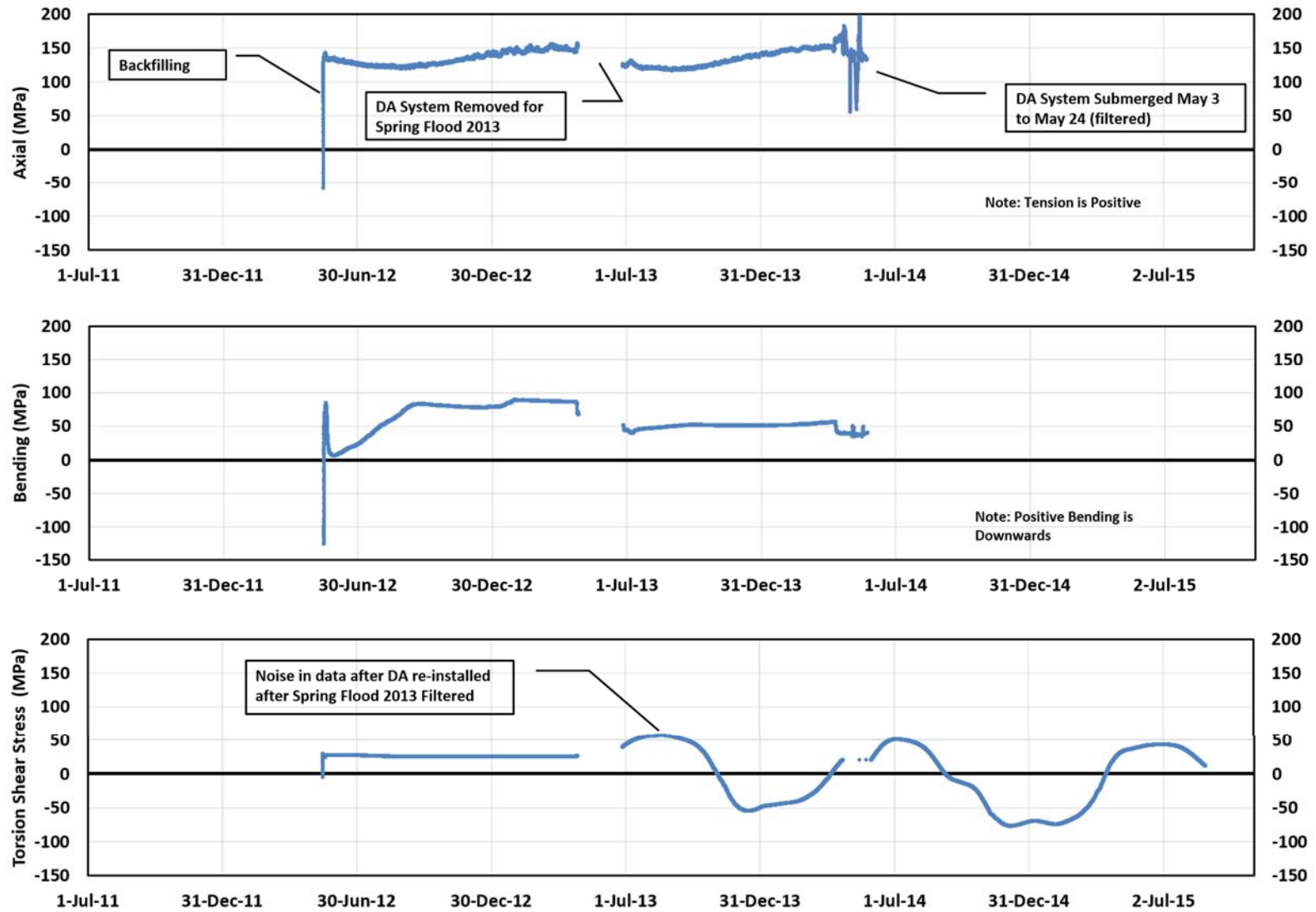


Figure 5-23 Pipe Stresses Plum River Along the Slope.

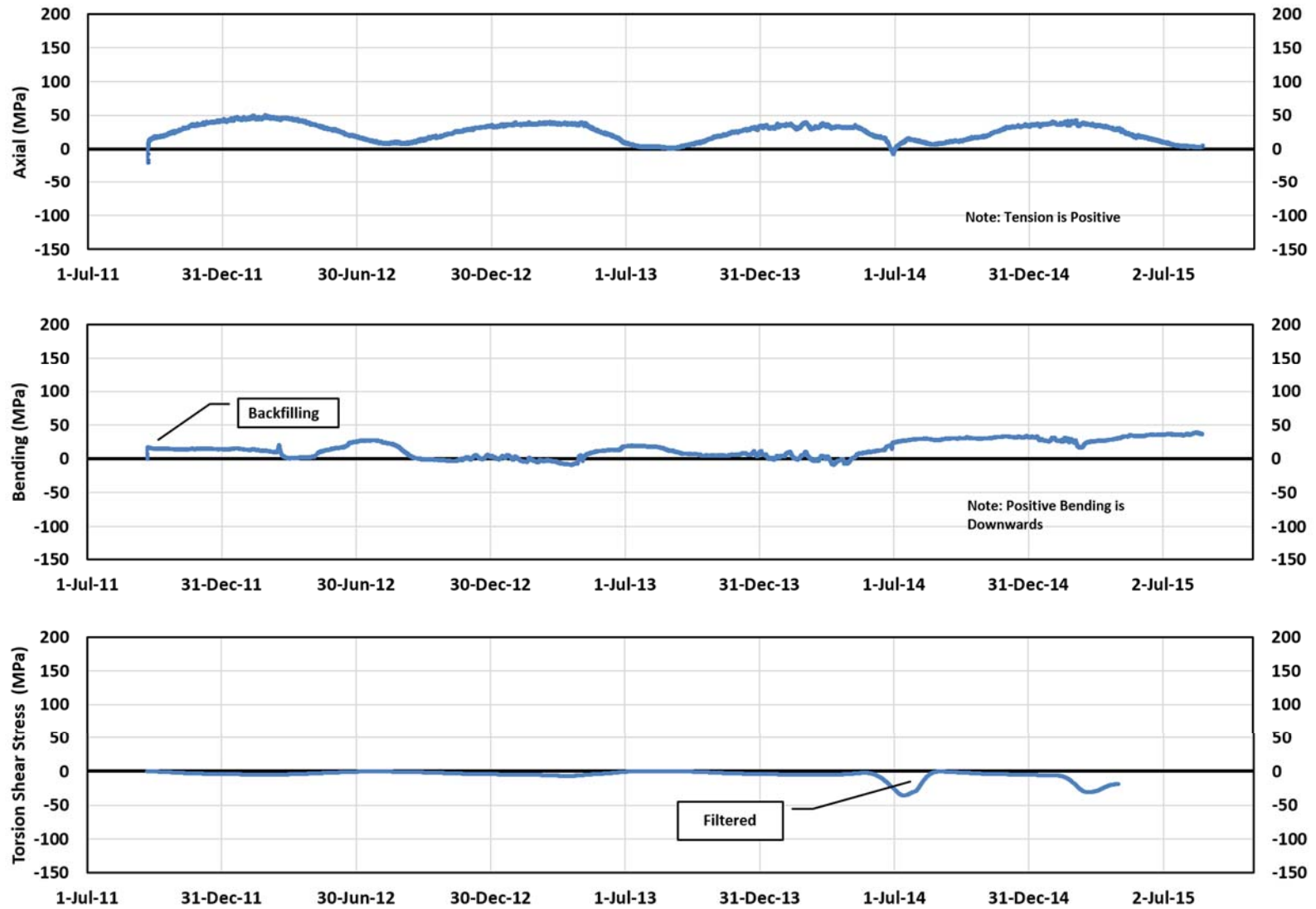


Figure 5-24 Pipe Stresses St-Lazare Top of Valley.

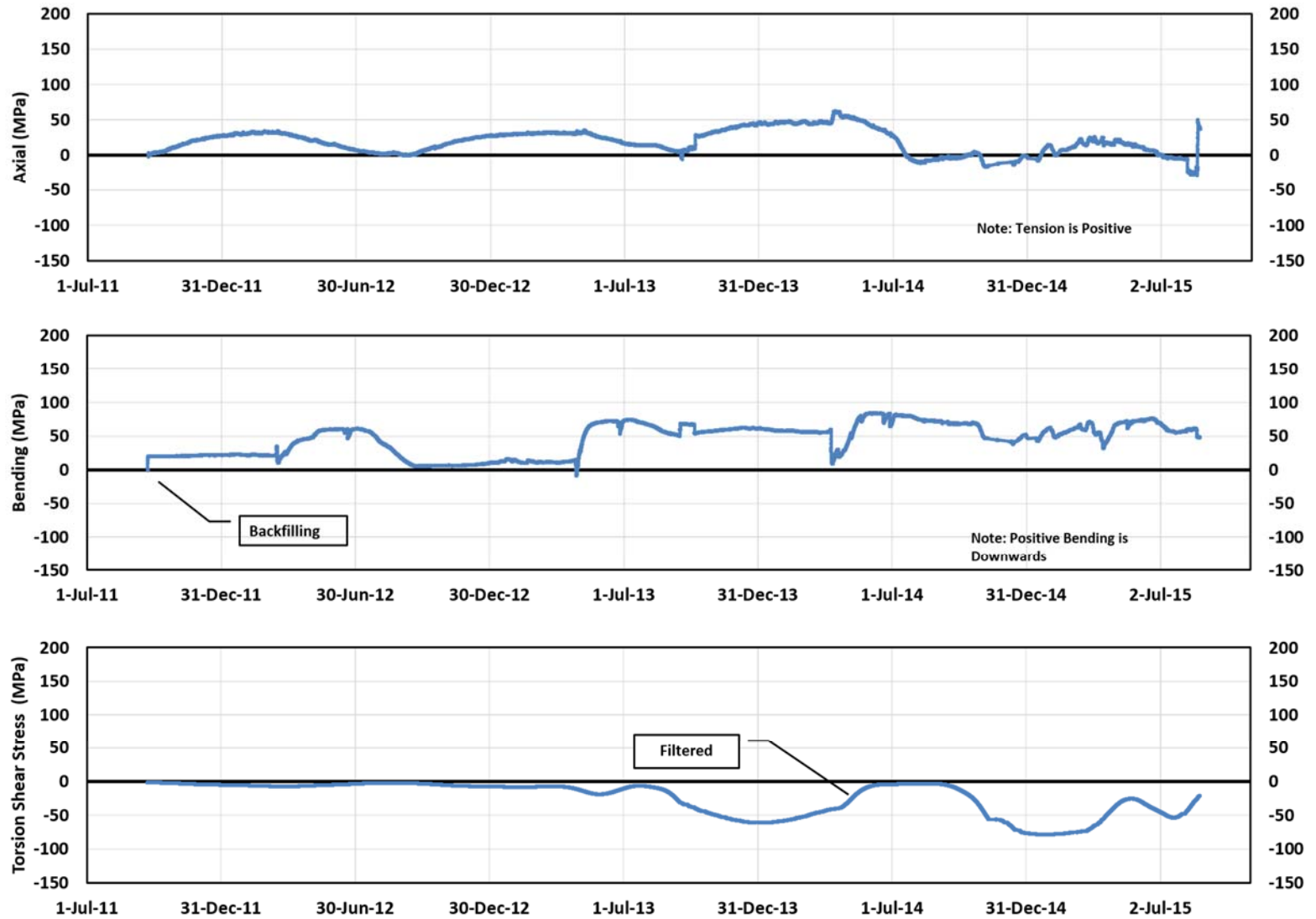


Figure 5-25 Pipe Stresses St-Lazare Middle of Valley.



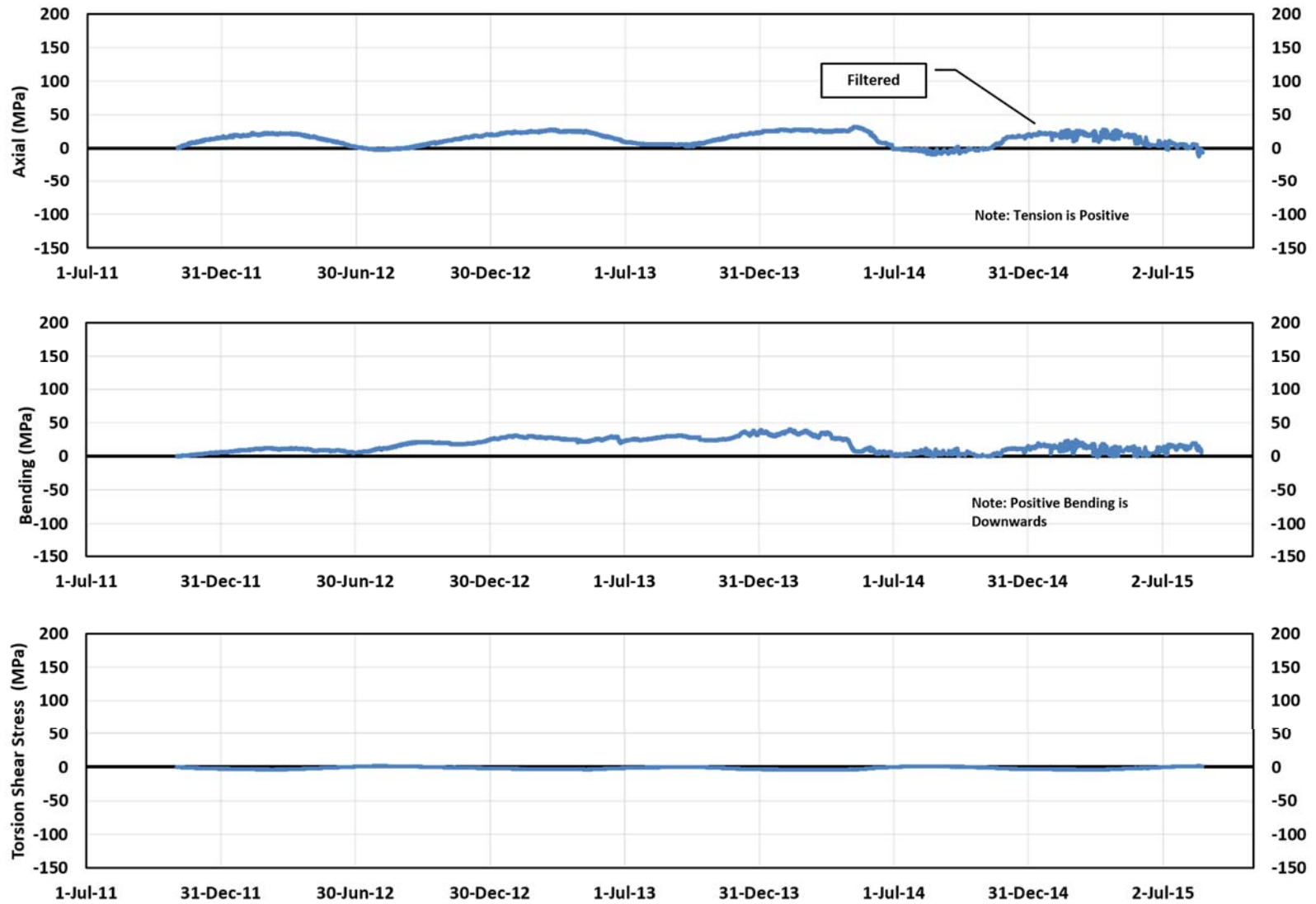


Figure 5-26 Pipe Stresses St-Lazare Bottom of Valley.

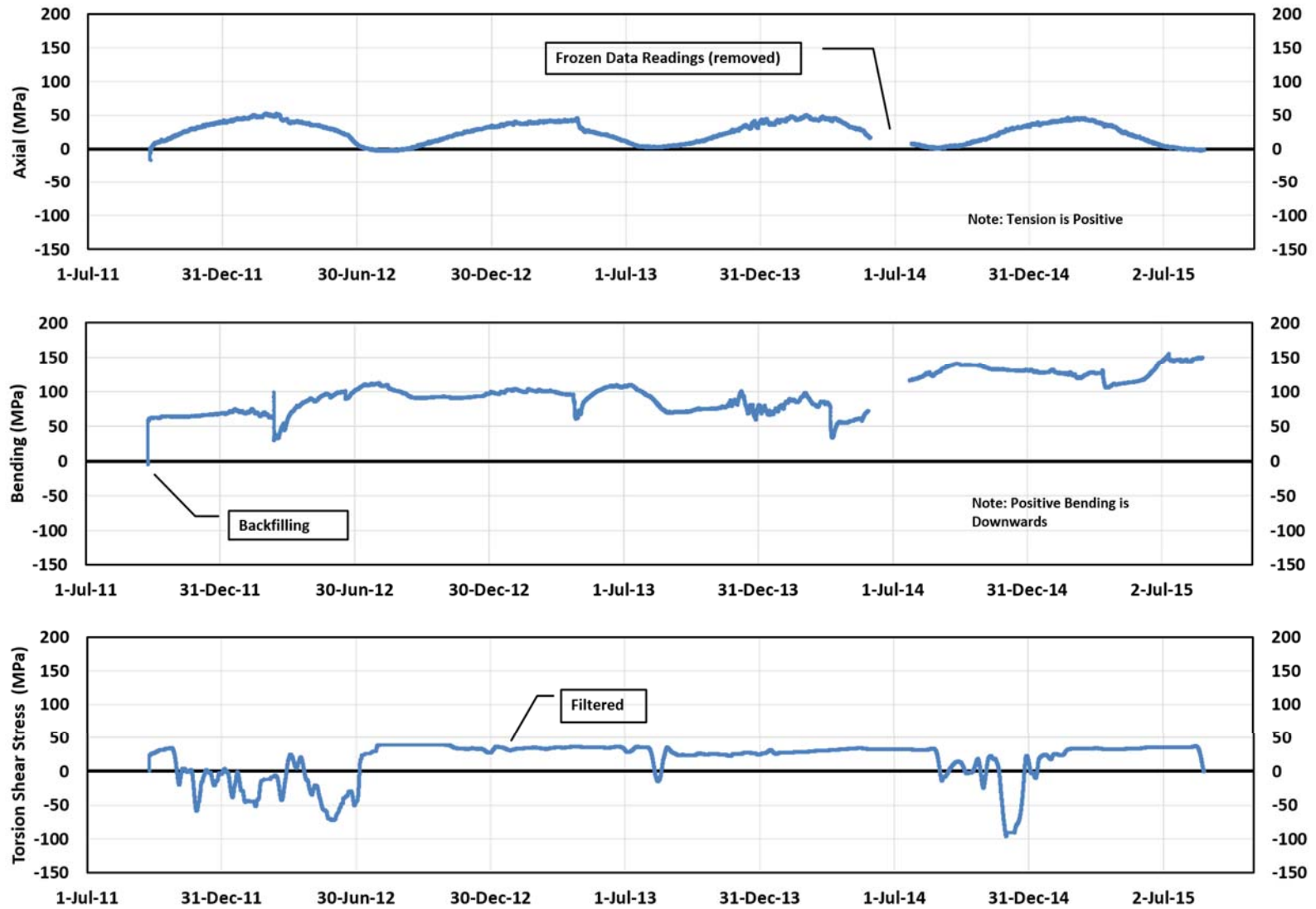


Figure 5-27 Pipe Stresses Harrowby Top of Valley.

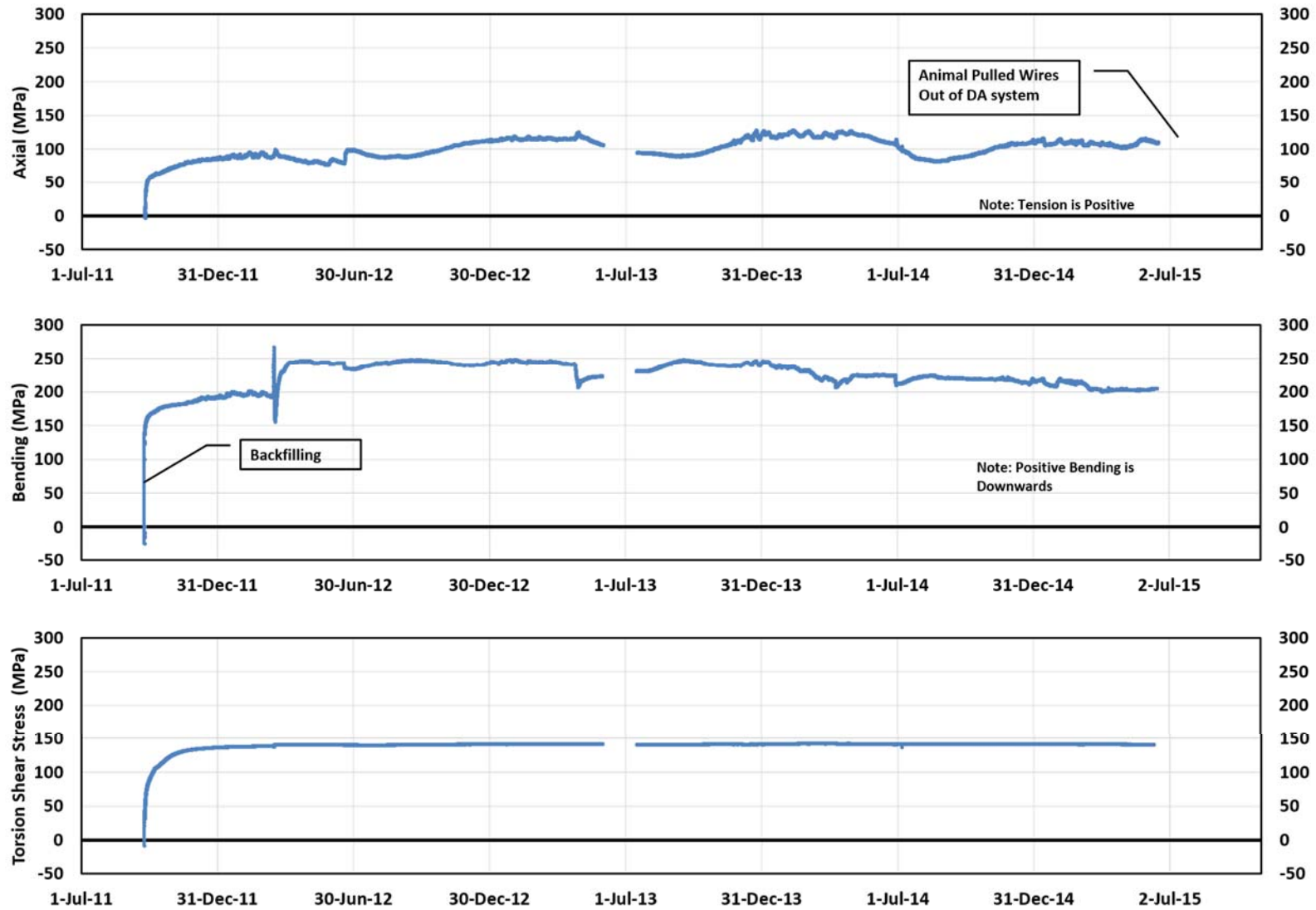


Figure 5-28 Pipe Stresses Harrowby Middle of Valley.

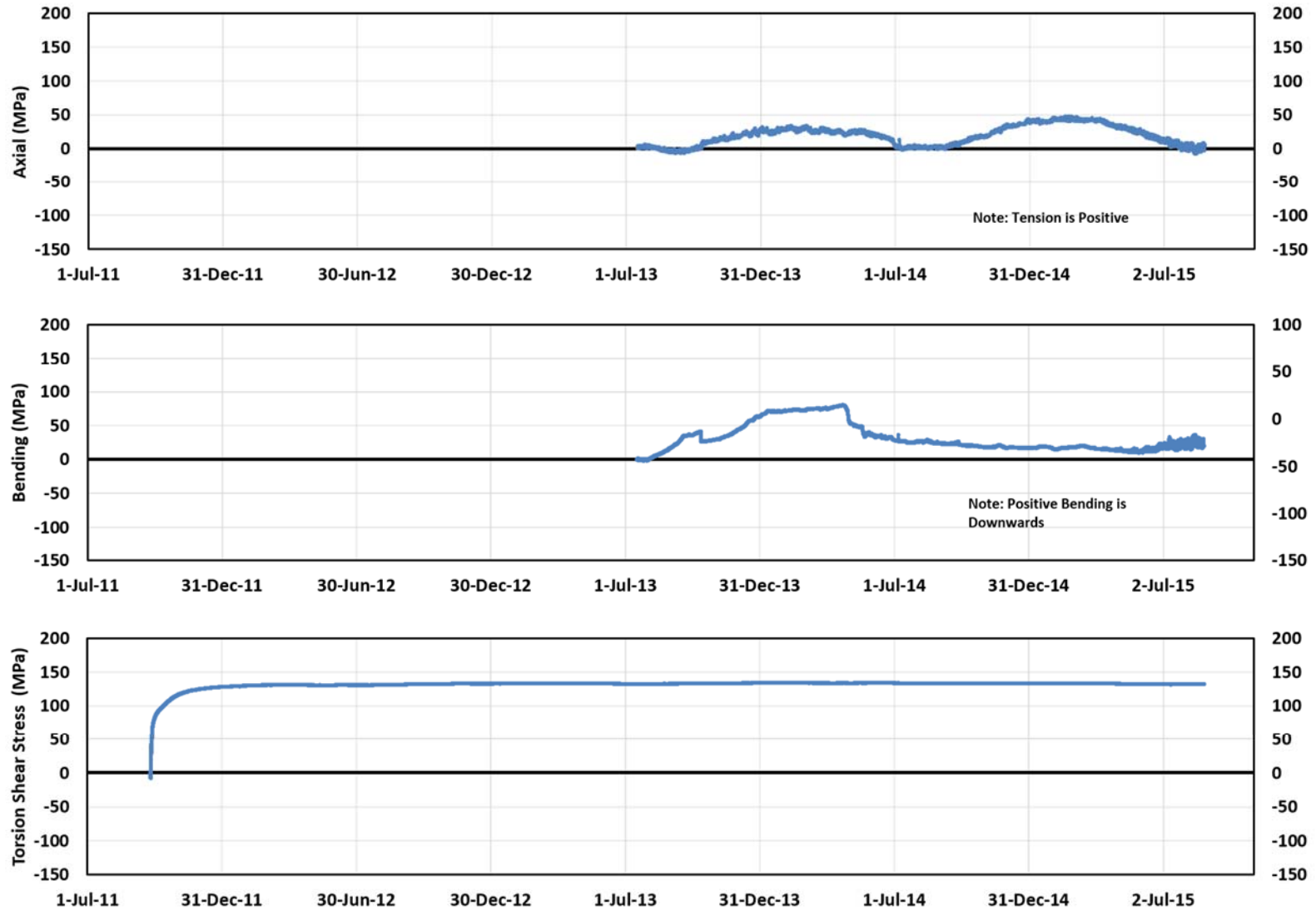


Figure 5-29 Pipe Stresses Harrowby Bottom of Valley.

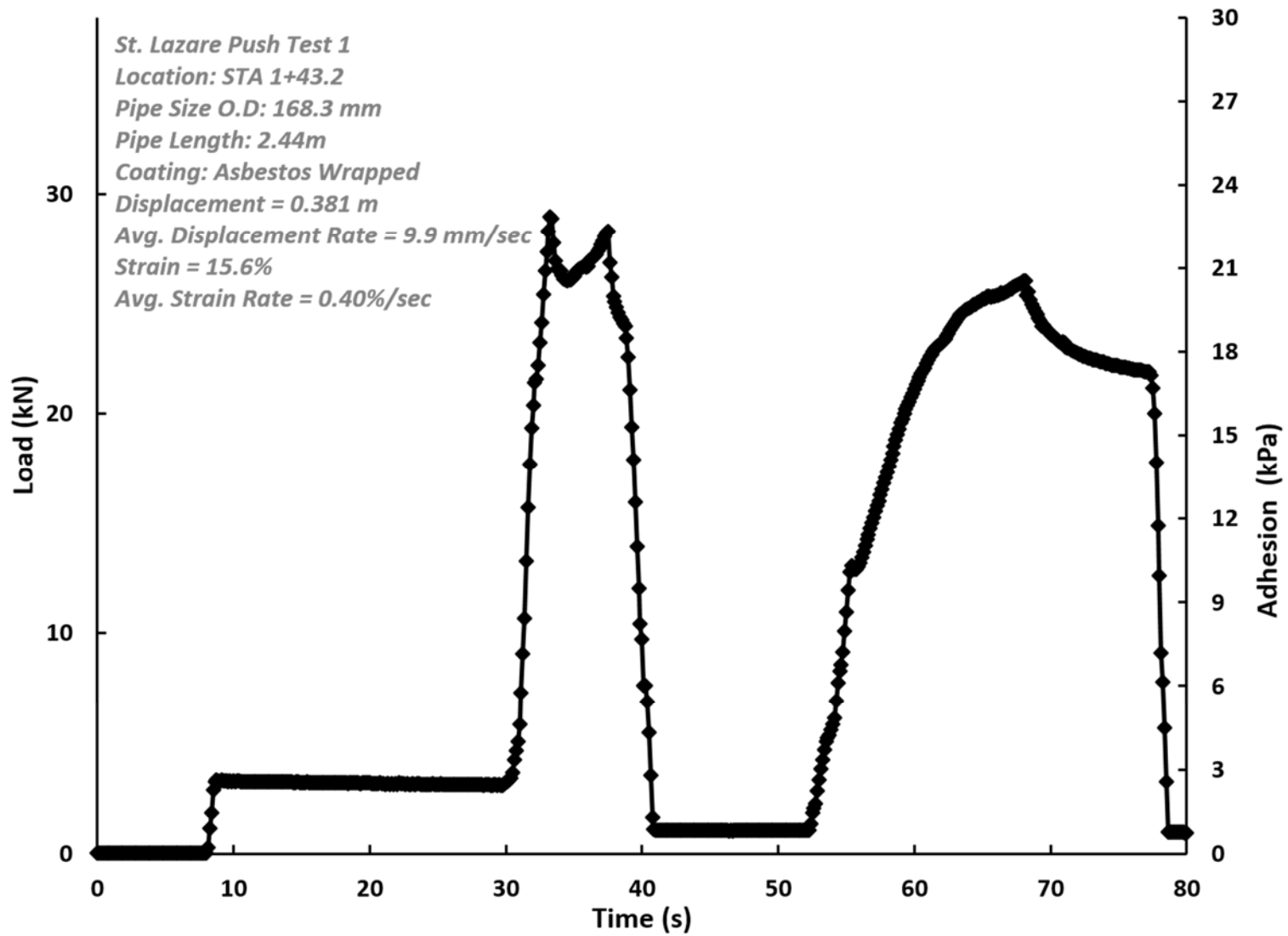


Figure 5-30 St-Lazare Pipe Push Test 1 Load versus Time.

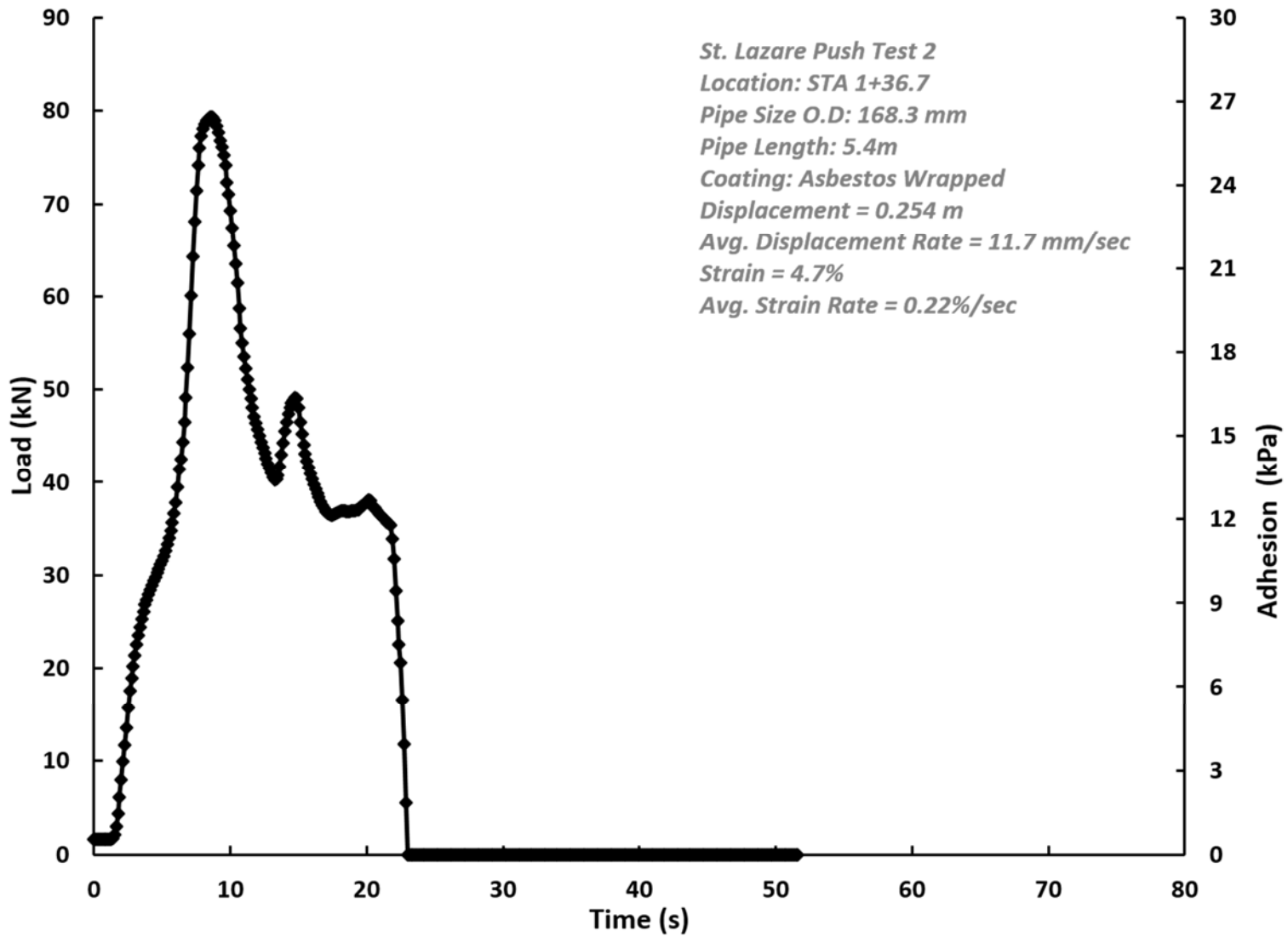


Figure 5-31 St-Lazare Pipe Push Test 2 Load versus Time.

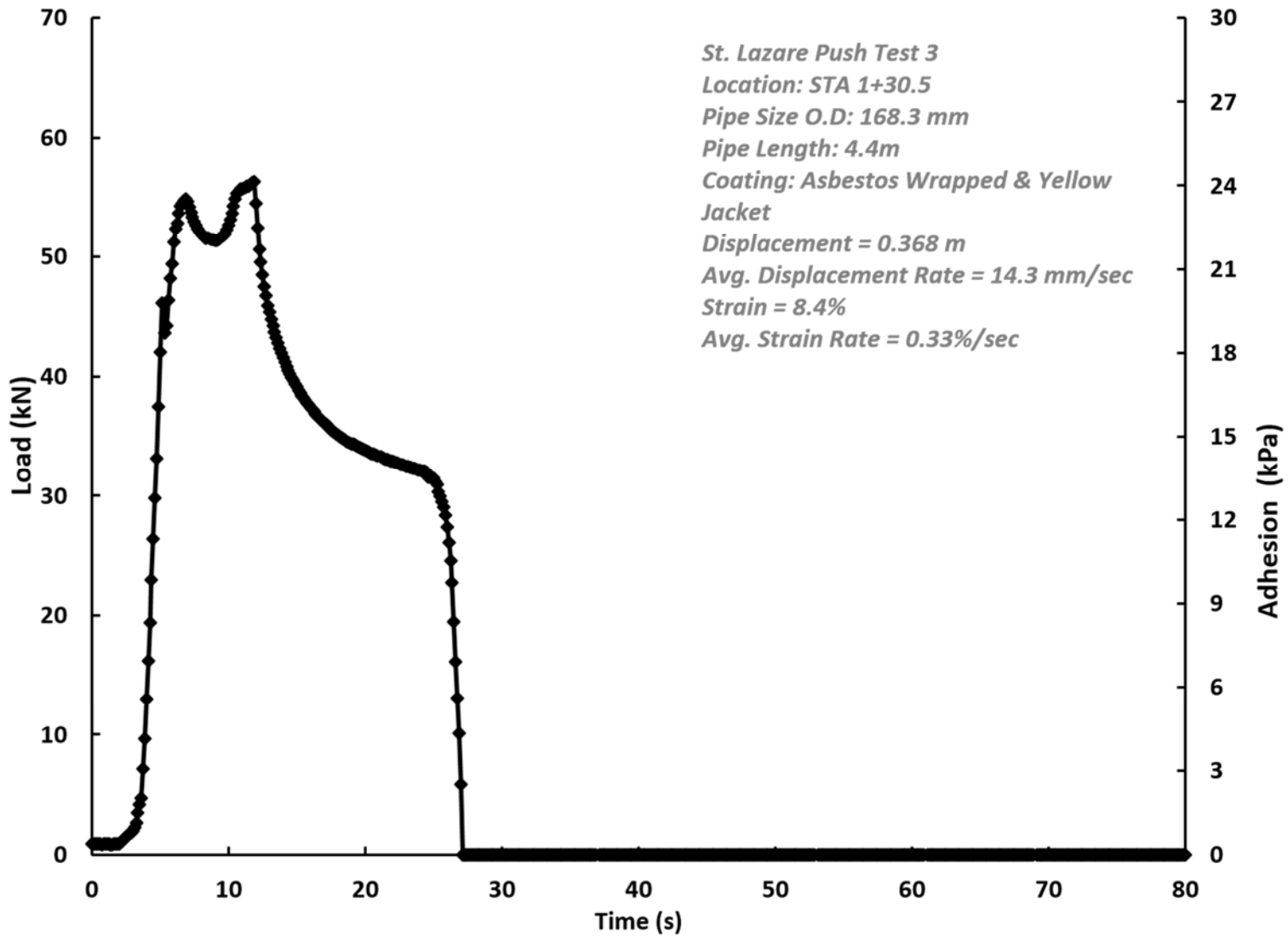


Figure 5-32 St-Lazare Pipe Push Test 3 Load versus Time.

Table 5-1 – Interruptions to Instrumentation Monitoring.

Site	Instrumentation	Dates Occurred	Cause/Condition	Action
All Sites	6 of 7 SIs	Between October 2010 and June 2011	Excessive ground movements resulted in SIs being impassable with the SI probe excluding SI10-04 at St-Lazare (Bottom of Valley).	Monitoring pins installed at ground surface to be surveyed as means to measure ground movement.
Plum River	VW1A & VW2A	May 14 <sup>th</sup> to June 7 <sup>th</sup> 2012	Lead wires were accidentally cut while installing strain gauges within the riverbank.	Lead wires were spliced together and protected
	VW1A & VW2A	June 7 <sup>th</sup> to November 1 <sup>st</sup> 2012	A new AVW200 2-Channel Vibrating Wire Spectrum Analyzer Module was replaced due to manufacture recall. It appeared the new AVW 200 was set-up properly but there was an issue with a device configuration software.	The issue with the AVW200 was identified at the next monitoring trip in November. The AVW200 device was flashed and re-configure which solved the problem.
	VW1A	November 11 <sup>th</sup> 2012 to March 24 <sup>th</sup> 2013	Sporadic false readings recorded	Unknown Problem
	All Instrumentation	April 25 <sup>th</sup> to June 26 <sup>th</sup> , 2013	Spring flood forecast predicated a river level at or above the height of the DA enclosure.	DA system removed for the flood and re-installed.
	VW1A	March 24 <sup>th</sup> to September 23 <sup>rd</sup> , 2013	No valid readings	No valid readings, DA program was re-uploaded and appears to have solved problem.
	Torsion Gauge Along the Slope	June 26 <sup>th</sup> 2013 to end of Monitoring (August 2015)	Realistic readings with false, unrealistic readings since re-installing the DA setup following the flood.	Unknown Problem
	VW1B	November 26 <sup>th</sup> , 2013 to December 20 <sup>th</sup> , 2013	Sporadic false readings recorded.	Unknown Problem
	VW1A and VW 1B	May 2 <sup>nd</sup> , 2014	DA enclosure under water (spring flood), estimated to be half way up the enclosure at its maximum level (~April 20, 2014). VW Instrumentation submerged and suspected to have shorted.	None



Table 5-1 – Interruptions to Instrumentation Monitoring (cont'd).

Site	Instrumentation	Dates Occurred	Cause/Condition	Action
Plum River	Strain Gauges and Ground Temperature Gauge	May 2 <sup>nd</sup> , 2014 to end of Monitoring (August 2015)	Box submerged during flood and salt build-up on wire connections due to excessive moisture in the box occurred after the box was under water. Strain gauge readings and ground temperature probe contain false readings and noisy realistic readings between May 2 <sup>nd</sup> and May 24 <sup>th</sup> . Top strain gauge along the slope set-up shorted around May 24 <sup>th</sup> , 2014. After May 24 <sup>th</sup> , readings for the strain gauges beyond crest and the bottom strain gauge along the slope generally cleared while ground temperature gauges is providing realistic readings with sporadic false readings. Bottom Strain Gauge along the slope stopped working June 7, 2015.	Salt building up removed, DA enclosure aired out, desiccator packages replaced.
St-Lazare	VW2A and VW2B at Top of Valley	Between June 2 <sup>nd</sup> , 2011 and September 1 <sup>st</sup> , 2011	VW readings indicate lead wires have been severed, suspected to be due to ground movements.	None
	VW4A at the Bottom of the valley	September 21 <sup>st</sup> , 2011 to November 1 <sup>st</sup> , 2011	The original code for the DA system did not include code to read the second VW.	Code updated and uploaded to the DA system.
	Strain Gauges at Bottom of Valley	September 21 <sup>st</sup> , 2011 to November 1 <sup>st</sup> , 2011	Noise in strain gauge readings. Cause unknown.	Noise was eliminated when the new program to include the second VW was uploaded.
	VW4B at Bottom of Valley	May 6 <sup>th</sup> , 2012 to October 30 <sup>th</sup> , 2012	False readings during this period. Cause unknown.	Realistic readings were measured when the program was re-sent to the DA system.

Table 5-1 – Interruptions to Instrumentation Monitoring (cont’d).

Site	Instrumentation	Dates Occurred	Cause/Condition	Action
St-Lazare	Torsion Gauge at Middle of Valley	September 15 <sup>th</sup> , 2013 to May 3 <sup>rd</sup> , 2014	Large somewhat realistic torsion strains were measured. The unusual reading may be due to construction activities in September and October 2013 at the valves nearby as part of the new river crossing pipeline including excavation work.	None
	Torsion Gauge at Top of Valley	June 13 <sup>th</sup> 2014 to end of Monitoring (August 2015)	Realistic readings with false, unrealistic readings. Cause unknown.	None
	Torsion Gauge at Middle of Valley	October 6 <sup>th</sup> , 2014 to end of Monitoring (August 2015)	Realistic readings with false, unrealistic readings. Cause unknown.	None
	Bottom of Pipe Gauge, Middle of Valley	October 26 <sup>th</sup> , 2014 to April 14 <sup>th</sup> , 2015	Realistic readings with false, unrealistic readings. Cause unknown.	None
	Bottom of Pipe Gauge at Bottom of Valley	July 14 <sup>th</sup> , 2014 to end of Monitoring (August 2015)	Realistic readings with false, unrealistic readings. Cause unknown.	None
Harrowby	VW7A at Bottom of Valley	Between June 6 <sup>th</sup> 2011 and September 24 <sup>th</sup> , 2011	VW readings indicate lead wires have been severed, suspected to be due to ground movements	None
	Torsion Gauge at Top of Valley	November 4 <sup>th</sup> , 2011 to October 30 <sup>th</sup> , 2012	Realistic readings with false, unrealistic readings. Cause unknown.	Realistic readings were measured when the program was re-sent to the DA system

Table 5-1 – Interruptions to Instrumentation Monitoring (cont'd).

Site	Instrumentation	Dates Occurred	Cause/Condition	Action
Harrowby	Strain Gauges at Middle of Valley	May 29 <sup>th</sup> , 2013 to July 17 <sup>th</sup> , 2013	Animal pulled on wiring into enclosure which pulled out the strain gauge wiring from the DA system	Strain gauges were re-wired and protective conduit was installed to protect wiring into the enclosure.
	VW7B at Bottom of Valley	June 21 <sup>st</sup> , 2012	VW readings indicate lead wires may have been severed, suspected to be due to ground movements	None
	Uniaxial Strain Gauges at Bottom of Valley	September 24 <sup>th</sup> , 2011 to July 16 <sup>th</sup> , 2013	Shortly after backfilling, false readings started but appeared to be realistic. Cause unknown	Realistic readings were measured when the program was re-sent to the DA system
	Strain Gauges at Top of Valley	May 29 <sup>th</sup> , 2014 to July 24 <sup>th</sup> , 2014	Frozen readings measured from strain gauges. Cause unknown.	Realistic readings were measured when the program was re-sent to the DA system
	Torsion Gauge at Top of Valley	June 10 <sup>th</sup> , 2014 to February 22 <sup>nd</sup> , 2015	Realistic readings with false, unrealistic readings. Cause unknown.	None
	Strain Gauges at Middle of Valley	June 9 <sup>th</sup> , 2015 to end of Monitoring (August 2015)	Animal pulled on wiring into enclosure which pulled out the strain gauge wiring from the DA system	None

Table 5-2 Slope Inclinator Operation Details.

Site	SI Label	Location	Date Installed	Inoperative Date	Depth Below Ground	Monitoring Events Recorded
Plum River	SI10-01	Along the Slope	August 2010	October 2010	3.9 m	Baseline
St-Lazare	SI10-02	Top of Valley		June 2011	7.3 m	Baseline
	SI10-03	Middle of Valley	September 2010	June 2011	4.0m	Baseline
	SI10-04	Bottom of Valley		Abandoned	-	4
Harrowby	SI10-05	Top of Valley			18.3 m	
	SI10-06	Middle of Valley	November 2010	June 2011	3.7 m	None
	SI10-07	Bottom of Valley			11.0 m	

Table 5-3 Summary of Post-Processing of Monitoring Data.

Site/Setup	Filtering			Comments	
	Gauge	False Readings	Unrealistic Values		Butterworth Filter
<b>Plum River</b>					
Beyond the Slope	Ground Temperature	Not Removed	Not Removed	-	No Processing Needed
Along the Slope	Top of Pipe	Removed	-	-	Occurred Between May 3 to 24, 2014
Along the Slope	Torsion	-	Truncated < Yield, Difference Between Readings < 3 Std. Dev	4 <sup>th</sup> Order Forward	-
Along the Slope	VW1A & VW1B	Removed	-	-	Occurred Between Mar 11, 2012 to Dec 20, 2013
<b>St-Lazare</b>					
Top of Valley	Torsion	-	Truncated < Yield, Difference Between Readings < 3 Std. Dev	4 <sup>th</sup> Order Forward	-

Table 5-3 Summary of Post-Processing of Monitoring Data (cont'd).

Site/Setup	Filtering				Comments
	Gauge	False Readings	Unrealistic Values	Butterworth Filter	
Middle of Valley	Bottom of Pipe	-	Negative Values Removed, Difference Between Readings < 3 Std. Dev of Top Gauge	4 <sup>th</sup> Order Forward with Bias	A bias was applied based on visual assessment on data
Middle of Valley	Torsion	-	Truncated < Yield, Difference Between Readings < 3 Std. Dev	4 <sup>th</sup> Order Forward	-
Bottom of Valley	Bottom of Pipe	-	Negative Values Removed, Difference Between Readings < 3 Std. Dev of Top Gauge	4 <sup>th</sup> Order Forward	-
Bottom of Valley	All Strain Gauges	Removed	-	-	Occurred up to November 1, 2011
Bottom of Valley	VW1B	Removed	-	-	Occurred between May 6 to Oct 30, 2013

Table 5-3 Summary of Post-Processing of Monitoring Data (cont'd).

Site/Setup	Gauge	Filtering			Comments
		False Readings	Unrealistic Values	Butterworth Filter	
<b>Harrowby</b>					
Top of Valley	Strain Gauges	Removed	-	-	Frozen Readings between May 29 to July 24, 2014
Top of Valley	Torsion	-	Truncated < Yield, Difference Between Readings < 3 Std. Dev	2 <sup>nd</sup> Order Forward	-
Bottom of Valley	Top of Pipe	Removed	-	-	Strain Gauge Monitoring up to July 16, 2013 not used in research
Bottom of Valley	Ground Temperature	Not Removed	Not Removed	-	No Processing Needed

Table 5-4 St-Lazare Pipe Push Test Results.

Location	Test #	Coating	O.D. (mm)	~ Wall t (mm)	Length (m)	Total Push Force (kN)	Force per meter (kN/m)	Maximum Adhesion (kPa)	Adhesion Factor <sup>1</sup> ( <i>in-situ</i> /recon.)
STA 1+43.2	1	Asbestos Wrapped	168.3	4.8	2.4	29.0	11.9	22.5	0.55/ 0.34
STA 1+36.7	2	Asbestos Wrapped	168.3	4.8	5.6	79.4	14.1	26.6	0.59/ 0.40
STA 1+30.5	3	Asbestos Wrapped/ Yellow Jacket	168.3	4.8	4.4	56.4	12.8	24.2	0.56/0.37
						<i>Avg.</i>	<i>12.9</i>	<i>24.4</i>	<i>0.57/.37</i>

<sup>1</sup> – Undrained shear strength of *in-situ* soil around the pipe = 43.4 kPa and reconstituted soil = 65.8 kPa



## **Chapter 6 Interpretation of Monitoring Data and Observations**

Interpretation of the monitoring data is presented in this chapter along with general observations that can be inferred from the monitoring results. The behaviour of the measured ground monitoring pin movements are discussed. Possible sources of load have been identified and quantified within the pipe stress monitoring data such as freeze/thaw and thermal expansion of pipe. Pipe stresses attributed to ground movements are also presented and discussed along with the response of pipe to other loading conditions such as backfilling.

### **6.1 Ground Movements**

The ground monitoring pins were surveyed using a RTK GPS on six occasions over a four year period. A summary of ground movements in tabular and graphical formats are presented in Figures 5-6 to Figure 5-9. In general, measured ground movements are downslope, oriented perpendicular or slightly perpendicular to the slope as shown on Figure 5-8 to Figure 5-13 as expected. Although movements are not entirely downslope, the major assumption that the ground movements are perpendicular to the valley slopes are considered to be valid and the strain gauges are orientated correctly to capture pipe strains based on the direction of observed ground movements. Ground monitoring Pins 1 to 8 for both valley sites have been monitored for a longer duration (over four years) and therefore the direction of measured movements is more discernable than those measured from the remaining monitoring pins, which have only been monitored for slightly over two years.

Some monitoring pins at St-Lazare (Pins 1, 4, 9, 11) were destroyed likely due to pipeline construction activities that occurred in the Fall of 2013. These pins were replaced in May of 2014. Additional construction activity occurred in this area again during the summer of 2015 which is suspected to have disturbed monitoring pins. The ground movement monitoring results for these pins appears random with no clear trend even when adjustments were made to the monitoring results following the monitoring pins being re-installed.

Ground monitoring pin results per valley site are summarized in Table 6-1 which include minimum, maximum and averages of the total movements and rates of movements per year. The results presented in Table 6-1 for the St-Lazare research site do not include Pins 1, 4, 9 and 11 since the monitoring results are questionable for these are pins. Pin 20 from the Harrowby site was also not included when calculating the values presented in Table 6-1 since it was destroyed early on, resulting in an insufficient amount of monitoring data.

The average rate of downslope movement is 25 mm/year and 40 mm/year for the Harrowby and St-Lazare sites, respectively. The valley sites are considered to be a very slow moving landslide (16 mm/year to 1.6 m/year) based on classification system develop by Cruden and Varnes (1996). Although considered to be very slow moving, the potential degree of damage to infrastructure is expected to be moderate based on work completed by Mansour et al. (2011) as shown in Figure 2-2. Cruden and Varnes (1996) classification system includes very rapid landslides (such as rock falls, and mud flows) within the system which has broadened the range of ground movement rates and has resulted in slow moving landslides being categorized with rates between 1.6 m/year to

160 m/year. These “slow” rates are considered to be moderate to fast moving for the types landslides that can occur in Manitoba. In this regard, the Cruden and Vanes (1996) classification for very slow moving landslides (16 mm/year to 1.6 mm/year) has been re-classified as representative of *slow moving* landslide movements within Manitoba in this thesis research.

The monitoring pins decreased in elevation an average of about 12 mm/year to 14 mm/year for the Harrowby and St-Lazare sites, respectively. The measured decrease in elevation is result of either translational landslide ground movements or rotational landslide ground movements or a combination thereof.

Slow moving landslides warrant further attention because of the potential for pipeline damage due to cumulative ground displacements over time (D.G. Honegger Consulting *et al.*, 2009). In historical landslide areas, ground movements tend to be slow following a first time failures, but moments of relatively rapid movements know as “surges” have occasionally occurred in many slow moving landslides (Baum 1998). It has been inferred from D.G. Honegger Consulting *et al.*, 2009 that slow moving landslides (including the occurrence of surges) do not necessarily lead to full reactivation of a landslide which is supported by the monitoring results in this thesis.

## **6.2 Temperature**

Ground temperatures measured ranged between lows of about -1°C to 2°C to highs of 12°C to 15°C depending on the research site (Figures 5-14 to 5-18). Only one site (Harrowby top of valley) measured temperatures below 0°C on two occasions, in 2012 for about a month and 2014 for about four months (Figure 5-17). The freezing

temperatures measured were only slightly below 0°C with minimum temperature of about -1°C for a short duration, likely not sufficient in magnitude and duration to freeze the ground in the vicinity of the pipe. Therefore, the ground in vicinity of the buried pipe does not freeze at the research sites and stresses induced on the pipe due to freezing was not examined in the research.

Pipe temperatures (outside of the pipe) mimic ground temperatures usually within  $\pm 1^\circ\text{C}$ . Higher initial temperatures were recorded while the shrink sleeve tape around the instrumentation was being heated during installation. Freezing temperatures on a pipe were recorded once for about two and half months at the Harrowby Top of Valley set-up with a recorded minimum temperature of  $-0.4^\circ\text{C}$  during that time (Figure 5-17).

At Plum River, several notable temperature changes and trends occurred as a result of the pipe being abandoned (Figure 5-14). The pipeline was cut about 50 m south of the pipe instrumentation (Plum River beyond the crest). A temperature drop was measured prior to the pipeline being cut, suspected to be due to pipeline being exposed to cold temperatures at the cut point and some cooling of the interior of the pipeline likely occurred through the open end of the pipe. Once the pipe was cut, the pipe and ground temperatures are virtually identical since there was no product flowing through the pipe influencing the pipe temperature.

### *6.2.1 Axial Pipe Stress due to Thermal Expansion*

The calculated axial stresses at the sites include a component of stress due to thermal expansion and contraction of the pipeline. These stresses have been removed from the axial stress data to determine axial stresses that may be attributed to landslide related

ground movements (Section 6.3.3). Thermal axial stresses can be calculated using the following equation:

$$\sigma_T = E\alpha(T_2 - T_1) \quad \text{eq. 6.1}$$

Where:

$\sigma_T$  = axial stress due temperature differential, MPa

$E$  = Young's modulus of steel, 207 GPa

$\alpha$  = coefficient of thermal expansion of steel,  $12 \times 10^{-6}$  m/m/°C

$T_2$  = measured pipe temperature, °C

$T_1$  = initial pipe temperature, °C

The thermal axial stress calculated using eq. 6.1 can be conservative since the equation assumes the buried pipe is of sufficient length where the soil-pipe interaction fully restricts the pipe (American Lifelines Alliance and American Society of Civil Engineers, 2001). Under these conditions, when the pipe temperature increases above the initial temperature at installation, the pipe material will try to expand, elongate along its length. But this movement is restricted by the soil holding on to the outside of the pipe by adhesion. This results in axial compressive stresses within the pipe member due to thermal changes (positive  $\sigma_T$ ).

At the research sites, the calculated thermal axial stress tended to be tensile in nature since the initial temperature at the start of monitoring ( $T_1$ ) was at or above the measured

pipe temperatures ( $T_2$ ). Therefore, the axial stresses that may be due to ground movements are for the most part lower than the measured axial stresses once the thermal expansion/contraction of the pipe is considered. Figure 6-1 plots an example of both the axial stresses measured and the axial stresses with the thermal stresses removed *versus* time and season for the valley sites set-ups.

The thermal effects on the pipe have resulted in a cyclic measured axial stress profile for all the sites with axial stress increasing in the fall/winter and decreasing in the spring/summer as shown in Figure 6-2 to Figure 6-4. Without the thermal stress, axial stresses at the research sites reduce by as much as 40 MPa resulting in many of the monitored locations showing axial stresses in and around zero suggesting little to no axial load is applied to the pipelines that maybe attributed to landslide movements. The axial stresses without thermal effects plotted does include the axial component of hoop stress ( $\nu\sigma_h$ ). However, the axial component of hoop stress is very low (less than a maximum of 1.5 MPa) and therefore, the axial stresses profile without thermal effects is essentially unchanged when removing the axial component of hoop stress.

The measured strains would have been drastically different if the pipe instrumentation was installed at colder temperatures and would be in general, compressive in nature if the initial pipe temperature was around 0°C. Also, the axial stress-state in the pipe prior to monitoring would be strongly influenced by the temperature at the time the pipeline was installed. The pipelines at the research sites were installed in the summer (Harrowby), Fall (St-Lazare) and winter (Plum River).

## 6.3 Pipe Stresses

### 6.3.1 Backfilling

An unexpected outcome of the monitoring is the magnitude of longitudinal pipe stresses induced on the pipelines due to backfilling of the excavations required to install the instrumentation. The excavations were sufficient in size and depth to safely install the pipe instrumentation. In general, the excavations were 1.5 to 3 m deep extending below the pipeline and tended to be 5 to 10 m wide at ground surface. Material excavated was used as backfill and the backfilling method consisted of placing material carefully around and beneath the pipe with an excavator. The material was compacted with the back of the excavator bucket and great care was taken to compact the material beneath the pipe as much as practically possible without risking damage to the pipe. The backfill above the pipe was not compacted until sufficient cover was placed (about 1 m) before the backfill was lightly compacted.

During installation of the first monitoring set-up at Plum River, the DA system was programmed to monitor pipe instrumentation every 10 minutes as a check to ensure the instrumentation was recording properly while the instrumentation was being wired into the DA. This check occurred while the excavation was being backfilled and the DA captured the strain change induced on the pipe during backfilling. The recorded strain data showed a large calculated downward bending stress (165 MPa) was induced on the pipe during backfilling. Consequently, backfilling was monitored for the remaining set-ups. Overall, backfilling induced strains on the pipe were measured at each of the set-ups with bending being the larger induced stress when compared to axial and torsion. Torsion

due to backfilling tended to be negligible or small when compared to other longitudinal pipe stresses. These backfill pipe stresses have either maintained levels, somewhat decreased, or have been released completely over the four years of pipeline monitoring. The largest backfill strains were measured at the middle of the valley at Harrowby and it appears these stresses have “locked-in” with calculated bending, axial, and shear backfill stresses of 170 MPa, 60 MPa, and 100 MPa, respectively.

These backfill stresses only occur at the set-up locations and when including residual backfill stresses in the probability analysis, would not reflect the actual stresses induced on the pipe beyond the set-up locations. In this regard, pipeline reliability calculations in this research will include and exclude backfill stresses.

### *6.3.2 Stress Relaxation After Pipeline Abandonment*

The gas pipeline at Plum River was cut and abandoned on December 17, 2012 and gas service was switched over to a new pipeline installed using directional drilling methods under the river. The gas pipeline was cut at a valve about 50 m back from the pipe instrumentation (beyond the crest set-up). Gas pipelines have been known to visibly move immediately after being cut based on discussions with Manitoba Hydro personnel. Prior to cutting the pipe, the monitoring interval was switched on the DA from one hour to one minute to capture any strain changes due to relaxation of the pipe. The monitoring results indicate there was little to no change in stress due to the pipe being cut and therefore any insight into the stress-state of the pipe prior to being instrumented was not realized.



At St-Lazare, a new pipeline river crossing was installed in the Summer/Fall 2013 with the switch over to the new pipeline occurring in August of 2015. The existing pipe was cut at the switch point, close to the river as shown on Figure 4-19. The St-Lazare bottom of valley was the closest monitoring set-up to the switch points, about 100 m away. Unfortunately, the monitoring results for one of the uniaxial gauges at this set-up contained noise at the time of the switch over. The monitoring noise would mask any strain release due pipe relaxation, unless the pipe relaxation resulted in changes in strain greater than the noise measured, which did not occur.

### *6.3.3 Ground Movements, and Environmental and Regional Affects*

Stain gauge monitoring data has revealed that changes in longitudinal pipe stresses (axial and bending) appear to be cyclic by season; spring, fall, winter, summer. Other environmental factors also seem to be influencing longitudinal pipe stresses such as changes in river levels at Plum River.

There also appears to be a connection with longitudinal stress changes at the valley sites on a regional scale, likely due to ground movements of the valley walls. Distinct changes in longitudinal stress over a short duration, particularly bending stress commonly occurs at roughly the same time at the two valley sites. Also, changes in longitudinal pipe stress over a longer duration (days and weeks) occurred at roughly the same time between the valley sites on several occasions and are referred to as notable changes in pipe stress. The nature of the distinct and notable changes in pipe stresses were either increases or decreases in axial tension or downward bending occurring separately or in several different combinations. These distinct and notable changes in longitudinal pipe stress are

either related to landslide ground movements or an unknown soil-pipe interaction mechanism is allowing the pipe to move within the soil mass releasing stresses. Of note, on several occasions monitored stress profiles shown distinct or notable decreases in downward bending and axial tension either stayed the same or decreased resulting a release of longitudinal stresses. This soil-pipe interaction mechanism is referred to as soil-pipe relaxation in this research and it is important to recognize that this pipeline response is within the elastic range of the structural pipe member and the soil-pipe relaxation observed is not due to plastic deformation of the pipeline. Hypothetical mechanisms that may be causing the soil-pipe relaxation observed are discussed in Chapter 8. Distinct and notable changes in pipe stress are discussed in detail for each site in Sections 6.3.3.1 to 6.3.3.3. The environmental and seasonal affects are also discussed in these sections.

Changes in longitudinal pipe stresses (axial and bending) can be indicators that landslide induced ground movements are causing pipe stresses, especially if the changes are distinct. The landslide ground movements measured at the valley sites are slow and assumed to be translational and/or rotational based on the valley slope geometry, ground pin monitoring results, failure depths of the SI's, and presence of ancestral large slump blocks which are the result of rotational type movements. At the Plum River site, ground movements were not measured, but landslide movements may still be occurring, and are assumed to be mostly rotational with the possibility of translational movements based on the failure depth of the SI, and a visual assessment of the remnants of past instabilities.

Bending and axial pipe stresses are plotted for each site with time and the seasons for comparison purposes. This allows for interpretation of trends related to pipeline

behaviour and changes in longitudinal stresses that may be attributed to ground movements (Figure 6-2 to 6-4). The axial stress profile without thermal effects have also been plotted with time and the seasons and included in the figures. Pipe torsion monitoring results have been excluded from the figures since pipe torsion is not as sensitive to ground movements when compared to longitudinal stresses, thus making it difficult to infer possible changes in torsion (shear stress) due to ground movements. Also, pipe torsion monitoring results are not fully discussed since the monitoring data set for pipe torsion is not complete (no torsion gauge at Plum River beyond the crest) or the data had to be heavily filtered.

Initially, the research intent was to compare/link pipe monitoring results to measured landslide ground movements between survey events to distinguish periods where notable ground movements occurred and then associate these movements with changes in pipe stress. Unfortunately, this comparison cannot be made given the amount of scatter in the ground monitoring pin survey data between individual surveys. Pipe stresses likely due to distinct or slow moving ground movements can therefore really only be inferred from the pipe stress profiles for axial and bending based on the understanding of how the buried pipeline is expected to respond to ground movements. This is done knowing, overall, ongoing ground movements are occurring at the annual rates measured at the two valley sites.

The monitored pipeline indirectly acts like a ground monitoring instrument that can identify subtle changes in applied strains because of the sensitive nature of strain gauges. Changes in pipe strains and thus calculated stresses are a result of the pipeline deforming in response to soil displacements of the surrounding backfill soil. These soil

displacements around the pipeline can be attributed to either landslide related ground movements or other soil-pipe interactions (soil-pipe relaxation). The following sections discuss the pipeline behaviour and changes in axial and bending stress that could be attributed to either landslide related ground movements or other factors such as soil-pipe relaxation. Distinct changes in pipe stress identified in the stress profiles (axial and bending) assumes sudden ground movements, potentially a “surge”, may be occurring while notable changes in longitudinal pipe stresses assume slower rates of ground movements may be occurring.

#### 6.3.3.1 Plum River

Figure 6-2 plots bending and axial stress profile with time and the seasons along with axial stresses without thermal effects. The pipe stress profile for the beyond the crest and along the slope set-up locations show similar trends.

During the spring floods of 2013 and 2014, a notable decrease in downward bending was measured at both monitoring locations. An increase in downward bending under the weight of floodwaters would be expected, especially for the along the slope monitoring point which is situated in about the middle of the riverbank slope.

The axial stresses beyond the crest and along the slope have essentially, identical trends where axial tension stress increased throughout the summer until the end of winter and decreased in the spring until early summer, mostly due to axial thermal effects. Axial tension stress appears to be increasing during the flood of 2013 and 2014. This is opposite to the downward bending stress profile which decreased during the floods.

The cause of changes in axial and bending stress during flood events is unknown, but what can be inferred is that river levels appear to be affecting pipe stresses, in particular during spring floods.

#### 6.3.3.2 St-Lazare

The axial and bending stress profiles with time exhibit similar magnitudes and trends between the three set-up locations at St-Lazare. Figure 6-3 plots bending, axial (measured and without thermal effects) with time and seasons.

The bending stress profiles are the most similar between the top and middle of the valley locations. At these locations, the bending stresses were relatively constant through the fall and winter. Downward bending increased in the spring into summer and then decreased between the summer and the fall.

A distinct change in bending stress has occurred at a least on set-up location each spring at essentially the same time as noted on Figure 6-3 and sometimes occurred in conjunction with an increase in axial tension. These distinct changes in longitudinal pipe stresses are either related to landslide ground movements or other mechanisms. The duration of these distinct changes can be as little as a few days or up to a couple of weeks. In general, the distinct changes in bending stress starts sometimes with a sharp increase in downward bending (likely due to landslide ground movements) followed by a sharp decrease in downward pipe bending (landslide movements or soil-pipe relaxation), and then followed by an increase downward bending usually over longer duration (weeks or months). A few other distinct changes in bending stress have occurred as noted on Figure 6-3 at the middle of the valley. Other notable changes in bending stress occurred

at this location for the last year of monitoring, but these changes in stress may be due to the construction activities which occurred close to middle of valley set-up during that time and may not be a result of ground movements. In addition, one of the uniaxial strain gauges contained noise for approximately six months within the last year, and the filtered axial and bending stress profiles may not accurately capture distinct stress changes as the filtering process attenuates both noisy and real data.

The bending stress profile for the bottom of the valley constantly increased for about two and half years (downward bending) until there was a distinct decrease in downward bending stress in the spring of 2014. This distinct change in stress also coincides in time with distinct changes in bending stress at the middle and top of the valley

The axial stress profile is strongly influenced by temperature change (thermal effects) of the steel pipe and the axial stress profile reflects this with increasing axial tension as the temperature decreases and decreasing axial tension with increasing temperature.

The axial stress profile changes when the thermal effects are removed as illustrated in the bottom plot of Figure 6-3. Axial stresses were generally constant for the first two years of monitoring. The distinct changes in bending stress observed did not translate into distinct changes in axial stress during this two year period. Distinct changes in axial stress in conjunction with changes in bending started to occur after September 2013 on a few occasions as noted on Figure 6-3. The distinct changes in axial stress were opposite to the changes in bending, *i.e.* a distinct decrease in downward bending with an increase in axial tension.

### 6.3.3.3 Harrowby

As with St-Lazare, the axial and bending stress profiles with time exhibit similar magnitudes and trends between the three instrumented locations at Harrowby. Figure 6-4 plots bending, axial (measured and without thermal effects) with time and the seasons.

Bending stresses were relatively constant through the fall and winter. Downward bending increased in the spring into summer and then decreased between the summer and the fall for the top and middle of the valley locations. This bending stress behaviour is consistent with the bending stress trends measured at St-Lazare at the top and middle of the valley locations where distinct changes in bending stress typically occurred each spring as noted on Figure 6-4.

The strain gauges at the bottom of the valley only became operational about two years after installation in July of 2013 and, as such, the bending stress profile with time is only available for a little over two years. The bending stress profile at the bottom of the valley increased through the summer and winter (downward bending) and decreased starting in the spring of 2014 and continued to decrease in general until the end of monitoring in August 2015.

Distinct changes in bending stress have occurred at a least one set-up location each spring, similar to St-Lazare. During the first two springs (2012 and 2013), distinct changes in bending stress occurred at the top and middle of the valley while during the spring of 2014, distinct changes in bending stress occurred at all three monitoring locations. During the spring of 2015, a distinct change in bending only occurred at the top of the valley set-up.

The axial stress profiles are strongly influenced by the temperature change except for the middle of the valley location where the axial stresses due to backfilling appear to be “locked-in”. The axial stress profiles without thermal effects at each set-up was generally constant or increased (increased tension) slightly between periods of distinct changes in axial stress at all three monitoring locations.

Distinct changes in axial stress occurred during the first two springs at the same time distinct changes in bending stress were also measured. At the middle of the valley, the axial tension stress increased while the downward bending stress increased and/or decreased in the first two springs (2012, 2013). This behaviour is consistent with bending and axial stress changes that occurred at St-Lazare. However, the opposite trend was observed at the top of valley where distinct decreases in axial tension occurred in the first two springs while the downward bending stress increased and/or decreased. A distinct change in axial stress also took place between June 18th and July 7th, 2013 at the top and middle of the valley, but were opposite in nature.

#### *6.3.4 Distinct Changes in Stresses at the Valley Sites*

Distinct changes in longitudinal pipe stress over a relatively short duration of time (a few days to a few weeks) have occurred at both valley sites during the spring seasons. Sometimes these distinct changes exhibit increased downward bending which is suspected to be due to landslide related ground movements or decreases in downward bending caused by either landslide movements or other soil-pipe interaction mechanisms. A soil-pipe interaction mechanisms may be causing release of pipe stresses, particularly in bending and these possible mechanisms are discussed in Chapter 8.



Table 6-2 summarizes the dates where distinct changes in bending stress occurred between the two valley research sites for the various set-up locations. It appears that distinct changes in bending stress occur every spring at roughly the same time between the two valley sites. Figure 6-5 plots the bending stress profile with time and seasons for both sites and notes when distinct changes in stress occur at both valley sites, typically each spring. Other notable changes in bending stress, but necessarily distinct, which occur at both valley sites are also noted on Figure 6-5. The closeness in time between when these changes in bending stress occurs between the two valley sites also suggest that ground movements may occur on a regional scale and are not limited to local conditions specific to a particular location.

#### **6.4 Pipe Push Tests**

Soil-pipeline adhesion influences the axial response of a pipeline. In particular, the axial stress in the pipeline may be limited to a maximum value if stresses at the soil-pipe interface are at or exceed the maximum soil-pipe adhesion, resulting in pipe slippage. Gradual and distinct decreases in axial tension strains were measured at the research sites and may be due to pipe slippage. It is important to determine if the axial stress profile is limited to the maximum pipe adhesion being achieved and pipe slippage is occurring. The results of the pipe push tests in combination with a simple finite element model were used to estimate the stresses that may be occurring at the soil-pipe interface based on the maximum monitored axial pipe stress at each site to determine if pipe adhesion is exceeded.

The adhesion factors from the push tests compared well with published experimental adhesion results (D.G. Honegger Consulting *et al.*, 2009) as shown on Figure 6-6. The pipe push test results compare best with the  $\sigma'_v = 40$  kPa overburden relationship developed by Cappelletto *et al.*, 1998 plotted on Figure 6-6 and this relationship is used to estimate the maximum soil-pipe adhesion stress at the research sites.

Undrained shear strength data of the *in-situ* pipe backfill is limited at the research sites. This is a result of a limited amount of good quality shallow soil samples obtained during the sub-surface investigation. Most of the soil samples retrieved were of poor quality and were not suitable for undrained shear strength testing. The undrained shear strength data available consists of one test on *in-situ* soil at a 3 m depth at the Harrowby site and undrained test results from reconstituted soil samples conducted on bulk samples of pipe backfill at the valley sites. The ratio of *in-situ* to reconstituted undrained shear strength is 0.61 based on two tests which was used to estimate the *in-situ* undrained shear strength at Plum River and St. Lazare (Table 6-3). Using the undrained strength data, the maximum adhesion value was estimated from Figure 6-6 for the research sites and the estimated values are included in Table 6-3. It is important to note that undrained shear strength, and therefore pipe adhesion, varies with changes in moisture and the measured moisture content of the backfill soil is assumed to be constant and not change over the monitoring period.

A simple finite element model (FEM) was developed to estimate the horizontal soil stress at the soil-pipe interface based on the highest axial pipe tension stress calculated from measured strain for each site. The estimated horizontal soil stress from the model can then be compared to the estimated maximum adhesion stress to determine if pipe slippage

is occurring at the sites. An idealized soil and pipeline section is used in the model as shown in Figure 6-7. The model consists of 10 m long portion of a pipeline (structural member) at a burial depth of 1 m. The pipeline structural properties were assigned to the structural member for each research site. A total stress constitutive model was used to represent the soil backfill and the Young's modulus of the soil was varied based on values consistent with the cohesive backfill soils present at the sites. A range of Young's modulus values was estimated using the equation presented by Bowles (1997) using the plasticity index ( $I_p$ ) of the backfill soil and the estimated undrained shear strength as follows:

Clay and Silty  $I_p > 30$  or organic

$$E = 100 \text{ to } 500S_u \quad \text{eq. 6.2}$$

Silty or Sandy Clay  $I_p < 30$  or stiff

$$E = 500 \text{ to } 1500S_u \quad \text{eq. 6.3}$$

A horizontal force was applied to one end of the pipeline within the model and adjusted until the average axial tension stress in the pipeline structural member matched the maximum axial pipe stress observed at each of the research sites. The boundary conditions in the model limited the pipeline movement to be horizontal and allowed for a shear zone to develop 0.3m on either side of the pipeline. The model requires strain compatibility between the soil and pipe, *i.e.* pipe slippage is not allowed, resulting in an upper bound prediction in horizontal soil stresses at the soil-pipe interface. The horizontal soil stress profile along the pipe was modelled for different Young's modulus values for

the maximum axial pipe stress observed at each site. Model output examples are presented in Figure 6-8 and Figure 6-9 showing pipe axial stress and horizontal stress at the soil-pipe interface along the 10 m long pipeline. Boundary effects can be seen to be affecting results at the ends of the pipeline. In this regard, the average axial pipe stress and average horizontal soil stress calculated ignored a 1m portion at each end of the pipe that were affected by boundary proximity in the numerical model.

Figures 6-10 to Figure 6-12 plots the modelled average horizontal soil stress along the pipe interface *versus* Young's modulus of the backfill for the three sites. The maximum estimated adhesion stress is also plotted on the figures. About half of Young's modulus values modelled predicted average horizontal soils stresses below the maximum adhesion at the Plum River and Harrowby sites. This suggests the pipeline at these two sites may or may not have slipped at the maximum axial tension stress observed. At the St-Lazare site, the predicted range of horizontal soil stress fell below the maximum adhesion stress and pipe slippage has likely not occurred based on the monitoring results.

## **6.5 Summary**

The monitoring data for the three research sites was assessed and interpreted with the following conclusions and observations:

- Ground pin movement is generally downslope and parallel to pipe alignment,
- Landslide movements at the valley sites is classified as slow (<50 mm per year) and could cause moderate damage to infrastructure,
- Soil in vicinity of the pipeline does not freeze,

- Pipe stresses due to pipe temperature changes dominate the axial stress profile, little to no axial stresses occurred without thermal effects,
- Insight into the initial stress-state of the pipeline prior to monitoring was not realized following two of the pipelines being cut,
- Backfilling around and below pipelines induce large stresses on the pipe which can either be “locked-in” or partially or fully released with time,
- A monitored pipeline using strain gauges acts like a sensitive ground movement monitoring tool,
- River levels affects measured longitudinal pipe stresses in riverbank areas,
- Distinct changes or notable changes in longitudinal pipe stresses are either due to landslide movements or a soil-pipe relaxation mechanism,
- Distinct changes in longitudinal pipe stresses occur at roughly the same time between the two valley sites, suggesting regional conditions affects pipe stresses,
- The adhesion factors from the push tests compared well with published experimental adhesion results.
- Soil-pipe adhesion may or may not have been exceeded during monitoring for the Harrowby and Plum River research sites and soil-pipe adhesion was likely not exceeded at the St-Lazare site. Therefore, pipe slippage may not be a possible explanation of distinct and notable decreases in monitored axial tension stresses.

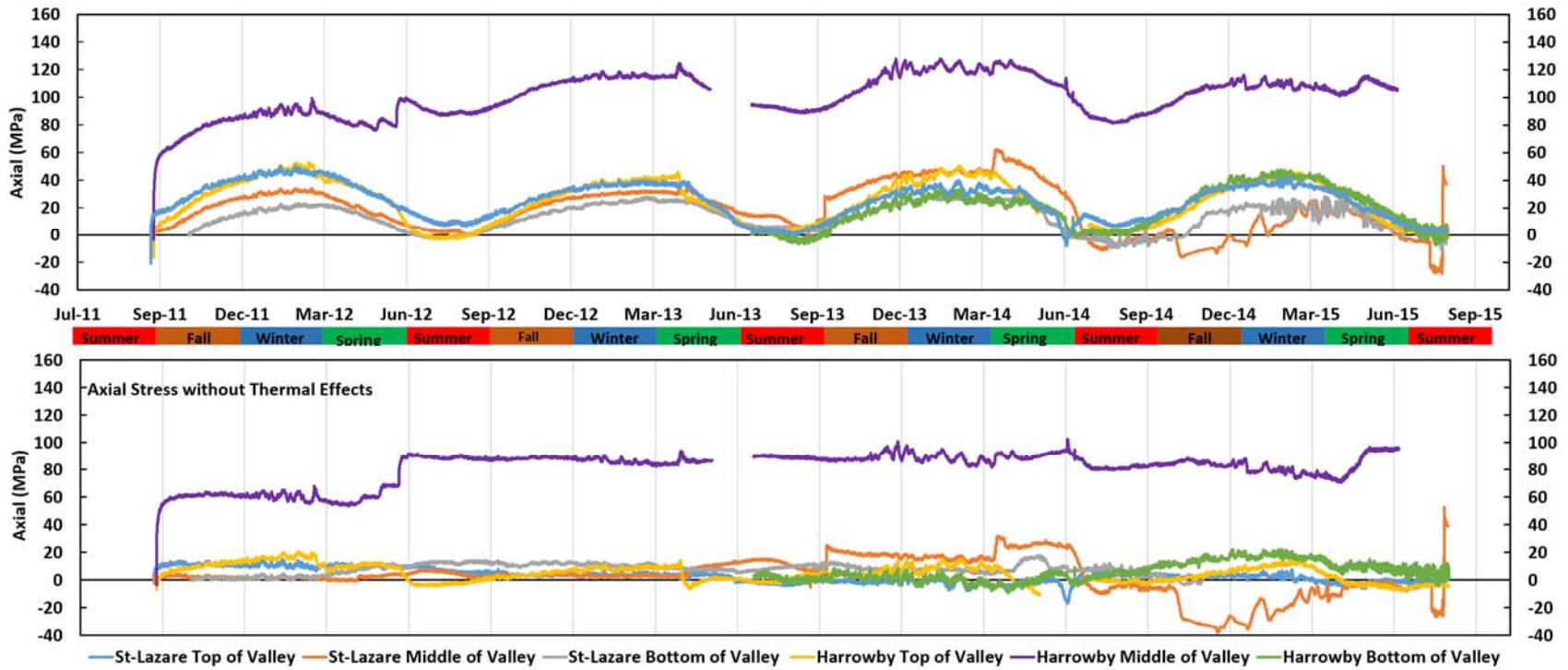


Figure 6-1 Calculated Axial Stress and Axial Stresses without Thermal Effects at the Valley Sites.

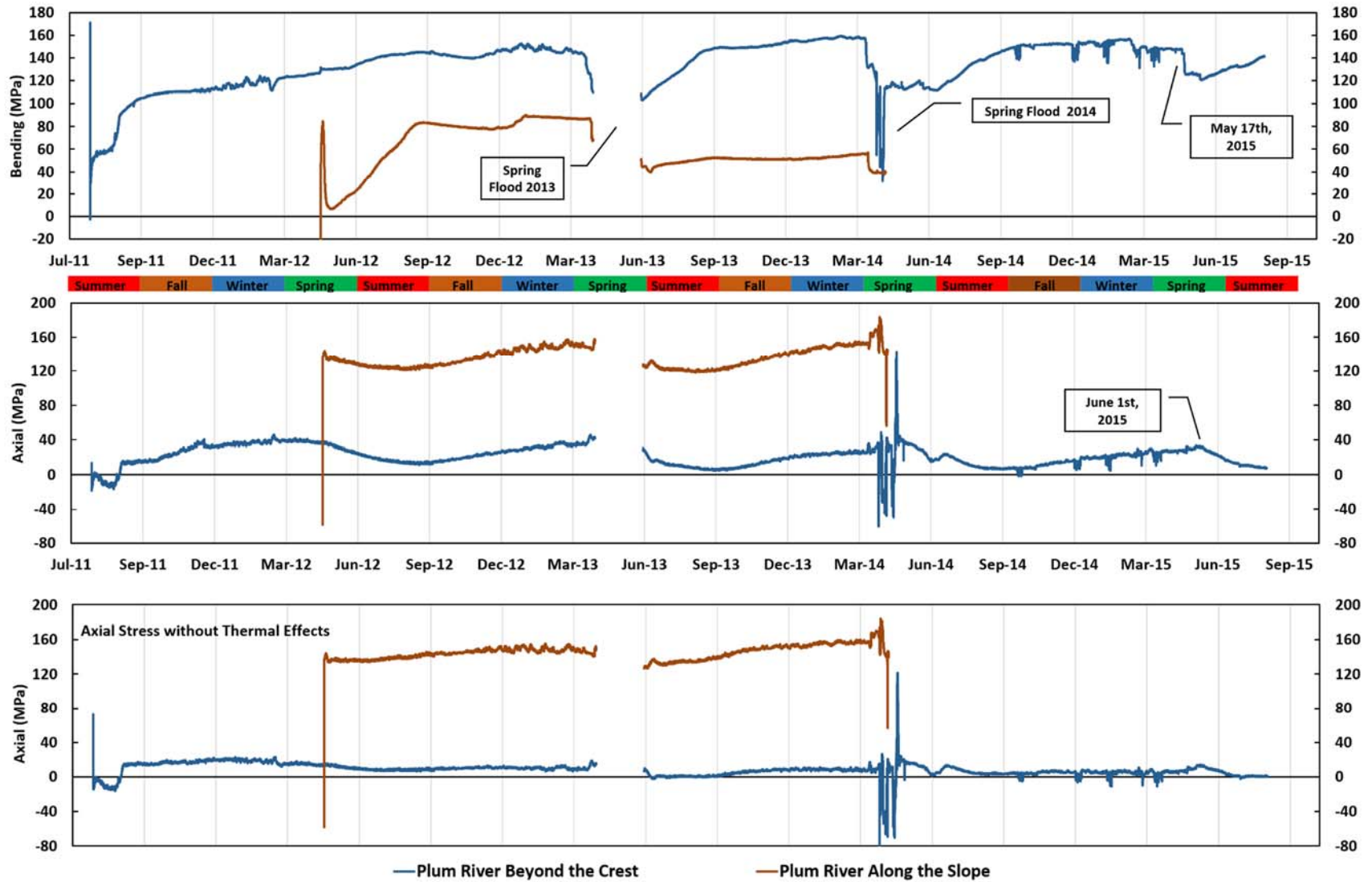


Figure 6-2 Plum River Bending and Axial Stresses with Time and Seasons.

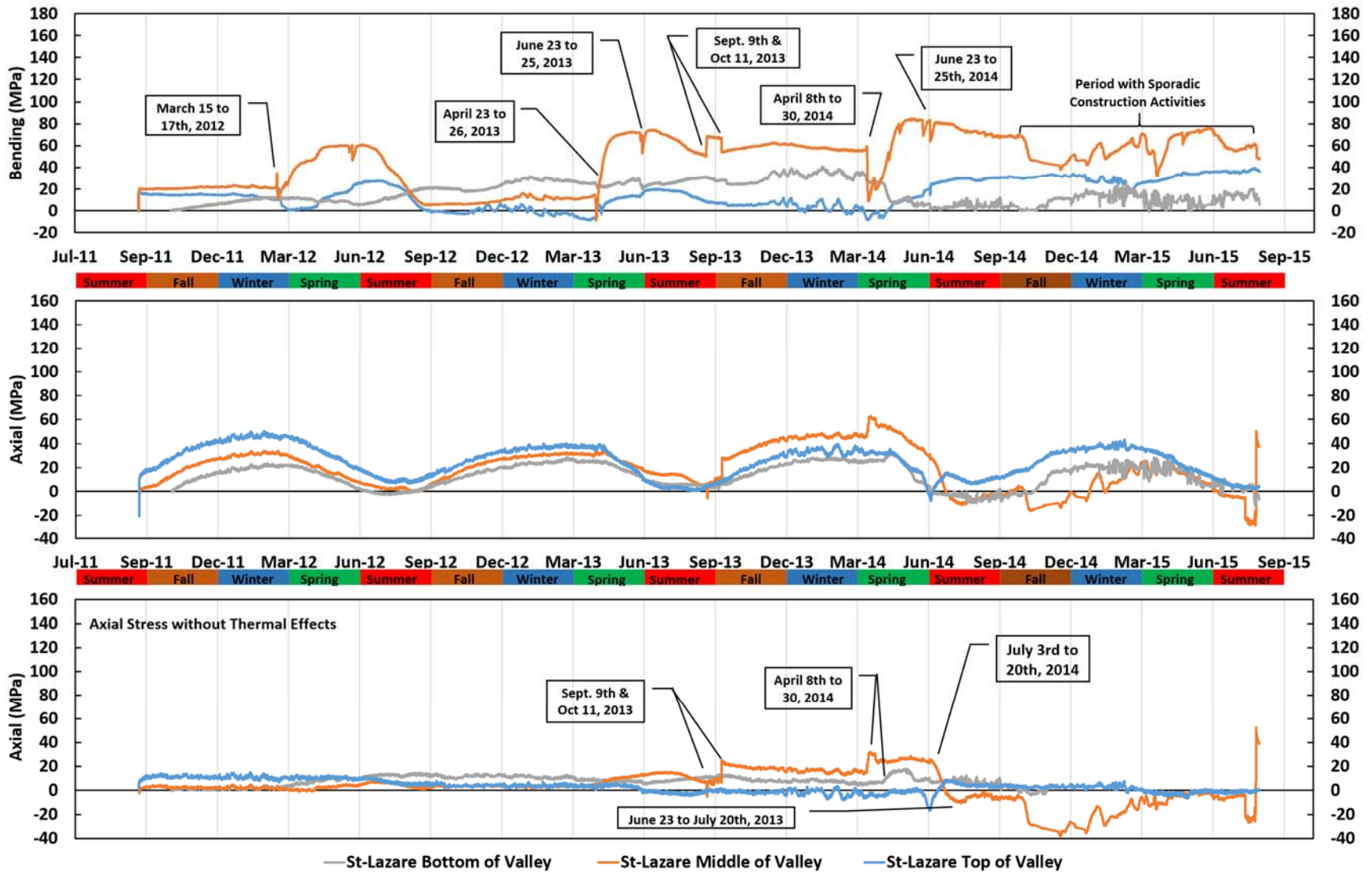


Figure 6-3 St-Lazare Bending and Axial Stresses with Time and Seasons.



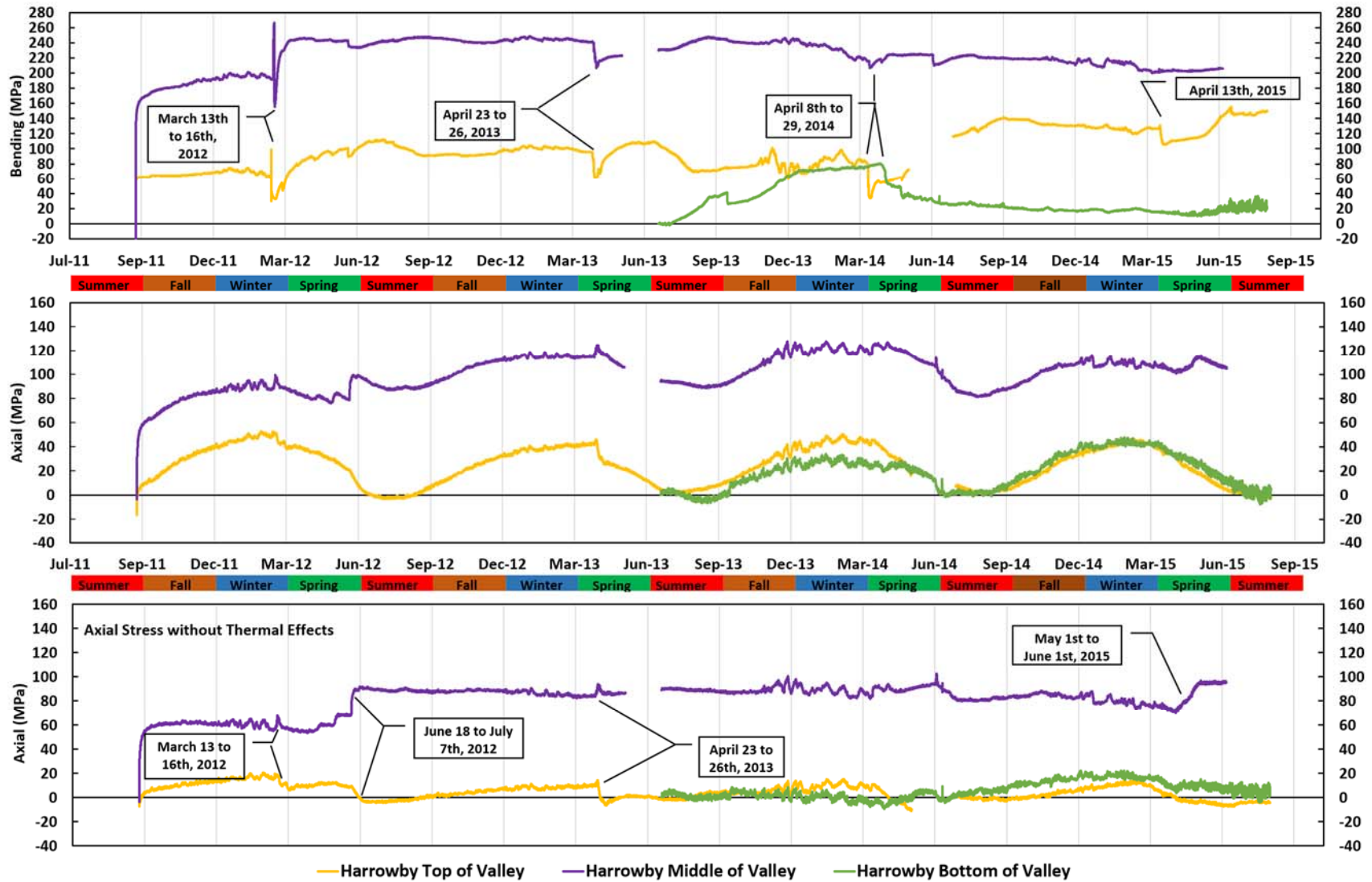


Figure 6-4 Harrowby Bending and Axial Stresses with Time and Seasons.

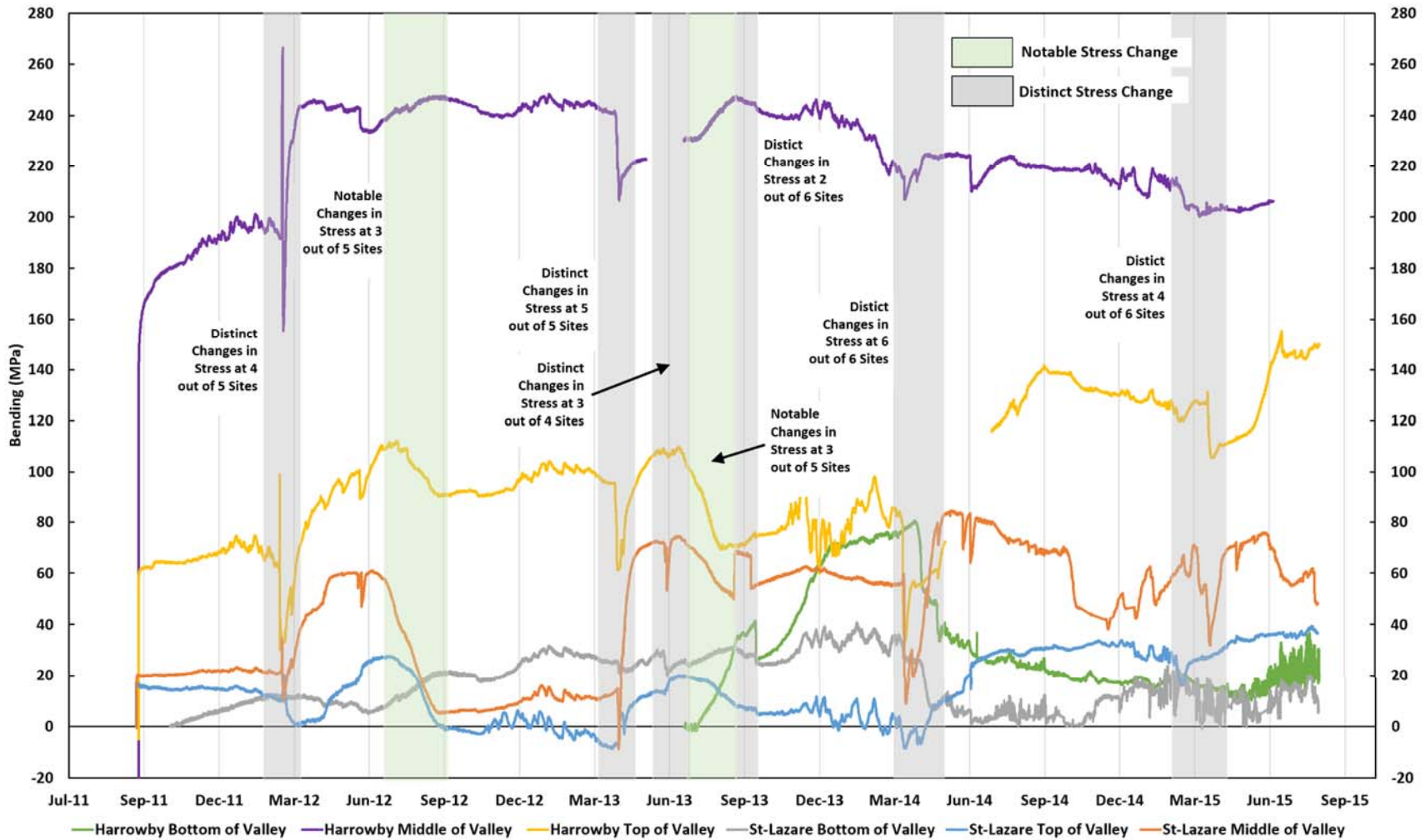


Figure 6-5 Bending Stress with Time and Season for the Valley Sites.

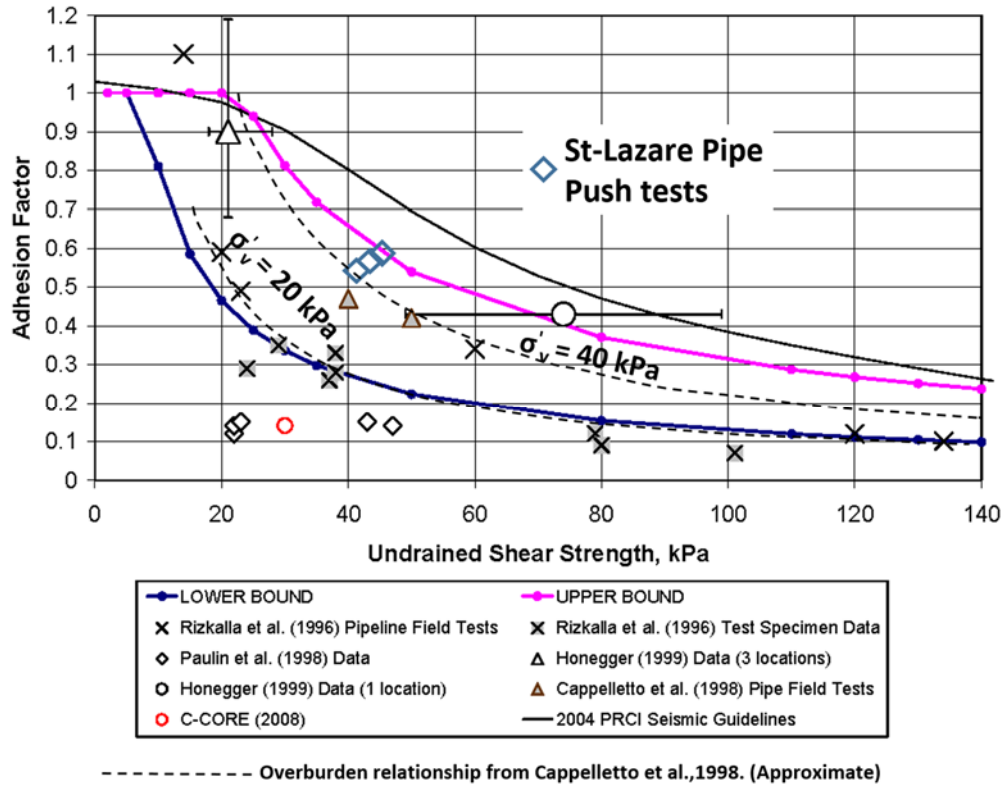


Figure 6-6 Comparison of  $\alpha$ -Su from St-Lazare pipe push test (modified from D.G. Honegger Consulting et al., 2009).

Risk to Gas Pipelines In Landside Areas  
 Pipe Adhesion Simulation  
 St-Lazare Pipe and Soil Properties  
 Backfill Young's Modulus (E): 10,000 kPa  
 File Name: St-Lazare 01.gsz

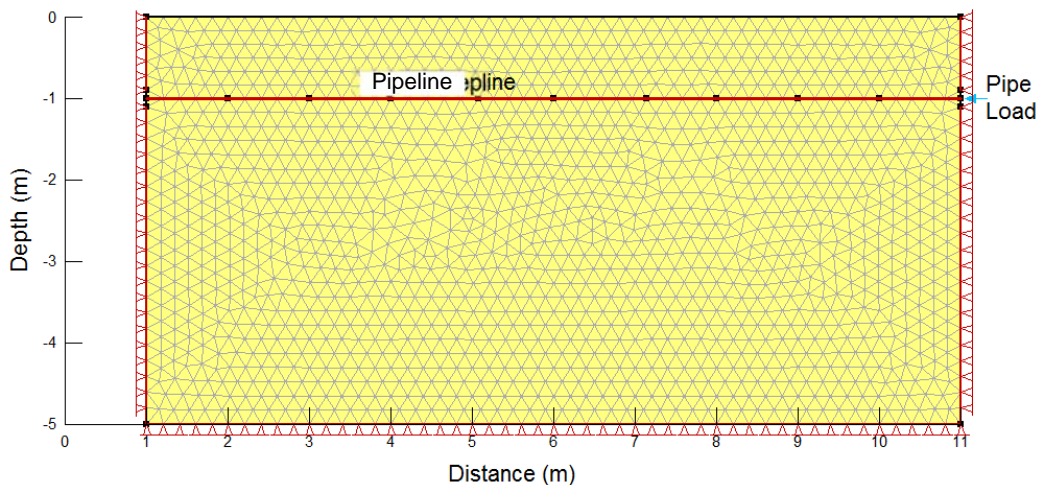


Figure 6-7 Example of Pipe Adhesion Simulation FEM Model Output.

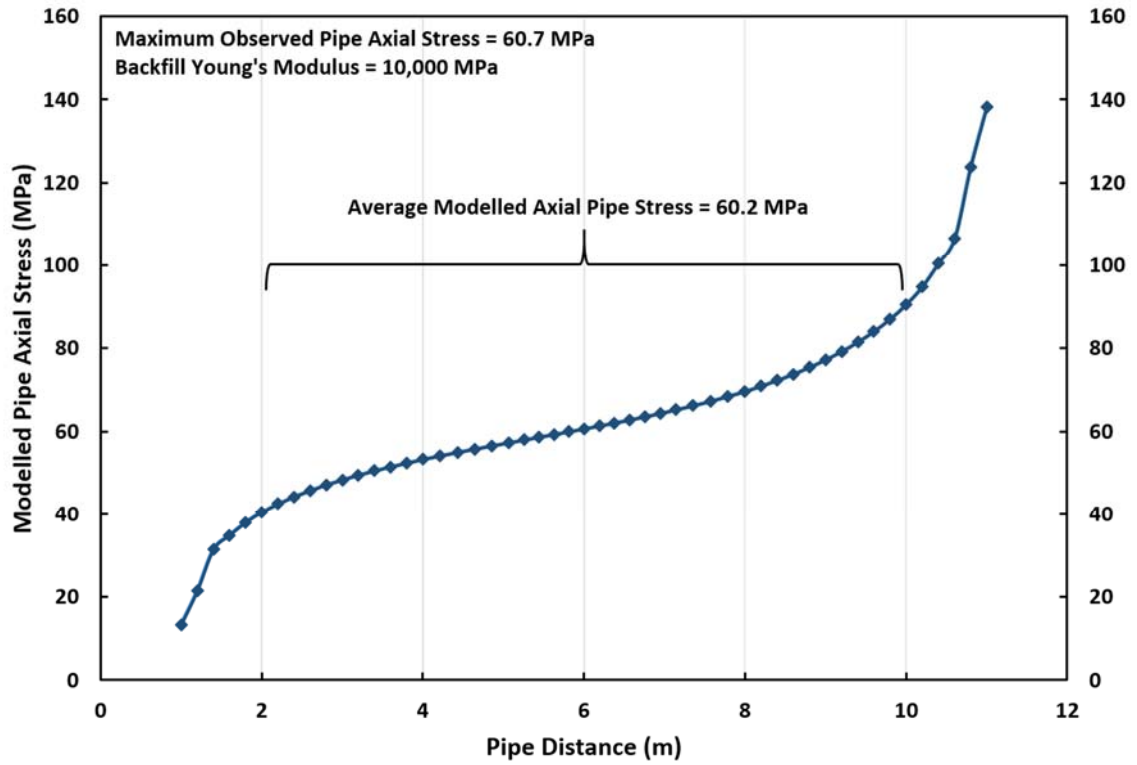


Figure 6-8 Modelled Axial Pipe Stress Along the Pipe for St-Lazare.

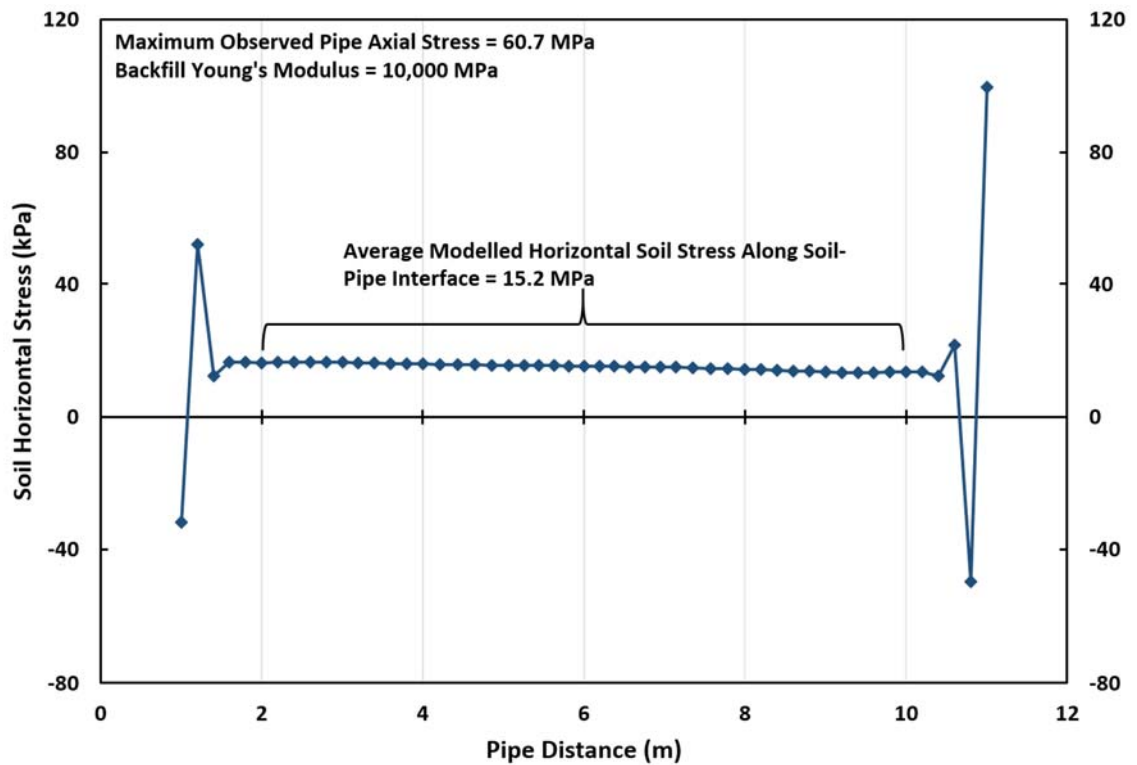


Figure 6-9 Modelled Horizontal Soil Stress at the Soil-Pipe Interface for St-Lazare.

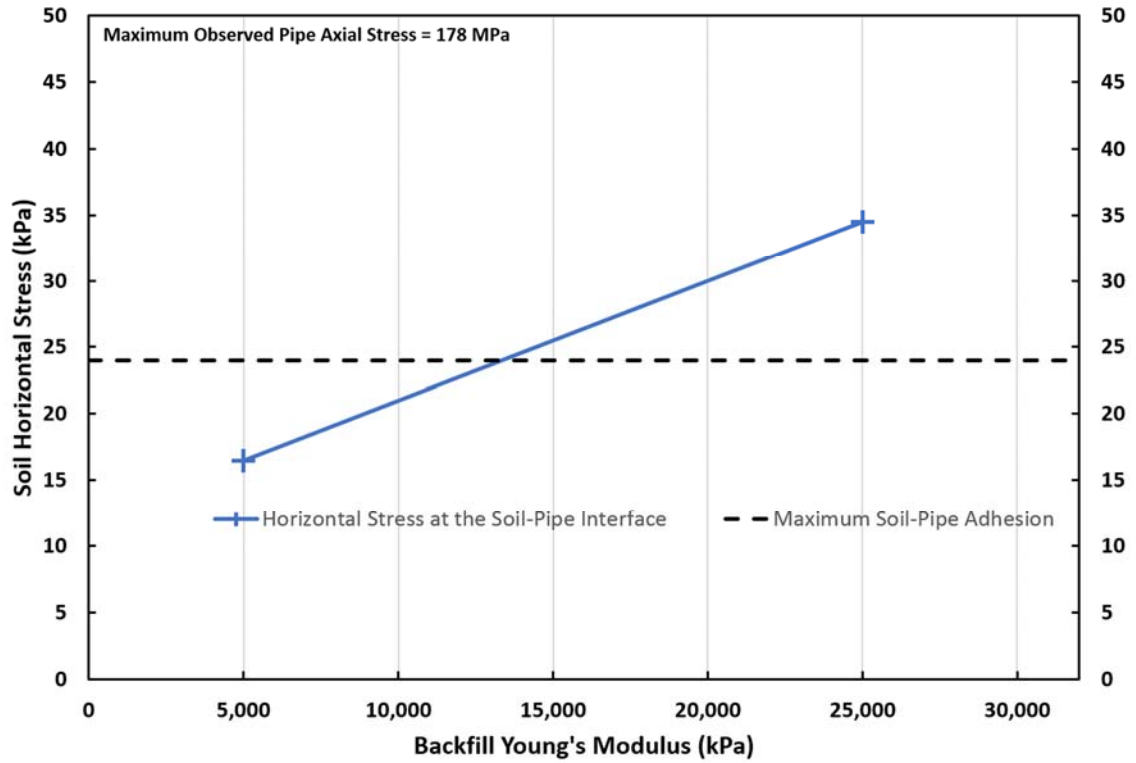


Figure 6-10 Modelled Horizontal Soil Stress *versus* Young's Modulus for Plum River.

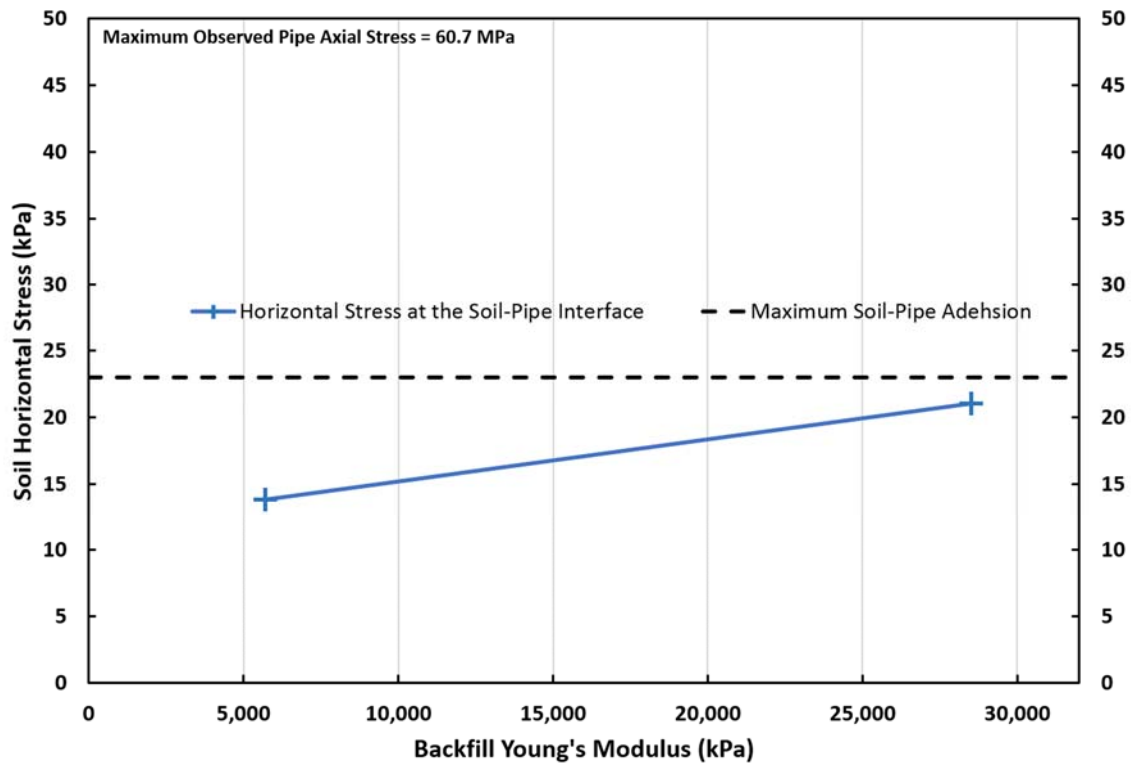


Figure 6-11 Modelled Horizontal Soil Stress *versus* Young's Modulus for St-Lazare.

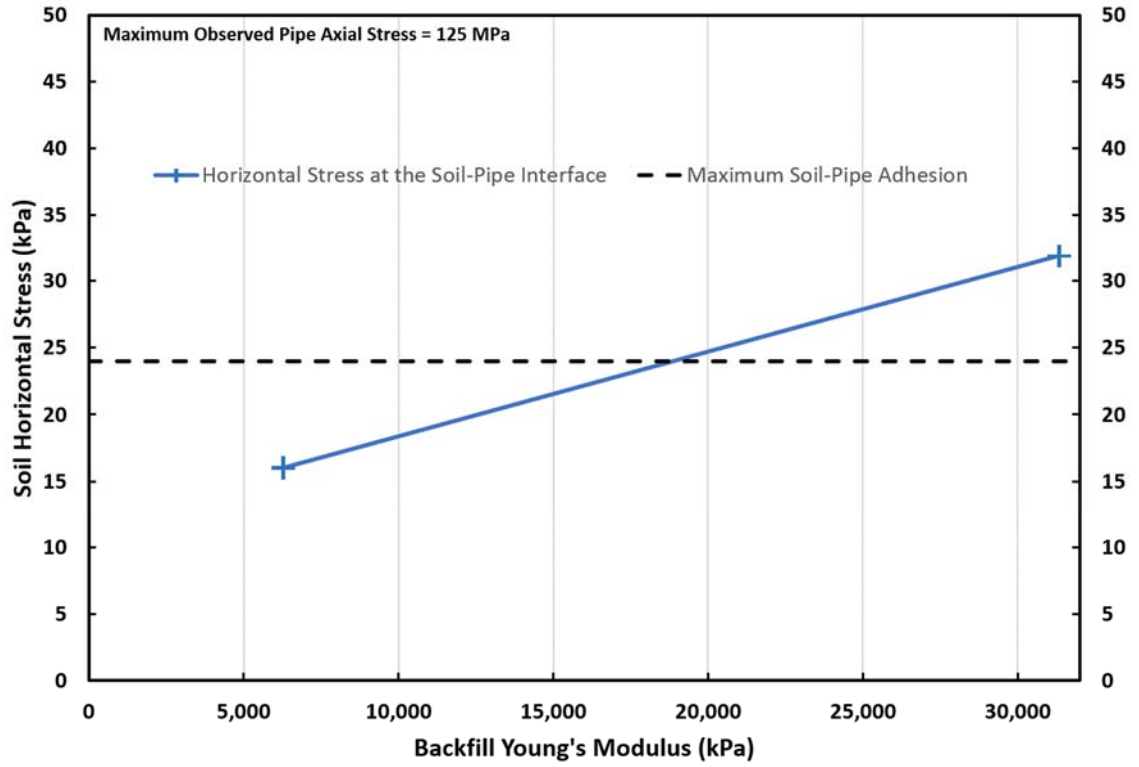


Figure 6-12 Modelled Horizontal Soil Stress *versus* Young's Modulus for Harrowby.

Table 6-1 Summary of Monitoring Pin Results for St. Lazare and Harrowby.

	Downslope Movement	(-) Change in Elevation	(+) Change in Elevation
<b>St-Lazare</b>			
Maximum (mm)	+582	-279	+26.0
Minimum (mm)	+17	-3	+21
<i>Average (mm)</i>	<b>+156</b>	<b>-56</b>	
Max. Rate (mm/year)	+137	-66	+11
Min. Rate (mm/year)	+4	-1	+10
<i>Avg. Rate (mm/year)</i>	<b>+40</b>	<b>-14</b>	
<b>Harrowby</b>			
Maximum (mm)	+236	-159	+35
Minimum (mm)	+17	-6	+4
<i>Average (mm)</i>	<b>+77</b>	<b>-36</b>	
Max. Rate (mm/year)	+56	-59	+16
Min. Rate (mm/year)	+8	-3	+2
<i>Avg. Rate (mm/year)</i>	<b>+25</b>	<b>-12</b>	

Note: (+) Downslope Movement/Increase in Elevation  
 (-) Upslope Movement/Decrease in Elevation

Table 6-2 –Distinct Changes in Bending Stress over Relatively Short Durations (Valley Sites).

Dates	St-Lazare			Harrowby		
	Top	Middle	Bottom	Top	Middle	Bottom
March 13 <sup>th</sup> to 17 <sup>th</sup> , 2012*	Mar 17 <sup>th</sup>	Mar 15 <sup>th</sup>	-	Mar 13 <sup>th</sup>	Mar 16 <sup>th</sup>	n/a
April 23 <sup>rd</sup> to May 1 <sup>st</sup> , 2013*	Apr 26 <sup>th</sup>	Apr 23 <sup>th</sup>	Apr 1 <sup>st</sup>	Apr 24 <sup>th</sup>	Apr 26 <sup>th</sup>	n/a
June 23 to 25 <sup>th</sup> , 2013	Jun 25 <sup>th</sup>	Jun 23 <sup>th</sup>	Jun 23 <sup>th</sup>	-	-	-
September 25 <sup>th</sup> to October 11 <sup>th</sup> , 2013	-	Sept 25 <sup>th</sup> and Oct 11 <sup>th</sup>	-	Oct 11 <sup>th</sup>	-	-
April 8 <sup>th</sup> to 30 <sup>th</sup> , 2014	Apr 16 <sup>th</sup>	Apr 9 <sup>th</sup>	Apr 8 to 30 <sup>th</sup>	Apr 8 <sup>th</sup>	-	Apr 25 <sup>th</sup>
March 5 <sup>th</sup> to April 16 <sup>th</sup> , 2015	Mar 5 <sup>th</sup> to 13 <sup>th</sup>	Mar 30 <sup>th</sup> to Apr 16 <sup>th</sup>	noise	Apr 13 <sup>th</sup>	Mar 9 <sup>th</sup> to 24 <sup>th</sup>	-

- No distinct or sudden changes in bending stress occurred close to the dates noted

\* Distinct changes in bending stress occurred days apart at both valley sites



Table 6-3 Maximum Pipe Adhesion Estimates

	Estimated Undrained Shear Strength, $S_u$ , (kPa)	$\sim$ Adhesion Factor <sup>1</sup>	Maximum Adhesion Stress (kPa)
<b>Plum River</b>	50*	0.42	21
<b>St-Lazare</b>	57*	0.40	23
<b>Harrowby</b>	63	0.38	24

<sup>1</sup> Based on  $\sigma'_v = 40$  kPa overburden relationship from Figure 6-6

\* Estimated undrained shear strength of pipe backfill

## **Chapter 7 Statistical Analysis and Probability of Pipeline Failure**

### **Estimates**

The statistical analysis completed at the three research sites is presented in this chapter. The probability of pipeline failure was calculated for various limit states failure modes and compared to the target probability of failures to determine if limit states target reliability values are exceeded at the research sites. Manitoba Hydro provided information on their pipeline network which was examined to determine if limit states are exceeded for different pipeline sections assuming these pipelines may be subjected to slow moving landslides and the results are presented herein.

#### **7.1 Limit States Reliability Targets**

CSA Z662-15 specifies limit states reliability targets ( $R=1-P_f$ ) for gas pipelines. The onshore gas pipeline industry has recently begun to shift to this approach where the probability of failure of a pipeline shall not exceed a target probability of failure based on an acceptable failure rate (Porter *et al.*, 2004).

##### *7.1.1 Ultimate Limit States Reliability Targets*

Ultimate limit states reliability risk targets are calculated based on potential loss of life due to a gas pipeline failure (per km-yr) within a zone of influence. The zone of influence, also referred to as assessment area is related to the size and operating pressure of the gas pipeline. These targets were developed based on known acceptable risk levels for individuals and society (Nessim *et al.*, 2004) as discussed in Section 2.2.

CSA Z662 defines two types of limit states reliability targets depending on if the hazard can occur anywhere within the pipeline network or whether it is location-specific. Geotechnical hazards such as landslides are location-specific hazards as long as the length of pipeline exposed to the geotechnical hazard is less than 1,600 m which is typically satisfied for landslides in Manitoba. The CSA Z662-15 standard provides the following equation to calculate location-specific limit states reliability targets:

$$R_{TLS} = \begin{cases} 1 - \frac{1650}{(\rho PD^3)^{0.66}} & \rho = 0 \\ 1 - \frac{197}{(\rho PD^3)^{0.66}} & \rho > 0 \end{cases} \quad \text{eq. 7.1}$$

Where:

$R_{TLS}$  = limit states target reliability, per km-yr

$P$  = pipeline pressure, MPa

$D$  = pipe diameter, mm

$\rho$  = average population density per hectare

The calculated reliability in eq.7.1 is applicable for a pipeline segment within a certain assessment area. The assessment area is 1,600 m long (evaluation length) by an evaluation width in meters is determined using the following equation:

$$\text{Evaluation Width} = 0.158\sqrt{PD^2} \quad \text{eq. 7.2}$$

The average population density parameter ( $\rho$ ) is the average number of occupants within all buildings and facilities within the assessment area. The assessment area is equal to a

length of 1,600 m along the pipeline and a width calculated using equation eq. 7.2. The occupancy patterns and numbers are assessed to determine the average number of people in a building or facility during normal use. If occupancy information is not available, CSA Z662-15 provides suggested average density populations depending on the pipeline class and the number and type of dwellings within the assessment area as show in Tables 7-1 and 7-2.

Limit states target reliability values can be converted ( $R_{TLS} = 1 - P_f$ ) into a target probability of pipeline failure and plotted for varying consequences as shown in Figure 7-1. At the research sites, the calculated probability of failure (tensile rupture and local buckling limit states) in a given year can be compared against the ultimate limit states target probability to determine compliance as follows:

$$P_f < P_t \quad \text{eq. 7.3}$$

Where:

$P_f$  = probability of failure for ultimate limit states failure modes, per km-yr

$P_t$  = limit states target reliability in the form of a probability of failure, per km-yr

For the three research sites the ultimate limit states probability of failure target is as follows:

- Plum River (Class 1) - 6.18E-02 per km-yr, evaluation length x width (1,600 m x 34.6 m)

- St-Lazare (Class 2) -  $9.50E-04$  per km-yr, evaluation length x width (1,600 m x 71.5 m)
- Harrowby (Class 2) -  $5.48E-03$  per km-yr, evaluation length x width (1,600 m x 26.1 m)

All three research sites fit within the evaluation length for a location-specific hazard. The Plum River site has the highest probability of failure target while St-Lazare has the lowest. For the pipeline information provided by Manitoba Hydro, the ultimate limit states probability of pipeline failure target is as low as  $2.28E-10$  per km-yr (Class 4) and as high as 0.105 per km-yr.

#### *7.1.2 Serviceability Limit States Reliability Targets*

CSAZ662-15 recommends a serviceability limit state probability target of 0.9 per km-year with the caveat that a higher reliability target (lower probability of failure) can be selected by the pipeline operator since the consequences of exceeding serviceability limit states are for the most part, economical. CSA Z662-15 also classifies pipe yielding as a serviceability limit states failure mode with the potential to progress to an ultimate limit states failure mode (product loss) if excessive deformation occurs. CSA Z662-15 does not define what is deemed to be excessive yielding and it has been inferred from the standard that defining this limit would be the responsibility of the pipeline operator. A target value of 0.9 was selected for this thesis research.

## 7.2 Statistical Analysis Results

### 7.2.1 *Statistical and Probability of Failure Results at Research Sites*

The statistical methods discussed in Section 2.6 were used to evaluate the statistical properties of the monitoring data for each of the applicable limit states failure modes using the equations presented in Section 2.5. Histograms and associated cumulative probability distributions functions (CDFs) for each limit states failure mode have been created for all the monitoring set-ups and are included in Appendix D. Appendix D also includes overall histograms and cumulative probability distribution based on monitoring results for each site for the various limit states failure modes. An example set of statistical results for one of the monitoring set-ups are presented in Figure 7-2 to Figure 7-7. All histogram bin sizes and ranges (x-axis) are consistent for each limit states failure mode for ease of comparison while the relative probability density function (PDF),  $f_X(x)$ , along y-axis was kept consistent for the most part with a few exceptions.

Theoretical probability distribution functions were applied to the measured data set to determine which of the functions provides the best-fit to the measured data. Some of the histograms exhibited a bimodal distribution due to backfill stresses in the data set. The probability distribution functions applied include normal, log normal, and gamma distributions. The best-fit of the three functions was assessed visually using the CDF plots which is a valid method to identify the best-fit (CSA Z662-15). The selected best-fit function is plotted on all the histogram and CDF plots. The best-fit theoretical probability distribution function was used to calculate the probability of exceedance for a particular limit states failure mode and then compared to the target limit states probability. Table 7-3

presents the predicted probability of failure for the research sites. Set-up locations where a limit states failure mode is exceeded are also noted in Table 7-3.

Although the overall probability of failure predications when examining each research site are higher than the individual set-ups, the predictions are considered not to be representative. This is because of the larger dispersion in the measured data when individual data sets are superimposed on each other. The strains and stresses induced on the pipe during backfilling also skewed the statistical analysis results since backfill loads differed in magnitude between set-ups and sometimes were sustained for different periods of time.

The calculated probability of failure from the data sets for each set-up is considered to be the probability of failure in a given year. The data set represents four years of data and the data collected contains time-dependent and time-independent random variables. Probability estimates using time-independent variables are representative of the true probability of failure regardless of the base unit of time (seconds, days, years) selected. Time independent variables at the research sites include constant, slow moving ground movements inducing stresses on the pipe. Time-dependent random variables should account for the time factor when determining probability of failure for a given period such as a year. This typically means scaling down the probability of failure estimate since adverse conditions that may cause failure are not consistently being applied to a particular element being examined. An example of this is high wind-loads which are typically presented based on a specified return period. The time dependent variables at the research sites vary seasonally such as temperature and gas pressure (demand), but are re-occurring at roughly the same time, year after year. The measured temperature profiles

and distinct stress changes based on the monitoring results each spring are examples of yearly re-occurring events. Therefore, the calculated probability of failure is essentially the probability of failure in a given year.

The results presented in Table 7-3 are based on the measured data and includes induced stresses and strains due to backfilling. The normal distribution function was usually the best-fit while the gamma distribution was the best-fit in a few instances, typically when examining the local buckling limit states failure mode. Many of the probability of failure estimates were statistically insignificant (tensile rupture and strain based buckling approaches) where the probability of failure was less than 1E-15 per km-yr, meaning exceeding limit states targets is improbable. Yielding and DNV load controlled buckling (2000) are the only limit states failure modes which produced meaningful probability of failures results. The DNV load controlled buckling (2000) incorporates bending moments along with axial forces and pipe pressures when predicting buckling. Set-up locations with higher measured bending stresses resulted in higher probability of failures as compared to the strain based approaches. The DNV load controlled buckling (2012) also incorporates bending loads, but the recently updated equation diminished the influence of axial forces and bending moments in buckling predictions, significantly lowering predicted probability of failure values.

The Harrowby middle of valley set-up produced the highest calculated probability of failure for the valley sites whereas the Plum River along the slope set-up had the highest values for the riverbank site. Yielding probability of failure estimates exceeded limit states targets at one set-up location, the Harrowby middle of the valley location. High backfill stresses were “locked-in” at this location which has resulted in the  $P_f$  estimate of



1.0. The highest predicted probability of failure related to local buckling occurred at the Plum River along the slope location while the Harrowby middle of valley set-up had the second highest predicted probability of failure for local buckling.

### *7.2.2 Probability of Failure Estimates without “locked-in” Stresses and Beyond the Set-Ups*

Probability of failure estimates when including “locked-in” backfill strains/stresses are not reflective of the actual probability of failure of the pipeline beyond the set-up locations at the research sites. Also, the set-up locations may not be located where the maximum pipe loading is occurring due to ground movements. It is believed the set-up locations are likely close to or perhaps at the location where the maximum pipe loads are occurring, however no data is available to verify this assumption. As such, calculating the probability of failure of the pipeline without “locked-in” backfill strain/stresses and for areas beyond the set-up locations is important in understanding the actual risk to pipeline at the research sites. The Harrowby middle of valley location measured the highest pipe loading of all the sites with and without “locked-in” backfill strains/stresses and this data set was used to determine the probability of failure without backfill loads. This data set was also used to determine the percent increase required to exceed limit states targets for yield and local buckling (DNV load controlled buckling, 2000) as a way to evaluate the risk of pipeline failure beyond the set-up locations. Limit states targets were exceeded for yielding at this set-up and therefore a percentage increase could not be calculated. An identical approach was applied to the Plum River along the slope data set, representing the riverbank case. The results are presented in Table 7-4.

The predicted probability of failure for yield and local buckling dropped several orders of magnitude when “locked-in” backfill stresses were removed from the data set. Probability of failure for yielding at the Harrowby middle of valley location dropped from 1.00 to  $3.36E-7$  per km-yr without backfill stresses and falls well below the serviceability limit states reliability targets for yielding. The large reduction in probability of failure estimates for yielding highlights the influence that “locked-in” backfill stresses have on probability of failure predications. An increase in the average pipe loading of about +45% to +509% is required to exceed limit states reliability targets for the two limit states failure modes examined for areas outside of the monitoring locations. A smaller percentage increase is required to exceed limit states targets when considering “locked-in” backfill stresses as opposed to a larger percent increase required to exceed limit states when backfill stresses are removed from the data sets.

Excluding areas where pipelines have been backfilled following installation, it is unlikely limit states targets are exceeded in areas beyond the monitoring locations based on the calculated percent increases in loading conditions required to exceed limit states. The ground and pipeline profile at the valley sites is relatively constant with only subtle changes in both profiles. Ground pin monitoring also did not reveal any distinct zones where higher ground movements were measured outside of the set-up locations. This implies pipe strains and stresses are likely relatively uniform along the pipeline along the valley slopes including the set-up locations. As for Plum River, the slope is relatively short (<5 m long) and the monitoring data from the middle of the slope is considered to be representative of the average pipeline strains and stresses along the slope length.

The probability of failure estimates are representative of relatively straight pipeline alignments within slow moving landslide areas. A higher concentration of strains and stresses tend to develop at pipeline bends when subjected to ground movements which are located at the crest and toe of the valley and riverbank sites. The limit states pipe failure modes examined may be exceeded at these locations.

### *7.2.3 Standard Error Estimates*

Theoretical distribution functions are estimators applying a statistical distribution to a sample set of a random variable. Therefore, the applied statistical distribution includes some inherent uncertainty in relation to the true statistical distribution of the random variable since the observed data set is finite and variable. Several methods exist to predict the statistical uncertainty of an applied statistical distribution to a particular sample set. Bootstrapping is one such method. Bootstrapping is a statistical re-sampling method that uses an approximation technique to simulate numerous frequency distributions to determine how these simulated distributions differ from the actual measured sample set. Bootstrapping is somewhat similar to a Monte-Carlo simulation approach, but is a statistical sampling model whereas the Monte-Carlo simulation is a deterministic model.

The Bootstrapping method proposed by Van Helden (2013) was used to estimate the standard error in the predicted probability of failure values. The method proposed is discussed in detail in Van Helden (2013) and is not presented herein. The standard error was estimated for yielding and local buckling probability of failure calculations for the Harrowby middle of valley and the Plum River along the slope locations since these locations had the highest predicted probability of failure values. Table 7-5 summarizes

the Bootstrapping results. The estimated standard errors are generally low, ranging from one order of magnitude to several orders of magnitude less than the predicted probability of failure. The inclusion of the calculated standard error in the probability of failure estimates does not change the outcome of statistical analysis and compliance with limit states target reliabilities.

#### 7.2.4 *Initial Pipe Stress-State*

The outcome of the statistical analysis assumes the initial stress-state of the pipe is at or near zero. This is a fair assumption given the periodic release of longitudinal stresses (axial and bending) observed in the monitoring data and the lack of reduction in pipe stresses following the pipelines being cut and abandoned at Plum River and St-Lazare. Longitudinal pipe stresses appear to be somewhat cumulative to point where stresses are released, suspected to be due to soil-pipe relaxation. In some instances, built-up pipe stresses (axial and bending) are fully released, dropping longitudinal pipe stresses to at or close to zero. There are a few instances where the release only results in a partial reduction in longitudinal pipe stresses suggesting the monitored pipe stresses are somewhat cumulative (*e.g.* Harrowby middle of valley set-up) or the soil-pipe relaxation mechanism was not sufficient in nature to completely reduce pipe stresses at that instance. The pipelines may have been initially stressed prior to monitoring of longitudinal pipe stresses within landslide areas are assumed to be somewhat cumulative. The results presented in Section 7.2.2 apply where the initial pipe stress-state would have to be sufficient enough to increase the average measured pipe loading by about +45% to +509% to exceed limit state targets for the failure modes examined when “locked-in” backfill strains/stresses are removed from the data. This percent increase is for the two

set-ups were the highest stresses were measured and implies that the structural capacity of the pipeline at the research sites can handle some initial pipe stresses in addition to the maximum measured pipe stresses before limit states failure modes are exceeded.

### **7.3 Manitoba Hydro Pipeline Network Assessment**

Manitoba Hydro's gas pipeline network contains pipelines with various pipe properties operating at different operating pressures. Many of these pipelines transverse potential landslide areas that may be subjected to ground movements similar in direction and magnitude to those measured at the research sites. Various pipelines were examined using the results from the research sites to determine if limit states target reliabilities are exceeded, focusing on yielding and local buckling limit states failure modes (DNV load controlled buckling, 2000). Manitoba Hydro provided a list encompassing the range of different pipelines within their network. Measured pipe strains and calculated stresses monitored at the valley sites (Harrowby middle of valley) and riverbank site (Plum River along the slope) sites were first converted into applied loads in the form of axial forces, bending moments and torsion. The applied loads measured at the research sites are representative of expected pipe loading in slow moving landslides for larger, deep valleys and riverbanks that have undergone past instabilities, but are likely still moving. The maximum operating pipeline pressure rating was used in the assessment which is conservative since operational line pressures are likely lower.

A summary of the pipeline network assessment is presented in Tables 7-6 and 7-7. The assessment was conducted including (Table 7-6) and excluding (Table 7-7) "locked-in" backfill stresses. Yielding limit states targets are exceeded for about 70% of the pipeline

network when “locked-in” backfill stresses are included in the analysis and local buckling targets are exceeded for about 20% of the pipeline network depending on the Class (Table 7-6).

Exceedance of limit states targets dwindles considerably when “locked-in” backfill stresses are excluded from the analysis (Table 7-7) with about seven pipelines remaining within Manitoba Hydro’s network. The majority of these pipelines exceed yielding limit states targets as a result of using maximum operating pressure (MOP) in the calculations. Limit states targets for yielding were satisfied with a 3 to 28% reduction in the assumed line pressure. At the research sites, the average operating pipeline pressure was about 30% to 40% lower than the MOP. Local buckling may occur for two pipelines (La Salle and Letellier) if these pipelines transverse valleys where slow moving landslides are occurring and are located within a densely populated area (Class 4).

#### **7.4 Summary**

Overall the probability of pipeline failure estimates are low and are typically well below limit states target reliability values. The structural capacity of the pipeline at the research sites can also handle some initial pipe stresses prior to monitoring in addition to the maximum measured pipe loading before limit states failure modes are exceeded. The potential for yielding above serviceability limit states targets is likely in areas where the pipeline has been backfilled and also may occur in other areas where pipeline pressures are operated at or near MOP. Local buckling may also occur in backfill areas, but is improbable outside of backfill areas except for pipelines which are similar to the La Salle and Letellier pipelines. These pipelines may exceed limit states targets for yielding and

local buckling depending on if these pipelines run through slow moving landslide areas and the class of the pipeline is high (Class 4). Longitudinal strains and stresses due to ground movements do not appear to be sustained and cumulative as has been typically assumed by other researchers. Measured longitudinal strains peak and then reduce (release) as discussed in Chapter 6. This has resulted in overall lower probability of failure values for the various limit states and somewhat implies that the initial stress-state of the pipelines was at or near zero prior to monitoring. The release of longitudinal pipe stresses may be attributed to what is referred to as soil-pipe relaxation in this thesis research. This hypothesized behaviour mechanism is discussed in detail Chapter 8.

Location Specific Probability Targets for Limit States Design

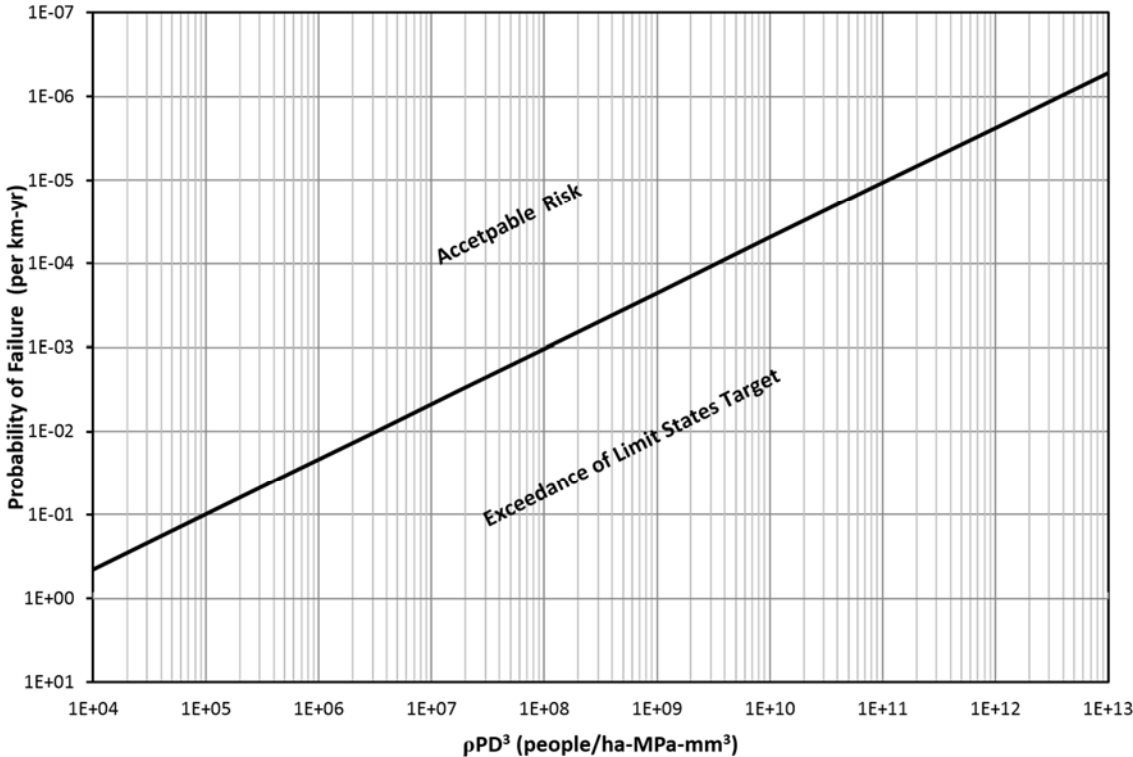


Figure 7-1 Target Probability of Failure ( $P_f$ ) for Varying Consequences.



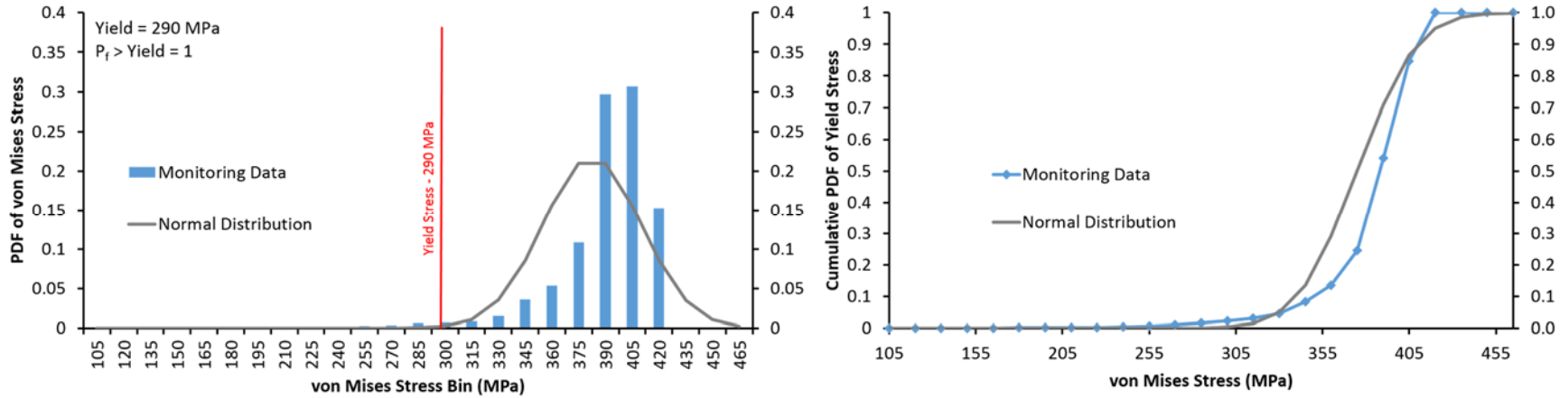


Figure 7-2 Yield statistics and Best-Fit Theoretical Distribution (Harowby Middle of Valley Histogram).

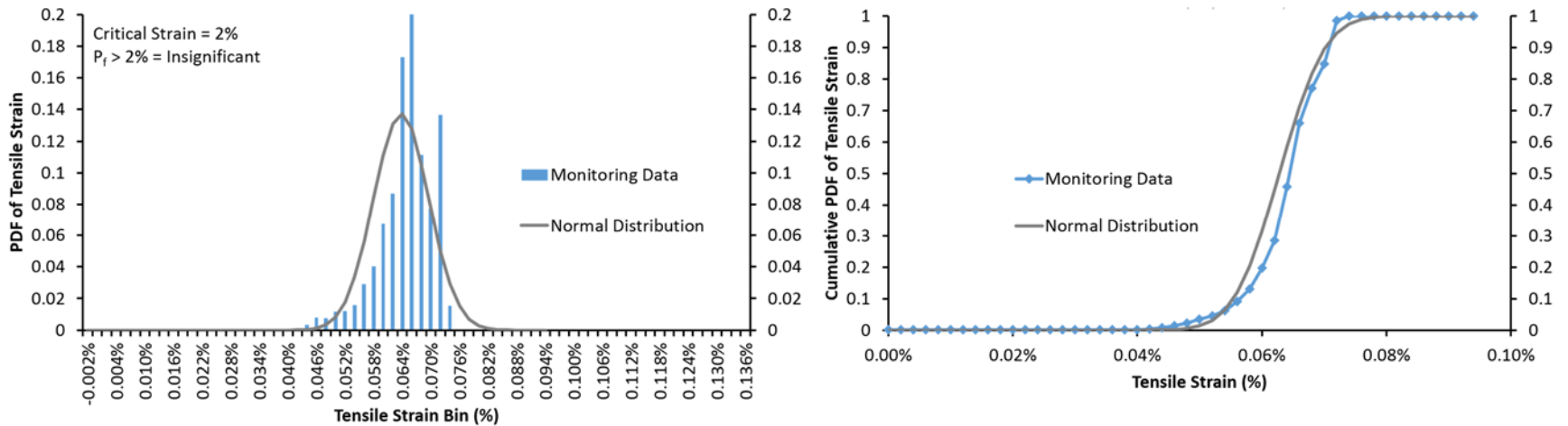


Figure 7-3 Tensile Rupture Statistics and Best-fit Theoretical Distribution (Harowby Middle of Valley Histogram).

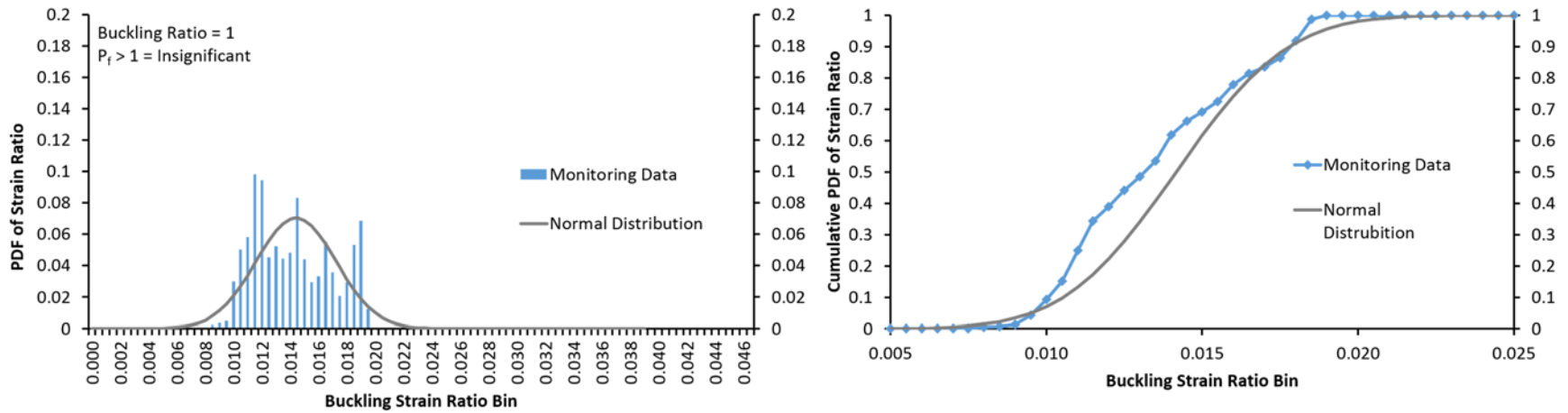


Figure 7-4 CSA Strain Buckling Statistics and Best-fit Theoretical Distribution (Harrowby Middle of Valley Histogram).

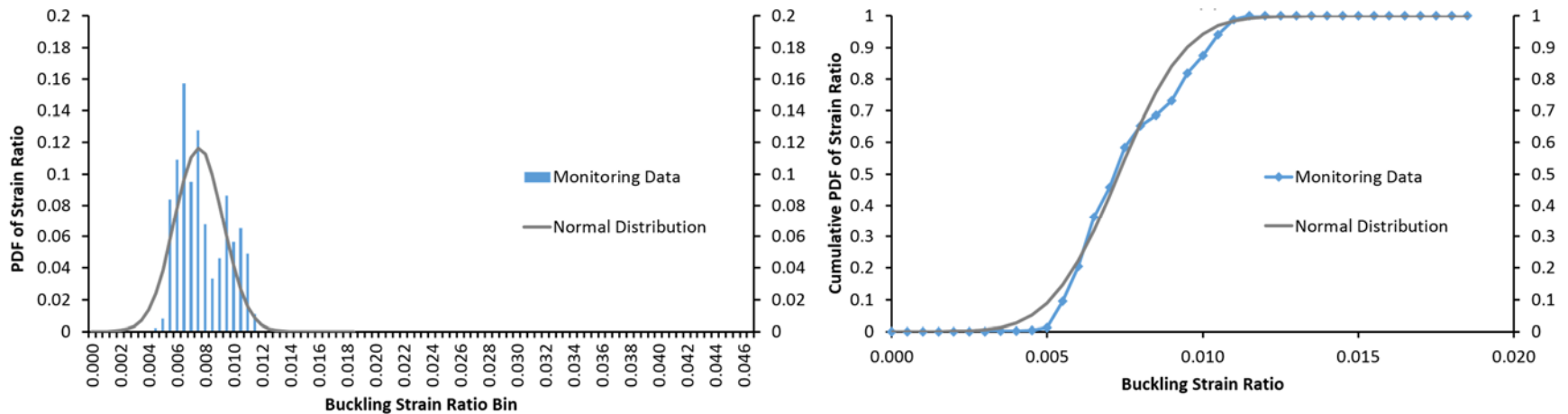


Figure 7-5 DNV Strain Buckling Statistics and Best-fit Theoretical Distribution (Harrowby Middle of Valley Histogram).

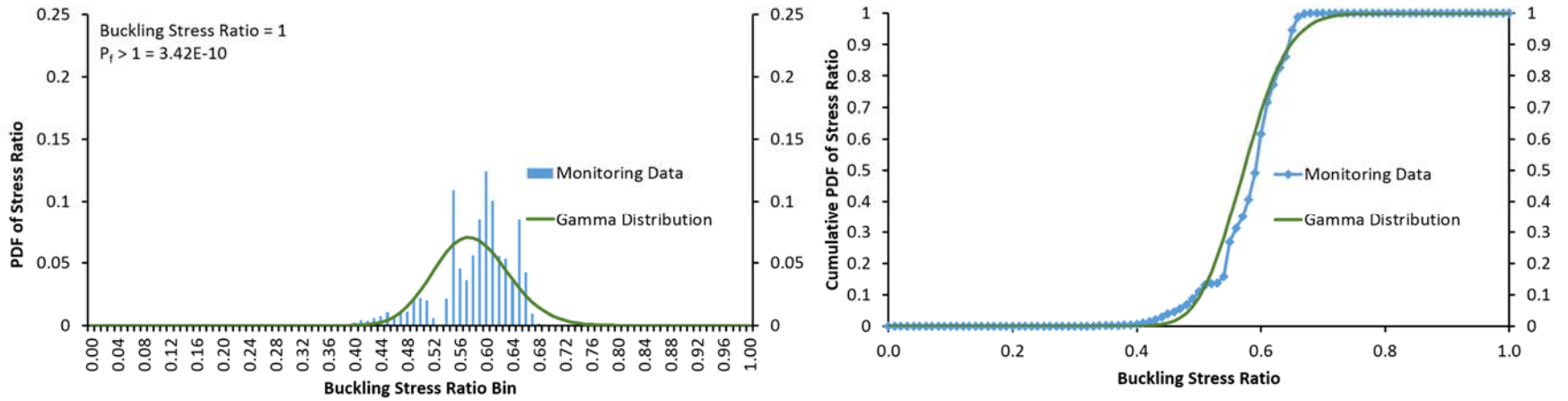


Figure 7-6 DNV (2000) Load Controlled Buckling Statistics and Best-fit Theoretical Dist. (Harrowby Middle of Valley Histogram)

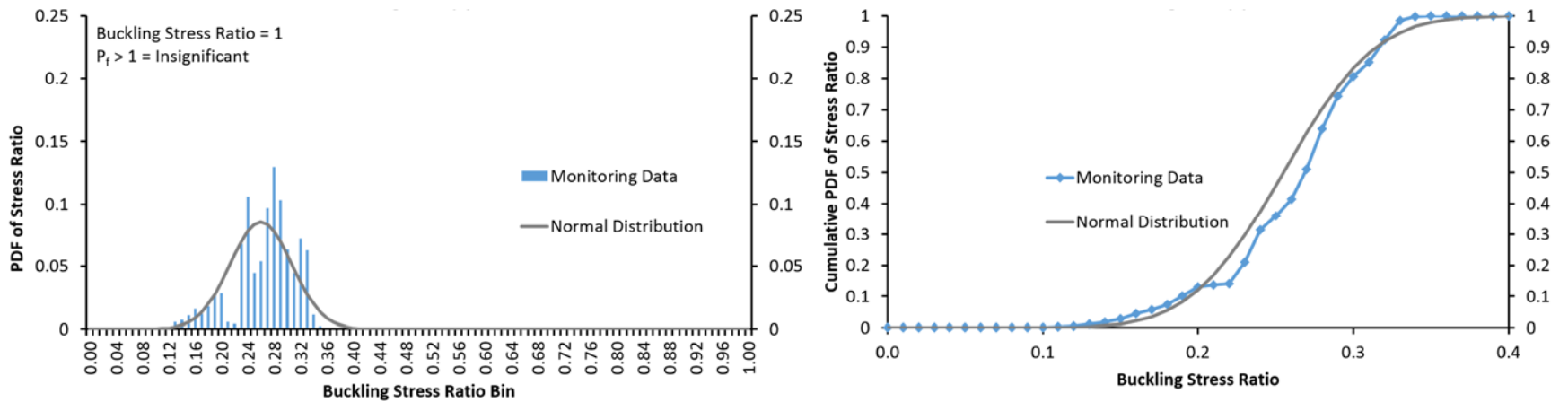


Figure 7-7 DNV (2012) Load Controlled Buckling Statistics and Best-fit Theoretical Dist. (Harrowby Middle of Valley Histogram)

Table 7-1 - Class Location Designators.

Development within the Class location assessment area	Class
None	Class 1
dwelling units $\leq$ 10	Class 1
One or more of the following:	Class2
a) industrial installation (e.g. chemical plant or a hazardous substance storage area) where release of pipeline product can cause the industrial installation to produce a dangerous or environmental condition	
b) 11 to 45 dwellings	
c) a building occupied by 20 or more persons during normal use	
d) a small, well-defined outside area occupied by 20 or more persons during normal use such as a playground, recreation area, outdoor theatre, or other place of public assembly	
46 or more dwelling units	Class 3
A prevalence of buildings intended for human occupancy with 4 or more storeys above ground:	Class 4

Notes: Each dwelling unit in a multiple unit building shall be counted separately. If future development within the class location designation increases the class, design, operating, and maintenance at this location shall follow the requirements of the higher future class. For buildings where rapid evacuation can be difficult (e.g. hospitals, nursing homes), Class selections shall take this into consideration.

Table 7-2 - Population Density by Location Class.

Class	Average Population Density (people per hectare)
1	0.04
2	3.3
3	18
4	100

Table 7-3 – Predicted Probability of Failure (per km-yr) for Various Limit States Failure Modes.

Site	Set-Up	"Locked-in" Backfill Loads	Yield (per km-yr)	Tensile Rupture	CSA Strain Limit	DNV Strain Limit 2012	DNC Load Controlled 2000	DNC Load Controlled 2012
<b>Plum River</b>	Beyond Crest	Partially (Bending)	5.36E-11 (1)	-- (1)	--(1)	-- (1)	-- (2)	-- (2)
	Along Slope	Partially (Axial)	1.50E-03 (1)	-- (1)	**No compression due to tension axial stresses		1.05E-07 (2)	-- (2)
<b>St-Lazare</b>	Top	No	2.84E-09 (1)	-- (1)	-- (2)	-- (2)	-- (1)	-- (1)
	Middle	No	8.42E-10 (1)	-- (1)	-- (1)	-- (1)	-- (1)	-- (1)
	Bottom	No	3.62E-09 (1)	-- (1)	-- (1)	-- (1)	-- (1)	-- (1)
<b>Harrowby</b>	Top	Partially (Bending)	2.78E-13 (1)	-- (1)	-- (2)	-- (2)	5.22E-15 (2)	-- (1)
	Middle	Full (Bending, Axial, Torsion)	<b>1.00*</b>	-- (1)	-- (1)	-- (1)	3.42E-10 (2)	-- (1)
	Bottom	Full (Torsion)	4.09E-11 (1)	-- (1)	-- (2)	-- (1)	1.79E-12 (2)	-- (2)

(1) - Normal distribution best-fit

(2) - Gamma distribution best-fit

-- statistically insignificant

\* - Limit States probability targets exceed

Table 7-4 Probability of Failure with and without “locked-in” Stresses and % Increase Required to Exceed Limit States Targets.

Set-Up	Yielding <sup>1</sup>		Local Buckling <sup>2</sup>	
	With “locked-in” backfill loads	Without backfill loads	With “locked-in” backfill loads	Without backfill loads
<b>Harrowby Middle of Valley (Valley Site)</b>				
Probability of failure per km-yr (P <sub>f</sub> )	1.00	3.36E-7	3.42E-10	<1.50E-15
% increase to exceed limit states reliability targets	-	+46%	+45%	+294%
<b>Plum River Along the Slope (Riverbank Site)</b>				
Probability of failure per km-yr (P <sub>f</sub> )	1.50E-3	<1.50E-15	1.05E-7	6.77E-15
% increase to exceed limit states reliability targets	+48%	+287%	+218%	+509%

<sup>1</sup> – Normal distribution function used to predict probability of failure

<sup>2</sup> – Gamma distribution function used to predict probability of failure

Table 7-5 – Bootstrapping Standard Error on Predicted Probability of Failures for Yield and Local Buckling at the Research Sites.

Set-Up	Yielding <sup>1</sup>		Local Buckling <sup>2</sup>	
	With “locked-in” backfill loads	Without backfill loads	With “locked-in” backfill loads	Without backfill loads
<b>Harrowby Middle of Valley (Valley Site)</b>				
Probability of Failure, $P_f$ , (per km-yr)	1.00	2.36E-07	3.42E-10	insignificant
Standard Error Estimate	± 4.74E-08	± 3.77E-08	± 8.96E-11	-
$P_f$ + Standard Error Estimate	1.00	2.74E-07	4.32E-10	-
<b>Plum River Along the Slope (Riverbank Site)</b>				
Probability of Failure, $P_f$ , (per km-yr)	1.50E-03	insignificant	1.05E-07	6.77E-15
Standard Error Estimate	± 8.36E-05	-	± 3.56E-08	± 2.48E-15
$P_f$ + Standard Error Estimate	1.59E-03	-	1.40E-07	9.25E-15

<sup>1</sup> – Normal distribution function used to predict probability of failure

<sup>2</sup> – Gamma distribution function used to predict probability of failure



Table 7-6 – Potential Exceedance of Limit States for Re-backfilled Pipeline within Slow Moving Landslide Areas.

Pipeline Location	Line Size	MOP <sup>1</sup> (kPa)	Wall Thickness (mm)	Pipe Grade (MPa)	Yield Target P <sub>f</sub> Exceeded	Local Buckling P <sub>f</sub> Target Exceeded By Class			
						Class 1	Class 2	Class 3	Class 4
IDC	406.4	4830	6.35	317					
Oak Bluff	406.4	4830	6.35	317					
La Salle	323.9	4830	6.35	290					
	219.1	4830	5.56	290					
	60.3	4830	3.18	290	V	V	V, R	V, R	V, R
Landmark	273	6900	5.56	317	V, R				
	219.1	6900	4.78	317					
Brandon	323.9	6070	6.35	290	V, R				
	323.9	6070	4.78	290	V, R				
	168.3	6070	3.96	290					
	273.1	4140	5.56	290					
	114.3	4140	3.18	317					

Table 7-6 Potential Exceedance of Limit States for Re-backfilled Pipeline within Slow Moving Landslide Areas (cont'd).

Pipeline Location	Line Size	MOP <sup>1</sup> (kPa)	Wall Thickness (mm)	Pipe Grade (MPa)	Yield P <sub>f</sub> Target Exceeded	Local Buckling P <sub>f</sub> Target Exceeded By Class			
						Class 1	Class 2	Class 3	Class 4
Brandon	273.1	4140	5.56	290					
South Loop	114.3	6070	3.18	290					
Morris	88.9	6070	3.18	241	V				V
Letellier	60.3	6070	3.18	290	V	V	V, R	V, R	V, R
Benito	168.3	7930	3.18	359	V, R				
Mintonas	88.3	7930	3.18	359	V				
St. Pierre	60.3	4830	3.91	317	V	V	V	V	V
Minell	168.3	7230	4.78	290					
Harrowby	88.9	3450	3.2	290	V				
Plum River	88.9	6070	3.2	241					

<sup>1</sup> - Maximum Operating Pressures (MOP) held constant for P<sub>f</sub> calculations

V- Valley Area

R- Riverbank Area

Table 7-7 Potential Exceedance of Limit States for Pipelines within Slow Moving Landslide Areas

Pipeline Location	Line Size	MOP <sup>1</sup> (kPa)	Wall Thickness (mm)	Pipe Grade (MPa)	Yield P <sub>f</sub> Target Exceeded	Local Buckling P <sub>f</sub> Target Exceeded By Class			
						Class 1	Class 2	Class 3	Class 4
La Salle	60.3	4830	3.18	290	V				V
Landmark	273	6900	5.56	317	L.P				
Brandon	323.9	6070	6.35	290	L.P				
		6070	4.78	290	L.P				
Letellier	60.3	6070	3.18	290	V				V
Benito	168.3	7930	3.18	359	L.P				

<sup>1</sup> - Maximum Operating Pressures (MOP) held constant for P<sub>f</sub> calculations

L.P - Line pressure at Maximum Operating Level is dominating von Mises yield stresses for valley and riverbank Areas. Yield is not exceeded when line pressure used in P<sub>f</sub> calculations is reduced to between 0.72 to 0.97 of MOP depending on pipeline properties.

## **Chapter 8 Changes in Pipe Stresses due to Ground Movements or Other Mechanisms**

Landslide movements have been linked to monitored changes in pipe stresses when both downward pipe bending stresses and axial tension (without thermal effects) increase. Distinct increases in longitudinal pipe stresses in the monitoring data are assumed to be the response of the pipe to more sudden landslide movements while slower landslide movements are assumed to reflect slower increases in axial tension and downward bending in the monitoring results. Mechanisms causing other combinations in axial and bending stress changes, however, is not as clear. Measured longitudinal strains are not sustained and cumulative and can decrease over time. Some of the observed decreases in axial tension and downward bending may be attributed to ground movements or could be due to a form of soil-pipe relaxation. The observed soil-pipe relaxation mechanism is not due to plastic deformation of the pipeline as the pipe response at the research sites are within the elastic range of the structural member. Decreases (reduction) in downward bending occurred more often in the monitoring data when compared to decreases in axial tension stresses and the decreases in downward bending also tended to be larger in magnitude. This chapter describes decreases in longitudinal pipe stresses that may be related to either ground movements or soil-pipe relaxation. Several hypothetical mechanisms that could be causing soil-pipe relaxation are discussed in this chapter.

## 8.1 Changes Pipe Stresses Attributed to Ground Movements

The pipe monitoring results (Figures 6-2 to 6-4) showed that there are roughly three general combinations of changes in longitudinal pipe stresses; 1) increased downward bending stresses and axial tension either increased or was relatively unchanged, 2) decreased downward bending and increased axial tension, and 3) decreased downward bending and axial tension either decreased or was relatively unchanged. The first two combinations are likely due to landslide ground movements and have been assumed to be as such within this thesis research. Figure 8-1 is a schematic illustration of the types of landslide related ground movements required to cause the first two combinations of stress changes.

Rotational landslide movements cause surficial ground movements that typically result in mostly downward soil displacements,  $\delta_d$ , with a smaller component of downslope displacements,  $\delta_a$  (Figure 8-1 a.). The pipeline response to these landslide movements is an increase in downward bending and possibly, an increase in axial tension (combination 1) depending on the point along the pipeline being examined in relation to the extent of the rotation landslide area. Downward ground movements are more prevalent at the extents of a rotational landslide than downslope movements, while a more balanced proportion of downward movements to downslope movements would be expected near the center of a rotational landslide. Therefore, axial tension stresses may or may not increase depending on the location along the pipeline profile within a rotational slide. The pipeline monitoring locations were placed within the top, relatively flat portion of the large ancestral slump blocks at the valley sites and this location would likely coincide with the extent of where the ancestral rotational landslide likely occurred. The ancestral

landslide areas are suspected to be active based on the depths where the SI's became inoperable.

Translational landslide movements occur at shallow depths resulting in downslope soil displacements as shown in Figure 8-1 b. The pipeline is not perfectly straight and translational ground movements cause a pull on the pipe in the longitudinal direction due to soil-pipe adhesion. The decrease in downward bending stresses measured at the sites may be a result of the pipe straightening out due to translational landslide ground movements. The deflected shape of the pipe would have to straighten out only very slightly to reduce bending stresses. This explanation is strengthened when increased axial tension stresses are measured on the pipe as downward bending stresses decrease. In this regard, the combination of decreased downward bending and increased axial tension (combination 2) is assumed to be due to landslide movements.

## **8.2 Soil-Pipe Relaxation Mechanisms**

Landslide movements cannot easily explain the pipe stress monitoring results where downward bending stresses decreased and axial tensions either decreased or were maintained (combination 3). However, several other soil-pipe interaction mechanisms may be causing the measured reduction in longitudinal strains. Three soil-pipe relaxation mechanisms have been proposed as possible explanations of the pipe behaviour observed. The three mechanisms focus on soil-pipe interactions where downward bending stresses would decrease and the mechanisms are as follows:

- Upward block movement
- Soil displaces around the pipeline
- Loss of soil-pipe contact due to soil volume change

The first two mechanisms are related to soil displacements around the pipeline in the downward direction which could explain the reduction of downward bending. The last mechanism is independent of soil displacement or ground movements and may account for the reduction in both downward bending stresses and axial tension observed at the research sites.

Several researchers have noted or indirectly commented on the possible existence of a soil-pipe relaxation mechanism not attributed to plastic deformation of pipe member. Cavanagh and Rizkalla (1992) while evaluating the results of a 16 year monitoring program for a pipeline in a landslide area where ground displacements were measured, commented on *“there were large, unresolved discrepancies between the ground movement trends observed in the slope indicators and the pipeline displacements as derived from the precise survey monitoring”*. Bruschi and Tomassini *et al.* (1995) remarked on the discrepancy between field (pipe strain and soil movement) monitoring results and the lack of pipeline rupture in the following statement *“the field experience shows that soil movements are not unequivocally linked to a potential for pipe rupture”*. The strongest supporting evidence of the existence of a soil-pipe relaxation mechanism in landslide areas comes from research conducted by Scarpelli *et al.* (1995) where four case studies of pipelines in landslide areas were examined that included pipe strain gauge and ground movement monitoring. In one of the cases studies, the pipeline did not show large strains due to ground movements and Scarpelli *et al.* (1995) commented as follows: *“It is*

*not clear yet how this observed behaviour, i.e. a small strain accumulation in spite of large and continuous soils displacements, can be explained”.*

### *8.2.1 Upward Block Movement*

The upward block movement mechanism is where the pipeline attempts to lift the overburden soil a small amount (Pedersen and Jensen, 1988) in response to downward soil displacement. The pipelines are buried at shallow depths (~1 m) at the research sites and the overburden soil above the pipe may not provide sufficient resistance to counter uplift forces. A free body diagram of the forces resulting from downward soil displacement is illustrated in Figure 8-2. As the soil mass around the pipe moves down, the pipe deflects downwards in response to these soil movements resulting in downward bending stresses in the pipeline. The pipe naturally attempts to straighten out to release the bending stresses, but is resisted by the overburden soils. This results in an upward pipe force,  $f_p$ , being applied to the soil at the soil-pipe interface which resists,  $R_s$ , the upward pipe force over the pipe width. Since the response of the pipeline is elastic in nature, the upward pipe force continues to be applied following ground movements unless the pipe displaces.

The soil resistance to upward pipe movement develops a passive soil wedge or block above the pipe that is dependent on the weight of the wedge and the mobilized strength of the soil between the wedge and the adjacent soil along two shear planes as shown in Figure 8-3. This idealized soil-pipe interaction behaviour is essentially identical to uplift buckling failure modes analyzed in offshore pipelines. High temperature changes in offshore pipelines produces high compressive strains in the pipeline, leading to potential



upheaval buckling. Upheave buckling is where the pipeline attempts to buckle upwards because of high compressive strains and since the backfill soil tends to be weaker and is at lower overburden stresses than the *in-situ* soil at the bottom of backfill trench. The pipeline tries to buckle upwards by applying an upward pipe force on the soil above the pipe. Failure occurs when the upward force exceeds the soil resistance of the passive wedge above the pipe and the pipeline and soil displace upwards (El-Gharbawy, 2006). The pipeline may even break out of the backfill soil (Pedersen and Jensen, 1988,). DNV provides a recommended design practice on buckling mechanisms, including upheaval buckling, for offshore pipelines resting on or buried within seabeds (DNV-RP-F110).

The main difference between the uplift block mechanism presented herein and the upheaval buckling failure mode, is the upward pipe force is not large in comparison and only small displacements are assumed to be occurring. However, the upward pipe force due to downward soil displacement may be large enough to exceed the weight of the soil wedge above the pipe and starts to mobilize the shear strength of the soil along the two shear planes of the wedge. It is speculated only a small amount of vertical straining at the shear planes is required to release some or all of the downward pipe bending stresses within the pipe. The mobilized shear strength can be either undrained (cohesive soil) if a quick loading condition is occurring or drained (cohesive, and non-cohesive soil) for slower loading rates.

The upward block movement mechanism could explain the soil-pipe relaxation observed at the research sites, especially where distinct, sharp increases in downward bending stresses are followed by a sharp decrease in downward bending within the monitoring data. This occurred at four out five set-ups at the valley sites in March 2012 (Figure 6-5).

Large increases in downward bending was followed by an even larger sudden release of downward bending stresses. A possible explanation for these drastic changes in bending stresses is the large increase in downward bending resulted in an upward pipe force large enough to slightly lift the overburden soil releasing downward bending stresses or maybe the pipeline moved through the soil where the soil above the pipe displaces (flows) around the pipe (Section 8.2.2), or combination thereof.

### *8.2.2 Soil Displaces around the Pipeline*

The upward pipe force due to downward soil displacements results in a stress on the soil at the soil-pipe contact resisted locally by the shear strength of the soil. A localized failure could occur when the upward pipe force exceeds the shear strength of the soil, displacing the soil near the contact around the pipe. This allows the pipe to deflect upwards and release downward bending stresses as shown in Figure 8-4. This soil-pipe interaction is another possible explanation to the soil-pipe relaxation mechanism being observed at the research sites. The soil-pipe interaction where the soil displaces (flows) around a pipeline was observed in research completed by Mahdavi (2013) and is essentially a localized bearing capacity failure mode in the reverse direction as described in DNV-RP-F110. DNV-RP-F110 recommends using bearing capacity equations (drained and undrained) to predict localized failure for soil being displaced around a pipeline.

As with the upward block mechanism, it is speculated only a small amount of soil displacement around the pipe is required to release some or all of the downward pipe bending stresses within the pipeline. Due to the pseudo-viscous nature of soils, especially

fine grained cohesive soils, soil creep under the applied load may also be occurring causing small soil displacements.

Both the soil displacements around the pipe and the upward block mechanisms are dependent on the shear strength of the soil. In the undrained scenario, the undrained shear strength is inversely proportional to the moisture content, *i.e.* high moisture content result in low undrained shear strength. Periods in time where higher moisture contents occur in the soil leads to a lower undrained shear strength and less resistance to soil displacing around the pipe or upward block movements and may be the reason that distinct, and quick changes in downward bending stress were more commonly observed in the spring (*e.g.* snow melt) at the valley sites.

### *8.2.3 Loss of Soil-Pipe Contact Due to Soil Volume Change*

The last soil-pipe relaxation mechanism is independent of ground movements and related to soil volume change due to moisture changes in the soil. This soil-pipe relaxation is considered to be the least plausible of the three proposed, but could provide an alternative explanation to measured decreases in axial tension that are not due to soil-pipe adhesion being exceeded (Section 6.4).

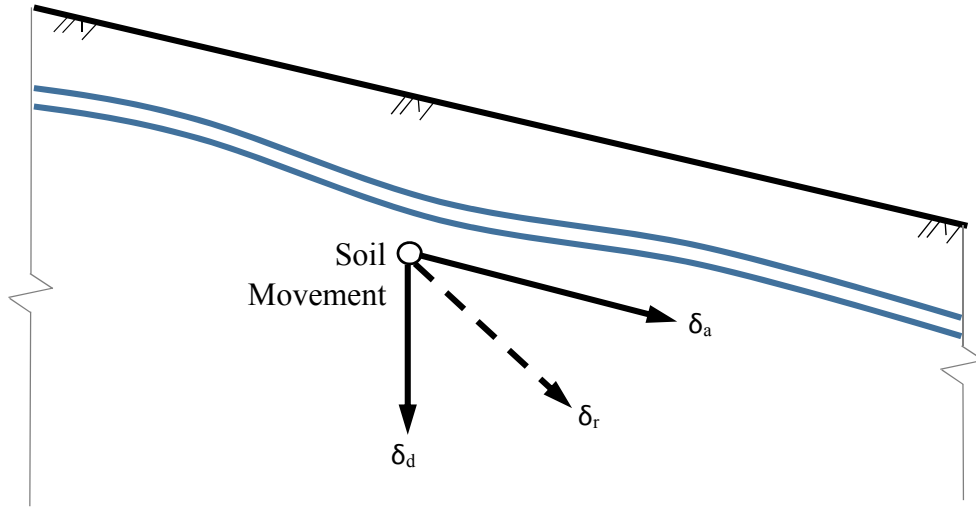
The fine grained cohesive backfill soils at the research sites are susceptible to notable volume changes as moisture conditions in the soils vary. Drying soil shrinks while wetting soils swell. Drying of the backfill could weaken the contact pressure between the soil and the pipe as the soil shrinks and pulls away from the pipe as shown in Figure 8-5. The ability for the soil to hold on to the pipeline also weakens as the contact pressure

weakens and axial tension forces in the pipe may be sufficiently high enough to cause the pipe to slip through the soil, reducing or releasing axial tension.

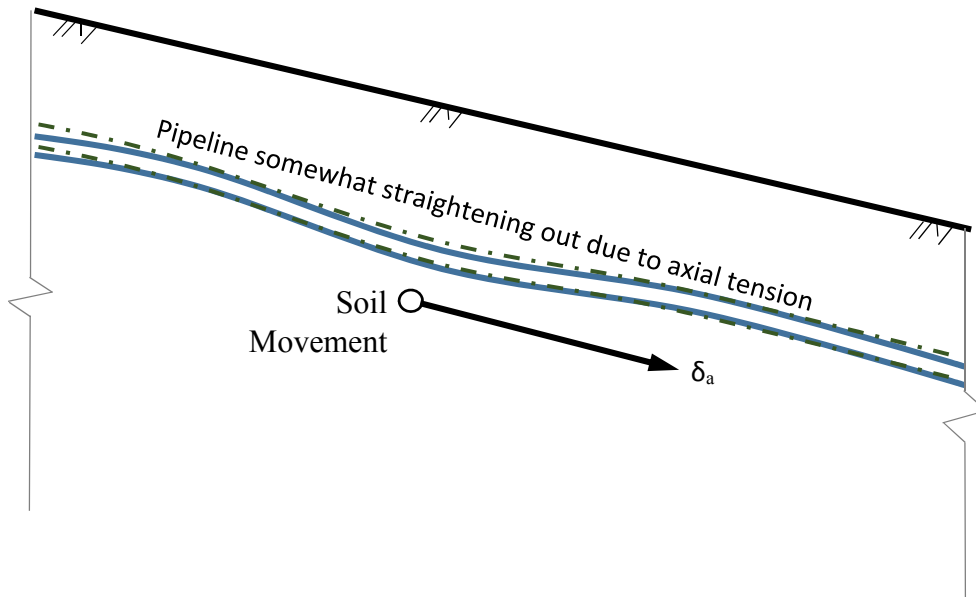
The weakening of the contact pressure, likely to a lesser degree, may also reduce the ability of the backfill soils to resist pipe movements in other directions. As the soil shrinks and pulls away from the pipe, a thin zone of weakened soil develops. Soil within this zone likely provides reduced resistance to pipe movements laterally or vertically, at least for small pipe displacements occurring within the weakened zone. The weakening of the soil around the pipe could be sufficient enough to allow the pipe to move vertically a small amount, possibly reducing or releasing downward bending in the pipeline. This is especially true in the event the soil-pipe contact is partially or completely lost due to excessive drying and the pipeline is free to move, but this scenario is unlikely.

### **8.3 Summary**

This chapter discusses changes in longitudinal pipe stresses attributed to ground movements or to a soil-pipe relaxation mechanism. Three hypothetical soil-pipe relaxation mechanism were presented as possible explanations to the measured pipe stresses which showed a decrease in downward bending while axial tension either decreased or was relatively unchanged. Any one of the soil-pipe relaxation models presented could be limiting longitudinal pipe strains and ultimately, lowering the probability of pipeline failure exceeding limit states failure modes for pipelines in landslide areas.



- a) Ground movements resulting in increased downward bending and increased axial tension,  $\delta_d$  = downward displacement causing pipe bending stresses,  $\delta_a$  = downslope displacement causing pipe axial tension stresses,  $\delta_r$  = resultant displacement.



- b) Ground movements resulting in decrease downward bending and increased axial tension,  $\delta_a$  = downslope displacement causing axial tension stresses in the pipeline.

Figure 8-1 Landslide Related Ground Movements at the Research Sites.

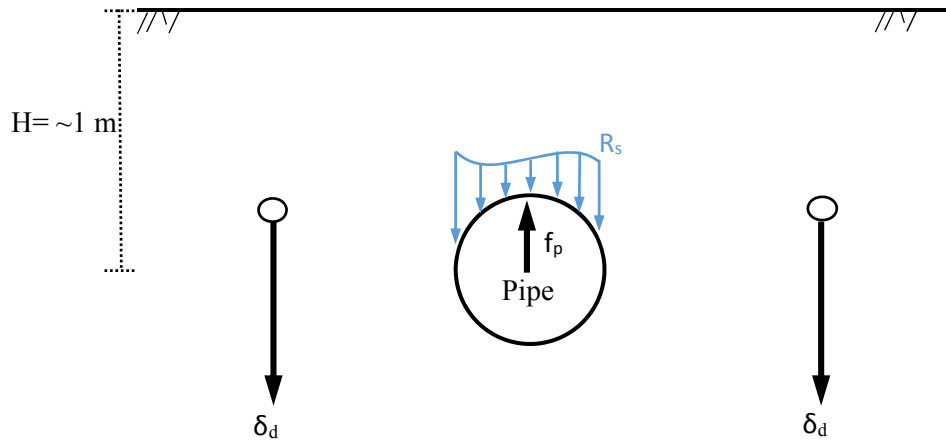


Figure 8-2 Free Body Diagram of Pipe Response to Downward Soil Displacements,  $\delta_d$ .  $f_p$  is Upward Pipe Force and  $R_s$  is the Soil Resisting Force Over the Width of the Pipe.

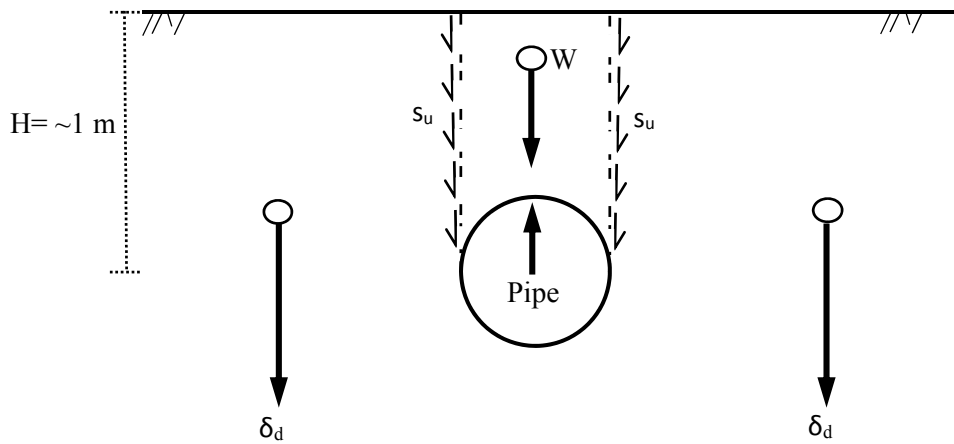


Figure 8-3 Upward Block Mechanism.  $W$  = Weight of the Overburden Soil,  $S_u$  = Undrained Shear Strength of the Soil.

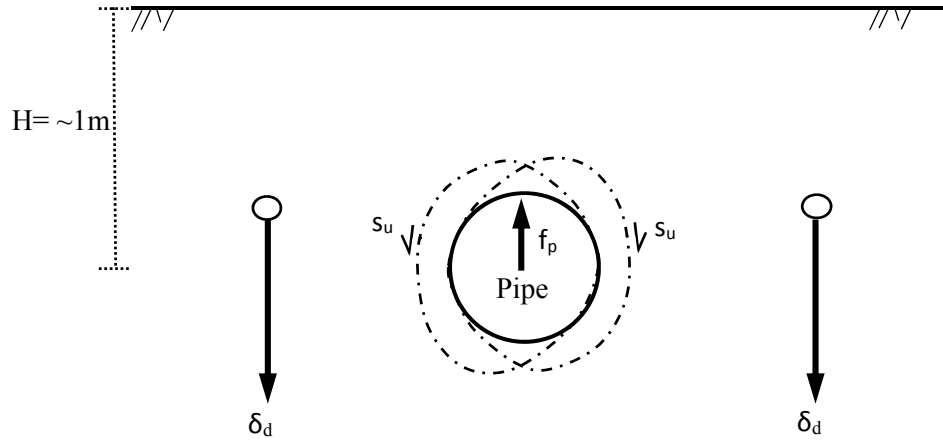


Figure 8-4 Soil Displaces Around the Pipe Mechanism.

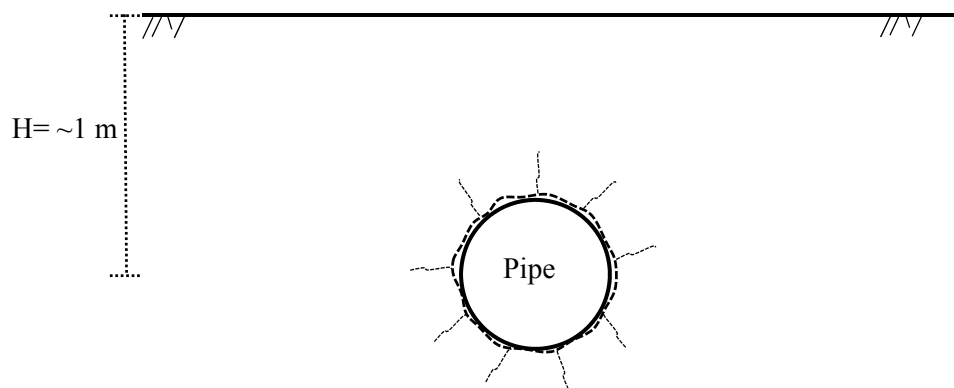


Figure 8-5 Loss of Soil-Pipe Contact due to Soil Volume Change Mechanism.

## **Chapter 9 Risk Management System**

Chapter 9 describes the risk management system developed to assess the risk to buried gas pipelines within ground movement areas such as landslide areas. This risk management system is referred to as the PipeHaz risk management system within this thesis research. The PipeHaz risk management system (PipeHaz) is intended to provide a simple and flexible risk management approach for gas pipelines in Manitoba that may be at-risk due to ground movements (geotechnical hazards). Specifically, risks associated with ground movements along natural slopes and at river crossings. PipeHaz uses a multi-phase approach which can be applied in full or in parts and complies with CSA standards for onshore gas pipelines (CSA Z662-15). The system relies on gathering and reviewing of pipeline and hazard information, subjective and statistical (from the results in Chapter 7) estimates of probability of pipeline failure for various types of ground movement, and vulnerability of the system to these movements. The probability of failure estimates are then compared to limit states target values. Probability of pipeline failure estimates exceeding limit states target probabilities of failure are considered to be unacceptable. PipeHaz utilizes two RBDA risk estimation methods in a staged approach. A quantitative risk indexing method is used earlier on in the risk management system to screen and categorize pipeline locations that may be at-risk. The second method is a statistical risk analysis approach using the outcome of this thesis research where the statistical parameters from the monitored pipe stresses/strain data are used in conjunction with theoretical probability distributions to predict probability of pipeline failure for other



pipelines in slow moving landslide areas. Other statistical methods are to be used to assess pipeline risk when subjected to sudden and significant landslide movements.

The main objectives of the PipeHaz system are to:

- encompass all possible geotechnical hazards that the pipeline may be subjected to at river crossings or along or near natural slopes,
- identify the extent of these hazards,
- estimate the likelihood of hazard occurrence, vulnerability of the system, and probability of failure along the pipeline,
- provide a method to rank and compare sites,
- enable comparison of the risks associated with geotechnical hazards to other geohazards (hydrotechnical) and other risks (i.e. corrosion),
- and develop measures to mitigate, reduce or eliminate risk and improve system reliability in a justifiable and effective manner.

### **9.1 Phased Approach to PipeHaz**

PipeHaz uses a five phased approach to identify, assess, and manage risks. With each phase of the system, the degree of uncertainty associated with the estimates of hazard likelihood and probability of pipeline failure decreases. The five phases are as follows:

- Phase 1 – Information gathering and review.
- Phase 2 – Hazard inventory, probability of pipeline failure estimations, and risk evaluation.
- Phase 3 – Risk control analysis and cost-benefit analysis.

- Phase 4 – Action - remedial works, monitoring, re-evaluation (probabilistic risk analysis).
- Phase 5 – System maintenance.

The PipeHaz risk management process is illustrated in Figure 9-1. The site monitoring process and later stages (site monitoring) within the PipeHaz system is quite detailed and the end process is illustrated in detail in Figure 9-2.

#### *9.1.1 Phase 1 – Information Gathering and Review*

Potential sites within owner/operator’s pipeline system exposed to geotechnical hazards are identified through review of air photos (most recent), maintenance records, and field site inspection reports. Potential sites are then combined with sites that have already been previously identified to determine the total number of at-risk sites. Once all at-risk sites have been identified, available relevant information is then gathered and reviewed such as pipeline characteristics (size, yield strength, year installed, burial depth), anecdotal information from local inspectors, line operating pressure, soils information, geological information, existing engineering reports, groundwater information, rainfall data and air photos from previous years. This creates an information inventory at each site to which the level of knowledge (calculated in Phase 2) can be estimated based on the type, quantity, and quality of information available. The level of knowledge is a way to estimate the uncertainty in a subjective probability of failure estimate and is similar to a standard error estimate.

### *9.1.2 Phase 2 – Hazard Inventory, Probability of Pipeline Failure Estimations, and Risk Evaluation*

Phase 2 implements a variation of a quantitative risk indexing method to estimate risk at a particular site. A risk indexing method is, in essence, a quantification of a Failure Mode and Effects Analysis (FMEA) method. The risk indexing method is explained in detail in Section 9.2 with an example application included in Appendix E. The PipeHaz system incorporates a quantitative risk indexing method for estimating probability of pipeline failure (referred to as probability of pipeline failure index) for each geotechnical hazard, but handles consequences separately through the reliability based limit states approach.

Each at-risk site is visited by qualified personnel to assess site conditions and determine the estimated probability of pipeline failure in a given year using the PipeHaz indexing method. The estimated probability of failure for each site is compared to target probabilities which is used to classify the site as either low, moderate, high risk, or exceeds limit states targets as illustrated in Figure 9-3. The extent for each zone was defined subjectively. An estimated probability of pipeline failure plotting within any of the zones defined will be within 50% (high), an order of magnitude (moderate), or two orders of magnitude (low) of the limit states target probability of pipeline failure.

The site classifications are reviewed and evaluated for sites that are deemed unacceptable and require further risk assessment (Phase 3 and Phase 4). Gas pipeline owner/operators may deem any risk level as unacceptable. It is suggested that sites with a high risk level or greater be deemed unacceptable. These sites are considered to be priority sites and would require further risk evaluations and may require site monitoring and higher level

risk assessments. Figure 9-4 presents a flow chart for priority sites. Site monitoring and higher level risk assessment should be skipped for sites that exceed limit states targets. These sites are automatically considered for remedial construction works (Phase 4) and are placed on a project planning list.

### *9.1.3 Phase 3 – Risk control analysis and cost-benefit analysis*

Phase 3 of the PipeHaz system involves development of conceptual risk control options for sites deemed unacceptable (priority sites) such as reduction of hazard likelihood, system vulnerability, and consequence. Risk control costs and effectiveness are estimated. The risk control options at each priority site are then evaluated and the most appropriate risk control option is selected for a cost-benefit analysis. A cost-benefit analysis is undertaken on the preferred control option.

### *9.1.4 Phase 4 – Action - remedial works, monitoring and re-evaluation*

Phase 4 of the PipeHaz system is discussed in the following sections.

#### **9.1.4.1 Project Planning List and Remedial Construction**

The outcome of the cost-benefit analysis is used to determine priority sites that require remedial works or monitoring. Priority sites with a cost-benefit ratio greater than unity are automatically placed on a project planning list for remedial works along with priority sites identified in Phase 2 (sites significantly exceed limit states targets) as shown in Figure 9-4. Within the planning list, sites are ranked in terms of their cost-benefit ratio, budget availability, importance of the pipeline to local, regional, and system operations. Intuitively, sites identified in Phase 2 which significantly exceed limit states targets will

be ranked high. Remedial works are implemented based on the ranking system accordingly. Remedial works may include erosion protection measures along water bodies, slope stabilization, adjustments to burial depth (*i.e.* directional drilling of deeper pipes at river crossings), pipe relaxation (through excavation, cutting and re-burial), and in extreme cases, pipeline re-alignment. Approvals for remedial works are easier to attain with results from a well-defined and systematic risk management system such as PipeHaz, thus helping to facilitate the approval process.

#### 9.1.4.2 Site Monitoring and Re-Evaluation of Risk

Priority sites with cost-benefit ratios less than one trigger site monitoring and re-evaluation of risk at a set frequency as a means to control risk (Figure 9-4). Site monitoring is essential to properly capture changes in site conditions over time, especially changes in conditions that increase the likelihood of hazard occurrence or increase the vulnerability of the pipeline. Monitoring of priority sites is to include scheduled site visits at an appropriate frequency by qualified personnel to re-assess the probability of failure as conditions change on site. In particular, the site monitoring schedule should capture factors that are seasonal and somewhat time dependent which significantly influence the probability of a hazard occurring such as the amount of erosion, and the extent and number of tension cracks in a landslide area. Ideally, qualified personnel are assigned to specific priority sites to monitor and do not switch sites. The risk estimate for the priority sites will be re-evaluated following each site visit using the quantitative risk indexing method as outlined in Phase 2. The frequency of the site visits will be dependent on the site classification and can be modified based on the results of

the re-assessed probability of failure estimates. The cost-benefit analysis (Phase 3) for a priority site may also be re-assessed based on the results of the site monitoring.

#### 9.1.4.3 Observed Ground Movements at Priority Sites

If ground movements are physically observed or landslide activities are suspected to be occurring during site monitoring, the priority site (with a cost-benefit  $< 1$ ) will be surveyed and instrumentation is to be installed to measure ground movements either at surface using monitoring pins, or at depth with slope inclinometers. The intent of the instrumentation is to confirm ground movements, and gain an understanding of the direction and rate of movements. Obtaining ground movement data will enable the use of more advanced risk estimation methods, some of which are based on the outcome of this thesis research. This allows for a higher level prediction of probability of pipeline failure. The risk estimation approach will differ for slow moving landslide areas *versus* areas with a potential for a sudden and significant landslide as shown in Figure 9-2.

Exceedance of limit states (yielding or local buckling) will be estimated using statistical methods based on the measured stress and strains at the Harrowby middle of valley and Plum River along the slope set-ups for priority sites where pipelines are within slow moving landslide areas with ground movements less than 50 mm/year. Tables 7-6 and Tables 7-7 can be used to quickly determine if yielding and local buckling limit states failure modes are exceeded for a particular pipeline for a certain class. Alternatively, the Probability of Failure Estimator spreadsheet included in the digital appendix can be used to determine if limit states are exceeded. Pipeline properties along with pipeline class are inputted into the spreadsheet and probability of failure estimates for valley areas and

riverbank areas are generated including and excluding “locked-in” backfill stresses. The generated probability of failure estimates are compared to target limit states values and compliance with limit states is determined in the spreadsheet. If the estimated probability of failure for a priority site exceeds limit states target probability of failure, the priority site will be added to the project planning list.

For landslide areas where ground movements are larger than 50 mm/year, Figure 2-2 from Mansour *et al.* (2011) is used to determine the potential degree of damage to infrastructure and if the risk to the pipeline is acceptable.

The probability of pipeline failure estimates presented in Chapter 7 assumes ground movements are relatively constant and does not consider the probability of a sudden, fast moving landslide, with significant ground movements (major landslide). The probability of a sudden, significant landslide and the risk to a pipeline within the landslide is a separate, independent set of probabilities. A qualified geotechnical engineer is required to assess the susceptibility of the pipeline to the occurrence of a major landslide to determine next steps. One option is to undertake a probabilistic slope stability analysis to determine the probability of a landslide occurring that encompasses the pipeline and then the probability of pipeline failure as result of the triggered landslide needs to be calculated. Calculating the probability of pipeline failure once a sudden, significant landslide occurs is not straightforward. The probability failure for pipelines within a major landslide could easily be close to unity, but is dependent on the nature of the landslide in terms of its mass, the location of pipeline relative to the slip surface of the slide, pipe geometries, etc. A simple approach is to assume the probability of pipeline failure once a major landslide occurs is unity and therefore, the calculated probability of a

major landslide encompassing the pipeline can be directly compared to the limit states target. Alternatively, other engineering tools or judgment can be used to estimate the probability of pipeline failure once a major landslide occurs. A deterministic slope stability analysis approach could also be used to predict the probability of landslide occurring at the pipeline, but this approach would require assumptions and subjective inputs by the geotechnical engineer. The outcome of engineering assessment will determine if remedial works are required and if so, the site will be ranked and placed on the project planning list.

#### *9.1.5 Phase 5 – System Maintenance*

The PipeHaz risk management system requires validation in the first few years of implementation and there will likely be adjustments and modifications required to the system. The PipeHaz system also requires regular maintenance and updates. The PipeHaz risk management system is somewhat of a living system since its ability to manage risk increases with time as long as the system is adjusted and upgraded to improve performance to suit the needs of the owner. In particular, subjective probabilities, weighted factors may need to be adjusted over time. A long term system management plan is key to the effectiveness and performance of the PipeHaz system and should include periodic “re-booting” of the entire system, starting at Phase 1. A “re-boot” allows for a fresh new look at all possible at-risk sites.

Gathering of additional information may be warranted for high risk sites with a large uncertainty in the probability of pipeline failure estimates to verify that these sites do not exceed limit states targets. Obtaining soil, groundwater, and geometric information at



these sites will significantly reduce the uncertainty and improve the accuracy of the probability of pipeline failure estimates.

## **9.2 Quantitative Risk Indexing Method**

The risk indexing method developed has been adapted from Ferris *et al.* (2003). A quantitative risk index entails identifying factors influencing hazard likelihood, vulnerability, and consequences where values for each factor are assigned subjectively. These values are combined to provide an estimate of failure probability and risk. The uncertainty in the estimated probability of failure is calculated using a separate index related to the level of knowledge of the site. An example of the risk indexing method for the Harrowby site is included in Appendix E.

### *9.2.1 Determination of Parameter Uncertainty*

The level of knowledge at a site is used to calculate the uncertainty or in other words, the accuracy in the probability of pipeline failure estimates. Table 9-1 presents a level of knowledge index and includes 12 categories of information types pertinent to assessing geotechnical hazards. Each category is weighted out of unity based on their influence in understanding geotechnical conditions at a site. The presence of engineering reports and ground movement monitoring are heavily weighted within the index with a total weight of 0.5 out of 1.0. All other information categories have been assigned a weight of 0.05. For each category, the level of knowledge (based on the information gathered in PipeHaz Phase 1) is determined from Table 9-2 as either negligible to low (0.01) to very high (0.9). The level of knowledge is multiplied by the weighted values and summed to produce the level of accuracy of the probability of pipeline failure estimated at a

particular site. The level of knowledge index produces uncertainty values in estimated probability ranging between 10% for a site with high levels of information for all 12 categories or within two orders of magnitude for a site with little to no information.

### *9.2.2 Subjective Probability of Failure Estimates for Geotechnical Hazard*

Geotechnical hazards are separated into two individual probability of pipeline failure indexes, one for landslides and the other for ground settlement, subsidence and soil heave. Each index includes a list of factors that can trigger geotechnical hazards (Tables 9-3 and 9-4). The factors are weighted out of unity based on how a particular factor contributes to the overall failure mechanism.

A subjective probability is then selected from Table 9-5 by qualified personnel for each factor based on the likelihood of the factor having an influence in a given year and the vulnerability of the system to the factor being examined. The selected subjective probability is multiplied by the weighted values and the summation of the products provides an estimate of probability of pipeline failure for that particular hazard. The summation of each individual probability of pipeline failure for each geotechnical hazard provides the overall probability of pipeline failure for geotechnical hazards.

The subjective probability matrix (Table 9-5) is adapted from Ferris et al. (2003) which was developed by an expert panel. The possible values within the matrix range from a probability of  $P_f = 1.0$  to a probability of  $10E-06$  per year depending on the likelihood of a factor having an influence on triggering a particular hazard (negligible to very high) and the vulnerability of the system to this factor (unlikely to likely vulnerable). The range of

subjective probabilities in Table 9-5 is also equivalent to the possible range of overall probability of pipeline failure outcomes for each index (Tables 9-4 and Tables 9-5).

The landslide index considers factors related to erosion (toe and scour), groundwater (seepage, external water source to slope), vegetation damage, external loads (loading at crest), evidence of ground movements (tension cracks, head scarps, compression ridges) and history of landslide activity at the site or nearby. Factors indicative of ground movement (tension cracks, head scarps/slump blocks, and compression ridges) account for a weighting of 0.45 out of 1.0 while historical landslide activity accounts for a weighting 0.2 out of 1.0. All other categories have been assigned a weight of 0.05 out of 1.

The index for ground settlement, subsidence and soil heave considers factors related to permafrost (thawing, discontinuous), volume change of the soil (frost heave, shrinking/swelling potential), and installation/maintenance (poor backfill techniques, sinkholes from poor directional drilling techniques). All factors have been assigned roughly equal weighting of 0.15 or 0.2 out of 1.0. The current PipeHaz risk management system only considers the probability of pipeline failure due to ground settlement, subsidence and soil heave at river crossings or along or near natural slopes, but can be expanded to assess this hazard along the entire length of the pipeline.

The risk indexing method evaluates geotechnical hazards at specific locations and therefore, location-specific limit states reliability targets values are applicable within the evaluation length calculated for each site (Section 7.1.1). The results the of risk indexing method are compared against limit states target probability of failure values to determine

compliance or exceedance and next steps in PipeHaz system will depend on the outcome of the comparison (Figure 9-1).

### **9.3 Summary**

The PipeHaz system incorporates the results of this thesis research in order to provide a higher level method of assessing risk and probability of pipeline failure. This risk management system is considered to be robust and comprehensive, but is simple enough to implement in full or individually. PipeHaz can be modified or adapted easily by the service provide to suit their needs and internal systems. The intent of the PipeHaz system is to illustrate a fully detailed risk management system in compliance with CSAZ662-15 and is in line with current industry standards.

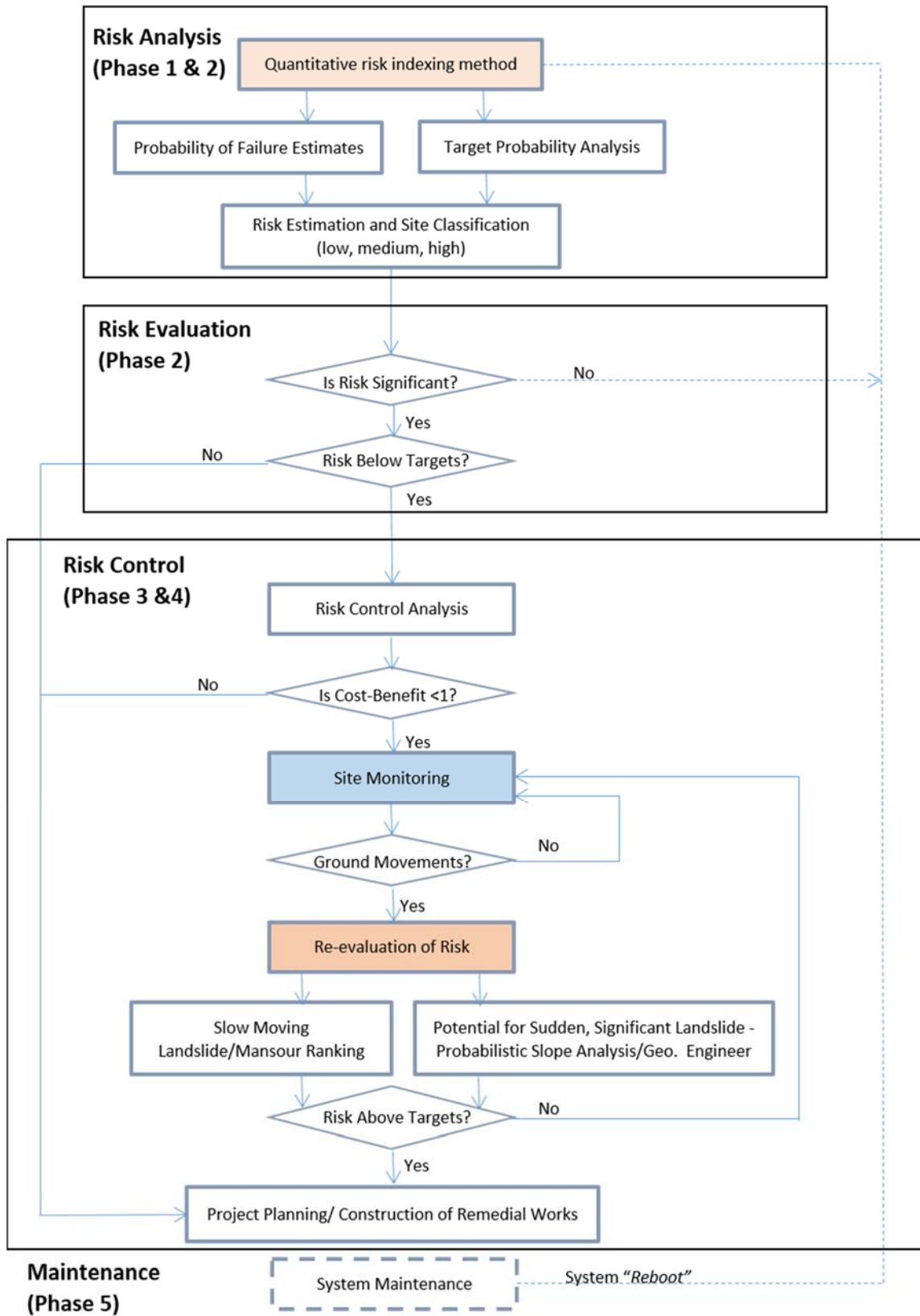


Figure 9-1 PipeHaz Risk Management Process.

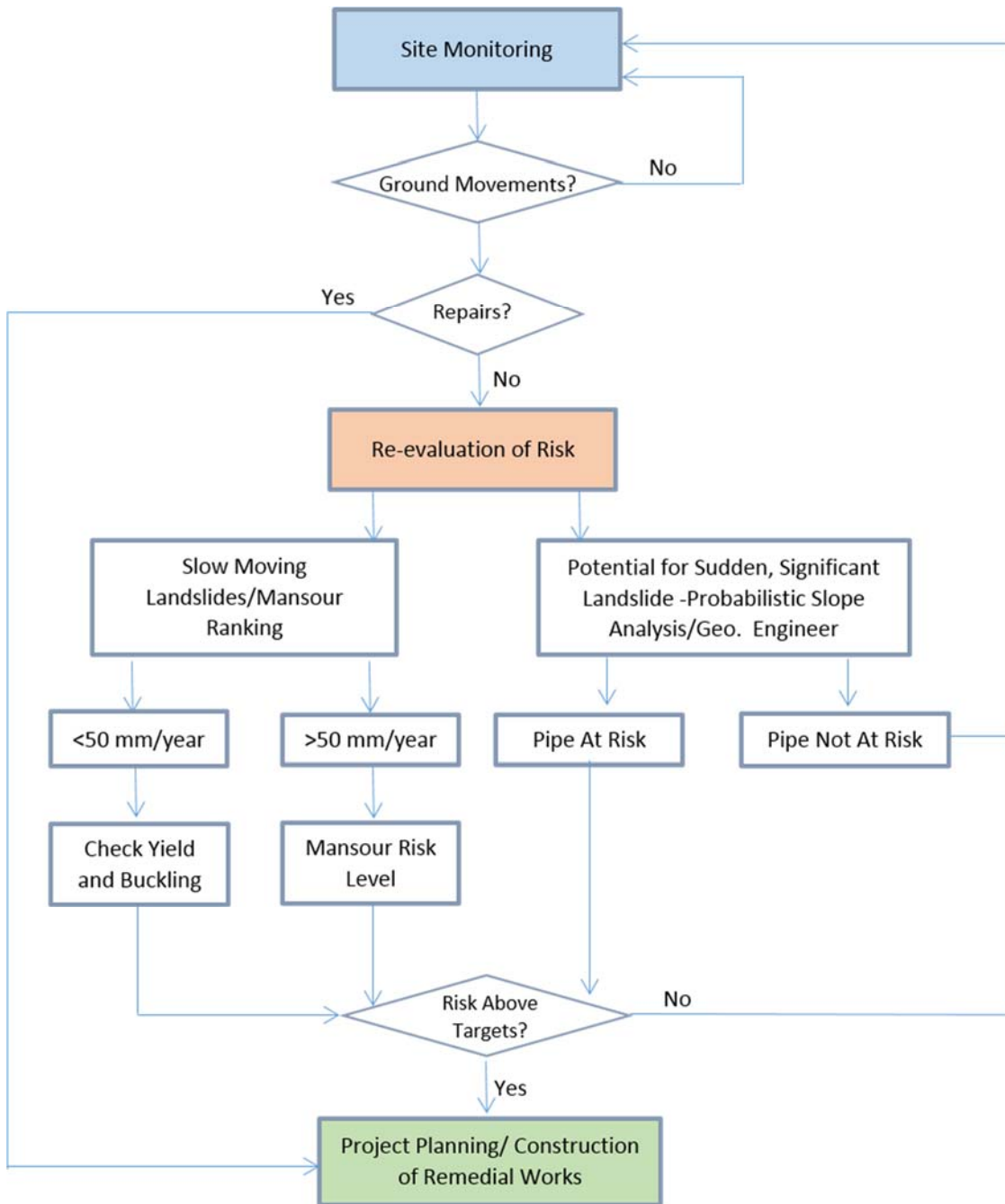


Figure 9-2 PipeHaz Detailed Site Monitoring Process.

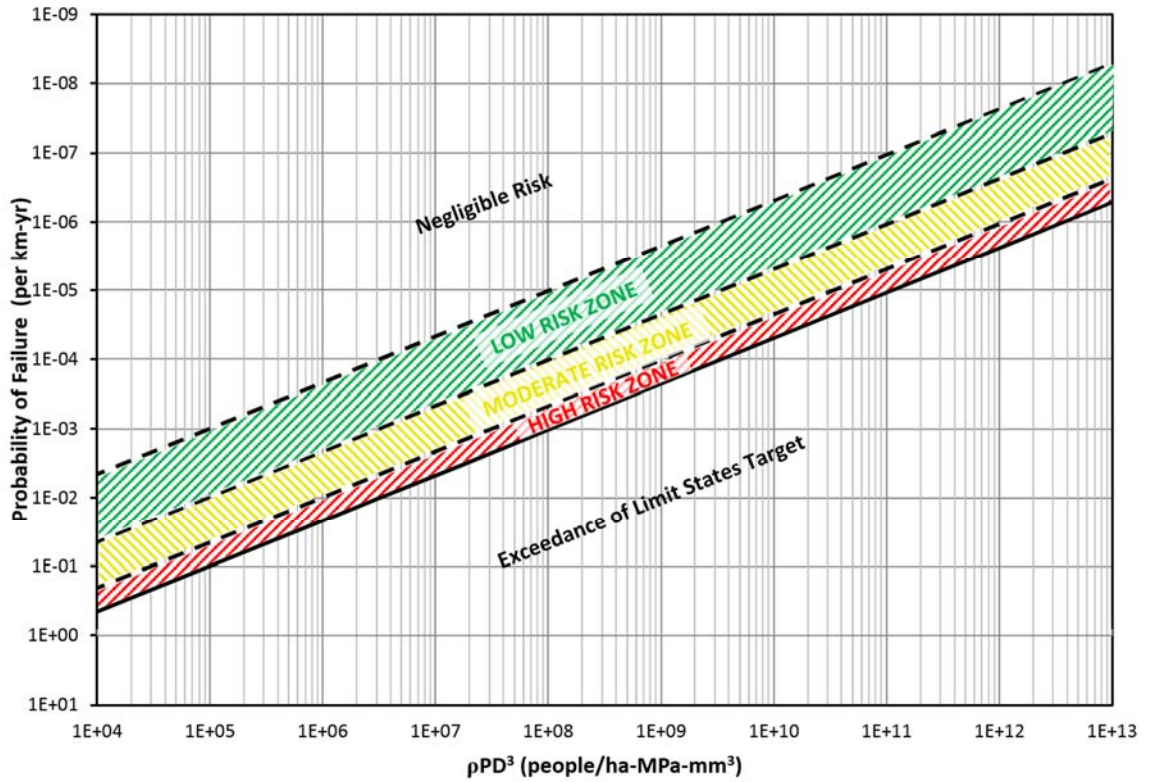


Figure 9-3 Risk Level for Site Probability of Failure Targets.

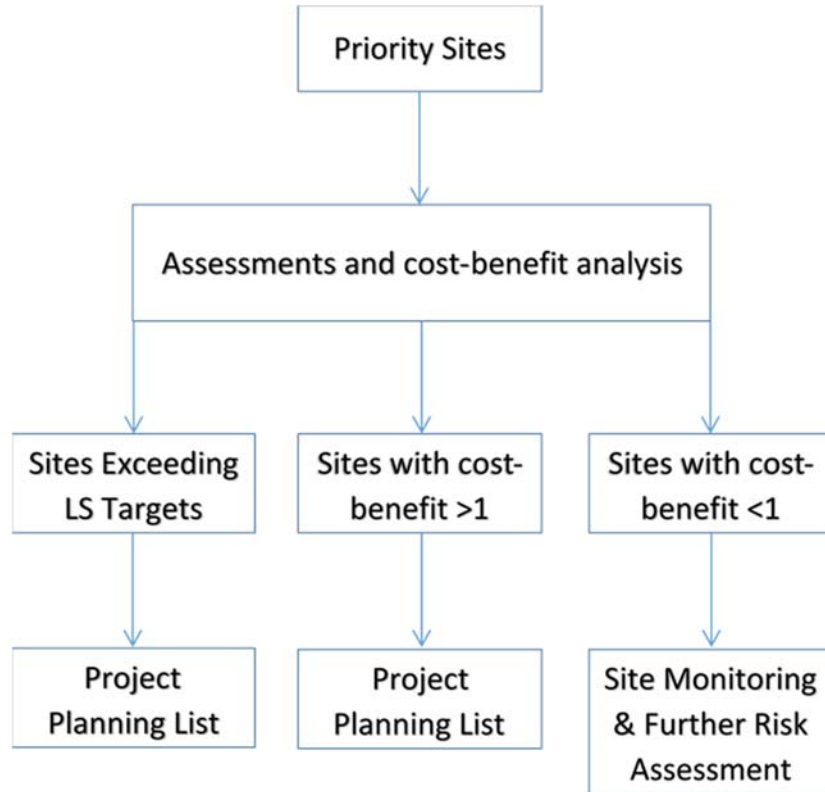


Figure 9-4 Priority Sites Flow Chart.

Table 9-1 – Level of Knowledge at a Site Index.

<b>Information</b>	<b>Description</b>	<b>Weighting</b>	<b>Level of value</b>	<b>Product &amp; Summation</b>
Natural hazard maps	Area covered by map and reviewed	0.05		
Aerial photos (various years)	Area covered by aerial and reviewed	0.05		
Geological maps	Area covered by map and reviewed	0.05		
Maintenance records	Quality and quantity	0.05		
Field inspection reports	Quality and quantity	0.05		
Groundwater information	Proximity to site and frequency of measurements	0.05		
Rainfall data	Proximity to site and frequency of measurements	0.05		
Soils information	Proximity of test holes and quality, area covered by soils map	0.05		
Existing eng. studies	Quality of study	0.30		
Ground movement monitoring	Survey pins, Slope inclinometers (quality and quantity)	0.20		
Pipe details and operation	Quantity and line pressure data available	0.05		
Anecdotal information	Quality of source	0.05		
<b>Total</b>		<b>1.00</b>	<b>±AP<sub>f</sub></b>	



Table 9-2 – Level of Value of Information.

Level of Information	Factor
Very High	0.9
High	0.50
Medium	0.10
No to Low	0.01

Table 9-3 – Landslides Probability of Pipeline Failure Estimate Index.

Hazard	Weighting	Subjective Probability	Product & Summation
Toe Erosion	0.05		
Scour	0.05		
Bank Failures	0.10		
Piezometric Conditions	0.10		
Seepage Exiting Face of Slope	0.05		
External Water Source to Slope	0.05		
Damage to Vegetation	0.05		
Loading at Crest	0.05		
Tension Cracks	0.10		
Head Scarp/ Slump Blocks	0.10		
Compression Ridges	0.10		
History of Landslide Activity at site or nearby	0.20		
<b>Total</b>	<b>1.00</b>	<b><math>P_f</math></b>	

Table 9-4 – Ground Settlement, Subsidence and Soil Heave Probability of Pipeline  
Failure Estimate Index.

<b>Hazard</b>	<b>Weighting</b>	<b>Subjective Probability</b>	<b>Product &amp; Summation</b>
Thawing Permafrost (Pingo)	0.15		
Area of Discontinuous Permafrost	0.20		
Frost Heave Susceptible Soils	0.20		
Shrinking/Swelling Potential Soils	0.15		
Poor Backfill Techniques	0.15		
Sinkholes from piping	0.15		
<b>Total</b>	<b>1.00</b>	<b><math>P_f</math></b>	

Table 9-5–Subjective Probability (in a Given Year).

Likelihood of Factor Having an Influence	State of the System		
	Unlikely Vulnerable	Moderately Vulnerable	Likely Vulnerable
Very High	1E-01	5E-01	1.0
High	1E-02	5E-02	1E-01
Moderate	1E-03	5E-03	1E-02
Low	1E-04	5E-04	1E-03
Negligible	1E-06	5E-06	1E-05

## **Chapter 10 Summary, Conclusions and Recommendations for Future Research**

### **10.1 Summary**

This thesis research investigated the risk of buried pipeline failure in landslide areas, in particular landslide movements along the longitudinal direction of a pipeline. The research assessed stress/strains induced on pipelines due to landslides focusing on the response of a pipeline and working towards linking it to ground movements. Probability theory in conjunction with a RBDA limit states approach was used to determine risk of pipeline failure.

Within Manitoba, natural gas pipeline sites that are at-risk to landslide movements were examined and three sites were selected for further research. The three research sites represent a range of landslide types (translational, rotational), are in different geological features, and are considered to be high risk within Manitoba Hydro's gas pipeline network. The three research sites selected were the Plum River crossing, Harrowby Assiniboine River valley, and St-Lazare Assiniboine River valley sites.

A comprehensive field and monitoring program was undertaken to identify and quantify possible sources of load that may be inducing strains/stresses on the pipelines and the sources examined include landslide ground movements, soil volume change due to freeze-thaw, and elongation/compression of the pipe due to temperature change. Soil and pipe instrumentation sets were installed at eight locations between the three research sites and the instrumentation monitored temperature changes (soil and pipe), groundwater

levels, and longitudinal and torsional pipe strains. Ground movements were initially to be measured using slope inclinometers (SIs), but the SIs became inoperable early on due to ground movements. The method to measure ground movements was switched to ground based survey of monitoring pins for the remainder of the research only at the valley sites. Alternative methods to measure ground movement measurements at Plum River were deemed to be inappropriate.

Soil, pipe, and ground movements were measured for about four years and a significant amount of data was recorded. Data filtering was required on some of the data to produce usable data for additional analysis. The soils in the vicinity of the pipelines did not freeze and loads associated with freeze/thaw on the pipeline were not examined further. Ground movements at the valley sites were generally downslope and perpendicular the valley slopes and are considered to be slow moving landslides (<50 mm/year).

Axial, bending and torsional stresses were calculated for each monitoring location and showed that backfilling, changes in river levels, thermal effects, a soil-pipe relaxation mechanism (speculated), and ground movements all affected pipe stresses and behaviour. Large backfill stresses were induced on the pipe at the monitoring locations and these stresses (predominantly bending) were “locked-in”, or dissipated partially or fully over the duration of the monitoring. Pipe thermal effects dominated the measured axial stress, with little to no axial stresses measured without thermal effects. Landslide ground movements and/or a soil-pipe relaxation mechanism appear to be inducing distinct and notable changes in pipeline axial and bending stresses. Some of these, in particular distinct changes in longitudinal pipe stresses, occur at roughly the same time (spring) between the two valley sites.

Pipe push tests were conducted to gain a better understanding of soil-pipe adhesion and to provide a possible explanation of the pipe behaviour observed in the monitoring data. The results of the pipe push tests in conjunction with finite element modelling suggests decreases in measured axial tension at some of the monitoring locations (Harrowby and Plum River) may or may not be due the pipeline slipping through the soil while pipe slippage has likely not occurred at the St-Lazare site.

Several ultimate and serviceability limit states pipe failure modes were examined using the measured pipe stresses such as tensile rupture, local buckling, and yielding. Statistical analysis was undertaken to calculate the probability of pipeline failure for the various limit states failure modes at each monitoring location. Probability of failure estimates were insignificant for tensile rupture and strain based local buckling.

The probability of failure estimates for yielding and stress based buckling were compared to limit states reliability targets and generally, satisfied limit states reliability targets when “locked-in” backfill stresses were removed. An increase in the average pipe loading of about +45% to +509% is required to exceed limit states reliability targets at the research sites and although the initial stress-state of the monitored pipeline was not released, the pipelines at the research sites could accommodate some initial pipe stresses or additional stresses in the future without exceeding limit states targets. Other pipelines were examined within Manitoba Hydro’s pipeline network and the majority of the pipelines would satisfy limit states if subjected to slow moving landslides when “locked-in” backfill stresses are not included.

The probability of failure estimates were generally insignificant or low and speculated to be due to a soil-pipe relaxation mechanism which is causing a release in longitudinal pipe stresses. Pipe monitoring results revealed a decrease in downward bending and axial tension that cannot be easily explained through landslide movements. Three hypothetical mechanisms were presented and discussed such as an upward block movement, soil displaces around the pipe, and loss of soil-pipe contact due to soil volume change.

The outcome of the research was used to develop a risk managements system (PipeHaz) to examine geotechnical hazards for a pipeline network. Specifically, risks associated with ground movements along natural slopes and at river crossings are examined within the system. Two RBDA based risk estimation methods in a staged approach are used to determine exceedance of limit states reliability targets. A quantitative risk indexing method is used earlier on while the second method utilizes the outcome of this thesis research to predict probability of pipeline failure for pipelines within slow moving landslides. The PipeHaz risk management system is a fully detailed risk management system in compliance with CSAZ662-15 and is in line with current industry standards.

## **10.2 Conclusions**

The conclusions of the research are:

1. The Assiniboine river valley walls are likely active in areas where ancestral landslides have occurred and are considered to be slow moving landslides (<50 mm/year).

2. Placing backfill around and below pipelines induces large pipe stresses, especially bending, regardless if good construction practice is used in backfilling of excavations. These backfill stresses may exceed limit states related to yielding and reduces the capacity of pipeline, especially when backfill stresses are “locked-in”.
3. The soil in the vicinity of buried gas pipelines does not freeze therefore freeze/thaw induce pipe stresses do not occur.
4. Pipe temperature changes dominate measured axial strains, and little to no axial stresses were measured without thermal effects.
5. A pipeline instrumented with strain gauges acts like a sensitive instrument which responds to very small soil movements.
6. Strain gauges provide useful data, but their reliability can be problematic and may require post processing to produce usable data.
7. Distinct changes in longitudinal pipe stresses occur in the spring within the Assiniboine River Valley, suggesting regional conditions indirectly effects pipe stresses.
8. Landslide related ground movements are causing distinct and notable changes in longitudinal pipe stresses as follows:
  - a. increased downward bending stresses and axial tension either increased or was relatively unchanged,
  - b. and decreased downward bending and increased axial tension.
9. Longitudinal pipe stresses and strains due to ground movements are not sustained and are not cumulative with additional ground movements as has been typically

assumed by other researchers. This has lowered probability of pipeline failures estimates for the various limit states.

10. A soil-pipe relaxation mechanism is causing a reduction or full release of longitudinal pipe stresses (downward bending and axial tension).
11. Pipe slippage (exceedance of soil-pipe adhesion) is a possible explanation for the observed decreases in axial tension.
12. Probability of pipeline failure is below limit states targets for various failure modes and for most of Manitoba Hydro's pipeline network for pipelines within slow moving landslide areas (<50 mm year). This is based on the monitoring results assuming the initial stress-state of the monitored pipeline was at or close to zero.
13. Pipelines may exceed limit states targets for yielding and local buckling depending on if these pipelines run through slow moving landslide areas and the class of the pipeline is high.
14. The risk management system developed using the outcome of the research is considered to be a comprehensive, robust, progressive and effective way to manage pipeline risk in areas where ground movements are suspected.

### **10.3 Recommendations for Future Research**

The following are recommendations for future:

1. Current backfilling techniques need to be assessed and modified to reduce the potential for imposing high pipe stresses during backfilling. New techniques should also be considered. Conducting field tests on modified or new techniques



would provide valuable insight into the response of the pipeline and is strongly recommended.

2. The initial stress-state of a pipeline could not be determined. Further research into this would allow a more representative estimate of probabilities of pipeline failures. The probability of failure estimates presented herein can then be recalculated including the initial stress-state of the pipelines.
3. Soil-pipe adhesion may be exceeded (pipe slippage) at two of the research sites, limiting the maximum axial tension stress on the pipelines. It would be valuable to confirm if pipe slippage is occurring through additional analysis as it is a reasonable explanation of the observed release of axial tension stresses in the pipeline.
4. Three hypothetical soil-pipe relaxation mechanisms were proposed based on the observed behaviour of the pipeline. Additional research work is needed to gain a better understanding of the pipe behaviour observed and the mechanisms causing a reduction and sometimes loss in downward bending and axial tension stresses.
5. The degree of soil-pipe relaxation varied between monitoring locations. Measured longitudinal pipe stresses at the Harrowby middle of valley set-up seem to be somewhat sustained and cumulative with additional ground movements. Understanding the conditions that result in soil-pipe relaxation occurring versus those that result in sustained and cumulative pipe stresses is key in evaluating the risk to buried gas pipelines.
6. The outcome of the research is applicable for buried pipelines subjected to slow moving landslides where ground movements are less than 50 mm/year. Higher

rates of ground movements may produce higher probability of failure estimates and should be examined further. The data collected in this thesis research would be well suited to develop a Finite Element Model to predict pipe response at higher rates of ground movements and the data collected can also be used to calibrate model. Careful consideration should be taken into how to handle soil-pipe relaxation and pipe slippage in the predicative model since any probability of pipeline failure estimates would be sensitive to these considerations.

7. Alternative methods to measure ground movements and pipe stresses should be considered if similar work is to be undertaken in the future. Vibrating wire strain gauges and fiber optic strain sensors are examples of alternative ways to measure pipe strain. Digital Image Correlation (Take, 2015) and Interferometric Synthetic Aperture Radar (InSAR) remote sensing could be used to measured ground movements in lieu of slope inclinometers or ground based survey.
8. The risk management system proposed should be tested and implemented since it is a more comprehensive, higher level approach to what is typically used in industry.

## Chapter 11 References

Acres Manitoba Ltd. 2000. Study of Slope Failures Along PTH41 St-Lazare, Manitoba. Report prepared for Manitoba Infrastructure and Transportation.

Allergro Energy Consulting. 2005. Safety Incidents on Natural Gas Distribution Systems: Understanding the Hazards. Office of Pipeline Safety U.S Department on Transportation.

American Lifelines Alliance and American Society of Civil Engineers. 2001. Guidelines for the Design of Buried Steel Pipelines. ASCE

Ang, A.H., Tang, W.H. 2007. Probability Concepts in Engineering: Emphasis on Applications to Civil and Environmental Engineering. 2nd edition, John Wiley and Sons.

ASTM D422-63. 2007. Standard Test Method for Particle-Size Analysis of Soils. ASTM, West Conshohocken, PA.

ASTM D2166-13. 2013. Standard Test Method for Unconfined Compressive Strength of Cohesive Soil. ASTM, West Conshohocken, PA.

ASTM D2216-10. 2010. Standard Test Methods for Lab Determination of Water Content of Soil. ASTM, West Conshohocken, PA.

ASTM D2487-11. 2011. Standard Practice for Classification of Soils for Engineering Purposes (Unified Soil Classification System). ASTM, West Conshohocken, PA.

ASTM D4318-10. 2010. Standard Test Methods for Liquid Limit, Plastic Limit, and Plasticity Index of Soils. ASTM, West Conshohocken, PA.

ASTM D6913-04. 2009. Standard Test Methods for Particle-Size Distribution (Gradation) of Soils Using Sieve Analysis. ASTM, West Conshohocken, PA.

Bai, Q., Bai, Y (2014), Seabed Pipeline Design, Analysis, and Installation. 1st edition, Elsevier Science: Burlington.

Baldwin, J.R. 2007. Development of a GIS-Based Landslide Management System for Western Manitoba's Highway Network. M.Sc. Thesis. University of Manitoba, Canada.

Becchi, R., Scarpelli, G., Cuscuna, S., Re, G., Tomassini, D. 1994. Safety and serviceability analysis of pipelines in unstable slope. In Proceedings International 13th Conference on Offshore Mechanics and Arctic Engineering. Houston, USA.

Blatz, J.A, Ferreira, N.J, Graham, J. 2004. Effects of Near-surface Environmental Conditions on Instability of an Unsaturated Soil Slope. Canadian Geotechnical Journal. Volume 41, 1111-1126.

Braun, J, Major, G, West, D., Bukovansky, M. 1998. Geological Hazard Evaluation Boosts Risk-Management Program for Western U.S Pipeline. Oil and Gas Journal. Volume 96, 73-79.

Brüggemann, H., Schermann, P., Kleindorf, C. (2005), Elasto-Plastic Bearing Behaviour of Steel Pipes Subjected to Internal Pressure and Bending. 3R International, Volume 44, Issue 7, 148-422.

Bruschi, R., Glavina, M., Spinazze, M., Tomassini, D. 1996. Pipelines subject to slow landslide movements structural modelling vs Field Measurements. In Proceedings 15th International Conference on Offshore Mechanics and Arctic Engineering. Houston, USA.

Bruschi, R., Monti, P., Bolzoni, G., Tagliaferri, R. 1995. Finite Element Method as Numerical Laboratory for Analyzing Pipeline Response under Internal Pressure. In Proceedings 14th International Conference on Offshore Mechanics and Arctic Engineering. Copenhagen, Denmark.

Bruschi, R., Tomassini, D., Cuscani, S., Venzi, S. 1995. Failure Modes for Pipelines in Landslide Areas. In Proceedings 14th International Conference on Offshore Mechanics and Arctic Engineering Copenhagen, Denmark, 1995

Bowels, J. 1997. Foundation Analysis and Design. 5th edition, The McGraw-Hill Companies Inc.

Calvetti, Francesco, Prisco, Claudio di, Nova, Roberto. 2004. Experimental and Numerical Analysis of Soil-Pipe Interaction. Journal of Geotechnical and Geoenvironmental Engineering. Volume 130, 1292-1299.

Canada. National Energy Board Onshore Pipeline Regulations. SOR/99-294.

Canadian Standards Association. (2001). CSA S16-01 Design of Steel Structures.

Canadian Standards Association. (2011). CSA Z662-11 Oil and Gas Pipeline Systems.

Canadian Standards Association. (2015). CSA Z662-15 Oil and Gas Pipeline Systems.

Cappelletto, A., Tagliaferri, R., Gianmario, G., Giuseppe, A., Furlani, G., Scarpelli, G. 1998. Field full scale tests on longitudinal pipeline-soil interaction. In Proceedings International Pipeline Conference, Calgary, Alberta.

Cavanagh, P.C., Rizkalla, M. 1992. The Development of an Alternate Approach for Pipeline Operation in Unstable Slopes: A Case History. In Proceedings 11th International Conference on Offshore Mechanics and Arctic Engineering, Calgary, Alberta.

Cocchetti, G., Prisco, C., di, Galli, A., Nova, R. 2009. Soil-Pipeline Interaction along Unstable Slopes – A Coupled Three-Dimensional Approach. Part 1: Theoretical Formulation. Canadian Geotechnical Journal. Volume 46, 1289 -1304.

Cocchetti, Giuseppe, Prisco, Claudio di, Galli, Andrea. 2009. Soil-Pipeline Interaction along Unstable Slopes – A Coupled Three-Dimensional Approach. Part 2: Numerical Analysis. Canadian Geotechnical Journal. Volume 46, 1305 -1321

Committee on Gas and Liquid Fuel Lines (CGL). 1984. Guidelines for the Seismic Design of Oil and Gas Pipeline Systems. Technical Council on Lifeline Earthquakes Engineering, ASCE, New York.

Couperthwaite, S.L., Marshall, R.G. 1989. Line Monitoring Instruments Prove Effective for Western U.S Areas Subject to Landslides. Oil and Gas Journal, Volume 87, 85-90.

Challamel, N., de Buhan, P. 2003. Mixed Modelling applied to Soil-Pipe Interaction. Computer and Geotechnics. Volume 30, 205-216.

Chan, P.D.S, Wong, R.C.K. 2004. Performance Evaluation of Buried Steel Pipe in a Moving Slope: A Case Study. Canadian Geotechnical Journal. Volume 41, 894-907.

Cruden, D.M., Varnes, D.J. 1996. Landslide types and processes. In: Turner A.K.; Shuster R.L. (eds) Landslides: Investigation and Mitigation. Special Report 247 Prepared for Transportation Research Board, National Research Council (US).

Det Norske Veritas A. 2007. DNV-RP-F110 October 2007. Global Buckling of Submarine Pipelines Structural Design Due to High Temperature/High Pressure.

Det Norske Veritas A. 2000. DNV-OS-F101 2001. Submarine Pipeline Systems.

Det Norske Veritas A. 2013. DNV-OS-F101 October 2013. Submarine Pipeline Systems.

D.G. Honegger Consulting, C-Core, and SSD Inc. 2009. Guideline for Construction Natural Gas and Liquid Hydrocarbon Pipelines in Areas Subject to Landslide and Subsidence Hazards. Catalog No. L52292(V). Construction & Operations Technical Committee of PRCI.

Dinovitzer, A., Fredj, A., Sen, M. 2014. Pipeline Stress Relief and Evaluation of Strain Measurement Technology at a Moving Slope. In Proceedings 10th International Pipeline Conference, Calgary, Alberta.

Dorey, A.B., Cheng, J.J.R., Murray, D.W. 2001. Critical Buckling Strains for Energy Pipelines. Structural Engineering Report No 203, Department of Civil Engineering, University of Alberta.

El-Gharbawy, S. 2006. Uplift Capacity of Buried Offshore Pipelines. In Proceedings 8th International Conference on Offshore and Polar Engineering, San Francisco, USA.

European Gas Pipeline Incident Data Group. December 2011. 8th EGIG-Report 1970 to 2010.

Fell, R. 1993. Landslide Risk Assessment and Acceptable risk. Canadian Geotechnical Journal. Volume 31, 261 – 272.

Ferris, Gerry, Samchek, Alan, Isherwood, Andy. 2003. Geotechnical Risk Assessment: Estimating Slope Failure Probability. In Proceedings of the ASCE International Conference on Pipeline Engineering and Construction.

Finlay, P.J., Fell, R. 1997. Landslides: Risk Perception and Acceptance. Canadian Geotechnical Journal. Volume 34, 169 – 188.

Greenwood, J., Bukovansky, M., Graeme, M., 1986. Line Monitoring Instruments Prove Effective for Western U.S Areas Subject to Landslides. Paper published in Oil and Gas Journal, Volume 84, 68,70-73

Gresnigt, A.M. 1986. Plastic Design of Buried Steel Pipelines. Heron, Vol 31, No. 4, The Netherlands.

Gresnigt, A.M., Steenbergen, H.M.G.M. 1998. Plastic Deformation and Local Buckling of Pipelines Loaded by Bending and Torsion. In Proceedings 8th International Conference on Offshore and Polar Engineering. Montreal, Canada.

Karbasian, H., Zimmerman, S., Marewski, U., Steiner, M. (2012) Combined Loading Capacity of Pipelines- Approaches Towards Compressive Strain Limits. In Proceedings 9th International Pipeline Conference. Calgary, Canada. 2012

Khatib, I.F, Maison, B.F., Powell G.H., Row, D.G., Swanson, J.D. 1992. Artic Pipelines Limit States for Secondary Loadings. In Proceedings 2nd International Conference on Offshore and Polar Engineering. San Francisco, USA.

Klassen, R.W. 1966. Bedrock Topography, Riding Mountain, West of Principal Meridian, Manitoba-Saskatchewan. Geological Survey of Canada, Preliminary Map 2-1966, doi: 10.4095/107626.



Klassen, R.W. 1979. Pleistocene Geology and Geomorphology of the Riding Mountain and Duck Mountain Areas, Manitoba-Saskatchewan. Geological Survey of Canada, Memoir 396.

Klassen, R.W. 1979. Surficial Geology, Riding Mountain, West of Principal Meridian, Manitoba-Saskatchewan. Geological Survey of Canada, "A" Series Map 1479A, doi: 10.4095/109198.

Klassen, R.W. 1972, Wisconsin Events and the Assiniboine and Qu'Appelle Valleys of Manitoba and Saskatchewan. Canadian Journal of Earth Sciences. Volume 9, 544-560.

Lee, S-J, Cha, J. Y., Kim, W-S, Kim, Y-P, Zi, G. 2014. Evaluation of Tensile Strain Capacity for Pipelines using Strain-based Design. In Proceedings 24th International Ocean and Polar Engineering Conference, Busan, Korea.

Mahdavi, H., Kenny, S., Phillips, R., Popescu, R. 2013. Significance of Geotechnical Loads on Local Buckling Response of Buried Pipelines with Respect to Conventional Practice. Canadian Geotechnical Journal. Volume 50, 68 – 80.

Mansour, M.F. 2009. Characteristic Behaviour of Slow Moving Slides. Ph.D. Thesis. University of Alberta, Canada.

Mohareb, M. 2002. Plastic Interaction Relations for Pipe Sections. Journal of Engineering Mechanics. Volume 128, 112 – 120.

Mohareb, M. 2003. Plastic Resistance of Pipe Sections: Upper Bound Solution. Journal of Structural Engineering. Volume 129, 41 – 48.

Mohareb, M., Elwi, A., Kulak, G.L., Murray, D.W. (1994), Deformational Behaviour of Line Pipe. Structural Engineering Report No 202, Department of Civil Engineering, University of Alberta.

National Energy Board. December 2011. Focus on Safety and Environment A Comparative Analysis of Pipeline Performance 2000- 2009.

Nessim, M. 2012. Limit States Design and Assessment of Onshore Pipelines. In Proceedings 9th International Pipeline Conference, Calgary, Alberta.

Nessim, M., Zhou, W., Zhou, J., Rothwell, B., McLamb, M. 2004. Target Reliability Levels for Design and Assessment of Onshore Natural Gas Pipelines. In Proceedings 5th International Pipeline Conference, Calgary, Alberta.

Nessim, M, Zimmerman, T, Glover, A., McLamb, M., Rothwell, B., Zhou, J. 2002. Reliability-based Limit States Design for Onshore Pipelines. In Proceedings 4th International Pipeline Conference, Calgary, Alberta.

Nobahar, A, Kenny, S., King, T., McKenna, R., Phillips, R. 2007. Analysis and Design of Buried Pipelines for Ice Gouging Hazard: a Probabilistic Approach. Journal of Offshore Mechanics and Arctic Engineering. Volume 129, 219-228.

O'Rourke, M.J, Nordberg, C., 1992. Longitudinal Permanent Ground Deformation Effects on Buried Continuous Pipelines. Technical Report NCEER-92-0014 prepared for National Center for Earthquake Engineering Research, Buffalo, NY.

Ozkan, I.F. 2008. Experimental and Numerical Analysis of Steel Pipes Subjected to Combined Loads. Ph.D. Thesis. University of Ottawa, Canada.

Ozkan, I.F., Mohareb, M. 2003. Testing of Steel Pipes under Bending, Twist, and Shear. *Journal of Structural Engineering*. Volume 129, 1350-1357

Paglietti, A. 2007. *Plasticity of Cold Worked Metals: A Deductive Approach*. Billerica, MA: WIT Press.

Pedersen, P., Juncher, J. 1988. Upheaval Creep of Buried Heated Pipelines with Initial Imperfections. *Journal of Marine Structures*. Volume 1, 11-22.

Porter, M., Logue, C., Savigny, W., Esford, F., Bruce, I. 2004. Estimating the Influence of Natural Hazards on Pipeline Risk and System Reliability. In *Proceedings 5th International Pipeline Conference*, Calgary, Alberta.

Porter, M., Savigny, W. 2002. Natural Hazard and Risk Management for South American Pipelines. In *Proceedings 4th International Pipeline Conference*, Calgary, Alberta, 2002

Rajani, B.B, Robertson, P.K., Morgenstern, N.R. 1995. Simplified Design Methods for Pipelines Subject to Transverse and Longitudinal Soil Movements. *Canadian Geotechnical Journal*. Volume 32, 309 – 323.

Rizkalla, M., Trigg, A., Simmonds, G. 1996. Recent Advances in the Modeling of Longitudinal Pipeline/Soil Interaction for Cohesive Soils. In *Proceedings 15th International Conference on Offshore Mechanics and Arctic Engineering*, Florence, Italy.

Scarpelli, G., Aleotti, P., Baldelli, P., Milani, G., Brambati, E. 1995. Field Experience of Pipelines in Geologically Unstable Areas. In *Proceedings International 14th Conference on Offshore Mechanics and Arctic Engineering*. Copenhagen, Denmark.

Scarpelli, G., Sakellariadi, E., Furlani, G. 1999. Longitudinal pipeline-soil interaction: results from field full scale and laboratory testing. In Proceedings 12th European conference on soil mechanics and geotechnical engineering, Amsterdam, Netherlands.

Simmonds, Gordon R, Zhou, Z. Joe, Samchek Alan T. 1996. A Rational Design and Operating Strategy for Pipelines Traversing Unstable Slopes. Paper presented in Proceedings 5th International Pipeline Conference, Calgary, Alberta.

Take, A. 2015. Thirty-sixth Canadian Geotechnical Colloquium: Advances in Visualization of Geotechnical Processes through Digital Image Correlation. Canadian Geotechnical Journal. Volume 52, 1199-1220

Teller, J.T., Thorleifson, L.H., Matile, G., Brisbin, W.C. 1996. Sedimentology, Geomorphology, and History of the Central Lake Agassiz Basin. Geological Association of Canada Field Trip Guidebook for GAC/MAC Joint Annual Meeting.

Trigg, A., Rizkalla, M., 1994. Development and Application of a Closed Form Technique for the Preliminary Assessment of Pipeline Integrity in Unstable Slopes. In Proceedings 13th International Conference on Offshore Mechanics and Arctic Engineering, Houston, USA.

Timoshenko, S.P., Goodier, J.N. 1970. Theory of Elasticity, 3rd edition, McGraw-Hill

US DOT. (2004). Office of Pipeline Safety Statistics for Gas Transmission Pipeline Incident, 1984 to 2002.

Van Helden, M.J. 2013. Measurement and Modeling of Anisotropic Spatial Variability of Soils for Probabilistic Stability Analysis of Earth Slopes. Ph.D. Thesis. University of Manitoba, Canada.

Wang, Y.-Y, Cheng, W., Horsley, D. 2004. Tensile Strain Limits of Buried Defects in Pipeline Girth Welds. In Proceedings 5th International Pipeline Conference, Calgary, Alberta.

Wang, Y.-Y, Horsley, D. 2003. Tensile Strain Limits of Pipelines. In Proceedings 14th biennial EPRG-PRCI-APIA joint technical meeting on pipeline research, Berlin. Paper 35.

Wijewickreme, D., Honegger, D., Mitchell, A., Fitzell, T. 2005. Seismic Vulnerability Assessment and Retrofit of a Major Natural Gas Pipeline System: A Case History. Earthquake Spectra. Volume 21, 539-567.

Wijewickreme, D., Karimian, H., Honegger, D. 2009. Response of Buried Steel Pipelines Subjected to Relative Axial Soil Movement. Canadian Geotechnical Journal. Volume 46, 735-752.

Winter, D. 2009. Biomechanics and Motor Control of Human Movement. 4th edition, John Wiley and Sons Inc.

Yong, Salina. 2003. A slide in the Harrowby Hills. M.Sc. Thesis. University of Alberta, Canada.

Yoosef-Ghodsi, N., Kulak, G.L., Murray, D.W. 1994. Behaviour of Girth-Welded Line Pipe. Structural Engineering Report No 203, Department of Civil Engineering, University of Alberta.

Yoosef-Ghodsi, N., Ozkan, I, Chen, Q. 2014. Comparison of Compressive Strain Equations. In Proceedings 7th International Pipeline Conference, Calgary, Alberta.

Yoosef-Ghodsi, N., Zhou, J., Murray, D.W. 2008. A Simplified Model for Evaluation Strain Demand in a Pipeline Subjected to Longitudinal Ground Movement. In Proceedings 7th International Pipeline Conference, Calgary, Alberta.

Young, W.C. 2002. Roark's Formula for Stress and Strain. 7th edition, McGraw-Hill

Yu. B., Gabriel, D., Noble, L., An, K-N. 1999. Estimate of the Optimum Cutoff Frequency for the Butterworth Low-pass Digital Filter. Journal of Applied Biomechanics. Volume 15, 319-329.

Zimmerman, T.J.E, Chen, Q., Pandey, M.D. 1996. Target Reliability Levels for Pipeline Limit States Design. In Proceedings 1st International Pipeline Conference, Calgary, Alberta.

Zimmerman, T.J.E, Colquhoun, I.R., Price, P. St. J., Smith, R.J. 1992. Development of a Limit States Guidelines for the Pipeline Industry. In Proceedings 13th International Conference on Offshore Mechanics and Arctic Engineering. Calgary, Canada.

Zimmerman, T.J.E, Stephens, M.J., DeGeer, D.D., Chen, Q. 1995. Compressive Strain Limit for Buried Pipelines. In 14th International Conference on Offshore Mechanics and Arctic Engineering. Copenhagen, Denmark.

Zhou, W. 2012. Reliability of Pressurized Pipelines Subjected to Longitudinal Ground Movement. Structure and Infrastructure Engineering. Volume 8, 1123-1135.

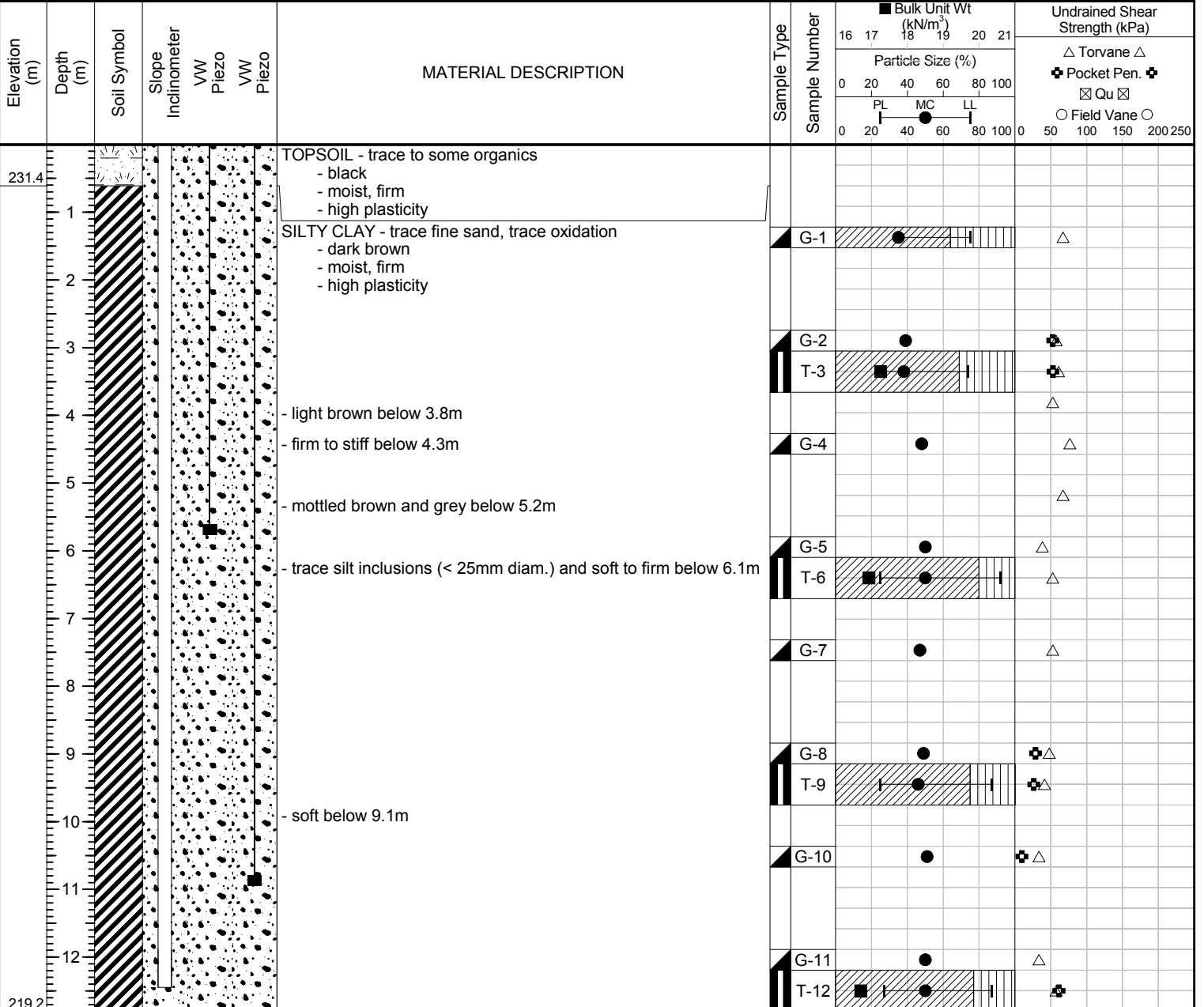
Zhou, W., Rothwell, B., Nessim, M., Zhou, W. 2009. Reliability-Based Design and Assessment Standards for Onshore Natural Gas Transmission Pipelines. Journal of Pressure Vessel Technology. Volume 131, 1-6

# Appendix A – Test Hole Logs

# Sub-Surface Log

**Client:** University of Manitoba **Project Number:** \_\_\_\_\_  
**Project Name:** Gas Pipeline Study **Location:** Plum River - Near Top of Bank  
**Contractor:** Paddock Drilling Ltd. **Ground Elevation:** 232.0 m  
**Method:** 125 mm Solid Stem Auger, RM 30 Track Mount **Date Drilled:** 23 August 2011

**Sample Type:** Grab Shelby Tube Split Spoon Split Barrel Core  
**Particle Size Legend:** Clay Silt Sand Gravel Cobbles Boulders  
**Backfill Legend:** Grout Grout Seal VW Cable SI Tip VW Tip



**END OF TEST HOLE AT 12.8m IN SILTY CLAY**  
**Notes:**  
 1. No seepage or sloughing observed  
 2. SI-01 installed to depth of 12.5m below ground. Vibrating Wire Piezometers VW-1A and VW-1B installed to depth of 6m and 11.7m, respectively.

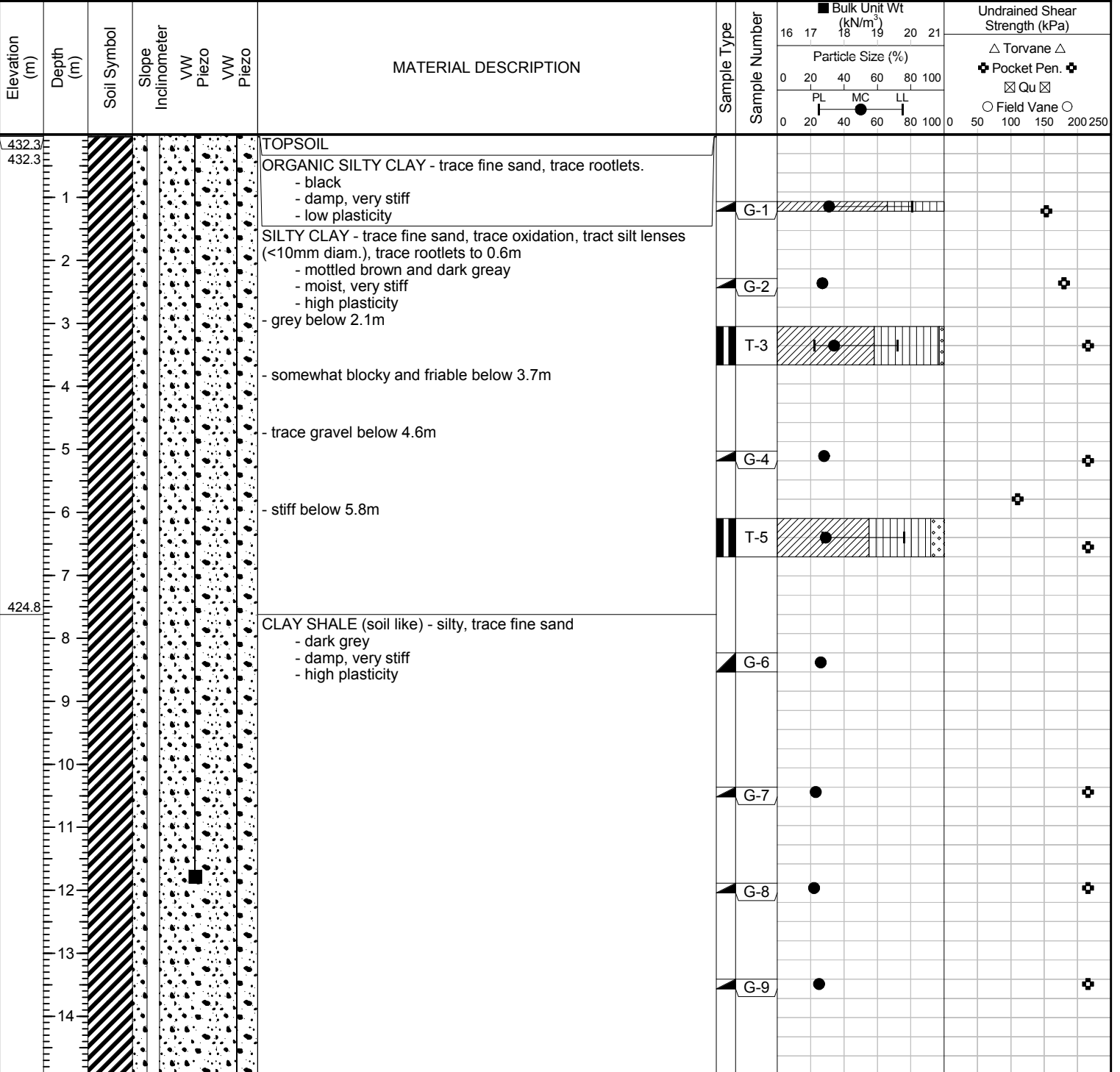
**Logged By:** N.J Ferreira **Reviewed By:** N.J Ferreira **Project Engineer:** Nelson Ferreira



# Sub-Surface Log

**Client:** University of Manitoba **Project Number:** \_\_\_\_\_  
**Project Name:** Gas Pipeline Study **Location:** St. Lazare - Near Top of Valley Wall  
**Contractor:** Paddock Drilling Ltd. **Ground Elevation:** 432.4 m  
**Method:** 125 mm Solid Stem Auger, Acker SS Track Mount **Date Drilled:** 1 September 2011

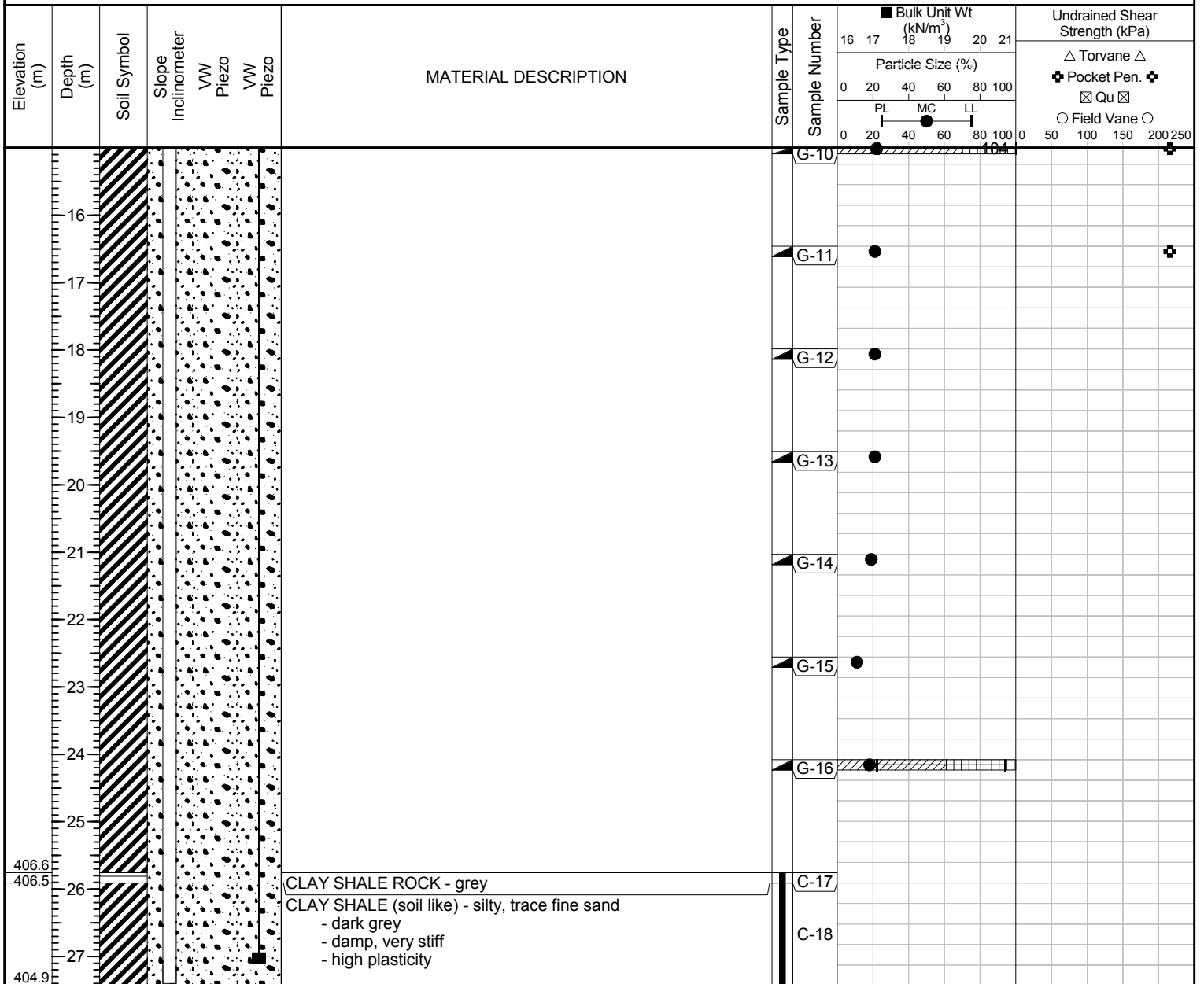
**Sample Type:** Grab  Shelby Tube  Split Spoon  Split Barrel  Core   
**Particle Size Legend:** Clay  Silt  Sand  Gravel  Cobbles  Boulders   
**Backfill Legend:** Grout  Grout Seal  VW Cable  SI Tip  VW Tip



SUB-SURFACE LOG PHD RESEARCH LOGS.GPJ TREK GEOTECHNICAL.GDT 9/5/16

**Logged By:** N.J Ferreira **Reviewed By:** N.J Ferreira **Project Engineer:** Nelson Ferreira

# Sub-Surface Log



END OF TEST HOLE AT 27.4m IN CLAY SHALE

Notes:

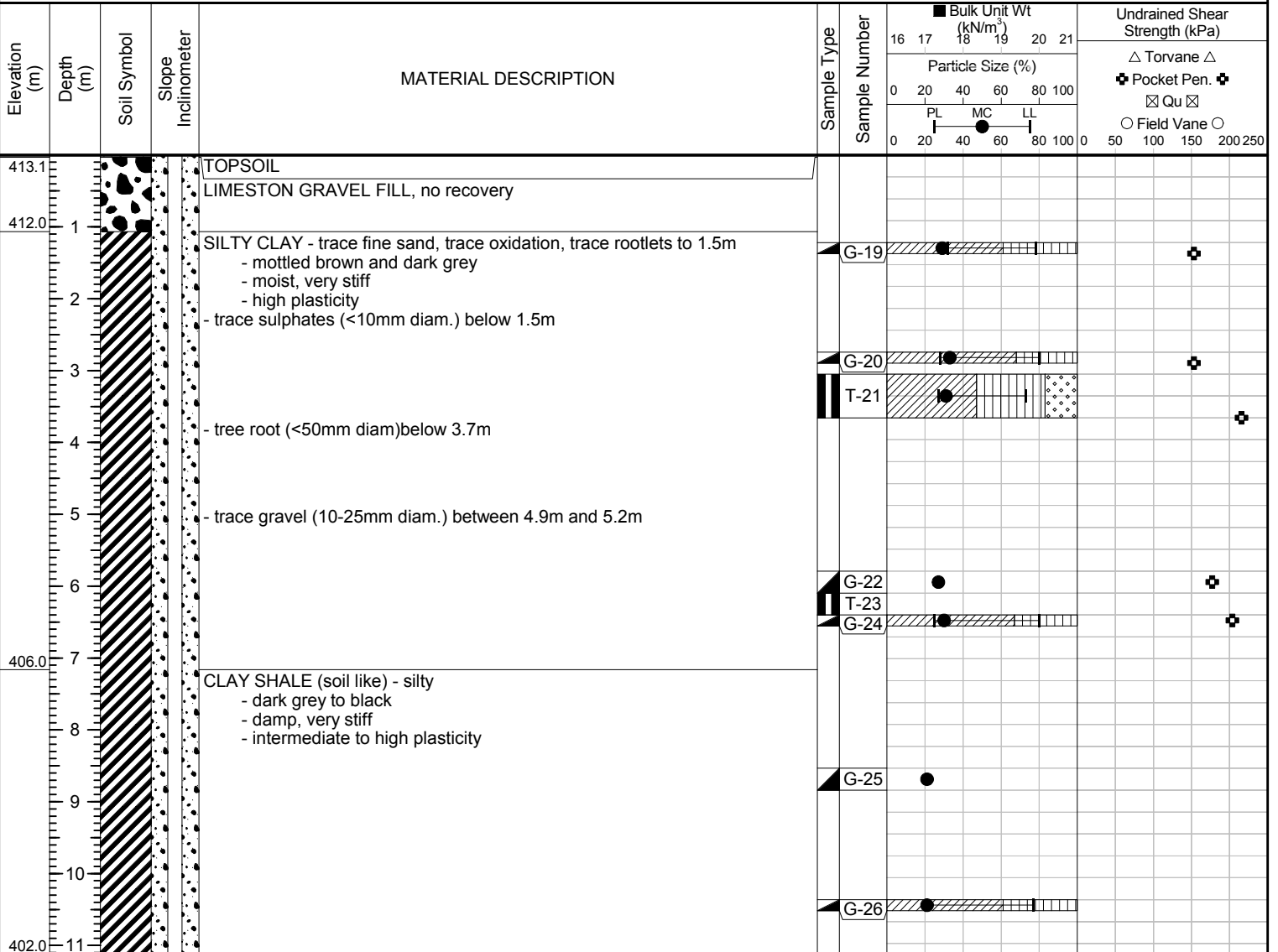
1. Power Auger Refusal at 25.8m, drilling method switched to NQ coring below 25.8m
2. No seepage or sloughing observed
3. Difficult drilling below 7.6m. The auger flights had to spinned slowly in order to continue drilling below this depth. This resulted in heavily disturbed grab samples.
4. SI-02 installed to depth of 27.4m below ground. Vibrating Wire Piezometers VW-2A and VW-2B installed to depth of 11.9m and 27.1m, respectively.

SUB-SURFACE LOG PHD RESEARCH LOGS.GPJ TREK GEOTECHNICAL.GDT 9/5/16

# Sub-Surface Log

**Client:** University of Manitoba **Project Number:** \_\_\_\_\_  
**Project Name:** Gas Pipeline Study **Location:** St. Lazare - Mid-Slope of Valley Wall  
**Contractor:** Paddock Drilling Ltd. **Ground Elevation:** 413.1 m  
**Method:** 125 mm Solid Stem Auger, Acker SS Track Mount **Date Drilled:** 2 September 2011

**Sample Type:**  Grab  Shelby Tube  Split Spoon  Split Barrel  Core  
**Particle Size Legend:**  Clay  Silt  Sand  Gravel  Cobbles  Boulders  
**Backfill Legend:**  Grout Seal



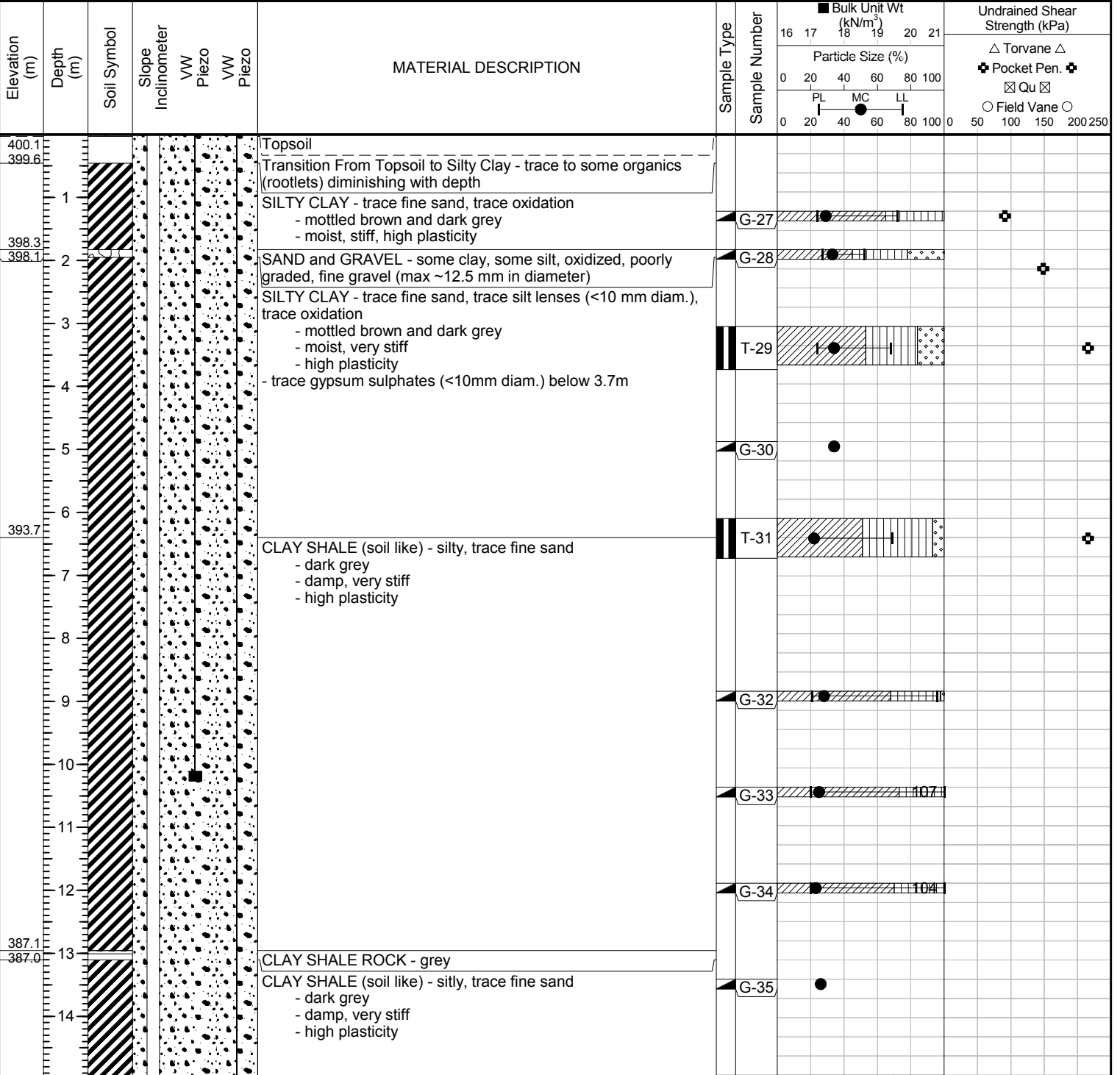
END OF TEST HOLE AT 11.1m IN CLAY SHALE  
 Notes:  
 1. No seepage or sloughing observed  
 2. SI-03 installed to depth of 11.1m below ground.

SUB-SURFACE LOG PHD RESEARCH LOGS.GPJ TREK GEOTECHNICAL.GDT 9/5/16

# Sub-Surface Log

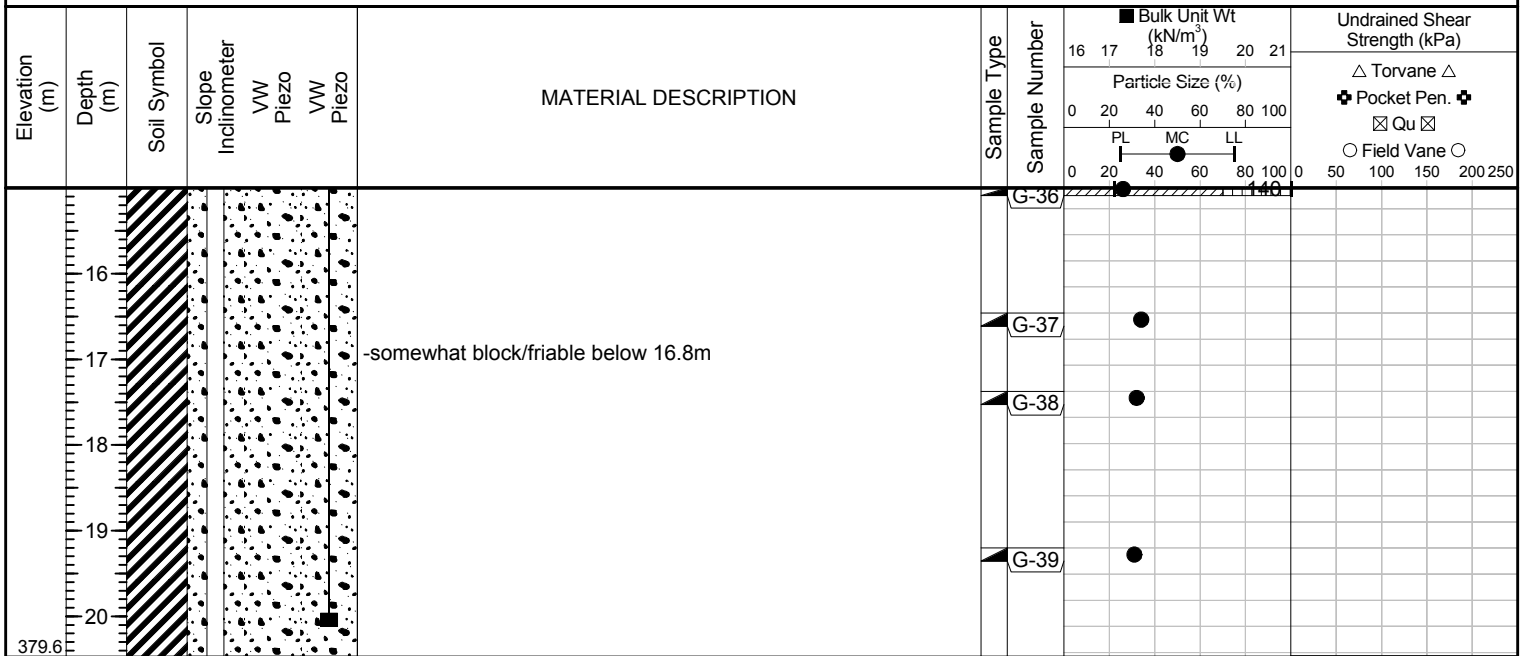
**Client:** University of Manitoba **Project Number:** \_\_\_\_\_  
**Project Name:** Gas Pipeline Study **Location:** St. Lazare - Lower Slope of Valley Wall  
**Contractor:** Paddock Drilling Ltd. **Ground Elevation:** 400.1 m  
**Method:** 125 mm Solid Stem Auger, Acker SS Track Mount **Date Drilled:** 3 September 2011

**Sample Type:** Grab Shelby Tube Split Spoon Split Barrel Core  
**Particle Size Legend:** Clay Silt Sand Gravel Cobbles Boulders  
**Backfill Legend:** Grout Grout Seal VW Cable VW Tip



**Logged By:** N.J Ferreira **Reviewed By:** N.J Ferreira **Project Engineer:** Nelson Ferreira

# Sub-Surface Log



END OF TEST HOLE AT 20.5m IN CLAY SHALE

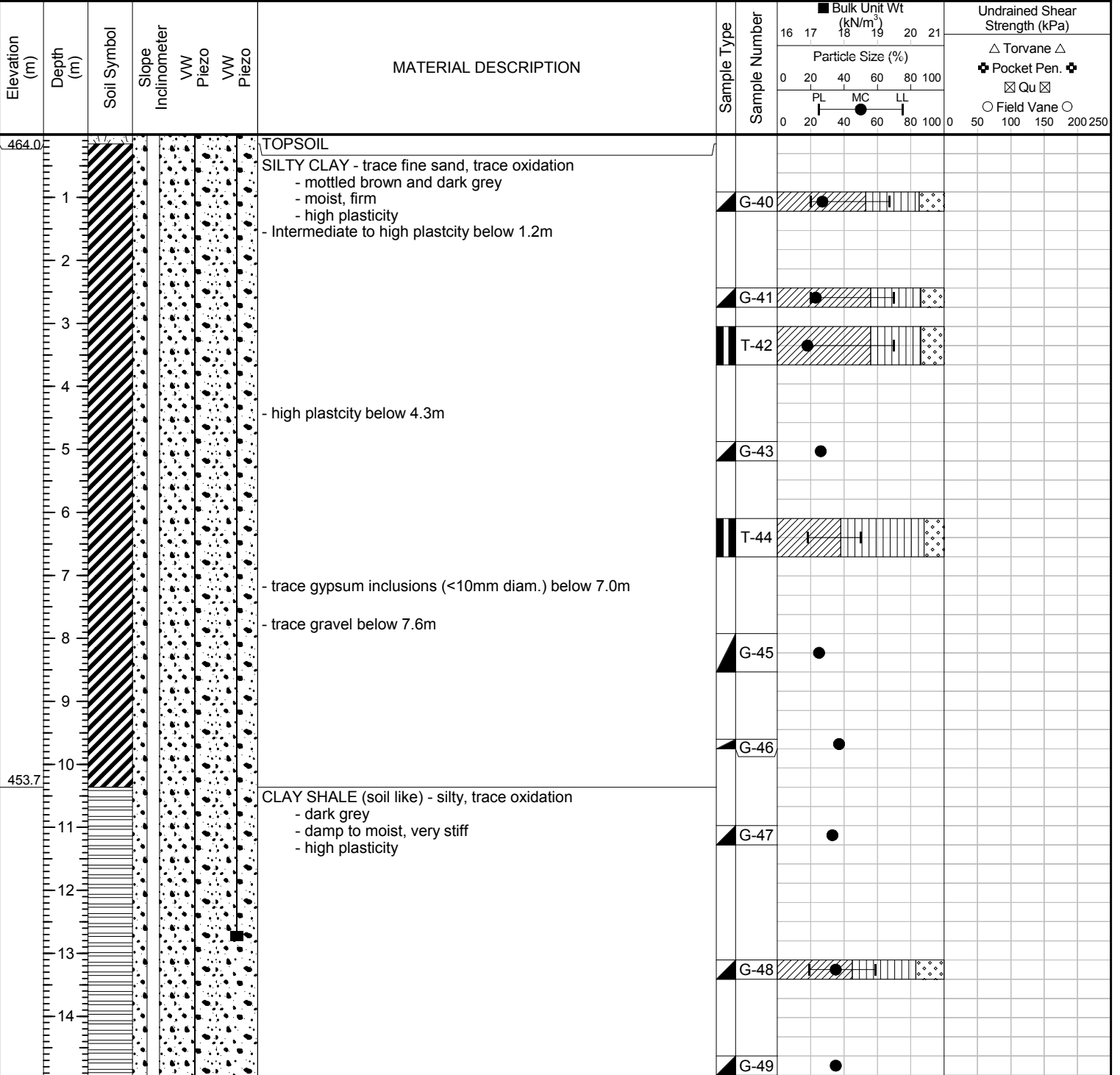
Notes:

1. No seepage or sloughing observed
3. Difficult drilling below 6.4m. The auger flights had to spinned slowly in order to continue drilling below this depth. This resulted in heavily disturbed grab samples.
4. SI-04 installed to depth of 20.5m below ground. Vibrating Wire Piezometers VW-4A and VW-4B installed to depth of 10.2m and 20.1m, respectively.

# Sub-Surface Log

**Client:** University of Manitoba **Project Number:** \_\_\_\_\_  
**Project Name:** Gas Pipeline Study **Location:** Harrowby - Near Top of Valley Wall  
**Contractor:** Paddock Drilling Ltd. **Ground Elevation:** 464.1 m  
**Method:** 125 mm Solid Stem Auger, CME 850 Track Mount **Date Drilled:** 23 November 2011

**Sample Type:** Grab Shelby Tube Split Spoon Split Barrel Core  
**Particle Size Legend:** Clay Silt Sand Gravel Cobbles Boulders  
**Backfill Legend:** Grout Grout Seal VW Cable SI Tip VW Tip



SUB-SURFACE LOG PHD RESEARCH LOGS.GPJ TREK GEOTECHNICAL.GDT 9/5/16

**Logged By:** N.J Ferreira **Reviewed By:** N.J Ferreira **Project Engineer:** Nelson Ferreira

# Sub-Surface Log

Elevation (m)	Depth (m)	Soil Symbol	Slope Inclinometer VW Piezo VW Piezo	MATERIAL DESCRIPTION	Sample Type	Sample Number	Bulk Unit Wt (kN/m <sup>3</sup> )	Undrained Shear Strength (kPa)	
							16 17 18 19 20 21	△ Torvane △	✚ Pocket Pen. ✚
							Particle Size (%)		⊠ Qu ⊠
							0 20 40 60 80 100		○ Field Vane ○
							PL MC LL	0 50 100 150 200 250	
							0 20 40 60 80 100		
16						G-50	●		
17									
18						G-51	●		
19									
20						G-52	●	▨	▨
21									
22									
23						G-53	●		
24									
25									
26						G-54	●		
27									
28									
29						G-55	●		
30	433.9								

END OF TEST HOLE AT 30.2m IN CLAY SHALE

Notes:

- Trace seepage at 10.1m and no sloughing observed
- Hard drilling below 6.1m. The auger flights had to be spun slowly in order to continue drilling below this depth. This resulted in heavily disturbed grab samples. Difficult drilling 18.9m to 20.4m and 25.9m to 26.2m
- SI-05 installed to depth of 29.6m below ground. Vibrating Wire Piezometers VW-5A and VW-5B installed to depth of 12.8m and 29.0m, respectively.

SUB-SURFACE LOG PHD RESEARCH LOGS.GPJ\_TREK GEOTECHNICAL.GDT 9/5/16

Logged By: N.J Ferreira

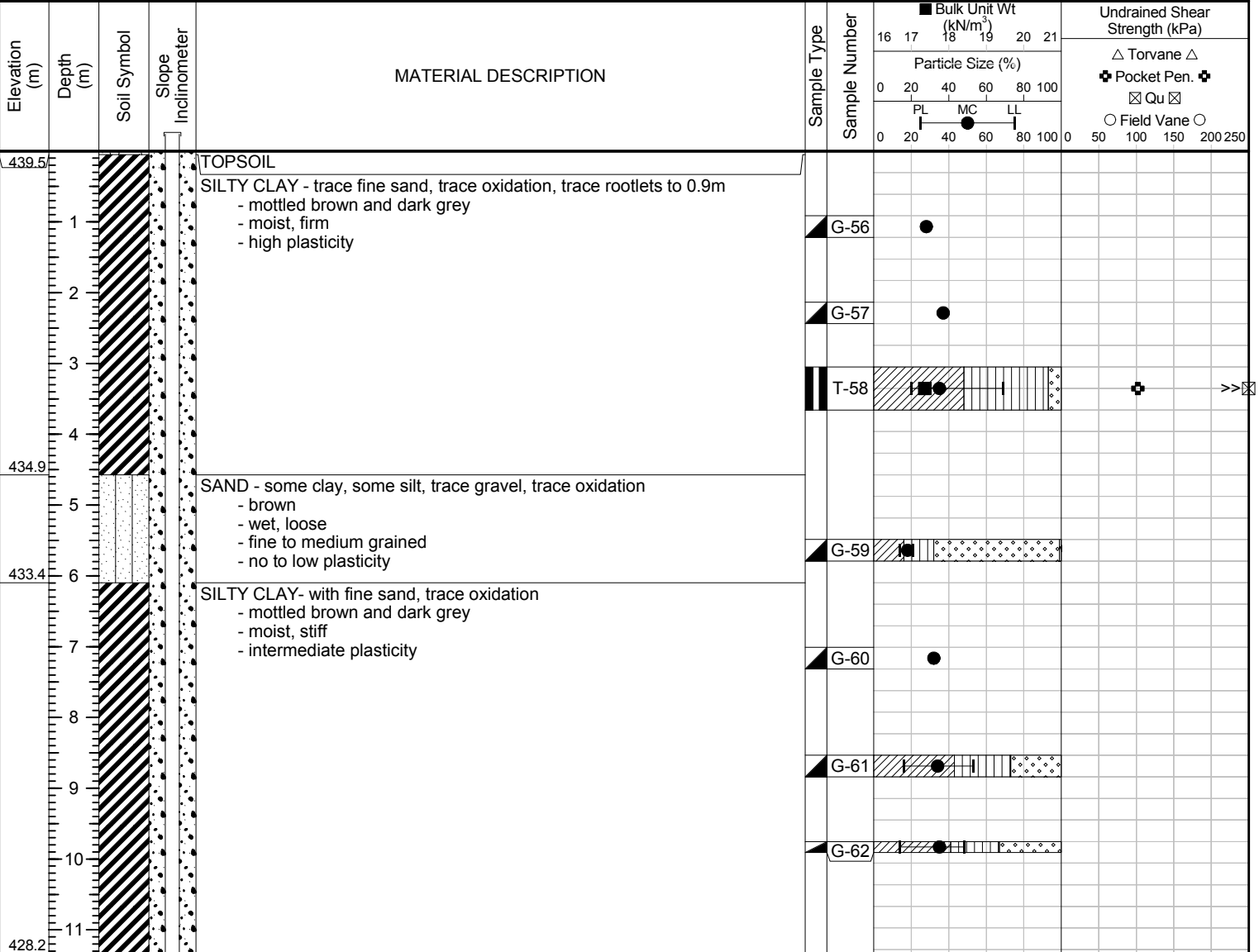
Reviewed By: N.J Ferreira

Project Engineer: Nelson Ferreira

# Sub-Surface Log

**Client:** University of Manitoba **Project Number:** \_\_\_\_\_  
**Project Name:** Gas Pipeline Study **Location:** Harrowby - Mid-Slope of Valley Wall  
**Contractor:** Paddock Drilling Ltd. **Ground Elevation:** 439.5 m  
**Method:** 125 mm Solid Stem Auger, CME 850 Track Mount **Date Drilled:** 24 November 2011

**Sample Type:** Grab  Shelby Tube  Split Spoon  Split Barrel  Core  
**Particle Size Legend:** Clay  Silt  Sand  Gravel  Cobbles  Boulders  
**Backfill Legend:** Grout Seal  Capped Riser



END OF TEST HOLE AT 11.3m IN SILTY CLAY

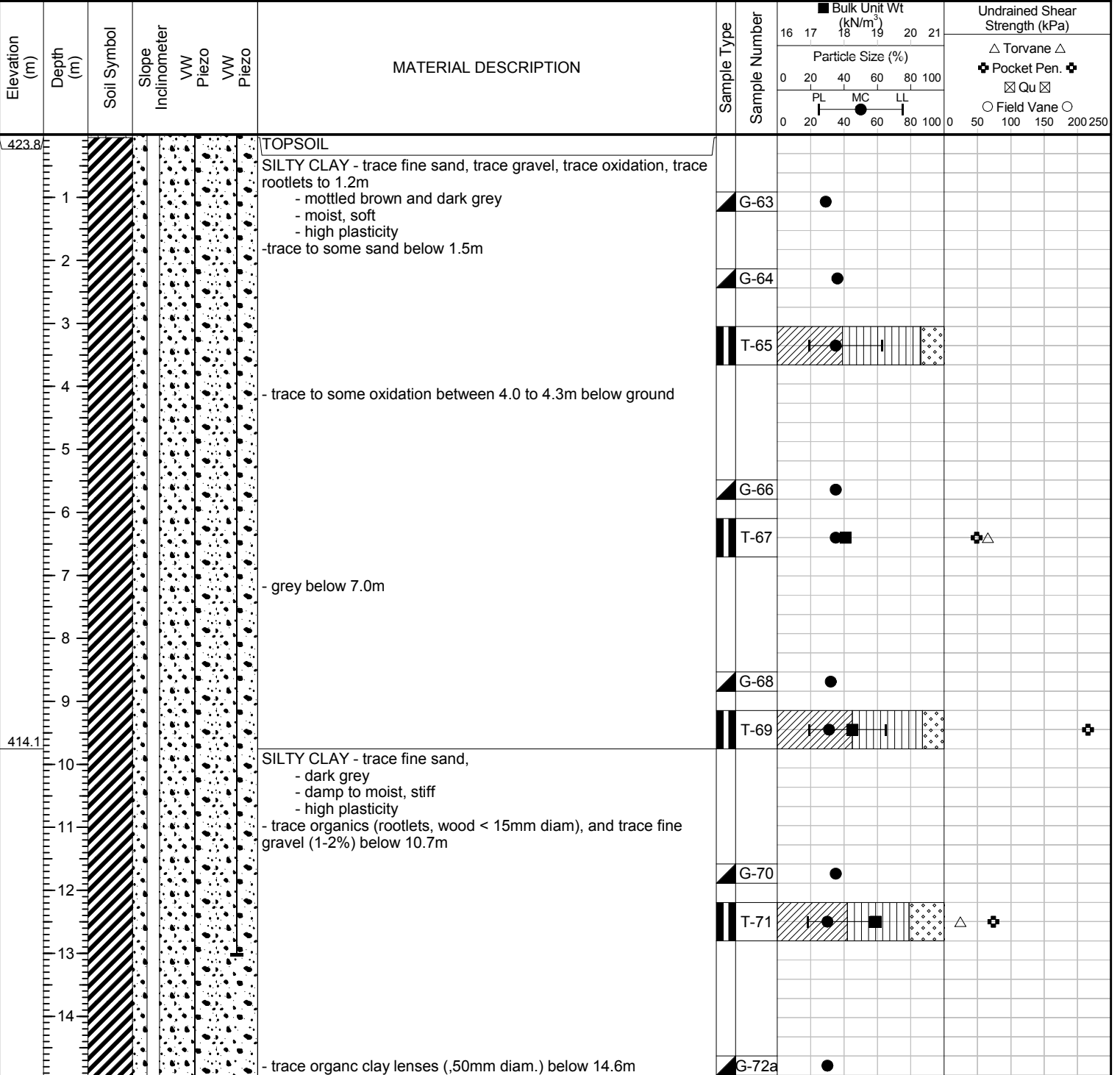
- Notes:
1. No seepage observed.
  2. Sloughing at 5.2m below ground.
  3. SI-06 installed to depth of 11.3m below ground.



# Sub-Surface Log

**Client:** University of Manitoba **Project Number:** \_\_\_\_\_  
**Project Name:** Gas Pipeline Study **Location:** Harrowby - Lower Slope of Valley Wall  
**Contractor:** Paddock Drilling Ltd. **Ground Elevation:** 423.9 m  
**Method:** 125 mm Solid Stem Auger, CME 850 Track Mount **Date Drilled:** 26 November 2011

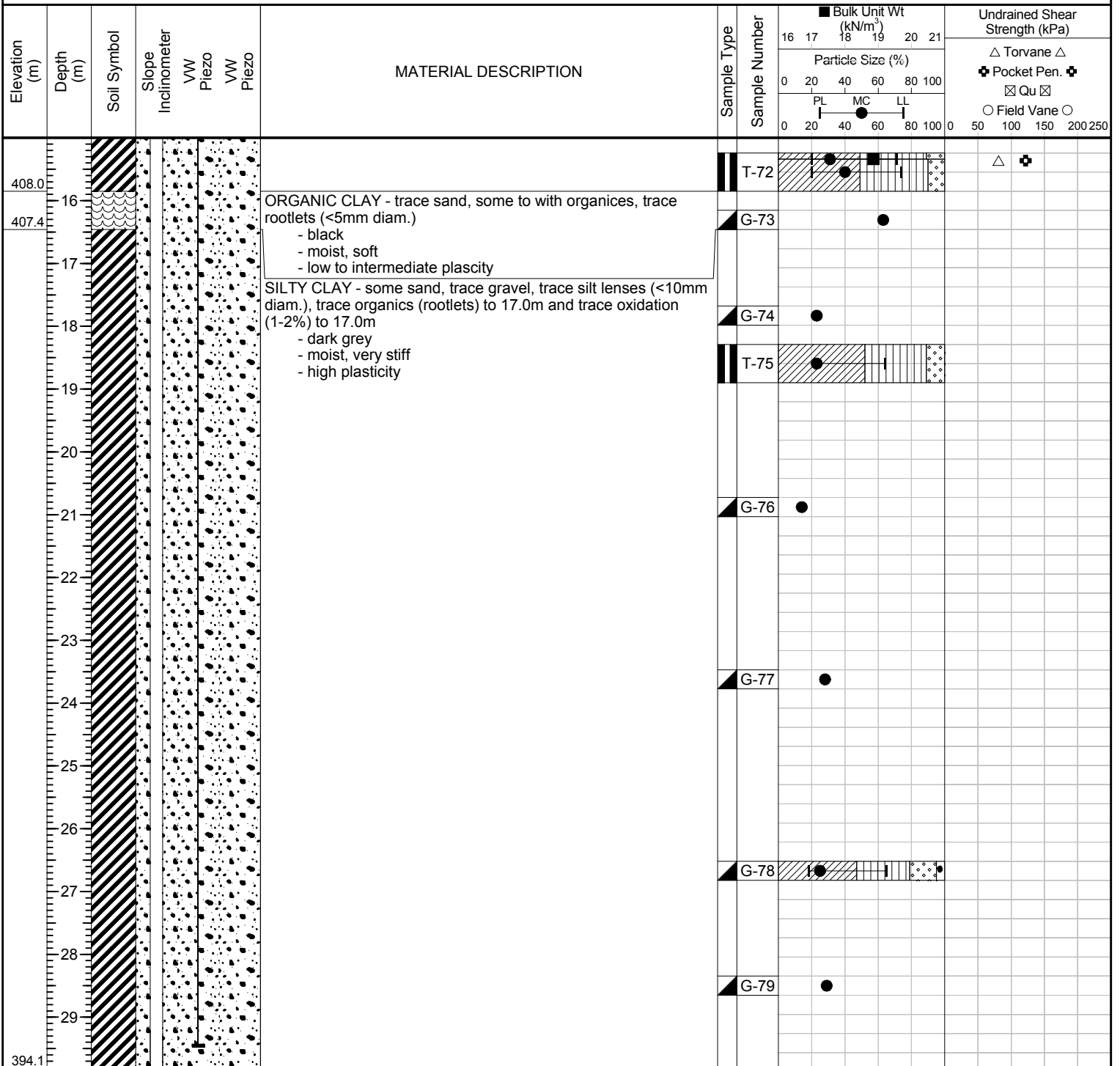
**Sample Type:** Grab Shelby Tube Split Spoon Split Barrel Core  
**Particle Size Legend:** Clay Silt Sand Gravel Cobbles Boulders  
**Backfill Legend:** Grout Grout Seal VW Cable SI Tip VW Tip



SUB-SURFACE LOG PHD RESEARCH LOGS.GPJ TREK GEOTECHNICAL.GDT 9/5/16

**Logged By:** N.J Ferreira **Reviewed By:** N.J Ferreira **Project Engineer:** Nelson Ferreira

# Sub-Surface Log



END OF TEST HOLE AT 29.8m IN SILTY CLAY

Notes:

1. No seepage or sloughing observed.
2. SI-07 installed to depth of 29.8m below ground. Vibrating Wire Piezometers VW-7A and VW-7B installed to depth of 13.0m and 29.5m, respectively.

SUB-SURFACE LOG PHD RESEARCH LOGS.GPJ TREK GEOTECHNICAL.GDT 9/5/16

Logged By: N.J Ferreira

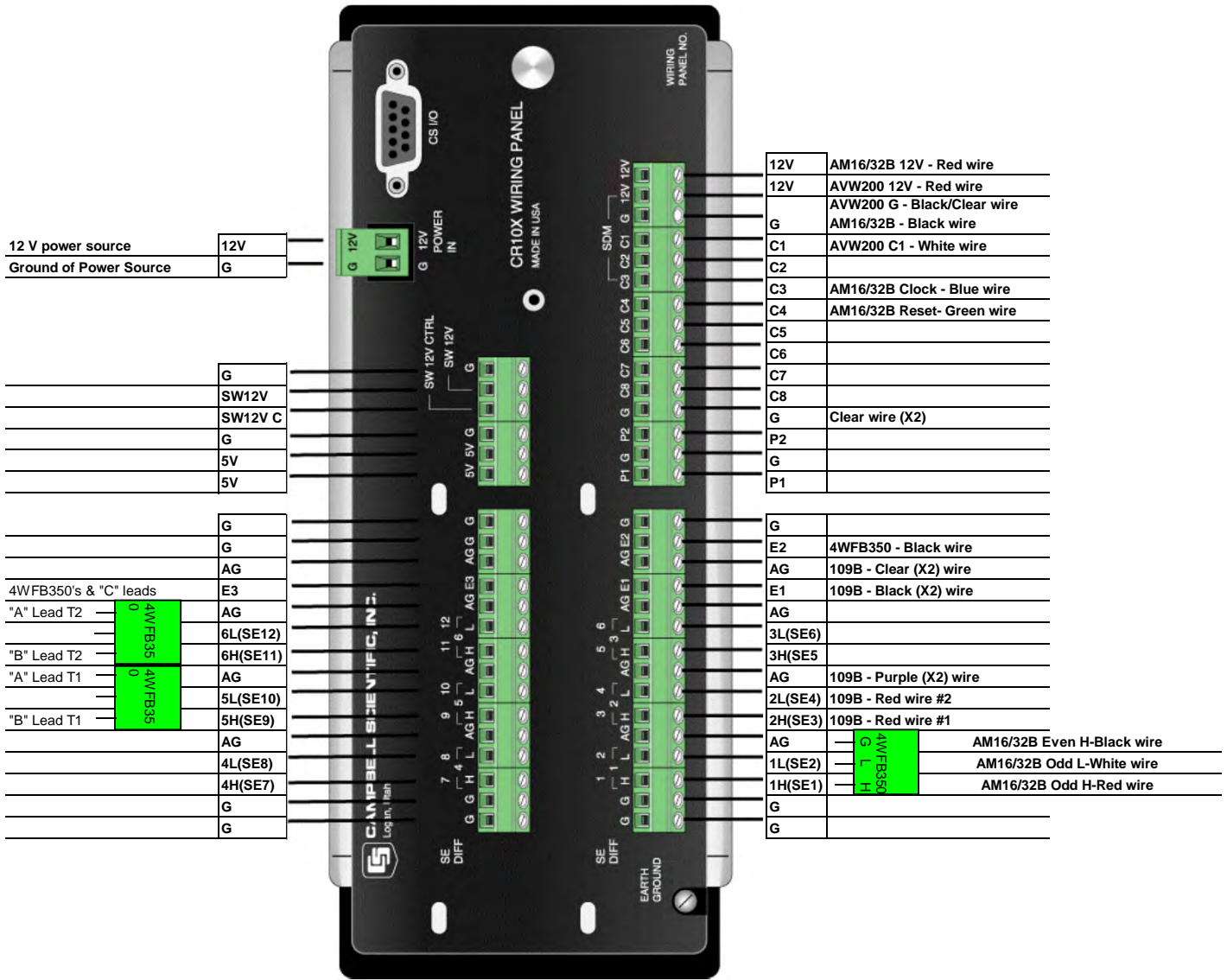
Reviewed By: N.J Ferreira

Project Engineer: Nelson Ferreira

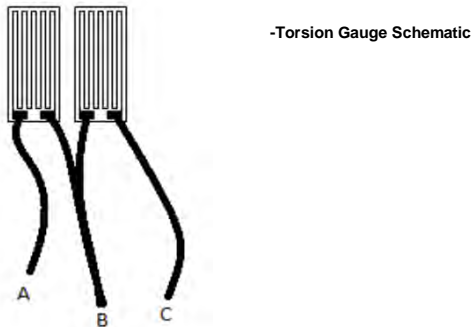
## Appendix B – DA Programming

# CR10X WIRING DIAGRAM

Company:	University of Manitoba
Project:	Nelson Ferreira - River Bank Site
Prepared By:	Ian Milne - Campbell Scientific Canada Corp.

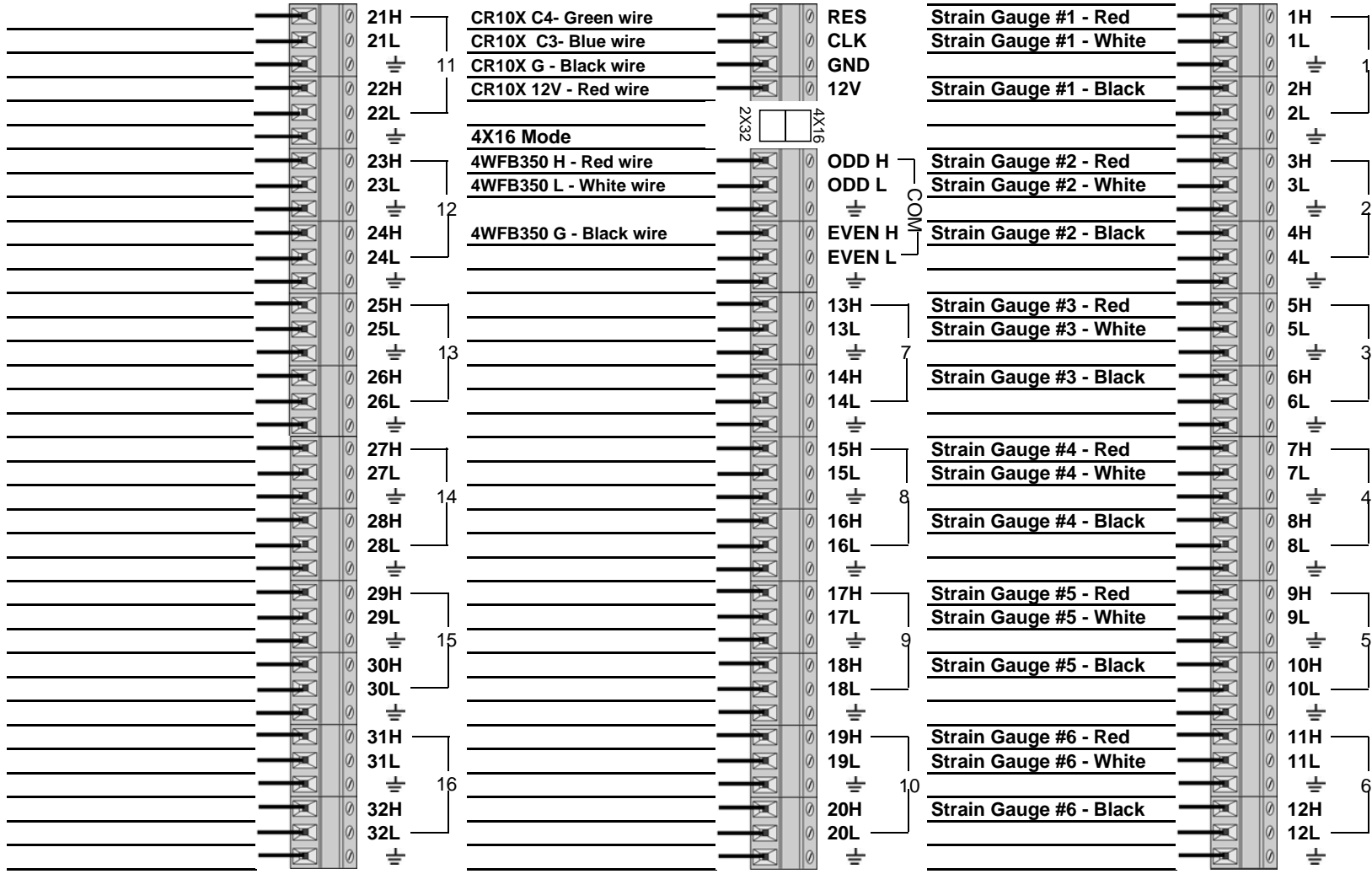


- NOTES:**
- \*\* Use FIN4COND-L cable for wiring AVW200 interface to datalogger\*\*
  - \*\*Use 2X FIN4COND-L cable for wiring AM16/32B to datalogger\*\*
  - \*\* Connect the "C" lead from both Torsion gauges to E3 as well as the black leads from the 4WFB350 modules
  - \*\* T1 = Torsion Gauge #1, T2 = Torsion Gauge #2



**AM16/32 WIRING DIAGRAM**

COMPANY: University of Manitoba  
 PROJECT: Nelson Ferreira  
 DOCUMENTED BY: Shannon Green, Campbell Scientific Canada



RIVERBANK\_PROGRAM\_REV1\_5.CSI, Table 1

;  
;{CR10X}

;Date: July 8, 2010

;Written by: Shannon Green

;Campbell Scientific Canada Corp.

;Station: River Bank

;REV 1 - Oct 7, 2010:

;By: Shannon Green, Campbell Scientific Canada Corp.

;Revised program wiring descriptions to match revised CR10X and AM16/32B wiring diagrams.

;Revised full bridge (P6) instruction to include Auto Range instead of fixed range of 2500 mV.

;Rev 1\_1 - June 6, 2011

;By: Ian Milne, Campbell Scientific Canada Corp.

;Revised Temperature calculation for 109B's

;REV 1\_2 - June 15, 2011

;By: Ian Milne, Campbell Scientific Canada Corp.

;Added Full Bridge instruction for torsion gauge

;REV 1\_3 - July 5, 2011

;By: Ian Milne, Campbell Scientific Canada Corp.

;Added one more Full Bridge instruction for torsion gauge

;REV 1\_4 - July 18, 2011

;By: Ian Milne, Campbell Scientific Canada Corp.

;Revised Temp calculation - it was inadvertently changed in a previous revision

;REV 1\_5 - August 5, 2011

;By: Ian Milne, Campbell Scientific Canada Corp.

;Changed Thermistor storage to High Resolution to prevent overflow

;Wiring:

;SE1 - Odd H AM16/32B (red wire) + 4WFB350 (H)

;SE2 - Odd L AM16/32B (White wire) + 4WFB350 (L)

;SE3 - 109B #1 (Red wire)

;SE4 - 109B #2 (Red wire)

;AG - 109B #1,#2 (Purple wire)

;EX1 - 109B #1,#2 (Black wire)

;AG - 109B #1, #2 (Clear wire)

;C1 - AVW200 (White wire) Using FIN6COND-L wire

;C3 - AM16/32B RES

;C4 - AM16/32B CLK

;12V - AVW200 (Red wire) Using FIN6COND-L wire

;12V - AM16/32B 12V (Red wire)

;G - AM16/32B (Black)

;G - AVW200 (Black,Clear wire)

;EX2 - 4FWB350 (Black wire)

;DIFF 4 - 4WFB350 - Torsion Gauge

;DIFF 5 - 4WFB350 - Torsion Gauge

;AM16/32B wiring:

;(4x16 mode)

;RES - CR10X C4 (Green wire)

```
;CLK - CR10X C3 (Blue wire)
;Odd H - 4WFB350 - H (RED wire)
;Odd L - 4WFB350 - L (White wire)
;Even H - 4WFB350 - GND (BLK wire)
;12V - CR10X 12V (Red wire)
;G - CR10X (Black wire)
;Strain Gauge #1 Red wire - 1H
;Strain Gauge #1 White wire - 1L
;Strain Gauge #1 Black wire - 2H
;Strain Gauge #2 Red wire - 3H
;Strain Gauge #2 White wire - 3L
;Strain Gauge #2 Black wire - 4H
;Strain Gauge #3 Red wire - 5H
;Strain Gauge #3 White wire - 5L
;Strain Gauge #3 Black wire - 6H
;Strain Gauge #4 Red wire - 7H
;Strain Gauge #4 White wire - 7L
;Strain Gauge #4 Black wire - 8H
;Strain Gauge #5 Red wire - 9H
;Strain Gauge #5 White wire - 9L
;Strain Gauge #5 Black wire - 10H
;Strain Gauge #6 Red wire - 11H
;Strain Gauge #6 White wire - 11L
;Strain Gauge #6 Black wire - 12H
```

```
;Executing scan rate of CR10X every hour to take measurments of sensors
;Reducing or increasing seconds will change the scan rate of the logger. Change rate as desired.
;NOTE: Reducing the scan rate to a faster execution interval will affect the power consumption by the logger.
```

```
*Table 1 Program
01: 3600 Execution Interval (seconds)
```

```
;Instructions for 109B Temperature sensor measurements. Values in Degrees Celcius.
```

```
1: AC Half Bridge (P5)
1: 2 Reps
2: 25 2500 mV 60 Hz Rejection Range
3: 3 SE Channel
4: 1 Excite all reps w/Exchan 1
5: 2500 mV Excitation
6: 1 -- Loc [ V_Vx ]
7: 1.0 Multiplier
8: 0.0 Offset
```

```
2: Beginning of Loop (P87)
1: 0000 Delay
2: 2 Loop Count
```

```
3: Z=1/X (P42)
1: 1 -- X Loc [ V_Vx ]
2: 3 Z Loc [ Vx_V ]
```

4: Z=X+F (P34)

1: 3 X Loc [ Vx\_V ]  
2: -1 F  
3: 4 Z Loc [ Vx\_V1 ]

5: Z=X\*F (P37)

1: 4 X Loc [ Vx\_V1 ]  
2: 24900 F  
3: 5 Z Loc [ Rtherm ]

6: Z=LN(X) (P40)

1: 5 X Loc [ Rtherm ]  
2: 6 Z Loc [ lnRt ]

7: Z=X\*F (P37)

1: 6 X Loc [ lnRt ]  
2: .001 F  
3: 7 Z Loc [ Sc\_lnRt ]

8: Polynomial (P55)

1: 1 Reps  
2: 7 X Loc [ Sc\_lnRt ]  
3: 8 F(X) Loc [ 1\_Tk ]  
4: .001129 C0  
5: .234108 C1  
6: 0.0 C2  
7: 87.7547 C3  
8: 0.0 C4  
9: 0.0 C5

9: Z=1/X (P42)

1: 8 X Loc [ 1\_Tk ]  
2: 9 Z Loc [ Tk ]

10: Z=X+F (P34)

1: 9 X Loc [ Tk ]  
2: -273.15 F  
3: 10 -- Z Loc [ Temp\_1 ]

11: End (P95)

;------End of 109B Measurements-----

;-Instructions for measuring Peizometers through the AVW200 interface-

12: SDI-12 Recorder (P105)

1: 0000 SDI-12 Address  
2: 0 Start Measurement (aM!)  
3: 1 Port  
4: 19 Loc [ Vw\_1\_Freq ]  
5: 1.0 Multiplier  
6: 0.0 Offset

;------End of Peizometer Measurements-----



;----- Enable multiplexer to measure resistive strain gauges -----

13: Do (P86)

1: 44 Set Port 4 High

;Delay for Mux to turn on

14: Excitation with Delay (P22)

1: 2 Ex Channel

2: 15 Delay W/Ex (0.01 sec units)

3: 0000 Delay After Ex (0.01 sec units)

4: 0000 mV Excitation

;Begin measurement loop on multiplexer

15: Beginning of Loop (P87)

1: 0000 Delay

2: 6 Loop Count

;Clock pulse to cycle mux

16: Do (P86)

1: 73 Pulse Port 3

17: Excitation with Delay (P22)

1: 1 Ex Channel

2: 2 Delay W/Ex (0.01 sec units)

3: 0 Delay After Ex (0.01 sec units)

4: 0 mV Excitation

;Measurement instruction for measuring 3 wire Vishay WK strain gauges.

18: Full Bridge (P6)

1: 1 Repts

2: 20 Auto 60 Hz Rejection Range (OS>1.09)

3: 1 DIFF Channel

4: 2 Excite all reps w/Exchan 2

5: 2500 mV Excitation

6: 25 -- Loc [ mVperV\_1 ]

7: 1.0 Multiplier

8: 0.0 Offset

19: End (P95)

20: Do (P86)

1: 54 Set Port 4 Low

;----- End of Strain Gauge Measurements -----

;----- Torsion Gauge Measurements -----

21: Full Bridge (P6)

1: 1 Reps  
2: 0 Auto Slow Range (OS>1.09)  
3: 5 DIFF Channel  
4: 3 Excite all reps w/Exchan 3  
5: 2500 mV Excitation  
6: 32 Loc [ mV\_V\_Tor1 ]  
7: 1 Multiplier  
8: 0 Offset

22: Full Bridge (P6)

1: 1 Reps  
2: 0 Auto Slow Range (OS>1.09)  
3: 6 DIFF Channel  
4: 3 Excite all reps w/Exchan 3  
5: 2500 mV Excitation  
6: 31 Loc [ mV\_V\_Tor2 ]  
7: 1 Multiplier  
8: 0 Offset

;----- OUTPUT SECTION -----

23: If time is (P92)

1: 0 Minutes (Seconds --) into a  
2: 60 Interval (same units as above)  
3: 10 Set Output Flag High (Flag 0)

24: Set Active Storage Area (P80)

1: 1 Final Storage Area 1  
2: 60 Array ID

25: Real Time (P77)

1: 1110 Year,Day,Hour/Minute (midnight = 0000)

26: Sample (P70)

1: 2 Reps  
2: 10 Loc [ Temp\_1 ]

27: Resolution (P78)

1: 1 High Resolution

28: Sample (P70)

1: 6 Reps  
2: 19 Loc [ Vw\_1\_Freq ]

29: Resolution (P78)

1: 0 Low Resolution

30: Sample (P70)

1: 6 Reps  
2: 25 Loc [ mVperV\_1 ]

RIVERBANK\_PROGRAM\_REV1\_5.CSI, Table 1

31: Sample (P70)

1: 1 Reps

2: 32 Loc [ mV\_V\_Tor1 ]

32: Sample (P70)

1: 1 Reps

2: 31 Loc [ mV\_V\_Tor2 ]

\*Table 2 Program

02: 0.0000 Execution Interval (seconds)

\*Table 3 Subroutines

End Program

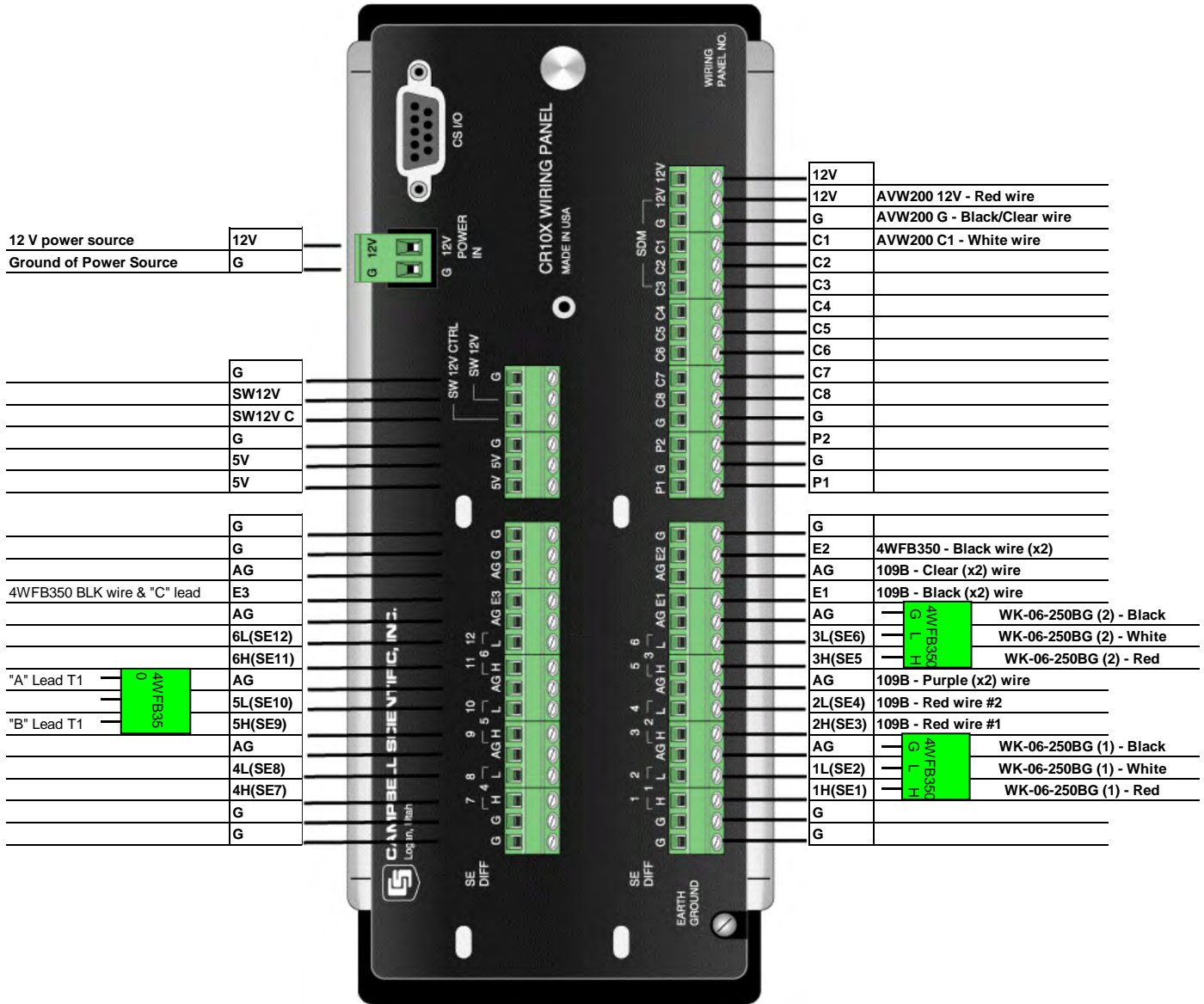
RIVERBANK\_PROGRAM\_REV1\_5.CSI, Input Locations

Addr	Name	Flags	# Reads	# Writes	Blocks
1	[ V_Vx ]	RW--	1	1	Start -----
2	[ V_Vx_2 ]	-W--	0	1	----- End
3	[ Vx_V ]	RW--	1	1	-----
4	[ Vx_V1 ]	RW--	1	1	-----
5	[ Rtherm ]	RW--	1	1	-----
6	[ InRt ]	RW--	1	1	-----
7	[ Sc_InRt ]	RW--	1	1	-----
8	[ 1_Tk ]	RW--	1	1	-----
9	[ Tk ]	RW--	1	1	-----
10	[ Temp_1 ]	RW--	1	1	-----
11	[ Temp_2 ]	R--	1	0	-----
12	[ _____ ]	----	0	0	-----
13	[ _____ ]	----	0	0	-----
14	[ _____ ]	----	0	0	-----
15	[ _____ ]	----	0	0	-----
16	[ _____ ]	----	0	0	-----
17	[ _____ ]	----	0	0	-----
18	[ _____ ]	----	0	0	-----
19	[ Vw_1_Freq ]	RWM-	1	1	Start -----
20	[ Vw_1_Res ]	R-M-	1	0	----- Member ---
21	[ Vw_1_Amp ]	R-M-	1	0	----- Member ---
22	[ Vw_2_Freq ]	R-M-	1	0	----- Member ---
23	[ Vw_2_Res ]	R-M-	1	0	----- Member ---
24	[ Vw_2_Amp ]	R-M-	1	0	----- End
25	[ mVperV_1 ]	RWM-	1	1	Start -----
26	[ mVperV_2 ]	R-M-	1	0	-----
27	[ mVperV_3 ]	R-M-	1	0	-----
28	[ mVperV_4 ]	R-M-	1	0	-----
29	[ mVperV_5 ]	R-M-	1	0	----- Member ---
30	[ mVperV_6 ]	R-M-	1	0	----- End
31	[ mV_V_Tor2 ]	RW--	1	1	-----
32	[ mV_V_Tor1 ]	RW--	1	1	-----

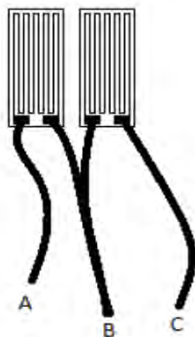
# CR10X WIRING DIAGRAM

Company:  
Project:  
Prepared By:

University of Manitoba  
Nelson Ferreira - Valley Site 1  
Ian Milne - Campbell Scientific Canada Corp.



**NOTES:** \*\* Use FIN4COND-L cable for wiring AVW200 interface to datalogger\*\*  
 \*\* Connect the "C" lead from both Torsion gauges to E3 as well as the black leads from the 4WFB350 modules  
 \*\* T1 = Torsion Gauge #1, T2 = Torsion Gauge #2



-Torsion Gauge Schematic

VALLEY\_1\_PROGRAM\_REV1\_3.CSI, Table 1

:{CR10X}

;Date: July 18, 2011

;Written by: Ian Milne

;Campbell Scientific Canada Corp.

;REV 1\_1 - August 5, 2011

;By: Ian Milne, Campbell Scientific Canada Corp.

;Changed Thermistor storage to High Resolution to prevent overflow

;REV 1\_2 - August 24th, 2011

;By: Ian Milne, Campbell Scientific Canada Corp.

;Fixed problem with Strain gauge 2 - incorrect channel being read due

;to use of REPS & conflict with wiring. Wiring remains the same.

;REV 1\_3 - September 26th, 2011

;By: Ian Milne, Campbell Scientific Canada Corp.

;Added in second AVW200 measurement to final storage.

;Station: Valley Site 1

;Wiring:

;SE1 - WK-06-250BG (red wire) / 4WFB350 (H)

;SE2 - WK-06-250BG (White wire) / 4WFB350 (L)

;AG - WK-06-250BG (Black wire) / WFB350 (G)

;SE3 - 109B #1 (Red wire)

;SE4 - 109B #2 (Red wire)

;AG - 109B #1,#2 (Purple wire)

;EX1 - 109B #1,#2 (Black wire)

;AG - 109B #1, #2 (Clear wire)

;C1 - AVW200 (White wire) Using FIN6COND-L wire

;12V - AVW200 (Red wire) Using FIN6COND-L wire

;G - AVW200 (Black,Clear wire)

;EX2 - 4FWB350 (Black wire)

;DIFF 4 - 4WFB350 - Torsion Gauge

;DIFF 5 - 4WFB350 - Torsion Gauge

;EX3 - 4WFB350 BLK wire + 'C lead' of WK-06-125TR-10CW

;Executing scan rate of CR10X every hour to take measurments of sensors

;Reducing or increasing seconds will change the scan rate of the logger. Change rate as desired.

;NOTE: Reducing the scan rate to a faster execution interval will affect the power consumption by the logger.

\*Table 1 Program

01: 3600 Execution Interval (seconds)

;Instructions for 109B Temperature sensor measurements. Values in Degrees Celcius.

1: AC Half Bridge (P5)

1: 2 Reps  
 2: 25 2500 mV 60 Hz Rejection Range  
 3: 3 SE Channel  
 4: 1 Excite all reps w/Exchan 1  
 5: 2500 mV Excitation  
 6: 1 -- Loc [ V\_Vx ]  
 7: 1.0 Multiplier  
 8: 0.0 Offset

2: Beginning of Loop (P87)

1: 0000 Delay  
 2: 2 Loop Count

3:  $Z=1/X$  (P42)

1: 1 -- X Loc [ V\_Vx ]  
 2: 3 Z Loc [ Vx\_V ]

4:  $Z=X+F$  (P34)

1: 3 X Loc [ Vx\_V ]  
 2: -1 F  
 3: 4 Z Loc [ Vx\_V1 ]

5:  $Z=X*F$  (P37)

1: 4 X Loc [ Vx\_V1 ]  
 2: 24900 F  
 3: 5 Z Loc [ Rtherm ]

6:  $Z=LN(X)$  (P40)

1: 5 X Loc [ Rtherm ]  
 2: 6 Z Loc [ lnRt ]

7:  $Z=X*F$  (P37)

1: 6 X Loc [ lnRt ]  
 2: .001 F  
 3: 7 Z Loc [ Sc\_lnRt ]

8: Polynomial (P55)

1: 1 Reps  
 2: 7 X Loc [ Sc\_lnRt ]  
 3: 8 F(X) Loc [ 1\_Tk ]  
 4: .001129 C0  
 5: .234108 C1  
 6: 0.0 C2  
 7: 87.7547 C3  
 8: 0.0 C4  
 9: 0.0 C5

9:  $Z=1/X$  (P42)

1: 8 X Loc [ 1\_Tk ]  
 2: 9 Z Loc [ Tk ]

10: Z=X+F (P34)  
1: 9 X Loc [ Tk ]  
2: -273.15 F  
3: 10 -- Z Loc [ Temp\_1 ]

11: End (P95)

;-----End of 109B Measurements-----

;----- Measure Peizometers through the AVW200 interface -----

12: SDI-12 Recorder (P105)  
1: 0000 SDI-12 Address  
2: 0 Start Measurement (aM!)  
3: 1 Port  
4: 19 Loc [ Vw\_1\_Freq ]  
5: 1.0 Multiplier  
6: 0.0 Offset

;-----End of Peizometer Measurements-----

;----- Measure resistive strain gauges -----

;Measurement instruction for measuring 2 wire Vishay WK strain gauges.

13: Full Bridge (P6)  
1: 1 Repts  
2: 20 Auto 60 Hz Rejection Range (OS>1.09)  
3: 1 DIFF Channel  
4: 2 Excite all reps w/Exchan 2  
5: 2500 mV Excitation  
6: 25 Loc [ mVperV\_1 ]  
7: 1.0 Multiplier  
8: 0.0 Offset

14: Full Bridge (P6)  
1: 1 Repts  
2: 20 Auto 60 Hz Rejection Range (OS>1.09)  
3: 3 DIFF Channel  
4: 2 Excite all reps w/Exchan 2  
5: 2500 mV Excitation  
6: 26 Loc [ mVperV\_2 ]  
7: 1.0 Multiplier  
8: 0.0 Offset

;----- End of Strain Gauge Measurements -----

;----- Torsion Gauge Measurement -----



15: Full Bridge (P6)  
1: 1 Reps  
2: 0 Auto Slow Range (OS>1.09)  
3: 5 DIFF Channel  
4: 3 Excite all reps w/Exchan 3  
5: 2500 mV Excitation  
6: 27 Loc [ mV\_V\_Tor1 ]  
7: 1 Multiplier  
8: 0 Offset

;----- OUTPUT SECTION -----

16: If time is (P92)  
1: 0 Minutes (Seconds --) into a  
2: 60 Interval (same units as above)  
3: 10 Set Output Flag High (Flag 0)

17: Set Active Storage Area (P80)  
1: 1 Final Storage Area 1  
2: 60 Array ID

18: Real Time (P77)  
1: 1110 Year,Day,Hour/Minute (midnight = 0000)

19: Sample (P70)  
1: 2 Reps  
2: 10 Loc [ Temp\_1 ]

20: Resolution (P78)  
1: 1 High Resolution

21: Sample (P70)  
1: 2 Reps  
2: 19 Loc [ Vw\_1\_Freq ]

22: Sample (P70)  
1: 2 Reps  
2: 22 Loc [ Vw\_2\_Freq ]

23: Resolution (P78)  
1: 00 Option

24: Sample (P70)  
1: 2 Reps  
2: 25 Loc [ mVperV\_1 ]

25: Sample (P70)  
1: 1 Reps  
2: 27 Loc [ mV\_V\_Tor1 ]

\*Table 2 Program  
02: 0.0000 Execution Interval (seconds)

\*Table 3 Subroutines

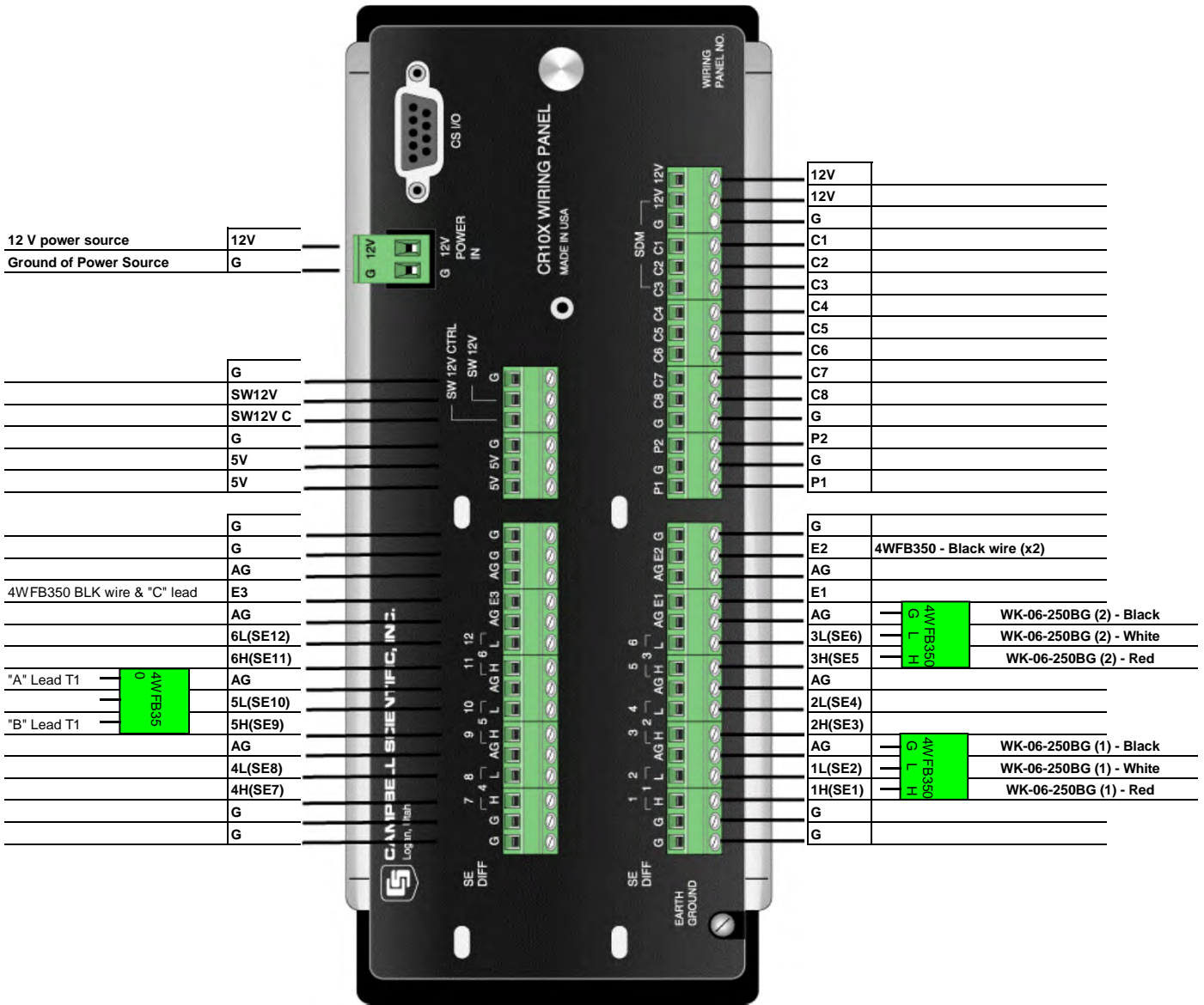
End Program

VALLEY\_1\_PROGRAM\_REV1\_3.CSI, Input Locations

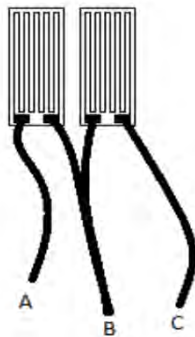
Addr	Name	Flags	# Reads	# Writes	Blocks
1	[ V_Vx ]	RW--	1	1	Start -----
2	[ V_Vx_2 ]	-W--	0	1	----- End
3	[ Vx_V ]	RW--	1	1	-----
4	[ Vx_V1 ]	RW--	1	1	-----
5	[ Rtherm ]	RW--	1	1	-----
6	[ InRt ]	RW--	1	1	-----
7	[ Sc_InRt ]	RW--	1	1	-----
8	[ 1_Tk ]	RW--	1	1	-----
9	[ Tk ]	RW--	1	1	-----
10	[ Temp_1 ]	RW--	1	1	-----
11	[ Temp_2 ]	R--	1	0	-----
12	[ _____ ]	----	0	0	-----
13	[ _____ ]	----	0	0	-----
14	[ _____ ]	----	0	0	-----
15	[ _____ ]	----	0	0	-----
16	[ _____ ]	----	0	0	-----
17	[ _____ ]	----	0	0	-----
18	[ _____ ]	----	0	0	-----
19	[ Vw_1_Freq ]	RWM-	1	1	Start -----
20	[ Vw_1_Res ]	R-M-	1	0	----- Member End
21	[ Vw_1_Amp ]	--M-	0	0	----- Member ---
22	[ Vw_2_Freq ]	R-M-	1	0	----- Member ---
23	[ Vw_2_Res ]	R-M-	1	0	----- Member ---
24	[ Vw_2_Amp ]	--M-	0	0	----- End
25	[ mVperV_1 ]	RWM-	1	1	Start -----
26	[ mVperV_2 ]	RWM-	1	1	-----
27	[ mV_V_Tor1 ]	RW--	1	1	-----
28	[ _____ ]	----	0	0	-----

# CR10X WIRING DIAGRAM

Company: University of Manitoba  
 Project: Nelson Ferreira - Valley Site 2  
 Prepared By: Ian Milne - Campbell Scientific Canada Corp.



**NOTES:** \*\* Connect the "C" lead from both Torision gauges to E3 as well as the black leads from the 4WFB350 modules  
 \*\* T1 = Torsion Gauge #1, T2 = Torsion Gauge #2



-Torsion Gauge Schematic

VALLEY\_2\_PROGRAM\_REV1\_1.CSI, Table 1

:{CR10X}

;Date: July 18, 2011

;Written by: Ian Milne

;Campbell Scientific Canada Corp.

;REV 1\_1 - August 24th, 2011

;By: Ian Milne, Campbell Scientific Canada Corp.

;Fixed problem with Strain gauge 2 - incorrect channel being read due

;to use of REPS & conflict with wiring. Wiring remains the same.

;Station: Valley Site 2

;Wiring:

;SE1 - WK-06-250BG (red wire) / 4WFB350 (H)

;SE2 - WK-06-250BG (White wire) / 4WFB350 (L)

;AG - WK-06-250BG (Black wire) / WFB350 (G)

;EX2 - 4WFB350 (Black wire)

;DIFF 4 - 4WFB350 - Torsion Gauge

;DIFF 5 - 4WFB350 - Torsion Gauge

;EX3 - 4WFB350 BLK wire + 'C lead' of WK-06-125TR-10CW

;Executing scan rate of CR10X every hour to take measurements of sensors

;Reducing or increasing seconds will change the scan rate of the logger. Change rate as desired.

;NOTE: Reducing the scan rate to a faster execution interval will affect the power consumption by the logger.

\*Table 1 Program

01: 3600 Execution Interval (seconds)

;----- Measure resistive strain gauges -----

;Measurement instruction for measuring 2 wire Vishay WK strain gauges.

1: Full Bridge (P6)

1: 1 Reps

2: 20 Auto 60 Hz Rejection Range (OS>1.09)

3: 1 DIFF Channel

4: 2 Excite all reps w/Exchan 2

5: 2500 mV Excitation

6: 25 Loc [ mVperV\_1 ]

7: 1.0 Multiplier

8: 0.0 Offset

2: Full Bridge (P6)

1: 1 Reps

2: 20 Auto 60 Hz Rejection Range (OS>1.09)

3: 3 DIFF Channel

4: 2 Excite all reps w/Exchan 2

5: 2500 mV Excitation

6: 26 Loc [ mVperV\_2 ]

7: 1.0 Multiplier

8: 0.0 Offset

;----- End of Strain Gauge Measurements -----

;----- Torsion Gauge Measurement -----

3: Full Bridge (P6)

- 1: 1 Reps
- 2: 0 Auto Slow Range (OS>1.09)
- 3: 5 DIFF Channel
- 4: 3 Excite all reps w/Exchan 3
- 5: 2500 mV Excitation
- 6: 27 Loc [ mV\_V\_Tor1 ]
- 7: 1 Multiplier
- 8: 0 Offset

;----- OUTPUT SECTION -----

4: If time is (P92)

- 1: 0 Minutes (Seconds --) into a
- 2: 60 Interval (same units as above)
- 3: 10 Set Output Flag High (Flag 0)

5: Set Active Storage Area (P80)

- 1: 1 Final Storage Area 1
- 2: 60 Array ID

6: Real Time (P77)

- 1: 1110 Year,Day,Hour/Minute (midnight = 0000)

7: Sample (P70)

- 1: 2 Reps
- 2: 25 Loc [ mVperV\_1 ]

8: Sample (P70)

- 1: 1 Reps
- 2: 27 Loc [ mV\_V\_Tor1 ]

\*Table 2 Program

- 02: 0.0000 Execution Interval (seconds)

\*Table 3 Subroutines

End Program



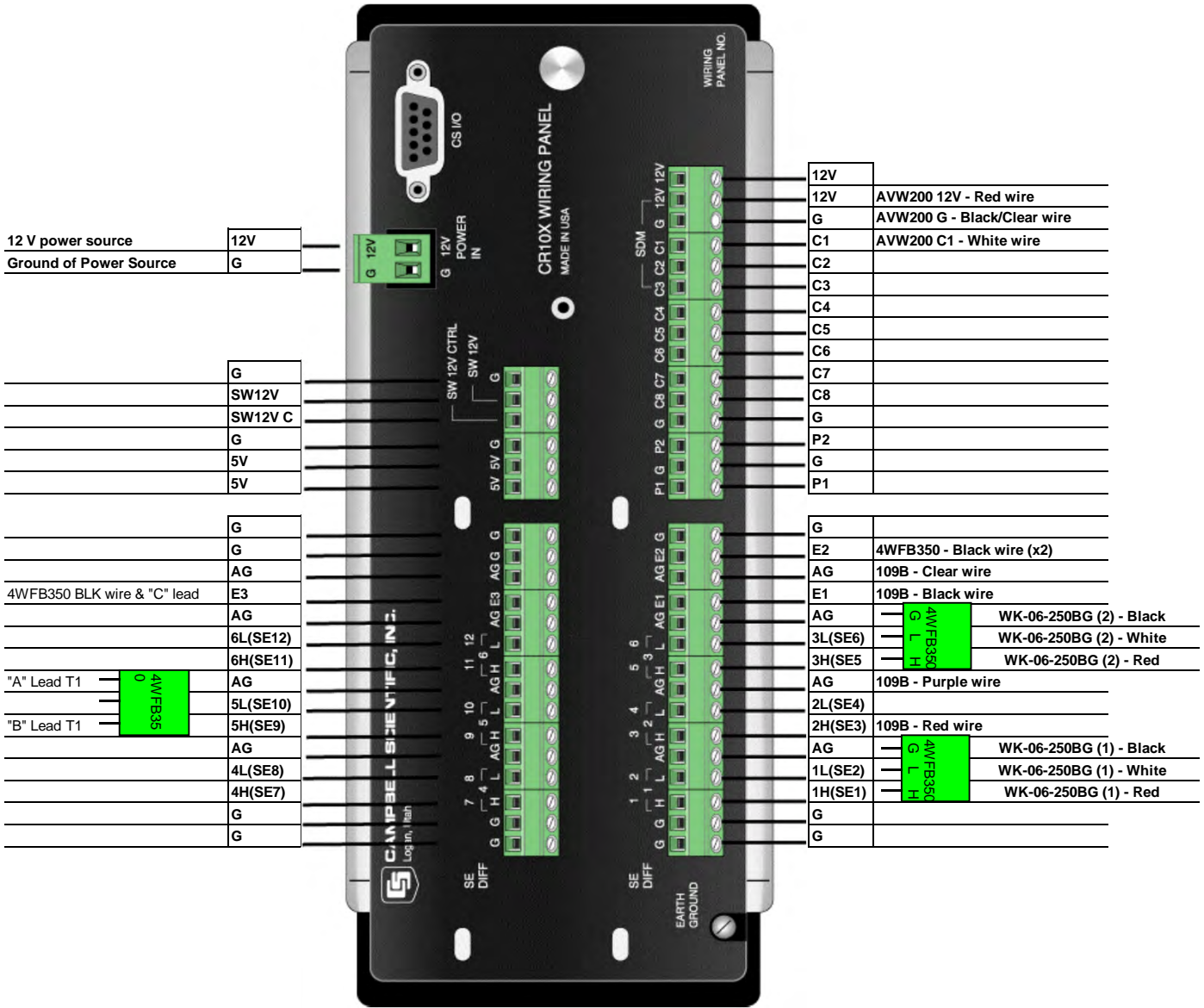
VALLEY\_2\_PROGRAM\_REV1\_1.CSI, Input Locations

Addr	Name	Flags	# Reads	# Writes	Blocks
1	[ _____ ]	----	0	0	-----
2	[ _____ ]	----	0	0	-----
3	[ _____ ]	----	0	0	-----
4	[ _____ ]	----	0	0	-----
5	[ _____ ]	----	0	0	-----
6	[ _____ ]	----	0	0	-----
7	[ _____ ]	----	0	0	-----
8	[ _____ ]	----	0	0	-----
9	[ _____ ]	----	0	0	-----
10	[ _____ ]	----	0	0	-----
11	[ _____ ]	----	0	0	-----
12	[ _____ ]	----	0	0	-----
13	[ _____ ]	----	0	0	-----
14	[ _____ ]	----	0	0	-----
15	[ _____ ]	----	0	0	-----
16	[ _____ ]	----	0	0	-----
17	[ _____ ]	----	0	0	-----
18	[ _____ ]	----	0	0	-----
19	[ Vw_1_Freq ]	--M-	0	0	-----
20	[ Vw_1_Res ]	--M-	0	0	----- Member End
21	[ Vw_1_Amp ]	--M-	0	0	----- Member ---
22	[ Vw_2_Freq ]	--M-	0	0	----- Member ---
23	[ Vw_2_Res ]	--M-	0	0	----- Member ---
24	[ Vw_2_Amp ]	--M-	0	0	----- End
25	[ mVperV_1 ]	RWM-	1	1	Start -----
26	[ mVperV_2 ]	RWM-	1	1	-----
27	[ mV_V_Tor1 ]	RW--	1	1	-----
28	[ _____ ]	----	0	0	-----

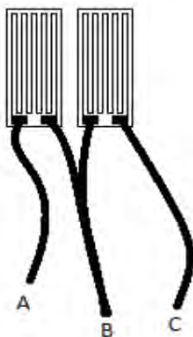


# CR10X WIRING DIAGRAM

Company:	University of Manitoba
Project:	Nelson Ferreira - Valley Site 3
Prepared By:	Ian Milne - Campbell Scientific Canada Corp.



**NOTES:** \*\* Use FIN4COND-L cable for wiring AVW200 interface to datalogger\*\*  
 \*\* Connect the "C" lead from both Torsion gauges to E3 as well as the black leads from the 4WFB350 modules  
 \*\* T1 = Torsion Gauge #1, T2 = Torsion Gauge #2



-Torsion Gauge Schematic

VALLEY\_3\_PROGRAM\_REV1\_3.CSI, Table 1

;  
;{CR10X}

;Date: July 18, 2011

;Written by: Ian Milne

;Campbell Scientific Canada Corp.

;REV 1\_1 - August 5, 2011

;By: Ian Milne, Campbell Scientific Canada Corp.

;Changed Thermistor storage to High Resolution to prevent overflow

;REV 1\_2 - August 24th, 2011

;By: Ian Milne, Campbell Scientific Canada Corp.

;Fixed problem with Strain gauge 2 - incorrect channel being read due

;to use of REPS & conflict with wiring. Wiring remains the same.

;REV 1\_3 - September 26th, 2011

;By: Ian Milne, Campbell Scientific Canada Corp.

;Added in second AVW200 measurement to final storage.

;Station: Valley Site 3

;Wiring:

;SE1 - WK-06-250BG (red wire) / 4WFB350 (H)

;SE2 - WK-06-250BG (White wire) / 4WFB350 (L)

;AG - WK-06-250BG (Black wire) / WFB350 (G)

;SE3 - 109B #1 (Red wire)

;AG - 109B #1 (Purple wire)

;EX1 - 109B #1 (Black wire)

;AG - 109B #1 (Clear wire)

;C1 - AVW200 (White wire) Using FIN6COND-L wire

;12V - AVW200 (Red wire) Using FIN6COND-L wire

;G - AVW200 (Black, Clear wire)

;EX2 - 4FWB350 (Black wire)

;DIFF 4 - 4WFB350 - Torsion Gauge

;DIFF 5 - 4WFB350 - Torsion Gauge

;EX3 - 4WFB350 BLK wire + 'C lead' of WK-06-125TR-10CW

;Executing scan rate of CR10X every hour to take measurements of sensors

;Reducing or increasing seconds will change the scan rate of the logger. Change rate as desired.

;NOTE: Reducing the scan rate to a faster execution interval will affect the power consumption by the logger.

\*Table 1 Program

01: 3600 Execution Interval (seconds)

;Instructions for 109B Temperature sensor measurements. Values in Degrees Celcius.

1: AC Half Bridge (P5)

1: 1 Reps

2: 25 2500 mV 60 Hz Rejection Range

3: 3 SE Channel

4: 1 Excite all reps w/Exchan 1

5: 2500 mV Excitation

6: 1 Loc [ V\_Vx ]

7: 1.0 Multiplier

8: 0.0 Offset

2: Z=1/X (P42)

1: 1 X Loc [ V\_Vx ]  
2: 2 Z Loc [ Vx\_V ]

3: Z=X+F (P34)

1: 2 X Loc [ Vx\_V ]  
2: -1 F  
3: 3 Z Loc [ Vx\_V1 ]

4: Z=X\*F (P37)

1: 3 X Loc [ Vx\_V1 ]  
2: 24900 F  
3: 4 Z Loc [ Rtherm ]

5: Z=LN(X) (P40)

1: 4 X Loc [ Rtherm ]  
2: 5 Z Loc [ lnRt ]

6: Z=X\*F (P37)

1: 5 X Loc [ lnRt ]  
2: .001 F  
3: 6 Z Loc [ Sc\_lnRt ]

7: Polynomial (P55)

1: 1 Reps  
2: 6 X Loc [ Sc\_lnRt ]  
3: 7 F(X) Loc [ 1\_Tk ]  
4: .001129 C0  
5: .234108 C1  
6: 0.0 C2  
7: 87.7547 C3  
8: 0.0 C4  
9: 0.0 C5

8: Z=1/X (P42)

1: 7 X Loc [ 1\_Tk ]  
2: 8 Z Loc [ Tk ]

9: Z=X+F (P34)

1: 8 X Loc [ Tk ]  
2: -273.15 F  
3: 9 Z Loc [ Temp\_1 ]

;----- End of 109B Measurement -----

;----- Measure Peizometers through the AVW200 interface -----

10: SDI-12 Recorder (P105)

1: 0000 SDI-12 Address  
2: 0 Start Measurement (aM!)  
3: 1 Port  
4: 19 Loc [ Vw\_1\_Freq ]  
5: 1.0 Multiplier  
6: 0.0 Offset

;-----End of Peizometer Measurements-----

;----- Measure resistive strain gauges -----

;Measurement instruction for measuring 2 wire Vishay WK strain gauges.

11: Full Bridge (P6)

1: 1 Reps  
2: 20 Auto 60 Hz Rejection Range (OS>1.09)  
3: 1 DIFF Channel  
4: 2 Excite all reps w/Exchan 2  
5: 2500 mV Excitation  
6: 25 Loc [ mVperV\_1 ]  
7: 1.0 Multiplier  
8: 0.0 Offset

12: Full Bridge (P6)

1: 1 Reps  
2: 20 Auto 60 Hz Rejection Range (OS>1.09)  
3: 3 DIFF Channel  
4: 2 Excite all reps w/Exchan 2  
5: 2500 mV Excitation  
6: 26 Loc [ mVperV\_2 ]  
7: 1.0 Multiplier  
8: 0.0 Offset

;----- End of Strain Gauge Measurements -----

;----- Torsion Gauge Measurement -----

13: Full Bridge (P6)

1: 1 Reps  
2: 0 Auto Slow Range (OS>1.09)  
3: 5 DIFF Channel  
4: 3 Excite all reps w/Exchan 3  
5: 2500 mV Excitation  
6: 27 Loc [ mV\_V\_Tor1 ]  
7: 1 Multiplier  
8: 0 Offset

;----- OUTPUT SECTION -----

14: If time is (P92)

1: 0 Minutes (Seconds --) into a  
2: 60 Interval (same units as above)  
3: 10 Set Output Flag High (Flag 0)

VALLEY\_3\_PROGRAM\_REV1\_3.CSI, Table 1

15: Set Active Storage Area (P80)

1: 1 Final Storage Area 1

2: 60 Array ID

16: Real Time (P77)

1: 1110 Year,Day,Hour/Minute (midnight = 0000)

17: Sample (P70)

1: 1 Reps

2: 9 Loc [ Temp\_1 ]

18: Resolution (P78)

1: 1 High Resolution

19: Sample (P70)

1: 2 Reps

2: 19 Loc [ Vw\_1\_Freq ]

20: Sample (P70)

1: 2 Reps

2: 22 Loc [ Vw\_2\_Freq ]

21: Resolution (P78)

1: 00 Option

22: Sample (P70)

1: 2 Reps

2: 25 Loc [ mVperV\_1 ]

23: Sample (P70)

1: 1 Reps

2: 27 Loc [ mV\_V\_Tor1 ]

\*Table 2 Program

02: 0.0000 Execution Interval (seconds)

\*Table 3 Subroutines

End Program



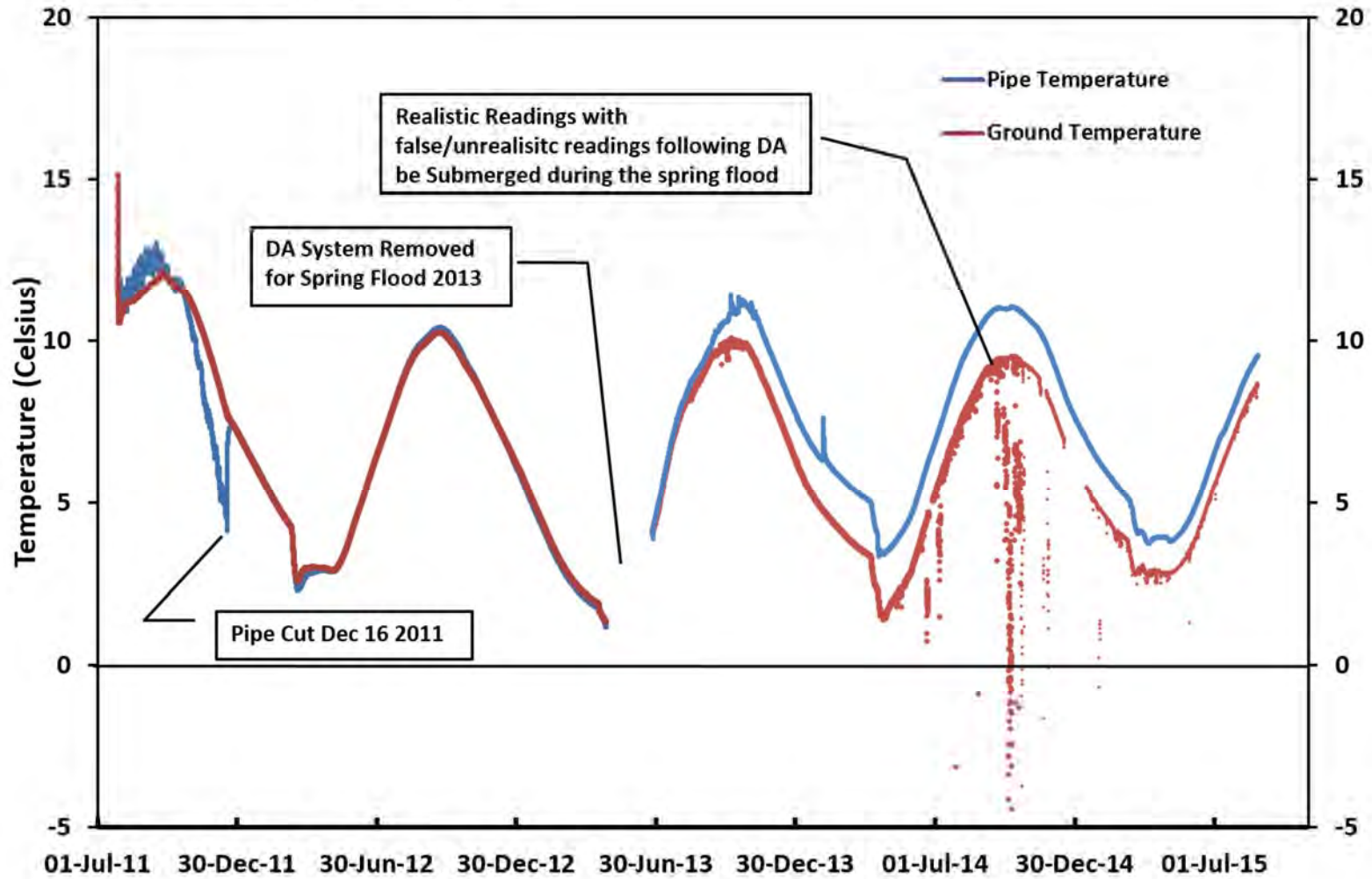
VALLEY\_3\_PROGRAM\_REV1\_3.CSI, Input Locations

Addr	Name	Flags	# Reads	# Writes	Blocks
1	[ V_Vx ]	RW--	1	1	-----
2	[ Vx_V ]	RW--	1	1	-----
3	[ Vx_V1 ]	RW--	1	1	-----
4	[ Rtherm ]	RW--	1	1	-----
5	[ InRt ]	RW--	1	1	-----
6	[ Sc_InRt ]	RW--	1	1	-----
7	[ 1_Tk ]	RW--	1	1	-----
8	[ Tk ]	RW--	1	1	-----
9	[ Temp_1 ]	RW--	1	1	-----
10	[ _____ ]	----	0	0	-----
11	[ _____ ]	----	0	0	-----
12	[ _____ ]	----	0	0	-----
13	[ _____ ]	----	0	0	-----
14	[ _____ ]	----	0	0	-----
15	[ _____ ]	----	0	0	-----
16	[ _____ ]	----	0	0	-----
17	[ _____ ]	----	0	0	-----
18	[ _____ ]	----	0	0	-----
19	[ Vw_1_Freq ]	RWM-	1	1	Start -----
20	[ Vw_1_Res ]	R-M-	1	0	----- Member End
21	[ Vw_1_Amp ]	--M-	0	0	----- Member ---
22	[ Vw_2_Freq ]	R-M-	1	0	----- Member ---
23	[ Vw_2_Res ]	R-M-	1	0	----- Member ---
24	[ Vw_2_Amp ]	--M-	0	0	----- End
25	[ mVperV_1 ]	RWM-	1	1	Start -----
26	[ mVperV_2 ]	RWM-	1	1	-----
27	[ mV_V_Tor1 ]	RW--	1	1	-----
28	[ _____ ]	----	0	0	-----

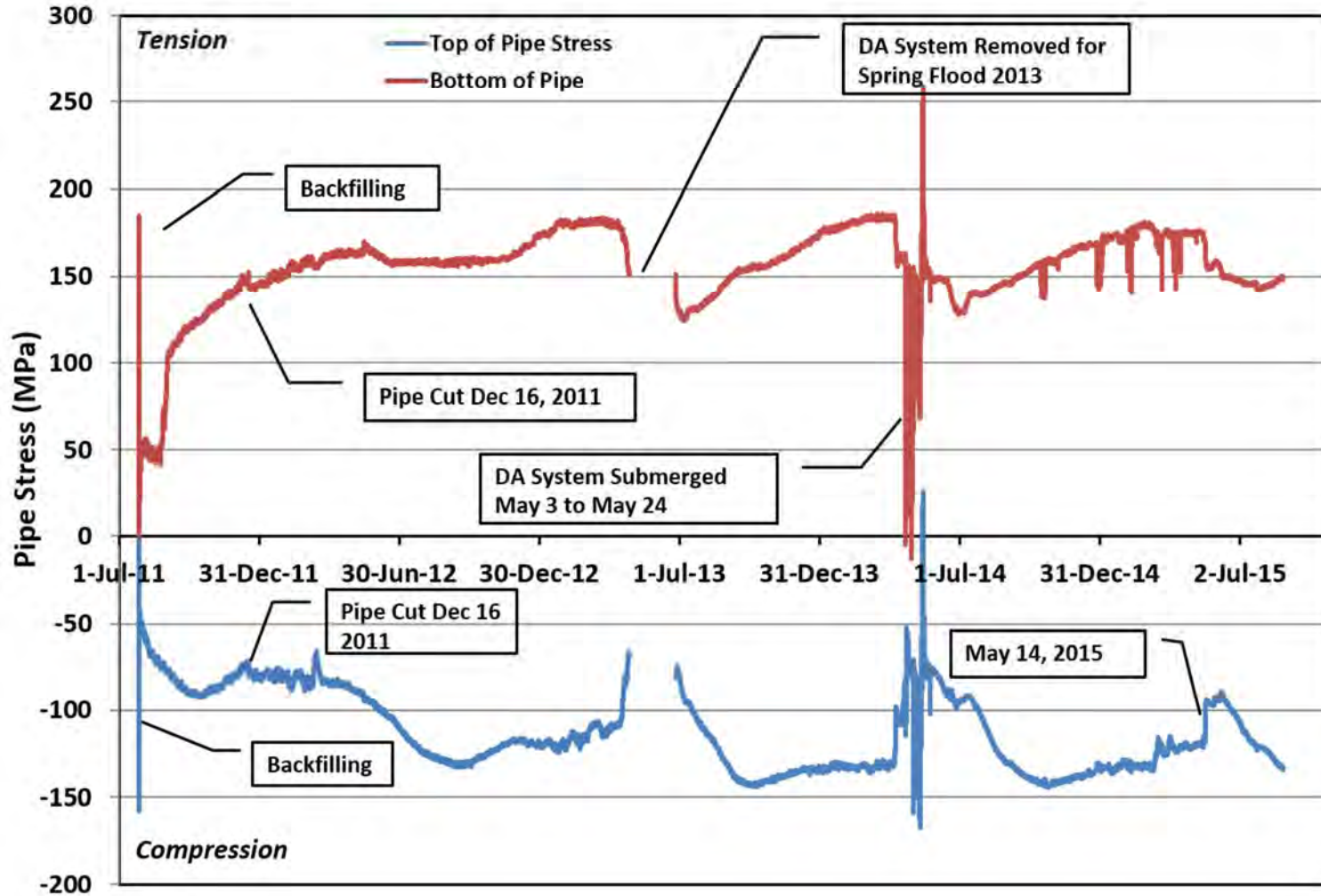
# Appendix C – DA Monitoring Results (Raw and Filtered)



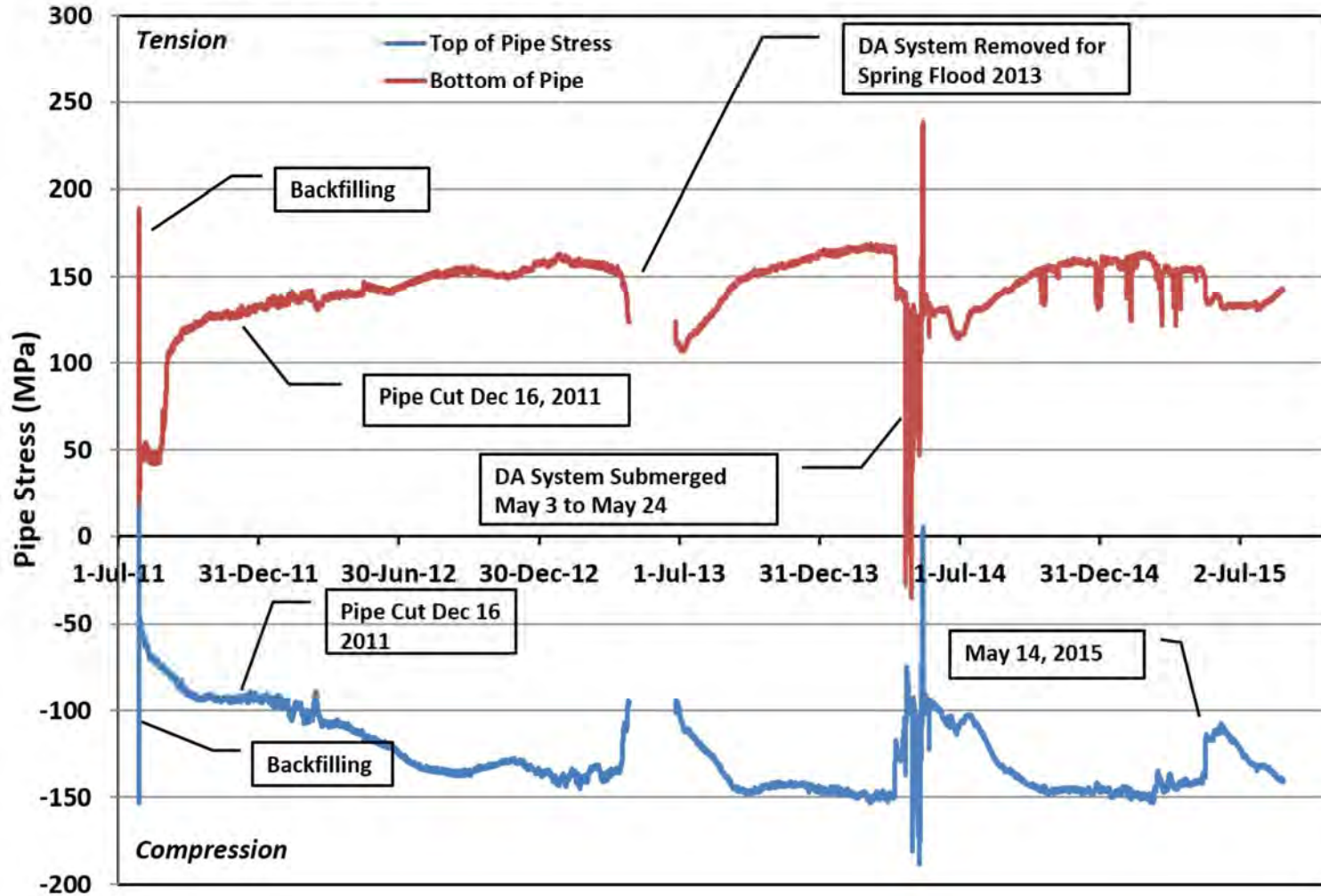
**Manitoba Hydro Gas Pipeline Research  
Plum River Test Site  
Beyond the Crest - Pipe/Ground Temperature**



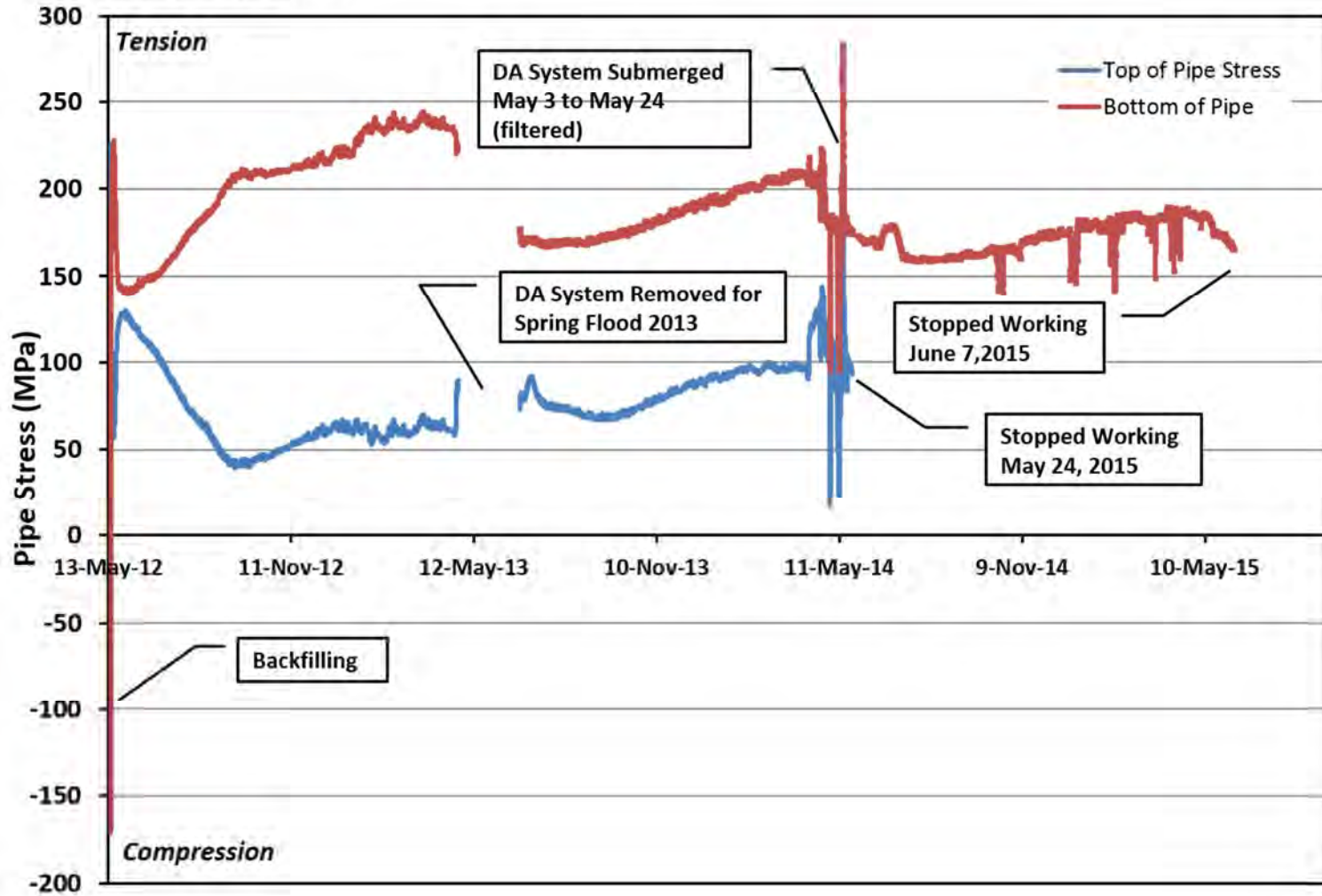
**Manitoba Hydro Gas Pipeline Research  
Plum River Test Site  
Beyond the Crest - Pipe Stresses**



**Manitoba Hydro Gas Pipeline Research  
 Plum River Test Site  
 Beyond the Crest - Pipe Stresses without Thermal Effects**

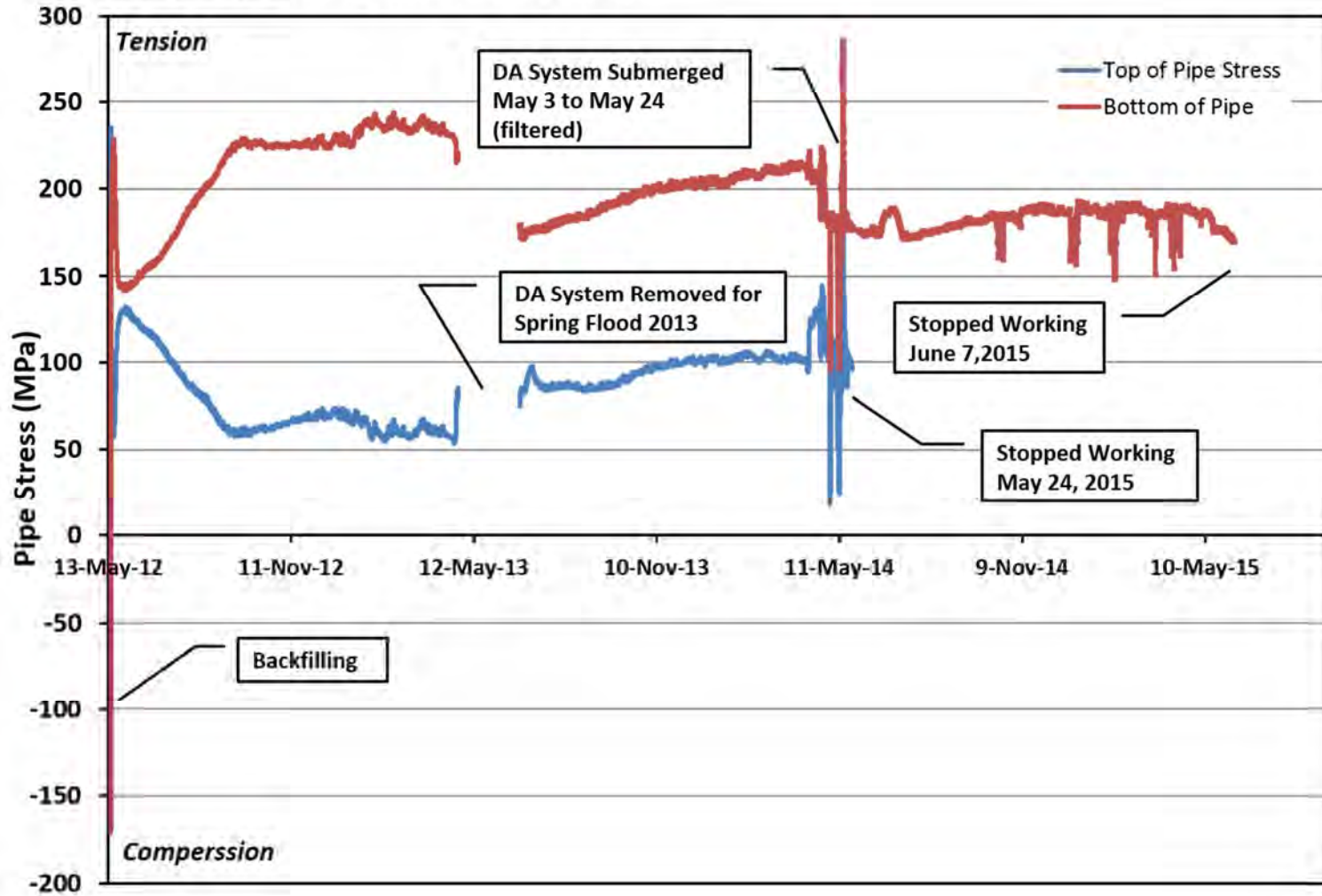


**Manitoba Hydro Gas Pipeline Research  
Plum River Test Site  
Along The Slope - Pipe Stresses**

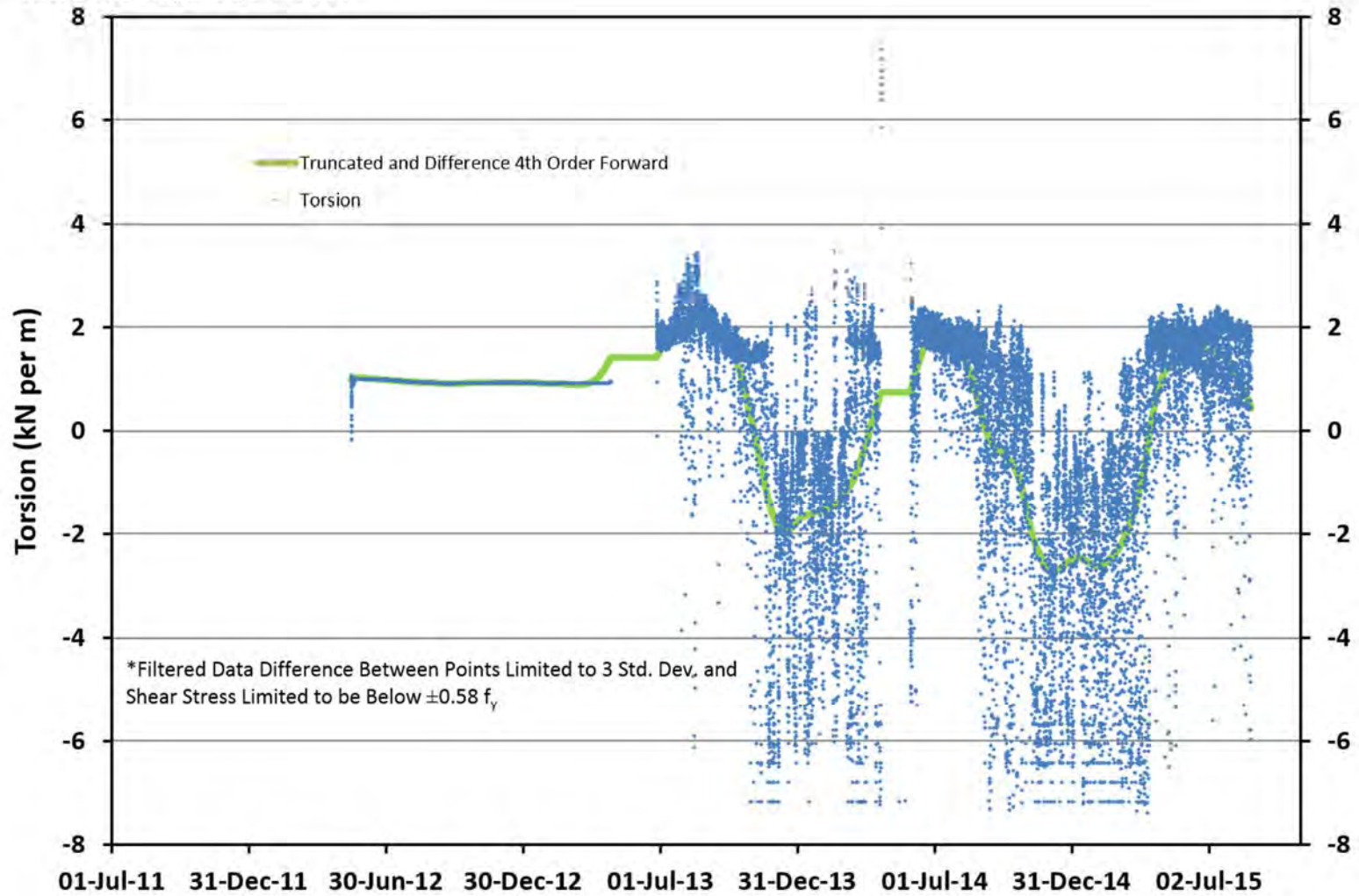




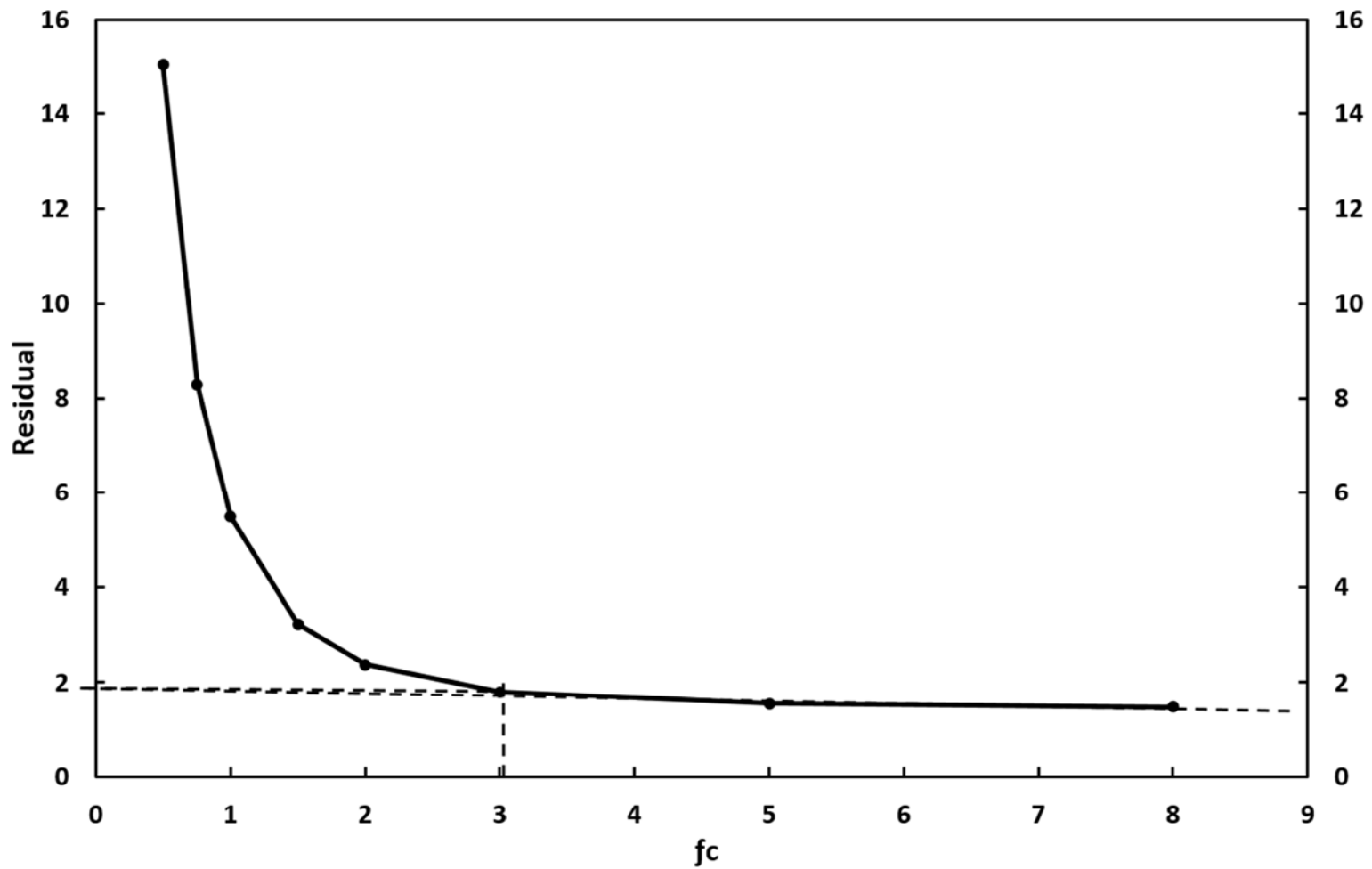
**Manitoba Hydro Gas Pipeline Research**  
**Plum River Test Site**  
**Along The Slope - Pipe Stresses without Thermal Effects**



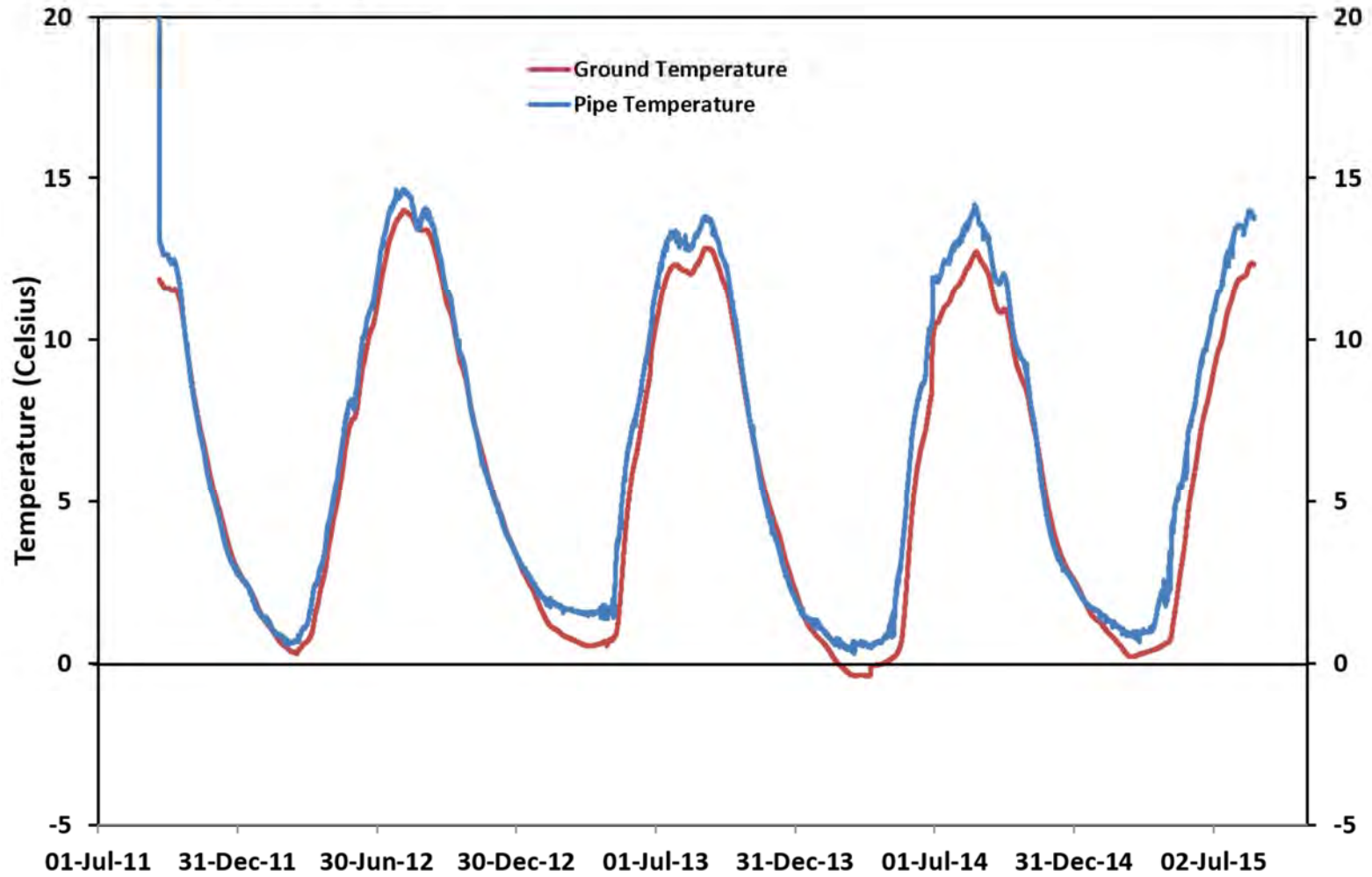
Manitoba Hydro Gas Pipeline Research  
Plum River Test Site  
Along The Slope - Pipe Torsion



Plum River Along the Slope  
Torsion Cut Off Frequency Truncated and Difference - Residuals

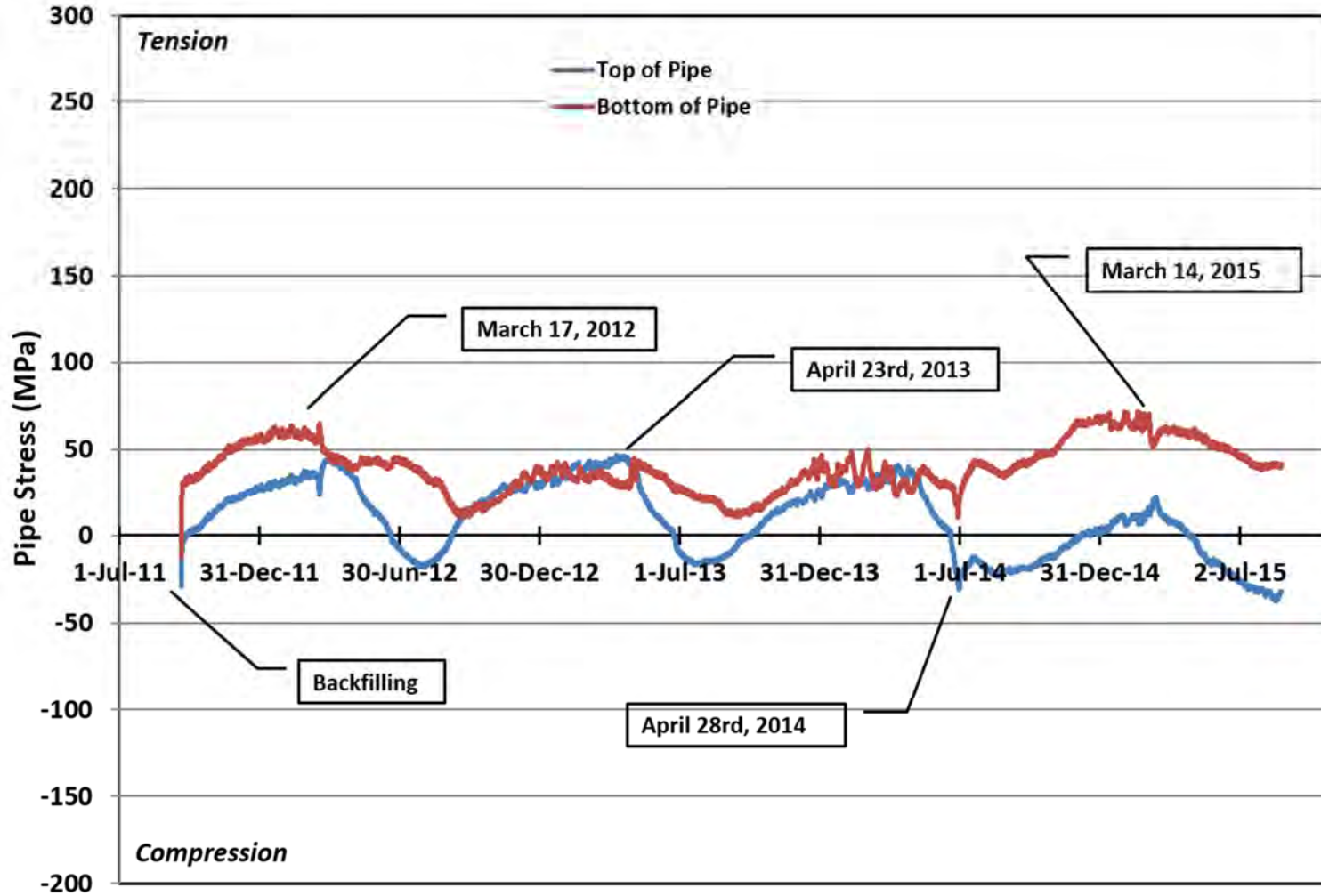


**Manitoba Hydro Gas Pipeline Research  
St. Lazare Test Site  
Top of Valley - Pipe/Ground Temperature**

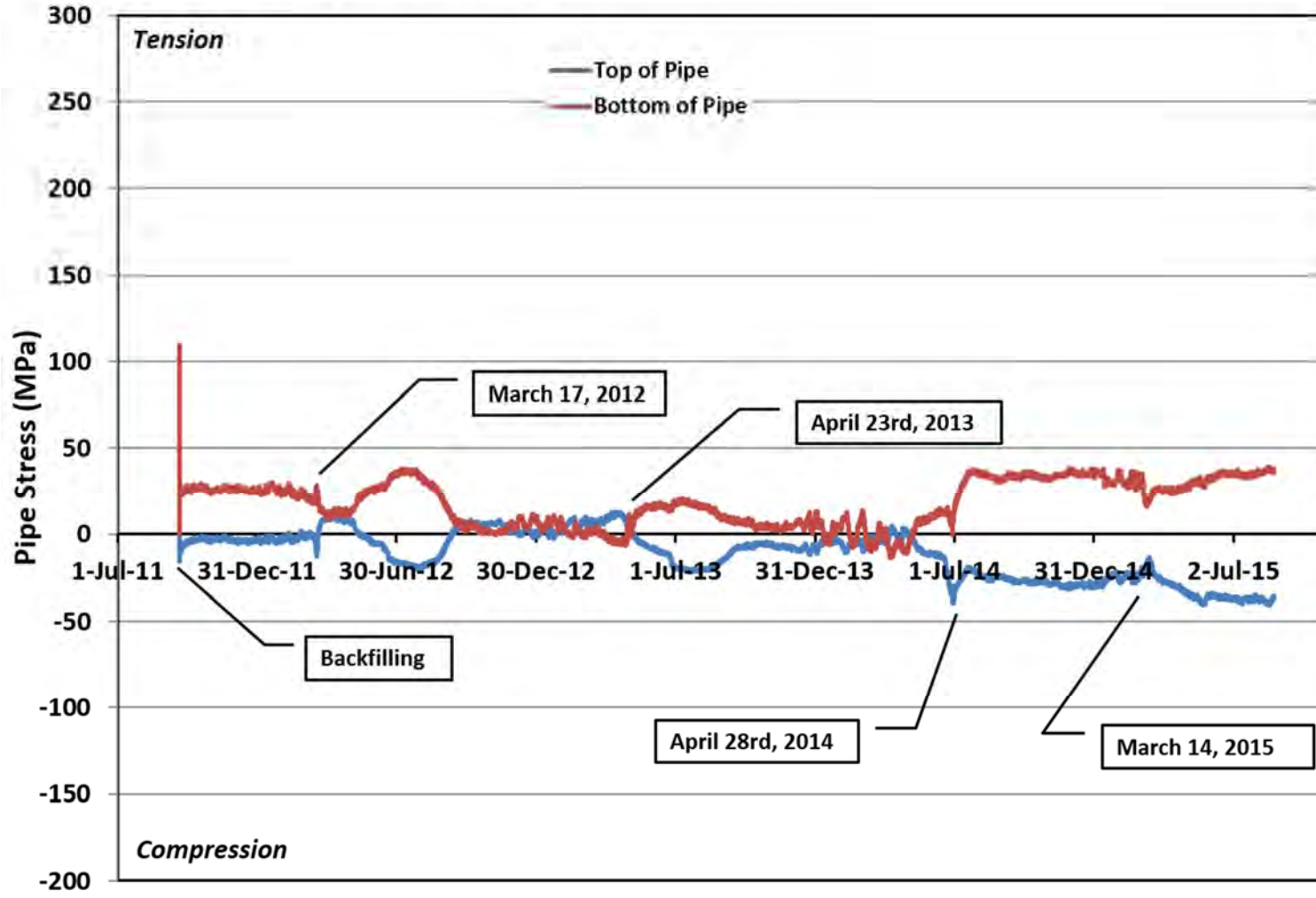




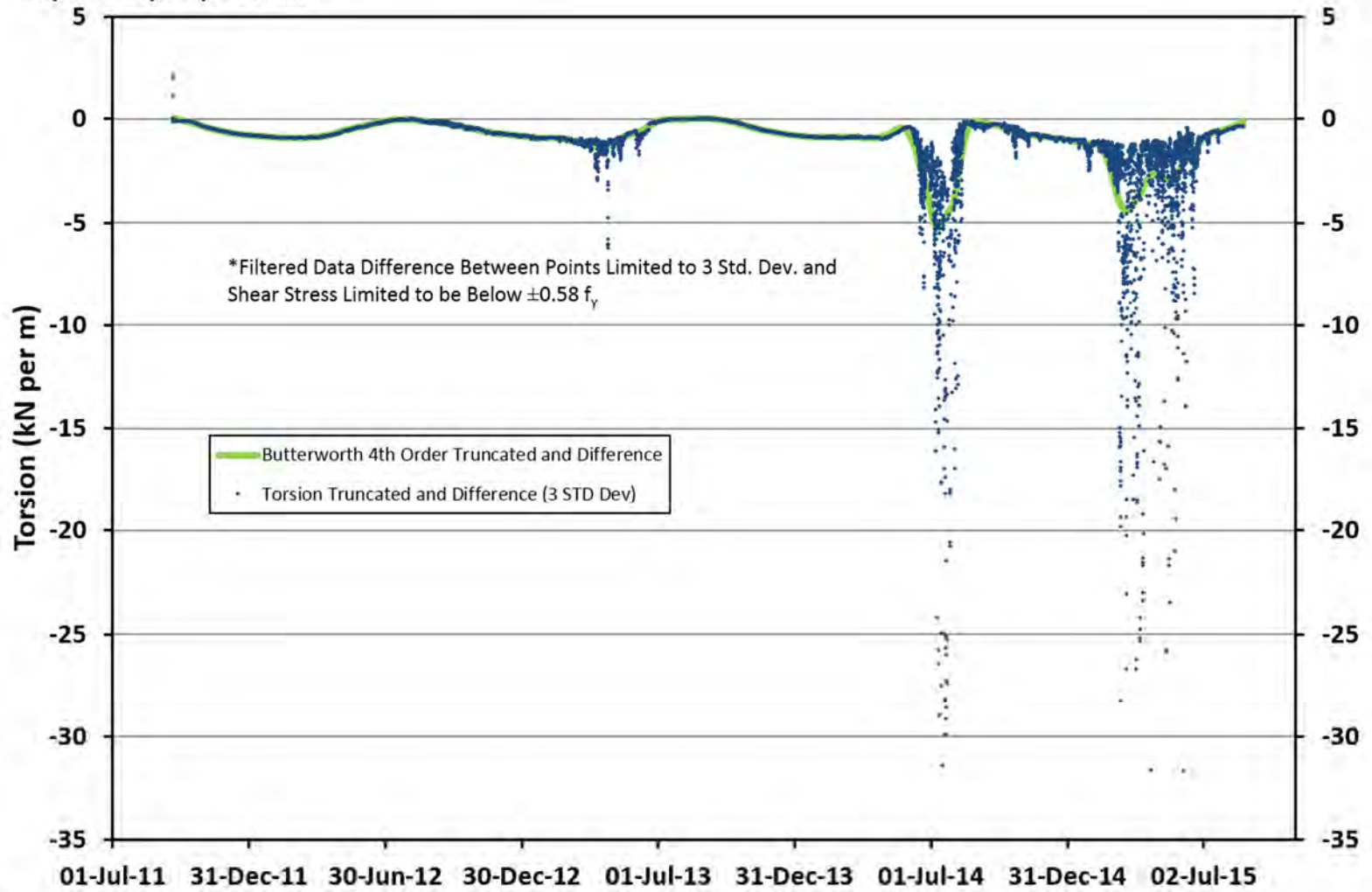
Manitoba Hydro Gas Pipeline Research  
St. Lazare Test Site  
Top of Valley - Pipe Stresses



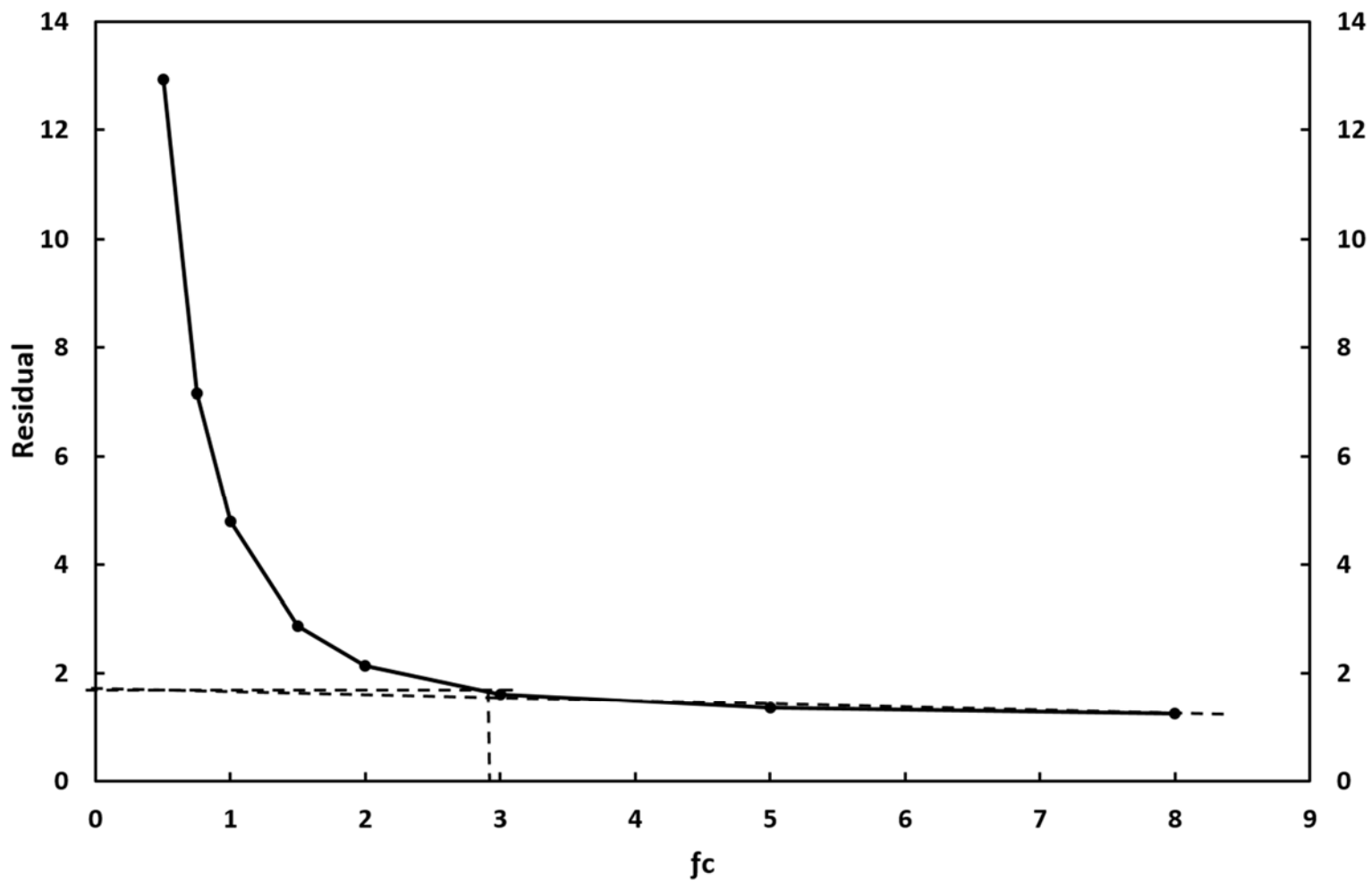
Manitoba Hydro Gas Pipeline Research  
St. Lazare Test Site  
Top of Valley - Pipe Stresses without Thermal Effects



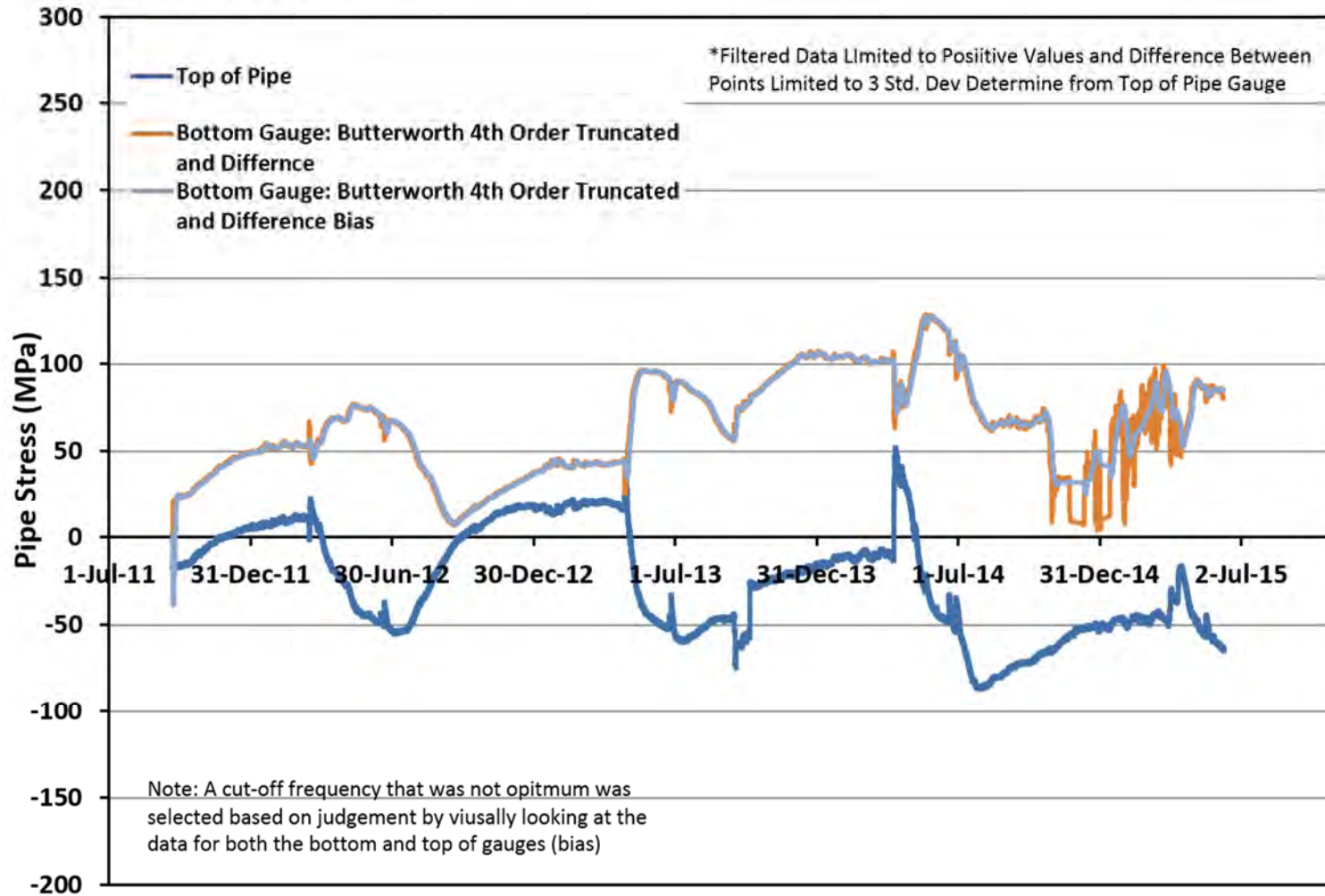
Manitoba Hydro Gas Pipeline Research  
St. Lazare Test Site  
Top of Valley - Pipe Torsion



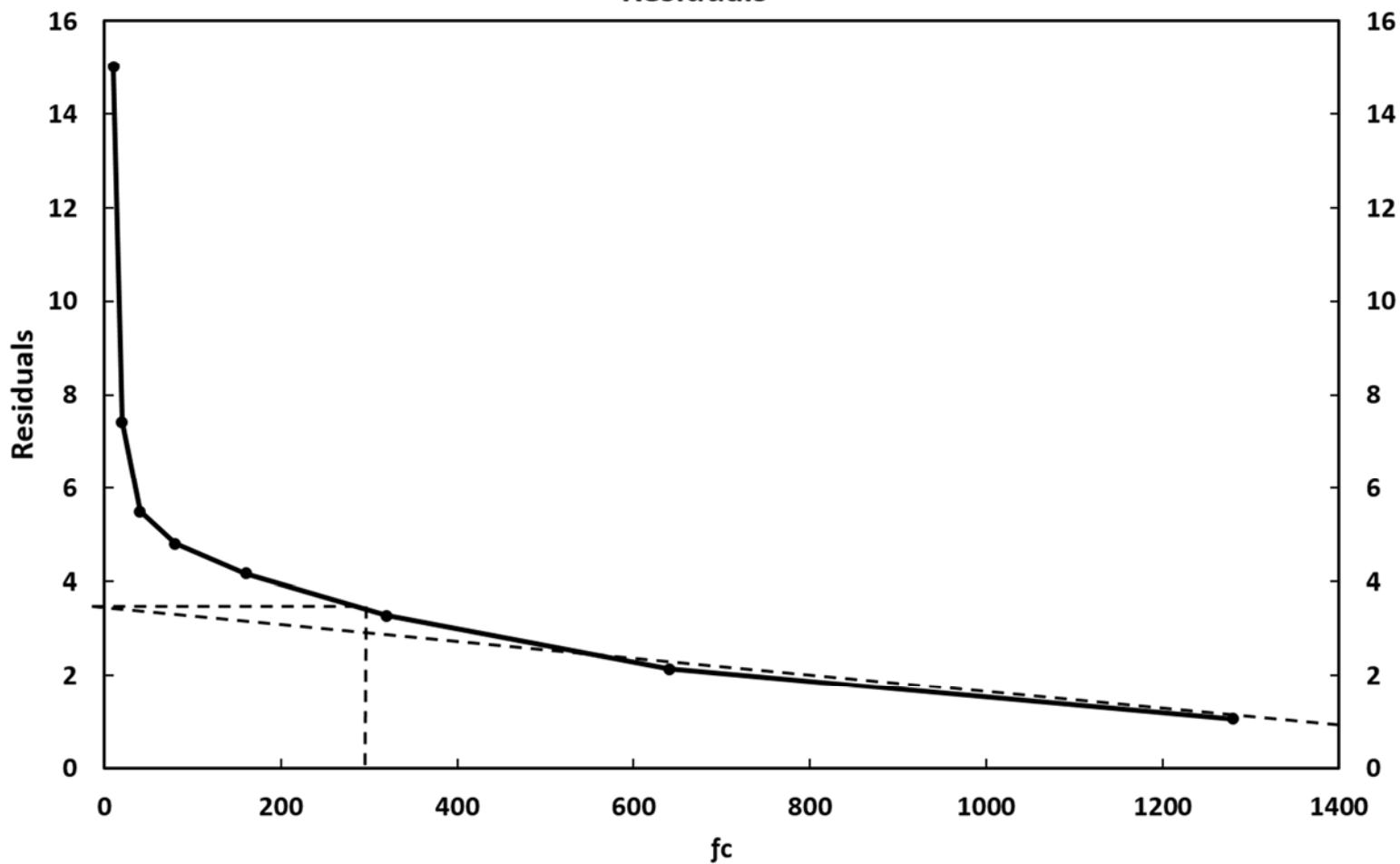
St-Lazare Top of Valley  
Torsion Cut Off Frequency Truncated and Difference - Residuals



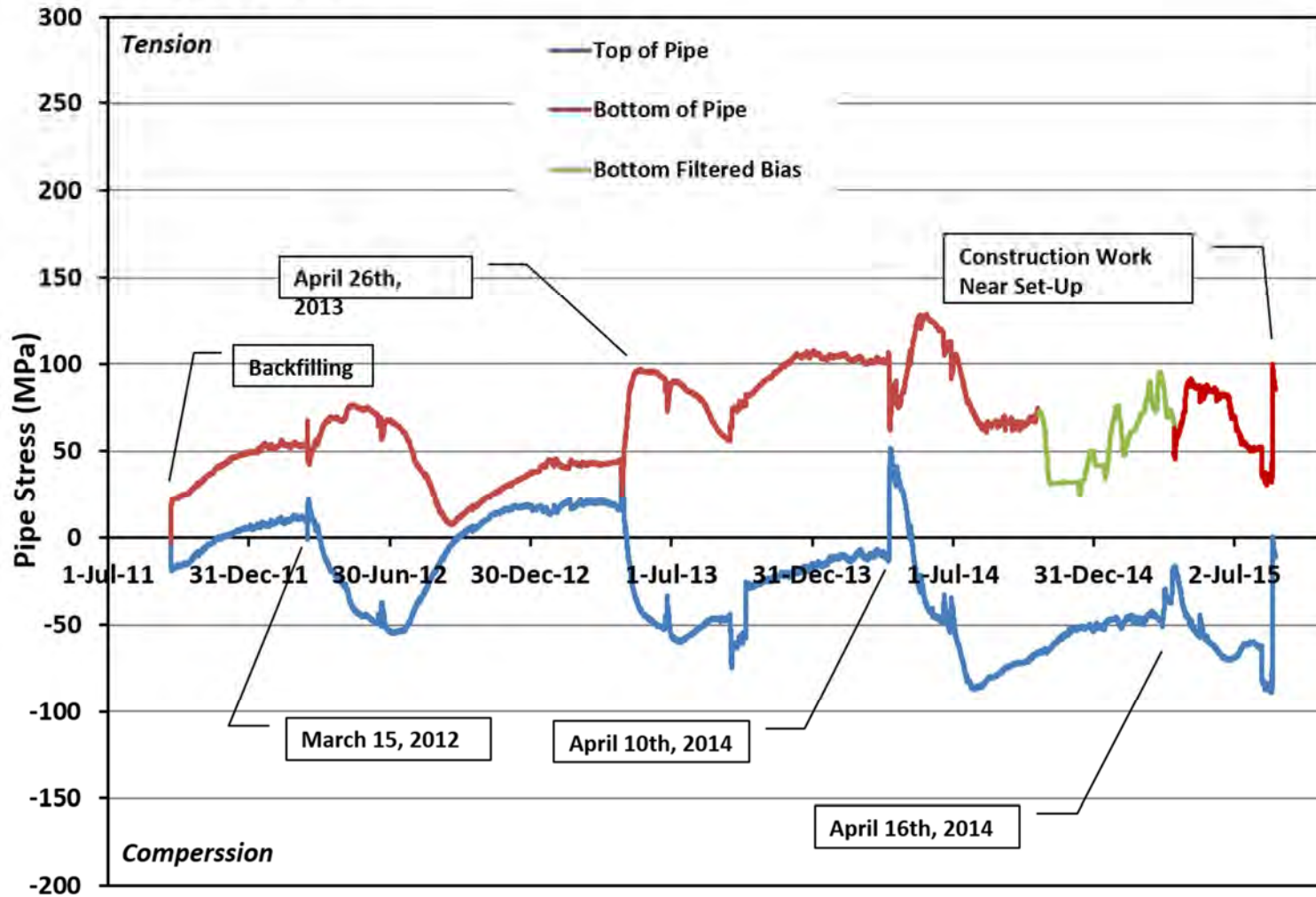
**Manitoba Hydro Gas Pipeline Research**  
**St. Lazare Test Site**  
**Middle of Valley - Pipe Stresses**



St-Lazare Middle of Valley  
Bottom Strain Gauge Cut Off Frequency Truncated and Difference -  
Residuals

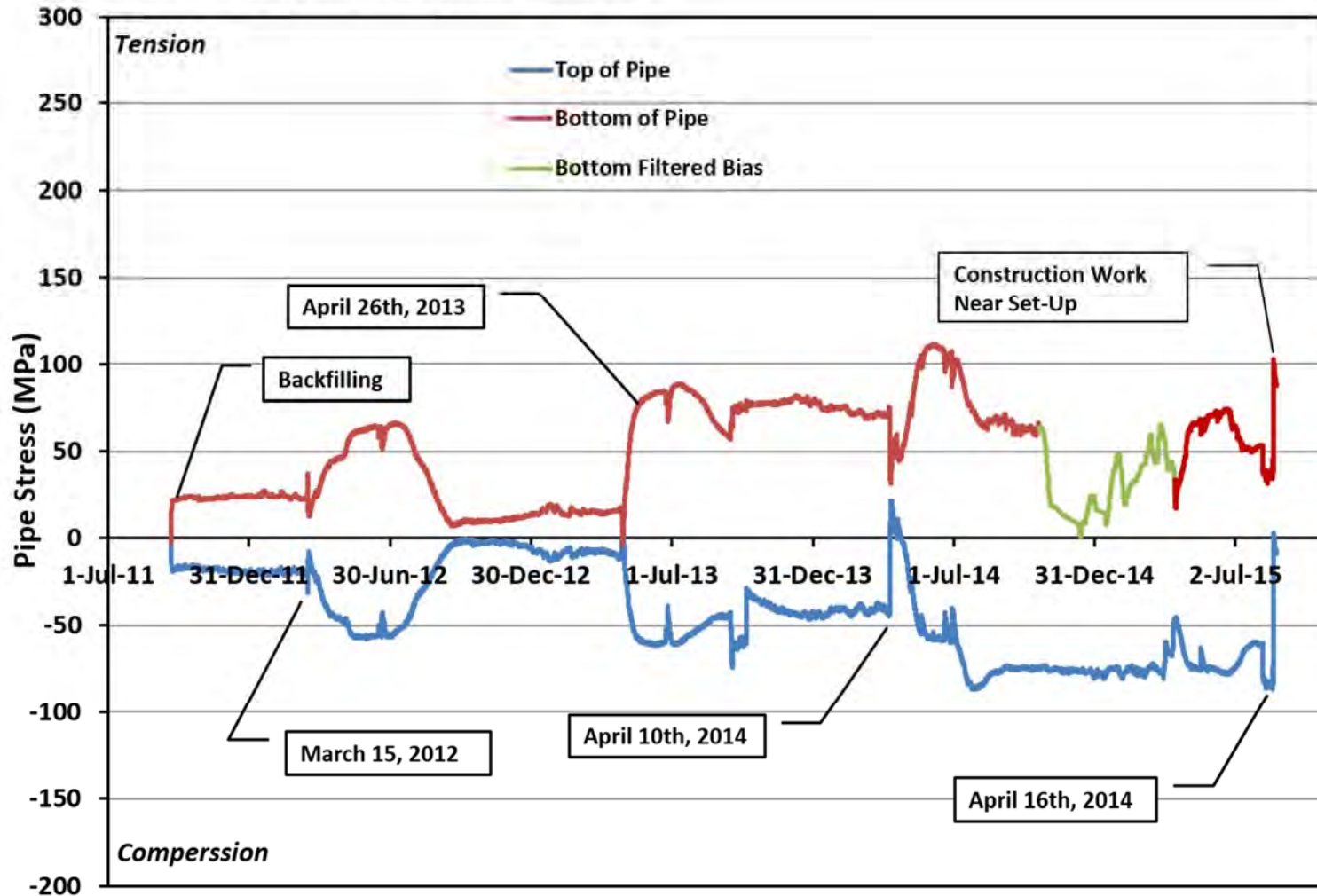


Manitoba Hydro Gas Pipeline Research  
St. Lazare Test Site  
Middle of Valley - Pipe Stresses



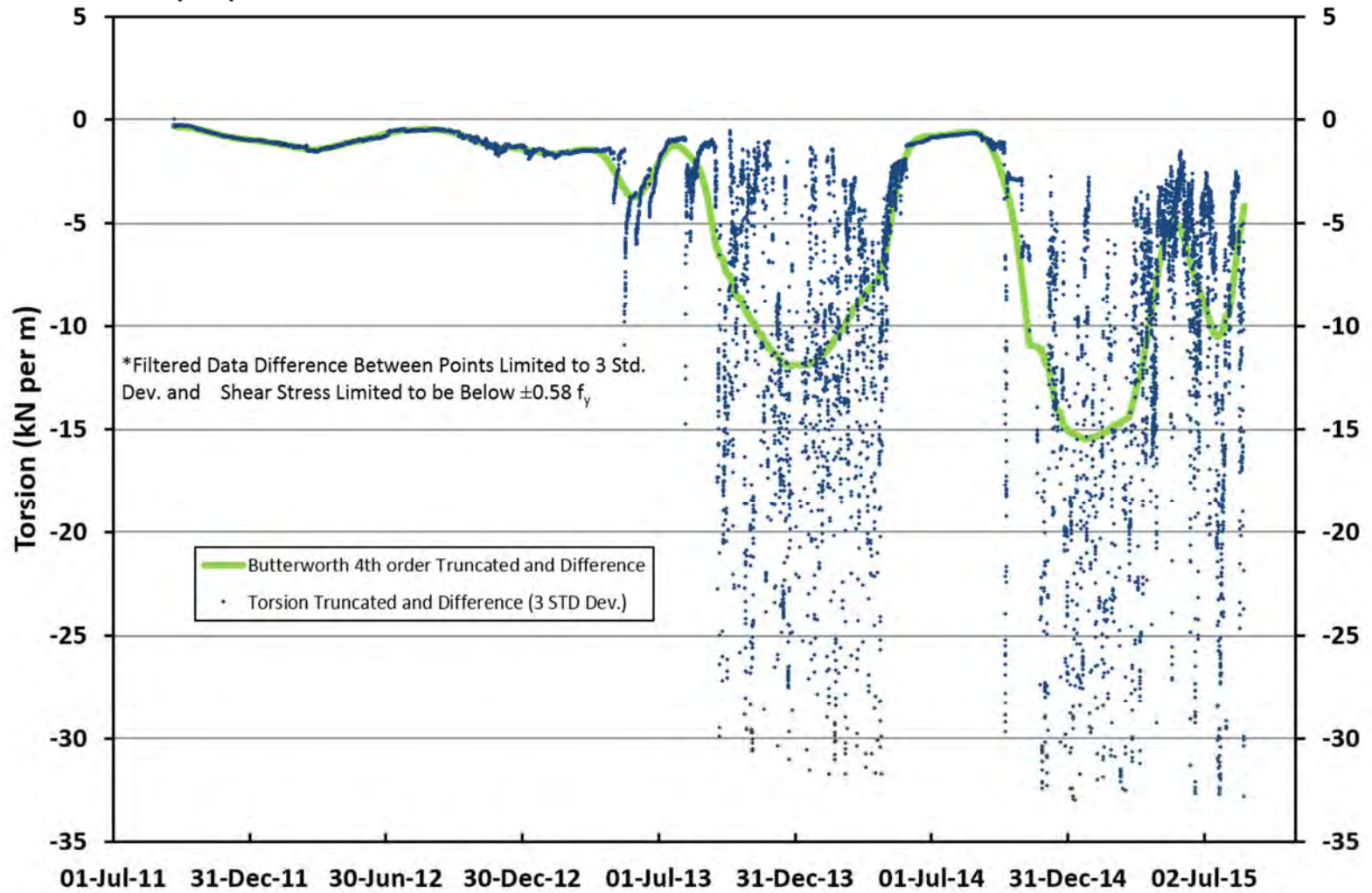


Manitoba Hydro Gas Pipeline Research  
 St. Lazare Test Site  
 Middle of Valley - Pipe Stresses without Thermal Effects

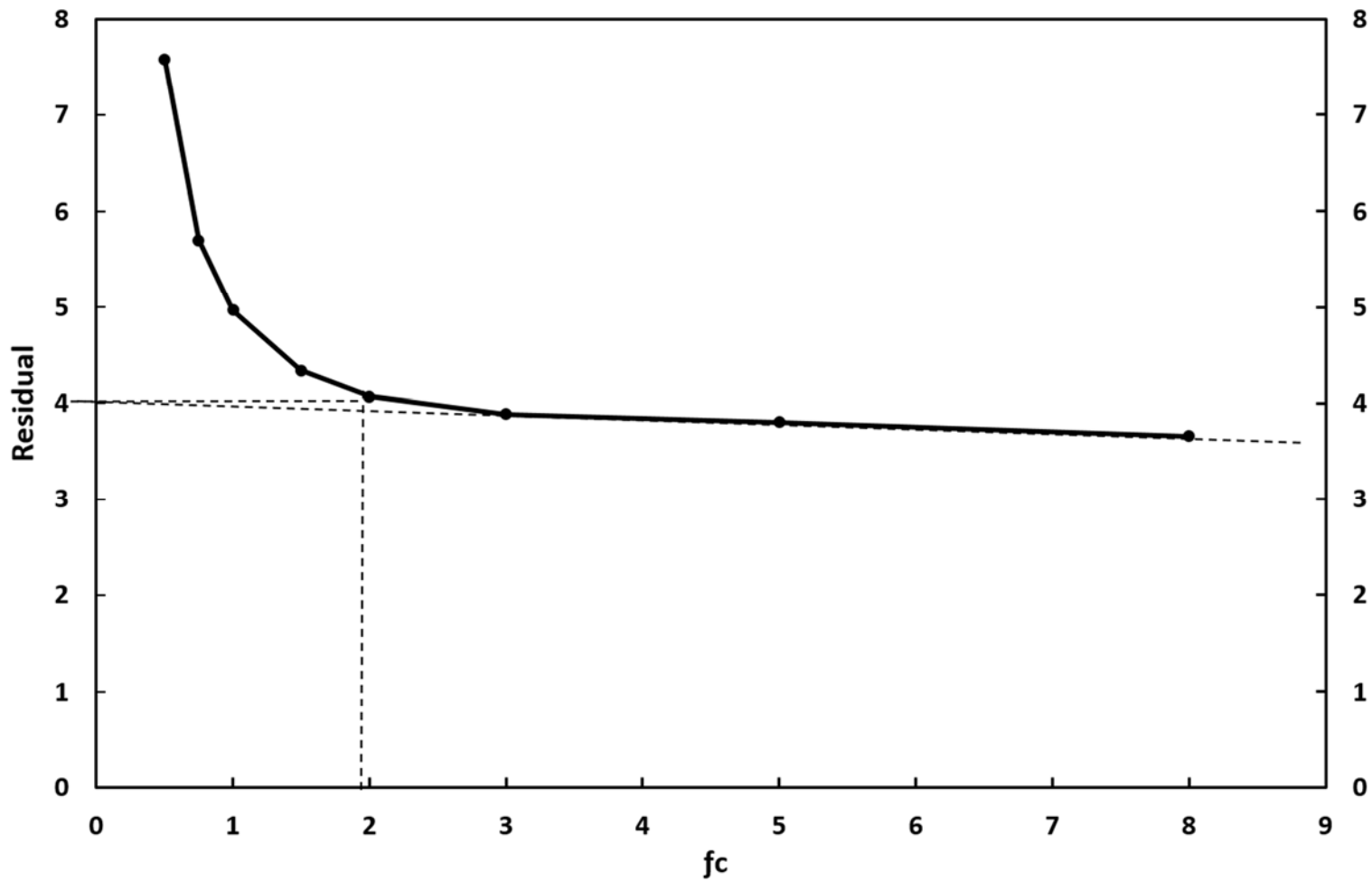




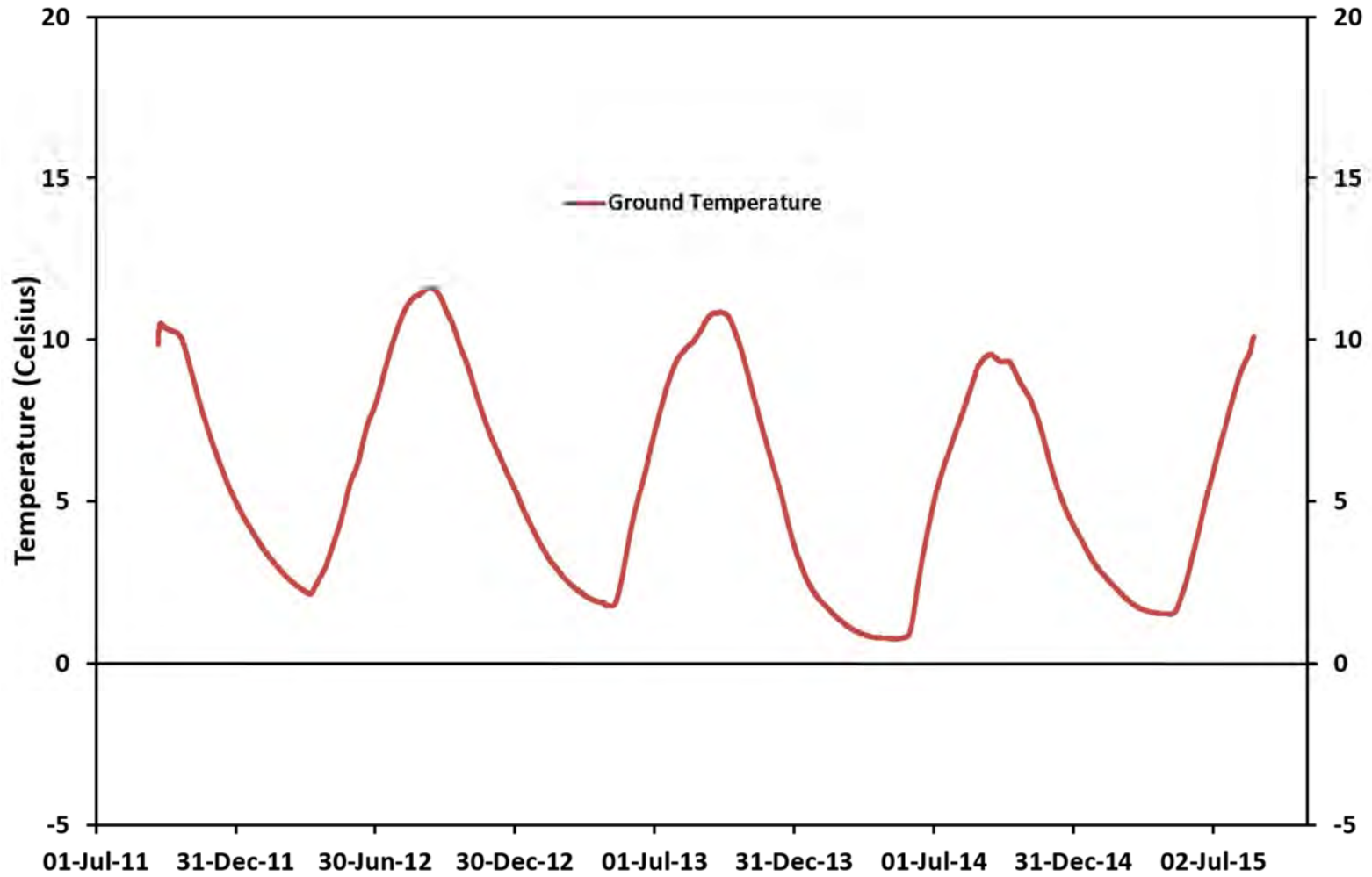
**Manitoba Hydro Gas Pipeline Research**  
**St. Lazare Test Site**  
**Middle of Valley - Pipe Torsion**



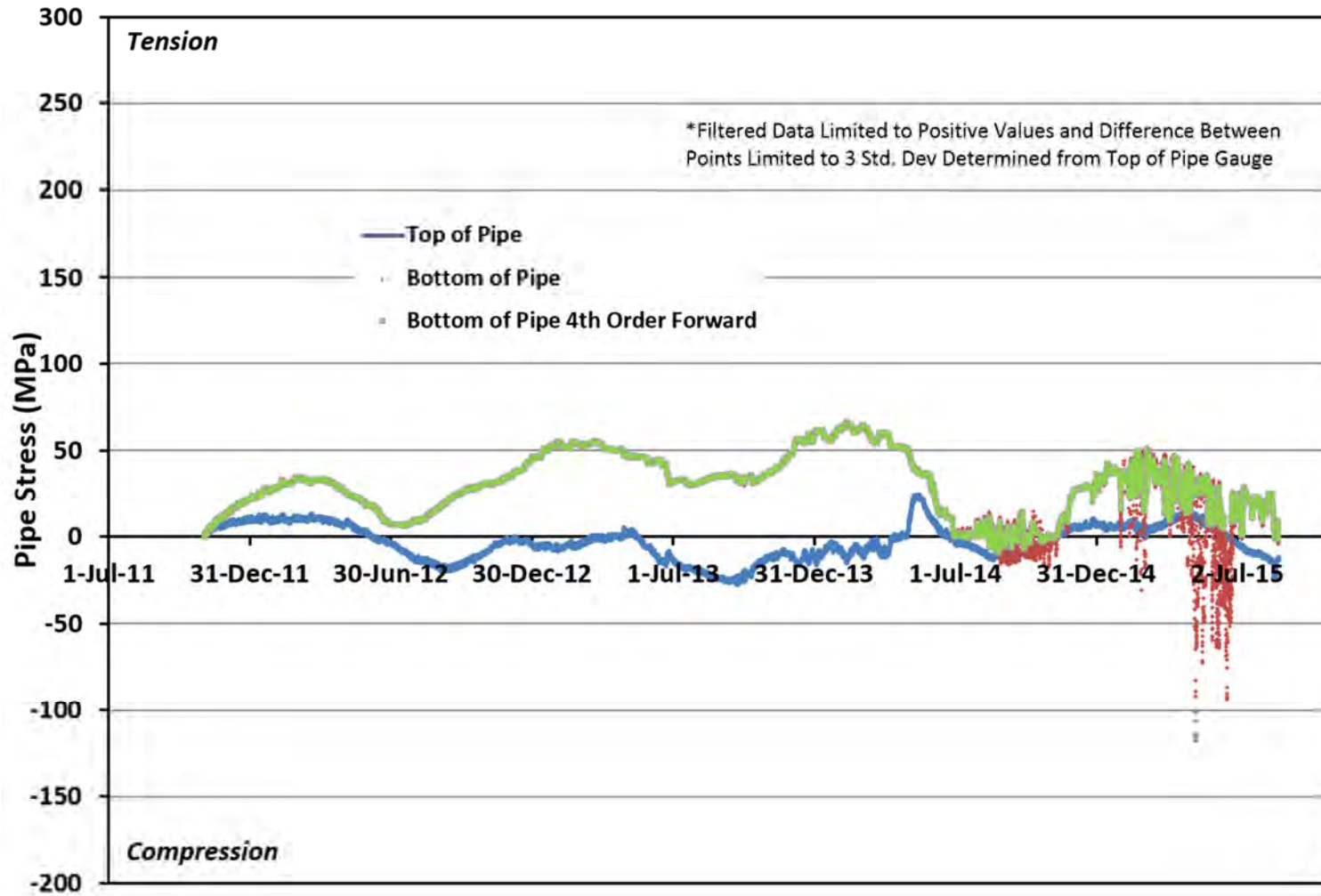
St-Lazare Middle of Valley  
Torsion Cut Off Frequency Truncated and Difference - Residuals



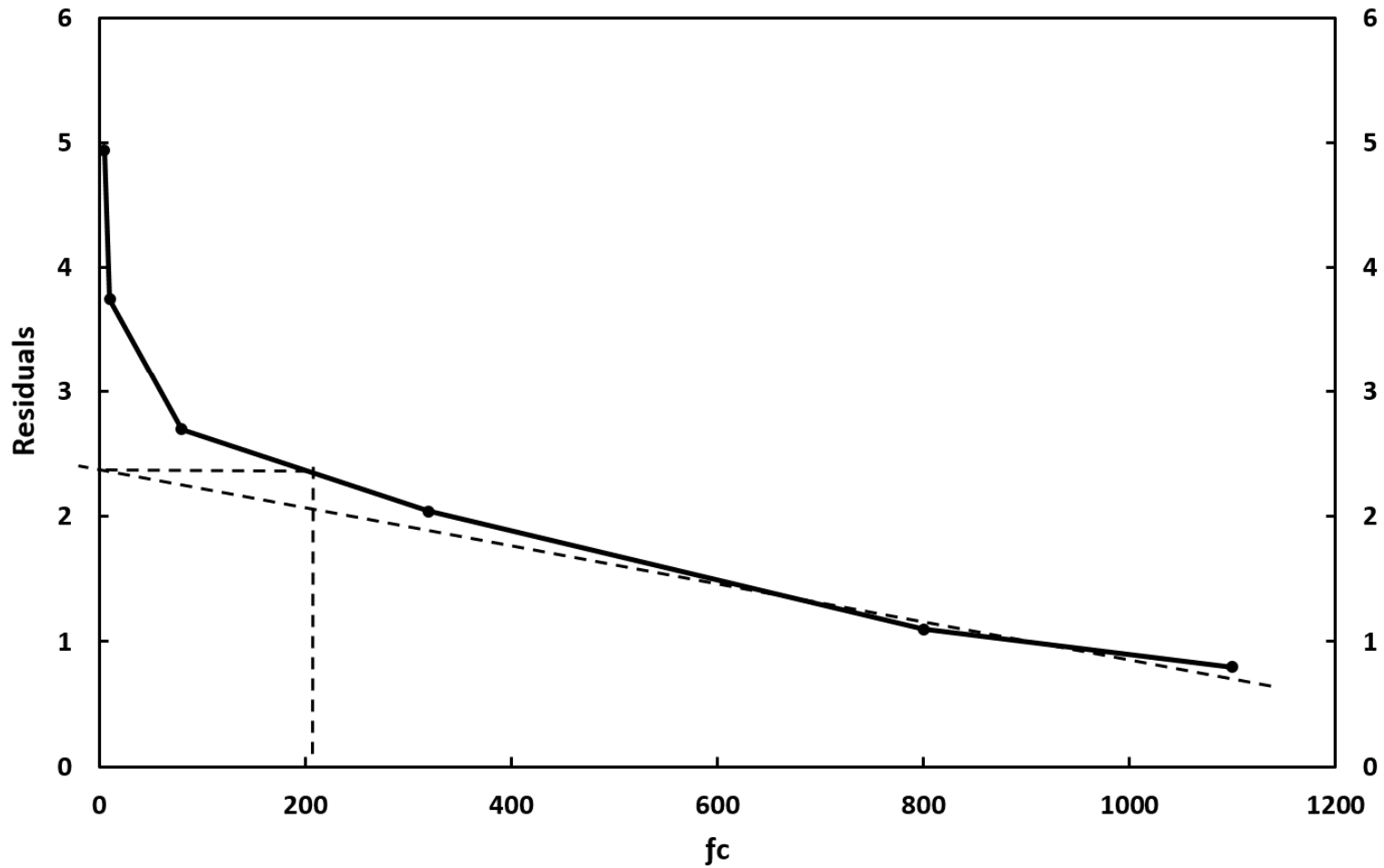
**Manitoba Hydro Gas Pipeline Research  
St. Lazare Test Site  
Bottom of Valley - Ground Temperature**



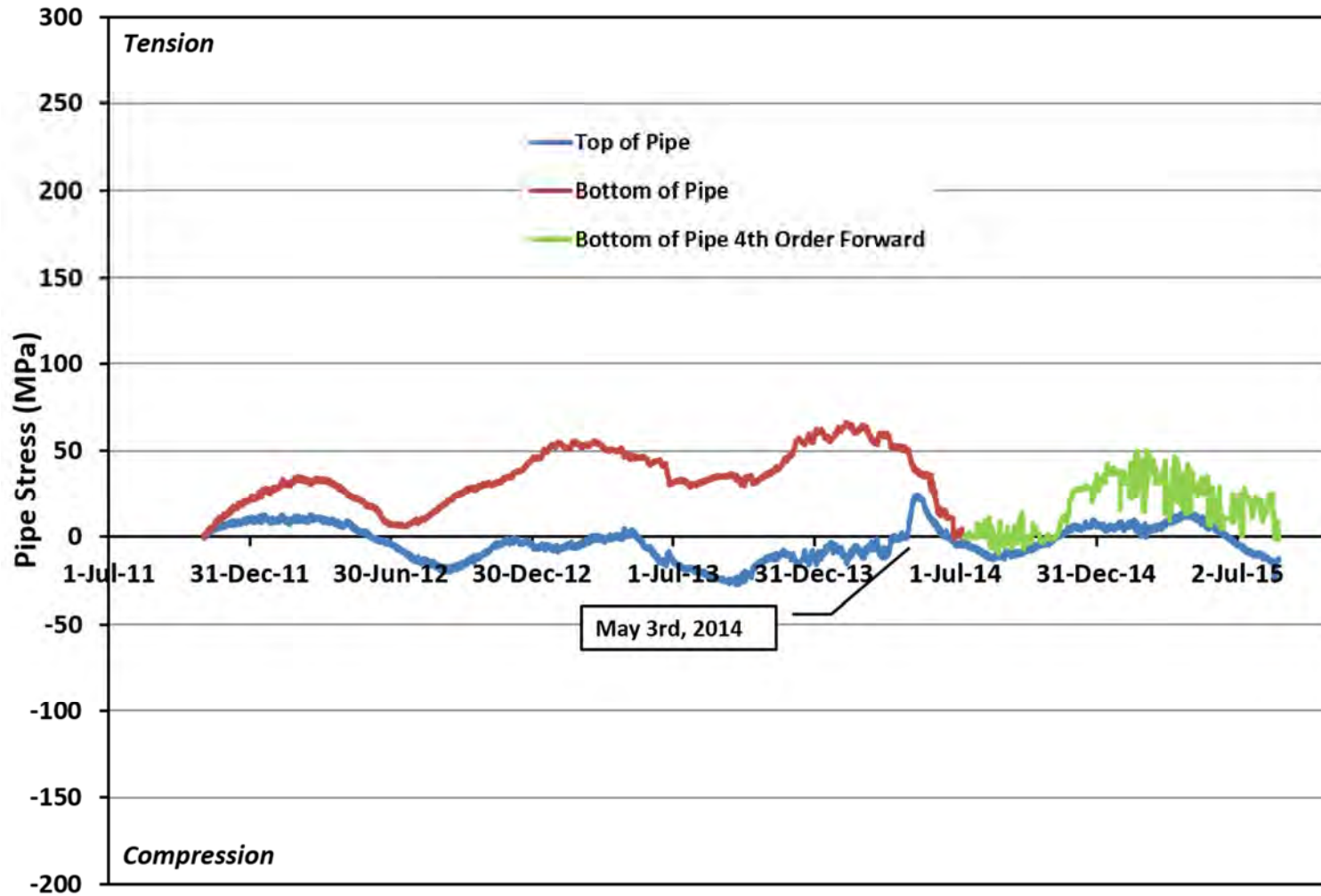
**Manitoba Hydro Gas Pipeline Research**  
**St. Lazare Test Site**  
**Bottom of Valley - Pipe Stresses**



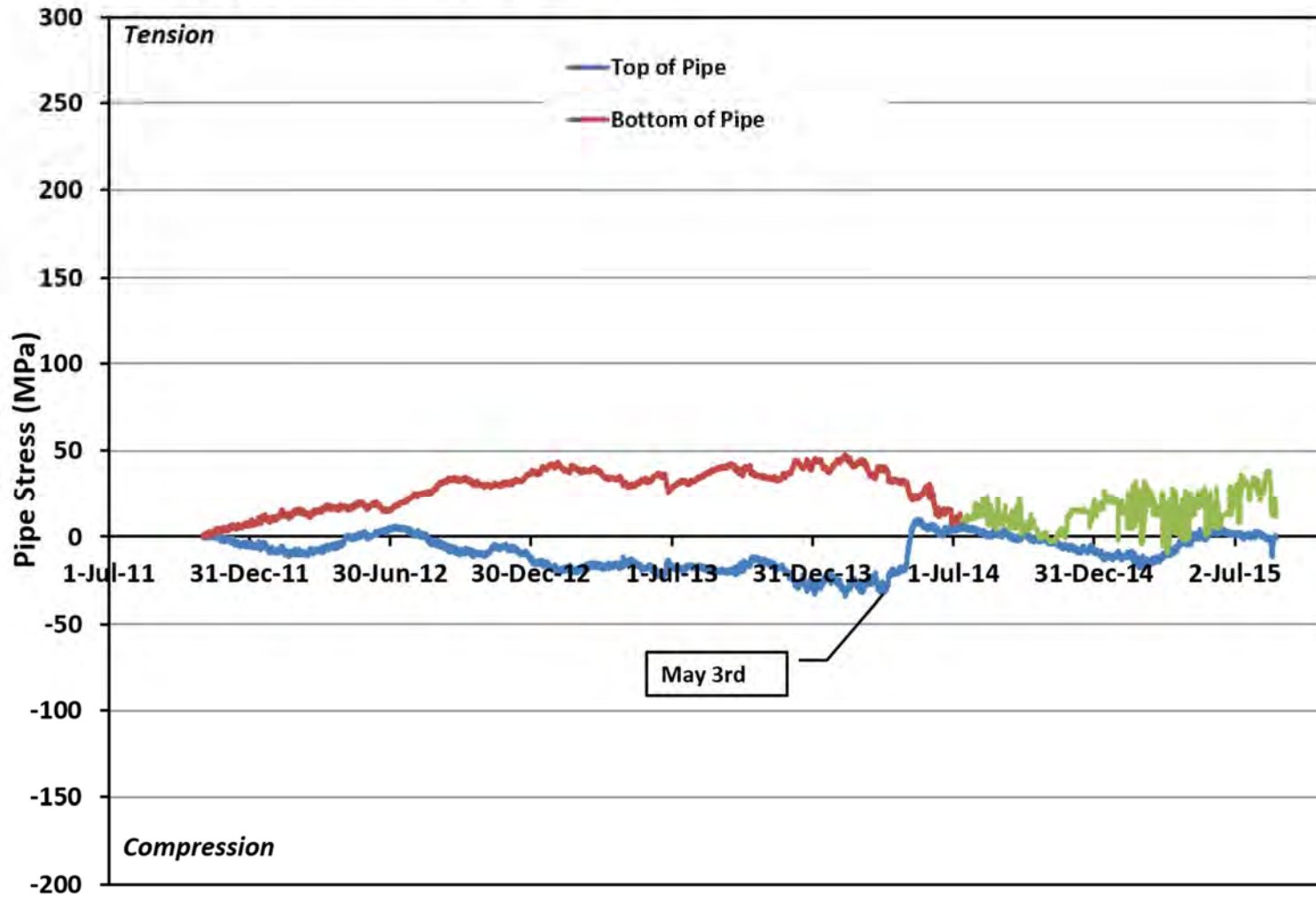
St-Lazare Bottom of Valley  
Bottom Strain Gauge Cut Off Frequency Truncated and Difference -  
Residuals



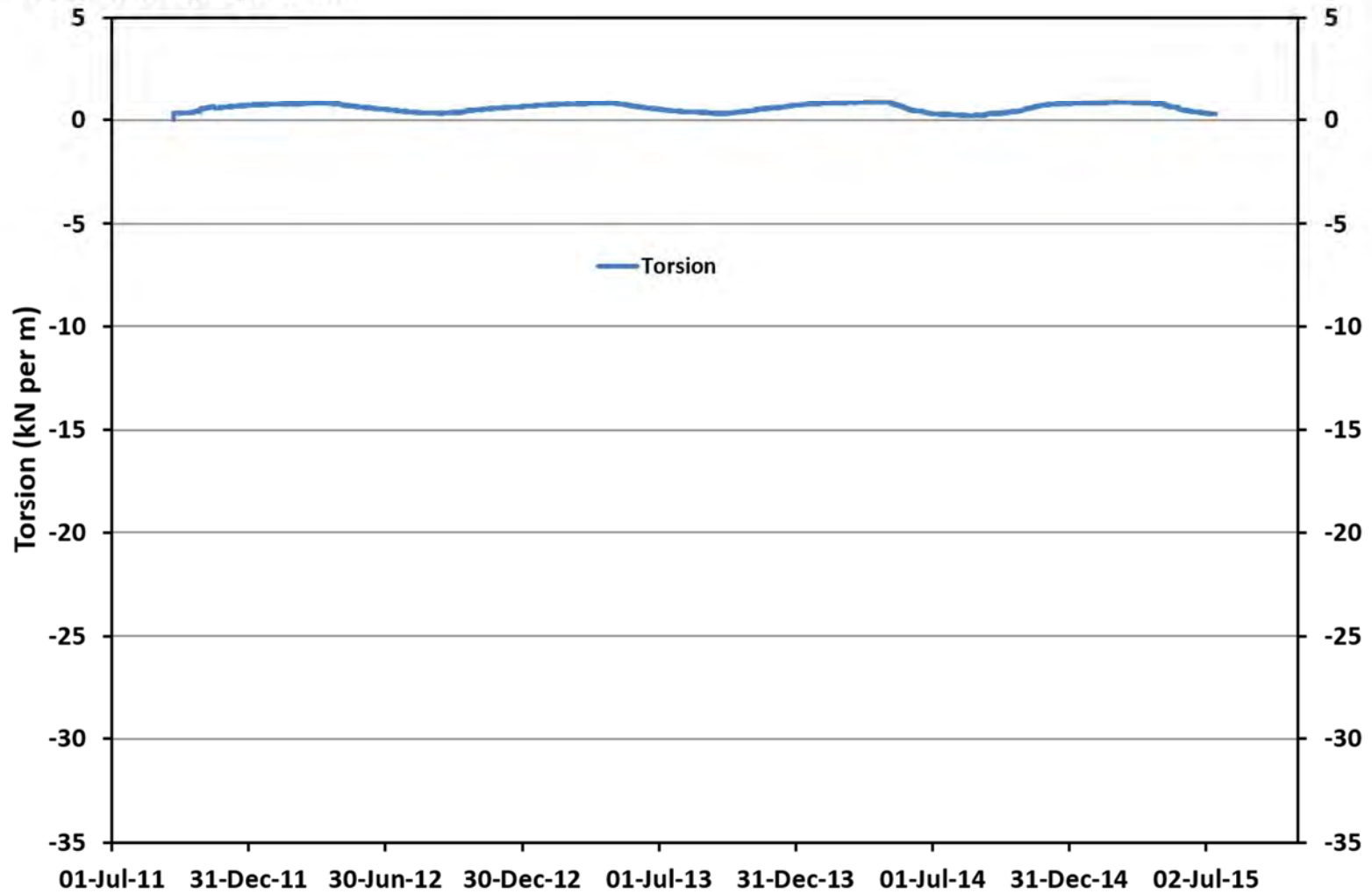
**Manitoba Hydro Gas Pipeline Research**  
**St. Lazare Test Site**  
**Bottom of Valley - Pipe Stresses**



**Manitoba Hydro Gas Pipeline Research**  
**St. Lazare Test Site**  
**Bottom of Valley - Pipe Stresses without Thermal Effects**

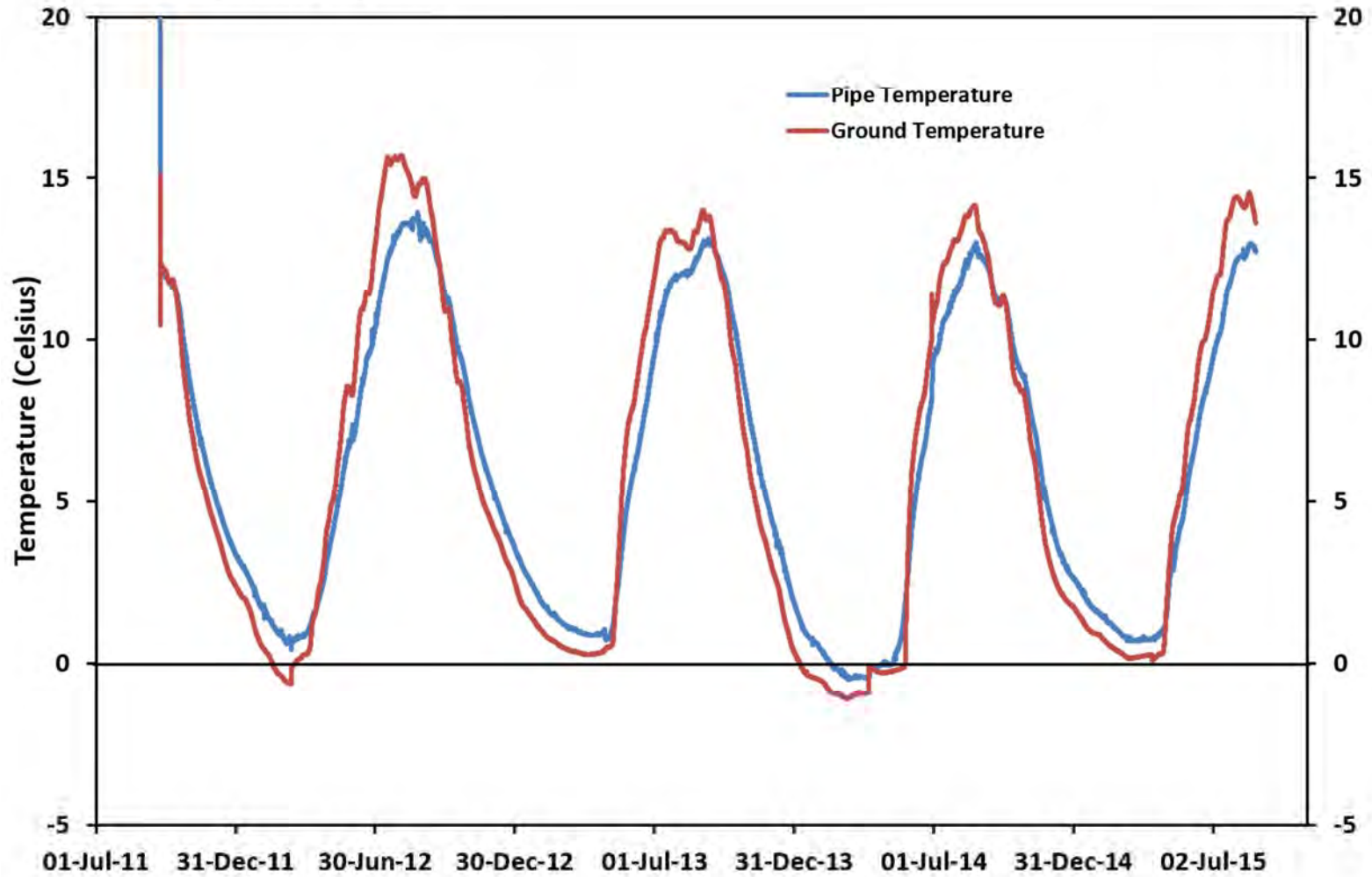


Manitoba Hydro Gas Pipeline Research  
St. Lazare Test Site  
Bottom of Valley - Pipe Torsion

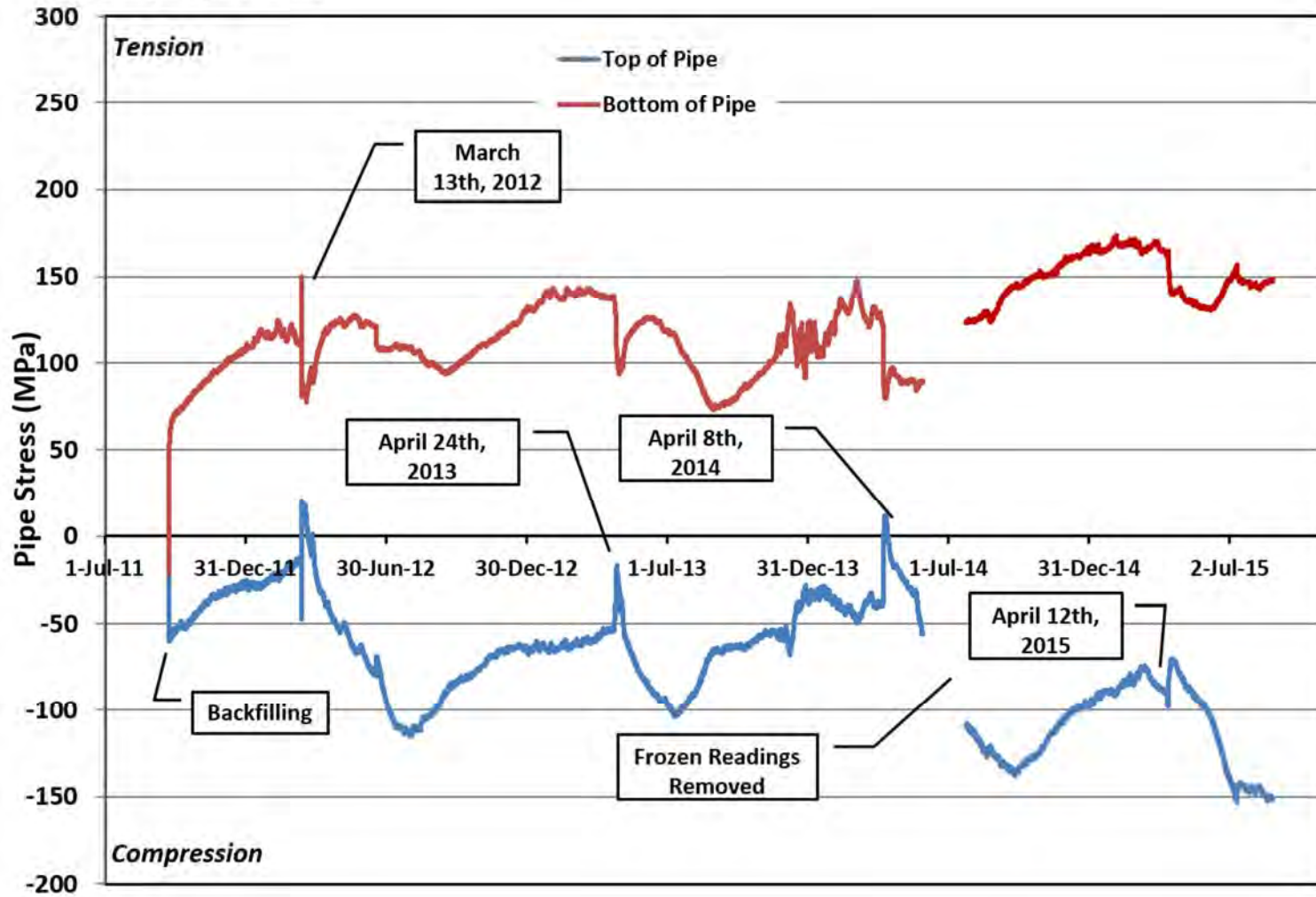




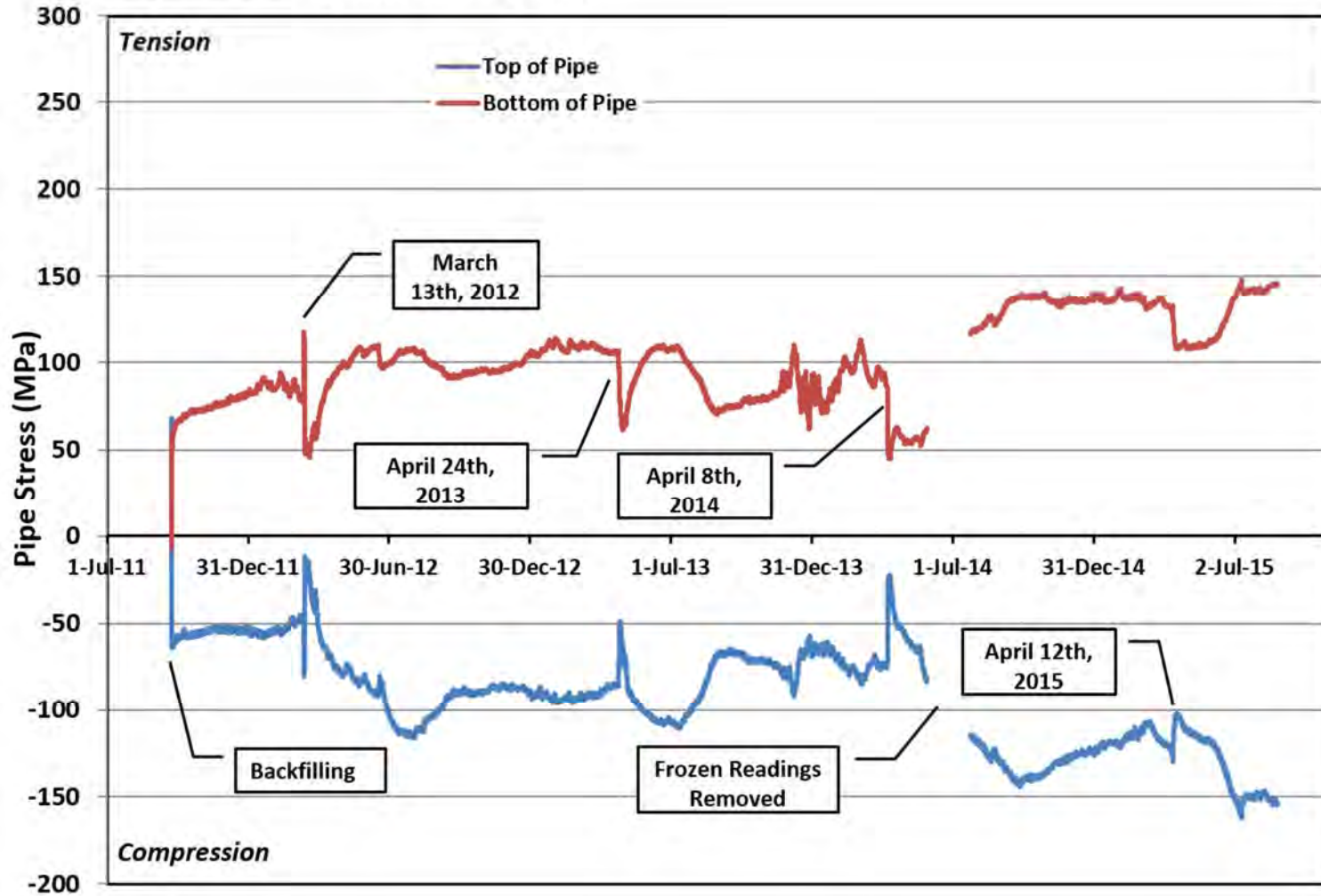
**Manitoba Hydro Gas Pipeline Research  
Harrowby Test Site  
Top of Valley - Pipe/Ground Temperature**



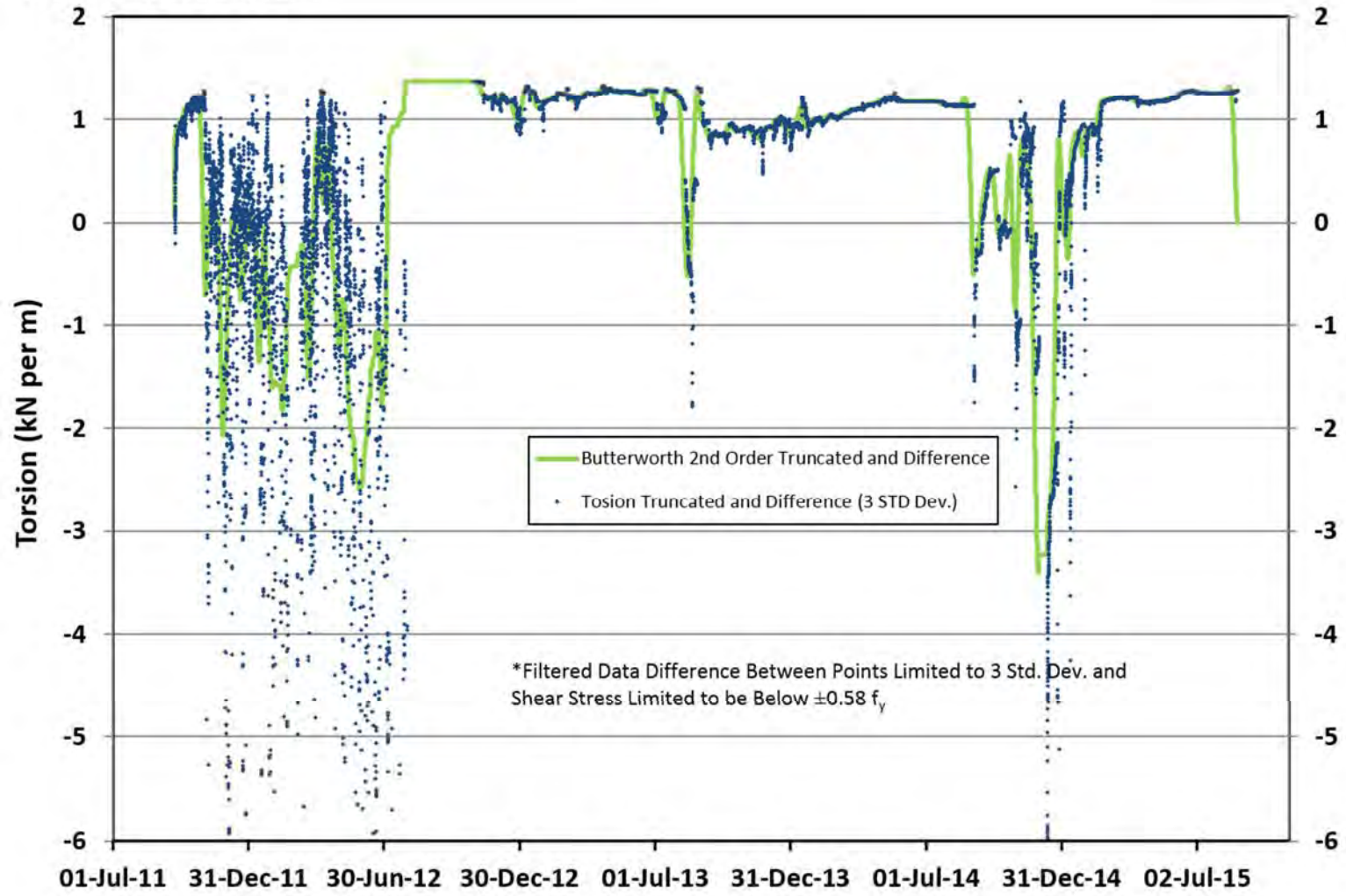
**Manitoba Hydro Gas Pipeline Research**  
**Harrowby Test Site**  
**Top of Valley - Pipe Stresses**



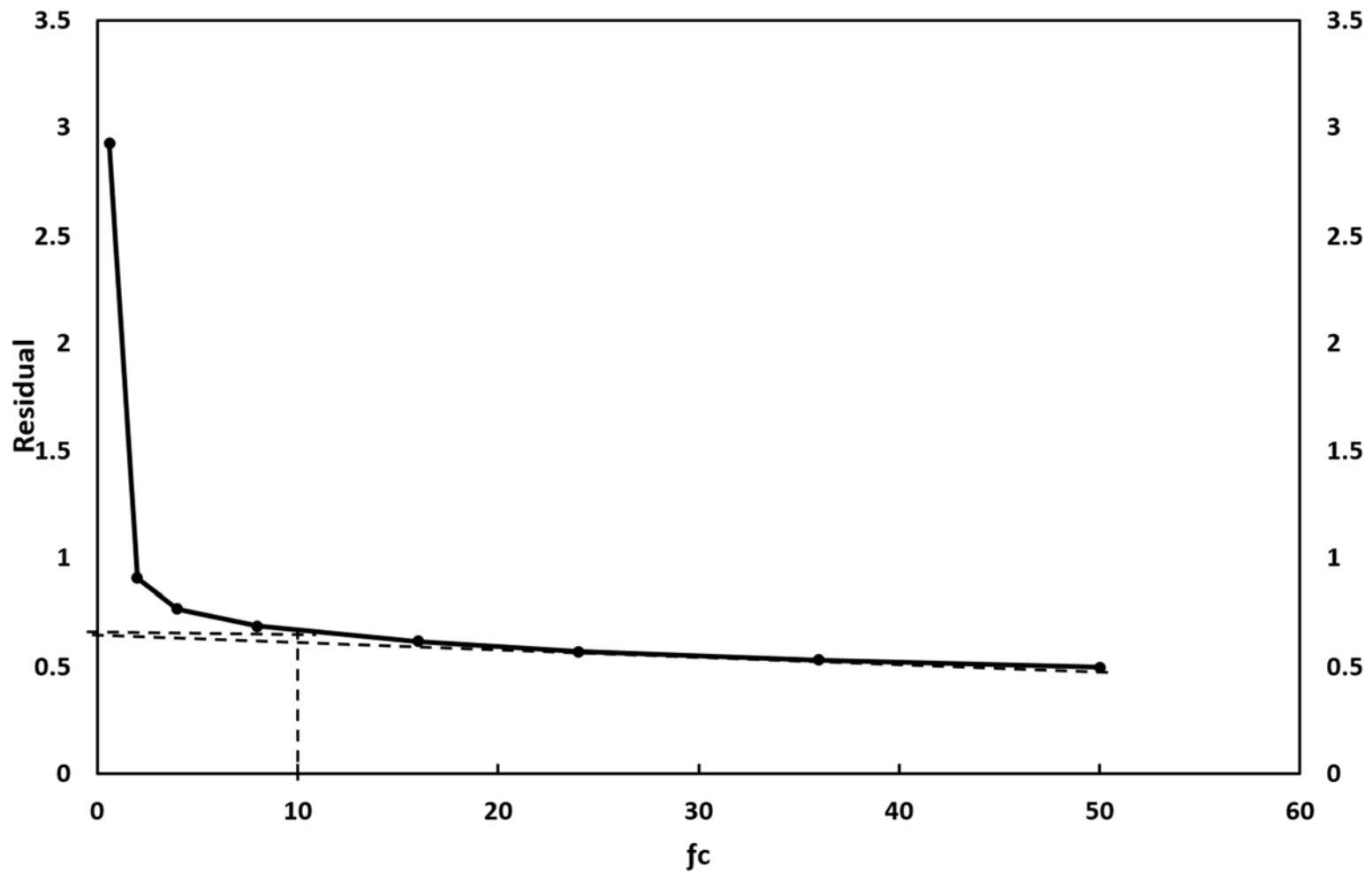
**Manitoba Hydro Gas Pipeline Research**  
**Harrowby Test Site**  
**Top of Valley - Pipe Stresses without Thermal Effects**



Manitoba Hydro Gas Pipeline Research  
Harrowby Test Site  
Top of Valley - Pipe Torsion

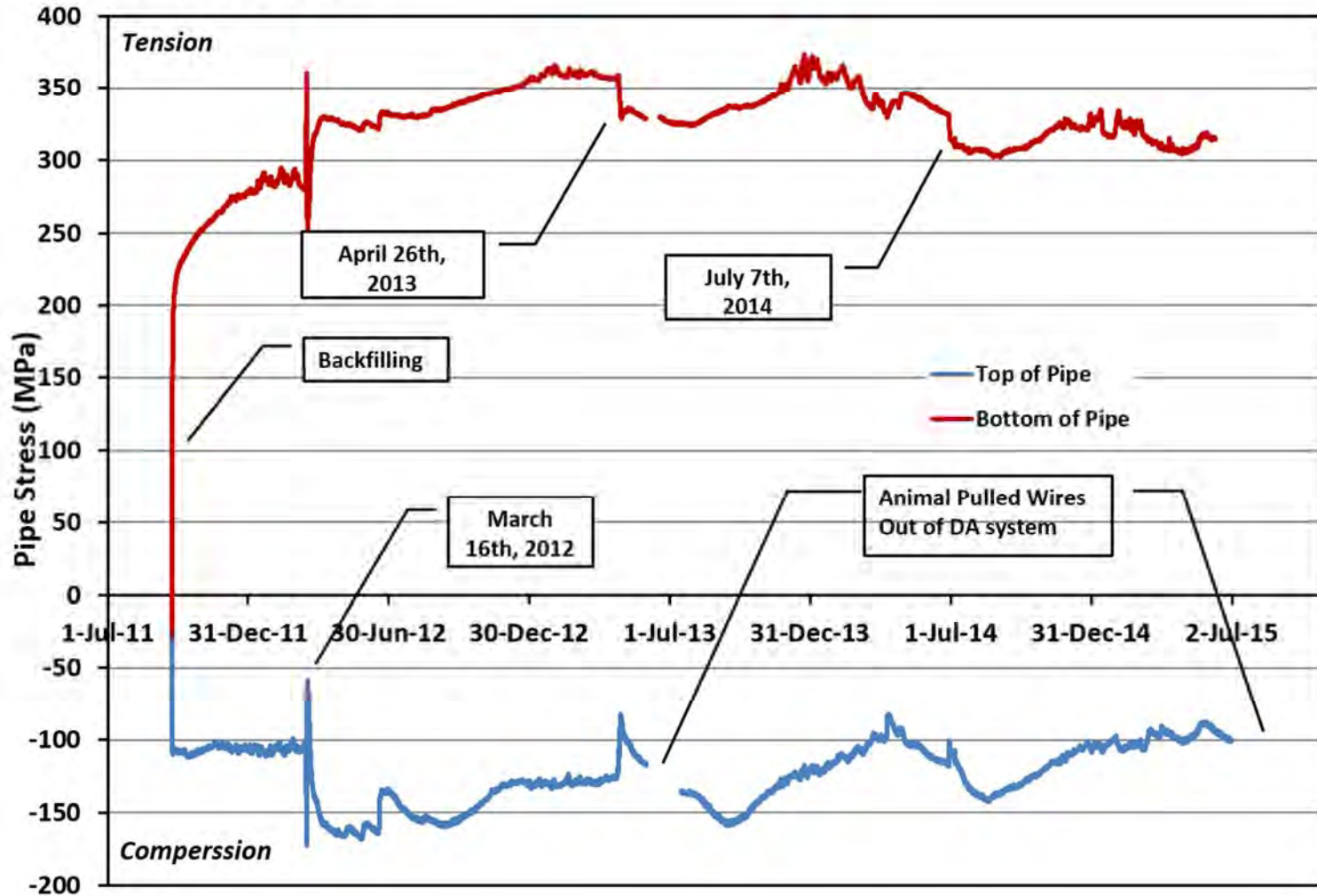


Harrowby Top of Valley  
Torsion Cut Off Frequency Truncated and Difference - Residuals

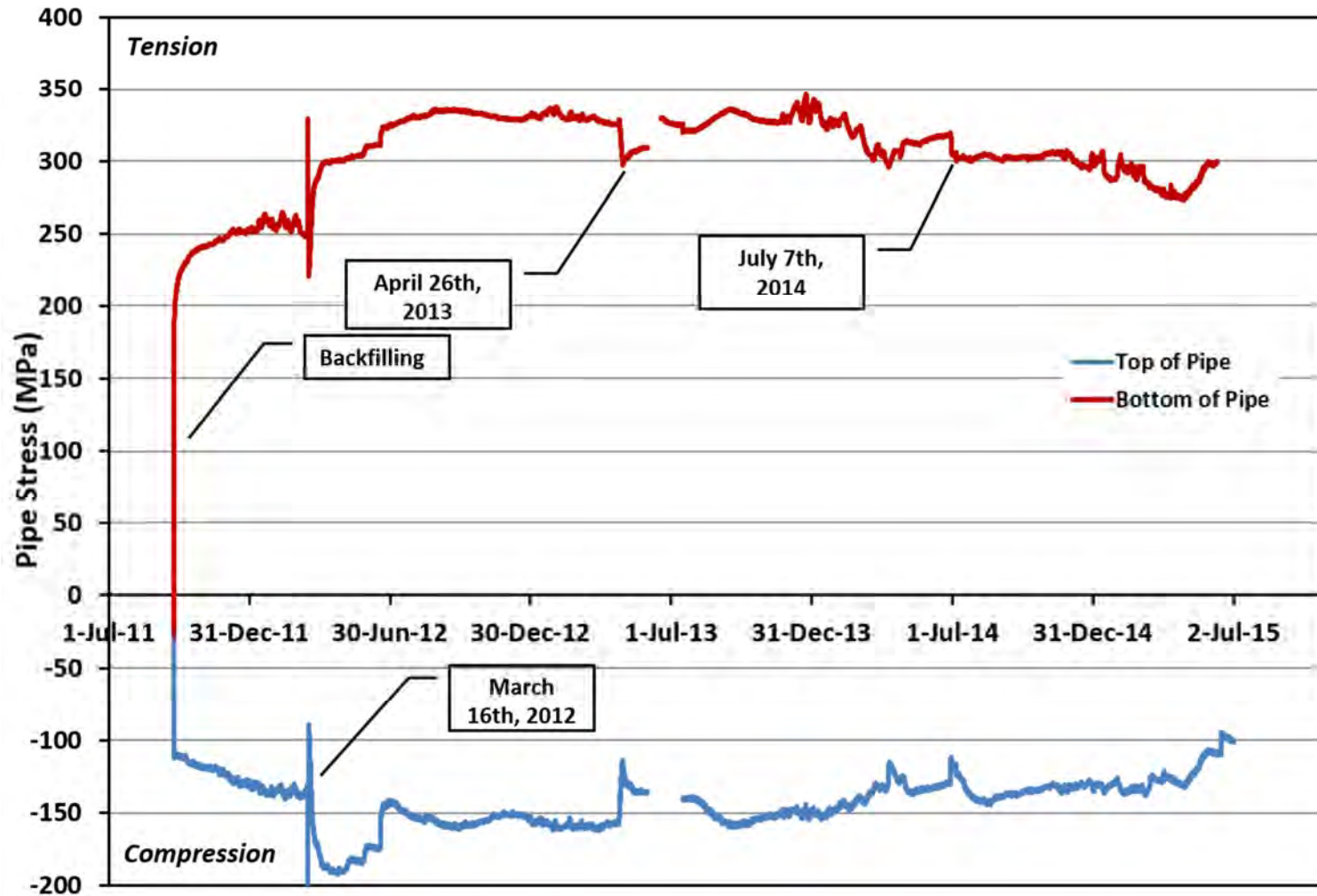




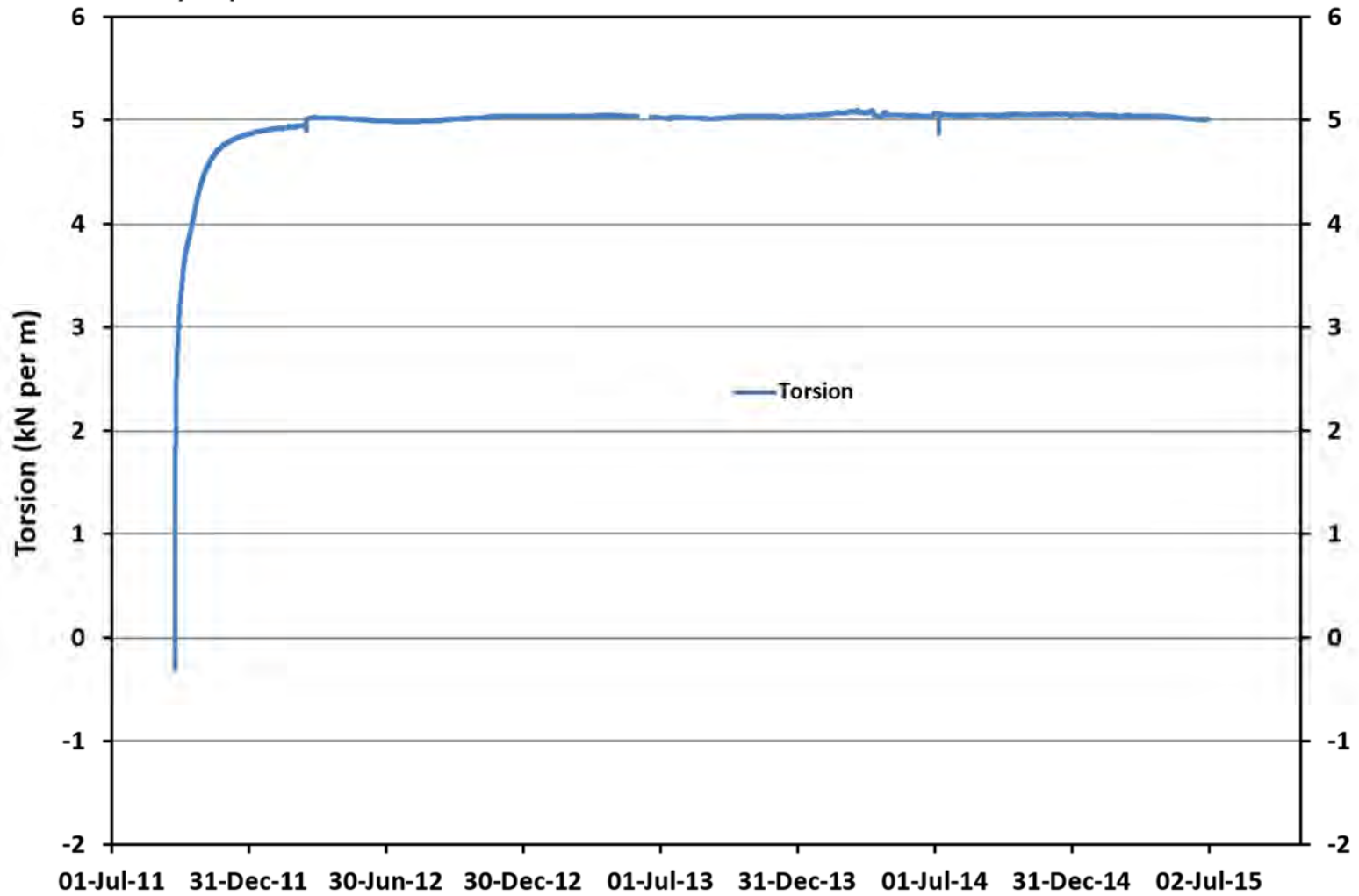
Manitoba Hydro Gas Pipeline Research  
Harrowby Test Site  
Middle of Valley - Pipe Stresses



Manitoba Hydro Gas Pipeline Research  
Harrowby Test Site  
Middle of Valley - Pipe Stresses

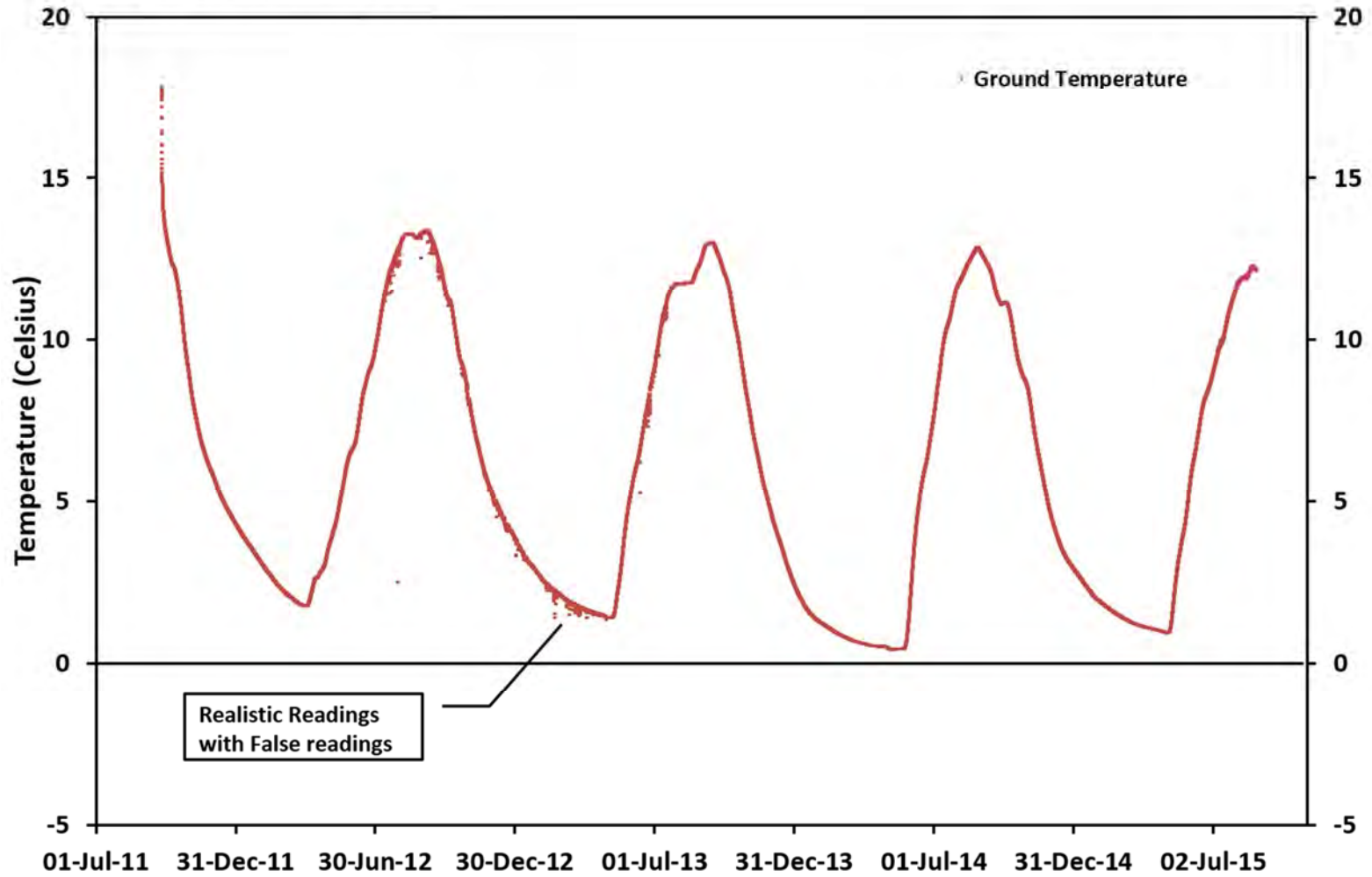


**Manitoba Hydro Gas Pipeline Research**  
**Harrowby Test Site**  
**Middle of Valley - Pipe Torsion**

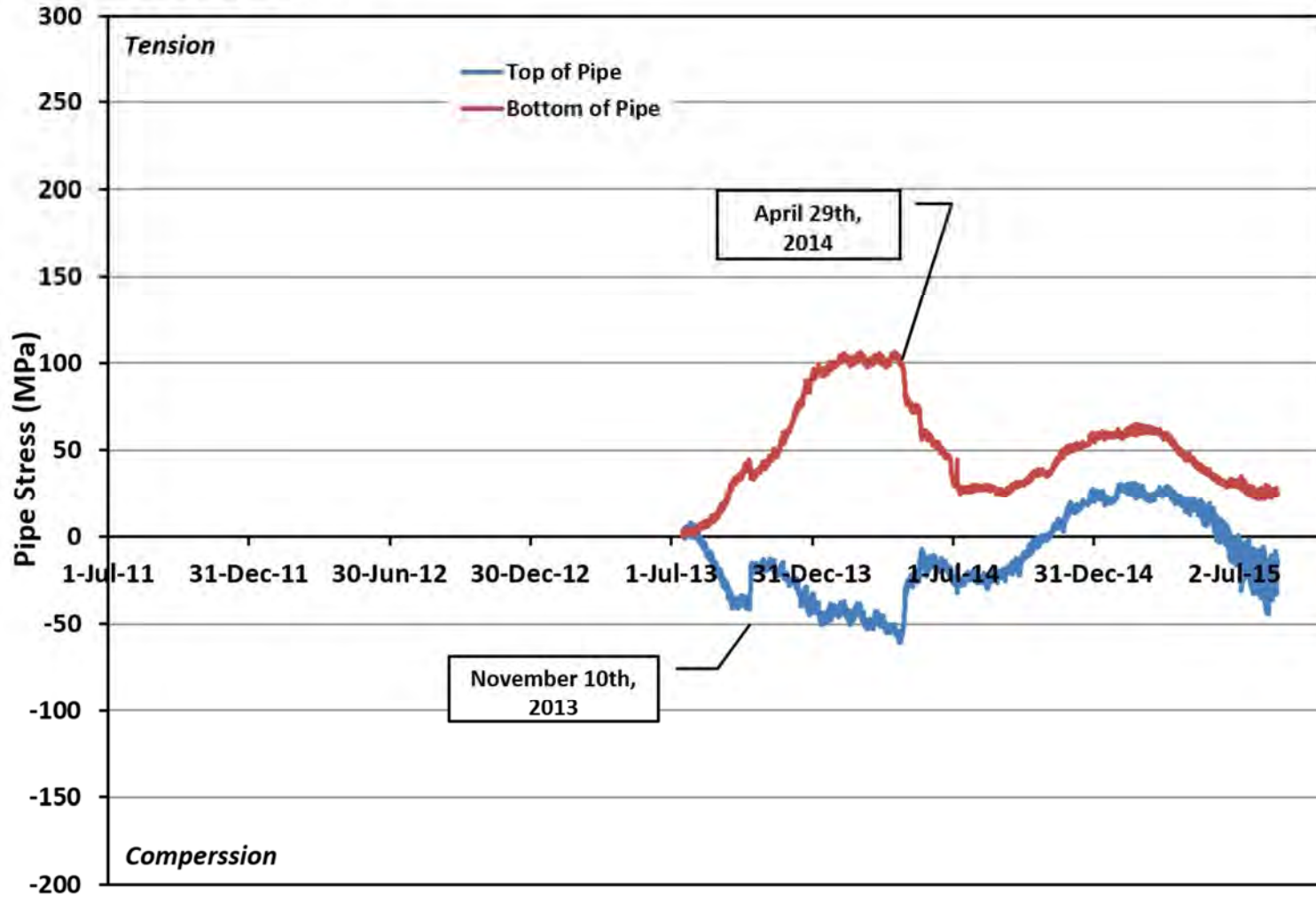




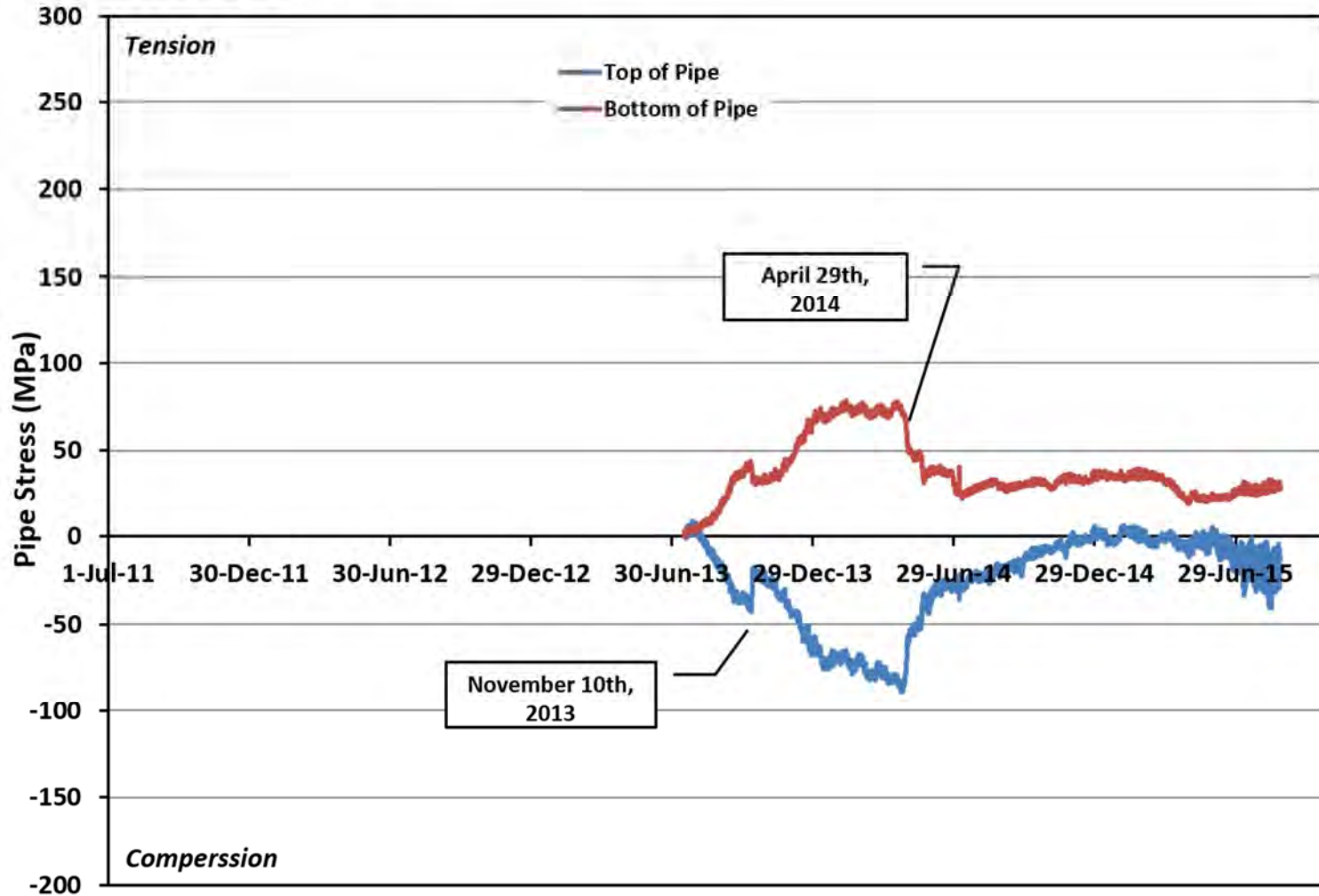
**Manitoba Hydro Gas Pipeline Research  
Harrowby Test Site  
Bottom of Valley - Ground Temperature**



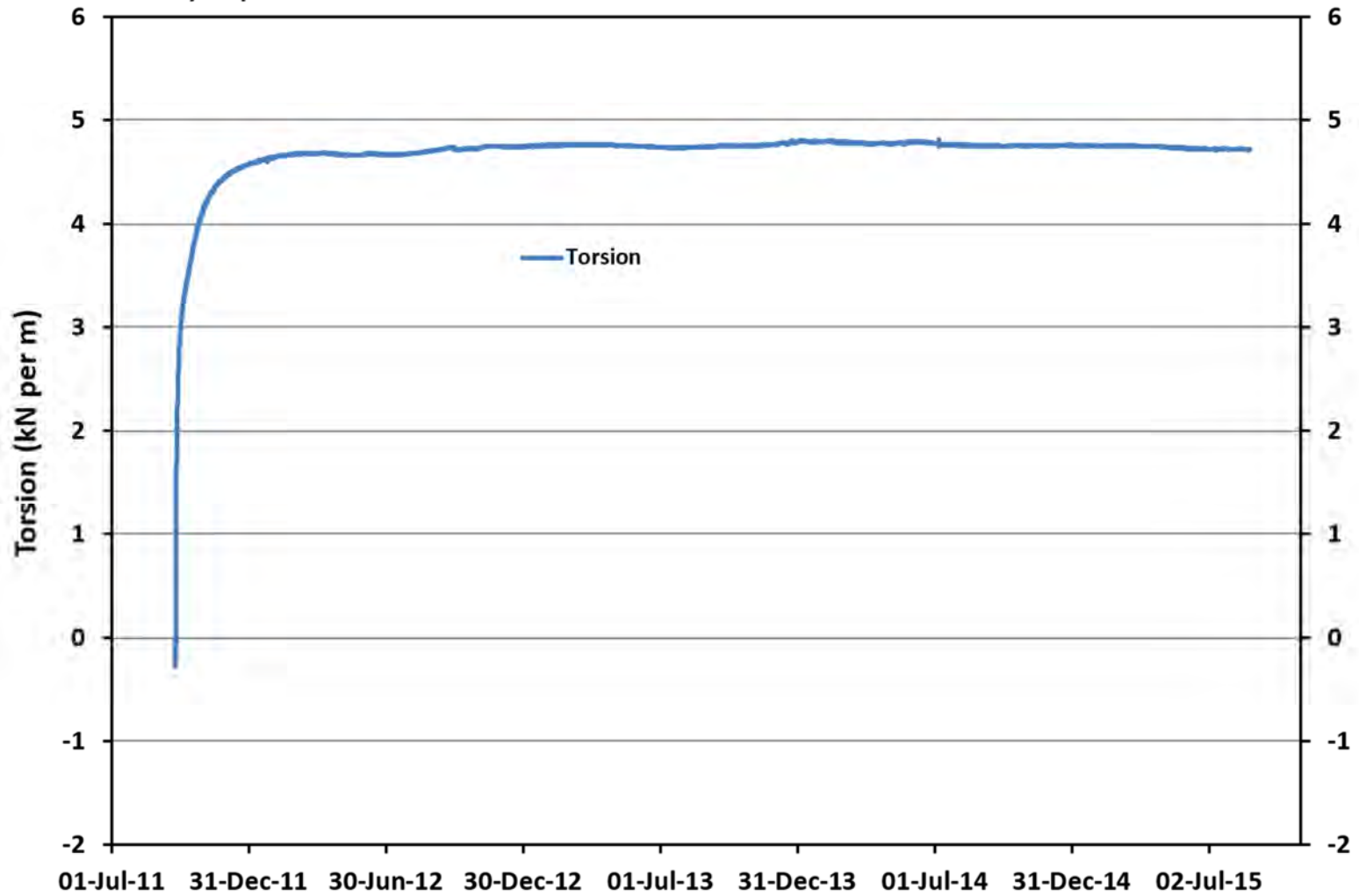
**Manitoba Hydro Gas Pipeline Research**  
**Harrowby Test Site**  
**Bottom of Valley - Pipe Stresses**



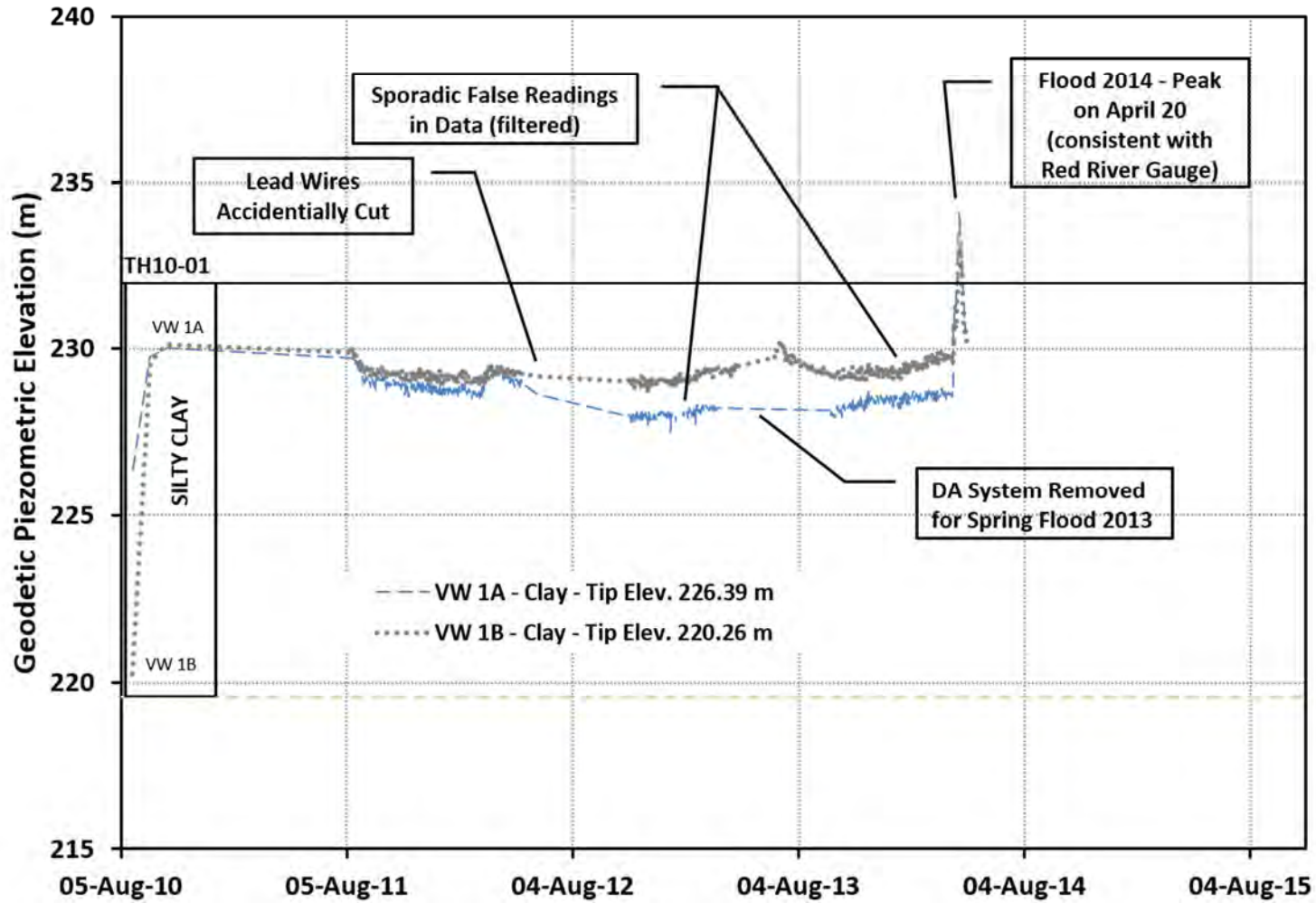
**Manitoba Hydro Gas Pipeline Research**  
**Harrowby Test Site**  
**Bottom of Valley - Pipe Stresses**



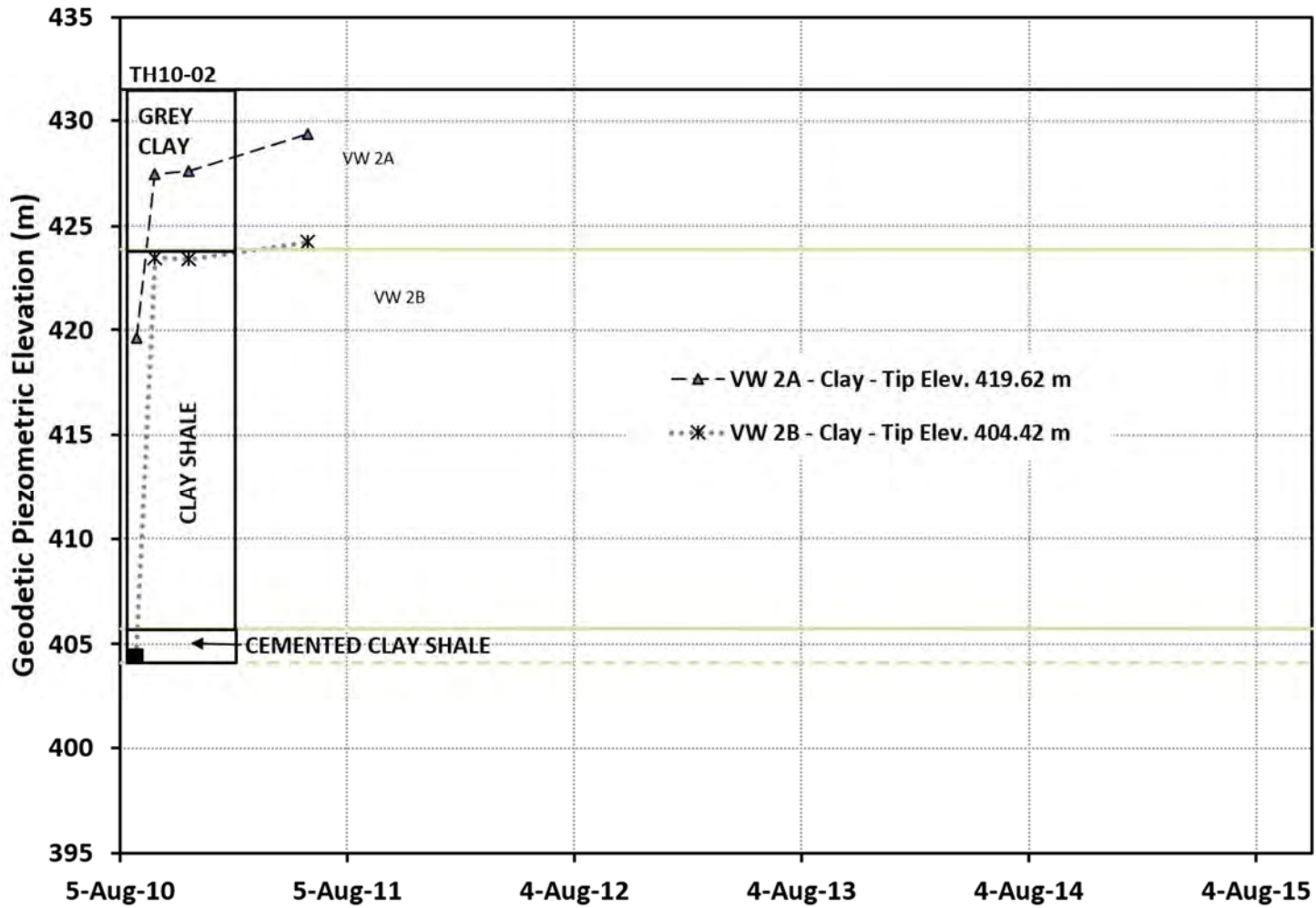
Manitoba Hydro Gas Pipeline Research  
Harrowby Test Site  
Bottom of Valley - Pipe Torsion



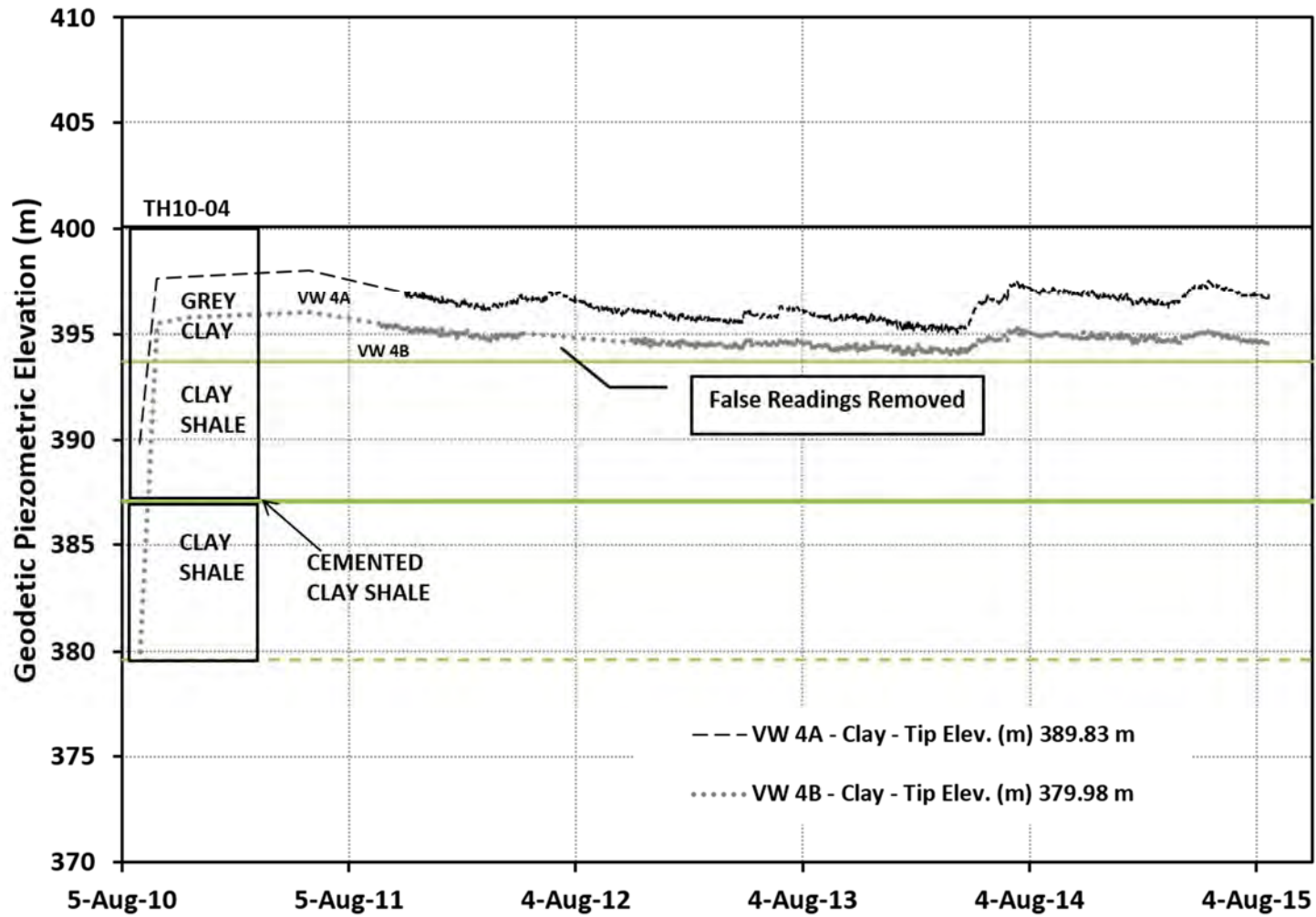
Manitoba Hydro Gas Pipeline Research  
Plum River Test Site  
Installation in TH10-01



Manitoba Hydro Gas Pipeline Research  
St. Lazare Test Site  
Top of Valley (TH10-02)

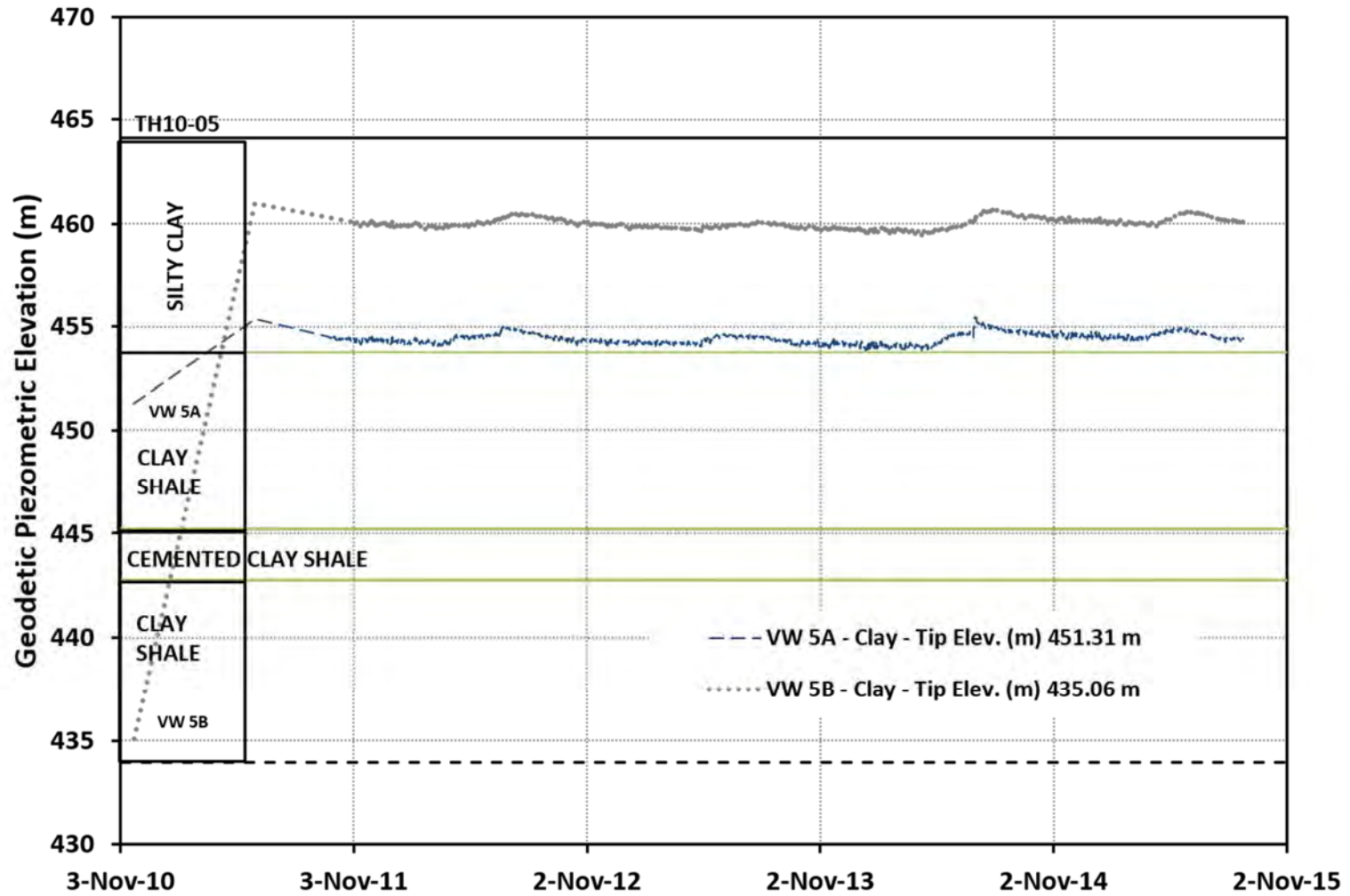


Manitoba Hydro Gas Pipeline Research  
St. Lazare Test Site  
Bottom of Valley (TH10-04)



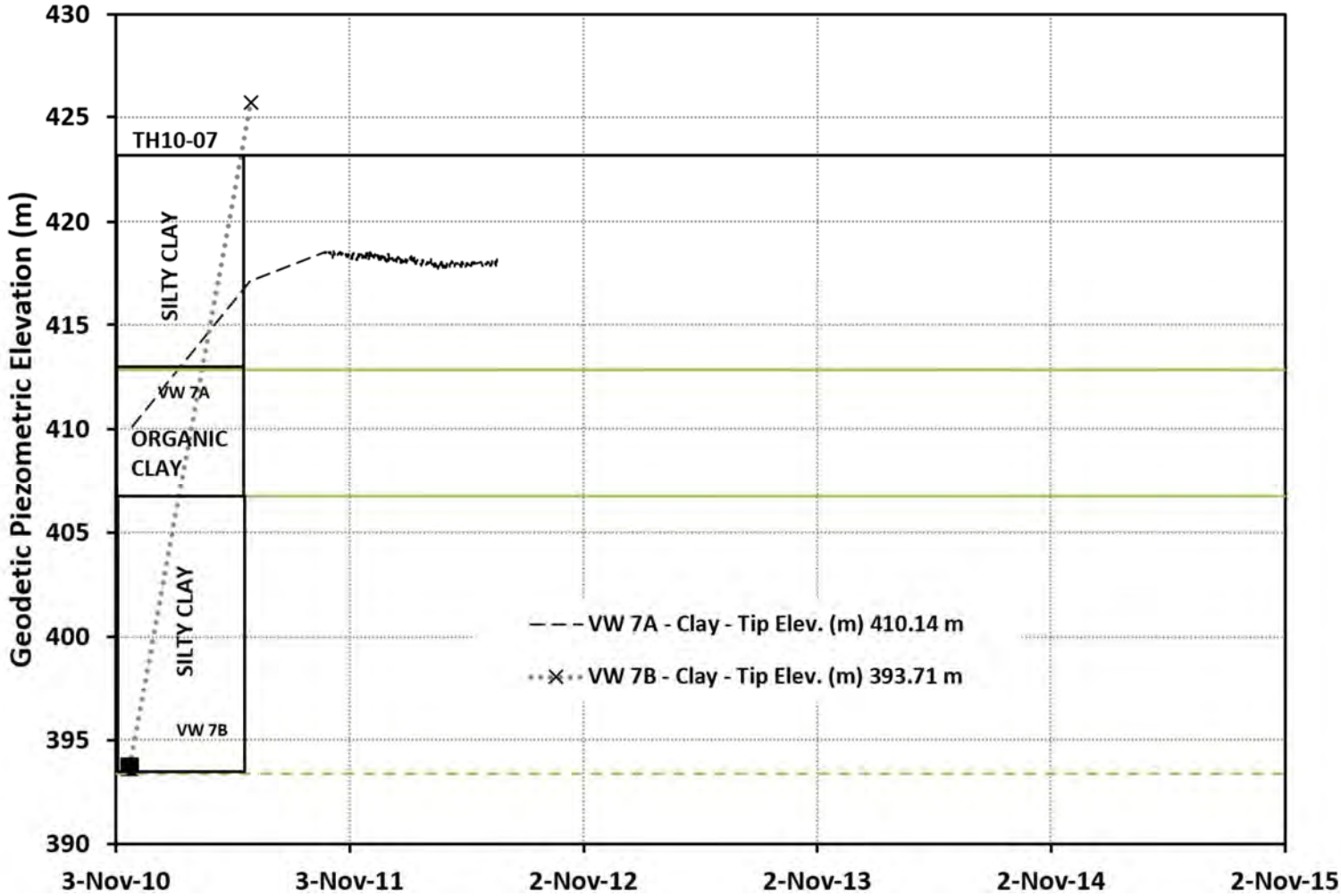


Manitoba Hydro Gas Pipeline Research  
Harrowby Test Site  
Top of Valley (TH10-05)





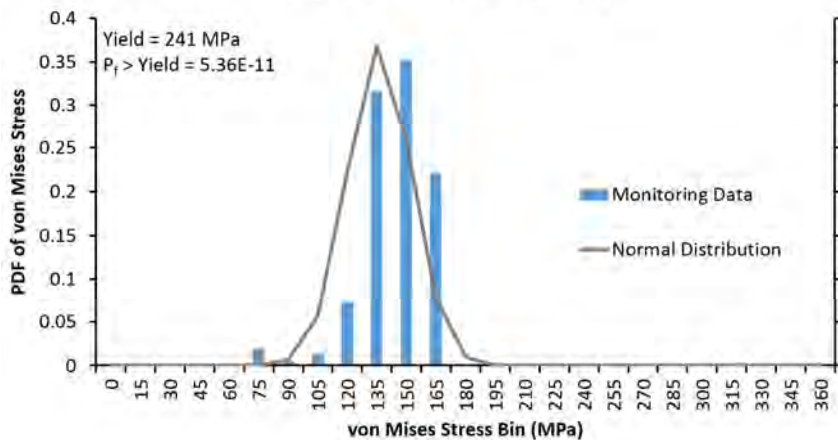
Manitoba Hydro Gas Pipeline Research  
Harrowby Test Site  
Bottom of Valley (TH10-07)



## Appendix D – Statistical Results

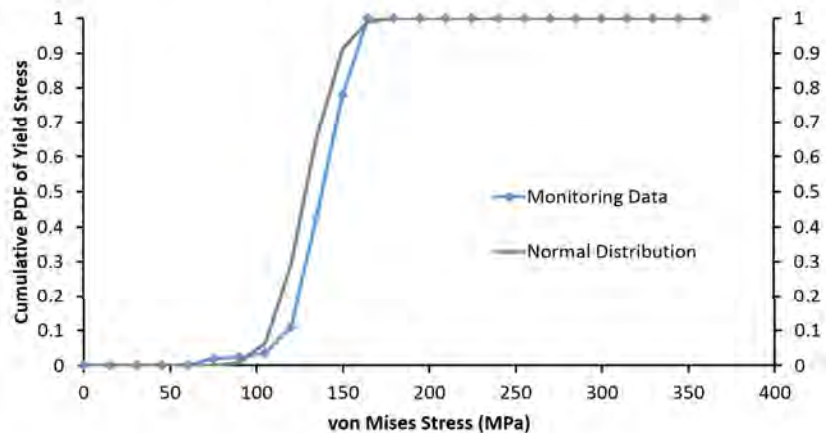
Plum River - Beyond the Crest

PDF von Mises (Yield 241 Mpa)



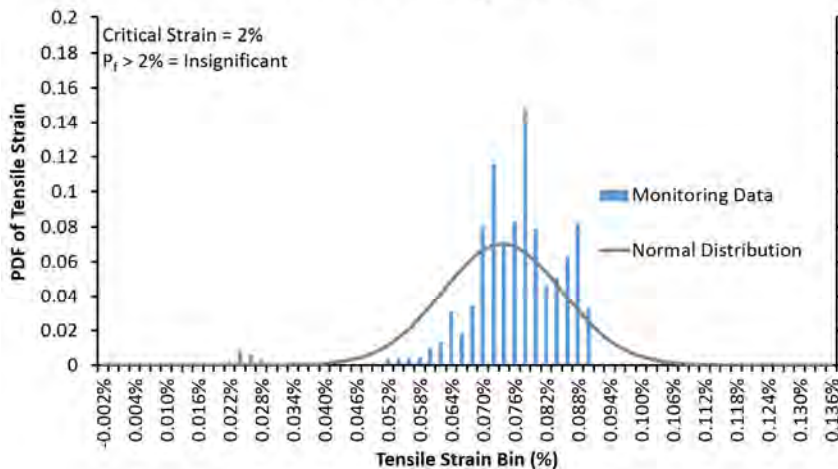
Plum River - Beyond the Crest

Cumulative PDF - Yield Stress



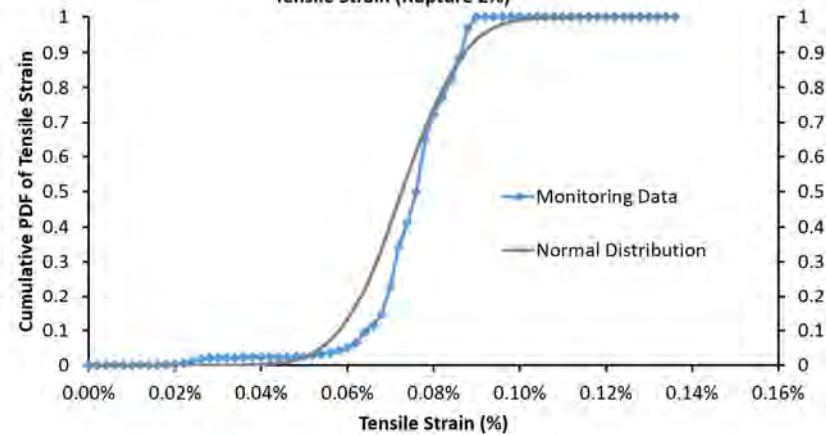
Plum River - Beyond the Crest

PDF - Tensile Strain (Rupture 2%)



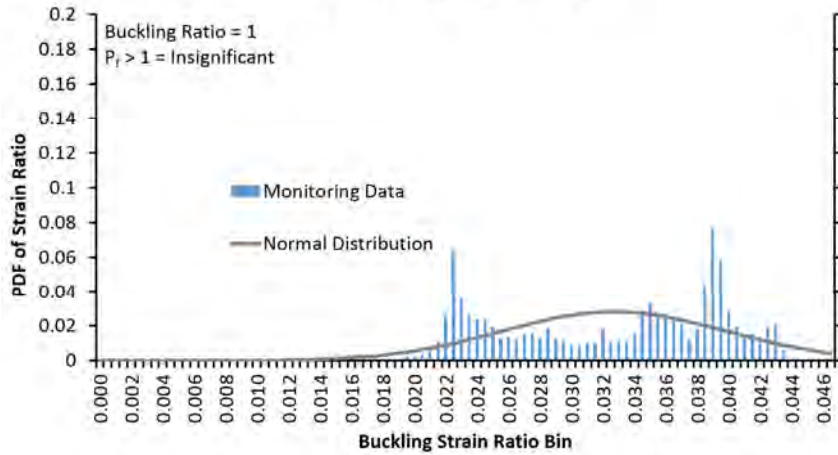
Plum River - Beyond the Crest

Cumulative PDF  
Tensile Strain (Rupture 2%)



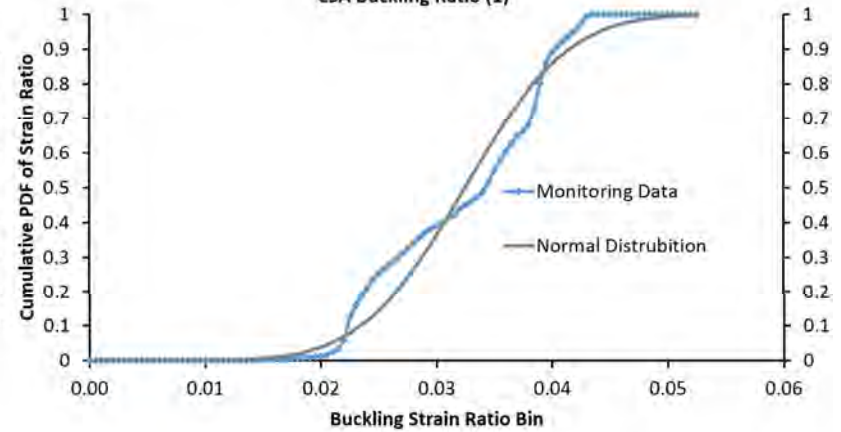
Plum River - Beyond the Crest

PDF - CSA Buckling Ratio (1)



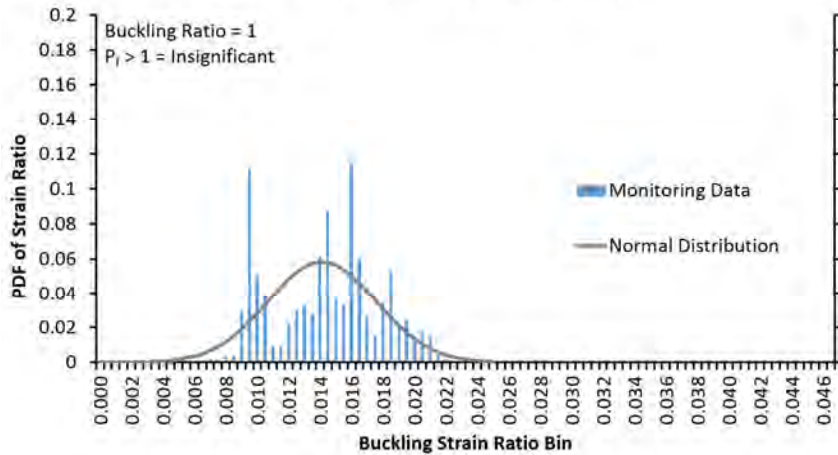
Plum River - Beyond the Crest

Cumulative PDF  
CSA Buckling Ratio (1)



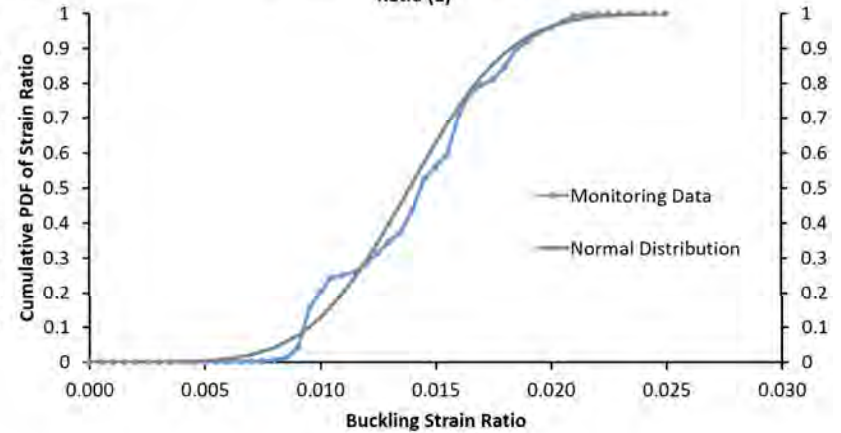
Plum River - Beyond the Crest

PDF - DNV Buckling 2012 Ratio (1)



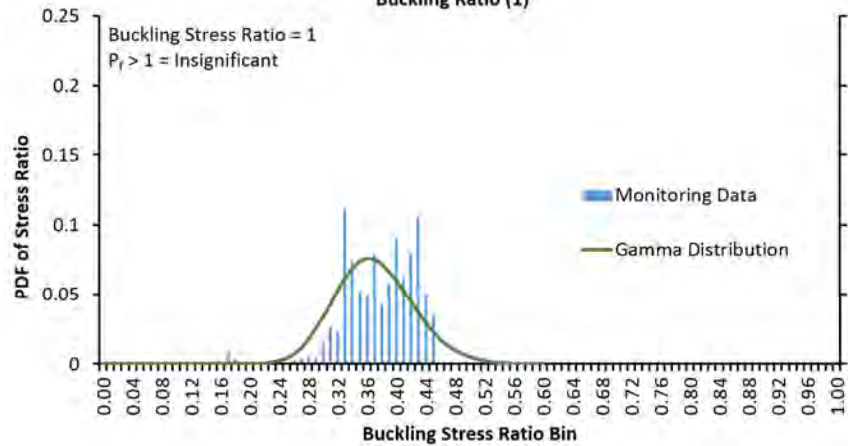
Plum River - Beyond the  
Crest

Cumulative PDF - DNV Buckling 2012  
Ratio (1)



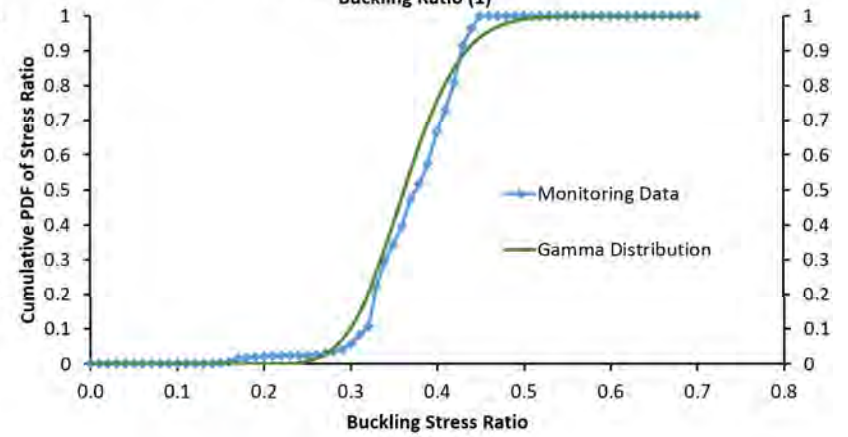
Plum River - Beyond Crest

PDF - DNV Stress Based Buckling Ratio (1)



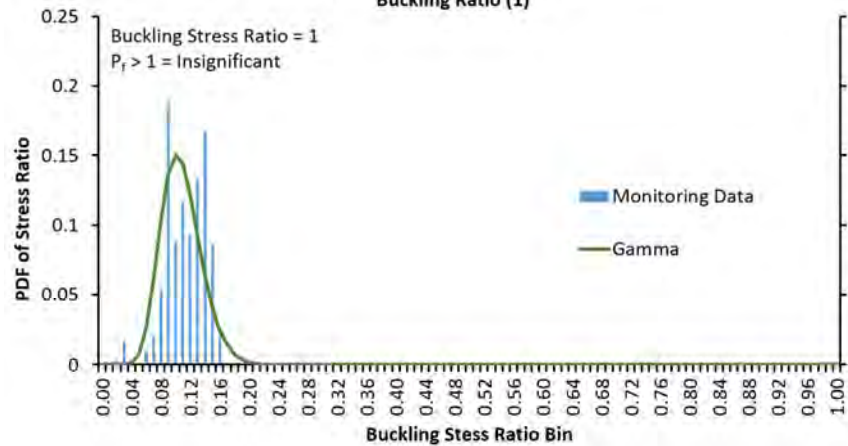
Plum River - Beyond Crest

Cumulative PDF - DNV Stress Based Buckling Ratio (1)



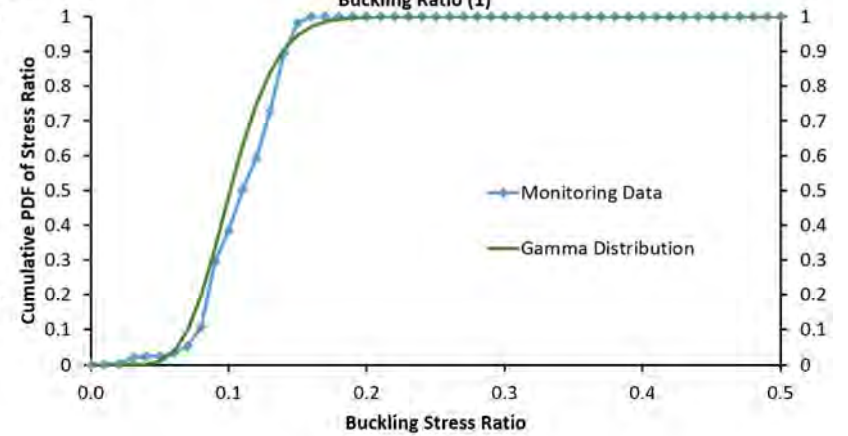
Plum River - Beyond the Crest

PDF - DNV Stress 2012 Based Buckling Ratio (1)



Plum River - Beyond the Crest

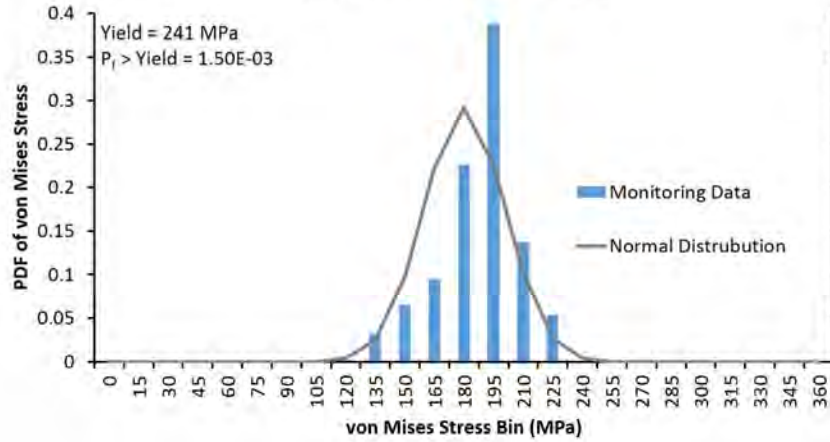
Cumulative PDF - DNV Stress 2012 Based Buckling Ratio (1)





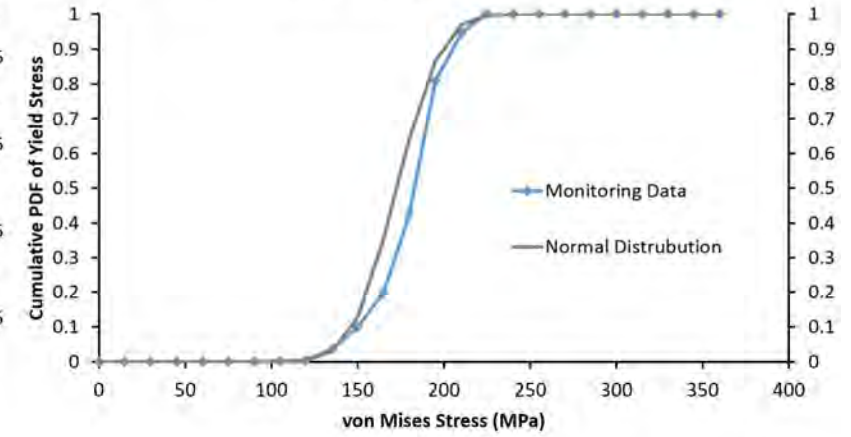
Plum River - Along the Slope

PDF von Mises (Yield 241 Mpa)



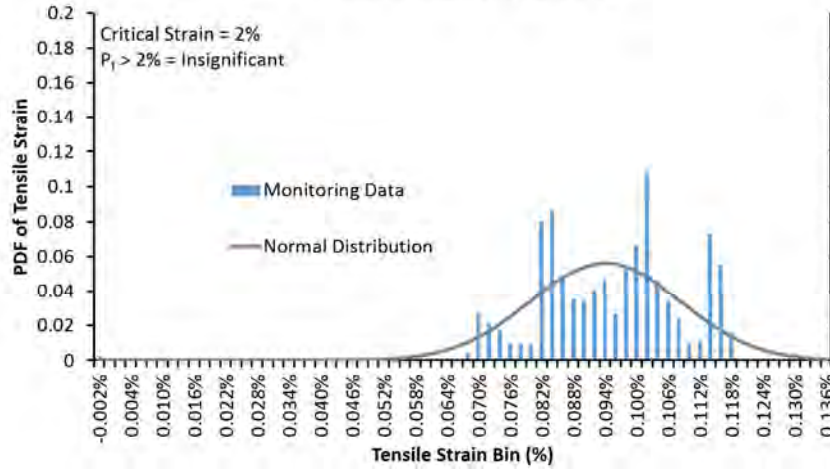
Plum River - Along the Slope

Cumulative PDF - Yield Stress



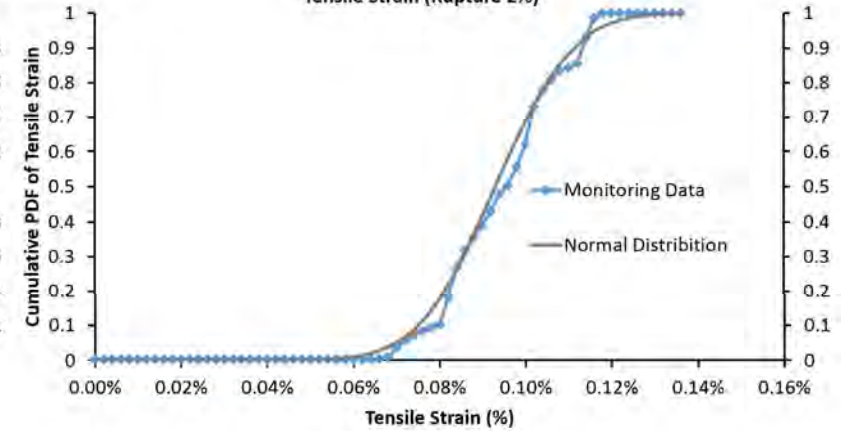
Plum River - Along the Slope

PDF - Tensile Strain (Rupture 2%)



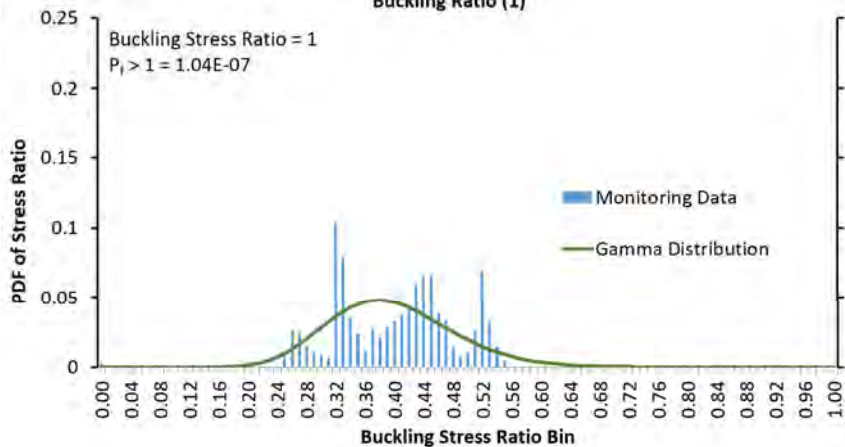
Plum River - Along the Slope

Cumulative PDF  
Tensile Strain (Rupture 2%)



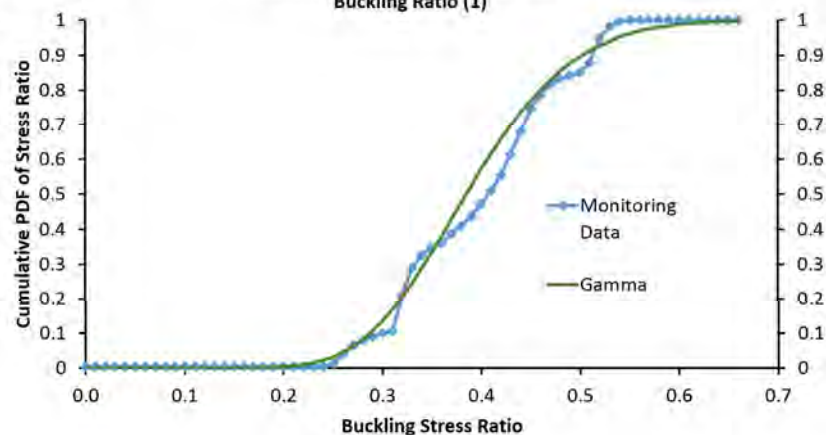
Plum River - Along the Slope

PDF - DNV Stress Based Buckling Ratio (1)



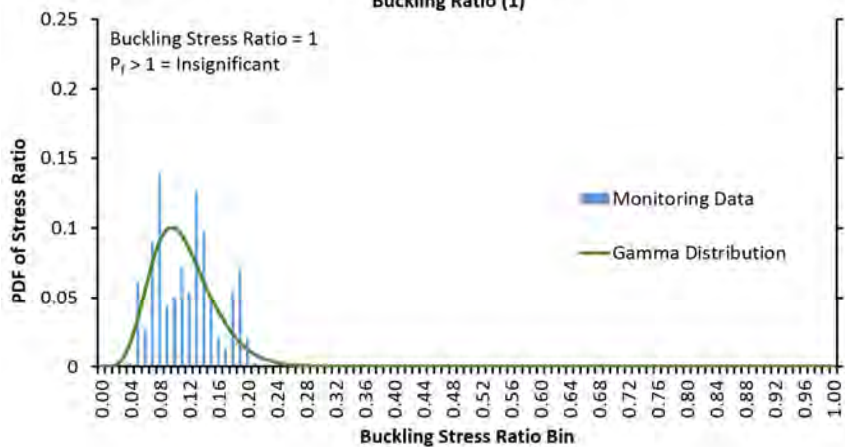
Plum River - Along the Slope

Cumulative PDF - DNV Stress Based Buckling Ratio (1)



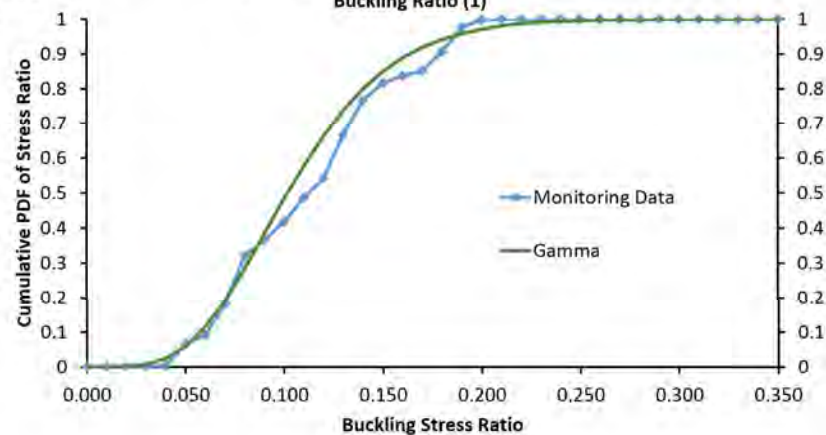
Plum River - Along the Slope

PDF - DNV Stress 2012 Based Buckling Ratio (1)



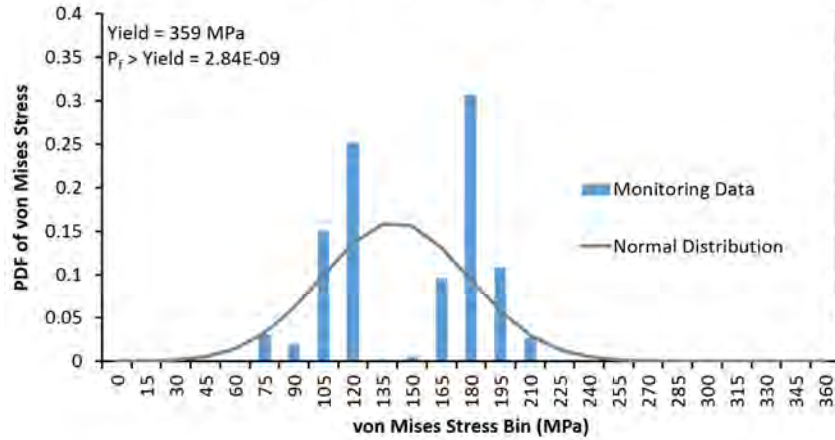
Plum River - Along the Slope

Cumulative PDF - DNV Stress 2012 Based Buckling Ratio (1)



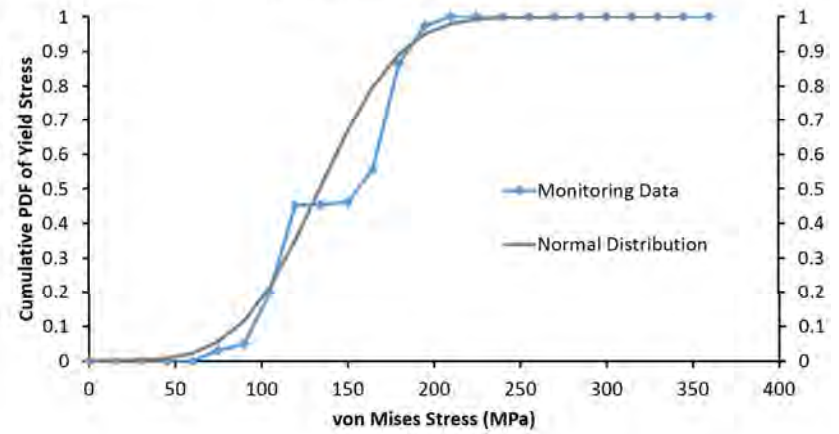
St. Lazare - Top of Valley

PDF von Mises (Yield 359 Mpa)



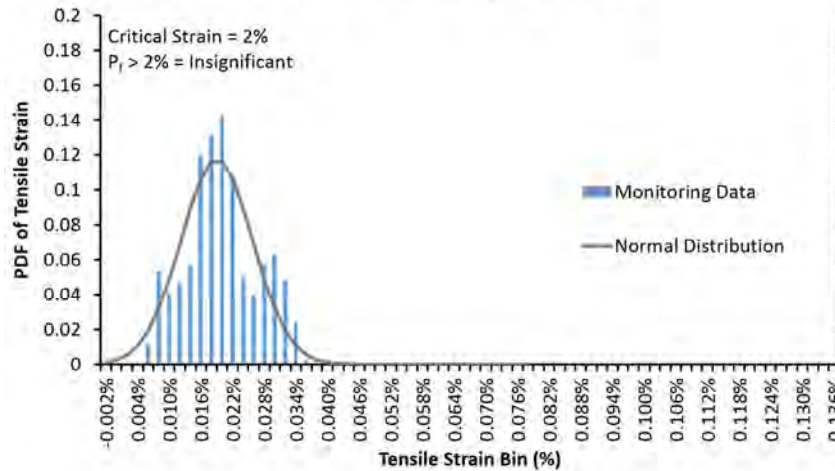
St. Lazare - Top of Valley

Cumulative PDF - Yield Stress



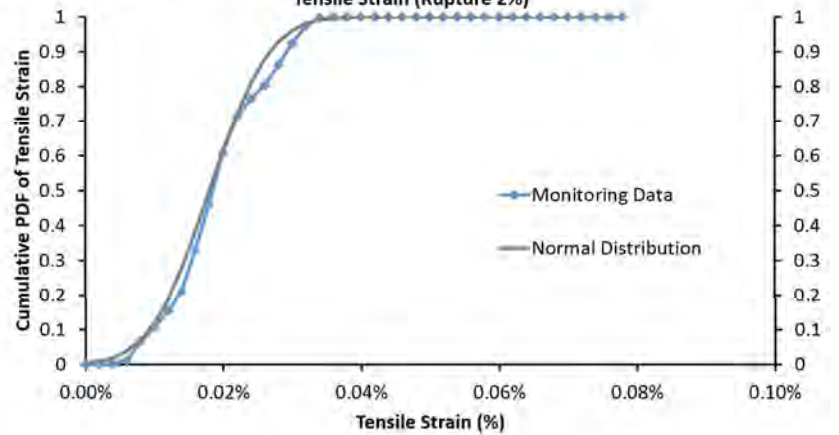
St. Lazare - Top of Valley

PDF - Tensile Strain (Rupture 2%)



St. Lazare - Top of Valley

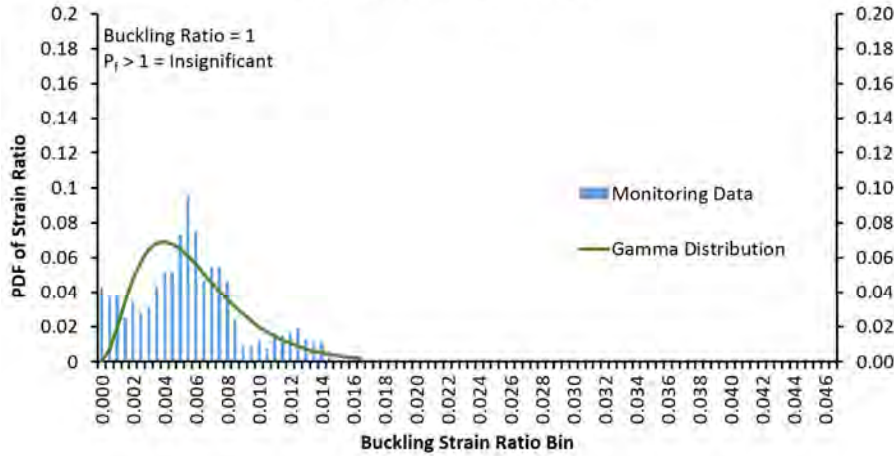
Cumulative PDF  
Tensile Strain (Rupture 2%)





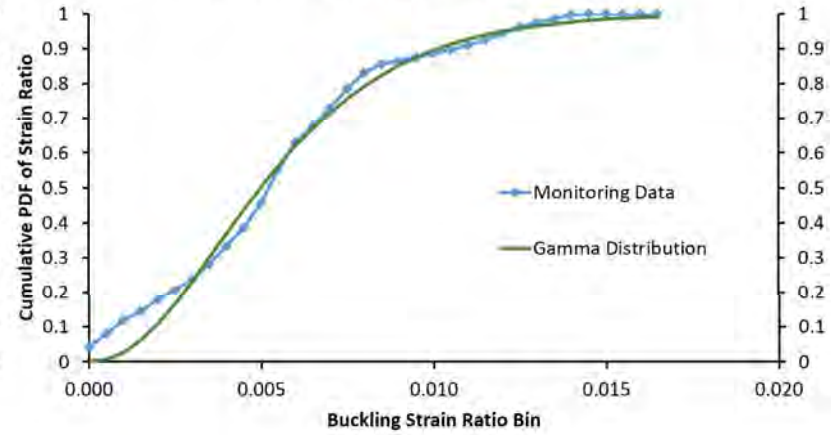
St. Lazare - Top of Valley

PDF - CSA Buckling Ratio (1)



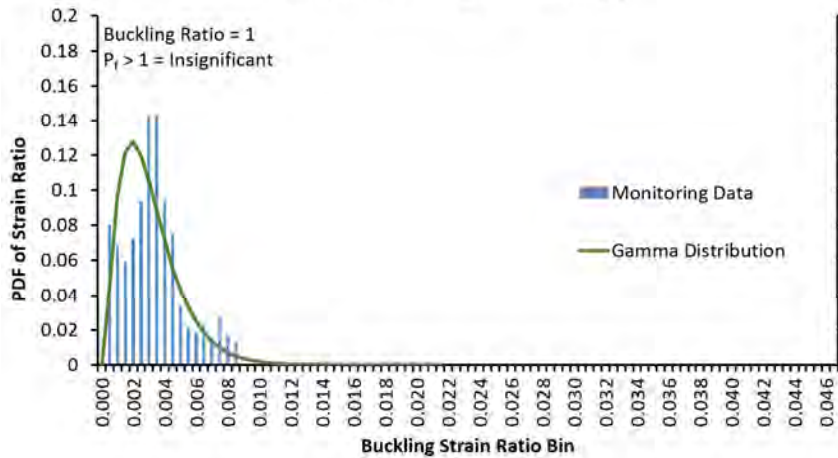
St. Lazare - Top of Valley

Cumulative PDF - CSA Buckling Ratio (1)



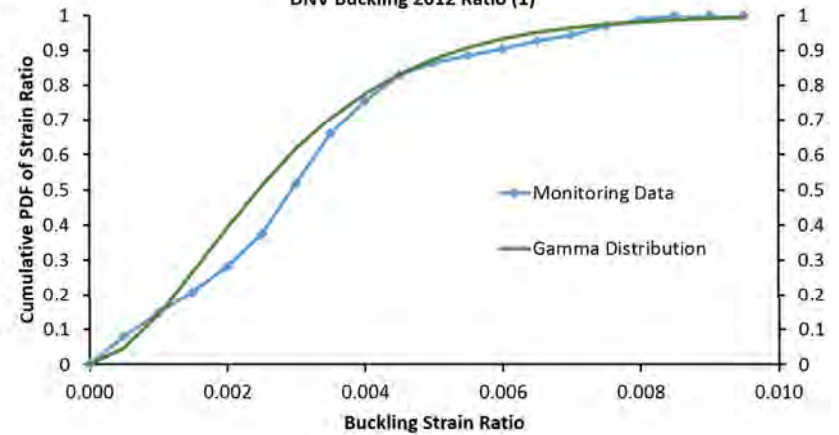
St. Lazare - Top of Valley

PDF - DNV Buckling Ratio 2012 (1)



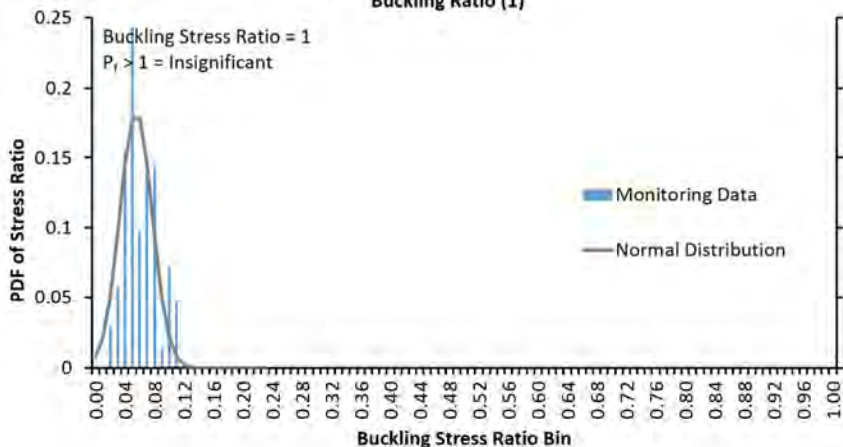
St. Lazare - Top of Valley

Cumulative PDF - DNV Buckling Ratio 2012 (1)



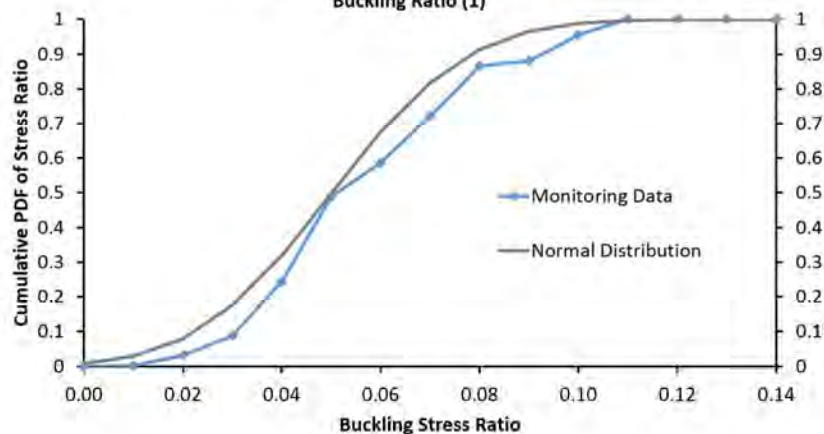
St. Lazare - Top of Valley

PDF - DNV 2000 Stress Based Buckling Ratio (1)



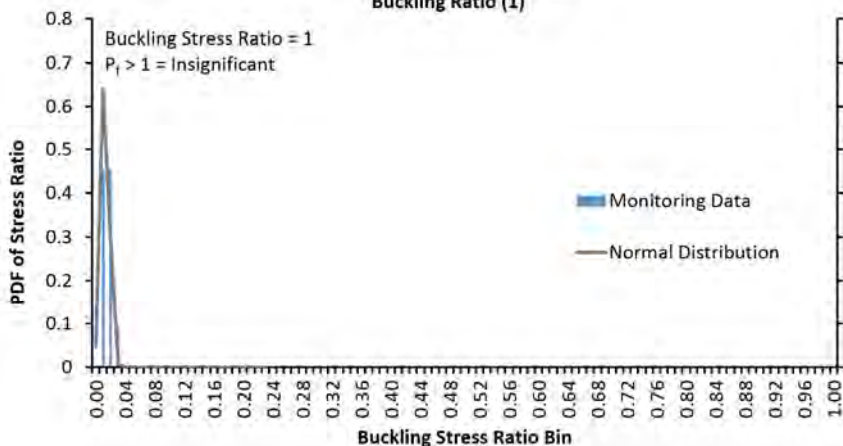
St. Lazare - Top of Valley

Cumulative PDF - DNV Stress Based Buckling Ratio (1)



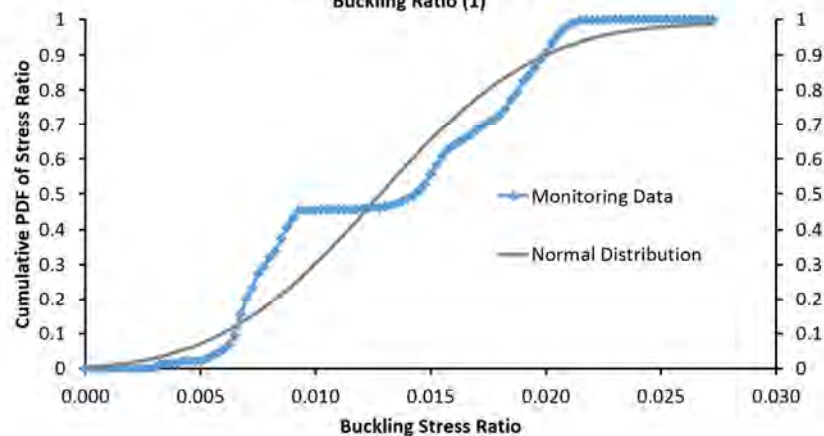
St. Lazare - Top of Valley

PDF - DNV 2012 Stress Based Buckling Ratio (1)



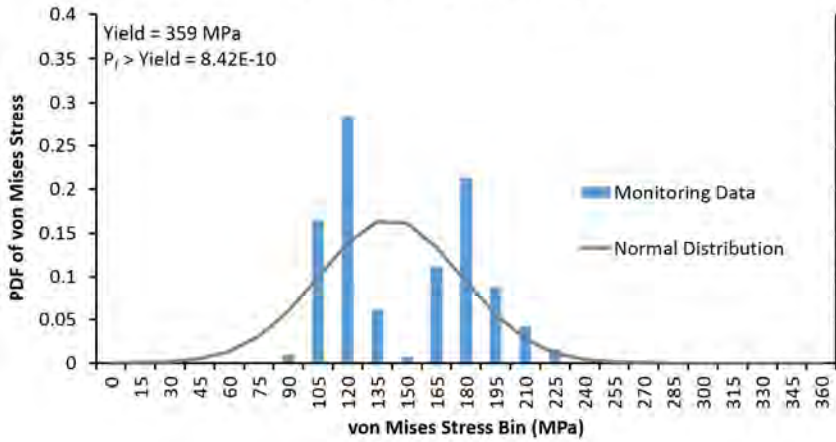
St. Lazare - Top of Valley

Cumulative PDF - DNV 2012 Stress Based Buckling Ratio (1)



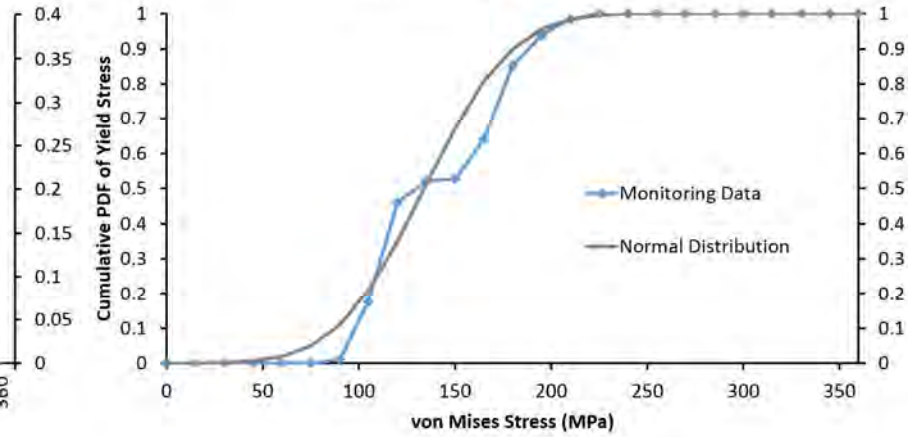
St. Lazare - Middle of Valley

PDF von Mises (Yield 359 Mpa)



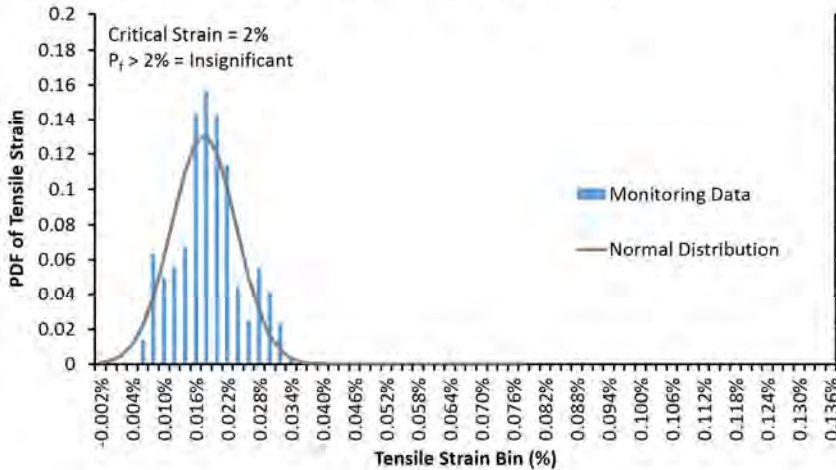
St. Lazare - Middle of Valley

Cumulative PDF - Yield Stress



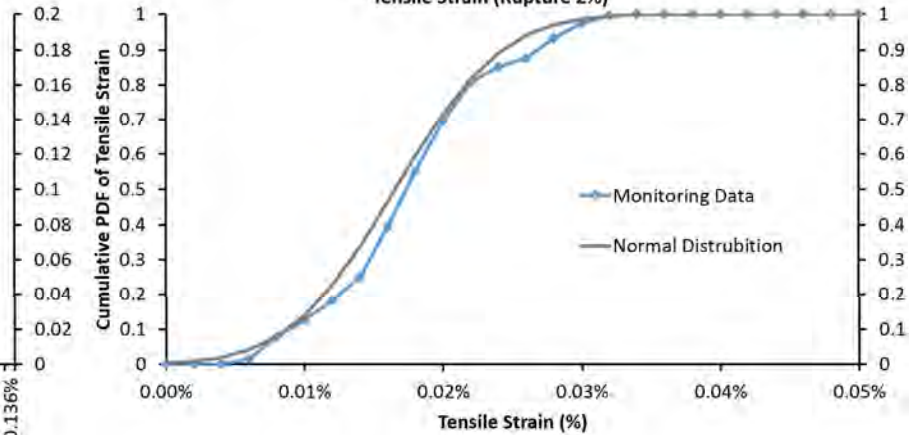
St. Lazare - Middle of Valley

PDF - Tensile Strain (Rupture 2%)



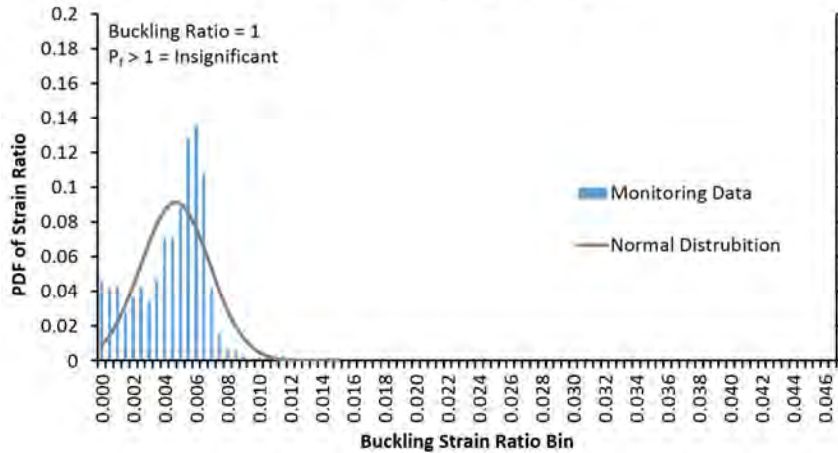
St. Lazare - Middle of Valley

Cumulative PDF  
Tensile Strain (Rupture 2%)



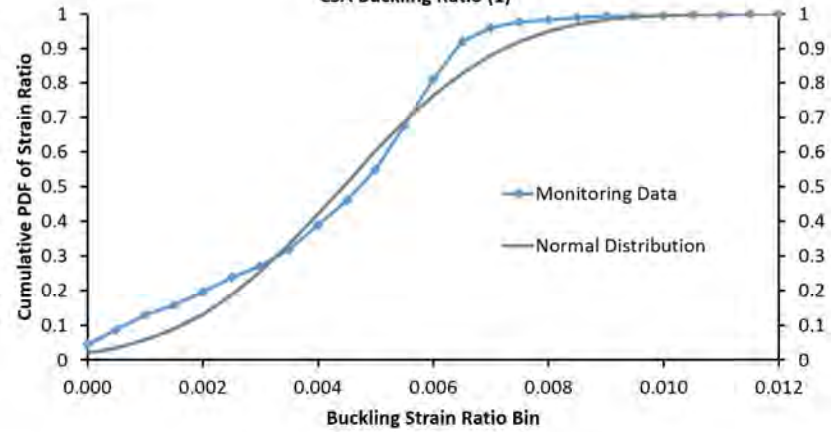
St. Lazare - Middle of Valley

PDF - CSA Buckling Ratio (1)



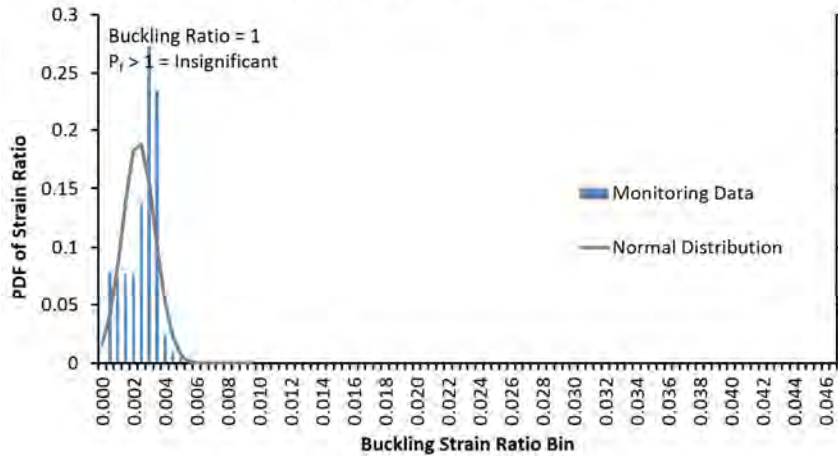
St. Lazare - Middle of Valley

Cumulative PDF  
CSA Buckling Ratio (1)



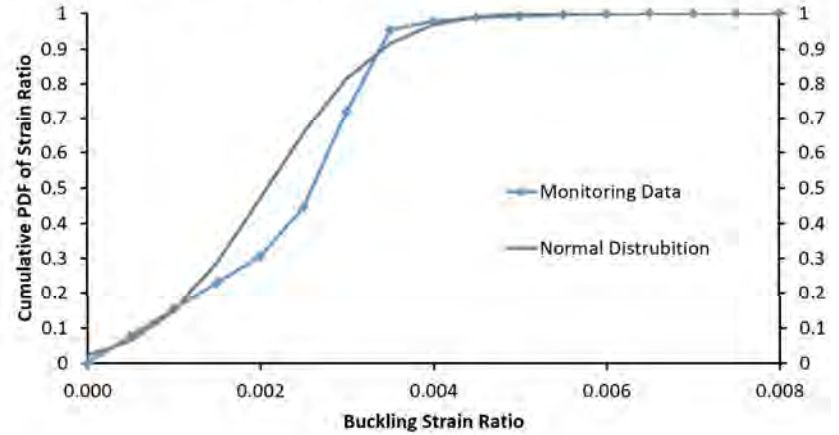
St. Lazare - Middle of Valley

PDF - DNV Buckling Ratio 2012 (1)



St. Lazare - Middle of Valley

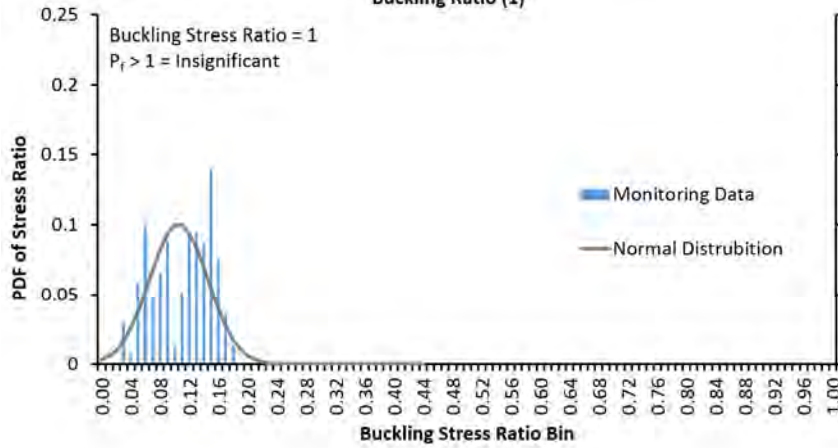
Cumulative PDF - DNV Buckling 2012 Ratio (1)





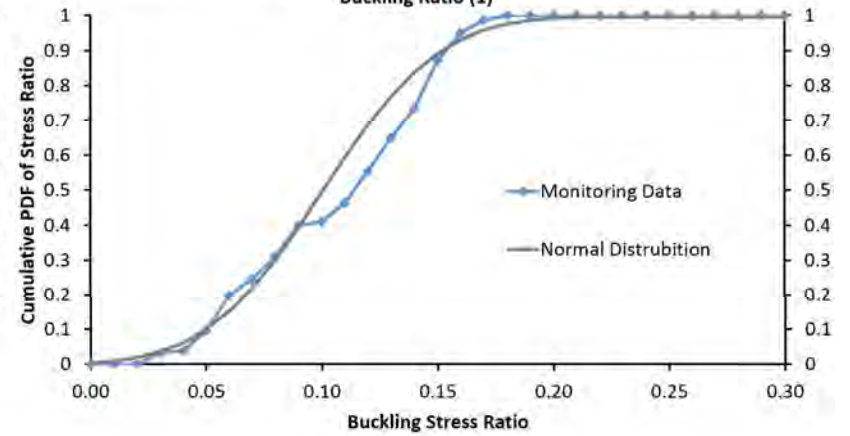
St. Lazare - Middle of Valley

PDF - DNV Stress Based Buckling Ratio (1)



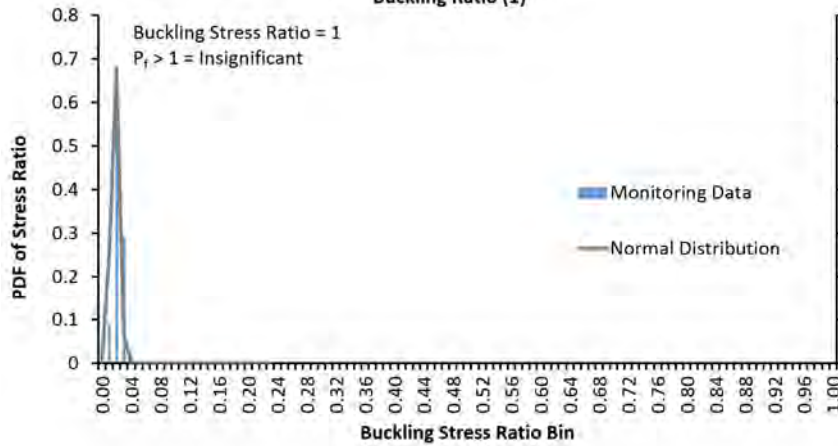
St. Lazare - Middle of Valley

Cumulative PDF - DNV Stress Based Buckling Ratio (1)



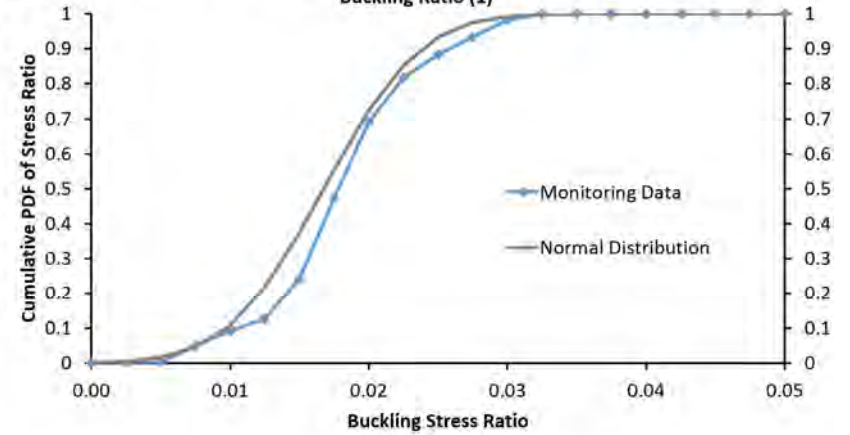
St. Lazare - Middle of Valley

PDF - DNV 2012 Stress Based Buckling Ratio (1)



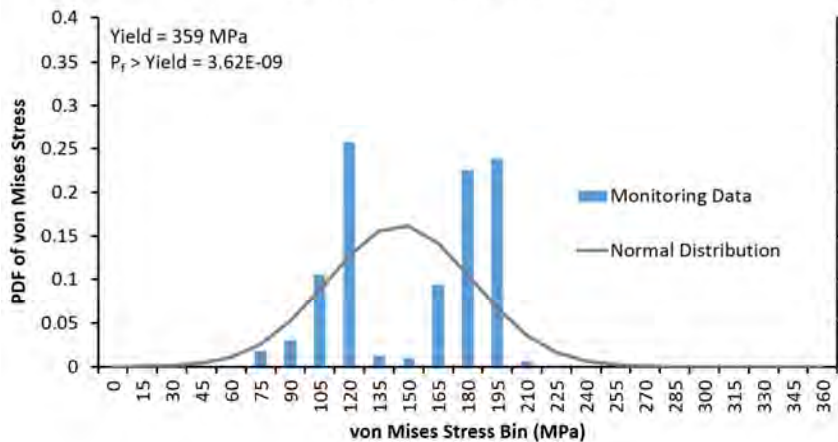
St. Lazare - Middle of Valley

Cumulative PDF - DNV 2012 Stress Based Buckling Ratio (1)



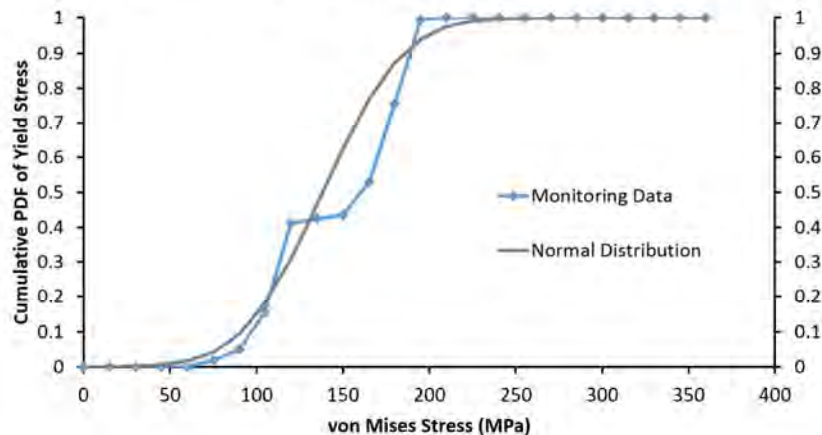
St. Lazare - Bottom of Valley

PDF von Mises (Yield 359 Mpa)



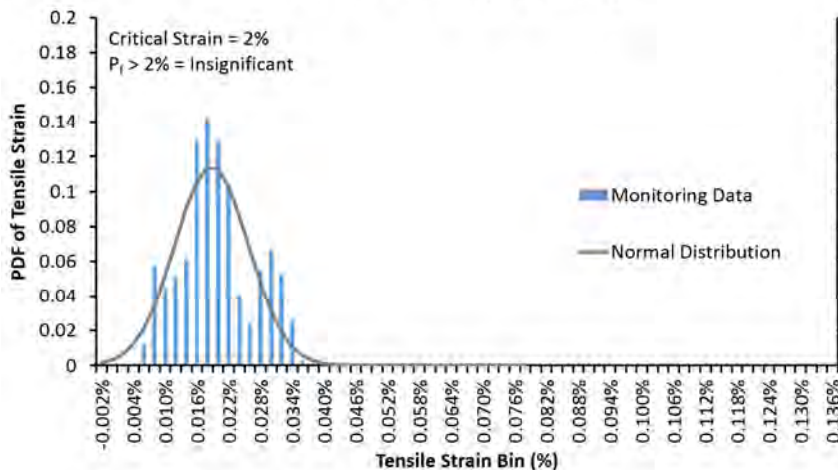
St. Lazare - Bottom of Valley

Cumulative PDF - Yield Stress



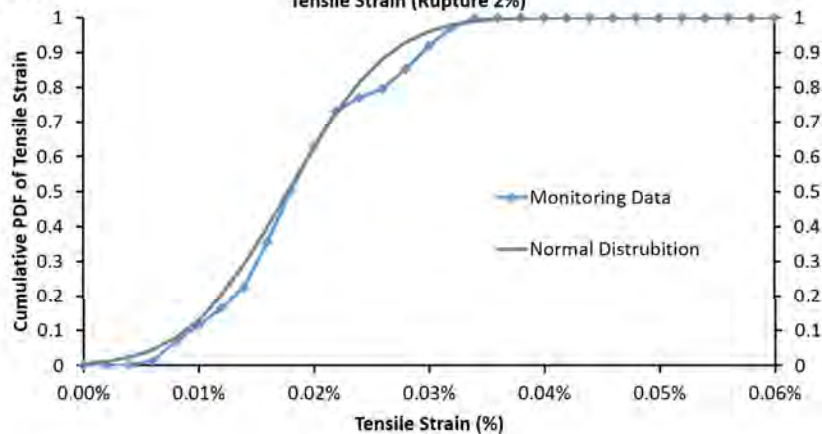
St. Lazare - Bottom of Valley

PDF - Tensile Strain (Rupture 2%)



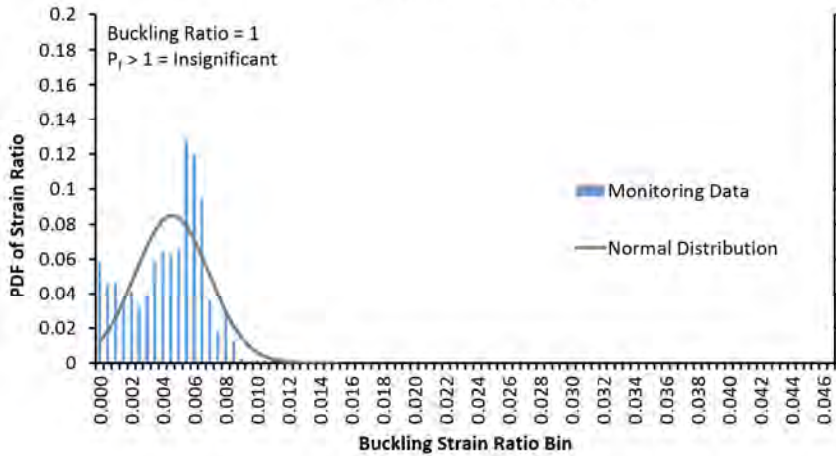
St. Lazare - Bottom of Valley

Cumulative PDF Tensile Strain (Rupture 2%)



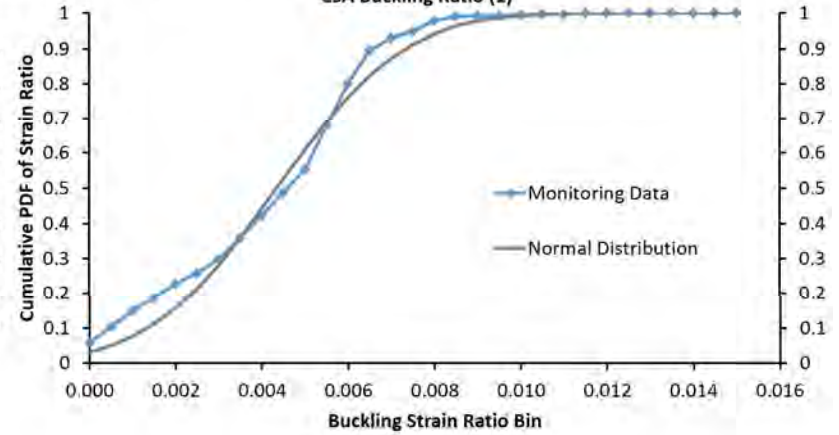
St. Lazare - Bottom of Valley

PDF - CSA Buckling Ratio (1)



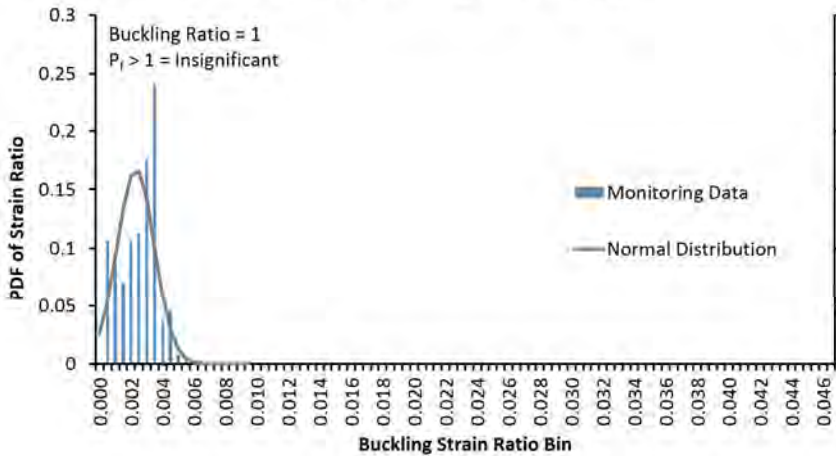
St. Lazare - Bottom of Valley

Cumulative PDF  
CSA Buckling Ratio (1)



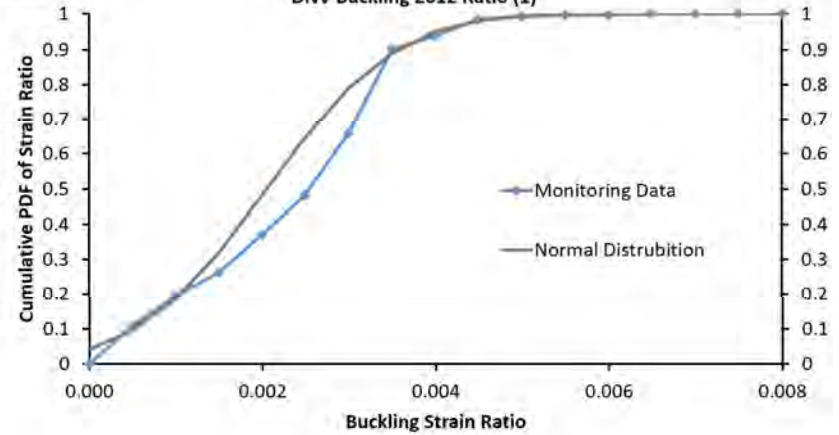
St. Lazare - Bottom of Valley

PDF - DNV Buckling Ratio 2012 (1)



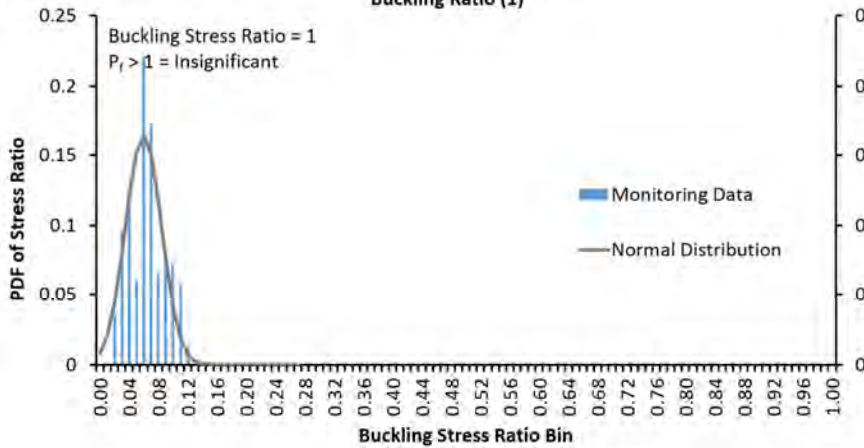
St. Lazare - Bottom of Valley

Cumulative PDF -  
DNV Buckling 2012 Ratio (1)



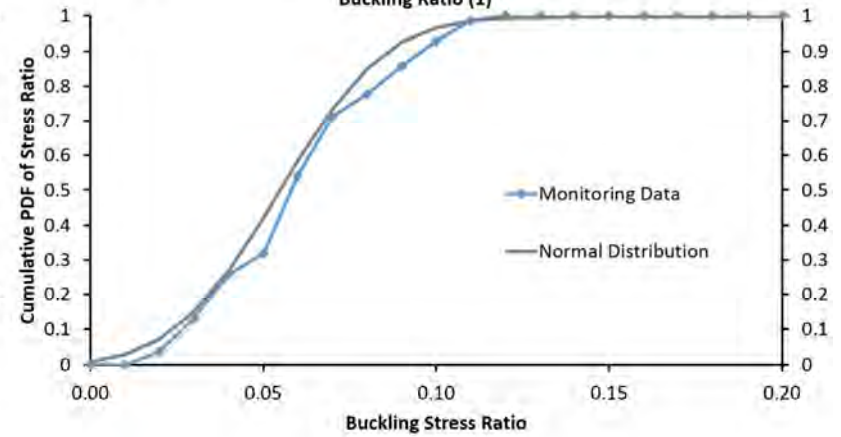
St. Lazare - Bottom of Valley

PDF - DNV Stress Based Buckling Ratio (1)



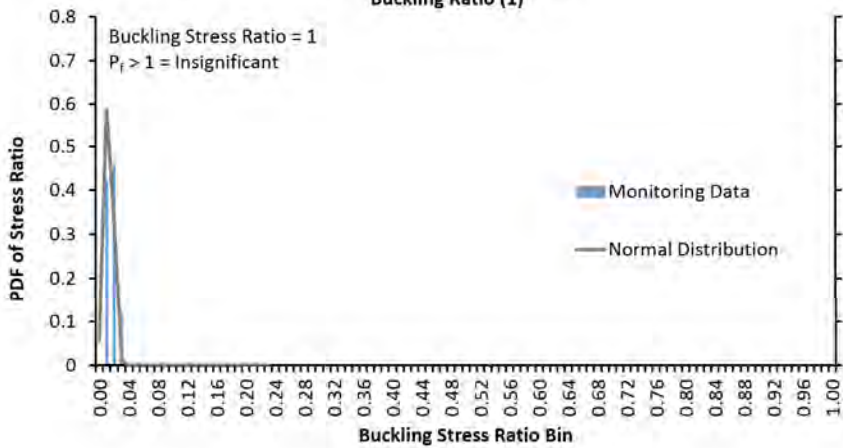
St. Lazare - Bottom of Valley

Cumulative PDF - DNV Stress Based Buckling Ratio (1)



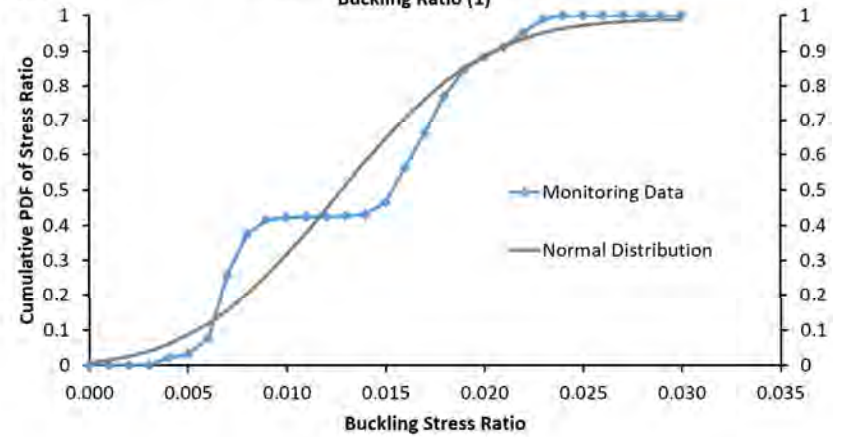
St. Lazare - Bottom of Valley

PDF - DNV 2012 Stress Based Buckling Ratio (1)



St. Lazare - Bottom of Valley

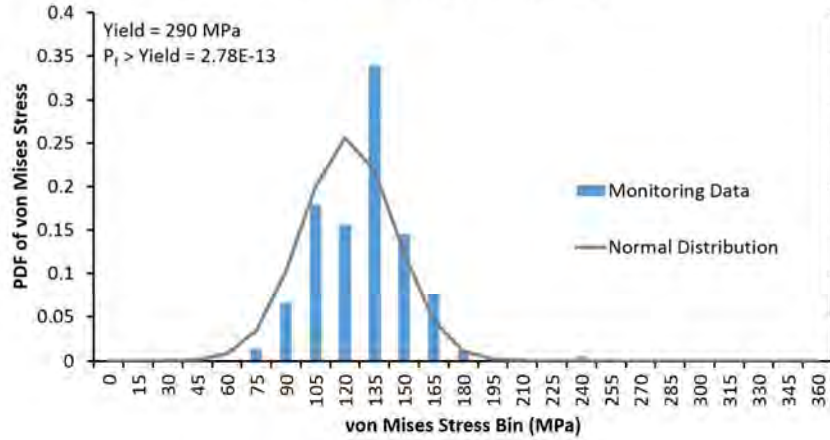
Cumulative PDF - DNV 2012 Stress Based Buckling Ratio (1)





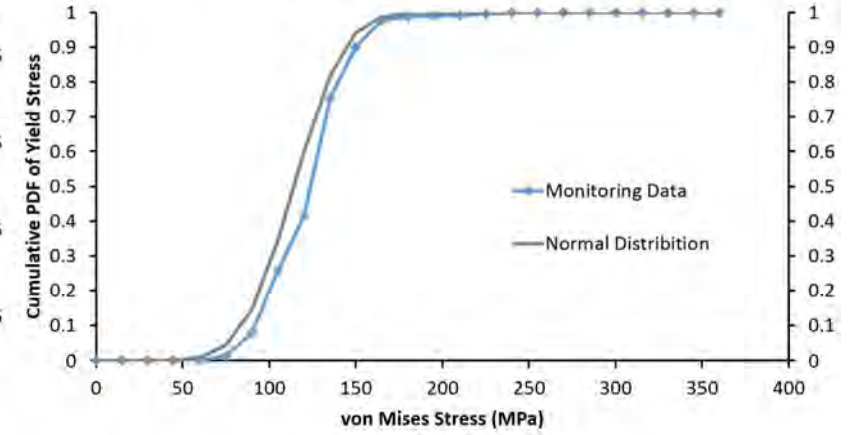
Harrowby - Top of Valley

PDF von Mises (Yield 290 Mpa)



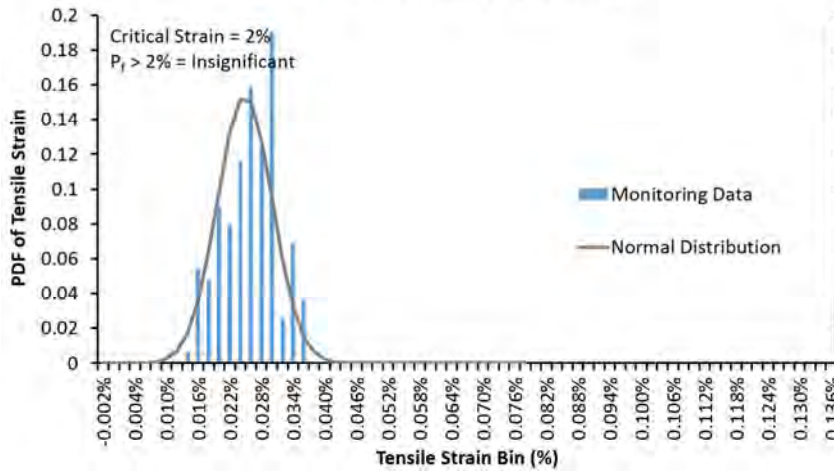
Harrowby- Top of Valley

Cumulative PDF - Yield Stress



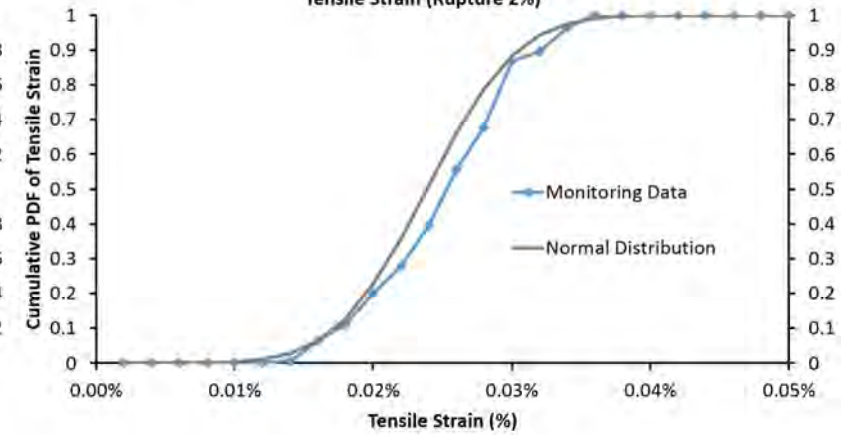
Harrowby - Top of Valley

PDF - Tensile Strain (Rupture 2%)



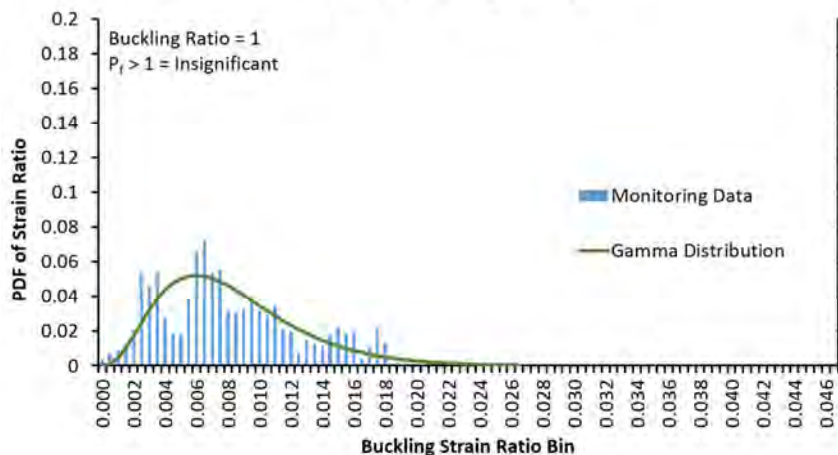
Harrowby - Top of Valley

Cumulative PDF  
Tensile Strain (Rupture 2%)



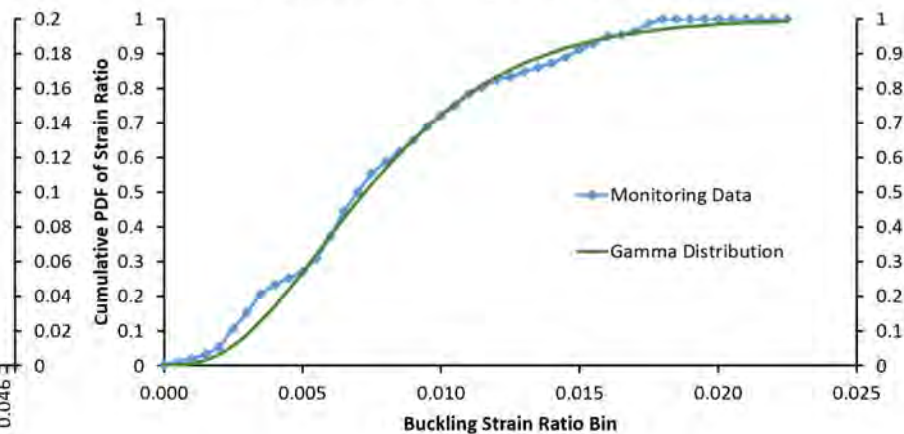
Harrowby - Top of Valley

PDF - CSA Buckling Ratio (1)



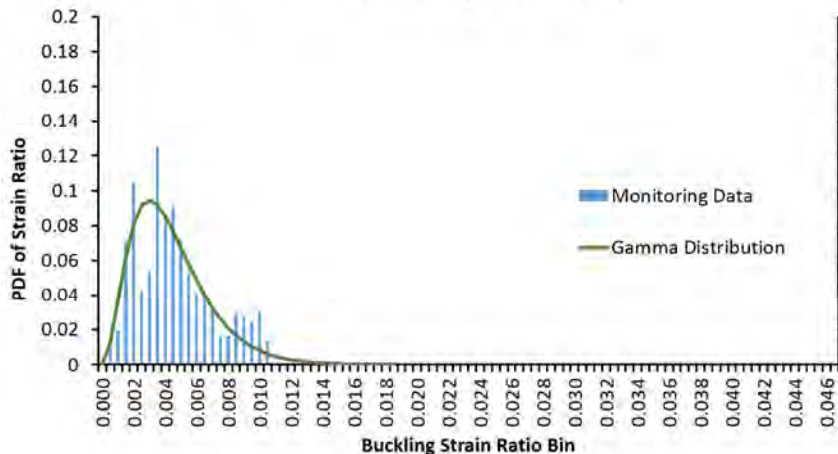
Harrowby - Top of Valley

Cumulative PDF - CSA Buckling Ratio (1)



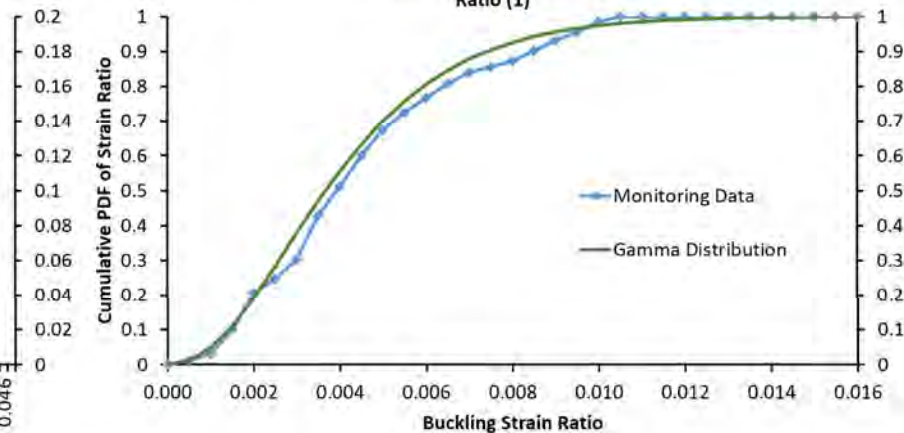
Harrowby - Top of Valley

PDF - DNV Buckling 2012 Ratio (1)



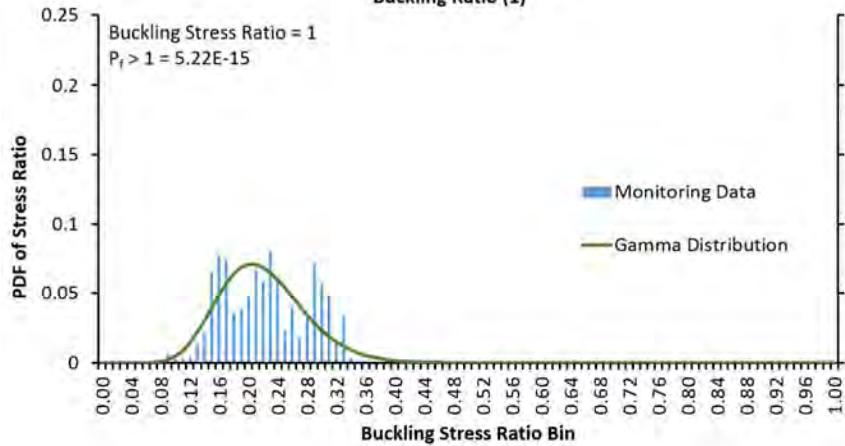
Harrowby - Top of Valley

Cumulative PDF - DNV Buckling 2012 Ratio (1)



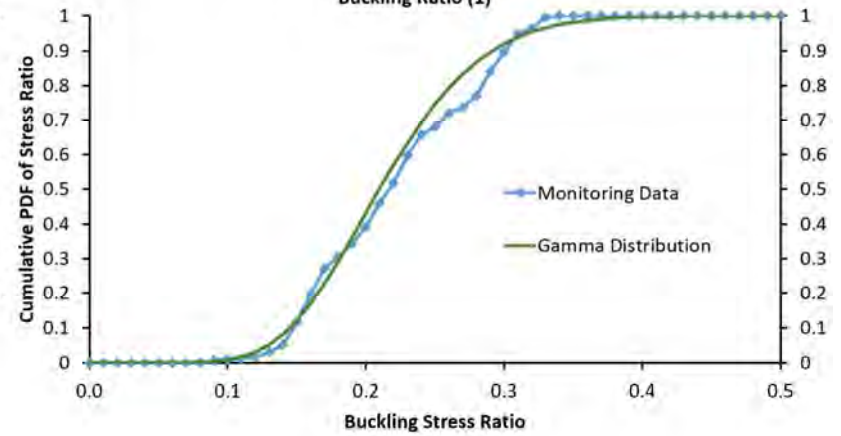
Harrowby - Top of Valley

PDF - DNV Stress Based Buckling Ratio (1)



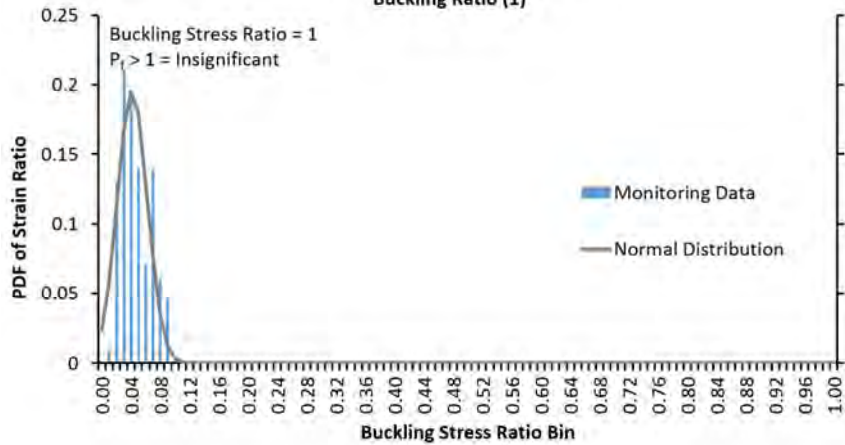
Harrowby- Top of Valley

Cumulative PDF - DNV Stress Based Buckling Ratio (1)



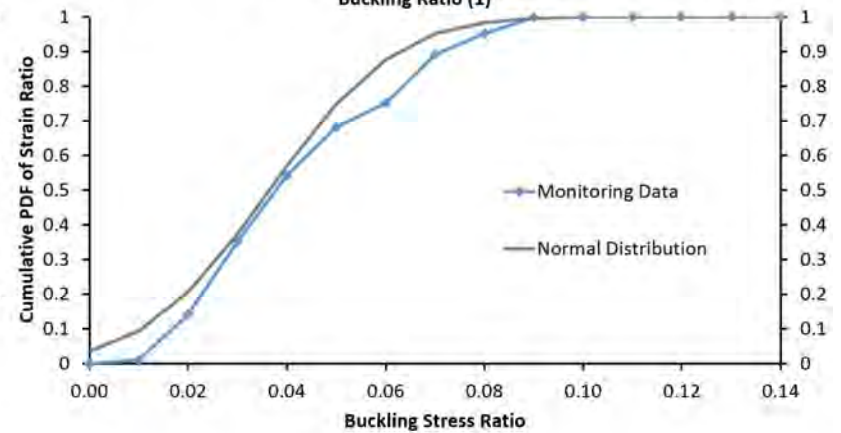
Harrowby - Top of Valley

PDF - DNV Stress 2012 Based Buckling Ratio (1)



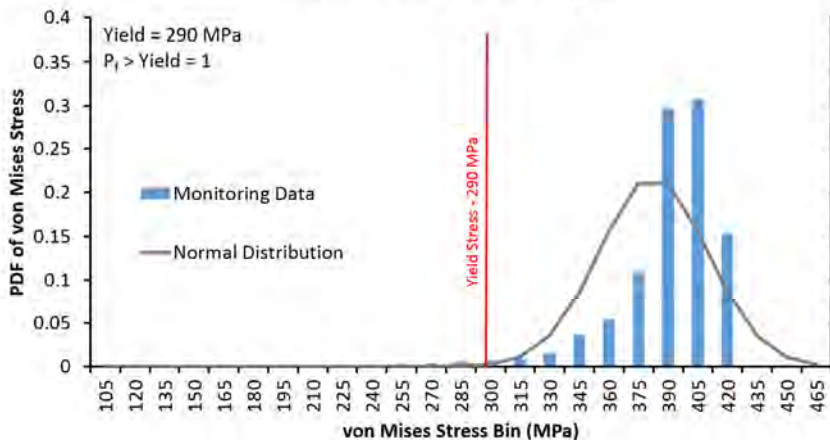
Harrowby- Top of Valley

Cumulative PDF - DNV Stress 2012 Based Buckling Ratio (1)



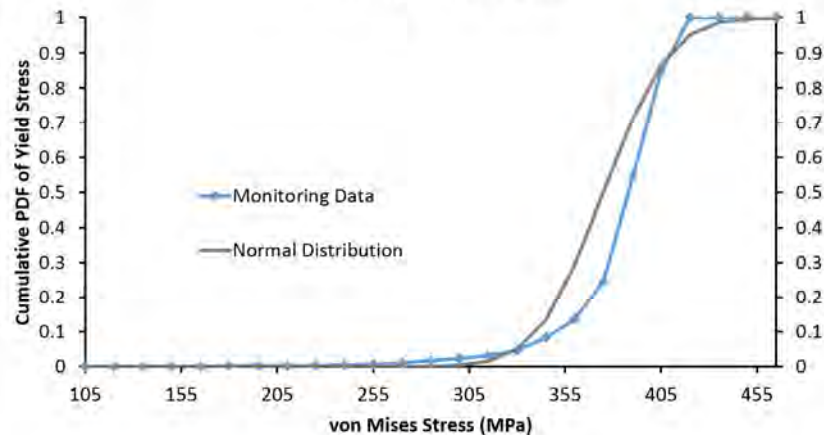
Harrowby - Middle of Valley

PDF von Mises (Yield 290 Mpa)



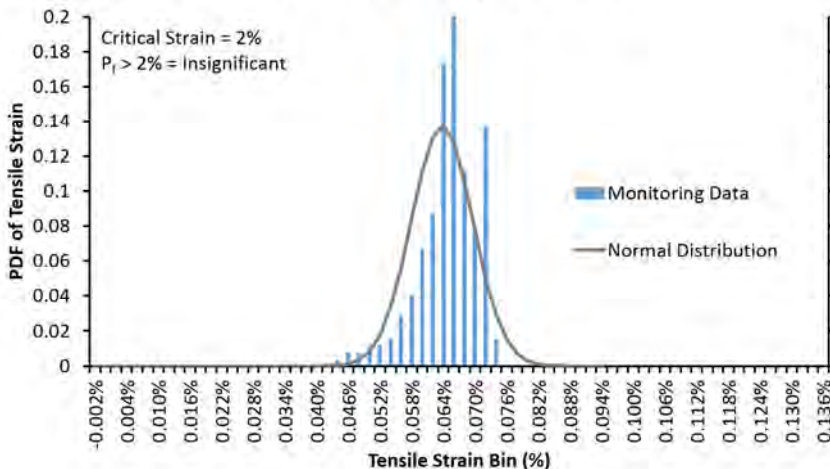
Harrowby - Middle of Valley

Cumulative PDF - Yield Stress



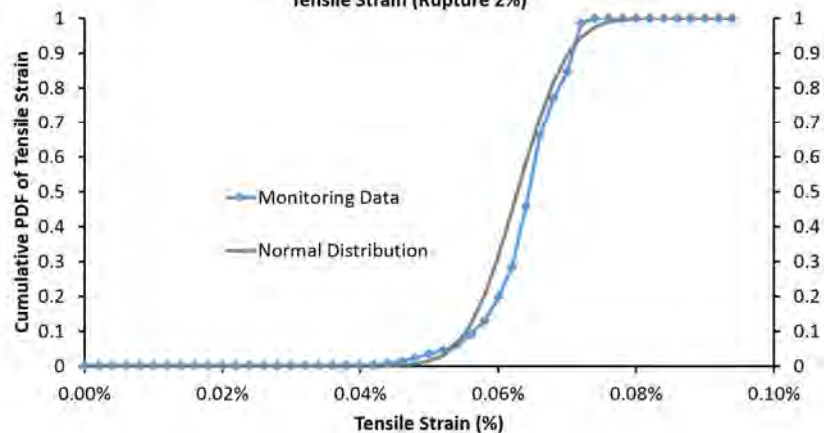
Harrowby - Middle of Valley

PDF - Tensile Strain (Rupture 2%)



Harrowby - Middle of Valley

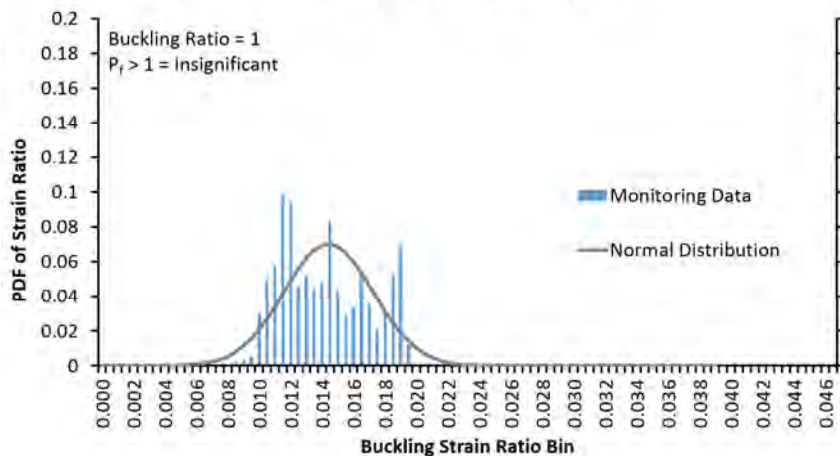
Cumulative PDF  
Tensile Strain (Rupture 2%)





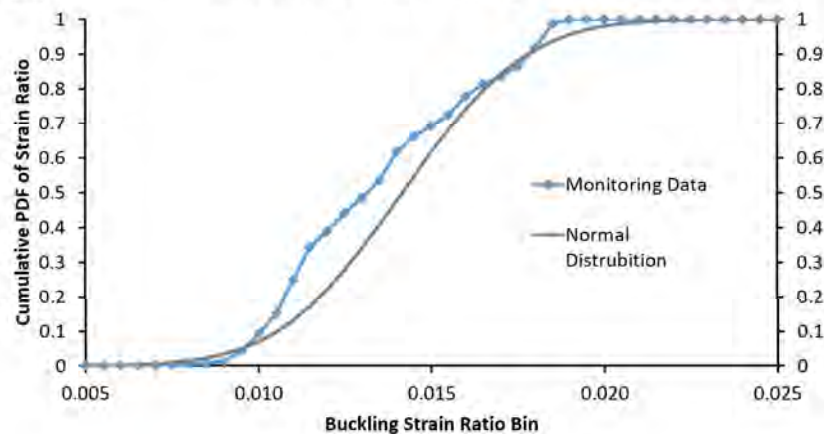
Harrowby - Middle of Valley

PDF - CSA Buckling Ratio (1)



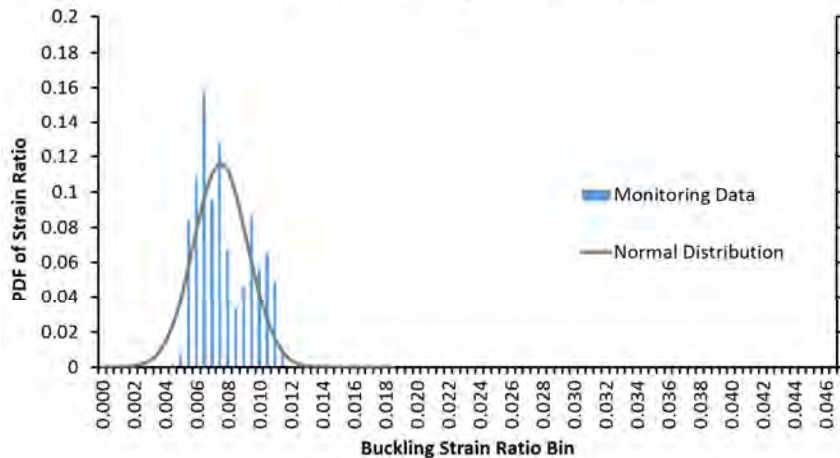
Harrowby - Middle of Valley

Cumulative PDF - CSA Buckling Ratio (1)



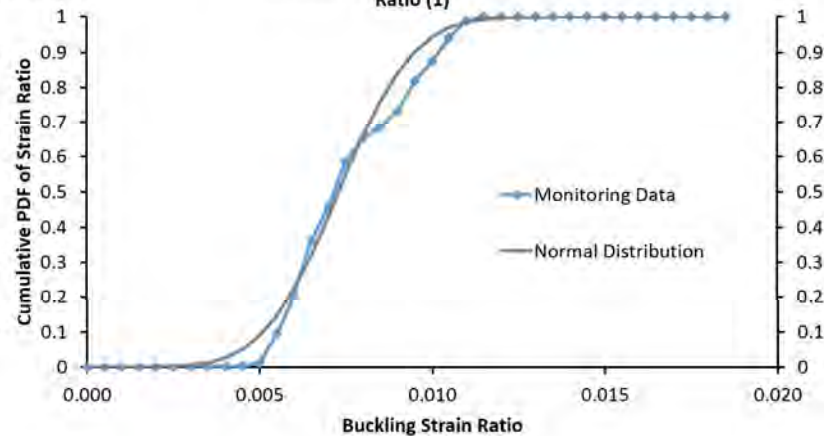
Harrowby - Middle of Valley

PDF - DNV Buckling 2012 Ratio (1)



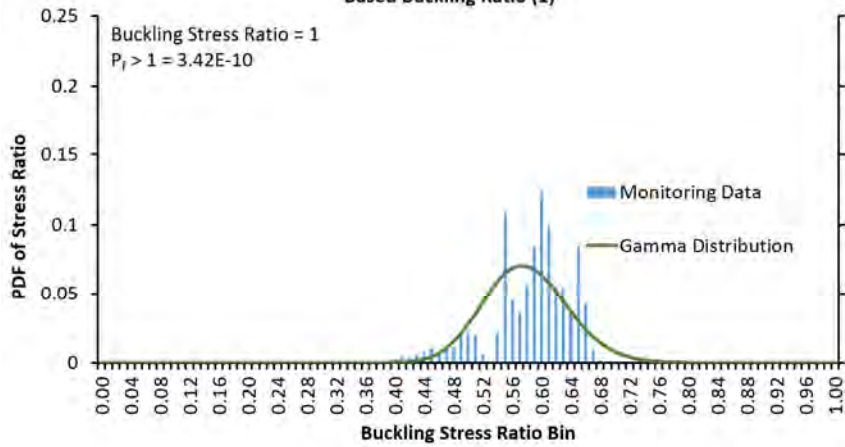
Harrowby - Middle of Valley

Cumulative PDF - DNV Buckling 2012 Ratio (1)



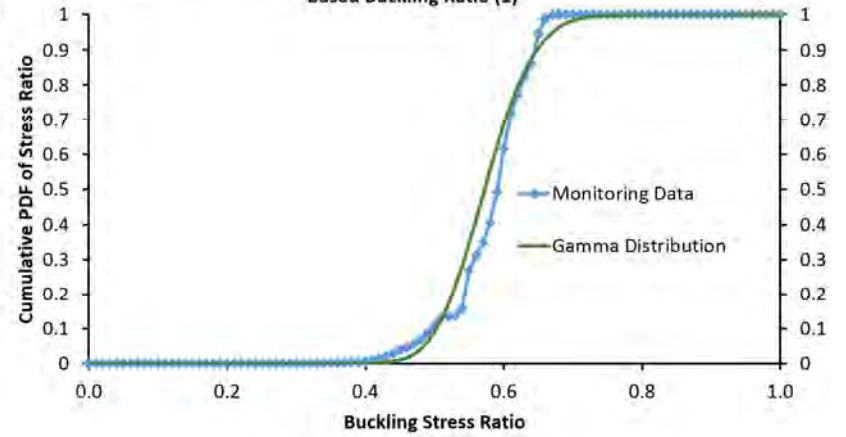
Harrowby - Middle of Valley

PDF - DNV Stress 2000  
Based Buckling Ratio (1)



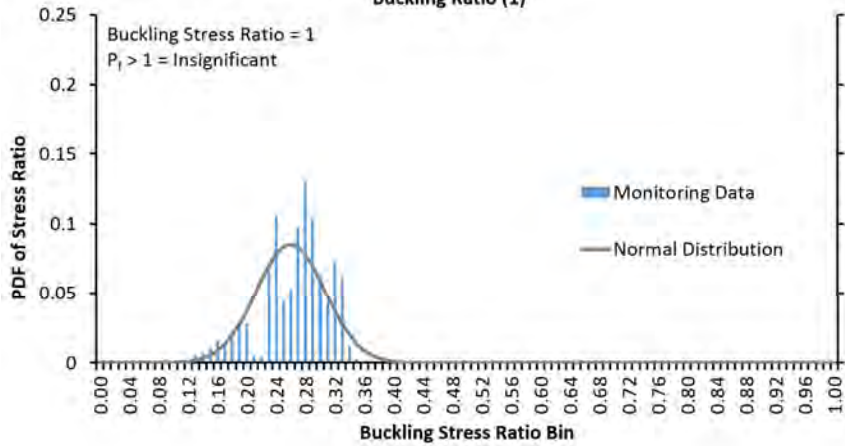
Harrowby- Middle of Valley

Cumulative PDF - DNV Stress 2000  
Based Buckling Ratio (1)



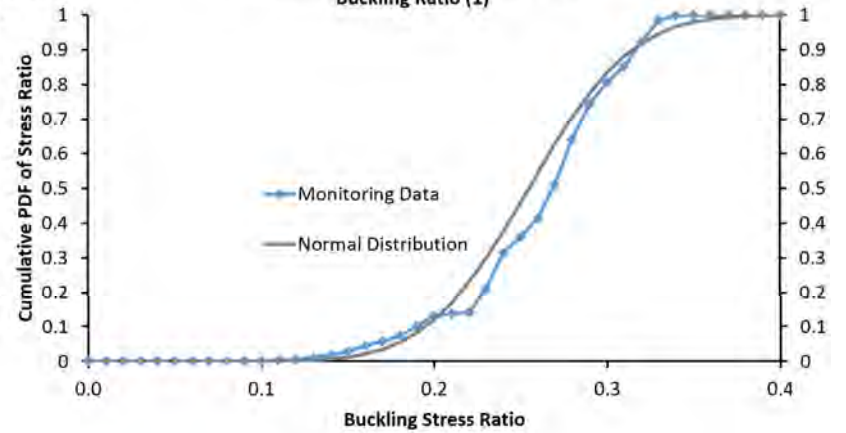
Harrowby - Middle of Valley

PDF - DNV Stress 2012 Based  
Buckling Ratio (1)



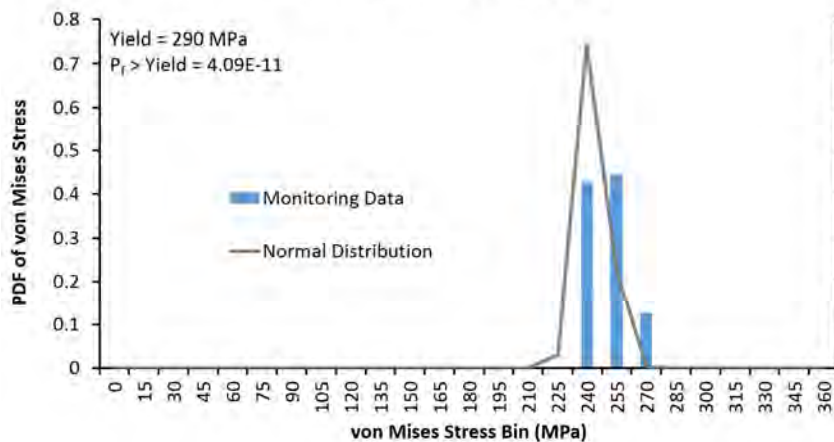
Harrowby- Middle  
of Valley

Cumulative PDF - DNV Stress 2012 Based  
Buckling Ratio (1)



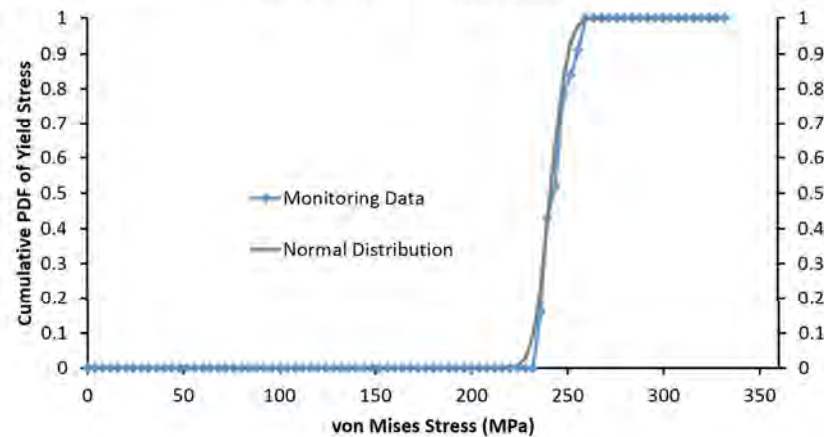
Harrowby - Bottom of Valley

PDF von Mises (Yield 290 Mpa)



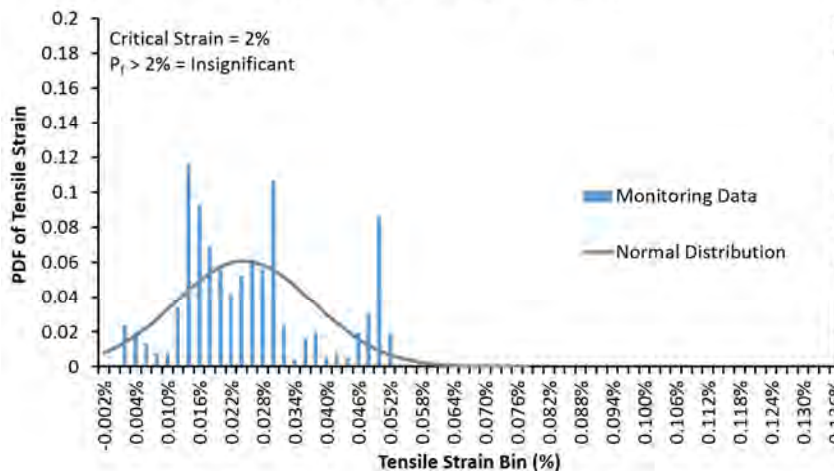
Harrowby- Bottom of Valley

Cumulative PDF - Yield Stress



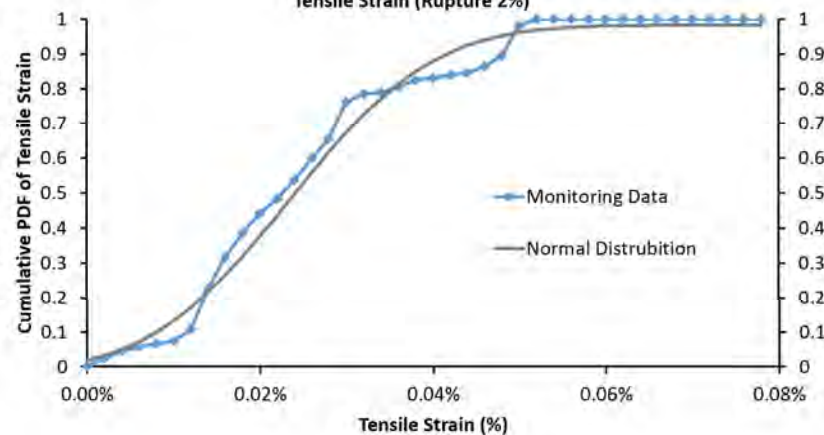
Harrowby - Bottom of Valley

PDF - Tensile Strain (Rupture 2%)



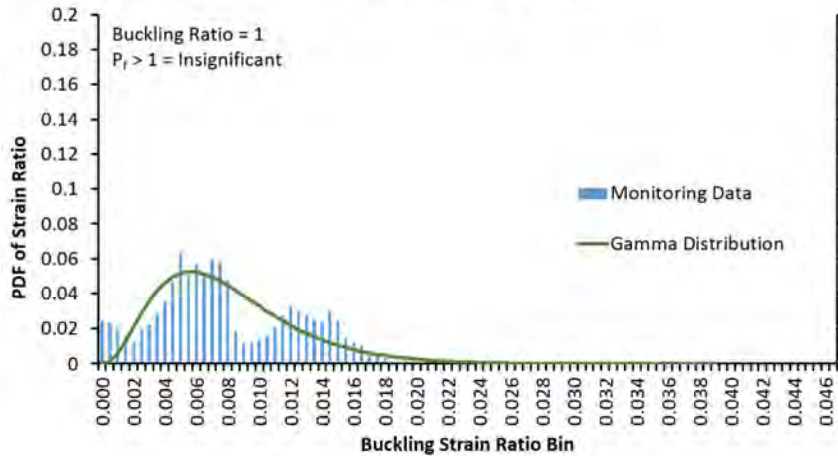
Harrowby - Bottom of Valley

Cumulative PDF  
Tensile Strain (Rupture 2%)



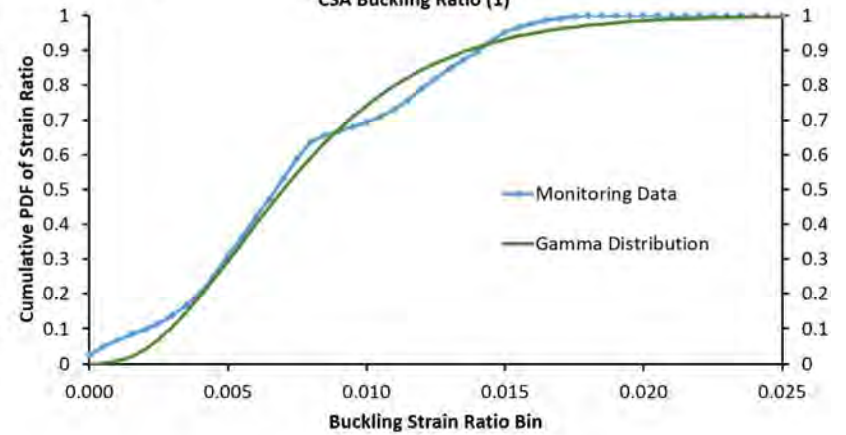
Harrowby - Bottom of Valley

PDF - CSA Buckling Ratio (1)



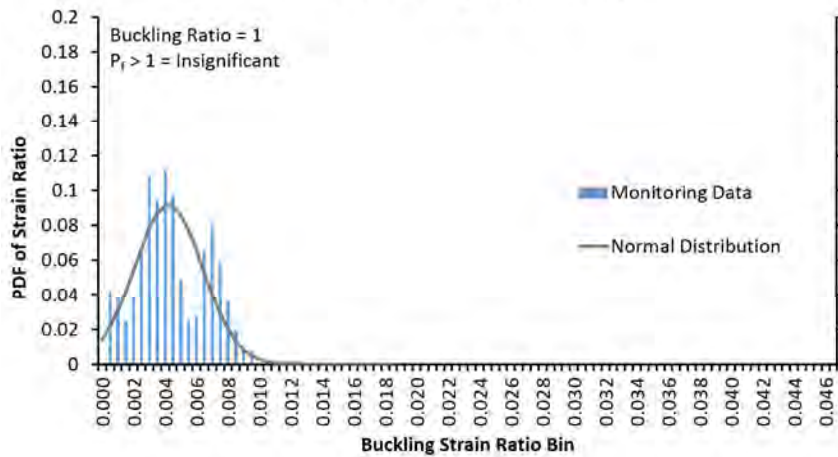
Harrowby - Bottom of Valley

Cumulative PDF  
CSA Buckling Ratio (1)



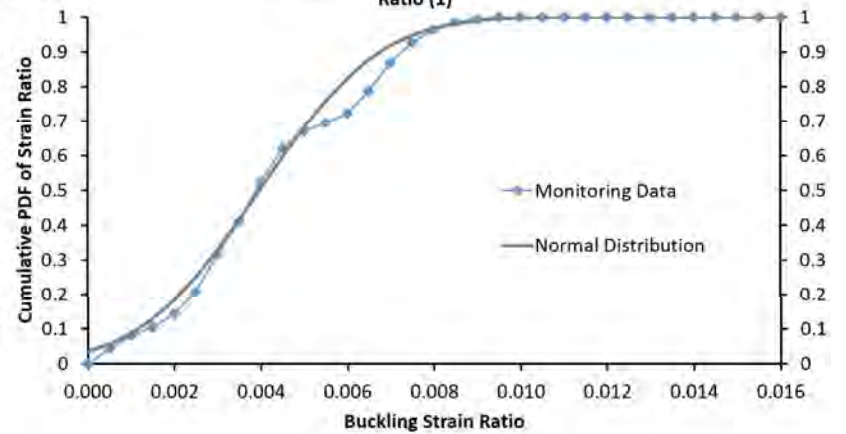
Harrowby - Bottom of Valley

PDF - DNV Buckling 2012 Ratio (1)



Harrowby- Bottom  
of Valley

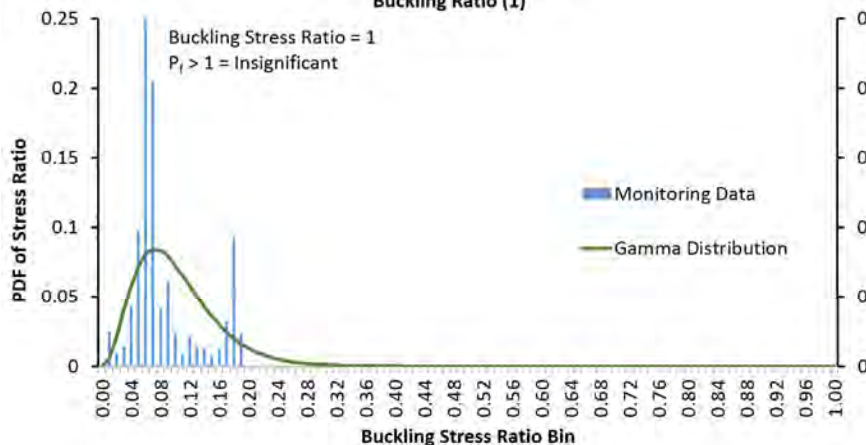
Cumulative PDF - DNV Buckling 2012  
Ratio (1)





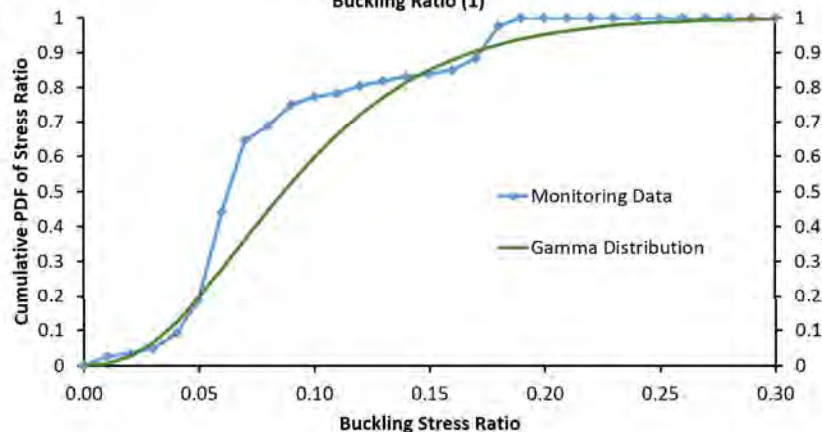
Harrowby - Bottom of Valley

PDF - DNV Stress 2000 Based  
Buckling Ratio (1)



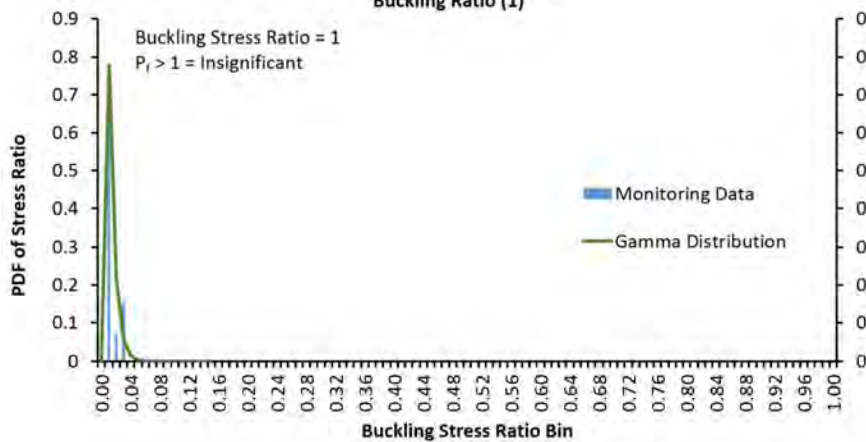
Harrowby- Bottom of Valley

Cumulative PDF - DNV Stress 2000 Based  
Buckling Ratio (1)



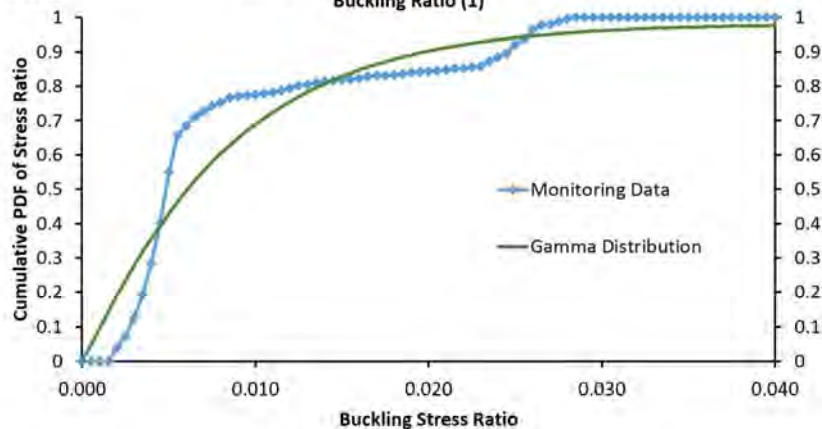
Harrowby - Bottom of Valley

PDF - DNV Stress 2012 Based  
Buckling Ratio (1)



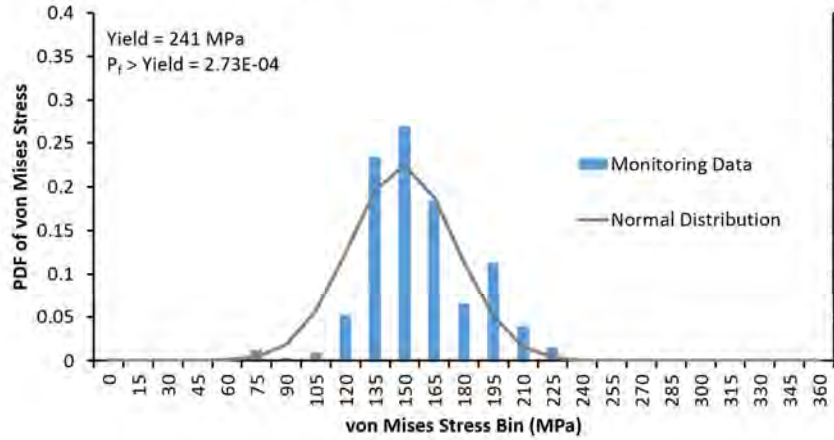
Harrowby- Bottom of Valley

Cumulative PDF - DNV Stress 2012 Based  
Buckling Ratio (1)



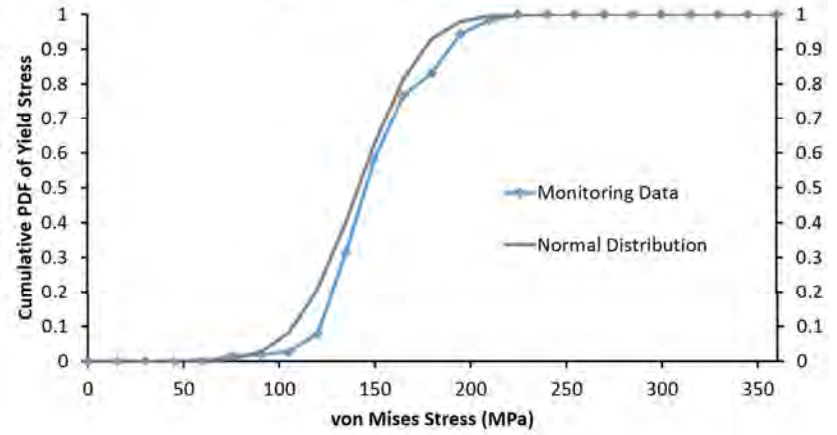
Plum River Summary

PDF von Mises (Yield 241 Mpa)



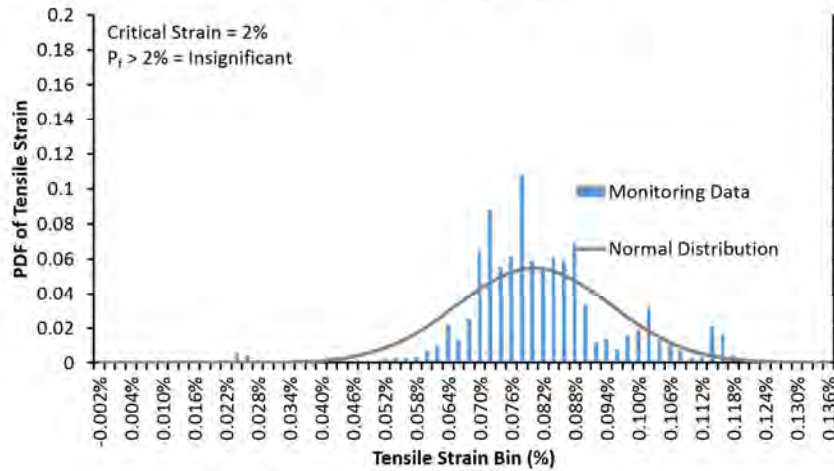
Plum River Summary

Cumulative PDF - Yield Stress



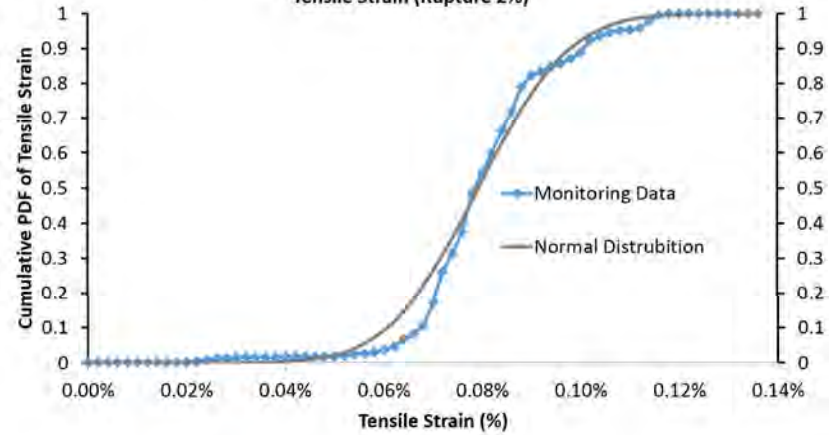
Plum River Summary

PDF - Tensile Strain (Rupture 2%)



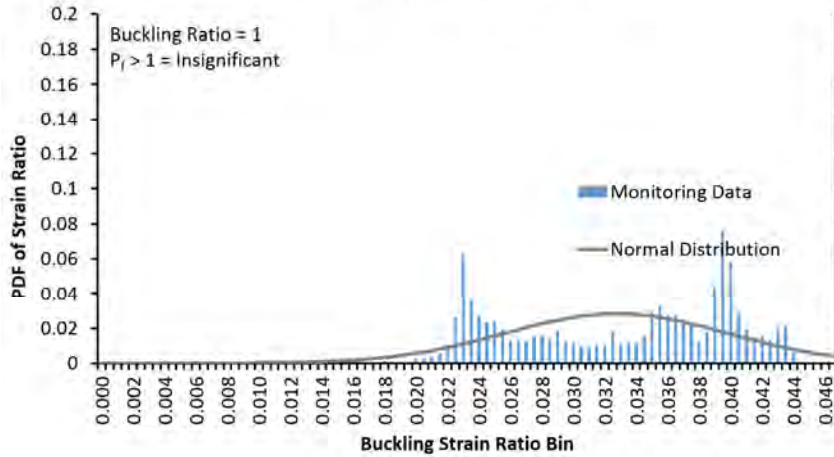
Plum River Summary

Cumulative PDF  
Tensile Strain (Rupture 2%)



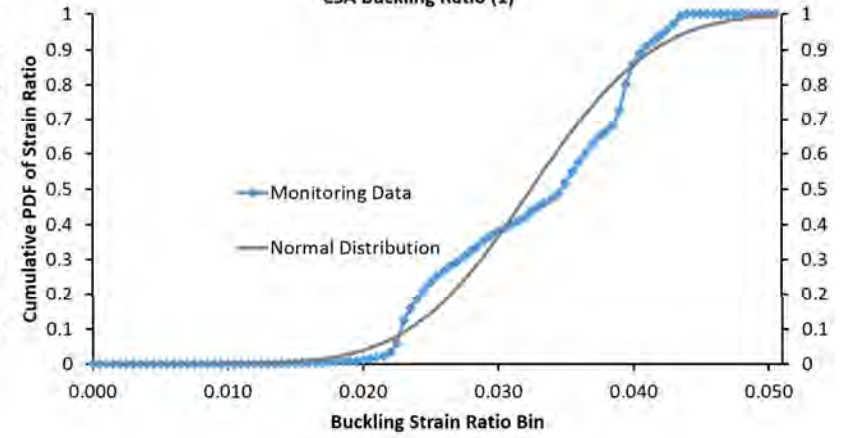
Plum River Summary

PDF - CSA Buckling Ratio (1)



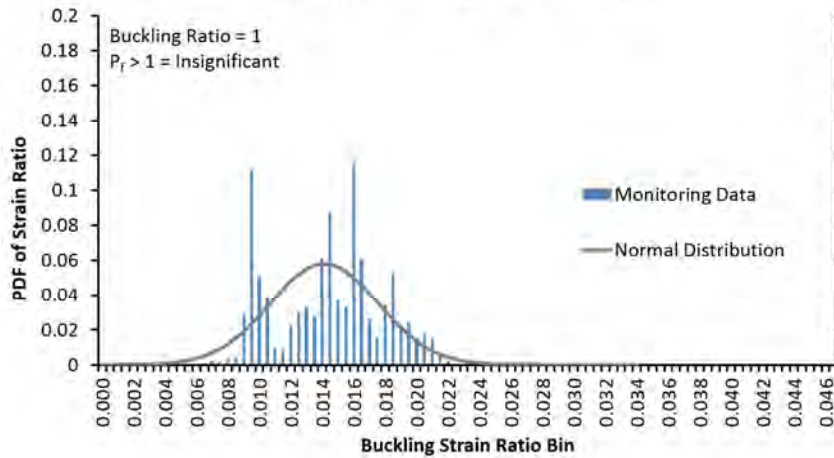
Plum River Summary

Cumulative PDF  
CSA Buckling Ratio (1)



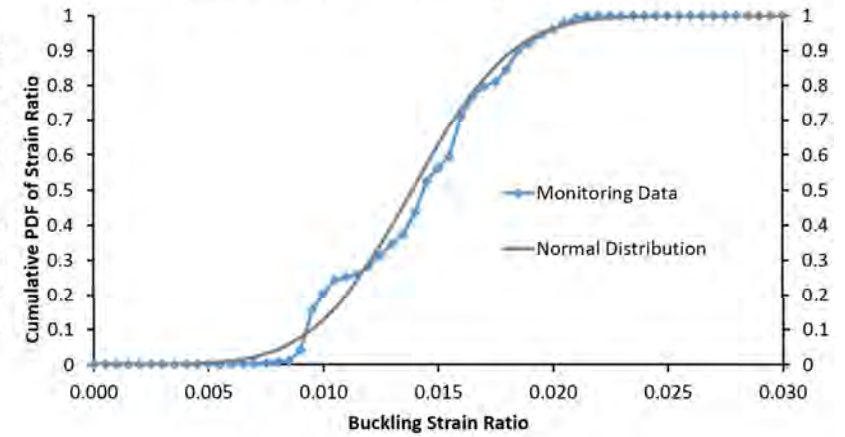
Plum River Summary

PDF - DNV Buckling Ratio 2012 (1)



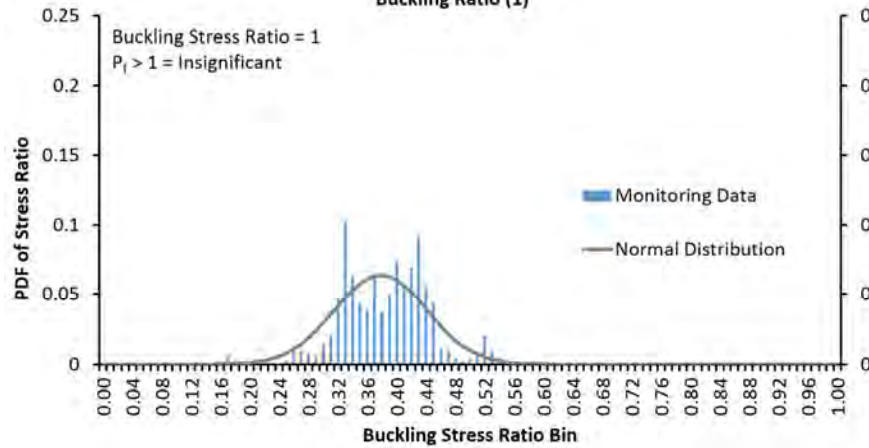
Plum River Summary

Cumulative PDF - DNV Buckling 2012 Ratio (1)



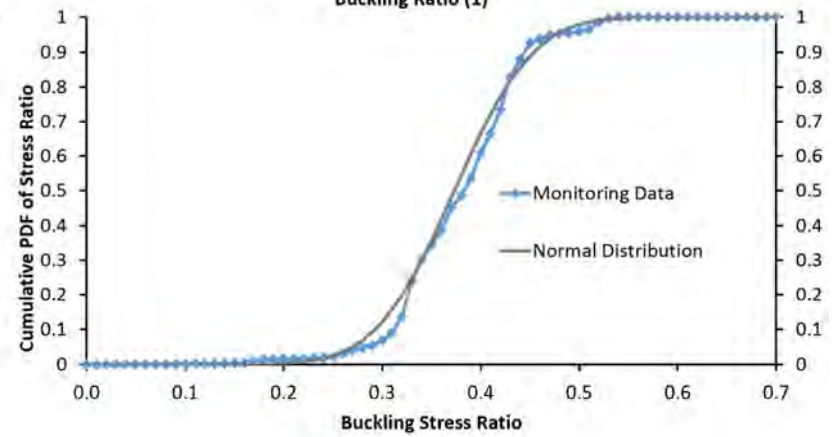
Plum River Summary

PDF - DNV Stress Based Buckling Ratio (1)



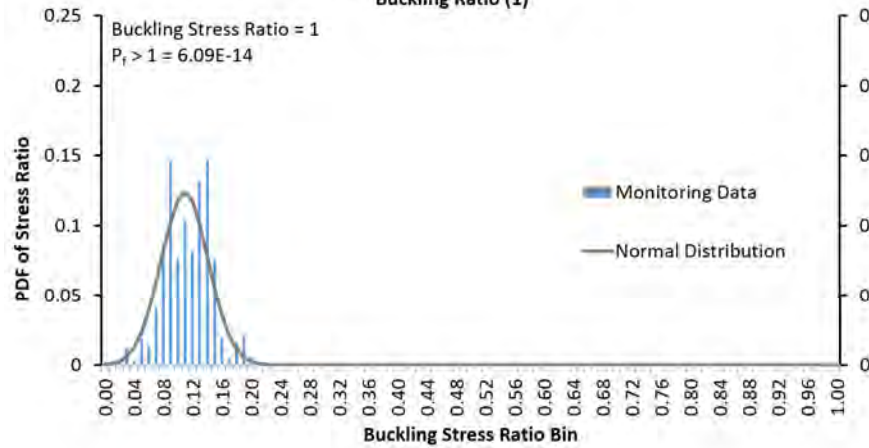
Plum River Summary

Cumulative PDF - DNV Stress Based Buckling Ratio (1)



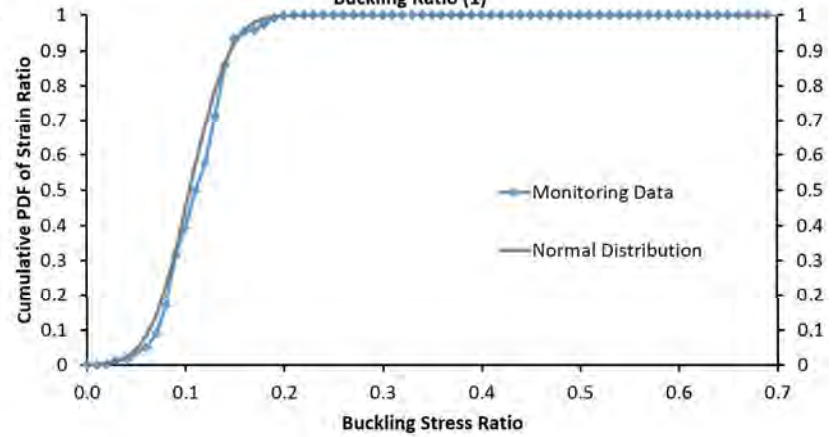
Plum River Summary

PDF - DNV 2012 Stress Based Buckling Ratio (1)



Plum River Summary

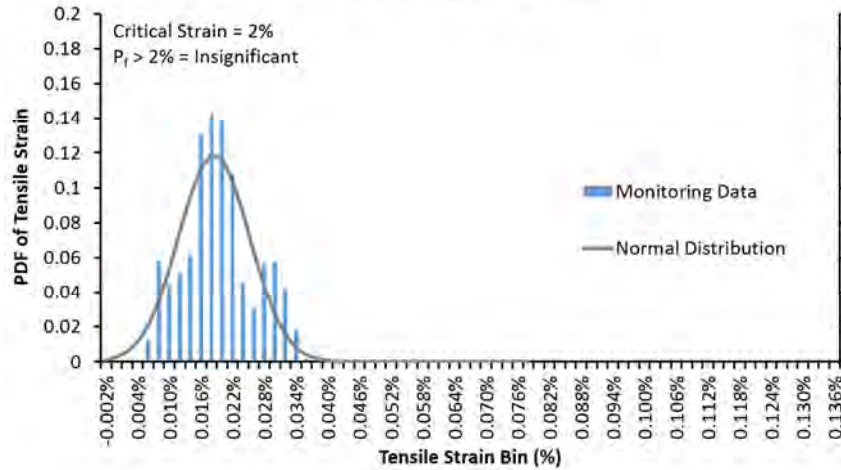
Cumulative PDF - DNV 2012 Stress Based Buckling Ratio (1)





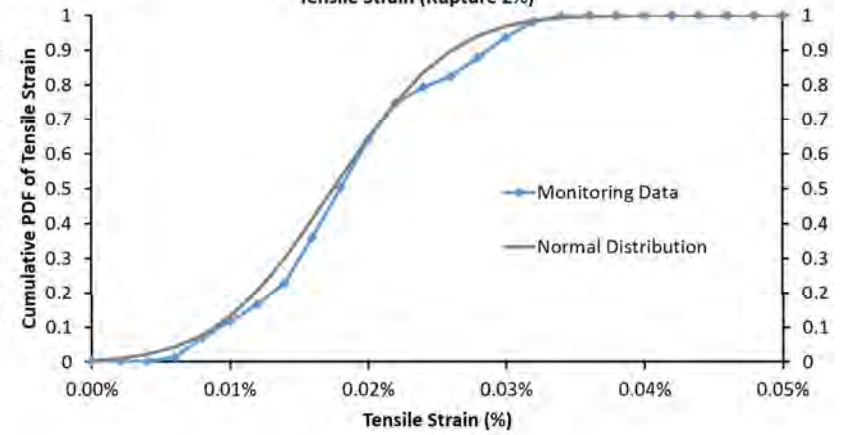
St. Lazare Summary

PDF - Tensile Strain (Rupture 2%)



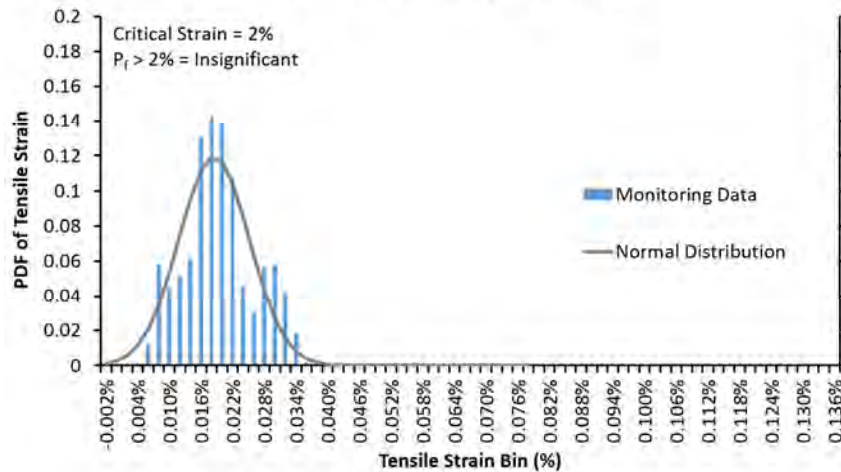
St. Lazare Summary

Cumulative PDF  
Tensile Strain (Rupture 2%)



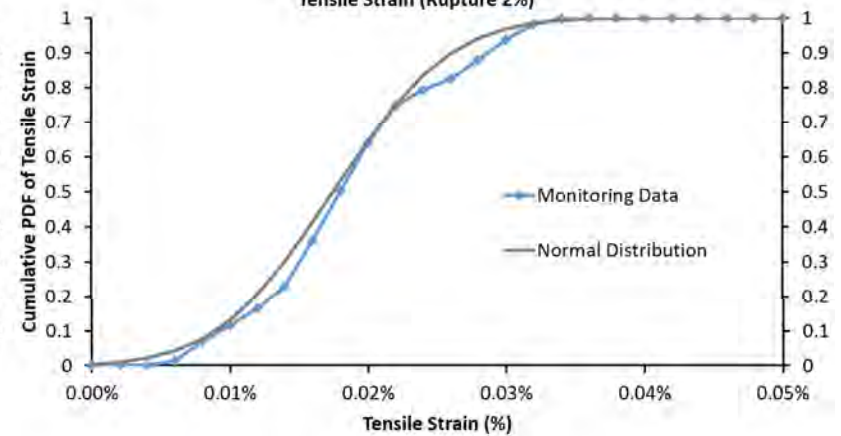
St. Lazare Summary

PDF - Tensile Strain (Rupture 2%)



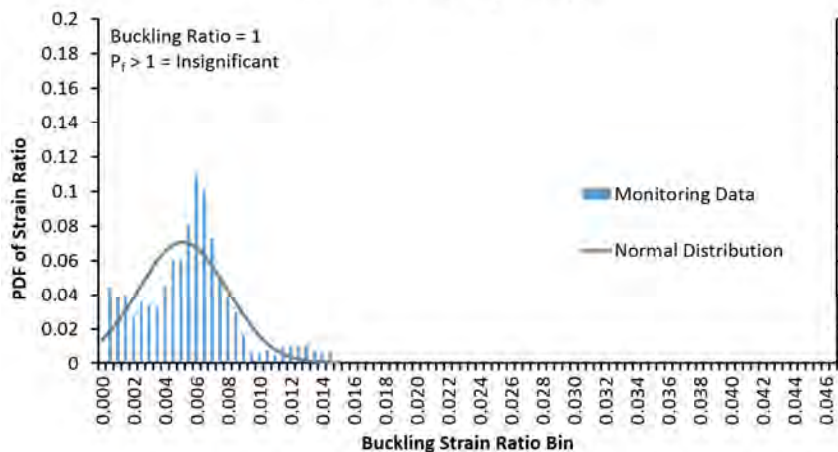
St. Lazare Summary

Cumulative PDF  
Tensile Strain (Rupture 2%)



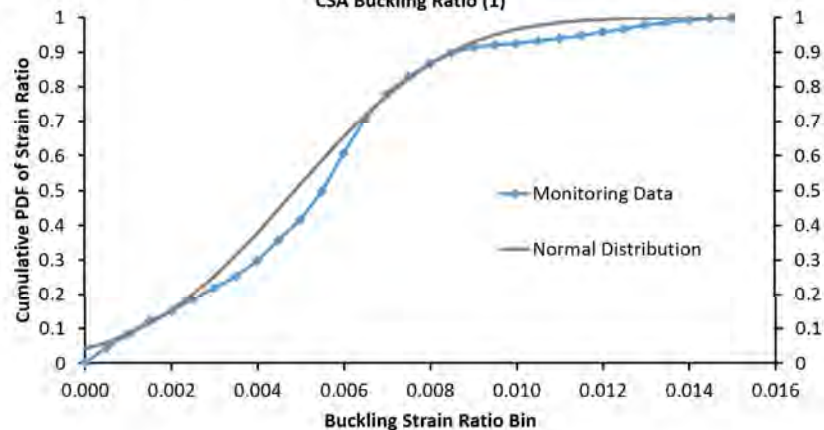
St. Lazare Summary

PDF - CSA Buckling Ratio (1)



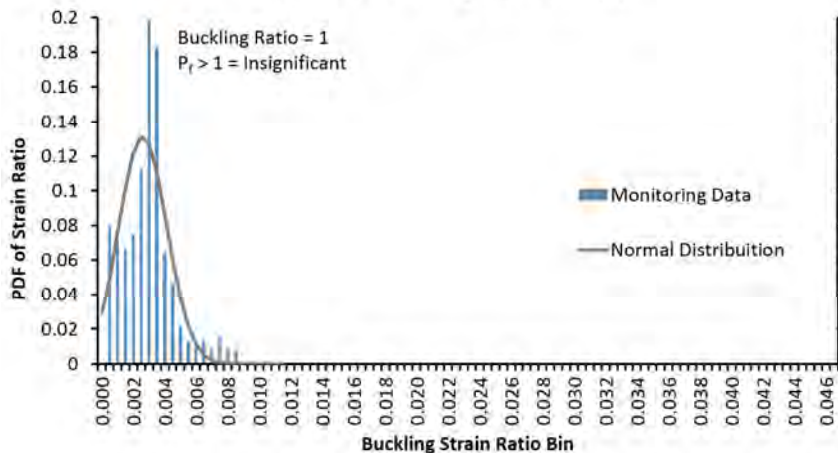
St. Lazare Summary

Cumulative PDF  
CSA Buckling Ratio (1)



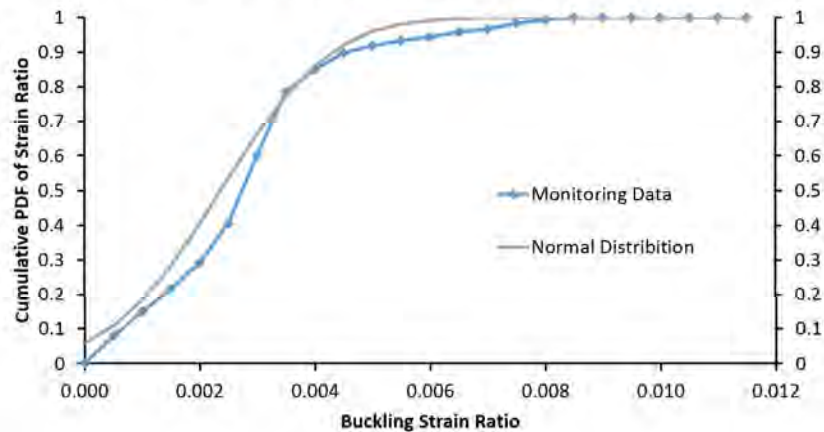
St. Lazare Summary

PDF - DNV Buckling Ratio 2012 (1)



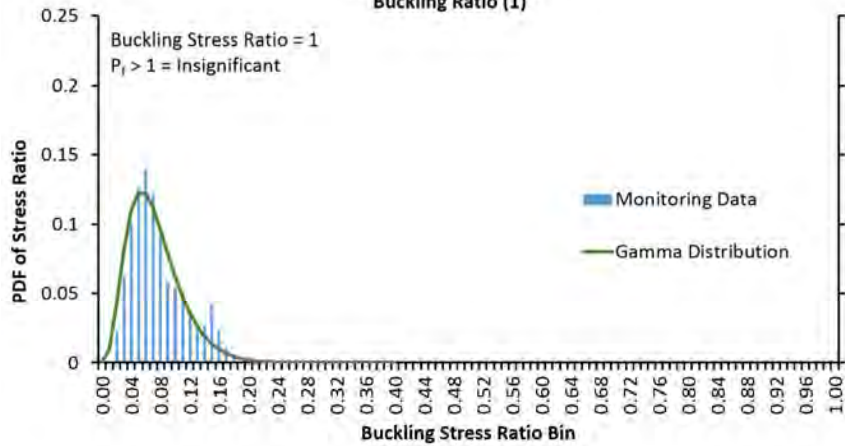
St. Lazare Summary

Cumulative PDF - DNV Buckling 2012 Ratio (1)



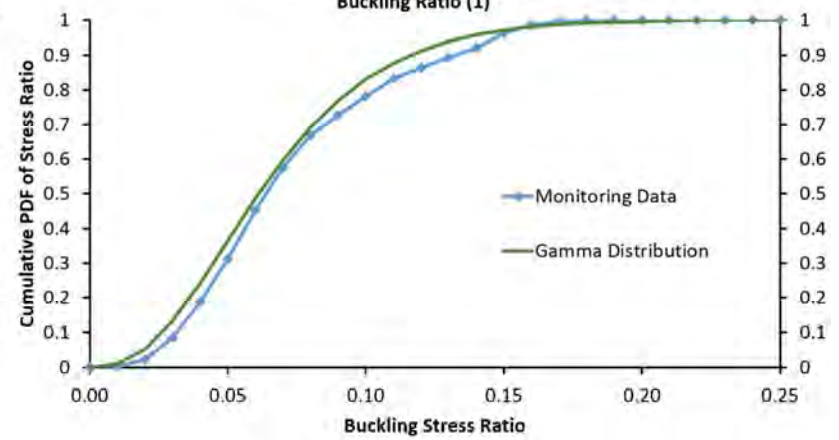
St. Lazare Summary

PDF - DNV Stress Based Buckling Ratio (1)



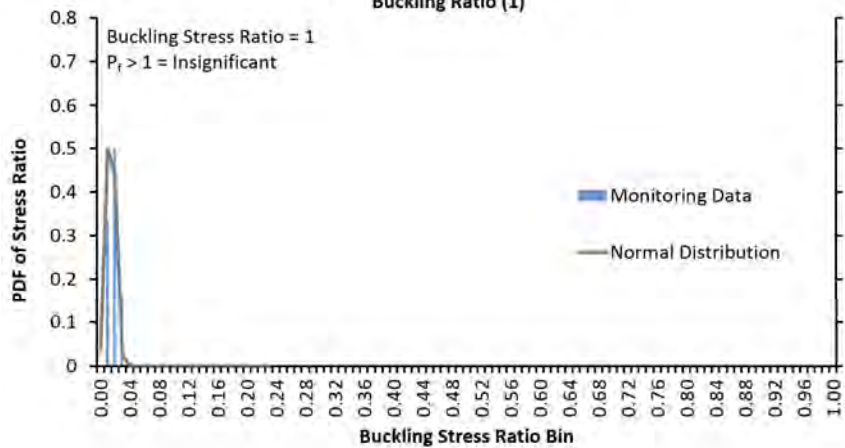
St. Lazare Summary

Cumulative PDF - DNV Stress Based Buckling Ratio (1)



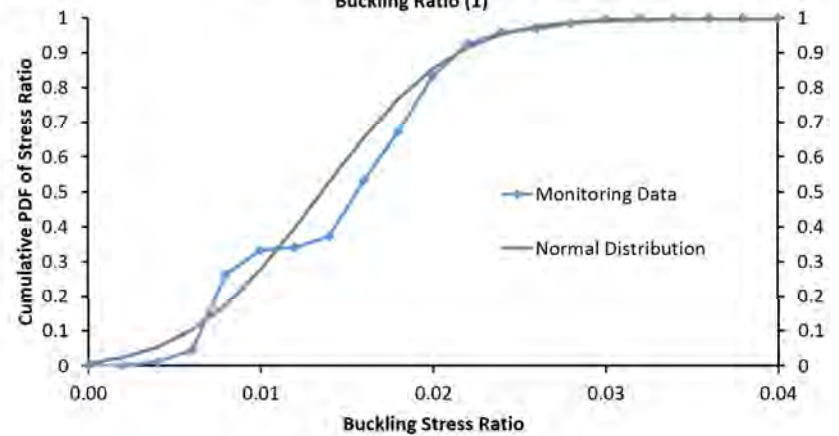
St. Lazare Summary

PDF - DNV 2012 Stress Based Buckling Ratio (1)



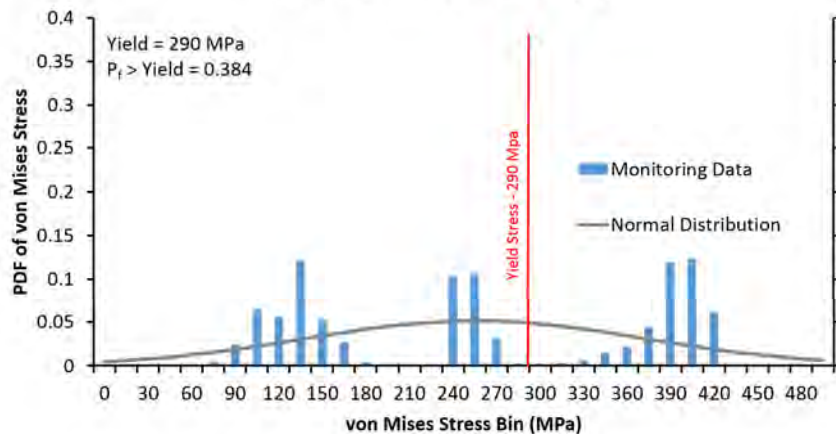
St. Lazare Summary

Cumulative PDF - DNV 2012 Stress Based Buckling Ratio (1)



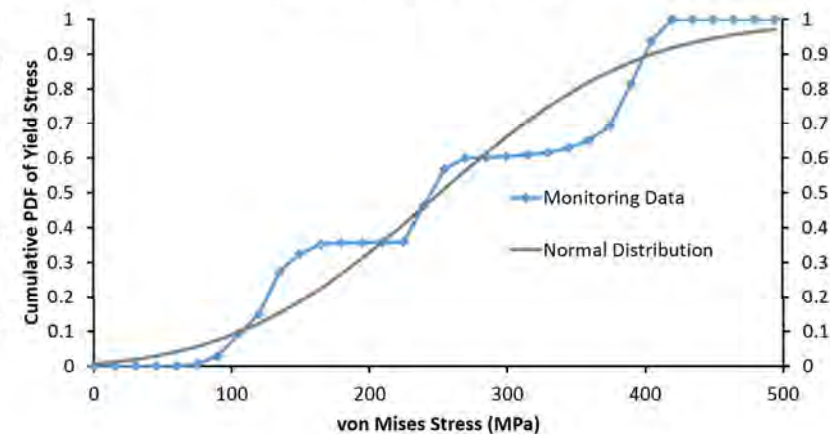
Harrowby Summary

PDF von Mises (Yield 290 Mpa)



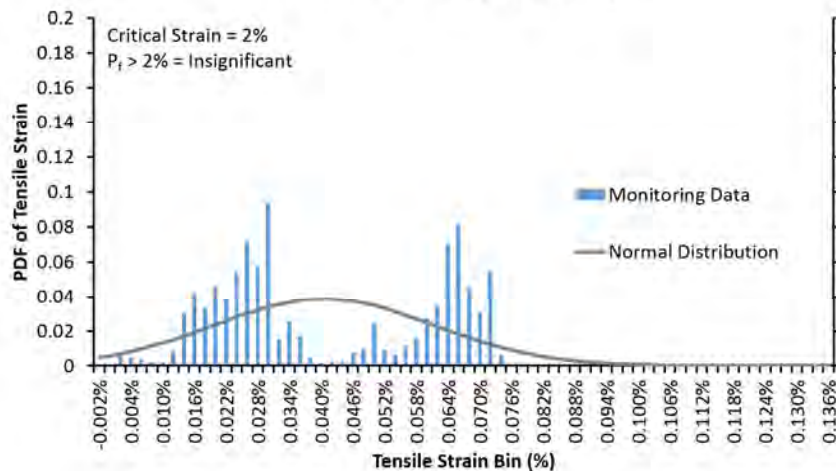
Harrowby Summary

Cumulative PDF - Yield Stress



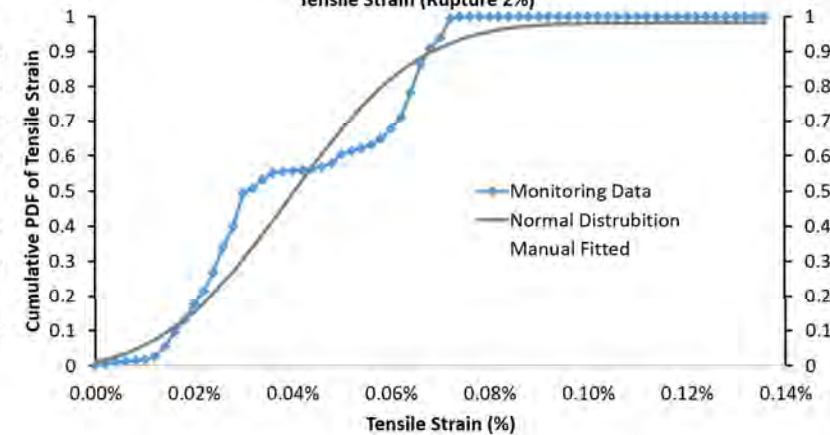
Harrowby Summary

PDF - Tensile Strain (Rupture 2%)



Harrowby Summary

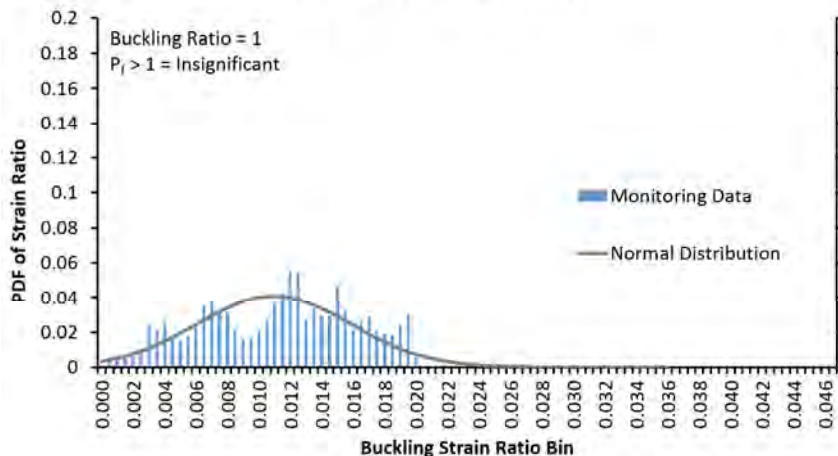
Cumulative PDF Tensile Strain (Rupture 2%)





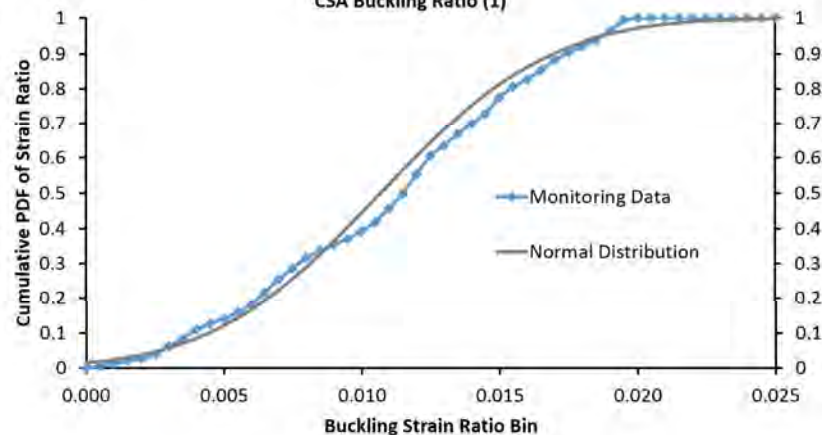
Harrowby Summary

PDF - CSA Buckling Ratio (1)



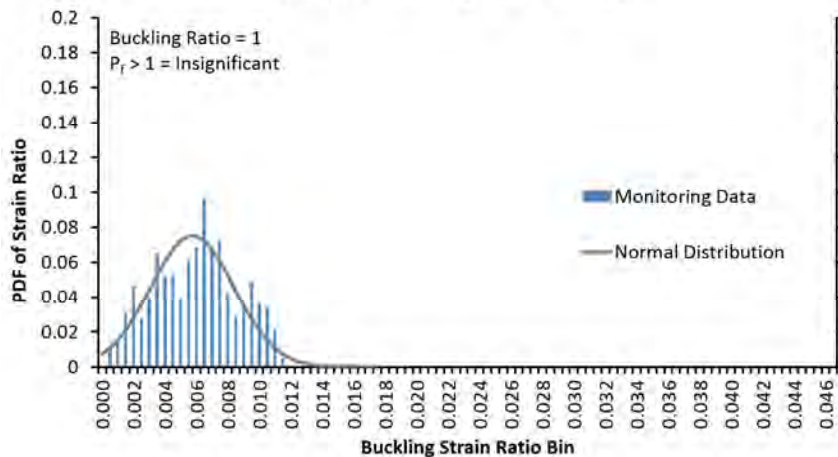
Harrowby Summary

Cumulative PDF  
CSA Buckling Ratio (1)



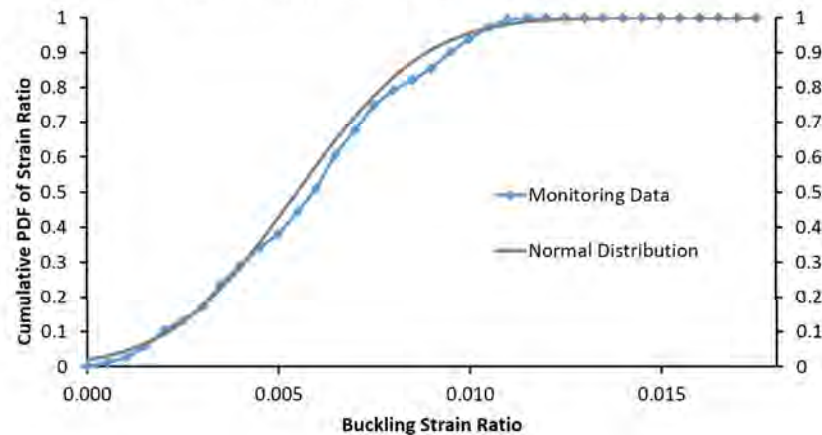
Harrowby Summary

PDF - DNV Buckling Ratio 2012 (1)



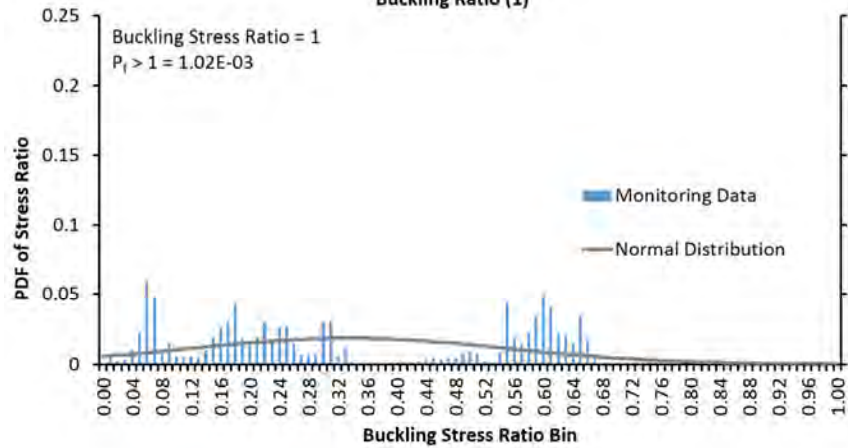
Harrowby Summary

Cumulative PDF - DNV Buckling 2012 Ratio (1)



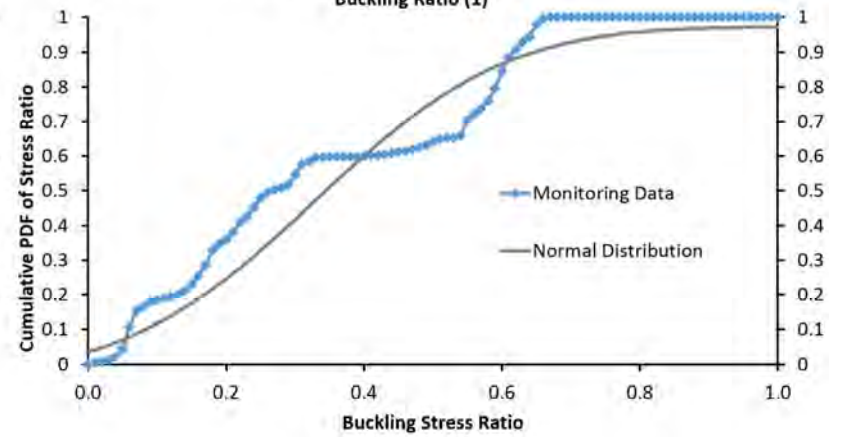
Harrowby Summary

PDF - DNV Stress Based Buckling Ratio (1)



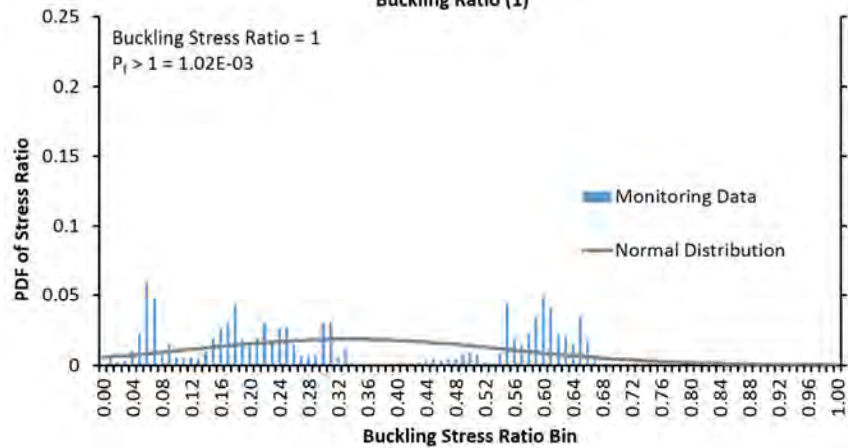
Harrowby Summary

Cumulative PDF - DNV Stress Based Buckling Ratio (1)



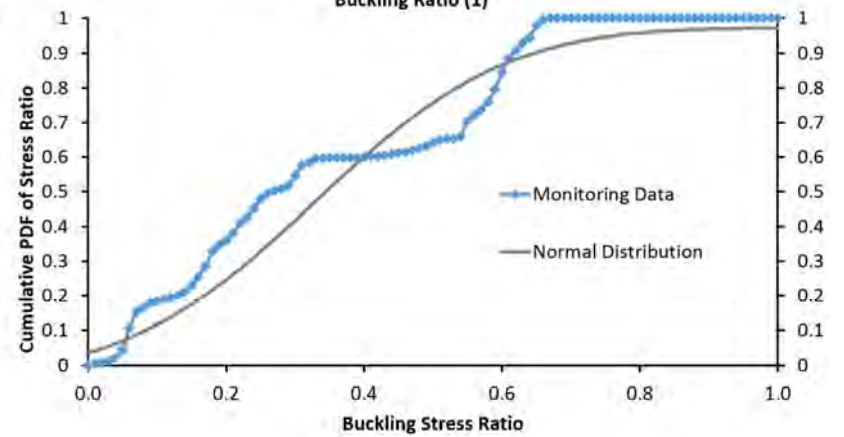
Harrowby Summary

PDF - DNV Stress Based Buckling Ratio (1)



Harrowby Summary

Cumulative PDF - DNV Stress Based Buckling Ratio (1)



## Appendix E – Example of Application of the Risk Indexing Method

## **Example Application of the Risk Indexing Method**

The example provided herein applies to Phase 1 and Phase 2 of the PipeHaz system for estimating risk from visual inspections completed at the Harrowby research site early on in the thesis research program. The probability of pipeline failure indices were filled out based on the knowledge and information available at the time of these visual inspections and does not consider additional information gathered through the course of the thesis research program.

### *Site Details*

During Phase 1 of the PipeHaz system all available information is gathered. Available information at the site includes aerial photos, geological maps, pipe information, existing engineering reports, and anecdotal information. Rainfall data is available near the site.

Once the information had been gathered and reviewed, the site was visited by a qualified inspector. The valley walls are about 100m high and 600m long which equates to a slope of 6H:1V. Figure 4-4 illustrates the site in plan and in cross-section. The right-of-way (ROW) was graded at a constant slope during installation of the pipeline. However, there are two terraces along the valley wall which are indicative of large slump block type movements which likely occurred after the pipeline was installed. Outside of the right-of-way, the valley wall is hummocky and scarred as a result of landslide activity. Groundwater seepage through the slope is present about a third of the way up the slope. Surficial soils consist of medium to high plastic silty clay, but can contain varying amounts of shale fragments, sand, and gravel which has likely been transported downslope over time.

The pipeline is 88.9 mm diameter (D) steel pipe buried at depth between 1.0 to 1.5m which is consistent with Manitoba Hydro's nominal burial depth of 1 m. The pipeline was installed in 1982 and operates at a line pressure (P) of 3.45 MPa, but fluctuates based on demand from the oat plant which the line services. The pipeline is considered a Class 2 (d) pipeline which has a design average population density ( $\rho$ ) of 3.3 people per hectare (Table 7-2). Table 01 summarizes the pipeline information required to calculate the  $\rho PD^3$  parameter. The calculation to determine Limit States probability of failure target (eq. 7.1) and evaluation length (7.2) are as follows:

$$\rho PD^3 = 8.00E+06 \text{ people/ha-MPa-mm}^3$$

$$P_f = \frac{197}{(\rho PD^3)^{0.66}}, P_f = 5.48E - 03 \text{ (per km - yr)}$$

$$\text{Evaluation Length} = 0.158\sqrt{PD^2}, \text{Evaluation Area} = 26 \text{ m wide x 1600 m long}$$

### *Example Results*

The level of knowledge weighting factors and subjective probabilities are presented in Table 02 and 03. This information is used to calculate the probability of failure estimate and the error in the probability estimate by multiplying the subjectively selected values from Table 02 and Table 03 within the indices tables (Table 04 to 07) and summarizing the products.

The completed probability of failure indices along with the results of the example are presented in Table 04 to Table 07 The level of knowledge (Table 04) is calculated to be 0.35 which would make the overall level of information available for the site between

medium to high level. A very high level research study within the Assiniboine valley was completed less than a kilometer down river. The study is a Master of Science thesis the valley wall stability and possible impacts on CP's rail line running near the bottom of the valley (Yong, 2003). The study included soils information (stratigraphy and properties), groundwater information, and stability analysis on the valley wall. The report and the contents of the report significantly improved the level of knowledge for the Harrowby site.

The probability of failure due to a landslide is calculated to be  $3.42E-03$  per km-yr (Table 05). The presence of slump blocks, seepage along the face, high groundwater conditions, retention ponds at the top of the valley and the history of landslide activity are the major contributors to a higher estimated probability of pipeline failure due to landslides. Site conditions around the river (toe erosion, scour and bank failures) had a minimal contribution to the estimated probability of pipeline failure along with damage to vegetation.

The probability of pipeline failure due to a ground settlement, subsidence and soil heave is lower than for landslides at  $1.08E-03$  per km-yr (Table 06). The shallow burial depth of the pipe and the *insitu* soils exposes the pipeline to potential stresses from shrinking/swelling and frost heave. These two factors are the major contributors to the estimated pipeline failure probability.

The example results are summarized in Table 07. The overall probability of pipeline failure is  $4.50E-03$  per km-yr which is slightly lower than the limit states target probability of pipeline failure of  $5.48E-03$  per km-yr. The site is classified as high risk

(Figure 01). The probability of pipeline failure estimate ranges between  $1.29\text{E-}02$  per km-yr and  $1.57\text{E-}03$  per km-yr based on the level of knowledge. These limits fall just within the moderate risk to exceedance of limit states risk zones. The evaluation width for which this estimate is applicable is 26 m of pipeline.

Table 01 – Harrowby Pipeline Information

	Value
Class 2 Pipe (People Per Hectare)	3.3
Operating Pressure	3.45 MPa
Diameter	88.9 mm

Table 03 – Level of Value of Information.

Level of Information	Factor
Very High	0.9
High	0.50
Medium	0.10
No to Low	0.01

Table 04- Subjective Probability (in a Given Year).

Likelihood of Factor Having an Influence	State of the System		
	Unlikely Vulnerable	Moderately Vulnerable	Likely Vulnerable
Very High	1E-01	5E-01	1.0
High	1E-02	5E-02	1E-01
Moderate	1E-03	5E-03	1E-02
Low	1E-04	5E-04	1E-03
Negligible	1E-06	5E-06	1E-05



Table 05 – Harrowby Level of Knowledge at a Site Index

<b>Information</b>	<b>Description</b>	<b>Weighting</b>	<b>Level of value</b>	<b>Product &amp; Summation</b>
Natural hazard maps	Area covered by map and reviewed	0.05	1.0E-02	5.0E-04
Aerial photos (various years)	Area covered by aerial and reviewed	0.05	1.0E-01	5.0E-03
Geological maps	Area covered by map and reviewed	0.05	1.0E-01	5.0E-03
Maintenance records	Quality and quantity	0.05	1.0E-02	5.0E-04
Field inspection reports	Quality and quantity	0.05	1.0E-02	5.0E-04
Groundwater information	Proximity to site and frequency of measurements	0.05	1.0E-01	5.0E-03
Rainfall data	Proximity to site and frequency of measurements	0.05	1.0E-01	5.0E-03
Soils information	Proximity of test holes and quality, area covered by soils map	0.05	1.0E-01	5.0E-03
Existing eng. studies	Quality of study	0.30	9.0E-01	2.7E-01
Ground movement monitoring	Survey pins, slope inclinometers (quality and quantity)	0.20	1.0E-02	2.0E-03
Pipe details and operation	Quantity and line pressure data available	0.05	5.0E-01	2.5E-02
Anecdotal information	Quality of source	0.05	5.0E-01	2.5E-02
<b>Total</b>		<b>1.00</b>	<b>±AP<sub>f</sub></b>	<b>±35%</b>

Table 06 – Harrowby Landslides Probability of Pipeline Failure Estimate Index

<b>Hazard</b>	<b>Weighting</b>	<b>Subjective Probability</b>	<b>Product &amp; Summation</b>
Toe erosion	0.05	1.0E-04	5.0E-06
Scour	0.05	1.0E-04	5.0E-06
Bank failures	0.10	1.0E-04	1.0E-05
Piezometric conditions	0.10	5.0E-04	5.0E-05
Seepage exiting face of slope	0.05	5.0E-03	2.5E-04
External water source to slope	0.05	5.0E-03	2.5E-04
Damage to vegetation	0.05	5.0E-06	2.5E-07
Loading at crest	0.05	5.0E-03	2.5E-04
Tension cracks	0.10	5.0E-04	5.0E-05
Head scarp/ slump blocks	0.10	5.0E-03	5.0E-04
Compression ridges	0.10	5.0E-04	5.0E-05
History of landslide activity at site or nearby	0.20	1.0E-02	2.0E-03
<b>Total</b>	<b>1.00</b>	<b><math>P_f</math></b>	<b>3.42E-03</b>

Table 07 – Harrowby Ground Settlement, Subsidence and Soil Heave Probability of Pipeline Failure Estimate Index

<b>Hazard</b>	<b>Weighting</b>	<b>Subjective Probability</b>	<b>Product &amp; Summation</b>
Thawing permafrost (Pingo)	0.15	1.0E-06	1.5E-07
Area of discontinuous permafrost	0.20	1.0E-06	2.0E-07
Frost heave susceptible soils	0.20	5.0E-03	1.0E-03

Shrinking/swelling potential soils	0.15	5.0E-04	7.5E-05
Poor backfill techniques	0.15	1.0E-06	7.5E-05
Sinkholes from piping	0.15	1.0E-06	1.5E-07
<b>Total</b>	<b>1.00</b>		<b><math>P_f</math></b>
			<b>1.08E-03</b>

Table 08 – Example Result Summary

	Value
Overall Probability of Failure Estimate	4.50E-03 (per km-yr)
Max Range of Probability of Failure	1.29E-02 (per km-yr)
Max Range of Probability of Failure	1.57E-03 (per km-yr)
$\rho PD^3$	7.95E+06 people/ha-MPa-mm <sup>3</sup>
Limit States Target Probability of Failure	5.48E-03 (per km-yr)
Assessment Area	1600 m along the pipe x 26 m wide

Site Probability Targets for Limit States Design ( Adapted from CSA Z662)

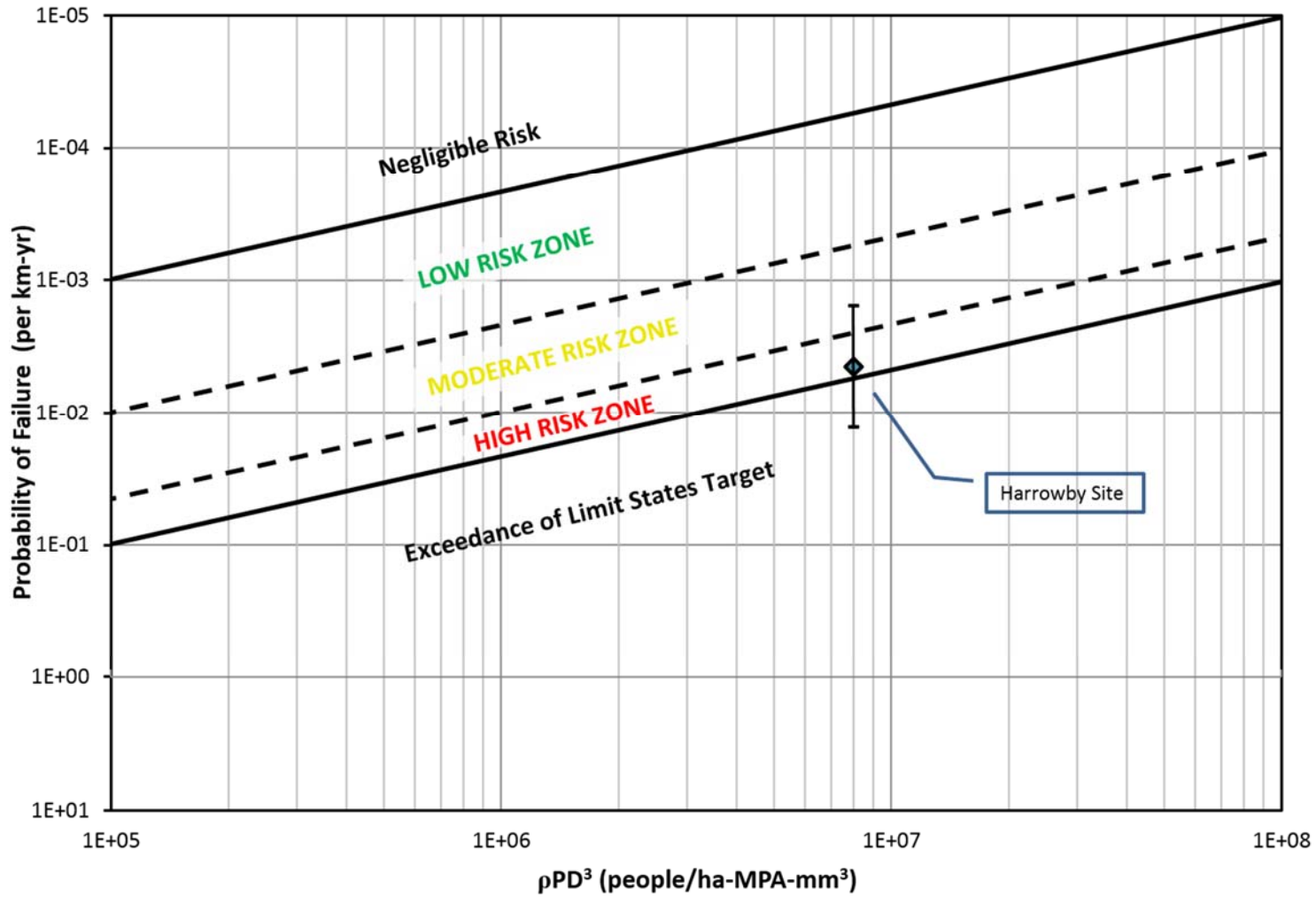


Figure 01 - Example Application Risk Classification